



Norwegian University  
of Life Sciences

**Master's Thesis 2024 30 ECTS**

Faculty of Science and Technology

# **A comparative study of soil temperature models, including machine learning models using two parameters**

**Mats Hoem Olsen**

Master of Science in Data Science

## Acknowledgements

I would like to thank all my friends who have supported me during the writing, and comforted me during the difficult times. A big thank you to Mahrin Tasfe, Emma Sofie Rikheim & Celine Hagen, Vegard Eriksen Sæther, Emilie Risdal Danielsen, and Sindre Stokke for making sure I didn't overwork myself, and was able to get a breather during this intense period.

I would also like to give a big thank you to the Student Life Center in Ås and Ås Health Station for the help and the services they give to students which I was able to use. Mental health is health and it showed during the writing, and am eternally grateful for the free services they offer.

I would also like to thank my supervisors; Mareile Astrid Wolff, Berit Nordskog, and Brita Linnestad for taking me as their master student and being patient with me while I figured things out along the way this semester. You have been the best advisors I could get, and I thank you for your patience.

## Contents

<b>1</b>	<b>Introduction</b>	<b>2</b>
<b>2</b>	<b>Theory</b>	<b>4</b>
2.1	Soil temperature . . . . .	4
2.2	Linear Regression . . . . .	5
2.3	Plauborg Regression . . . . .	5
2.4	Long Short Term-Memory (LSTM) model . . . . .	6
2.5	Gated Recurrent Unit (GRU) . . . . .	7
2.6	Bidirectional models . . . . .	9
<b>3</b>	<b>Method</b>	<b>10</b>
3.1	Source of data . . . . .	10
3.2	Dataset . . . . .	10
3.2.1	Selection process . . . . .	10
3.2.2	Collection of data . . . . .	11
3.2.3	Storage of data . . . . .	14
	Data structure . . . . .	14
3.3	Data cleaning and treatment . . . . .	14
3.3.1	Outlier detection and removal . . . . .	15
3.3.2	Missing value imputation . . . . .	16
3.3.3	Summary of data . . . . .	16
3.4	Setup of models . . . . .	17
3.4.1	Basic Linear model . . . . .	18
3.4.2	Plauborg . . . . .	18
3.4.3	LSTM . . . . .	18
3.4.4	GRU . . . . .	18
3.4.5	Bidirectional layer . . . . .	18
3.5	Metrics . . . . .	19
3.5.1	Confidence eclipses . . . . .	20
3.6	Model training . . . . .	21
3.7	Use of AI . . . . .	22
<b>4</b>	<b>Results</b>	<b>23</b>
4.1	Linear model . . . . .	26
4.2	Plauborg daily . . . . .	29
4.3	Plauborg hourly . . . . .	29
4.4	Long Short Term-Memory (LSTM) . . . . .	34
4.5	Bi-Directional Long Short Term-Memory (LSTM) . . . . .	37
4.6	Gated Recurrent Unit (GRU) . . . . .	37
4.7	Bi-directional Gated Recurrent Unit (GRU) . . . . .	43
<b>5</b>	<b>Discussion</b>	<b>46</b>
5.1	The Autumn discrepancy . . . . .	46
5.1.1	Temperature seasons . . . . .	46
5.2	Regression model performance . . . . .	46
5.3	Discussion of good results of Plauborg . . . . .	47
5.4	Modification of Plauborg . . . . .	47
	5.4.1 RNN results compared to other studies . . . . .	51

## LIST OF FIGURES

5.5 Deep learning model performance . . . . .	51
5.6 Future work . . . . .	51
<b>6 Conclusion</b>	<b>53</b>
6.1 Discussion of research goals . . . . .	53
6.2 Limitations . . . . .	54
<b>7 Bibliography</b>	<b>a</b>
<b>A Plots</b>	<b>g</b>
A.1 Difference plots of model performance per region . . . . .	g
A.2 Data visiulation of data before treatment . . . . .	cy
A.3 Data visiulation of data after treatment . . . . .	ev
<b>B Tables</b>	<b>gs</b>
B.1 Model performance . . . . .	gs
B.2 Data summary . . . . .	hf

## List of Algorithms

1 Randommised $\kappa$ algorithm . . . . .	20
2 Find Non-NULL Ranges (Abstract) . . . . .	21

## List of Figures

1 LSTM cell, From: Chevalier [20] . . . . .	6
3 Bi-directional model diargam . . . . .	8
2 GRU model sketch . . . . .	8
4 Diagram sketching three procedures used in this study. . . . .	10
5 Visual representation of Øsaker untreated . . . . .	12
6 Visual representation of Øsaker treated . . . . .	13
7 Simple Interpolation outlier detection . . . . .	16
8 Difference plots of extremal regions Linear Regression . . . . .	27
9 Plots showing ground truth vs predicted values from the linear Regression models with their 68%, 95%, and 99% confidence eclipses. The confidence eclipses function the same as confidence intervals but in two dimensions, meaning the area covered by the eclipse denotes where one can expect the points to be with a given confidence percent. These plots contain a subset of the data, however the ellipses and $\lambda_0$ are calculated with all the data. . . . .	29
10 Difference plots of extremal regions daily Plauborg . . . . .	30
11 Plots showing ground truth vs predicted values from the daily Plauborg models with their 68%, 95%, and 99% confidence eclipses. The confidence eclipses function the same as confidence intervals but in two dimensions, meaning the area covered by the eclipse denotes where one can expect the points to be with a given confidence percent. These plots contain a subset of the data, however the ellipses and $\lambda_0$ are calculated with all the data. . . . .	30
12 Difference plot for daily Plauborg model in year 2022 and region Innlandet for 20cm soil temperature. . . . .	32

## LIST OF FIGURES

13	Difference plots of extremal regions hourly Plauborg . . . . .	32
14	Plots showing ground truth vs predicted values from the hourly Plauborg models with their 68%, 95%, and 99% confidence eclipses. The confidence eclipses function the same as confidence intervals but in two dimensions, meaning the area covered by the eclipse denotes where one can expect the points to be with a given confidence percent. These plots contain a subset of the data, however the ellipses and $\lambda_0$ are calculated with all the data. . . . .	34
15	Difference plots of extremal regions LSTM . . . . .	35
16	Plots showing ground truth vs predicted values from the LSTM models with their 68%, 95%, and 99% confidence eclipses. The confidence eclipses function the same as confidence intervals but in two dimensions, meaning the area covered by the eclipse denotes where one can expect the points to be with a given confidence percent. These plots contain a subset of the data, however the ellipses and $\lambda_0$ are calculated with all the data. . . . .	35
17	Performance graphs displaying the developments of Mean Square Error and Explained Variance ( $R^2$ ) for each epoch. . . . .	37
18	Difference plots of extremal regions BiLSTM . . . . .	38
19	Plots showing ground truth vs predicted values from the BiLSTM models with their 68%, 95%, and 99% confidence eclipses. The confidence eclipses function the same as confidence intervals but in two dimensions, meaning the area covered by the eclipse denotes where one can expect the points to be with a given confidence percent. These plots contain a subset of the data, however the ellipses and $\lambda_0$ are calculated with all the data. . . . .	38
20	Performance graphs displaying the developments of Mean Square Error and Explained Variance ( $R^2$ ) for each epoch. . . . .	40
21	Difference plots of extremal regions GRU . . . . .	40
22	Plots showing ground truth vs predicted values from the GRU models with their 68%, 95%, and 99% confidence eclipses. The confidence eclipses function the same as confidence intervals but in two dimensions, meaning the area covered by the eclipse denotes where one can expect the points to be with a given confidence percent. These plots contain a subset of the data, however the ellipses and $\lambda_0$ are calculated with all the data. . . . .	42
23	Performance graphs displaying the developments of Mean Square Error and Explained Variance ( $R^2$ ) for each epoch. . . . .	42
24	Difference plots of extremal regions BiGRU . . . . .	43
25	Plots showing ground truth vs predicted values from the BiGRU models with their 68%, 95%, and 99% confidence eclipses. The confidence eclipses function the same as confidence intervals but in two dimensions, meaning the area covered by the eclipse denotes where one can expect the points to be with a given confidence percent. These plots contain a subset of the data, however the ellipses and $\lambda_0$ are calculated with all the data. . . . .	45
26	Performance graphs displaying the developments of Mean Square Error and Explained Variance ( $R^2$ ) for each epoch. . . . .	45
27	Comperasion of daily versus hourly predictions . . . . .	49
28	Diff plot for Linear Regression, region Innlandet, year 2021, at depth 10 . . . . .	g
29	Diff plot for Linear Regression, region Innlandet, year 2022, at depth 10 . . . . .	h
30	Diff plot for Linear Regression, region Innlandet, year 2021, at depth 20 . . . . .	i
31	Diff plot for Linear Regression, region Innlandet, year 2022, at depth 20 . . . . .	j
32	Diff plot for Linear Regression, region Trøndelag, year 2021, at depth 10 . . . . .	k

## LIST OF FIGURES

33	Diff plot for Linear Regression, region Trøndelag, year 2022, at depth 10 . . . . .	1
34	Diff plot for Linear Regression, region Trøndelag, year 2021, at depth 20 . . . . .	m
35	Diff plot for Linear Regression, region Trøndelag, year 2022, at depth 20 . . . . .	n
36	Diff plot for Linear Regression, region Østfold, year 2021, at depth 10 . . . . .	o
37	Diff plot for Linear Regression, region Østfold, year 2022, at depth 10 . . . . .	p
38	Diff plot for Linear Regression, region Østfold, year 2021, at depth 20 . . . . .	q
39	Diff plot for Linear Regression, region Østfold, year 2022, at depth 20 . . . . .	r
40	Diff plot for Linear Regression, region Vestfold, year 2021, at depth 10 . . . . .	s
41	Diff plot for Linear Regression, region Vestfold, year 2022, at depth 10 . . . . .	t
42	Diff plot for Linear Regression, region Vestfold, year 2021, at depth 20 . . . . .	u
43	Diff plot for Linear Regression, region Vestfold, year 2022, at depth 20 . . . . .	v
44	Diff plot for Plauborg (day), region Innlandet, year 2021, at depth 10 . . . . .	w
45	Diff plot for Plauborg (day), region Innlandet, year 2022, at depth 10 . . . . .	x
46	Diff plot for Plauborg (day), region Innlandet, year 2021, at depth 20 . . . . .	y
47	Diff plot for Plauborg (day), region Innlandet, year 2022, at depth 20 . . . . .	z
48	Diff plot for Plauborg (day), region Trøndelag, year 2021, at depth 10 . . . . .	aa
49	Diff plot for Plauborg (day), region Trøndelag, year 2022, at depth 10 . . . . .	ab
50	Diff plot for Plauborg (day), region Trøndelag, year 2021, at depth 20 . . . . .	ac
51	Diff plot for Plauborg (day), region Trøndelag, year 2022, at depth 20 . . . . .	ad
52	Diff plot for Plauborg (day), region Østfold, year 2021, at depth 10 . . . . .	ae
53	Diff plot for Plauborg (day), region Østfold, year 2022, at depth 10 . . . . .	af
54	Diff plot for Plauborg (day), region Østfold, year 2021, at depth 20 . . . . .	ag
55	Diff plot for Plauborg (day), region Østfold, year 2022, at depth 20 . . . . .	ah
56	Diff plot for Plauborg (day), region Vestfold, year 2021, at depth 10 . . . . .	ai
57	Diff plot for Plauborg (day), region Vestfold, year 2022, at depth 10 . . . . .	aj
58	Diff plot for Plauborg (day), region Vestfold, year 2021, at depth 20 . . . . .	ak
59	Diff plot for Plauborg (day), region Vestfold, year 2022, at depth 20 . . . . .	al
60	Diff plot for Plauborg (hour), region Innlandet, year 2021, at depth 10 . . . . .	am
61	Diff plot for Plauborg (hour), region Innlandet, year 2022, at depth 10 . . . . .	an
62	Diff plot for Plauborg (hour), region Innlandet, year 2021, at depth 20 . . . . .	ao
63	Diff plot for Plauborg (hour), region Innlandet, year 2022, at depth 20 . . . . .	ap
64	Diff plot for Plauborg (hour), region Trøndelag, year 2021, at depth 10 . . . . .	aq
65	Diff plot for Plauborg (hour), region Trøndelag, year 2022, at depth 10 . . . . .	ar
66	Diff plot for Plauborg (hour), region Trøndelag, year 2021, at depth 20 . . . . .	as
67	Diff plot for Plauborg (hour), region Trøndelag, year 2022, at depth 20 . . . . .	at
68	Diff plot for Plauborg (hour), region Østfold, year 2021, at depth 10 . . . . .	au
69	Diff plot for Plauborg (hour), region Østfold, year 2022, at depth 10 . . . . .	av
70	Diff plot for Plauborg (hour), region Østfold, year 2021, at depth 20 . . . . .	aw
71	Diff plot for Plauborg (hour), region Østfold, year 2022, at depth 20 . . . . .	ax
72	Diff plot for Plauborg (hour), region Vestfold, year 2021, at depth 10 . . . . .	ay
73	Diff plot for Plauborg (hour), region Vestfold, year 2022, at depth 10 . . . . .	az
74	Diff plot for Plauborg (hour), region Vestfold, year 2021, at depth 20 . . . . .	ba
75	Diff plot for Plauborg (hour), region Vestfold, year 2022, at depth 20 . . . . .	bb
76	Diff plot for BiLSTM, region Innlandet, year 2021, at depth 10 . . . . .	bc
77	Diff plot for BiLSTM, region Innlandet, year 2022, at depth 10 . . . . .	bd
78	Diff plot for BiLSTM, region Innlandet, year 2021, at depth 20 . . . . .	be
79	Diff plot for BiLSTM, region Innlandet, year 2022, at depth 20 . . . . .	bf
80	Diff plot for BiLSTM, region Trøndelag, year 2021, at depth 10 . . . . .	bg
81	Diff plot for BiLSTM, region Trøndelag, year 2022, at depth 10 . . . . .	bh

## LIST OF FIGURES

82	Diff plot for BiLSTM, region Trøndelag, year 2021, at depth 20 . . . . .	bi
83	Diff plot for BiLSTM, region Trøndelag, year 2022, at depth 20 . . . . .	bj
84	Diff plot for BiLSTM, region Østfold, year 2021, at depth 10 . . . . .	bk
85	Diff plot for BiLSTM, region Østfold, year 2022, at depth 10 . . . . .	bl
86	Diff plot for BiLSTM, region Østfold, year 2021, at depth 20 . . . . .	bm
87	Diff plot for BiLSTM, region Østfold, year 2022, at depth 20 . . . . .	bn
88	Diff plot for BiLSTM, region Vestfold, year 2021, at depth 10 . . . . .	bo
89	Diff plot for BiLSTM, region Vestfold, year 2022, at depth 10 . . . . .	bp
90	Diff plot for BiLSTM, region Vestfold, year 2021, at depth 20 . . . . .	bq
91	Diff plot for BiLSTM, region Vestfold, year 2022, at depth 20 . . . . .	br
92	Diff plot for LSTM, region Innlandet, year 2021, at depth 10 . . . . .	bs
93	Diff plot for LSTM, region Innlandet, year 2022, at depth 10 . . . . .	bt
94	Diff plot for LSTM, region Innlandet, year 2021, at depth 20 . . . . .	bu
95	Diff plot for LSTM, region Innlandet, year 2022, at depth 20 . . . . .	bv
96	Diff plot for LSTM, region Trøndelag, year 2021, at depth 10 . . . . .	bw
97	Diff plot for LSTM, region Trøndelag, year 2022, at depth 10 . . . . .	bx
98	Diff plot for LSTM, region Trøndelag, year 2021, at depth 20 . . . . .	by
99	Diff plot for LSTM, region Trøndelag, year 2022, at depth 20 . . . . .	bz
100	Diff plot for LSTM, region Østfold, year 2021, at depth 10 . . . . .	ca
101	Diff plot for LSTM, region Østfold, year 2022, at depth 10 . . . . .	cb
102	Diff plot for LSTM, region Østfold, year 2021, at depth 20 . . . . .	cc
103	Diff plot for LSTM, region Østfold, year 2022, at depth 20 . . . . .	cd
104	Diff plot for LSTM, region Vestfold, year 2021, at depth 10 . . . . .	ce
105	Diff plot for LSTM, region Vestfold, year 2022, at depth 10 . . . . .	cf
106	Diff plot for LSTM, region Vestfold, year 2021, at depth 20 . . . . .	cg
107	Diff plot for LSTM, region Vestfold, year 2022, at depth 20 . . . . .	ch
108	Diff plot for GRU, region Innlandet, year 2021, at depth 10 . . . . .	ci
109	Diff plot for GRU, region Innlandet, year 2022, at depth 10 . . . . .	cj
110	Diff plot for GRU, region Innlandet, year 2021, at depth 20 . . . . .	ck
111	Diff plot for GRU, region Innlandet, year 2022, at depth 20 . . . . .	cl
112	Diff plot for GRU, region Trøndelag, year 2021, at depth 10 . . . . .	cm
113	Diff plot for GRU, region Trøndelag, year 2022, at depth 10 . . . . .	cn
114	Diff plot for GRU, region Trøndelag, year 2021, at depth 20 . . . . .	co
115	Diff plot for GRU, region Trøndelag, year 2022, at depth 20 . . . . .	cp
116	Diff plot for GRU, region Østfold, year 2021, at depth 10 . . . . .	cq
117	Diff plot for GRU, region Østfold, year 2022, at depth 10 . . . . .	cr
118	Diff plot for GRU, region Østfold, year 2021, at depth 20 . . . . .	cs
119	Diff plot for GRU, region Østfold, year 2022, at depth 20 . . . . .	ct
120	Diff plot for GRU, region Vestfold, year 2021, at depth 10 . . . . .	cu
121	Diff plot for GRU, region Vestfold, year 2022, at depth 10 . . . . .	cv
122	Diff plot for GRU, region Vestfold, year 2021, at depth 20 . . . . .	cw
123	Diff plot for GRU, region Vestfold, year 2022, at depth 20 . . . . .	cx
124	Visual representation of station 17 untreated for TM . . . . .	cz
125	Visual representation of station 17 untreated for TJM10 . . . . .	da
126	Visual representation of station 17 untreated for TJM20 . . . . .	db
127	Visual representation of station 11 untreated for TM . . . . .	dc
128	Visual representation of station 11 untreated for TJM10 . . . . .	dd
129	Visual representation of station 11 untreated for TJM20 . . . . .	de
130	Visual representation of station 26 untreated for TM . . . . .	df

## LIST OF FIGURES

131	Visual representation of station 26 untreated for TJM10 . . . . .	dg
132	Visual representation of station 26 untreated for TJM20 . . . . .	dh
133	Visual representation of station 27 untreated for TM . . . . .	di
134	Visual representation of station 27 untreated for TJM10 . . . . .	dj
135	Visual representation of station 27 untreated for TJM20 . . . . .	dk
136	Visual representation of station 15 untreated for TM . . . . .	dl
137	Visual representation of station 15 untreated for TJM10 . . . . .	dm
138	Visual representation of station 15 untreated for TJM20 . . . . .	dn
139	Visual representation of station 57 untreated for TM . . . . .	do
140	Visual representation of station 57 untreated for TJM10 . . . . .	dp
141	Visual representation of station 57 untreated for TJM20 . . . . .	dq
142	Visual representation of station 34 untreated for TM . . . . .	dr
143	Visual representation of station 34 untreated for TJM10 . . . . .	ds
144	Visual representation of station 34 untreated for TJM20 . . . . .	dt
145	Visual representation of station 39 untreated for TM . . . . .	du
146	Visual representation of station 39 untreated for TJM10 . . . . .	dv
147	Visual representation of station 39 untreated for TJM20 . . . . .	dw
148	Visual representation of station 37 untreated for TM . . . . .	dx
149	Visual representation of station 37 untreated for TJM10 . . . . .	dy
150	Visual representation of station 37 untreated for TJM20 . . . . .	dz
151	Visual representation of station 41 untreated for TM . . . . .	ea
152	Visual representation of station 41 untreated for TJM10 . . . . .	eb
153	Visual representation of station 41 untreated for TJM20 . . . . .	ec
154	Visual representation of station 52 untreated for TM . . . . .	ed
155	Visual representation of station 52 untreated for TJM10 . . . . .	ee
156	Visual representation of station 52 untreated for TJM20 . . . . .	ef
157	Visual representation of station 118 untreated for TM . . . . .	eg
158	Visual representation of station 118 untreated for TJM10 . . . . .	eh
159	Visual representation of station 118 untreated for TJM20 . . . . .	ei
160	Visual representation of station 30 untreated for TM . . . . .	ej
161	Visual representation of station 30 untreated for TJM10 . . . . .	ek
162	Visual representation of station 30 untreated for TJM20 . . . . .	el
163	Visual representation of station 38 untreated for TM . . . . .	em
164	Visual representation of station 38 untreated for TJM10 . . . . .	en
165	Visual representation of station 38 untreated for TJM20 . . . . .	eo
166	Visual representation of station 42 untreated for TM . . . . .	ep
167	Visual representation of station 42 untreated for TJM10 . . . . .	eq
168	Visual representation of station 42 untreated for TJM20 . . . . .	er
169	Visual representation of station 50 untreated for TM . . . . .	es
170	Visual representation of station 50 untreated for TJM10 . . . . .	et
171	Visual representation of station 50 untreated for TJM20 . . . . .	eu
172	Visual representation of station 17 treated for TM . . . . .	ew
173	Visual representation of station 17 treated for TJM10 . . . . .	ex
174	Visual representation of station 17 treated for TJM20 . . . . .	ey
175	Visual representation of station 11 treated for TM . . . . .	ez
176	Visual representation of station 11 treated for TJM10 . . . . .	fa
177	Visual representation of station 11 treated for TJM20 . . . . .	fb
178	Visual representation of station 26 treated for TM . . . . .	fc
179	Visual representation of station 26 treated for TJM10 . . . . .	fd

## LIST OF TABLES

180	Visual representation of station 26 treated for TJM20 . . . . .	fe
181	Visual representation of station 27 treated for TM . . . . .	ff
182	Visual representation of station 27 treated for TJM10 . . . . .	fg
183	Visual representation of station 27 treated for TJM20 . . . . .	fh
184	Visual representation of station 15 treated for TM . . . . .	fi
185	Visual representation of station 15 treated for TJM10 . . . . .	fj
186	Visual representation of station 15 treated for TJM20 . . . . .	fk
187	Visual representation of station 57 treated for TM . . . . .	fl
188	Visual representation of station 57 treated for TJM10 . . . . .	fm
189	Visual representation of station 57 treated for TJM20 . . . . .	fn
190	Visual representation of station 34 treated for TM . . . . .	fo
191	Visual representation of station 34 treated for TJM10 . . . . .	fp
192	Visual representation of station 34 treated for TJM20 . . . . .	fq
193	Visual representation of station 39 treated for TM . . . . .	fr
194	Visual representation of station 39 treated for TJM10 . . . . .	fs
195	Visual representation of station 39 treated for TJM20 . . . . .	ft
196	Visual representation of station 37 treated for TM . . . . .	fu
197	Visual representation of station 37 treated for TJM10 . . . . .	fv
198	Visual representation of station 37 treated for TJM20 . . . . .	fw
199	Visual representation of station 41 treated for TM . . . . .	fx
200	Visual representation of station 41 treated for TJM10 . . . . .	fy
201	Visual representation of station 41 treated for TJM20 . . . . .	fz
202	Visual representation of station 52 treated for TM . . . . .	ga
203	Visual representation of station 52 treated for TJM10 . . . . .	gb
204	Visual representation of station 52 treated for TJM20 . . . . .	gc
205	Visual representation of station 118 treated for TM . . . . .	gd
206	Visual representation of station 118 treated for TJM10 . . . . .	ge
207	Visual representation of station 118 treated for TJM20 . . . . .	gf
208	Visual representation of station 30 treated for TM . . . . .	gg
209	Visual representation of station 30 treated for TJM10 . . . . .	gh
210	Visual representation of station 30 treated for TJM20 . . . . .	gi
211	Visual representation of station 38 treated for TM . . . . .	gj
212	Visual representation of station 38 treated for TJM10 . . . . .	gk
213	Visual representation of station 38 treated for TJM20 . . . . .	gl
214	Visual representation of station 42 treated for TM . . . . .	gm
215	Visual representation of station 42 treated for TJM10 . . . . .	gn
216	Visual representation of station 42 treated for TJM20 . . . . .	go
217	Visual representation of station 50 treated for TM . . . . .	gp
218	Visual representation of station 50 treated for TJM10 . . . . .	gq
219	Visual representation of station 50 treated for TJM20 . . . . .	gr

## List of Tables

1	Staion information for each station/w location and MET-ID . . . . .	11
2	software version description . . . . .	14
3	Request to servers about stations . . . . .	14
4	Table of station statistics . . . . .	17
5	LSTM standard paramters . . . . .	18

## LIST OF TABLES

6	GRU standard parameters . . . . .	19
7	Bidirectional method parameters . . . . .	19
8	Model parameters . . . . .	22
9	Model performance for each station at 10cm, part 1 . . . . .	23
10	Model performance for each station at 10cm, part 2 . . . . .	24
11	Model performance for each station at 20cm, part 1 . . . . .	25
12	Model performance for each station at 20cm, part 2 . . . . .	26
13	Performance table for Linear Regression at 10 cm depth and 20 cm depth. The station names can be found in table 1. . . . .	28
14	Performance table for daily values Plauborg model at 10 cm depth and 20 cm depth. The station names can be found in table 1. . . . .	31
15	Performance table for hourly values Plauborg model at 10 cm depth and 20 cm depth. The station names can be found in table 1. . . . .	33
16	Performance table for LSTM model at 10 cm depth and 20 cm depth. The station names can be found in table 1. . . . .	36
17	Performance table for BiLSTM model at 10 cm depth and 20 cm depth. The station names can be found in table 1. . . . .	39
18	Performance table for GRU model at 10 cm depth and 20 cm depth. The station names can be found in table 1. . . . .	41
19	Performance table for BiGRU model at 10 cm depth and 20 cm depth. The station names can be found in table 1. . . . .	44
20	Hourly Plauborg model results. . . . .	50
21	Daily Plauborg model results. . . . .	50
22	Plauborg-hour-model results for 20cm depth . . . . .	gs
23	Plauborg-hour-model results for 10cm depth . . . . .	gt
24	Plauborg-day-model results for 20cm depth . . . . .	gu
25	Plauborg-day-model results for 10cm depth . . . . .	gy
26	Linear Regression results for 20cm depth . . . . .	gw
27	Linear Regression results for 10cm depth . . . . .	gx
28	GRU results for 20cm depth . . . . .	gy
29	GRU results for 10cm depth . . . . .	gz
30	BiGRU results for 20cm depth . . . . .	ha
31	BiGRU results for 10cm depth . . . . .	hb
32	BiLSTM results for 20cm depth . . . . .	hc
33	BiLSTM results for 10cm depth . . . . .	hd
34	LSTM results for 20cm depth . . . . .	he
35	LSTM results for 10cm depth . . . . .	hf
36	Table of station statistics for air part 1 . . . . .	hg
37	Table of station statistics for soil 10cm part 1 . . . . .	hh
38	Table of station statistics for soil 20cm part 1 . . . . .	hi
39	Table of station statistics for air part 2 . . . . .	hj
40	Table of station statistics for soil 10cm part 2 . . . . .	hk
41	Table of station statistics for soil 20cm part 2 . . . . .	hl
42	Table of station statistics for air part 3 . . . . .	hm
43	Table of station statistics for soil 10cm part 3 . . . . .	hn
44	Table of station statistics for soil 20cm part 3 . . . . .	ho
45	Table of station statistics for air part 4 . . . . .	hp
46	Table of station statistics for soil 10cm part 4 . . . . .	hq
47	Table of station statistics for soil 20cm part 4 . . . . .	hr



---

## **Todo list**



## Abstract

This comparative study examines the efficacy of three established models for predicting soil temperatures at depths of 10cm and 20cm across four Norwegian regions: Innlandet, Østfold, Vestfold, and Trøndelag. To ensure comprehensive regional representation, four monitoring stations were strategically placed within each region. Utilizing data from Nibio, including hourly air temperature at 2m and soil temperatures at 10cm and 20cm depths, the study evaluated seven models cited in existing literature.

These models included Linear Regression, Plauborg's Linear Regression for daily and hourly values, LSTM, bidirectional LSTM, GRU, and bidirectional GRU. The findings revealed improved performance of bidirectional models over unidirectional ones and comparable results between the hourly extension and Plauborg's original daily model. Notably, deep learning models exhibited a dual-mode operation to adapt to the transitional Autumn/Spring and stable Summer periods.

It was found that the bidirectional models performed the best and that bidirectional LSTM worked best for 10 cm soil temperature while Bidirectional GRU worked best for 20 cm soil temperature. It was also found that the inclusion of time in regression models improved the models predictive capabilities.

The author of this current study advocates for further research into bidirectional models and suggests broadening the feature set beyond two variables to capture additional predictive variations.

## Oppsummering

Denne sammenlignings studien undersøker effekten av tre etablerte modeller for å forutsi jordtemperaturer på dybder på 10 cm og 20 cm i fire norske regioner: Innlandet, Østfold, Vestfold og Trøndelag. For å sikre helhetlig regional representasjon ble fire målestasjoner strategisk plassert innenfor hver region. Ved å bruke data fra Nibio, inkludert timelig lufttemperatur ved 2m og jordtemperaturer på 10cm og 20cm dybder, evaluerte studien syv modeller sitert i eksisterende litteratur.

Disse modellene inkluderte lineær regresjon, Plauborgs lineære regresjon for daglige og timebaserte verdier, LSTM, toveis LSTM, GRU og toveis GRU. Funnen avslørte forbedret ytelse av toveismodeller i forhold til enveismodeller og sammenlignbare resultater mellom timeforlengelsen og Plauborgs opprinnelige daglige modell. Spesielt viste dyplæringsmodeller en dual-mode-operasjon for å tilpasse seg overgangsperiodene høst/vår og stabile sommerperioder.

Det ble funnet at toveismodellene fungerte best og at toveis LSTM fungerte best for 10 cm jordtemperatur mens toveis GRU fungerte best for 20 cm jordtemperatur. Det ble også funnet at inkludering av tid i regisjons modellen hadde en positiv påvirkning av modelens prediknings evne.

Forfatteren av denne nåværende studien tar til orde for videre forskning på toveismodeller og foreslår å utvide funksjonssettet utover to variabler for å fange opp ytterligere prediktive variasjoner.

*Keywords:* LSTM, GRU, RNN, Soil temperature, Machine learning, regression, hourly, weather forecasting data

## 1 Introduction

Soil temperature is an important element in agriculture, impacting pest management, and yield forecasting. Accurate soil temperature readings offer insights into effective water management, as highlighted by [1], and are useful in predicting potential crop yields, as discussed by [2]. Furthermore, soil temperature is essential for calculating plant growth, a process noted by [3], and for anticipating the hatching of insect eggs, which is crucial for pest control measures [4, 5].

The ability to predict soil temperature days in advance can provide early warnings of potential flooding and erosion [6], and can indicate the optimal time for seed sprouting [3]. It also sheds light on nitrogen processes within the soil, which are essential for soil health [7].

With the ongoing challenges posed by climate change, understanding soil temperatures at specific depths has become increasingly important. This knowledge not only aids in immediate agricultural decisions but also contributes to the long-term adaptation of farming practices to evolving environmental conditions.

If it's important, why don't institutions measure it everywhere? There are several reasons for this, but a common reason is that it's expensive to install new equipment on old weather stations. Furthermore, it is unfeasible to install sensors absolutely everywhere at any depth, however it is not necessary with full coverage of an area as it is sufficient to have a few samples here and there to get an overview of the current state of the soil. Another thing is that it might be impractical to install sensors in some areas due to climate, soil quality (or lack thereof), or the misrepresentation of the area if it's a geographical or meteorological special case.

Sometimes the weather station do have the sensors in the fields reading soil temperature at given levels, but due to technical misadventures and unforeseen phenomena there might be gaps or misreadings that need to be replaced with approximations or NULL values<sup>1</sup>.

Previous research has investigated soil heat conductivity, leading to the formulation of differential equations [8]. However, these mathematical statements, which involve heat transfer, are computationally demanding and challenging to simulate or calculate [8, 9]. Numerical solutions are not the only obstacle; the dynamic nature of heat within the soil also plays a crucial role. For instance, frost in Scandinavian countries significantly alters soil heat conductivity [6], further complicating accurate calculations. As part of this study, data will be collected from Norway, situated within the Scandinavian region.

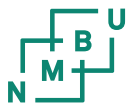
A beneficial model would be one using the fewest number of parameters as possible while returning results within acceptable tolerances. This study will consider models that can use only time and air temperature as those two features are the most common measurements measured at weather stations, since soil temperature is not necessarily calculated as stated earlier. A good metric in this study will be considered to be a combination of Root Mean Square Error and Explained Variance (see section 3.5).

This study aims to address the following key questions:

- Achieving Good Results with Minimal Parameters: Can satisfactory predictions be obtained using a limited set of meteorological and chronological parameters?
- Deep Learning Models for Soil Temperature Prediction: Is it feasible to employ deep learning models for predicting soil temperatures?
- Complexity of Deep Learning Models: Is it necessary to utilize complex deep learning architectures when predicting soil temperatures?
- Suitable model for Nordic climate: Is there a model that fits for the Scandinavian climate?

---

<sup>1</sup>These values are different from 0 as they represent "no data" and can't be used to do calculations.



---

## 1 INTRODUCTION

Regarding deep learning models, this study primarily focuses on Recurrent Neural Network networks and explores various compositions of this technology. The definition of a "good result" will be relative to the performance of other models in the field and to similar studies that employ comparable architectures. Additionally, the Gated Recurrent Unit (GRU) has been considered as an alternative to LSTM in this context due to its simplicity, and yet mechanically similar to the LSTM.

## 2 Theory

This section discusses the theory behind the models used in the study, with the first section being general information about the soil and use cases of soil temperature in agriculture.

### 2.1 Soil temperature

The difficult in predicting the soil temperature comes from that the environment is highly variant and radically different from each other. A farmer in Sunndal in Middle-Norway would have to do different considerations than a farmer in Bergen in Sør-Norge simple due to different climate and soil profile. There exist methods to help farmers get an local estimate of current soil state, one of which are using a soil thermometer. These methods works to make on-the-spot decision to when plant crops, water the crops, or when to harvest. A better approach is to have a model to predict the upcoming temperatures so farmers have a window of time to prepare for crop harvest or planting.

An application of the soil temperature is used as a mean of agricultural advise is the study conducted by Nibio where they look at the mean five-day air temperature compaired to the mean five-day soil temperature to asses when it is useful to start sowing the seeds[10].

A way to measure soil temperature is to insert a rod into the ground and measure, however to measure multiple depths there are usually three ways to do it; one rod to measure all the depths, one rod for each depth, and a hybrid solution of the first and the second method. There are two sensors that are being used

1. Model 107 Temperature Probe[11]

- Tolerance:  $\pm 0.2^\circ C$  (over the  $0^\circ C$  to  $50^\circ C$  range)
- Measuring Range:  $-50^\circ C$  to  $+100^\circ C$
- Probe Diameter: 0.76 cm (0.3 in.)

2. PT500 temperature sensor[12]

- Measuring Range: They have a broad measuring range, usually from  $-50^\circ C$  to  $+400^\circ C$
- Long-term Stability: PT500 sensors are known for their high long-term stability, making them reliable for continuous use over long periods.
- Construction: These sensors are constructed with platinum, which contributes to their precise measurements and robustness.

There are a few depths to choose to monitor, on of those ranges are 5 cm to 15 cm range that is the root zone[13]. The root zone is an range where the roots of plants where the highest density of roots are, and at the end of the root zone researchers can gather information about droughts and snow-melts that are filling up og depleting the root system.

A simple naive way to predict soil temperature would be to use the equation found by [14]

$$\text{daily soil temperature} \approx \tilde{T}_{\text{soil},\text{year}} + e^{-z/D} \sin(\omega t - z/D + \phi) \quad (1)$$

This analytical formula has its limitations as it does not take into account rain fall, snow melt, freezing, and re-freezing. Further more, the formula does not incorporate the importance of the surface temperature and its impact on the soil layers over time. An ideal formula would incorporate all of these elements and possibly more, but that would require more computation power than currently available.

## 2 THEORY

An expansion of this solution was expanded by [15] by including the solar movement to predict daily soil temperatures. The sun does heat up the soil differently depending on its angle over horizon and the clouds blocking or not hiding the sun. It is commented by the author of [15] that this simple model does not describe the soil temperature the effect of snow cover or precipitations effects.

From current understanding of soil physics a modern model researches incorporate the saturated hydraulic conductivity and the unfrozen water content to their equations[6]. Some of these formulas contain nested exponentials[6]. This formulation introduces numerical limitations as the estimation at the center of the formula would be amplified as the computation continues. A commonly used approach is Finite Difference Method (FDM) where a differential equation gets decomposed to several equations that get mapped to a grid with boundary conditions[7, 16, 17].

### 2.2 Linear Regression

Air temperature has a direct connection to soil temperature as the main source of thermal energy next to solar radiation. This study chose this model for its simplicity and being the simplest model to be considered. A primitive relation between air temperature and soil temperature at a given depth would be the equation (2).

$$T_{\text{Soil, n cm}} \approx \beta_{n \text{ cm}} T_{\text{Air}} + \vec{\varepsilon} \quad (2)$$

The  $\beta_{n \text{ cm}}$  represent the scaling factor for the air-soil relation. The regression model will be for the sake of convenience be expressed as the following expression

$$\vec{F}(\mathbf{A})\vec{\beta} = \vec{y} + \vec{\varepsilon}. \quad (3)$$

Where  $\vec{F}$  is a vector function with following domain  $\vec{F} : \mathbb{R}^{n \times m} \rightarrow \mathbb{R}^{n \times p}$  where  $m, n, p \in \mathbb{N}$ ,  $\mathbf{A}$  is the data in matrix form with dimensions  $\mathbb{R}^{n \times m}$ ,  $\vec{\beta}$  is the regression terms with shape  $\mathbb{R}^{p \times 1}$ ,  $\vec{y}$  is the target (TJM10 or TJM20) with shape  $\mathbb{R}^{n \times 1}$ , and  $\vec{\varepsilon}$  is the residual error with the same shape as  $\vec{y}$ .

This will function as the base model to compare to the Plauborg model in section 2.3.

### 2.3 Plauborg Linear Regression model with Fourier terms

The model developed by [18] was trained in Denmark and has shown promising results for a Scandinavian model. For that reason it was included in this study

An improvement over an time independent Linear Regression model would be a time dependent Linear Regression model that takes not only current time into account of the calculations but also previous measurements. It is current knowledge that soil temperatures depends on previous temperatures and meteorological phenomena. In the paper Plauborg [18] extend the features from only air temperature at current time to include also previous days of year and the air temperature from those days as an extension of [15]. This means the following F function that Plauborg used would be

$$\vec{F} := [air_t, air_{t-1}, air_{t-2}, air_{t-3}, \sin(\omega t), \cos(\omega t), \sin(2 * \omega t), \cos(2 * \omega t)]^T.$$

Where  $air_t$  is the air temperature at time  $t$  expressed in day of the year (0-365),  $\omega$  is the angular frequency in radians per hour or radians per day, depending on the time unit. The sine/cosine elements in the F function represent the variations through the day by fitting  $\vec{\beta}$  to the yearly variation. To adapt the authors model to an hourly time unit would be to either

1. Extend the F function to include a larger  $\omega$  coefficient to reflect hourly oscillations in conjunction with daily fluctuation
2. Refit the Fourier terms with a larger  $\omega$  coefficient to make the oscillations more representative of daily temperature changes.

The larger coefficient could be expressed as  $2\pi/24$  while the smaller  $\omega$  for daily values would be rescaled to  $2\pi/365$ .

The problem with this approach would be Fourier Sine-Cosine series approximation which would suggest that Plauborg's method could be subject to overfitting with addition of more terms on a small dataset. On the other hand it gives us a way to compute the coefficients  $\alpha_i$  and  $\gamma_i$  for sine and cosine terms respectively, though it would be more numerically stable with a pseudo-inverse computation or a max log likelihood approach. However, the python module used in this study utilizes a different algorithm described in this paper [19] that performs an iterative method of solving  $\underset{\beta}{\operatorname{argmin}} |X\vec{\beta} - \vec{y}|$ .

## 2.4 Long Short Term-Memory (LSTM) model

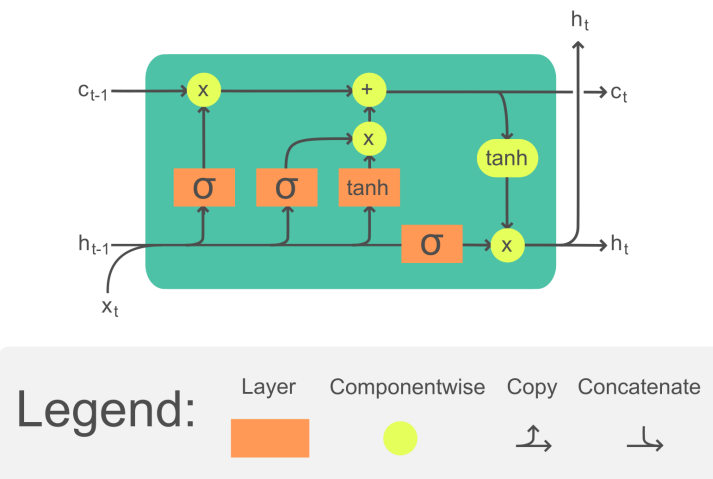


Figure 1: LSTM cell, From: Chevalier [20]

When modelling soil temperature it is important to know the air temperatures at the previous hours or days to predict the next soil temperature time step, for this a natural selection for a data driven model is a recurrent network. This type of deep learning models makes prediction based on previous time steps in the data, however the longer timespan the model takes into account the less important are the earlier time-steps become according to the model. The LSTM model has been tried in Türkiye [21], Belgium [22], United States of America [3] and their findings suggest it is a good model for predicting soil temperature, however it has also been used on a broader dataset spanning 3 continents [23].

LSTM[24] was developed in the field of Economy to predict the rise and fall of stocks, but has shown to be applicable to other problems that rely on time-series. It has been used to predict soil temperatures[3, 22, 23, 25–30] and utilizes a method of storing information across



## 2 THEORY

the timesteps to preserve information better when predicting, and sending information backwards during training so the earlier weights get adjusted more efficiently. This method is an attempt to solve the problem of the vanishing gradient problem.

The most common problem in training Neural networks is the vanishing gradient problem where updating the first few layers of a large network becomes exponentially more difficult since the adjustments gets smaller and smaller for each layer towards the start rather than the reverse. Long Short Term-Memory changes this by carrying information from the previous cells forward thereby allowing updating earlier cells with bigger impact than the standard approach[24]. LSTM is part of a family of Recurrent Neural Network's that passes information to other cells in the same layer.

LSTMs have proven effective in various tasks outside of economics such as natural language processing, speech recognition, and time series prediction. They provide a powerful mechanism for modeling sequential data while mitigating the vanishing gradient problem commonly encountered in basic RNNs.

### 2.5 Gated Recurrent Unit (GRU)

The complexity of soil temperatures and its dependency of previous time-steps make Recurrent Neural Network's a natural chose of a deep learning model, but the intricacy of an LSTM makes it difficult to fine tune. An alternative to LSTM is the GRU model[31] that has fewer parameters to adjust however it has a memory mechanism that allows it to forget and remember information that is passes to other cells in the model. It has been used in Turkey[21], and China[32]

The Gated Recurrent Unit (GRU)[31] was developed in the field of natural language modeling to make translation predictions, however it has been shown that this model is also applicable in other applications than language translation.

GRU is a simplification of the LSTM cell with fewer total gates, and no output gate. This makes it quicker to train and better for memory deficient computers/servers.

GRU shares similarities with LSTM networks but simplifies the architecture by using two gates: the update gate and the reset gate. These gates allow GRU to selectively retain relevant information from previous time steps while avoiding keeping unnecessary information. The update gate determines how much past information should be passed to the future, while the reset gate controls how much past information to forget. GRU has been effective in various sequence modeling tasks.

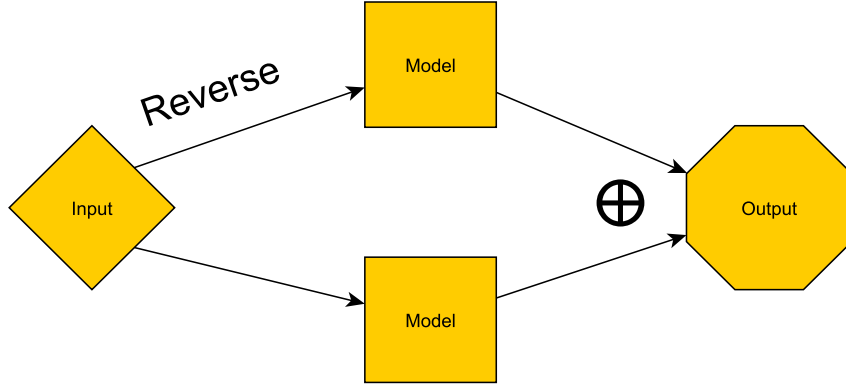


Figure 3: A diagram of the bidirectional method. The reverse indicates that the input data get reversed before it gets inserted into the model, while the bottom model gets the data. At the end the operator  $\oplus$  get invoked that combines the output data from both model to a single output. The specifics of this operator can be any operation that combines two vectors to a single vector. In this study the operation is averaging the values.

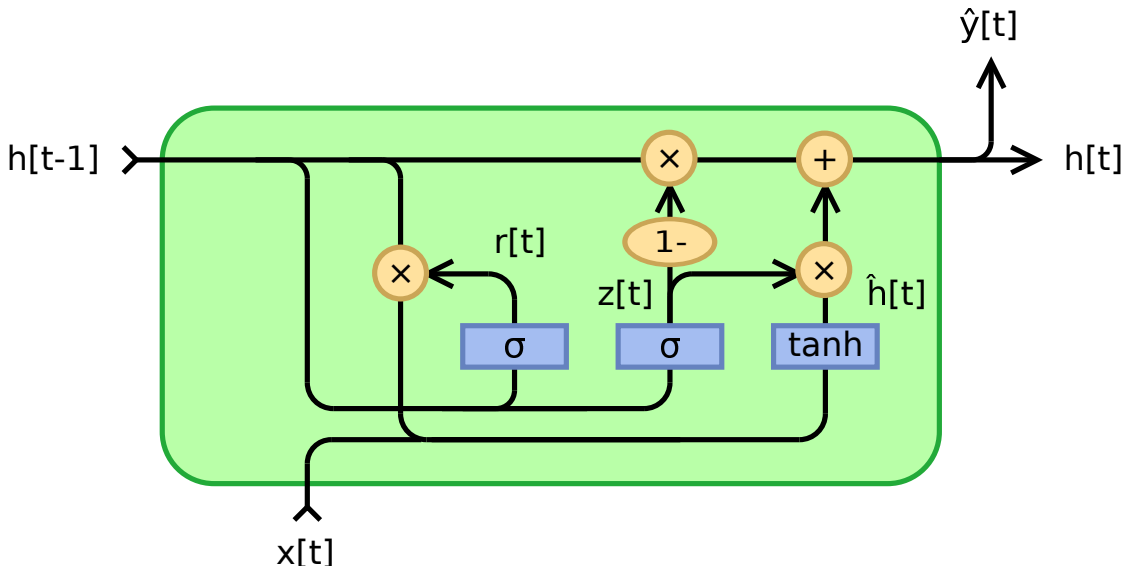


Figure 2: The GRU model where the memory cell gets more efficiently adjusted by the update gate ( $z$ ) and appended information via the reset gate ( $r$ ). From: [33]

The GRU model offers several advantages over LSTM. It is smaller, converges more efficiently due to the integrated memory and prediction layer, and has fewer gates. These fewer tunable parameters make it faster to train and store the model weights.

## 2.6 Bidirectional models

When making predictions with air temperatures as input, it would be useful not only to make predictions based only on air temperature from  $t_0$  to  $t_{max}$  since there is information to be found in the reverse time direction,  $t_{max}$  to  $t_0$ . This technique has been applied in other studies with noteworthy performance increase, therefore will be used in this study for both LSTM model and GRU model using the TensorFlow Keras module.

For the rest of the study a model with the prefix "Bi" indicates that it is a bidirectional model.

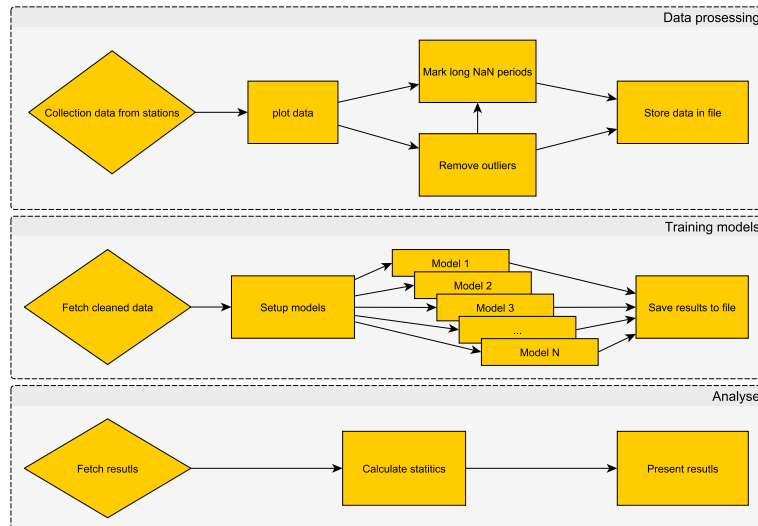


Figure 4: A surface level diagram of the methodology.

### 3 Method

#### 3.1 Source of data

For this comparative study the following data sources will be used

1. Norwegian Institute of Bioeconomy Research Agrometeorology service (Nibio)
2. Norwegian Institute of Bioeconomy Research Agrometeorology service (Nibio) (LMT)
3. The Norwegian Meteorological Institute (MET)

#### 3.2 Dataset

The dataset is chosen from four regions in Norway; Innlandet, Vestfold, Trøndelag, and Østfold. From each region are four stations picked shown in table 1

The dataset created from all stations, spanning the period of 1st of March to 31st of October, annually from 2016 through 2022. This timeframe was selected to capture the critical growing seasons across various regions. The specific features extracted for analysis include the mean hourly soil temperature at a depth of 10cm (denoted as TJM10), the mean hourly soil temperature at 20cm (TJM20), and the mean hourly air temperature measured at 2 meters above ground level. These parameters were collected from the Norwegian Institute of Bioeconomy Research Agrometeorology service (Nibio) (LMT) database.

##### 3.2.1 Selection process

An array of stations was provided by LMT based on their possession of the necessary data. All stations were reviewed, checked for missing data, and those with excessive gaps were removed from the list or replace with another station. After compiling a list of stations, each one was re-examined to identify outliers present in the data and eliminate them accordingly. If certain stations had an excessive number of missing values after the outlier check, nearby stations were sought, and the affected station was replaced and the outlier check was re-done. Table 5 is

### 3 METHOD

Region	Name	ID	Drain type	MET name	Latitude	Longdetude	Altitude [m.a.s.l.]
Innlandet	Apelsvoll	11	Self-drained	SN11500	60,70024	10,86952	262
Innlandet	Fåvang	17	Self-drained	SN13150	61,45822	10,18720	184
Innlandet	Ilseng	26	Self-drained	SN12180	60,80264	11,20298	182
Innlandet	Kise	27	Saturated	SN12550	60,77324	10,80569	129
Trøndelag	Kvitthamar	57	Saturated	SN69150	63,48795	10,87994	28
Trøndelag	Frosta	15	Self-drained	SN69655	63,56502	10,69298	18
Trøndelag	Mære	34	Self-drained	SN71320	63,94244	11,42527	59
Trøndelag	Rissa	39	Saturated	SN71320	63,58569	9,97007	23
Vestfold	Lier	30	Saturated	SN19940	59,79084	10,25962	38
Vestfold	Sande	42	Saturated	SN26990	59,61620	10,22339	35
Vestfold	Tjølling	50	Self-drained	SN27780	59,04641	10,12513	19
Vestfold	Ramnes	38	Saturated	SN27315	59,38081	10,23970	39
Østfold	Rakkestad	37	Saturated	SN3290	59,38824	11,39042	102
Østfold	Rygge	41	Self-drained	SN17380	59,39805	10,75427	35
Østfold	Tomb	52	Saturated	SN17050	59,31893	10,81449	12
Østfold	Øsaker	118	Saturated	SN3370	59,31936	11,04221	45

Table 1: Station information from stations used in this study. The MET names was found by looking at the coordinates of the station and finding the closest MET station coordinates. m.a.s.l stands for Meters above sea level. The ID will be used in the text, tables, and figures for convenience and it was used in the code for something.

showing Øsaker before treatment, and table 6 shows the same station cleaned and ready for being used as training/testing data.

The data plots (see figure 5 and 6 as example) shows all the raw data plotted as a blue line from 03-01 to 10-31. The yellow markings is placed there by computer algorithmns (see section 3.3.1 for in-depth explanation of the outlier detection methods) as potential outliers in the data. These markings have been looked over and verified weather or not they are genuine outliers or not. Further more the red lines are indicators of missing values, the number of missing values longer or shorter than 5 hours<sup>2</sup> are noted on the side bare with the total number of missing values regardless of length. The bottom bar are all the years laid on top of each other to highlight any years or periods that deviates for a particulate year compared to all the other years. There will be two versions of these plots, one for the untreated data and one for the treated data to show the difference the interpolation does to the data (see seciotn 3.3.2 for further details.).

#### 3.2.2 Collection of data

In the tabel 2 are the software programs used in this study and in the collection and treatment of the data. The program used in the collection of meteorological measurements is PowerShell in combination with Curl. Using hyperlinks gathered from inspecting LMT's web page using the browser (Microsoft Edge) built-in inspector tool to get the relevant links to send data requests. The presise URL's can be reviewed on GitHub in the studies GitHub repository<sup>3</sup>. For a more surfac level description on what was requested of the servers see table 3.

<sup>2</sup>The threshold for rain is 3 hours due to the high variance.

<sup>3</sup>Link: <https://github.com/ConAltDelete/MT24CS>

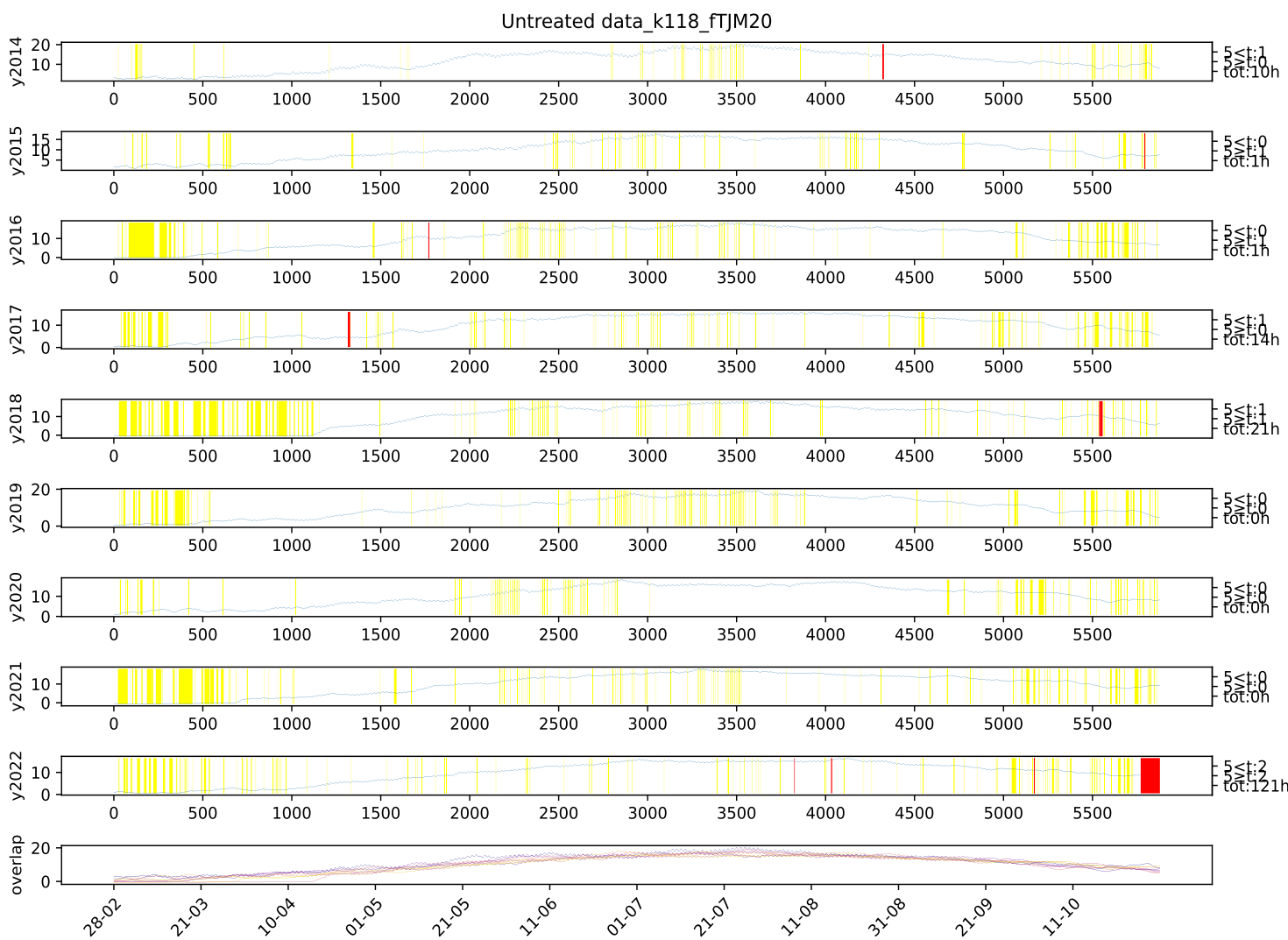


Figure 5: Visual representation of missing values at Øsaker from 2014 to 2022 at the parameter "TJM20". The left numbers indicated how many hours that are missing and how many of them are shorter than or longer than 5 hours. The yellow markings indicate possible outliers based on the given year, all markings was checked if they were actual outliers. The red colouring indicate missing values in the data (represented in the data with code "NULL").

### 3 METHOD

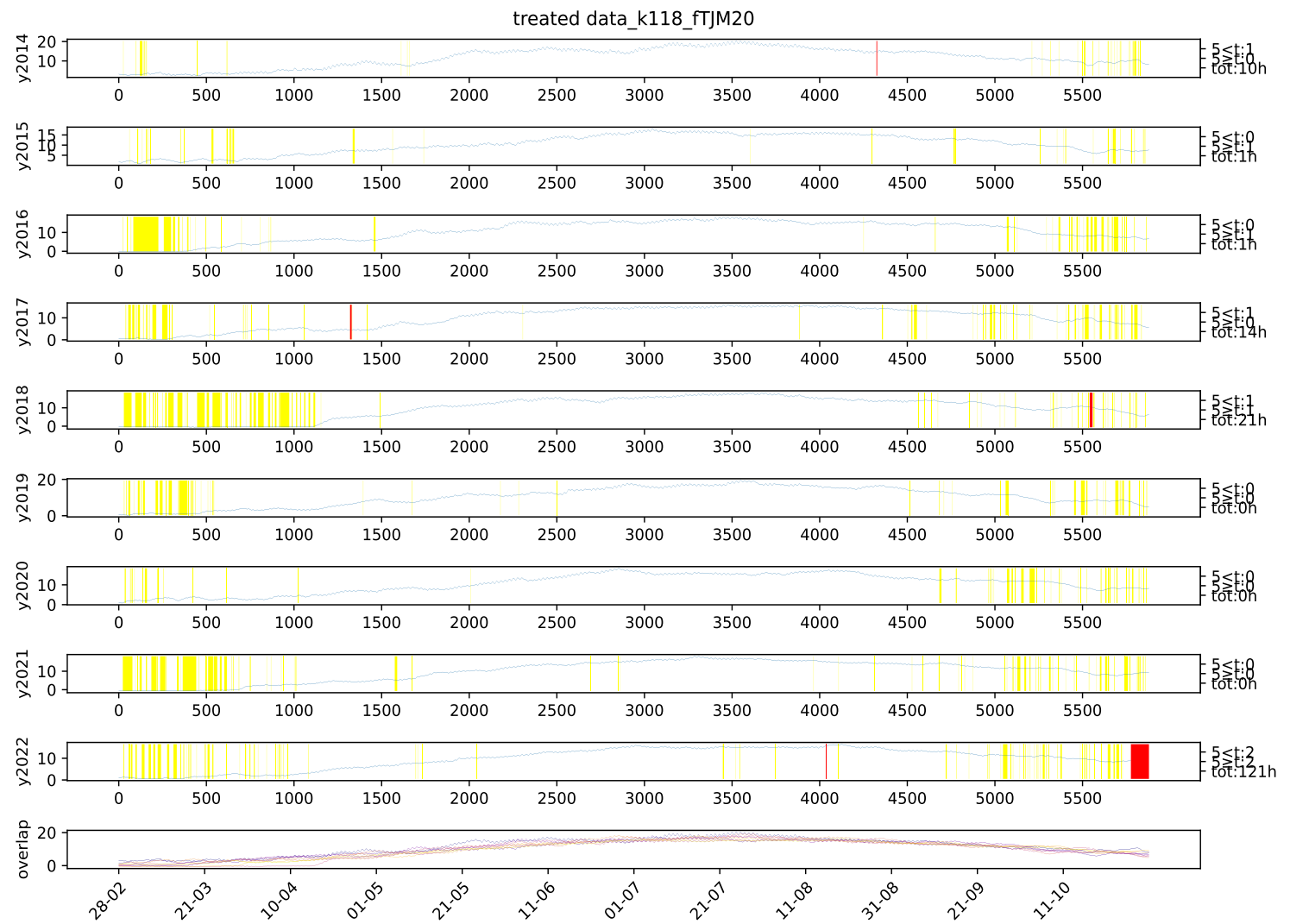


Figure 6: Visual representation of missing values at Øsaker from 2014 to 2022 at the parameter "TJM20" after treating for outliers. The left numbers indicated how many hours that are missing and how many of them are longer or shorter than 5 hours, however for this visualization they indicate the untreated version of the data. The yellow markings indicate possible outliers based on the given year, all markings was checked if they were actual outliers. The red colouring indicate missing values in the data (represented in the data with code "NULL"). The years 2014 and 2015 was removed from the dataset but not coloured in due to technical limitations of reusable code, and furthermore half of 2016 was removed due to suspicion of misreading from sensor at this station.

Name	version	description
PowerShell	7.3.11	Windows native scripting language
Curl	8.4.0 (windows) libcurl/8.4.0 Schannel WinIDN	Command line tool to communicate with servers using http.
Python	3.9.11	popular Scripting language

Table 2: The description the software used in this study

FROST	Description
Station ID	Sendt a request to LMT for station information using their remote API.
LMT	Description
Meteorological data	Requested soil temperature from 10cm depth, and 20cm depth and air temperature (2m), from 2014-03-01 to 2022-10-31.

Table 3: Description of what was requested from each server (MET, Nibio).

#### 3.2.3 Storage of data

The storage of the data is done through two data structures; Hashmap and DataFrame from the package pandas. The transformation of data is done with a customized data-type called "DataFileHandler" which is converted to a module for convenience. The keys for the hashmap is chosen by the naming of the data files and the pattern given to the class. To escalate the loading of the data it will also be exported to a binary file for faster retrieval.

**Technical overview of custom data structure** The data structure used to store the data from the different stations is called "DataFileHandler" and stores the data in a nested dictionary which can be interpreted as the data structure "tree". The main features of "DataFileHandler" is

1. Simple syntax for partitioning the data
2. Grouping the data after loading
3. Transforming all the data with the same function
4. loading and unloading of a large collection of data

This tree-structure uses recursion to search the dictionary to find the appropriate dataset to output.

### 3.3 Data cleaning and treatment

To use the data in this study it must be cleaned and treated for training. Though the data has been examined by the supplier, however it still had outliers that needed to be treated before

### 3 METHOD

---

modelling. For this reason several steps and methods is utilized in the prepossessing steps. The selection process for finding these station can be compiled into these steps

1. Recommendation from Norwegian Institute of Bio-economy Research
2. Find the missing values in the data using algorithm 2
3. Analyse missing values
4. Searching LMT database for alternative station candidates if current data is insufficient
5. If some station was replaced the repeat step 2

#### 3.3.1 Outlier detection and removal

Though the data fetched from Nibio is treated and controlled the external data from MET might not be, and this research project incorporated raw, untreated data from Nibio to fill inn missing values.

The method to quickly find obvious outliers was to look at the following z-score condition

$$|z(|\Delta T|)| = \left| \frac{|\Delta T| - E(|\Delta T|)}{\sqrt{Var(|\Delta T|)}} \right| > 2.35. \quad (4)$$

Where  $E()$  represents the expected value, which is a measure of the average of a set,  $Var()$  denotes the variance, which quantifies the spread or dispersion of the data points around the mean. The condition in equation 4 examines the absolute difference between successive measurements to compute the z-score for each data point then checks if it excised a score of 2.35, which translates to a check if a point performs a jump that deviates more than top  $\sim 1\%$  of all the other data points that year.

The z-score is a statistical measure that normalizes the dataset. It is calculated by subtracting the mean from an individual data point and then dividing the result by the standard deviation. This process transforms the data so that the new mean of the dataset is 0 and the standard deviation is 1. By converting data to z-scores, also known as standard scores, it becomes easier to compare different datasets and identify outliers, as the data is now on a standardized scale. This technique is particularly useful in fields like finance, research, and quality control where relative comparisons are essential.

The premise behind temperature analysis assumes that temperature fluctuations should be bounded, limiting how much they change from one time step to the next. To identify potential anomalies, an additional technique employed is the "out of line" method. This approach involves the program determining a projected point, denoted as  $C^*$ , and then quantifying the deviation of the actual observed data point from this projection. For a graphical illustration of this method, refer to figure 7, which visually depicts the extent of deviation of an observed temperature from its expected temperature.

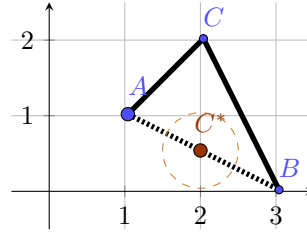


Figure 7: An simple outlier detection method utilizing a simple line to estimate where the expected point ( $C^*$ ,red dotted circle) is supposed to be. If observed point C falls outside the tolerance level (green circle) then it is marked as an outlier.

### 3.3.2 Missing value imputation

The data has missing values, however it is still possible to impute some reasonable values that does not deviate too much from what is expected. When interpolating values the method chosen is a linear interpolation with a maximum period of 5 consecutive hours for soil temperatures, and 3 consecutive hours for air temperatures. The reasoning for this is that the soil temperatures are more reliable making it safer to interpolate without loosing too much information, while air temperatures has a higher variance making it more difficult to interpolate without cutting values. Due to a technical oversight in the coding of this study some large periods that should not be imputed get interpolated at the beginning of the interval.

### 3.3.3 Summary of data

Following the processes of outlier removal and missing value interpolation, the statistics for the refined dataset are presented in table 4. For an in-depth year-by-year breakdown, please refer to the summaries located in appendix B.2.

### 3 METHOD

station ID	TM [°C]		TJM10 [°C]		TJM20 [°C]	
50	$\mu:11.43$	max:31.3 $\sigma:6.16$ min:-14.0	$\mu:11.11$	max:21.9 $\sigma:5.35$ min:-0.3	$\mu:10.71$	max:19.3 $\sigma:5.16$ min:0.0
42	$\mu:11.04$	max:33.0 $\sigma:6.83$ min:-14.5	$\mu:11.27$	max:23.2 $\sigma:5.93$ min:-0.4	$\mu:11.16$	max:20.6 $\sigma:5.62$ min:-0.1
38	$\mu:11.11$	max:32.3 $\sigma:6.81$ min:-19.7	$\mu:11.13$	max:22.8 $\sigma:5.89$ min:0.1	$\mu:10.96$	max:21.7 $\sigma:5.71$ min:0.3
30	$\mu:11.11$	max:32.5 $\sigma:6.92$ min:-16.8	$\mu:11.24$	max:27.6 $\sigma:5.98$ min:-3.3	$\mu:11.14$	max:23.5 $\sigma:5.66$ min:-3.3
118	$\mu:11.15$	max:33.1 $\sigma:6.61$ min:-16.6	$\mu:10.61$	max:21.8 $\sigma:5.47$ min:-0.9	$\mu:10.42$	max:20.3 $\sigma:5.22$ min:-0.7
52	$\mu:11.01$	max:32.6 $\sigma:6.78$ min:-18.0	$\mu:11.71$	max:23.2 $\sigma:5.51$ min:-1.0	$\mu:11.67$	max:24.2 $\sigma:5.41$ min:-0.6
41	$\mu:11.24$	max:33.7 $\sigma:6.68$ min:-19.2	$\mu:11.65$	max:25.9 $\sigma:6.02$ min:-0.8	$\mu:11.32$	max:22.2 $\sigma:5.7$ min:-0.3
37	$\mu:10.15$	max:31.6 $\sigma:6.84$ min:-20.1	$\mu:10.59$	max:22.0 $\sigma:5.58$ min:-1.5	$\mu:10.49$	max:20.5 $\sigma:5.46$ min:-0.7
39	$\mu:9.62$	max:31.4 $\sigma:5.94$ min:-15.1	$\mu:9.29$	max:19.6 $\sigma:4.9$ min:-0.9	$\mu:9.18$	max:18.5 $\sigma:4.79$ min:-0.3
34	$\mu:9.34$	max:32.7 $\sigma:6.55$ min:-19.5	$\mu:8.79$	max:19.3 $\sigma:4.9$ min:-1.3	$\mu:8.69$	max:17.9 $\sigma:4.73$ min:-0.2
57	$\mu:9.73$	max:32.8 $\sigma:6.41$ min:-21.4	$\mu:9.39$	max:22.2 $\sigma:5.23$ min:-1.3	$\mu:9.13$	max:19.1 $\sigma:5.07$ min:-0.9
15	$\mu:10.07$	max:33.5 $\sigma:6.1$ min:-15.4	$\mu:9.19$	max:20.2 $\sigma:4.76$ min:-0.2	$\mu:9.07$	max:18.7 $\sigma:4.6$ min:0.0
27	$\mu:9.97$	max:33.0 $\sigma:6.99$ min:-23.2	$\mu:10.55$	max:23.9 $\sigma:6.25$ min:-2.7	$\mu:10.21$	max:21.4 $\sigma:5.97$ min:-2.2
26	$\mu:9.64$	max:32.4 $\sigma:7.31$ min:-26.3	$\mu:9.53$	max:22.6 $\sigma:6.17$ min:-3.0	$\mu:9.51$	max:20.6 $\sigma:6.1$ min:-2.2
17	$\mu:9.19$	max:29.9 $\sigma:7.63$ min:-25.9	$\mu:9.64$	max:22.8 $\sigma:6.44$ min:-2.4	$\mu:9.35$	max:19.9 $\sigma:6.09$ min:-1.4
11	$\mu:9.76$	max:30.2 $\sigma:6.9$ min:-21.4	$\mu:10.15$	max:23.3 $\sigma:6.17$ min:-1.6	$\mu:10.0$	max:21.6 $\sigma:5.91$ min:-1.1

Table 4: The table shows the statistics of each station for each feature except for Time as it is a strictly monotonic sequence. The station names can be found in table 1.  $\mu$  Denotes the mean temperature,  $\sigma$  denotes the standard deviation, "min" is the minimum temperature, and "max" is the maximum temperature. All values in the table have the unit degree Celsius.

### 3.4 Setup of models

The models are set up in according to the relevant paper the model is fetched from, alternatively reuse the code made by the author. When importing the data to the model there will be modifying to the original code to facilitate for the model as far as it goes. Any modifications will be in the appendix under section ???. For the convenience of the reader all code is using the sklearn estimator class to make all the models discusses in this study more user friendly and compatible with sklearns other functions. The details of the models will be discussed in section

Parameter	value	Parameter	value
activation	"tanh"	kernel_constraint	None
recurrent_activation	"sigmoid"	recurrent_constraint	None
use_bias	True	bias_constraint	None
kernel_initializer	"glorot_uniform"	dropout	0.0
recurrent_initializer	"orthogonal"	recurrent_dropout	0.0
bias_initializer	"zeros"	seed	None
unit_forget_bias	True	return_sequences	False
kernel_regularizer	None	return_state	False
recurrent_regularizer	None	go_backwards	False
bias_regularizer	None	stateful	False
activity_regularizer	None	unroll	False
use_cudnn	"auto"		

Table 5: All the hyperparameters that are available to the Keras LSTM Layer and the standard options that this study chose to remain unchanged

2, this section discusses the setup and implementation of the models.<sup>4</sup>

#### 3.4.1 Basic Linear model

The linear model (section 2.2) utilises in the study is created from the python model sklearn (or scikit-learn according to pythons package manager). The model is setup with standard parameters, and the data is fed into the model without scaling with fitted intercept coefficient.

#### 3.4.2 Plauborg

The Plauborg regression will be formulated as a Linear Regression problem so that the 'Linear-Regression' function in the Sci-kit module can be used. For the parameters used in the paper[18] the F function defined in section 2.3 will be formulated with loops to give rise 3 more parameters for fine-tuning the model. NULL-values generated from the procedure get replaced with 0, since the data fed to the model is significantly larger than 10h (the minimum for the training is 24h).

#### 3.4.3 LSTM

The LSTM used in this study came from the keras module using standard settings.

#### 3.4.4 GRU

The GRU model used in this study is fetched from TensorFlow-Keras python module with standard settings. The model class used in this study is the Keras default GRU layer. The model settings can be reviewed in table 6 which is the standard settings for the keras class.

#### 3.4.5 Bidirectional layer

The Bi-directional layer used in this study came from the keras module using standard settings except for "merge\_mode" which is set to "ave" for averaging the output values. This was done

---

<sup>4</sup>Caution to the reader; The code used was run on the Linux subsystem (Debian) on windows due to the fact that the current version of tensorflow can't run on Windows.

### 3 METHOD

Parameter	value	Parameter	value
activation	"tanh"	recurrent_constraint	None
recurrent_activation	"sigmoid"	bias_constraint	None
use_bias	True	dropout	0.0
kernel_initializer	"glorot_uniform"	recurrent_dropout	0.0
recurrent_initializer	"orthogonal"	seed	None
bias_initializer	"zeros"	return_sequences	False
kernel_regularizer	None	return_state	False
recurrent_regularizer	None	go_backwards	False
bias_regularizer	None	stateful	False
activity_regularizer	None	unroll	False
kernel_constraint	None	reset_after	True
use_cudnn	"auto"		

Table 6: All the hyperparameters that are available to the Keras GRU Layer and the standard options that this study chose to remain unchanged

Parameter	value
merge_mode	"ave"
weights	None
backward_layer	None

Table 7: The adjustable parameters of the bidirectional layer from Keras.

since there are no other layers to get those values. The table of configurations can be found in table 7.

### 3.5 Metrics

The metrics used in this study are

- Root Mean Square Error (RMSE)
- Mean Absolut Error (MAE)
- Explained Variance ( $R^2$ )
- Bias
- Log Condition number ( $\log(\kappa)$ )
- digit sensitivity

Soil temperature as a different behaviour than air temperature since energy (temperature) though the soil gets dampen and delayed. Since the data used in this study has outliers that was not caught during data treatment, which has been addressed, the author of this study decided to include two more metrics that are not usually included in the evaluation; The log condition number, and digit sensitivity. Both metrics are based on the calculation of the condition number defined in formula 5.

$$\kappa = \lim_{\varepsilon \rightarrow 0^+} \sup_{|\partial x| \leq \varepsilon} \frac{|f(x + \partial x) - f(x)|}{|f(x)|} * \frac{|x|}{|\partial x|} \quad (5)$$

Calculating this directly is impossible due to the limitations of handling infinitesimally small numbers in simulations. However, this paper uses a own designed algorithm (referred to as  $\kappa$ ) to estimate this value for all the models. See algorithm 1 for the pseudocode of the algorithm.

---

**Algorithm 1:** Method for calculating  $\kappa$ .  $\mathcal{U}$  is a uniform random distribution in a range.

---

```

Data: Data
Result: log( $\kappa$ )
1 Let  $\kappa_f$  be the function 5;
2  $\kappa \leftarrow 0$ ;
3 for  $i \in 1 \dots |Data|$  do
4    $\partial x \leftarrow \mathcal{U}_{[-\sqrt{\varepsilon/|Data|}, \sqrt{\varepsilon/|Data|}]}$ ;
5    $k \leftarrow$  calculate with  $\kappa_f$  from  $x$  and  $x + \partial x$ ;
6   if  $k > \kappa$  then
7      $\kappa \leftarrow k$ ;
8   end if
9 end for
10 return  $\kappa$ 
```

---

The normal use case for  $\kappa$  is to check the sensitivity of matrices for small changes in the input,

The digit sensitivity is included to give an intuitive understanding of  $\kappa$  and is computed simply as  $\log_e(\kappa) + 1$ . This number tells us the significant digit generated from the model. If the number is less than 0 then it's the nth digit after the decimal point.

For the rest of the metrics, they are defined as follows

- RMSE

$$\sqrt{\frac{\sum(y_{\text{pred}} - y_{\text{truth}})^2}{n}} \quad (6)$$

- MAE

$$\frac{\sum|y_{\text{pred}} - y_{\text{truth}}|}{n} \quad (7)$$

- bias

$$\frac{\sum(y_{\text{pred}} - y_{\text{truth}})}{n} \quad (8)$$

- $R^2$

$$1 - \frac{\sum(y_{\text{pred}} - y_{\text{truth}})^2}{\sum(y_{\text{pred}} - \bar{y})^2} \quad (9)$$

Where  $\bar{y}$  is the mean of the target,  $y_{\text{pred}}$  is the predicted data, and  $y_{\text{truth}}$  is the observed soil temperature.

#### 3.5.1 Confidence eclipses

To see goodness of fit to the ground truth (soil temperature) confidence eclipses will be calculated for the results. This is done by calculating the singular values of the predicted soil temperature and the observed ground truth. A way to define it would be with equation (10).

$$\left| \begin{bmatrix} Y & \tilde{Y} \end{bmatrix}^T \begin{bmatrix} Y & \tilde{Y} \end{bmatrix} - \lambda I \right| = 0 \quad (10)$$

Where  $Y$  is the soil temperature,  $\tilde{Y}$  is the predicted soil temperature,  $[...]^T$  is the transpose of a matrix,  $\lambda$  is a diagonal matrix with the entries being the singular values, and  $I$  is the identity matrix. The interpretation of the singular values would be the width and height of the eclipse

that covers 1 standard deviation of the data in two dimensions. In section 4 only the smallest singular value will be shown, denoted  $\lambda_0$ , as it will be half the width of the ellipse and will show if a model fits to the symmetry line. Furthermore, the figures of the confidence eclipses will also show 2nd standard deviation, and 3rd standard deviation for completeness.

### 3.6 Model training

When training the model's data from 2014 to 2020 get used as the training data and the years 2021 to 2022 will be used as the test set. Normally data sets get split up into multiple training sets and test sets known as cross-validation however since this study have collected a large amount of data this technique is not necessary for the analyses. However, since the study utilizes the GridSearchCV class for finding optimal parameters cross-validation will be performed anyway within the training set by default.

The models get trained on air temperature, however the precise input for each model is not the same for all. The features used for each model are described in table 8 and their transformation in table 8.

The models get a sample of the training data at the time due to the size and the amount for missing data (for example figure 5) The algorithm used to fetch reliable indexes are demonstrated at algorithm 2.

---

**Algorithm 2:** Find Non-NUL Ranges (Abstract)

---

**Input :** Input data data  
**Output:** List of tuples: ranges

```

1 FindNonNULLRanges(data) ranges  $\leftarrow$  empty list;
2 start  $\leftarrow$  None;
3 for item in data do
4   if item is not NULL then
5     if start is None then
6       | start  $\leftarrow$  item;
7     end if
8   end if
9   else
10    if start is not None then
11      | Add (start, item index - 1) to ranges;
12      | start  $\leftarrow$  None;
13    end if
14  end if
15 end for
16 if start is not None then
17   | Add (start, Last index) to ranges;
18 end if
19 return ranges;

```

---

After the missing values has been identified rows get removed in such a way that if any of the features or target values is missing then that row get removed. At the end all the rows get concatenated , so there is just one complete dataset for the training.

### 3 METHOD

Model name	features	target	transformations
Linear Regression	TM	TJM10, TJM20	—
Plauborg	Time, TM	TJM10, TJM20	Time get translated in two way; the current day since new year if looking at daily values, and hours since new year if looking at hourly predictions. When converting TM to daily values the hourly data get averaged in 24 hour periods from midnight to 23:00
Deep learning models	Time, TM	TJM10, TJM20	Time get translated to hours since new year by taking the day of the year and multiplying it by 24 and adding the hour.

Table 8: Parameters used for predicting soil temperatures at depth 10cm and 20cm. The deep learning models encapsulated in the "Deep learing models" are LSTM, BiLSTM, GRU, and BiGRU.

### 3.7 Use of Artificial Intelligence in this paper

In this paper there has been used Artificial Intelligence (AI), specifically Bing Chat / Copilot hosted by Microsoft Cooperation according to the current guidelines for use of artificial intelligence at the faculty of The Norwegian University of Life Science (NMBU), for the following purposes:

1. Formalizing sentences and rephrasing sentences.
2. Spellchecking
3. Code generation of basic concepts and structures (tree traversal, template for generic classes)

It is important to emphasize that my engagement with AI have been actively curated and verified with known sources. All code underwent rigorous manual inspection within a dedicated testing environment. Furthermore, no confidential or sensitive information was shared with the AI; my interactions focused solely on broad topics and general inquiries. To validate the accuracy of AI-generated responses, it has been cross-checked with established research papers and textbooks.

## 4 Results

In this section will the outcome of the training be presented. The result for each model will be presented individually as the cooperation between the models will be discussed in section 5. The statistical analysis is based on the data from year 2021 and 2022, which was used as the test dataset. It is to be noted that the difference plots presented in this section is only showing results from 2022, the reasoning for this is that the results are similar enough that 2022 reflects also 2021. Plots for 2021 are available in the appendix in section A.

model		52	37	50	38	57	34	27	17	average
Linear model 10cm	$R^2$	0.22	0.47	0.58	0.39	0.3	-1.39	0.55	0.5	0.42
	MAE	2.89	3.5	2.7	3.74	3.36	3.42	3.24	3.43	3.27
	RMSE	3.68	4.5	3.61	4.81	4.29	4.26	4.27	4.52	4.23
	bias	1.23	2.07	1.77	2.5	2.77	3.18	2.08	2.51	2.3
Plauborg model (daily values) 10cm	$R^2$	0.66	0.87	0.94	0.85	0.85	0.4	0.9	0.88	0.86
	MAE	1.84	1.76	1.11	1.91	1.55	1.69	1.63	1.78	1.62
	RMSE	2.42	2.21	1.4	2.42	1.98	2.14	2.06	2.26	2.07
	bias	-0.64	0.37	-0.05	0.67	1.11	1.53	0.4	0.92	0.61
Plauborg model (hourly values) 10cm	$R^2$	0.64	0.86	0.88	0.75	0.68	-0.19	0.87	0.83	0.79
	MAE	1.96	1.8	1.47	2.37	2.26	2.31	1.72	1.98	1.93
	RMSE	2.51	2.34	1.91	3.05	2.91	3.01	2.28	2.65	2.53
	bias	-0.35	0.24	0.56	1.36	0.68	0.85	0.16	0.06	0.6
BiLSTM 10cm	$R^2$	0.75	0.96	0.96	0.95	0.92	0.69	0.95	0.95	0.93
	MAE	1.48	1.01	0.86	1.03	1.11	1.17	1.13	1.11	1.11
	RMSE	2.08	1.22	1.06	1.43	1.4	1.56	1.36	1.4	1.42
	bias	-1.08	-0.17	-0.48	0.18	0.42	0.75	-0.11	0.46	0.06
LSTM 10cm	$R^2$	0.71	0.92	0.94	0.89	0.86	0.52	0.91	0.92	0.89
	MAE	1.72	1.49	1.11	1.48	1.46	1.47	1.56	1.43	1.47
	RMSE	2.25	1.77	1.39	2.01	1.91	1.92	1.89	1.81	1.87
	bias	-0.81	0.02	-0.05	0.54	0.55	0.88	0.04	0.46	0.3
GRU 10cm	$R^2$	0.7	0.91	0.93	0.89	0.91	0.64	0.91	0.9	0.89
	MAE	1.69	1.53	1.18	1.57	1.19	1.31	1.49	1.54	1.42
	RMSE	2.29	1.89	1.44	2	1.5	1.69	1.85	1.98	1.81
	bias	-1.19	-0.15	-0.72	0.02	0.59	1.03	-0.14	0.5	0.03
BiGRU 10cm	$R^2$	0.69	0.93	0.95	0.92	0.88	0.62	0.92	0.93	0.9
	MAE	1.69	1.37	1.05	1.34	1.38	1.34	1.44	1.31	1.36
	RMSE	2.31	1.66	1.29	1.78	1.74	1.73	1.77	1.69	1.72
	bias	-1.15	-0.31	-0.4	0.23	0.23	0.55	-0.3	0.08	-0.04

Table 9: Statistics of the models for depth 10, part 1. The numbers are for year 2021, and 2022 collectively, and the average column is for all the stations in the year 2021, and 2022. The station names can be found in table 1.

#### 4 RESULTS

model		41	118	42	30	39	15	26	11	average
Linear model 10cm	$R^2$	0.59	0.31	0.51	0.59	0.21	-0	0.46	0.51	0.42
	MAE	3.07	3.49	3.52	3.11	3.19	3.14	3.65	2.71	3.27
	RMSE	3.98	4.5	4.57	4.05	4.06	3.92	4.71	3.57	4.23
	bias	1.49	2.93	2.11	1.73	2.83	2.8	2.9	1.53	2.3
Plauborg model (daily values) 10cm	$R^2$	0.9	0.84	0.88	0.91	0.83	0.79	0.86	0.86	0.86
	MAE	1.59	1.7	1.75	1.52	1.46	1.43	1.94	1.5	1.62
	RMSE	1.98	2.17	2.24	1.91	1.9	1.81	2.43	1.88	2.07
	bias	-0.29	1.14	0.33	-0.05	1.19	1.11	1.25	0.34	0.61
Plauborg model (hourly values) 10cm	$R^2$	0.9	0.71	0.85	0.89	0.63	0.56	0.84	0.82	0.79
	MAE	1.52	2.32	1.88	1.55	2.15	1.99	1.92	1.67	1.93
	RMSE	1.94	2.93	2.5	2.07	2.77	2.59	2.53	2.15	2.53
	bias	0.15	1.64	0.7	0.35	0.7	0.9	0.82	0.04	0.6
BiLSTM 10cm	$R^2$	0.94	0.94	0.95	0.95	0.88	0.89	0.95	0.93	0.93
	MAE	1.2	1.07	1.1	1.13	1.24	1.02	1.2	1.08	1.11
	RMSE	1.47	1.32	1.4	1.44	1.59	1.3	1.49	1.34	1.42
	bias	-0.76	0.64	-0.17	-0.56	0.5	0.44	0.74	-0.12	0.06
LSTM 10cm	$R^2$	0.91	0.88	0.9	0.91	0.83	0.8	0.91	0.87	0.89
	MAE	1.54	1.41	1.59	1.52	1.4	1.37	1.58	1.5	1.47
	RMSE	1.85	1.87	2	1.88	1.85	1.75	1.96	1.85	1.87
	bias	-0.37	1.05	0.2	-0.18	0.62	0.67	0.87	-0.05	0.3
GRU 10cm	$R^2$	0.9	0.91	0.9	0.91	0.88	0.87	0.89	0.89	0.89
	MAE	1.6	1.29	1.64	1.51	1.21	1.09	1.65	1.37	1.42
	RMSE	1.98	1.62	2.06	1.88	1.55	1.4	2.08	1.72	1.81
	bias	-0.94	0.44	-0.31	-0.7	0.67	0.53	0.77	-0.19	0.03
BiGRU 10cm	$R^2$	0.91	0.92	0.92	0.92	0.87	0.84	0.93	0.88	0.9
	MAE	1.5	1.2	1.46	1.44	1.29	1.26	1.39	1.47	1.36
	RMSE	1.81	1.55	1.82	1.76	1.66	1.56	1.74	1.8	1.72
	bias	-0.72	0.71	-0.14	-0.51	0.28	0.33	0.51	-0.37	-0.04

Table 10: Statistics of the models for depth 10, part 2. The numbers are for year 2021, and 2022 collectively, and the average column is for all the stations in the year 2021, and 2022. The station names can be found in table 1.

#### 4 RESULTS

model		52	37	50	38	57	34	27	17	average
Linear model 20cm	$R^2$	0.6	0.39	0.43	0.31	0.13	-2.25	0.42	0.34	0.31
	MAE	2.84	3.68	3.03	3.68	3.64	3.67	3.55	3.84	3.47
	RMSE	3.56	4.75	4.05	4.83	4.65	4.58	4.67	5.05	4.5
	bias	0.56	2.17	2.21	2.6	3.15	3.47	2.53	2.94	2.49
Plauborg model (daily values) 20cm	$R^2$	0.83	0.91	0.95	0.91	0.86	0.32	0.9	0.84	0.88
	MAE	1.87	1.5	0.98	1.37	1.54	1.84	1.53	1.91	1.54
	RMSE	2.33	1.88	1.25	1.72	1.84	2.1	1.92	2.45	1.91
	bias	-1.4	0.35	0.1	0.52	1.43	1.82	0.75	1.4	0.64
Plauborg model (hourly values) 20cm	$R^2$	0.8	0.83	0.84	0.74	0.62	-0.55	0.84	0.76	0.76
	MAE	1.98	1.94	1.7	2.32	2.42	2.43	1.89	2.27	2.06
	RMSE	2.5	2.51	2.18	2.98	3.08	3.16	2.46	3.02	2.68
	bias	-1.2	0.07	0.82	1.15	0.74	0.8	0.34	0.14	0.53
BiLSTM 20cm	$R^2$	0.8	0.92	0.95	0.93	0.9	0.59	0.93	0.91	0.9
	MAE	2.07	1.44	0.99	1.24	1.23	1.23	1.38	1.51	1.35
	RMSE	2.49	1.72	1.2	1.54	1.6	1.64	1.66	1.88	1.7
	bias	-1.79	-0.25	-0.13	0.19	0.53	0.81	0.13	0.59	0.07
LSTM 20cm	$R^2$	0.83	0.94	0.96	0.95	0.87	0.41	0.92	0.85	0.89
	MAE	1.99	1.28	0.88	1.08	1.33	1.54	1.36	1.8	1.36
	RMSE	2.35	1.55	1.09	1.33	1.77	1.96	1.77	2.37	1.76
	bias	-1.61	0.13	-0.17	0.31	1.11	1.48	0.6	1.3	0.42
GRU 20cm	$R^2$	0.8	0.95	0.96	0.96	0.9	0.5	0.93	0.86	0.9
	MAE	2.15	1.15	0.85	0.99	1.19	1.49	1.2	1.63	1.29
	RMSE	2.52	1.41	1.06	1.22	1.57	1.83	1.63	2.33	1.7
	bias	-1.81	-0.04	-0.35	0.14	0.98	1.34	0.36	1.11	0.24
BiGRU 20cm	$R^2$	0.79	0.93	0.96	0.94	0.91	0.63	0.94	0.93	0.92
	MAE	2.13	1.28	0.83	1.09	1.2	1.23	1.21	1.21	1.24
	RMSE	2.57	1.56	1.05	1.38	1.53	1.58	1.52	1.63	1.57
	bias	-1.91	-0.4	-0.15	0.11	0.55	0.81	0.04	0.43	0.01

Table 11: Statistics of the models for depth 20, part 1. The numbers are for year 2021, and 2022 collectively, and the average column is for all the stations in the year 2021, and 2022. The station names can be found in table 1.

model		41	118	42	30	39	15	26	11	average
Linear model 20cm	$R^2$	0.49	0.16	0.39	0.46	0.08	-0.24	0.3	0.35	0.31
	MAE	3.29	3.65	3.74	3.43	3.39	3.34	4.01	2.92	3.47
	RMSE	4.25	4.73	4.86	4.46	4.31	4.2	5.17	3.82	4.5
	bias	1.68	3.21	2.36	2.02	3.08	3.01	3.28	1.69	2.49
Plauborg model (daily values) 20cm	$R^2$	0.91	0.89	0.9	0.91	0.85	0.8	0.83	0.87	0.88
	MAE	1.41	1.38	1.54	1.47	1.47	1.41	2.1	1.44	1.54
	RMSE	1.75	1.74	1.97	1.82	1.73	1.68	2.53	1.74	1.91
	bias	-0.37	1.14	0.35	-0.01	1.4	1.22	1.58	0.46	0.64
Plauborg model (hourly values) 20cm	$R^2$	0.87	0.66	0.81	0.86	0.61	0.48	0.8	0.76	0.76
	MAE	1.67	2.42	2.1	1.71	2.19	2.09	2.11	1.85	2.06
	RMSE	2.14	3.03	2.74	2.28	2.79	2.71	2.76	2.35	2.68
	bias	0.13	1.72	0.75	0.43	0.63	0.83	0.89	-0.02	0.53
BiLSTM 20cm	$R^2$	0.91	0.92	0.92	0.92	0.89	0.86	0.9	0.88	0.9
	MAE	1.45	1.16	1.46	1.38	1.12	1.08	1.57	1.33	1.35
	RMSE	1.74	1.5	1.78	1.67	1.5	1.4	1.91	1.61	1.7
	bias	-0.68	0.82	-0.03	-0.4	0.46	0.43	0.89	-0.21	0.07
LSTM 20cm	$R^2$	0.93	0.92	0.93	0.93	0.86	0.81	0.86	0.84	0.89
	MAE	1.34	1.12	1.34	1.31	1.25	1.2	1.8	1.42	1.36
	RMSE	1.61	1.48	1.64	1.61	1.68	1.62	2.32	1.9	1.76
	bias	-0.58	0.92	0.16	-0.18	1.01	0.89	1.49	0.43	0.42
GRU 20cm	$R^2$	0.92	0.94	0.93	0.92	0.88	0.84	0.87	0.84	0.9
	MAE	1.36	0.96	1.31	1.33	1.22	1.14	1.59	1.34	1.29
	RMSE	1.64	1.26	1.63	1.66	1.56	1.52	2.19	1.87	1.7
	bias	-0.78	0.73	-0.03	-0.37	0.92	0.76	1.25	0.24	0.24
BiGRU 20cm	$R^2$	0.93	0.93	0.93	0.93	0.9	0.88	0.93	0.9	0.92
	MAE	1.32	1.06	1.26	1.28	1.1	1.05	1.31	1.2	1.24
	RMSE	1.57	1.35	1.59	1.55	1.4	1.31	1.68	1.47	1.57
	bias	-0.75	0.76	-0.1	-0.46	0.51	0.49	0.76	-0.22	0.01

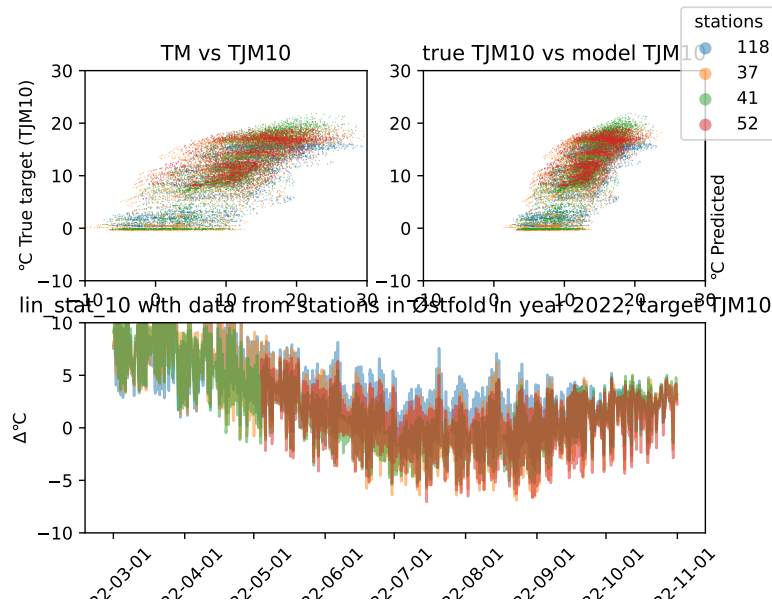
Table 12: Statistics of the models for depth 20, part 2. The numbers are for year 2021, and 2022 collectively, and the average column is for all the stations in the year 2021, and 2022. The station names can be found in table 1.

#### 4.1 Linear model

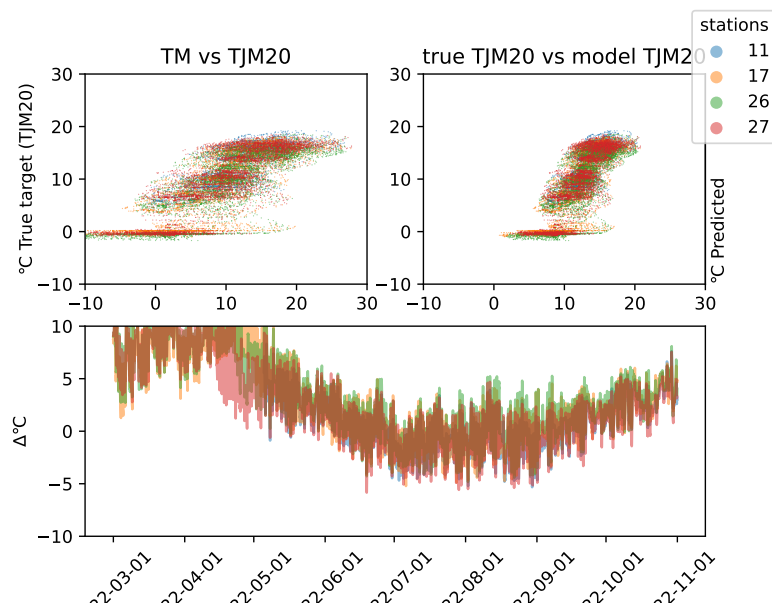
From figure 8 there is a large difference from March to late April and from there hovers around  $0^\circ C$  in difference. There is also a clear distinction in seasons in figure 8b when looking at air temperature versus soil temperature at 20 cm depth. Furthermore, when looking at ground truth versus predicted values there is a repetition in shape from the air versus soil temperature.

From the tables 13 it is clear that the model does not fit well with the data on the background of low  $R^2$  (less than 0.5). The model consistently overestimates the soil temperature regardless of the station. Furthermore, the digit sensitivity shows that the model is sensitive to small changes.

From the confidence ellipses in figure 9 it is clear that the model does not fit well to the data due to being off the symmetry line and having a large  $\lambda_0$ .



(a) Difference plot for Linear Regression model in year 2022 and region Østfold with the lowest RMSE.



(b) Difference plot for Linear Regression model in year 2022 and region Innlandet with the highest RMSE.

Figure 8: Difference plots of the extremal regions based on the RMSE measure. The station names can be found in table 1.

## 4 RESULTS

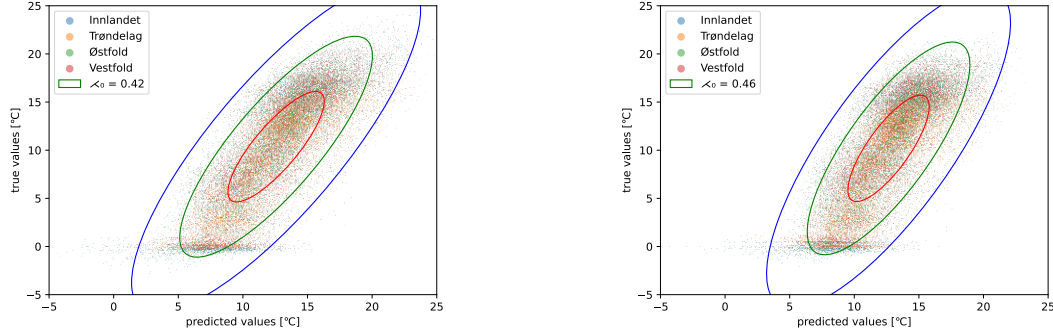
scope	spesific scope	RMSE [°C]	MAE [°C]	bias [°C]	$\log(\kappa(\text{model}))$	digit sensitivity	R <sup>2</sup>
global	—	4.504	3.474	2.487	-0.796	-1	0.308
region	Østfold	4.348	3.363	1.901	-0.796	-1	0.424
region	Vestfold	4.564	3.47	2.297	-0.796	-1	0.397
region	Trøndelag	4.438	3.508	3.175	-0.796	-1	-0.194
region	Innlandet	4.688	3.568	2.601	-0.796	-1	0.353
local	52	3.556	2.841	0.559	-0.796	-1	0.604
local	41	4.248	3.286	1.677	-0.796	-1	0.491
local	37	4.754	3.675	2.174	-0.796	-1	0.391
local	118	4.726	3.654	3.208	-0.796	-1	0.162
local	50	4.048	3.025	2.207	-0.796	-1	0.434
local	42	4.863	3.741	2.364	-0.796	-1	0.393
local	38	4.832	3.682	2.601	-0.796	-1	0.308
local	30	4.465	3.433	2.015	-0.796	-1	0.456
local	57	4.655	3.636	3.153	-0.796	-1	0.125
local	39	4.31	3.39	3.083	-0.796	-1	0.081
local	34	4.583	3.675	3.471	-0.796	-1	-2.248
local	15	4.198	3.342	3.006	-0.796	-1	-0.241
local	27	4.672	3.547	2.535	-0.796	-1	0.415
local	26	5.17	4.009	3.282	-0.796	-1	0.302
local	17	5.049	3.84	2.939	-0.796	-1	0.336
local	11	3.821	2.924	1.692	-0.796	-1	0.35

(a) Performance table for Linear Regression 20cm. Negative numbers in  $R^2$  should be treated as an indicator that the particular station/scope is not well-fitted to the data.

scope	spesific scope	RMSE [°C]	MAE [°C]	bias [°C]	$\log(\kappa(\text{model}))$	digit sensitivity	R <sup>2</sup>
global	—	4.231	3.267	2.303	-0.638	-1	0.423
region	Østfold	4.236	3.28	2.015	-0.638	-1	0.45
region	Vestfold	4.277	3.26	2.019	-0.638	-1	0.517
region	Trøndelag	4.133	3.274	2.893	-0.638	-1	0.028
region	Innlandet	4.282	3.254	2.246	-0.638	-1	0.504
local	52	3.679	2.889	1.226	-0.638	-1	0.221
local	41	3.976	3.07	1.494	-0.638	-1	0.593
local	37	4.501	3.503	2.07	-0.638	-1	0.473
local	118	4.5	3.486	2.93	-0.638	-1	0.306
local	50	3.611	2.702	1.766	-0.638	-1	0.584
local	42	4.571	3.525	2.109	-0.638	-1	0.506
local	38	4.815	3.741	2.502	-0.638	-1	0.388
local	30	4.053	3.106	1.733	-0.638	-1	0.588
local	57	4.293	3.356	2.775	-0.638	-1	0.295
local	39	4.057	3.193	2.835	-0.638	-1	0.213
local	34	4.262	3.415	3.176	-0.638	-1	-1.386
local	15	3.918	3.141	2.799	-0.638	-1	-0.003
local	27	4.272	3.236	2.078	-0.638	-1	0.551
local	26	4.714	3.651	2.902	-0.638	-1	0.456
local	17	4.518	3.432	2.506	-0.638	-1	0.501
local	11	3.567	2.713	1.529	-0.638	-1	0.51

(b) Performance table for Linear Regression 10cm. Negative numbers in  $R^2$  should be treated as an indicator that the particular station/scope is not well-fitted to the data.

Table 13: Performance table for Linear Regression at 10 cm depth and 20 cm depth. The station names can be found in table 1.



(a) The plot shows the ground truth against the predicted value of Linear Regression. The eclipses demonstrate the 68% (inner eclipse), 95% (middle eclipse), and 99% (outer eclipse) confidence interval for the model.

(b) The plot shows the ground truth against the predicted value of Linear Regression. The eclipses demonstrate the 68% (inner eclipse), 95% (middle eclipse), and 99% (outer eclipse) confidence interval for the model.

Figure 9: Plots showing ground truth vs predicted values from the linear Regression models with their 68%, 95%, and 99% confidence eclipses. The confidence eclipses function the same as confidence intervals but in two dimensions, meaning the area covered by the eclipse denotes where one can expect the points to be with a given confidence percent. These plots contain a subset of the data, however the ellipses and  $\lambda_0$  are calculated with all the data.

### 4.2 Plauborg daily

Figure 10 shows that the model fit well to the data by staying close to the symmetry line. The high RMSE plot in figure 10b shows a difference between the Autumn months and Summer months where there is an high difference in Autumn and an increase in difference in Spring while during Summer it stays around  $0^{\circ}\text{C}$  in difference.

Performance notes from table 14:

- Daily Plauborg can explain most of the variation in the data.
- It's a balanced model that does not overestimate more than  $0.8^{\circ}\text{C}$  in general.

Figure 11 shows that it is a good fit for the models.

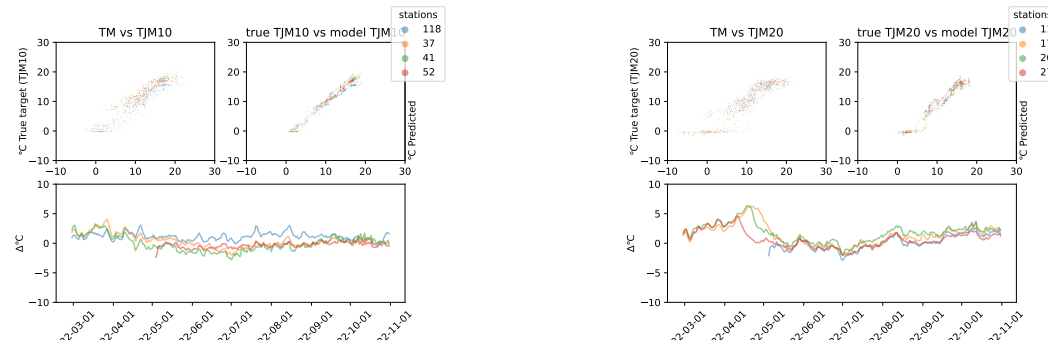
The Plauborg model follows strongly the soil temperature and thereby has good prediction, except for a few stations. There are two stations that do not follow the same trend as the other stations, those are station Fåværing in year 2021 predicting soil temperatures at 10cm (see figure ?? and ??) and Apelsvoll in year 2022 and year 2021 (see figure ?? and ??).

### 4.3 Plauborg hourly

Notes on figure 13:

- The difference plot show that there is a shift from Autumn month to the rest of the year.
- There is a seasonal grouping as described in Linear Regression (see 4.1)

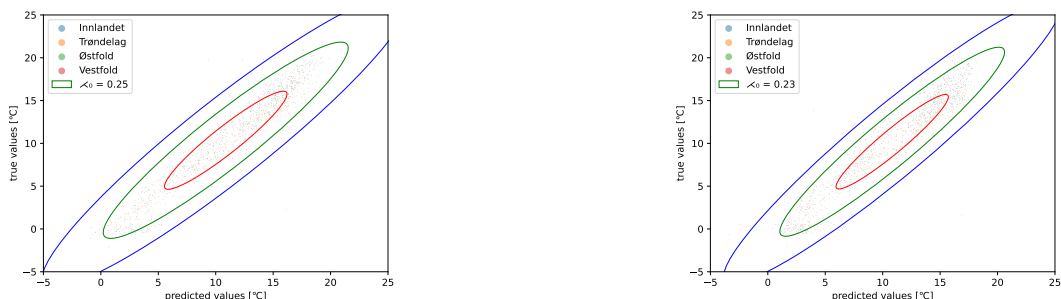
Notes on tabel 15:



(a) Difference plot for daily Plauborg model with the lowest RMSE in year 2022 and region Østfold.

(b) Difference plot for daily Plauborg model with the highest RMSE in year 2022 and region Innlandet.

Figure 10: Difference plots of the extremal regions based on the RMSE measure. The station names can be found in table 1.



(a) The plot shows the ground truth against the predicted value of daily values Plauborg model. The ellipses demonstrates the 65% (inner ellipse), 95% (middle ellipse), and 99% (outer ellipse) confidence interval for the model.

(b) The plot shows the ground truth against the predicted value of daily values Plauborg model. The ellipses demonstrates the 65% (inner ellipse), 95% (middle ellipse), and 99% (outer ellipse) confidence interval for the model.

Figure 11: Plots showing ground truth vs predicted values from the daily Plauborg models with their 68%, 95%, and 99% confidence ellipses. The confidence ellipses function the same as confidence intervals but in two dimensions, meaning the area covered by the ellipse denotes where one can expect the points to be with a given confidence percent. These plots contain a subset of the data, however the ellipses and  $\lambda_0$  are calculated with all the data.

## 4 RESULTS

scope	spesific scope	RMSE [°C]	MAE [°C]	bias [°C]	log( $\kappa$ (model))	digit sensitivity	R <sup>2</sup>
global	—	1.91	1.536	0.644	-1.913	-2	0.876
region	Østfold	1.94	1.541	-0.073	-1.918	-2	0.885
region	Vestfold	1.71	1.341	0.236	-1.907	-2	0.915
region	Trøndelag	1.843	1.56	1.461	-1.911	-2	0.794
region	Innlandet	2.16	1.735	1.02	-1.913	-2	0.863
local	52	2.33	1.873	-1.402	-1.906	-2	0.83
local	41	1.748	1.409	-0.371	-1.913	-2	0.914
local	37	1.877	1.496	0.353	-1.906	-2	0.905
local	118	1.742	1.384	1.139	-1.914	-2	0.886
local	50	1.251	0.985	0.096	-1.91	-2	0.946
local	42	1.966	1.54	0.346	-1.904	-2	0.901
local	38	1.721	1.367	0.515	-1.904	-2	0.912
local	30	1.817	1.471	-0.014	-1.908	-2	0.91
local	57	1.841	1.538	1.427	-1.915	-2	0.863
local	39	1.729	1.468	1.402	-1.906	-2	0.852
local	34	2.104	1.836	1.816	-1.912	-2	0.316
local	15	1.681	1.411	1.215	-1.914	-2	0.801
local	27	1.924	1.534	0.753	-1.91	-2	0.901
local	26	2.528	2.101	1.578	-1.916	-2	0.833
local	17	2.448	1.911	1.401	-1.912	-2	0.844
local	11	1.735	1.443	0.463	-1.909	-2	0.866

(a) Performance table for daily values Plauborg model 20cm

scope	spesific scope	RMSE [°C]	MAE [°C]	bias [°C]	log( $\kappa$ (model))	digit sensitivity	R <sup>2</sup>
global	—	2.074	1.621	0.608	-1.271	-2	0.861
region	Østfold	2.168	1.704	0.24	-1.256	-2	0.856
region	Vestfold	2.022	1.564	0.219	-1.265	-2	0.892
region	Trøndelag	1.957	1.528	1.235	-1.266	-2	0.782
region	Innlandet	2.165	1.71	0.714	-1.265	-2	0.873
local	52	2.418	1.837	-0.636	-1.257	-2	0.664
local	41	1.975	1.587	-0.293	-1.273	-2	0.9
local	37	2.206	1.755	0.373	-1.265	-2	0.873
local	118	2.165	1.697	1.137	-1.266	-2	0.839
local	50	1.395	1.105	-0.046	-1.261	-2	0.938
local	42	2.239	1.75	0.333	-1.263	-2	0.881
local	38	2.42	1.908	0.667	-1.264	-2	0.845
local	30	1.914	1.519	-0.046	-1.264	-2	0.908
local	57	1.978	1.547	1.108	-1.266	-2	0.85
local	39	1.896	1.455	1.193	-1.269	-2	0.828
local	34	2.143	1.687	1.535	-1.271	-2	0.397
local	15	1.806	1.428	1.114	-1.267	-2	0.787
local	27	2.063	1.627	0.396	-1.256	-2	0.895
local	26	2.43	1.937	1.251	-1.269	-2	0.855
local	17	2.26	1.78	0.921	-1.264	-2	0.875
local	11	1.879	1.504	0.339	-1.261	-2	0.864

(b) Performance table for daily values Plauborg 10cm

Table 14: Performance table for daily values Plauborg model at 10 cm depth and 20 cm depth.  
The station names can be found in table 1.

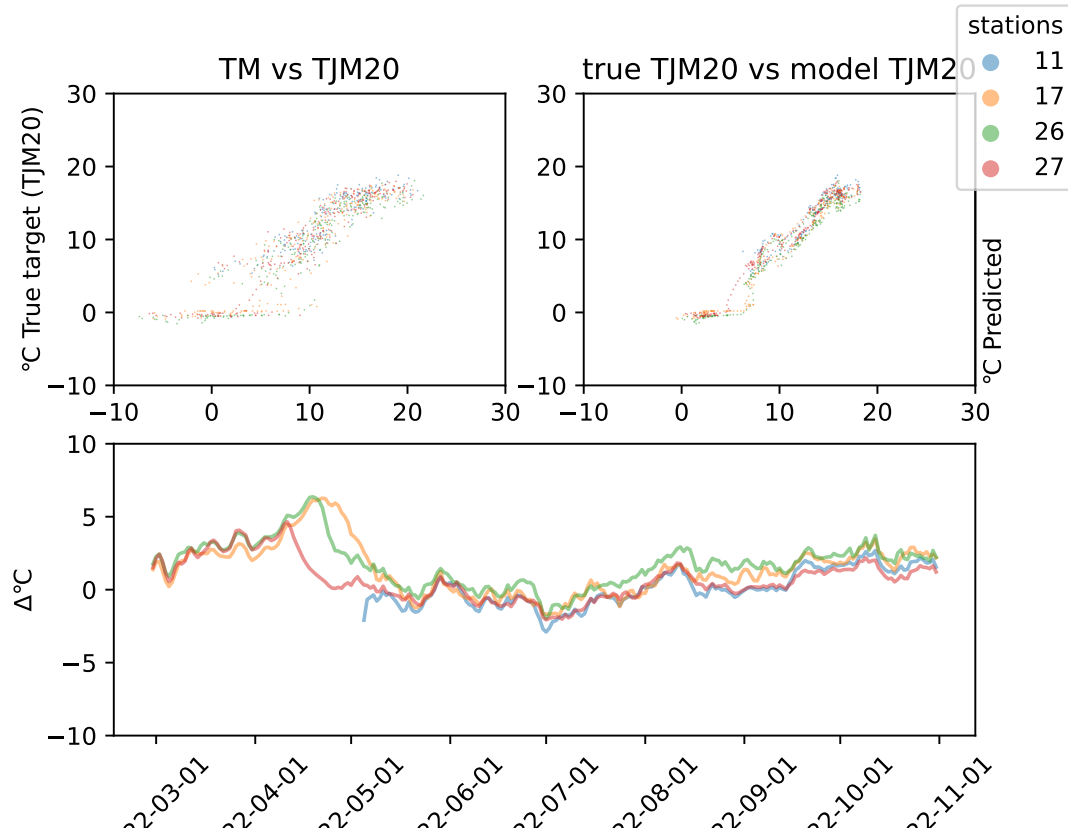
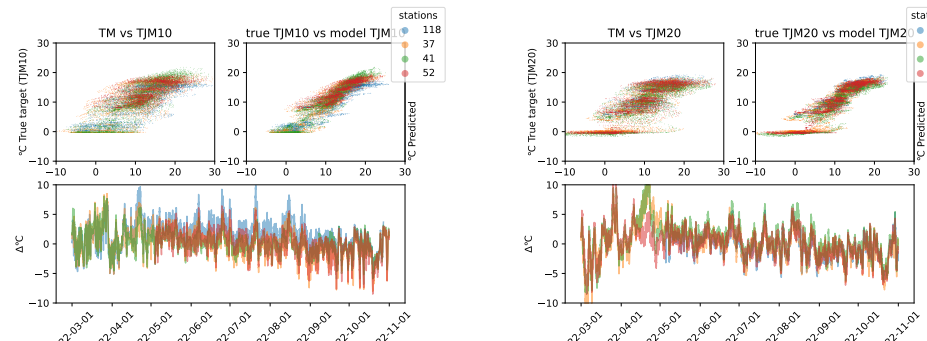


Figure 12: Difference plot for daily Plauborg model in year 2022 and region Innlandet for 20cm soil temperature.



(a) Difference plot for hourly Plauborg model with the lowest RMSE in year 2022 and region Østfold.  
(b) Difference plot for hourly Plauborg model with the highest RMSE in year 2022 and region Innlandet.

Figure 13: Difference plots of the extremal regions based on the RMSE measure. The station names can be found in table 1.

## 4 RESULTS

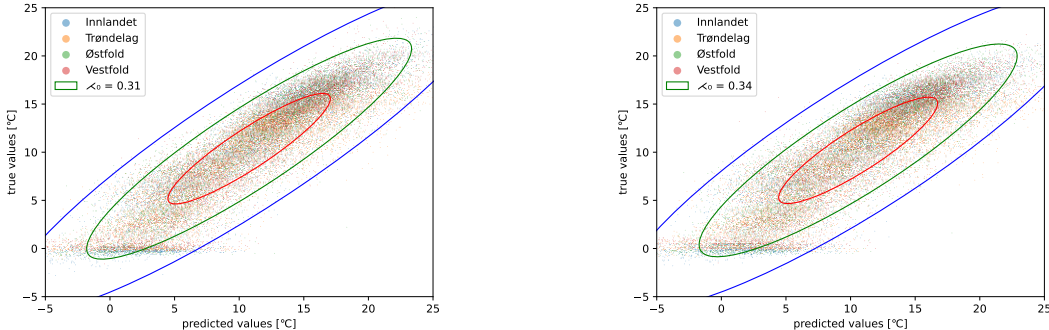
scope	spesific scope	RMSE [°C]	MAE [°C]	bias [°C]	log( $\kappa$ (model))	digit sensitivity	R <sup>2</sup>
global	—	2.676	2.06	0.528	-0.325	-1	0.756
region	Østfold	2.564	2	0.176	-0.327	-1	0.8
region	Vestfold	2.565	1.958	0.785	-0.329	-1	0.81
region	Trøndelag	2.938	2.279	0.75	-0.331	-1	0.477
region	Innlandet	2.612	1.997	0.379	-0.328	-1	0.799
local	52	2.504	1.976	-1.2	-0.324	-1	0.803
local	41	2.135	1.665	0.13	-0.324	-1	0.872
local	37	2.513	1.938	0.067	-0.33	-1	0.83
local	118	3.029	2.422	1.722	-0.329	-1	0.656
local	50	2.176	1.7	0.815	-0.329	-1	0.836
local	42	2.739	2.099	0.746	-0.321	-1	0.807
local	38	2.983	2.323	1.149	-0.327	-1	0.736
local	30	2.276	1.708	0.428	-0.333	-1	0.859
local	57	3.079	2.419	0.744	-0.319	-1	0.617
local	39	2.79	2.186	0.633	-0.323	-1	0.615
local	34	3.163	2.427	0.797	-0.328	-1	-0.547
local	15	2.706	2.094	0.827	-0.326	-1	0.484
local	27	2.455	1.885	0.335	-0.321	-1	0.839
local	26	2.757	2.105	0.892	-0.326	-1	0.801
local	17	3.023	2.265	0.137	-0.327	-1	0.762
local	11	2.346	1.847	-0.023	-0.325	-1	0.755

(a) Performance table for daily values Plauborg model 20cm

scope	spesific scope	RMSE [°C]	MAE [°C]	bias [°C]	log( $\kappa$ (model))	digit sensitivity	R <sup>2</sup>
global	—	2.529	1.926	0.597	-0.434	-1	0.794
region	Østfold	2.448	1.894	0.512	-0.434	-1	0.816
region	Vestfold	2.412	1.81	0.733	-0.444	-1	0.846
region	Trøndelag	2.822	2.176	0.781	-0.442	-1	0.547
region	Innlandet	2.382	1.805	0.312	-0.449	-1	0.847
local	52	2.514	1.964	-0.349	-0.445	-1	0.636
local	41	1.938	1.519	0.151	-0.444	-1	0.903
local	37	2.344	1.804	0.237	-0.439	-1	0.857
local	118	2.928	2.322	1.639	-0.442	-1	0.706
local	50	1.908	1.472	0.558	-0.448	-1	0.884
local	42	2.501	1.885	0.703	-0.44	-1	0.852
local	38	3.055	2.368	1.363	-0.442	-1	0.754
local	30	2.072	1.555	0.354	-0.436	-1	0.892
local	57	2.906	2.263	0.677	-0.448	-1	0.677
local	39	2.77	2.151	0.701	-0.438	-1	0.633
local	34	3.013	2.306	0.845	-0.444	-1	-0.193
local	15	2.589	1.991	0.903	-0.443	-1	0.562
local	27	2.277	1.724	0.163	-0.444	-1	0.872
local	26	2.532	1.918	0.821	-0.44	-1	0.843
local	17	2.649	1.979	0.065	-0.45	-1	0.828
local	11	2.146	1.666	0.038	-0.445	-1	0.823

(b) Performance table for hourly values Plauborg model 10cm

Table 15: Performance table for hourly values Plauborg model at 10 cm depth and 20 cm depth.  
The station names can be found in table 1.



(a) The plot shows the ground truth against the predicted value of hourly values Plauborg model. The eclipses demonstrate the 68% (inner eclipse), 95% (middle eclipse), and 99% (outer eclipse) confidence interval for the model.

(b) The plot shows the ground truth against the predicted value of hourly values Plauborg model. The eclipses demonstrates the 68% (inner eclipse), 95% (middle eclipse), and 99% (outer eclipse) confidence interval for the model.

Figure 14: Plots showing ground truth vs predicted values from the hourly Plauborg models with their 68%, 95%, and 99% confidence eclipses. The confidence eclipses function the same as confidence intervals but in two dimensions, meaning the area covered by the eclipse denotes where one can expect the points to be with a given confidence percent. These plots contain a subset of the data, however the ellipses and  $\lambda_0$  are calculated with all the data.

- From  $R^2$  measure it shows that the model captured much of the variance in the data.
- It tends to overestimate by  $0.5^\circ C$  on average.
- It is sensitive to small changes to the input as shown by the digit sensitivity measure.

The hourly Plauborg shows high variance but promising explained variance. During May and April the model shows a rise in prediction difference, likely due to the effect of snow keeping the temperature relative constant and therefore getting a copy-effect of the air temperature. Figure 14 shows that the model is a good fit as the confidence ellipse lines up with the symmetry line.

### 4.4 Long Short Term-Memory (LSTM)

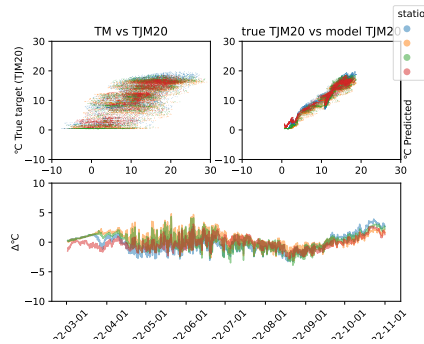
Figure 15 shows that the LSTM has two modes, one for Autumn and one for the remaining year. In Spring it starts to overestimate the soil predictions.

Figure 16 shows that the LSTM is good at capturing the variation, and is not sensitive to small changes. It has a consistent RMSE over all scopes on around  $1.6^\circ C$ .

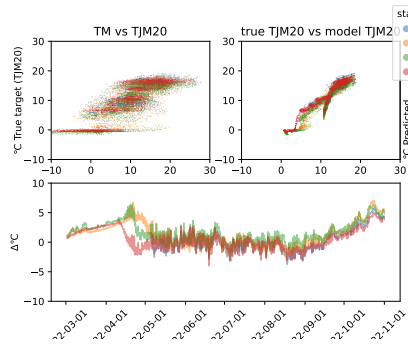
Figure 16 shows that the LSTM fits well to the data, however there is a clear deviation when the true soil temperature is between  $5^\circ C$  and  $20^\circ C$ .

The LSTM shows a great fit to the data except for the May/April month where there is a trend of constant over estimation with a constant value with few stations showing a spike in difference error in April. Figure 17 shows that LSTM quickly converges and does not need many epochs to give good results, however it does take longer to converge for soil temperature 20 cm depth.

## 4 RESULTS

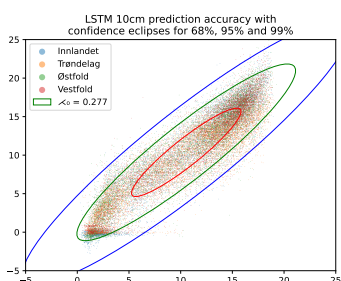


(a) Difference plot for LSTM model with the highest RMSE in year 2022 and region Vestfold.

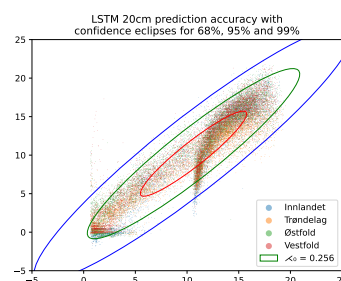


(b) Difference plot for LSTM model with the lowest RMSE in year 2022 and region Innlandet

Figure 15: Difference plots of the extremal regions based on the RMSE measure. The station names can be found in table 1.



(a) The plot shows the ground truth against the predicted value of LSTM model. The ellipses demonstrate the 68% (inner ellipse), 95% (middle ellipse), and 99% (outer ellipse) confidence interval for the model.



(b) The plot shows the ground truth against the predicted value of LSTM model. The ellipses demonstrate the 68% (inner ellipse), 95% (middle ellipse), and 99% (outer ellipse) confidence interval for the model.

Figure 16: Plots showing ground truth vs predicted values from the LSTM models with their 68%, 95%, and 99% confidence ellipses. The confidence ellipses function the same as confidence intervals but in two dimensions, meaning the area covered by the ellipse denotes where one can expect the points to be with a given confidence percent. These plots contain a subset of the data, however the ellipses and  $\lambda_0$  are calculated with all the data.

## 4 RESULTS

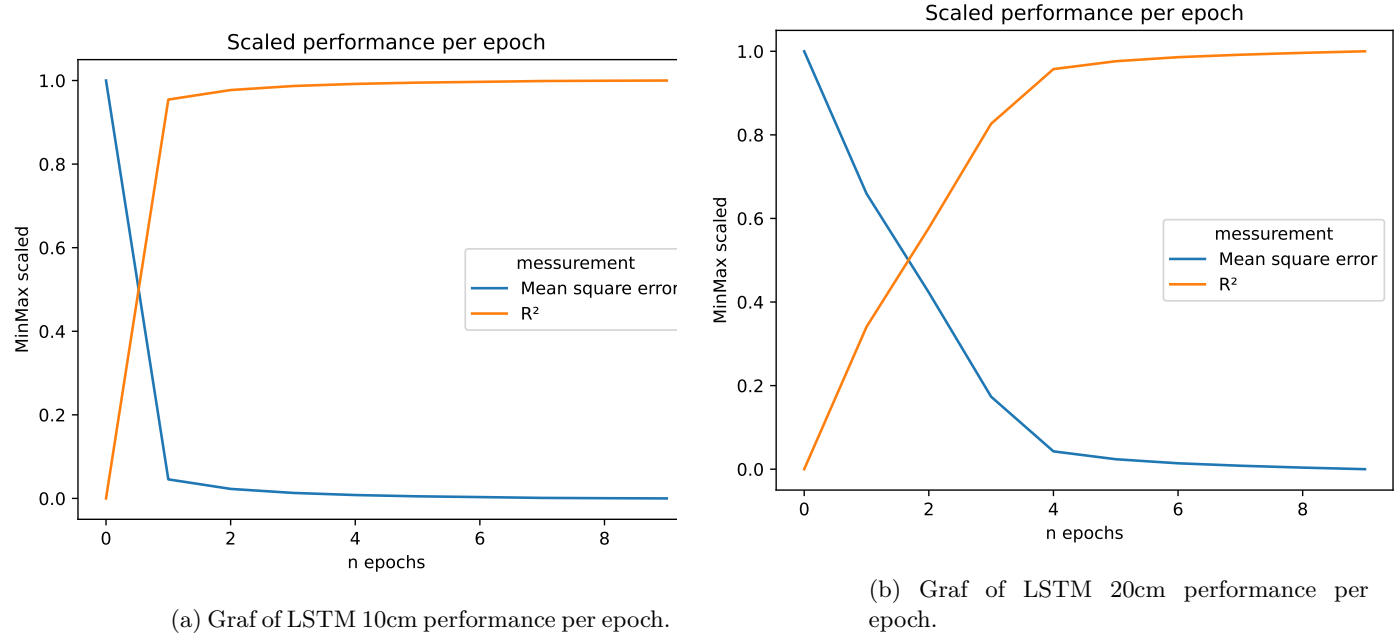
scope	spesific scope	RMSE [°C]	MAE [°C]	bias [°C]	$\log(\kappa(\text{model}))$	digit sensitivity	R <sup>2</sup>
global	—	1.762	1.363	0.423	-2.168	-3	0.893
region	Østfold	1.781	1.432	-0.288	-2.108	-3	0.902
region	Vestfold	1.433	1.153	0.033	-2.169	-3	0.94
region	Trøndelag	1.758	1.329	1.116	-2.177	-3	0.812
region	Innlandet	2.073	1.572	0.925	-2.165	-3	0.873
local	52	2.346	1.985	-1.611	-2.156	-3	0.826
local	41	1.609	1.339	-0.577	-2.15	-3	0.926
local	37	1.547	1.281	0.131	-2.132	-3	0.935
local	118	1.48	1.119	0.921	-2.149	-3	0.917
local	50	1.092	0.88	-0.165	-2.167	-3	0.958
local	42	1.637	1.343	0.163	-2.173	-3	0.931
local	38	1.326	1.082	0.31	-2.173	-3	0.947
local	30	1.606	1.308	-0.176	-2.147	-3	0.929
local	57	1.766	1.334	1.113	-2.133	-3	0.873
local	39	1.678	1.253	1.006	-2.158	-3	0.859
local	34	1.959	1.538	1.48	-2.165	-3	0.413
local	15	1.624	1.203	0.887	-2.173	-3	0.812
local	27	1.772	1.363	0.597	-2.137	-3	0.915
local	26	2.318	1.798	1.491	-2.153	-3	0.859
local	17	2.374	1.797	1.304	-2.103	-3	0.853
local	11	1.903	1.419	0.428	-2.164	-3	0.838

(a) Performance table for LSTM model 20cm

scope	spesific scope	RMSE [°C]	MAE [°C]	bias [°C]	$\log(\kappa(\text{model}))$	digit sensitivity	R <sup>2</sup>
global	—	1.871	1.472	0.302	-1.544	-2	0.886
region	Østfold	1.904	1.522	0.067	-1.571	-2	0.888
region	Vestfold	1.834	1.422	0.119	-1.565	-2	0.91
region	Trøndelag	1.859	1.423	0.675	-1.57	-2	0.803
region	Innlandet	1.893	1.534	0.328	-1.552	-2	0.903
local	52	2.254	1.725	-0.807	-1.544	-2	0.705
local	41	1.85	1.544	-0.372	-1.581	-2	0.911
local	37	1.773	1.495	0.023	-1.565	-2	0.917
local	118	1.872	1.412	1.047	-1.6	-2	0.879
local	50	1.388	1.106	-0.047	-1.593	-2	0.938
local	42	2.002	1.591	0.199	-1.517	-2	0.905
local	38	2.014	1.477	0.537	-1.559	-2	0.892
local	30	1.876	1.518	-0.182	-1.581	-2	0.911
local	57	1.906	1.463	0.549	-1.592	-2	0.86
local	39	1.855	1.397	0.616	-1.596	-2	0.834
local	34	1.923	1.466	0.877	-1.609	-2	0.52
local	15	1.754	1.371	0.669	-1.581	-2	0.797
local	27	1.894	1.561	0.043	-1.568	-2	0.911
local	26	1.964	1.585	0.869	-1.568	-2	0.905
local	17	1.809	1.433	0.464	-1.535	-2	0.92
local	11	1.854	1.503	-0.048	-1.553	-2	0.867

(b) Performance table for LSTM model 10cm

Table 16: Performance table for LSTM model at 10 cm depth and 20 cm depth. The station names can be found in table 1.



(a) Graf of LSTM 10cm performance per epoch.

(b) Graf of LSTM 20cm performance per epoch.

Figure 17: Performance graphs displaying the developments of Mean Square Error and Explained Variance ( $R^2$ ) for each epoch.

#### 4.5 Bi-Directional Long Short Term-Memory (LSTM)

Figure 18 shows a good fit, however figure 18a shows that station 52 underperforms compared to the other stations which is numerically shown in table 17.

Except for station 52, BiLSTM fits well with the data and is balance around  $0^\circ C$  in difference as shown in table 17.

The confidence eclipses as shown in figure 19 suggests a good fit with the data, however there seems to be a hard limit that the model has developed from  $0^\circ C$  to  $7^\circ C$  for some part of the year.

The LSTM shows a great fit to the data except for the May/April month when there is a high variance in the transition from one month to the other. In the BiLSTM epoch performance graph its shows that the model is quick to converge after 2 epochs.

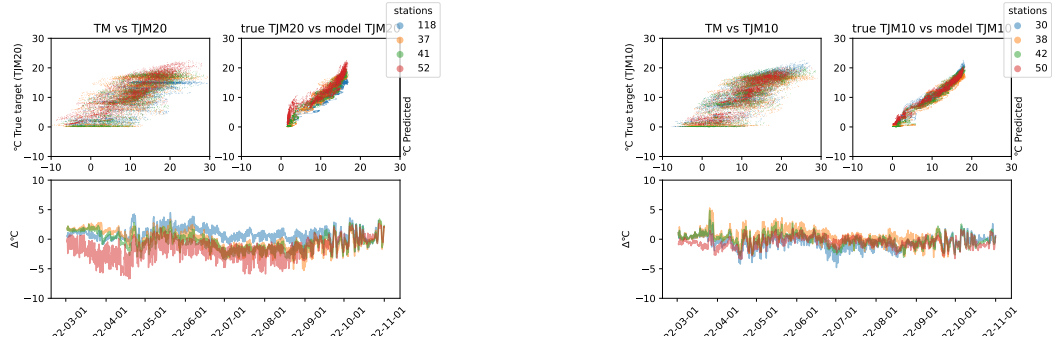
#### 4.6 Gated Recurrent Unit (GRU)

Figure 21 shows that GRU model is a good fit with the data, and demonstrates a different behaviour in Autumn compared to the rest of the year.

Table 18 show good performance, and is a balanced model. There is one station that stands out, that being station 52, 26, and 17 with the highest RMSE.

The confidence eclipses in figure 22 show that it is a good fit to the data, however it also shows that it has developed a hard limit at  $0^\circ C$  and at  $10^\circ C$ .

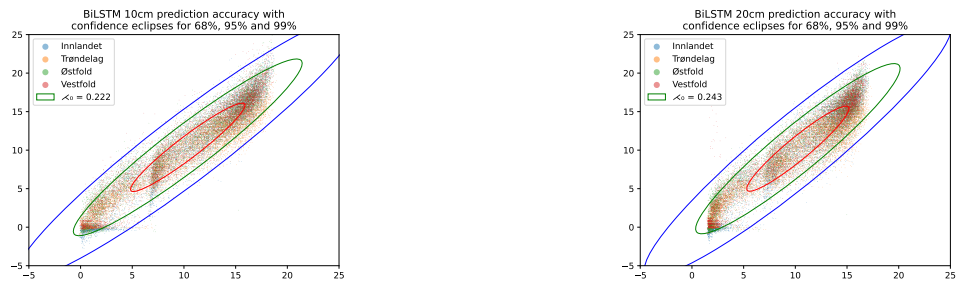
The GRU model demonstrates encouraging outcome with few notable stations and year. One of which is station Øsaker who overestimates the soil temperature at both depth (10 cm and 20



(a) Difference plot for BiLSTM model in year 2022 and region Østfold with highest RMSE.

(b) Difference plot for BiLSTM model in year 2022 and region Vestfold with lowest RMSE.

Figure 18: Difference plots of the extremal regions based on the RMSE measure. The station names can be found in table 1.



(a) The plot shows the ground truth against the predicted value of BiLSTM model. The ellipses demonstrate the 68% (inner ellipse), 95% (middle ellipse), and 99% (outer ellipse) confidence interval for the model.

(b) The plot shows the ground truth against the predicted value of BiLSTM model. The ellipses demonstrate the 68% (inner ellipse), 95% (middle ellipse), and 99% (outer ellipse) confidence interval for the model.

Figure 19: Plots showing ground truth vs predicted values from the BiLSTM models with their 68%, 95%, and 99% confidence ellipses. The confidence ellipses function the same as confidence intervals but in two dimensions, meaning the area covered by the ellipse denotes where one can expect the points to be with a given confidence percent. These plots contain a subset of the data, however the ellipses and  $\lambda_0$  are calculated with all the data.

## 4 RESULTS

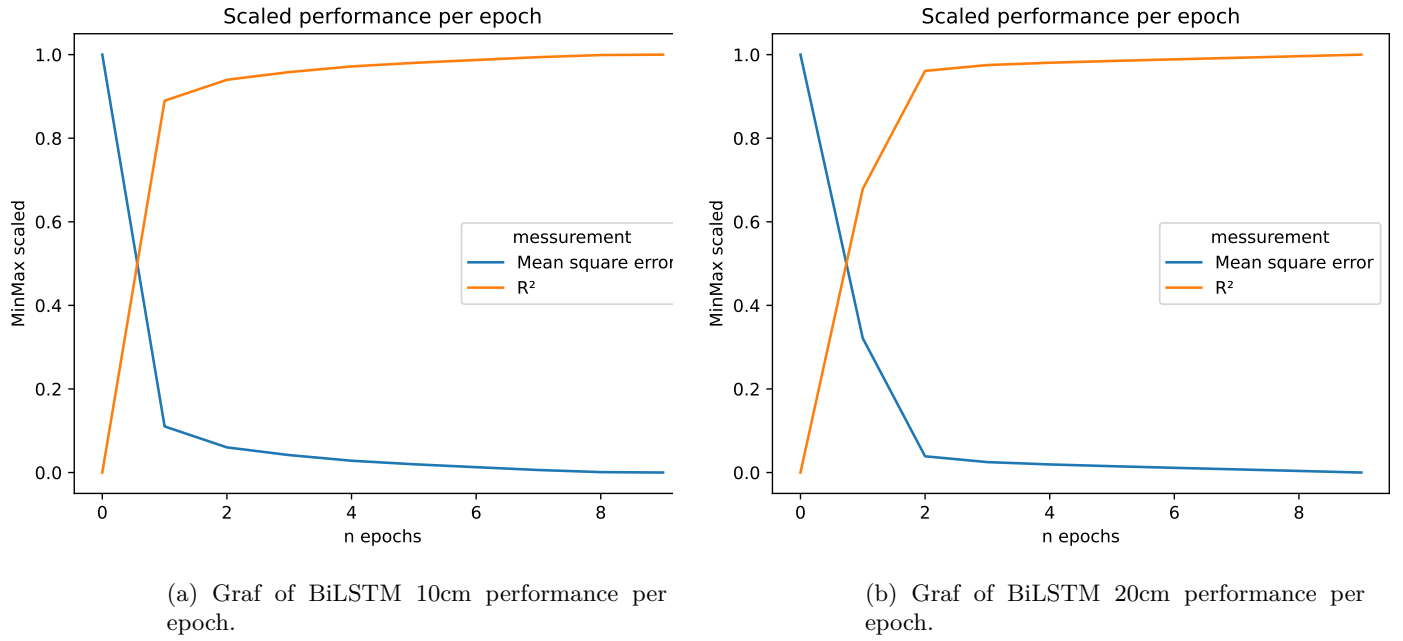
scope	spesific scope	RMSE [°C]	MAE [°C]	bias [°C]	log( $\kappa$ (model))	digit sensitivity	R <sup>2</sup>
global	—	1.695	1.349	0.068	-1.797	-2	0.901
region	Østfold	1.902	1.532	-0.479	-1.831	-2	0.889
region	Vestfold	1.563	1.268	-0.093	-1.796	-2	0.929
region	Trøndelag	1.538	1.166	0.557	-1.787	-2	0.856
region	Innlandet	1.76	1.444	0.339	-1.786	-2	0.908
local	52	2.495	2.067	-1.788	-1.819	-2	0.803
local	41	1.745	1.455	-0.675	-1.755	-2	0.913
local	37	1.716	1.439	-0.255	-1.813	-2	0.92
local	118	1.497	1.162	0.82	-1.814	-2	0.915
local	50	1.201	0.986	-0.131	-1.832	-2	0.95
local	42	1.781	1.463	-0.034	-1.814	-2	0.918
local	38	1.54	1.244	0.189	-1.808	-2	0.929
local	30	1.67	1.379	-0.396	-1.818	-2	0.923
local	57	1.6	1.233	0.534	-1.823	-2	0.896
local	39	1.504	1.123	0.464	-1.83	-2	0.887
local	34	1.64	1.233	0.808	-1.819	-2	0.589
local	15	1.405	1.08	0.435	-1.807	-2	0.86
local	27	1.664	1.385	0.13	-1.822	-2	0.925
local	26	1.91	1.567	0.894	-1.801	-2	0.904
local	17	1.884	1.508	0.589	-1.835	-2	0.907
local	11	1.607	1.333	-0.207	-1.805	-2	0.885

(a) Performance table for BiLSTM model 20cm

scope	spesific scope	RMSE [°C]	MAE [°C]	bias [°C]	log( $\kappa$ (model))	digit sensitivity	R <sup>2</sup>
global	—	1.423	1.111	0.06	-1.858	-2	0.934
region	Østfold	1.483	1.154	-0.252	-1.869	-2	0.932
region	Vestfold	1.341	1.03	-0.264	-1.832	-2	0.952
region	Trøndelag	1.467	1.133	0.524	-1.864	-2	0.877
region	Innlandet	1.4	1.135	0.225	-1.896	-2	0.947
local	52	2.08	1.479	-1.078	-1.838	-2	0.749
local	41	1.473	1.203	-0.757	-1.891	-2	0.944
local	37	1.221	1.006	-0.167	-1.88	-2	0.961
local	118	1.324	1.071	0.64	-1.893	-2	0.94
local	50	1.061	0.858	-0.475	-1.859	-2	0.964
local	42	1.403	1.103	-0.169	-1.861	-2	0.953
local	38	1.429	1.026	0.178	-1.878	-2	0.946
local	30	1.443	1.132	-0.559	-1.87	-2	0.947
local	57	1.405	1.106	0.419	-1.813	-2	0.924
local	39	1.592	1.239	0.496	-1.84	-2	0.878
local	34	1.557	1.171	0.749	-1.829	-2	0.685
local	15	1.3	1.018	0.445	-1.836	-2	0.888
local	27	1.356	1.126	-0.115	-1.836	-2	0.954
local	26	1.487	1.2	0.744	-1.848	-2	0.946
local	17	1.401	1.112	0.459	-1.875	-2	0.952
local	11	1.344	1.084	-0.118	-1.869	-2	0.93

(b) Performance table for BiLSTM model 10cm

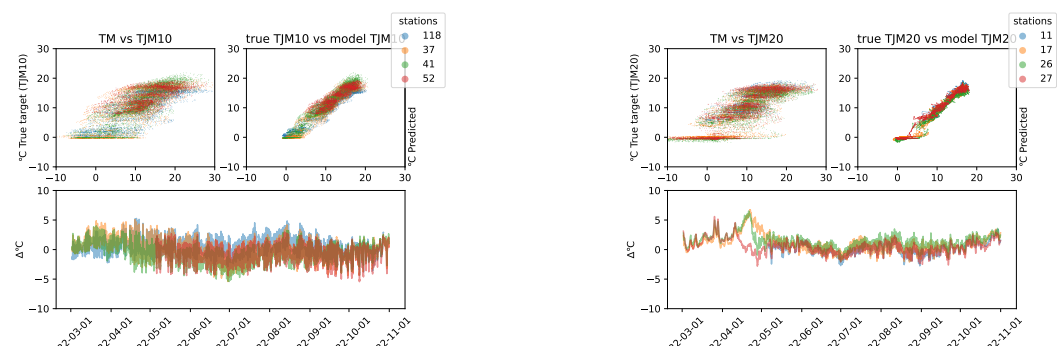
Table 17: Performance table for BiLSTM model at 10 cm depth and 20 cm depth. The station names can be found in table 1.



(a) Graf of BiLSTM 10cm performance per epoch.

(b) Graf of BiLSTM 20cm performance per epoch.

Figure 20: Performance graphs displaying the developments of Mean Square Error and Explained Variance ( $R^2$ ) for each epoch.



(a) Difference plot for GRU model in year 2022 and region Østfold with lowest RMSE

(b) Difference plot for GRU model in year 2022 and region Innlandet with highest RMSE

Figure 21: Difference plots of the extremal regions based on the RMSE measure. The station names can be found in table 1.

## 4 RESULTS

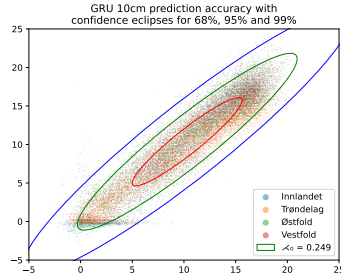
scope	spesific scope	RMSE [°C]	MAE [°C]	bias [°C]	log( $\kappa$ (model))	digit sensitivity	R <sup>2</sup>
global	—	1.7	1.294	0.244	-2.662	-3	0.901
region	Østfold	1.778	1.405	-0.482	-2.682	-3	0.903
region	Vestfold	1.417	1.118	-0.152	-2.646	-3	0.941
region	Trøndelag	1.622	1.255	0.993	-2.65	-3	0.841
region	Innlandet	1.979	1.419	0.706	-2.654	-3	0.884
local	52	2.517	2.148	-1.806	-2.633	-3	0.8
local	41	1.638	1.358	-0.779	-2.665	-3	0.924
local	37	1.414	1.146	-0.036	-2.639	-3	0.946
local	118	1.258	0.955	0.727	-2.629	-3	0.941
local	50	1.06	0.854	-0.355	-2.641	-3	0.961
local	42	1.628	1.307	-0.032	-2.655	-3	0.931
local	38	1.224	0.985	0.145	-2.664	-3	0.955
local	30	1.66	1.325	-0.368	-2.657	-3	0.924
local	57	1.575	1.194	0.982	-2.642	-3	0.899
local	39	1.563	1.217	0.917	-2.66	-3	0.878
local	34	1.831	1.489	1.339	-2.684	-3	0.502
local	15	1.518	1.138	0.763	-2.63	-3	0.836
local	27	1.626	1.2	0.362	-2.652	-3	0.929
local	26	2.187	1.595	1.246	-2.667	-3	0.874
local	17	2.335	1.634	1.106	-2.663	-3	0.857
local	11	1.869	1.344	0.244	-2.627	-3	0.844

(a) Performance table for GRU model 20cm

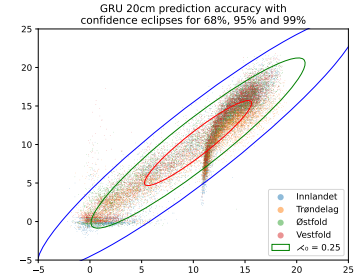
scope	spesific scope	RMSE [°C]	MAE [°C]	bias [°C]	log( $\kappa$ (model))	digit sensitivity	R <sup>2</sup>
global	—	1.807	1.418	0.027	-0.013	-1	0.894
region	Østfold	1.917	1.507	-0.377	-0.042	-1	0.887
region	Vestfold	1.861	1.474	-0.435	-0.044	-1	0.908
region	Trøndelag	1.537	1.199	0.699	0.014	-1	0.866
region	Innlandet	1.911	1.513	0.212	-0.03	-1	0.901
local	52	2.289	1.686	-1.195	-0.034	-1	0.696
local	41	1.983	1.6	-0.937	0.008	-1	0.898
local	37	1.89	1.528	-0.155	-0.027	-1	0.906
local	118	1.619	1.288	0.439	-0.002	-1	0.911
local	50	1.442	1.183	-0.719	-0.036	-1	0.933
local	42	2.062	1.645	-0.309	-0.032	-1	0.899
local	38	2.005	1.569	0.018	-0.013	-1	0.893
local	30	1.881	1.507	-0.695	-0.029	-1	0.91
local	57	1.5	1.19	0.589	-0.045	-1	0.914
local	39	1.553	1.214	0.671	-0.014	-1	0.884
local	34	1.69	1.315	1.031	-0.033	-1	0.639
local	15	1.404	1.086	0.533	-0.028	-1	0.87
local	27	1.853	1.486	-0.139	-0.021	-1	0.915
local	26	2.081	1.654	0.765	-0.011	-1	0.893
local	17	1.976	1.54	0.499	-0.002	-1	0.904
local	11	1.722	1.367	-0.189	-0.027	-1	0.885

(b) Performance table for GRU model 10cm

Table 18: Performance table for GRU model at 10 cm depth and 20 cm depth. The station names can be found in table 1.

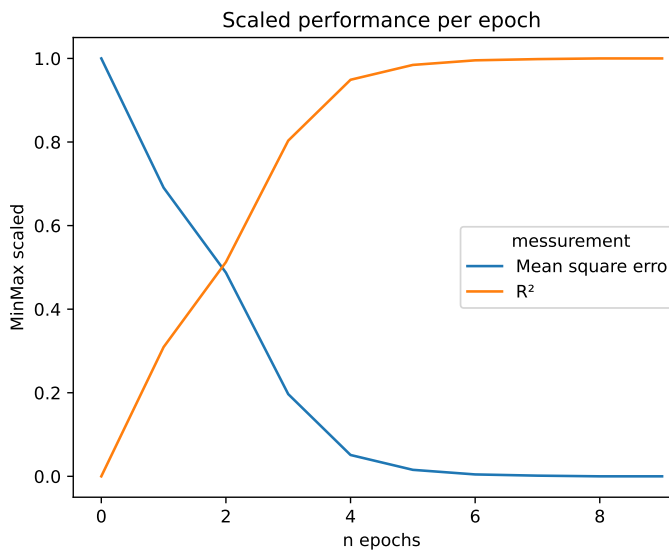


(a) The plot shows the ground truth against the predicted value of GRU model. The eclipses demonstrate the 68% (inner eclipse), 95% (middle eclipse), and 99% (outer eclipse) confidence interval for the model.

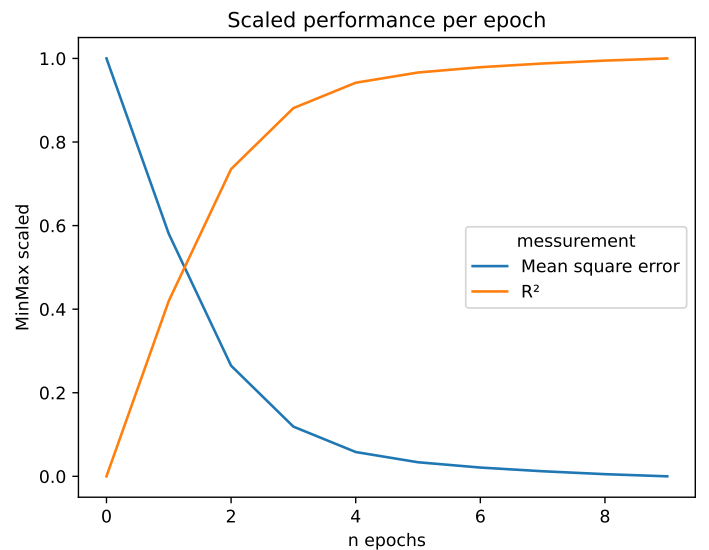


(b) The plot shows the ground truth against the predicted value of GRU model. The eclipses demonstrate the 68% (inner eclipse), 95% (middle eclipse), and 99% (outer eclipse) confidence interval for the model.

Figure 22: Plots showing ground truth vs predicted values from the GRU models with their 68%, 95%, and 99% confidence eclipses. The confidence eclipses function the same as confidence intervals but in two dimensions, meaning the area covered by the ellipse denotes where one can expect the points to be with a given confidence percent. These plots contain a subset of the data, however the ellipses and  $\lambda_0$  are calculated with all the data.



(a) Graf of GRU 10cm performance per epoch.



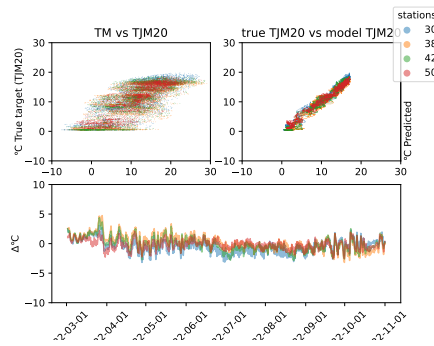
(b) Graf of GRU 20cm performance per epoch.

Figure 23: Performance graphs displaying the developments of Mean Square Error and Explained Variance ( $R^2$ ) for each epoch.

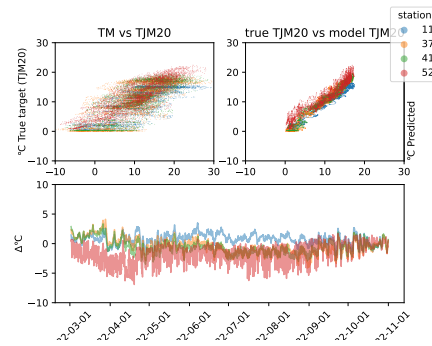
cm). The epoch graphs in figure 23 shows that it takes time to converge and has a slow learning rate.

All station shows an seasonal sensitivity, as all stations tend to incrementally overestimate in May before falling down towards  $0 \Delta^\circ C$  around April month.

### 4.7 Bi-directional Gated Recurrent Unit (GRU)



(a) Difference plot with the lowest RMSE for BiGRU model in year 2022 and region Vestfold



(b) Difference plot with the highest RMSE for BiGRU model in year 2022 and region Østfold

Figure 24: Difference plots of the extremal regions based on the RMSE measure. The station names can be found in table 1.

Figure 24 shows a reasonable fit, except for station 52 that underestimates the soil temperature. In both figure 24a and 24b there are two periods, Autumn with consistent overestimation and the rest of the year.

Table 19 shows that the model fits well to the data and can explain the variance in the data, except for station 52 that has a high RMSE compared to the other stations.

The confidence ellipses in figure 25 shows a good fit with the data, and does not have any learned hard limits in temperature.

Figure 26 shows that the model has a small learning rate however converges quickly after 4 epochs.

## 4 RESULTS

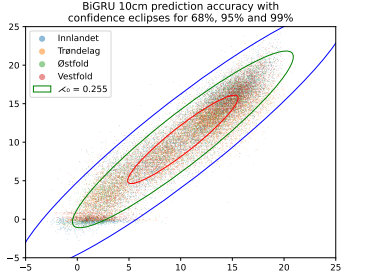
scope	spesific scope	RMSE [°C]	MAE [°C]	bias [°C]	$\log(\kappa(\text{model}))$	digit sensitivity	R <sup>2</sup>
global	—	1.575	1.236	0.012	-2.01	-3	0.915
region	Østfold	1.828	1.452	-0.583	-1.981	-2	0.898
region	Vestfold	1.409	1.112	-0.149	-1.981	-2	0.942
region	Trøndelag	1.456	1.141	0.584	-1.953	-2	0.872
region	Innlandet	1.572	1.236	0.247	-1.997	-2	0.927
local	52	2.565	2.131	-1.905	-2.004	-3	0.792
local	41	1.574	1.319	-0.749	-1.96	-2	0.93
local	37	1.562	1.283	-0.397	-1.996	-2	0.934
local	118	1.351	1.063	0.756	-1.943	-2	0.932
local	50	1.051	0.825	-0.151	-1.97	-2	0.961
local	42	1.585	1.259	-0.096	-2	-2	0.935
local	38	1.381	1.088	0.113	-1.996	-2	0.943
local	30	1.553	1.275	-0.464	-1.981	-2	0.934
local	57	1.527	1.198	0.549	-1.965	-2	0.905
local	39	1.404	1.095	0.514	-1.952	-2	0.902
local	34	1.578	1.228	0.807	-1.969	-2	0.63
local	15	1.311	1.052	0.486	-2.003	-3	0.878
local	27	1.52	1.205	0.037	-1.971	-2	0.938
local	26	1.677	1.314	0.763	-1.99	-2	0.926
local	17	1.629	1.208	0.434	-1.962	-2	0.931
local	11	1.467	1.199	-0.219	-1.975	-2	0.904

(a) Performance table for BiGRU model 20cm

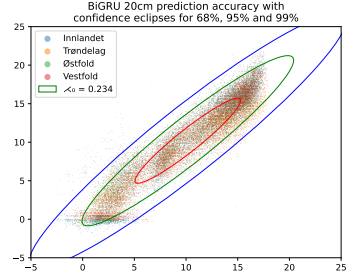
scope	spesific scope	RMSE [°C]	MAE [°C]	bias [°C]	$\log(\kappa(\text{model}))$	digit sensitivity	R <sup>2</sup>
global	—	1.722	1.36	-0.037	-1.734	-2	0.904
region	Østfold	1.793	1.408	-0.277	-1.717	-2	0.901
region	Vestfold	1.673	1.32	-0.211	-1.685	-2	0.925
region	Trøndelag	1.672	1.313	0.345	-1.7	-2	0.842
region	Innlandet	1.758	1.411	-0.023	-1.68	-2	0.916
local	52	2.31	1.687	-1.149	-1.7	-2	0.69
local	41	1.81	1.498	-0.716	-1.719	-2	0.915
local	37	1.659	1.369	-0.313	-1.705	-2	0.928
local	118	1.552	1.196	0.709	-1.681	-2	0.918
local	50	1.288	1.049	-0.397	-1.696	-2	0.947
local	42	1.818	1.455	-0.139	-1.709	-2	0.921
local	38	1.777	1.34	0.229	-1.731	-2	0.916
local	30	1.76	1.436	-0.507	-1.702	-2	0.922
local	57	1.736	1.377	0.226	-1.719	-2	0.884
local	39	1.659	1.286	0.283	-1.735	-2	0.867
local	34	1.732	1.336	0.554	-1.709	-2	0.621
local	15	1.562	1.256	0.334	-1.74	-2	0.839
local	27	1.774	1.438	-0.304	-1.716	-2	0.922
local	26	1.739	1.386	0.51	-1.658	-2	0.925
local	17	1.693	1.311	0.077	-1.705	-2	0.93
local	11	1.796	1.467	-0.375	-1.704	-2	0.875

(b) Performance table for BiGRU model 10cm

Table 19: Performance table for BiGRU model at 10 cm depth and 20 cm depth. The station names can be found in table 1.

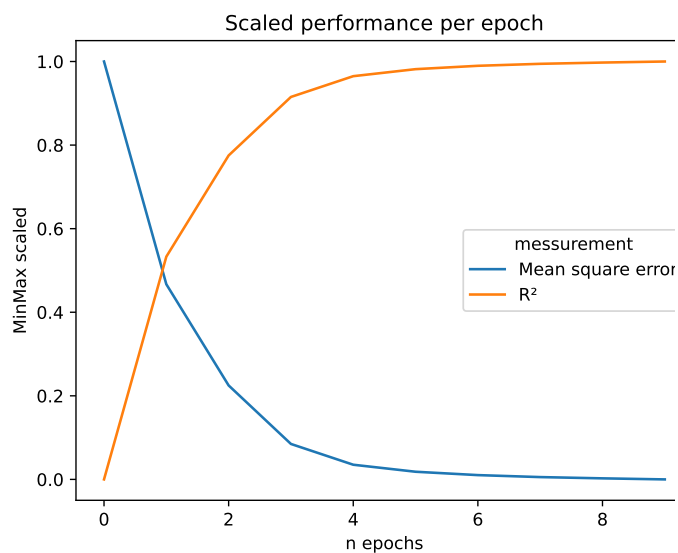


(a) The plot shows the ground truth against the predicted value of BiGRU model. The ellipses demonstrate the 68% (inner eclipse), 95% (middle eclipse), and 99% (outer eclipse) confidence interval for the model.

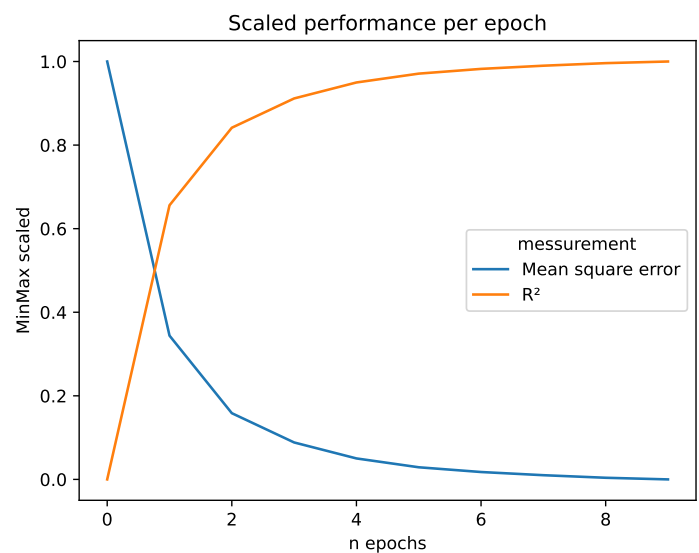


(b) The plot shows the ground truth against the predicted value of BiGRU model. The ellipses demonstrate the 68% (inner eclipse), 95% (middle eclipse), and 99% (outer eclipse) confidence interval for the model.

Figure 25: Plots showing ground truth vs predicted values from the BiGRU models with their 68%, 95%, and 99% confidence ellipses. The confidence ellipses function the same as confidence intervals but in two dimensions, meaning the area covered by the ellipse denotes where one can expect the points to be with a given confidence percent. These plots contain a subset of the data, however the ellipses and  $\lambda_0$  are calculated with all the data.



(a) Graf of BiGRU 10cm performance per epoch.



(b) Graf of BiGRU 20cm performance per epoch.

Figure 26: Performance graphs displaying the developments of Mean Square Error and Explained Variance ( $R^2$ ) for each epoch.

## 5 Discussion

### 5.1 The Autumn discrepancy

A phenomenon that arose during performance evaluations was that the linear models struggles with, and that the deep learning models treated differently was Autumn. The difference graphs showed a clear over or under estimation that are larger than  $10\sigma$ . This discrepancy can be contributed to the intercept coefficient that during low temperature ( $< 5^{\circ}\text{C}$ ) giving either an over estimation or an under approximation. Furthermore, when removing the calculation of the intercept the same phenomenon is still present possibility due to the model adapting better to Summer that has stable temperatures for a longer period than Autumn and Spring.

The deep learning models seems to have learned that there is a difference between winter season and the other seasons, and this effect can be observed in the difference plots in appendix A . but to a lesser exstent where it overestimates at a few periods during the Mars month. This can be due to snow covering the soil forming an thermal isolator keeping the soil temperature constant while the air temperature is fluctuating at relative normal rates giving the models a false sense of generality when predicting this period, however the GRU model seems to interoperate a sense of season awareness allowing it to have a more constant temperature prediction in the autumn and return to "normal" operation during Summer and Spring.

#### 5.1.1 Temperature seasons

It can be observed that in the "TM vs TJM10" and "TM vs TJM20" that there signs of seasons where in the air temperature range -10 to 10 and the soil temperature 0 to 5 represents winter / snow season, the air temperature range 0 to 20 and soil temperature 5 to 12 represent Autumn / Spring, and the air temperature 5 to 30 and soil temperature 12 to 22 represents Summer. This seems reasonable as when the temperature in the air rises there will be a lag period before the soil temperature gets warmed up to the appropriate temperature.

It can be observed in the raw data and in the diff plots (see figure ?? as an example) that the seasons can be shown though the temperatures and stable periods. The flat areas can be explained by snow covers that create a thermal isolation layer that dampens the effect of sudden changes in the air temperature. There exist models in the literature that takes this effect into account[7, 34] to make a more accurate prediction of soil temperature when there is snow present or frozen soil, however these models require knowledge about the soil that gets simulated or some other properties such as the specific heat capacity of the soil being simulated or the water content of the soil.

### 5.2 Regression model performance

The findings in the results, as detailed in the tables from (24) to (27), underscore the limitations of predicting soil temperatures without factoring in temporal elements. The study reveals that omitting time from the modelling process leads to inefficiencies and inaccuracies, a conclusion that is shown in the doubling of RMSE and halving of  $R^2$ , by the basic Linear Regression model compared to the Plauborg models.

This study looked into the adaptability of the original model, which was initially trained for daily mean temperature predictions. The model underwent a shift in coefficients to facilitate hourly forecasts, with the objective of determining whether the foundational formula could maintain its efficacy on smaller timescales, from daily mean values to hourly mean values in this case. A comparative analysis of the outcomes, as presented in tables (23) and (22), with their daily equivalents, revealed a consistency in values. This consistency suggests that the modelling

approach introduced by Plauborg in 2002 [18] is versatile enough to be applied to hourly data series, thereby expanding its utility beyond daily temperature estimations.

In the region Østfold year 2021 there is a divergence in the PLauborg models when predicting the 10 cm soil temperature, this arises as an effect from an old code used to plot the graph of this model. In the old code the NULL values was set by default to 0 meaning when calculation the difference between predicted values and ground truth it in essence created a copy of the air temperature.

### 5.3 Discussion of good results of Plauborg

It is found that incorporating historical temperature data significantly enhances the accuracy of predictions, even on an hourly scale. The coefficients for both daily and hourly predictions are noted to be less than one, which suggests that they represent an average temperature. The Fourier terms are employed to approximate the soil temperature function, as indicated in Equation (11), referenced from Holt' work [36] on estimating soil temperatures in 2008.

$$E_{\text{air,year}}(T) + e^{-z/D} \sin(\omega t - z/D + \phi) \quad (11)$$

The expected value of the soil temperature is denoted by  $E_{\text{soil,year}}$ , and  $T$  represents the collection of time (  $t$  ) and corresponding air temperature. As the term  $e^{z/D}$  is a constant, the estimation focuses on  $\sin(\omega t - Q)$ , which is expressed as  $\sin(\omega t) \cos(Q) - \sin(Q) \cos(\omega t)$ . Here,  $Q$  is  $z/D - \phi$  and is considered a constant. This leads to an extrapolation to a simple sum of sines and cosines, as the model does. The Plauborg model estimates the soil temperature equation (11) with the approximation given in Equation (12). The inclusion of extra terms is useful to account for external factors that influence temperature, such as rainfall, soil type, and atmospheric conditions.

$$E_{\text{air,period}}(T) + \sum \alpha_i e^{z/D} \sin(-Q_i) \cos(i\omega t_i) + \sum \beta_j e^{z/D} \cos(-Q_j) \sin(i\omega t_j) + \varepsilon \quad (12)$$

The term  $E_{\text{air, period}}$  is the expected value of air temperature over a designated period, which is distinct from an annual calculation.

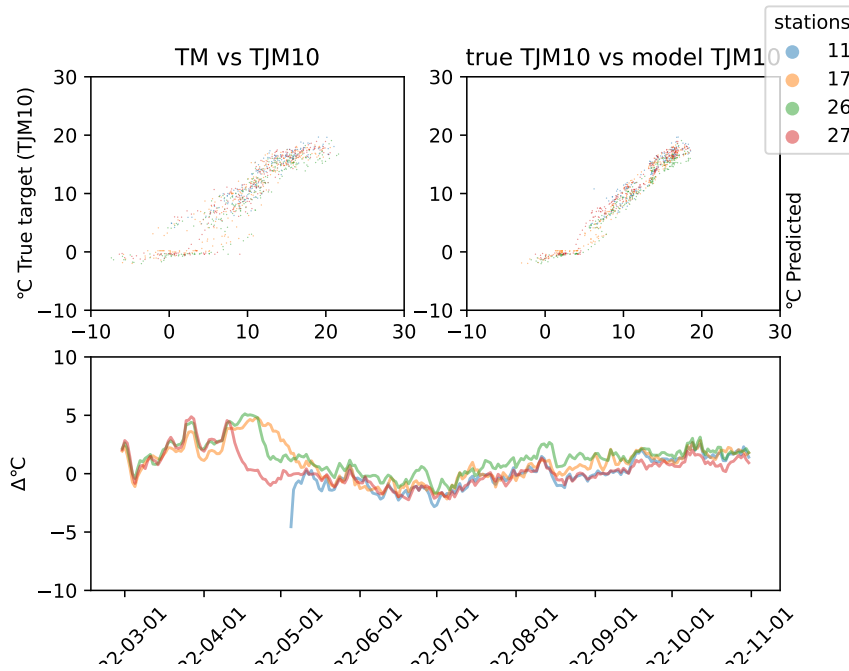
By focusing on shorter periods, the model can more accurately reflect the immediate environmental conditions, which is important for applications such as agricultural planning, where precise temperature forecasts can influence crop management decisions.

The differences between actual and predicted values in the Pluborg models could be due to the varying soil types at different stations. For the purpose of formulating a more precise model, it might be beneficial to incorporate a broader spectrum of meteorological measurements. These could include factors such as air pressure, humidity, and specific characteristics of the soil, like its type and texture. Additionally, the integration of non-linear variables—such as the square root of the temperature or the ratio of temperature change over a given time interval—might offer further refinement to the model's predictive capabilities. By incorporating these enhancements, the model can better grasp the complicated interactions between different metrological, and soil factors that influence temperature readings.

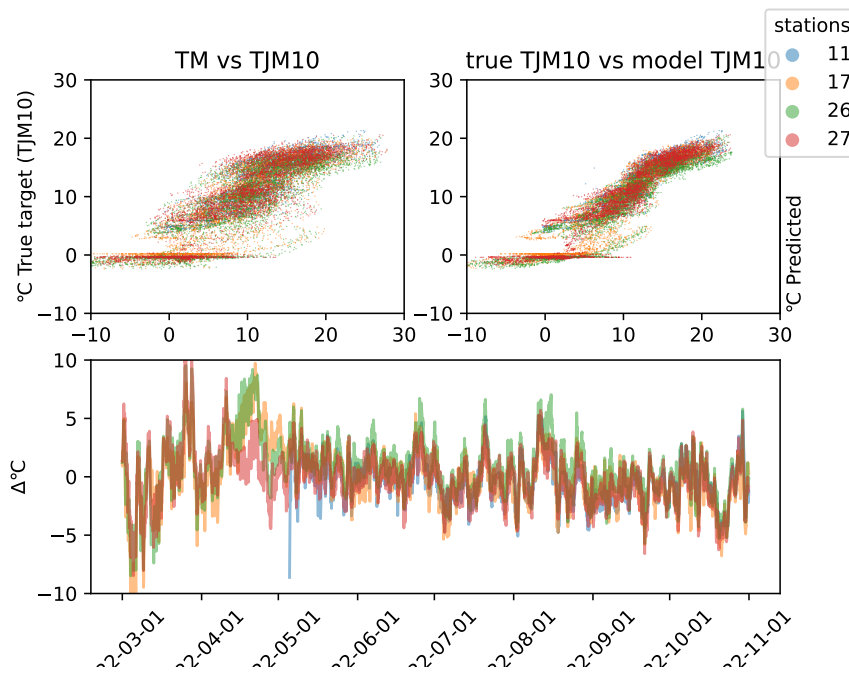
### 5.4 Modification of Plauborg

The Plauborg model trained in Norway was found to only need 3 days ( $t_0, t_{-1}, t_{-2}$ ) compared to [18] that needed 4 days ( $t_0, t_{-1}, t_{-2}, t_{-3}$ ). However, for the Fourier terms both models (hourly version and the daily version) required 2 sine and cosine terms. For the 20cm target the models

diverge in the sense of quantity of terms. It was found that the 20cm model needs 14 sine terms and 2 cosine terms, however only needs 2 days.



(a) The daily model of Plauborg model. The model uses daily average temperatures to predict soil temperatures.



(b) The hourly model of Plauborg model. The model uses hourly temperature data.

Figure 27: Comparison of daily versus hourly predictions

## 5 DISCUSSION

The modification to Plauborg's model is minor, by replacing the  $\omega$  with a larger coefficient it can be used with hourly data. As seen in figure 27b the variation is stronger than 27a however the overall performance is comparable as seen in table 25 and table 23.

scope	spesific scope	RMSE [°C]	MAE [°C]	bias [°C]	log( $\kappa$ (model))	digit sensitivity	R <sup>2</sup>
global	—	2.529	1.926	0.597	-0.434	-1	0.794
region	Østfold	2.448	1.894	0.512	-0.434	-1	0.816
region	Vestfold	2.412	1.81	0.733	-0.444	-1	0.846
region	Trøndelag	2.822	2.176	0.781	-0.442	-1	0.547
region	Innlandet	2.382	1.805	0.312	-0.449	-1	0.847
local	52	2.514	1.964	-0.349	-0.445	-1	0.636
local	41	1.938	1.519	0.151	-0.444	-1	0.903
local	37	2.344	1.804	0.237	-0.439	-1	0.857
local	118	2.928	2.322	1.639	-0.442	-1	0.706
local	50	1.908	1.472	0.558	-0.448	-1	0.884
local	42	2.501	1.885	0.703	-0.44	-1	0.852
local	38	3.055	2.368	1.363	-0.442	-1	0.754
local	30	2.072	1.555	0.354	-0.436	-1	0.892
local	57	2.906	2.263	0.677	-0.448	-1	0.677
local	39	2.77	2.151	0.701	-0.438	-1	0.633
local	34	3.013	2.306	0.845	-0.444	-1	-0.193
local	15	2.589	1.991	0.903	-0.443	-1	0.562
local	27	2.277	1.724	0.163	-0.444	-1	0.872
local	26	2.532	1.918	0.821	-0.44	-1	0.843
local	17	2.649	1.979	0.065	-0.45	-1	0.828
local	11	2.146	1.666	0.038	-0.445	-1	0.823

Table 20: Hourly Plauborg model results.

scope	spesific scope	RMSE [°C]	MAE [°C]	bias [°C]	log( $\kappa$ (model))	digit sensitivity	R <sup>2</sup>
global	—	2.074	1.621	0.608	-1.271	-2	0.861
region	Østfold	2.168	1.704	0.24	-1.256	-2	0.856
region	Vestfold	2.022	1.564	0.219	-1.265	-2	0.892
region	Trøndelag	1.957	1.528	1.235	-1.266	-2	0.782
region	Innlandet	2.165	1.71	0.714	-1.265	-2	0.873
local	52	2.418	1.837	-0.636	-1.257	-2	0.664
local	41	1.975	1.587	-0.293	-1.273	-2	0.9
local	37	2.206	1.755	0.373	-1.265	-2	0.873
local	118	2.165	1.697	1.137	-1.266	-2	0.839
local	50	1.395	1.105	-0.046	-1.261	-2	0.938
local	42	2.239	1.75	0.333	-1.263	-2	0.881
local	38	2.42	1.908	0.667	-1.264	-2	0.845
local	30	1.914	1.519	-0.046	-1.264	-2	0.908
local	57	1.978	1.547	1.108	-1.266	-2	0.85
local	39	1.896	1.455	1.193	-1.269	-2	0.828
local	34	2.143	1.687	1.535	-1.271	-2	0.397
local	15	1.806	1.428	1.114	-1.267	-2	0.787
local	27	2.063	1.627	0.396	-1.256	-2	0.895
local	26	2.43	1.937	1.251	-1.269	-2	0.855
local	17	2.26	1.78	0.921	-1.264	-2	0.875
local	11	1.879	1.504	0.339	-1.261	-2	0.864

Table 21: Daily Plauborg model results.

## 5 DISCUSSION

With modification to the model to accept hourly data it still performs approximately as well as the daily data version. With a average error of  $0.597^{\circ}\text{C} \pm 2.529^{\circ}\text{C}$  for TJM10 and  $0.528^{\circ}\text{C} \pm 2.676^{\circ}\text{C}$  for TJM20. It was found that the modified Plauborg model only needs 2 sine terms to make a good prediction and 12h of air temperature which would translate to half a day instead of 3 days.

### 5.4.1 RNN results compared to other studies

The findings of this research are consistent with the numerical trends observed in previous studies, such as those conducted by [23, 25, 26, 28, 29]. However, it is noteworthy that these studies incorporated a broader set of predictive features—including air moisture, rainfall, solar radiation, and wind speed—to enhance the accuracy of soil temperature predictions. The inclusion of these additional meteorological parameters has been shown to improve model performance, underscoring the importance of a comprehensive feature set in predictive modelling of soil temperature.

### 5.5 Deep learning model performance

It is observed in the epoch graphs of the deep learning models that there is a boost in learning rate when implementing the bidirectional technique rather than learning from the data in one time direction. Similarly, it is found that the general performance of the models gets improved by making them bidirectional.

By analysing the model performance table in section 4 it shows that BiLSTM did better than the other models in terms predicting soil temperature at 10 cm depth, however BiGRU did perform better at 20 cm depth.

### 5.6 Future work

The models chosen in this study is not a representative sample of current knowledge of soil temperature modelling, and this study did not aim for optimizing the models beyond what the original authors have already done with the exception for base models used for comparison purposes. A more comprehensive is needed of more complex models that utilises cutting edge technologies, techniques, and theory. One of which is logic based models, for instance ASPER[37] that tries to incorporate logical descriptions of the problem and limits the model for better or equal results based on fewer samples[38]. Another approach is to use the newest deep learning method of the attention mechanism[39] combined with recurrent neural networks to elevate the accuracy and speed of the model. As the author of the paper [23] has show some promise with that approach.

Furthermore, the models presented in this study are not optimised as far as they can as there are more parameters one can include in the model, and Hyper-Parameter one can fine tune to improve the predictive capability of the models such as

- The type of loss function
- the learning rate
- the optimizer
- the activation function used
- weight regulation
- adding a dropout rate

This are a small collection of techniques that can be utilised to furter optimize the models for better predictive performance.

There have been significant developments in model types, including Answer Set Programming-enhanced Entity-Relation (ASPER). ASPER combines logical statements<sup>5</sup> with deep learning models to achieve results comparable to or better than "non-logical" deep learning models, but with fewer samples [37]. A study demonstrated that the ASPER model can reduce the required number of samples/observations by a factor of 1/1000 [38] and studies that uses this knowledge based approach shows to improve the predictive ability of the model to predict soil temperatures[1, 40]. In an interview with the study researcher [41], it was found that while the model requires strict rules, it is possible to incorporate Bayesian statistics to enhance its generality for various applications. By relaxing the ruleset and acknowledging that the given rules may not be 100% accurate, the model can be adapted to other applications using approximation rule-sets. Its the belife of the author of current study that this model can be adapted to soil temperature prediction when incorporating Bayesian statistics.

Additionally, attention-awareness, a method developed by the Google cooperation [39] also used in ChatGPT and other modern AI technologies, has been employed to predict soil temperatures and soil moisture[23] and has shown promising results in predicting soil temperatures by dynamically putting emphases on some of the features, particular days, and combinations of these when predicting.

---

<sup>5</sup>Statements can be thought of as formulas, natural laws, or knowledge about the solution

## 6 Conclusion

Soil temperature significantly impacts agriculture, influencing pest prevention, conservation, yield prediction, and more. Despite its importance, widespread measurement remains challenging due to cost limitations and technical issues. Interpolating missing data using methods like global mean approximation is common but has drawbacks including requiring previous measurements of the soil temperature. Incorporating other features can improve soil temperature estimation to account for the variations that are not explained by air temperature alone. Advancements in prediction and measurement are crucial for sustainable agriculture and accurate climate models.

Method used in this study are

1. Fetch available data to use as training and testing set
2. Compile the data and treat it to be used in the model
3. Train all the models on the same training data, data from 2014 to 2020
4. calculate and plot relevant statistics using 2021 to 2022 test data
5. compile the results

The results of this study show that promising results can be achieved with few parameters, however further studies need to be done to see the effect of adding more parameters or making the models more complex by adding more structure<sup>6</sup>. As for regression modelling; Adding time to a regression model does improve the model predictive power over a time independent model. This make a simple model to predict soil temperatures in areas with no soil temperature measurement.

There is a clear advantage to data-driven modelling to further the investigation into deep learning models as the models shows comparable results to analytical models, as is show in other studies[3, 23, 26]. However, to improve the model performance more features is recommended to make the model more general and adaptable to other local environments outside the nortic climate. It was found in this study that none of the models had an RMSE less than 1 for any station or region, suggesting there are more variation in the data that is not captured by only time and air temperature alone.

### 6.1 Discussion of research goals

This study wanted to answer four questions;

1. Achieving Good Results with Minimal Parameters: Can satisfactory predictions be obtained using a limited set of meteorological and chronological parameters?
2. Deep Learning Models for Soil Temperature Prediction: Is it feasible to employ deep learning models for predicting soil temperatures?
3. Complexity of Deep Learning Models: Is it necessary to utilize complex deep learning architectures when predicting soil temperatures?
4. Suitable model for Nordic climate: Is there a model that fits for the Scandinavian climate?

To address each research question in order

<sup>6</sup>Structure as in more layers, augmentations of input and performing feature extraction as part of the model.

## 6 CONCLUSION

1. This study found that satisfactory results can be achieved with few parameters however there will be variations that the model will not be able to explain.
2. Yes, deep learning models has shown to have the capacity to capture difficult patterns in the data and to adapt to the seasons from only Time, and air temperature.
3. This study did not go deeper into adding more complexity to the models due to limitations in this study, see section 6.2 for more details. However, it was found that making the models bidirectional improved the deep learning models.
4. It is found in this study that the bidirectional models performed better than only training in one time direction. The BiLSTM performed the best in predicting 10 cm soil temperature, however BiGRU did perform better in predicting soil temperature at 20 cm depth. It is recommended that Bidirectional models should be further researched at a broader range of depths. However, due to the limitations of this study it is also recommended that further research being conducted into alternative models and newer deep learning techniques.

### 6.2 Limitations

This study faced a multitude of technical difficulties including,

- Trying to get the models to run properly
- Finding proper parameters to limit memory usage and time
- Insufficient computing power for some parameters
- Getting TensorFlow to work on Windows 10/11<sup>7</sup>

This study would be more comprehensive if these unforeseen difficulties did not occur, and it is recommended that it would be done a new study going more in depth into other type of deep learning models suitable for time-series data and investigating other potential features to include in the modelling.

---

<sup>7</sup>This was later found in the study that the TensorFlow project had moved from being Windows compatible to being exclusively runnable on Linux unless choosing an outdated version of TensorFlow.

## 7 Bibliography

### References

- [1] Meysam Alizamir, Ozgur Kisi, Ali Najah Ahmed, Cihan Mert, Chow Ming Fai, Sungwon Kim, Nam Won Kim, and Ahmed El-Shafie, “Advanced machine learning model for better prediction accuracy of soil temperature at different depths,” *PLOS ONE*, volume 15, number 4, Lei Lin, Ed., page 25, Apr. 14, 2020, ISSN: 1932-6203. DOI: 10.1371/journal.pone.0231055. [Online]. Available: <https://dx.plos.org/10.1371/journal.pone.0231055> (visited on 09/29/2023).
- [2] Ha Seon Sim, Dong Sub Kim, Min Gyu Ahn, Su Ran Ahn, and Sung Kyeom Kim, “Prediction of strawberry growth and fruit yield based on environmental and growth data in a greenhouse for soil cultivation with applied autonomous facilities,” *Korean Journal of Horticultural Science and Technology*, volume 38, number 6, pages 840–849, Dec. 31, 2020, ISSN: 1226-8763, 2465-8588. DOI: 10.7235/HORT.20200076. [Online]. Available: <https://www.hst-j.org/articles/doi/10.7235/HORT.20200076> (visited on 10/05/2023).
- [3] Cong Li, Yaonan Zhang, and Xupeng Ren, “Modeling hourly soil temperature using deep BiLSTM neural network,” *Algorithms*, volume 13, number 7, page 173, Jul. 17, 2020, ISSN: 1999-4893. DOI: 10.3390/a13070173. [Online]. Available: <https://www.mdpi.com/1999-4893/13/7/173> (visited on 03/17/2023).
- [4] Ornella Nanushi, Vasileios Sitokonstantinou, Ilias Tsoumas, and Charalampos Kontoes, *Pest presence prediction using interpretable machine learning*, May 16, 2022. arXiv: 2205.07723 [cs]. [Online]. Available: <http://arxiv.org/abs/2205.07723> (visited on 05/09/2024).
- [5] Scott N. Johnson, Peter J. Gregory, James W. McNicol, Yasmina Oodally, Xiaoxian Zhang, and Philip J. Murray, “Effects of soil conditions and drought on egg hatching and larval survival of the clover root weevil (*Sitona lepidus*),” *Applied Soil Ecology*, volume 44, number 1, pages 75–79, Jan. 1, 2010, ISSN: 0929-1393. DOI: 10.1016/j.apsoil.2009.10.002. [Online]. Available: <https://www.sciencedirect.com/science/article/pii/S0929139309001887> (visited on 05/09/2024).
- [6] Joris C. Stuurop, Sjoerd E.A.T.M. Van Der Zee, and Helen Kristine French, “The influence of soil texture and environmental conditions on frozen soil infiltration: A numerical investigation,” *Cold Regions Science and Technology*, volume 194, page 103456, Feb. 2022, ISSN: 0165232X. DOI: 10.1016/j.coldregions.2021.103456. [Online]. Available: <https://linkinghub.elsevier.com/retrieve/pii/S0165232X21002378> (visited on 01/31/2024).
- [7] Katri Rankinen, Tuomo Karvonen, and D. Butterfield, “A simple model for predicting soil temperature in snow-covered and seasonally frozen soil: Model description and testing,” *Hydrology and Earth System Sciences*, volume 8, number 4, pages 706–716, Aug. 31, 2004, ISSN: 1607-7938. DOI: 10.5194/hess-8-706-2004. [Online]. Available: <https://hess.copernicus.org/articles/8/706/2004/> (visited on 03/17/2023).
- [8] Tuomo Karvonen, *A model for predicting the effect of drainage on soil moisture, soil temperature and crop yield*. Otaniemi, Finland: Helsinki University of Technology, Laboratory of Hydrology and Water Resources Engineering, 1988, xvi, 215, Open Library ID: OL15197205M.
- [9] Jean Baptiste Joseph Fourier and Alexander Freeman, *The analytical theory of heat*. New York: Cambridge University Press, 2009, OCLC: 880311398, ISBN: 978-1-108-00178-6.

- [10] Berit Nordskog, Anne Kjersti Bakken, and Halvard Hole, *Jordtemperatur og spredning av husdyrgjødsel - Utredning av om jordtemperatur kan brukes som skranke for spredning av husdyrgjødsel på eng i Farsund kommune*. NIBIO, Jun. 13, 2018, Accepted: 2018-06-14T10:40:43Z ISSN: 2464-1162 Journal Abbreviation: Jordtemperatur og spredning av husdyrgjødsel - Utredning av om jordtemperatur kan brukes som skranke for spredning av husdyrgjødsel på eng i Farsund kommune Publication Title: 18, ISBN: 978-82-17-02114-8. [Online]. Available: <https://nibio.brage.unit.no/nibio-xmlui/handle/11250/2501555> (visited on 05/08/2024).
- [11] “107 - temperature probe.” (), [Online]. Available: <https://www.campbellsci.com/107> (visited on 05/12/2024).
- [12] Kamstrup. “Dokumentasjon for to-tråds Pt500 temperatursensorer.” (), [Online]. Available: <https://www.kamstrup.com/no-no/varmeloesninger/varmemaalere/temperature-sensors/2-wire-pt500-temperature-sensors/documents> (visited on 05/12/2024).
- [13] Jones SB. “3.5 soil temperature – ClimEx handbook.” (), [Online]. Available: <https://climexhandbook.w.uib.no/2019/11/05/soil-temperature-thermal-regime/> (visited on 05/12/2024).
- [14] Van Wijk, WR and De Vries, DA, *Periodic temperature variations in a homogeneous soil*, in *Physics of plant environment*, 1963, pages 103–143. [Online]. Available: [https://scholar.google.com/scholar\\_lookup?title=Periodic%20temperature%20variations%20in%20a%20homogeneous%20soil&author=W.R.%20Van%20Wijk&publication\\_year=1963&pages=103-143](https://scholar.google.com/scholar_lookup?title=Periodic%20temperature%20variations%20in%20a%20homogeneous%20soil&author=W.R.%20Van%20Wijk&publication_year=1963&pages=103-143) (visited on 05/07/2024).
- [15] J. Roodenburg, “Estimating 10-cm soil temperatures under grass,” *Agricultural and Forest Meteorology*, volume 34, number 1, pages 41–52, Feb. 1, 1985, ISSN: 0168-1923. DOI: 10.1016/0168-1923(85)90053-X. [Online]. Available: <https://www.sciencedirect.com/science/article/pii/016819238590053X> (visited on 05/09/2024).
- [16] Ravirajan Kumar Singh and Ram Vinoy Sharma, “Numerical analysis for ground temperature variation,” *Geothermal Energy*, volume 5, number 1, page 22, Nov. 1, 2017, ISSN: 2195-9706. DOI: 10.1186/s40517-017-0082-z. [Online]. Available: <https://doi.org/10.1186/s40517-017-0082-z> (visited on 05/07/2024).
- [17] Peter John Cleall, José Javier Muñoz-Criollo, and Stephen William Rees, “Analytical solutions for ground temperature profiles and stored energy using meteorological data,” *Transport in Porous Media*, volume 106, number 1, pages 181–199, Jan. 1, 2015, ISSN: 1573-1634. DOI: 10.1007/s11242-014-0395-3. [Online]. Available: <https://doi.org/10.1007/s11242-014-0395-3> (visited on 05/07/2024).
- [18] Finn Plauborg, “Simple model for 10 cm soil temperature in different soils with short grass,” *European Journal of Agronomy*, volume 17, number 3, pages 173–179, Oct. 2002, ISSN: 11610301. DOI: 10.1016/S1161-0301(02)00006-0. [Online]. Available: <https://linkinghub.elsevier.com/retrieve/pii/S1161030102000060> (visited on 03/17/2023).
- [19] Mark H. Van Benthem and Michael R. Keenan, “Fast algorithm for the solution of large-scale non-negativity-constrained least squares problems,” *Journal of Chemometrics*, volume 18, number 10, pages 441–450, 2004, \_eprint: <https://onlinelibrary.wiley.com/doi/pdf/10.1002/cem.889> ISSN: 1099-128X. DOI: 10.1002/cem.889. [Online]. Available: <https://onlinelibrary.wiley.com/doi/abs/10.1002/cem.889> (visited on 05/10/2024).
- [20] Guillaume Chevalier, *English: Schematic of the long-short term memory cell, a component of recurrent neural networks*, May 16, 2018. [Online]. Available: [https://commons.wikimedia.org/wiki/File:LSTM\\_Cell.svg](https://commons.wikimedia.org/wiki/File:LSTM_Cell.svg) (visited on 12/10/2023).

- [21] Ihsan Uluocak and Mehmet Bilgili, "Daily air temperature forecasting using LSTM-CNN and GRU-CNN models," *Acta Geophysica*, volume 72, number 3, pages 2107–2126, Jun. 1, 2024, ISSN: 1895-7455. DOI: 10.1007/s11600-023-01241-y. [Online]. Available: <https://doi.org/10.1007/s11600-023-01241-y> (visited on 05/12/2024).
- [22] Furkan Elmaz, Reinout Eyckerman, Wim Casteels, Steven Latré, and Peter Hellinckx, "CNN-LSTM architecture for predictive indoor temperature modeling," *Building and Environment*, volume 206, page 108327, Dec. 1, 2021, ISSN: 0360-1323. DOI: 10.1016/j.buildenv.2021.108327. [Online]. Available: <https://www.sciencedirect.com/science/article/pii/S0360132321007241> (visited on 04/11/2024).
- [23] Qingliang Li, Yuheng Zhu, Wei Shangguan, Xuezhi Wang, Lu Li, and Fanhua Yu, "An attention-aware LSTM model for soil moisture and soil temperature prediction," *Geoderma*, volume 409, page 115651, Mar. 2022, ISSN: 00167061. DOI: 10.1016/j.geoderma.2021.115651. [Online]. Available: <https://linkinghub.elsevier.com/retrieve/pii/S001670612100731X> (visited on 10/05/2023).
- [24] Sepp Hochreiter and Jürgen Schmidhuber, "Long short-term memory," *Neural Computation*, volume 9, number 8, pages 1735–1780, Nov. 1, 1997, ISSN: 0899-7667, 1530-888X. DOI: 10.1162/neco.1997.9.8.1735. [Online]. Available: <https://direct.mit.edu/neco/article/9/8/1735-1780/6109> (visited on 10/18/2023).
- [25] Hatice Citakoglu, "Comparison of artificial intelligence techniques for prediction of soil temperatures in turkey," *Theoretical and Applied Climatology*, volume 130, number 1, pages 545–556, Oct. 2017, ISSN: 0177-798X, 1434-4483. DOI: 10.1007/s00704-016-1914-7. [Online]. Available: <http://link.springer.com/10.1007/s00704-016-1914-7> (visited on 09/28/2023).
- [26] Yu Feng, Ningbo Cui, Weiping Hao, Lili Gao, and Daozhi Gong, "Estimation of soil temperature from meteorological data using different machine learning models," *Geoderma*, volume 338, pages 67–77, Mar. 2019, ISSN: 00167061. DOI: 10.1016/j.geoderma.2018.11.044. [Online]. Available: <https://linkinghub.elsevier.com/retrieve/pii/S0016706118311200> (visited on 03/17/2023).
- [27] Janani Kandasamy, Yuan Xue, Paul Houser, and Viviana Maggioni, "Performance of different crop models in simulating soil temperature," *Sensors*, volume 23, number 6, page 2891, Mar. 7, 2023, ISSN: 1424-8220. DOI: 10.3390/s23062891. [Online]. Available: <https://www.mdpi.com/1424-8220/23/6/2891> (visited on 11/07/2023).
- [28] Qingliang Li, Huibowen Hao, Yang Zhao, Qingtian Geng, Guangjie Liu, Yu Zhang, and Fanhua Yu, "GANs-LSTM model for soil temperature estimation from meteorological: A new approach," *IEEE Access*, volume 8, pages 59427–59443, 2020, ISSN: 2169-3536. DOI: 10.1109/ACCESS.2020.2982996. [Online]. Available: <https://ieeexplore.ieee.org/document/9045947/> (visited on 12/05/2023).
- [29] Xuezhi Wang, Wenhui Li, Qingliang Li, and Xiaoning Li, "Modeling soil temperature for different days using novel quadruplet loss-guided LSTM," *Computational Intelligence and Neuroscience*, volume 2022, Xin Ning, Ed., pages 1–17, Feb. 17, 2022, ISSN: 1687-5273, 1687-5265. DOI: 10.1155/2022/9016823. [Online]. Available: <https://www.hindawi.com/journals/cin/2022/9016823/> (visited on 12/05/2023).
- [30] Saeid Mehdizadeh, Farshad Ahmadi, and Ali Kozekalani Sales, "Modelling daily soil temperature at different depths via the classical and hybrid models," *Meteorological Applications*, volume 27, number 4, e1941, 2020, \_eprint: <https://onlinelibrary.wiley.com/doi/pdf/10.1002/met.1941>, ISSN: 1469-8080. DOI: 10.1002/met.1941. [Online]. Available: <https://onlinelibrary.wiley.com/doi/abs/10.1002/met.1941> (visited on 05/08/2024).

- [31] Kyunghyun Cho, Bart van Merriënboer, Caglar Gulcehre, Dzmitry Bahdanau, Fethi Bougares, Holger Schwenk, and Yoshua Bengio, *Learning phrase representations using RNN encoder-decoder for statistical machine translation*, Sep. 2, 2014. arXiv: 1406.1078[cs, stat]. [Online]. Available: <http://arxiv.org/abs/1406.1078> (visited on 05/07/2024).
- [32] Xinxing Li, Lu Zhang, Xiangyu Wang, and Buwen Liang, “Forecasting greenhouse air and soil temperatures: A multi-step time series approach employing attention-based LSTM network,” *Computers and Electronics in Agriculture*, volume 217, page 108602, Feb. 1, 2024, ISSN: 0168-1699. DOI: 10.1016/j.compag.2023.108602. [Online]. Available: <https://www.sciencedirect.com/science/article/pii/S0168169923009900> (visited on 05/12/2024).
- [33] Jeblad, *English: Gradient recurrent unit, type 2. variation on example in recurrent neural network (RNN) – part 5: Custom cells, to encompass the type difference from gate-variants of gated recurrent unit (GRU) neural networks*. Feb. 8, 2018. [Online]. Available: [https://commons.wikimedia.org/wiki/File:Gated\\_Recurrent\\_Unit,\\_type\\_2\\_.svg](https://commons.wikimedia.org/wiki/File:Gated_Recurrent_Unit,_type_2_.svg) (visited on 05/12/2024).
- [34] Joris C. Stuurop, Sjoerd E. A. T. M Van Der Zee, Clifford I. Voss, and Helen Kristine French, “Simulating water and heat transport with freezing and cryosuction in unsaturated soil: Comparing an empirical, semi-empirical and physically-based approach,” *Advances in Water Resources*, volume 149, page 103846, Mar. 2021, ISSN: 03091708. DOI: 10.1016/j.advwatres.2021.103846. [Online]. Available: <https://linkinghub.elsevier.com/retrieve/pii/S0309170821000014> (visited on 01/31/2024).
- [35] Charles C. Holt, “Forecasting seasonals and trends by exponentially weighted moving averages,” *International Journal of Forecasting*, volume 20, number 1, pages 5–10, Jan. 2004, ISSN: 01692070. DOI: 10.1016/j.ijforecast.2003.09.015. [Online]. Available: <https://linkinghub.elsevier.com/retrieve/pii/S0169207003001134> (visited on 10/20/2023).
- [36] T. R. H. Holmes, M. Owe, R. A. M. De Jeu, and H. Kooi, “Estimating the soil temperature profile from a single depth observation: A simple empirical heatflow solution,” *Water Resources Research*, volume 44, number 2, 2007WR005994, Feb. 2008, ISSN: 0043-1397, 1944-7973. DOI: 10.1029/2007WR005994. [Online]. Available: <https://agupubs.onlinelibrary.wiley.com/doi/10.1029/2007WR005994> (visited on 04/29/2024).
- [37] Trung Hoang Le, Huiping Cao, and Tran Cao Son, *ASPER: Answer set programming enhanced neural network models for joint entity-relation extraction*, version: 1, May 24, 2023. arXiv: 2305.15374[cs]. [Online]. Available: <http://arxiv.org/abs/2305.15374> (visited on 03/12/2024).
- [38] Fadi Al Machot, *Bridging logic and learning: A neural-symbolic approach for enhanced reasoning in neural models (ASPER)*, Dec. 18, 2023. arXiv: 2312.11651[cs]. [Online]. Available: <http://arxiv.org/abs/2312.11651> (visited on 03/12/2024).
- [39] Ashish Vaswani, Noam Shazeer, Niki Parmar, Jakob Uszkoreit, Llion Jones, Aidan N. Gomez, Łukasz Kaiser, and Illia Polosukhin, *Attention is all you need*, 2017. arXiv: 1706.03762[cs]. [Online]. Available: <http://arxiv.org/abs/1706.03762> (visited on 04/16/2024).
- [40] Olufemi P. Abimbola, George E. Meyer, Aaron R. Mittelstet, Daran R. Rudnick, and Trenton E. Franz, “Knowledge-guided machine learning for improving daily soil temperature prediction across the united states,” *Vadose Zone Journal*, volume 20, number 5, e20151, 2021, \_eprint: <https://onlinelibrary.wiley.com/doi/pdf/10.1002/vzj2.20151>, ISSN: 1539-1663. DOI: 10.1002/vzj2.20151. [Online]. Available: <https://onlinelibrary.wiley.com/doi/abs/10.1002/vzj2.20151> (visited on 05/08/2024).

- 
- [41] *A discussion of ASPER and possible further developments.* In collaboration with Fadi Al Machot, Mar. 7, 2024.

## Glossary

**D | H | L | R**

**D**

**DataFrame**

A table of values. The name is from the python library Pandas used in this study.. 13

**H**

**Hashmap**

A list of items where their unique placmnt in the list is detemend by their unique refrence key using a function that maps the key to a placement in the list.. 13

**Hyper-Parameter**

A parameter in a deep-learning model that adjusts the learning prosess.. 46

**L**

**Long Short Term-Memory**

A Recurrent Neural Network with a memory cell to distribute information along the other RNN cells.. 6

**R**

**Recurrent Neural Network**

A Neural network that passes information between cells in the same layers.. 2, 6, f

## Acronyms

**Symbols | A | F | G | L | M | N | R**

**Symbols**

$R^2$

Explained Variance. 17, 18, 37, 39, 40, V

$\log(\kappa)$

Log Condition number. 17

**A**

**ASPER**

Answer Set Programming-enhanced Entity-Relation. 46

**F**

**FDM**

Finite Difference Method. 4

**G**

**GRU**

Gated Recurrent Unit. 2, 6, 28, 33, III

**L**

**LMT**

Norwegian Institute of Bioeconomy Research Agrometeorology service (Nibio). 9, 10

**LSTM**

Long Short Term-Memory. 5, 6, 28, 33, III

**M**

**MAE**

Mean Absolut Error. 17, 18

**MET**

The Norwegian Meteorological Institute. 9, 13, 14

**N**

**Nibio**

Landbruksmeteorologisk Tjeneste. 1

**Nibio**

Norwegian Institute of Bioeconomy Research Agrometeorology service. 1, 3, 9, 13, 14, f

**NMBU**

The Norwegian University of Life Science. 19

**R**

**RMSE**

Root Mean Square Error. 17, 18, 33

## A Plots

### A.1 Difference plots of model performance per region

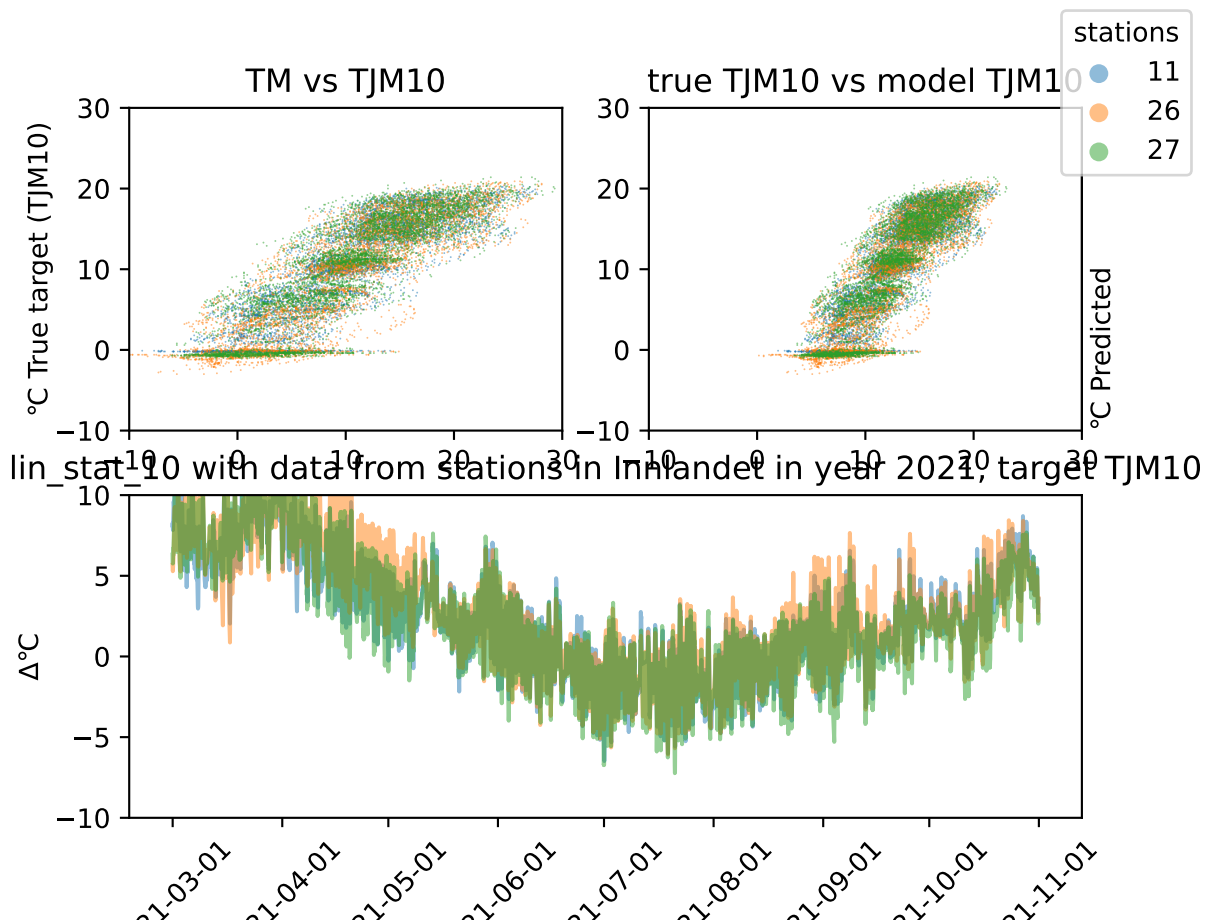


Figure 28: Difference plot for Linear Regression model in year 2021 and region Innlandet depth 10. The station names can be found in table 1.

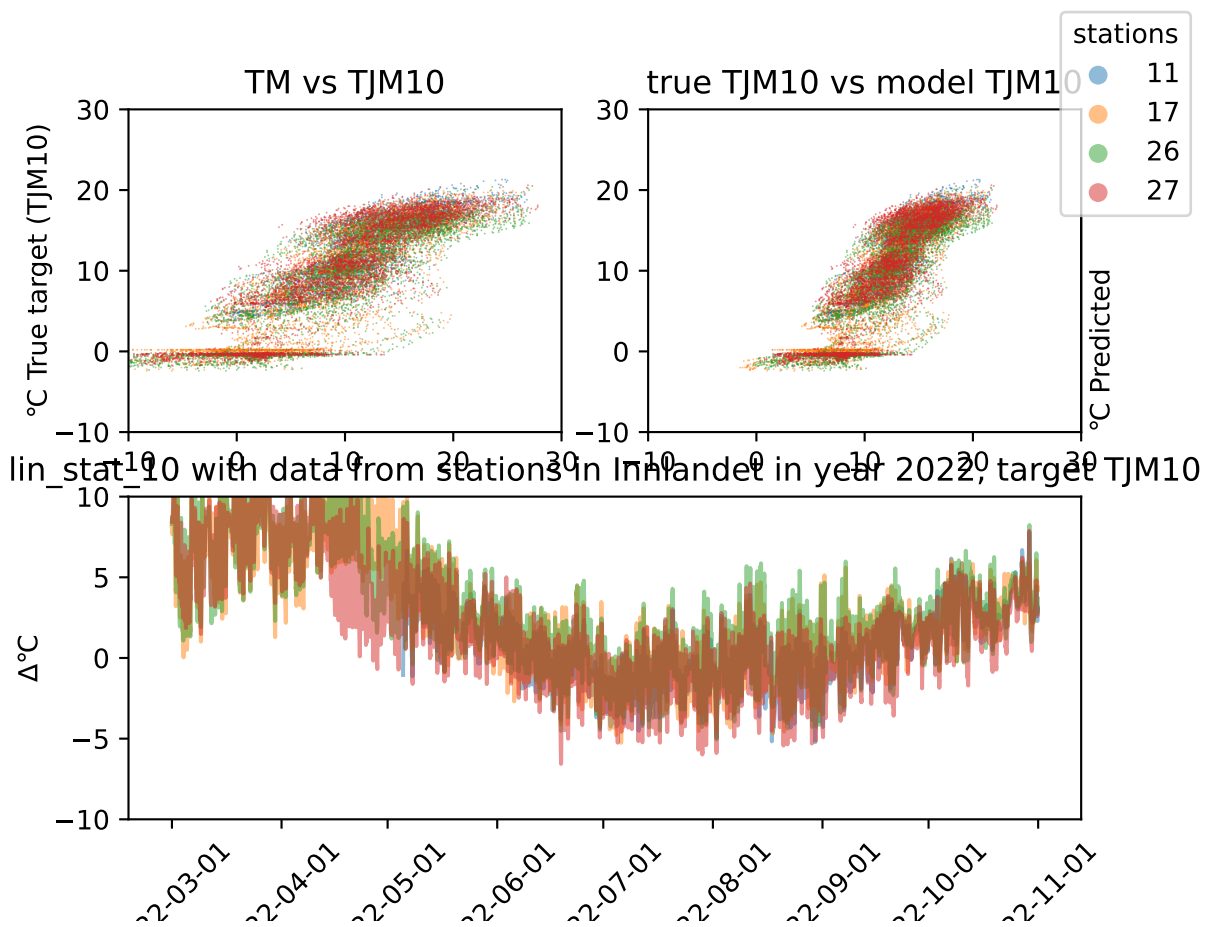


Figure 29: Difference plot for Linear Regression model in year 2022 and region Innlandetat depth 10. The station names can be found in table 1.

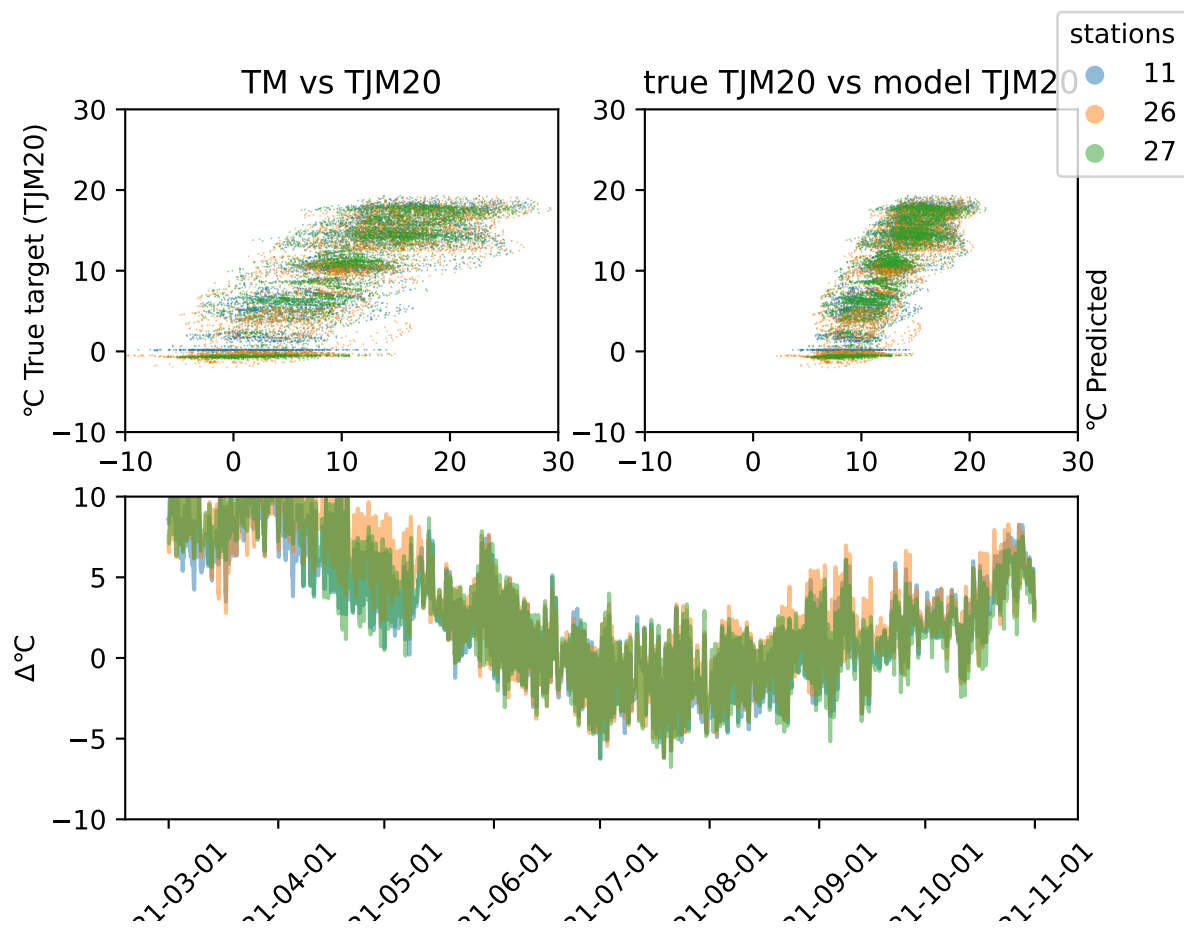


Figure 30: Difference plot for Linear Regression model in year 2021 and region Innlandet at depth 20. The station names can be found in table 1.

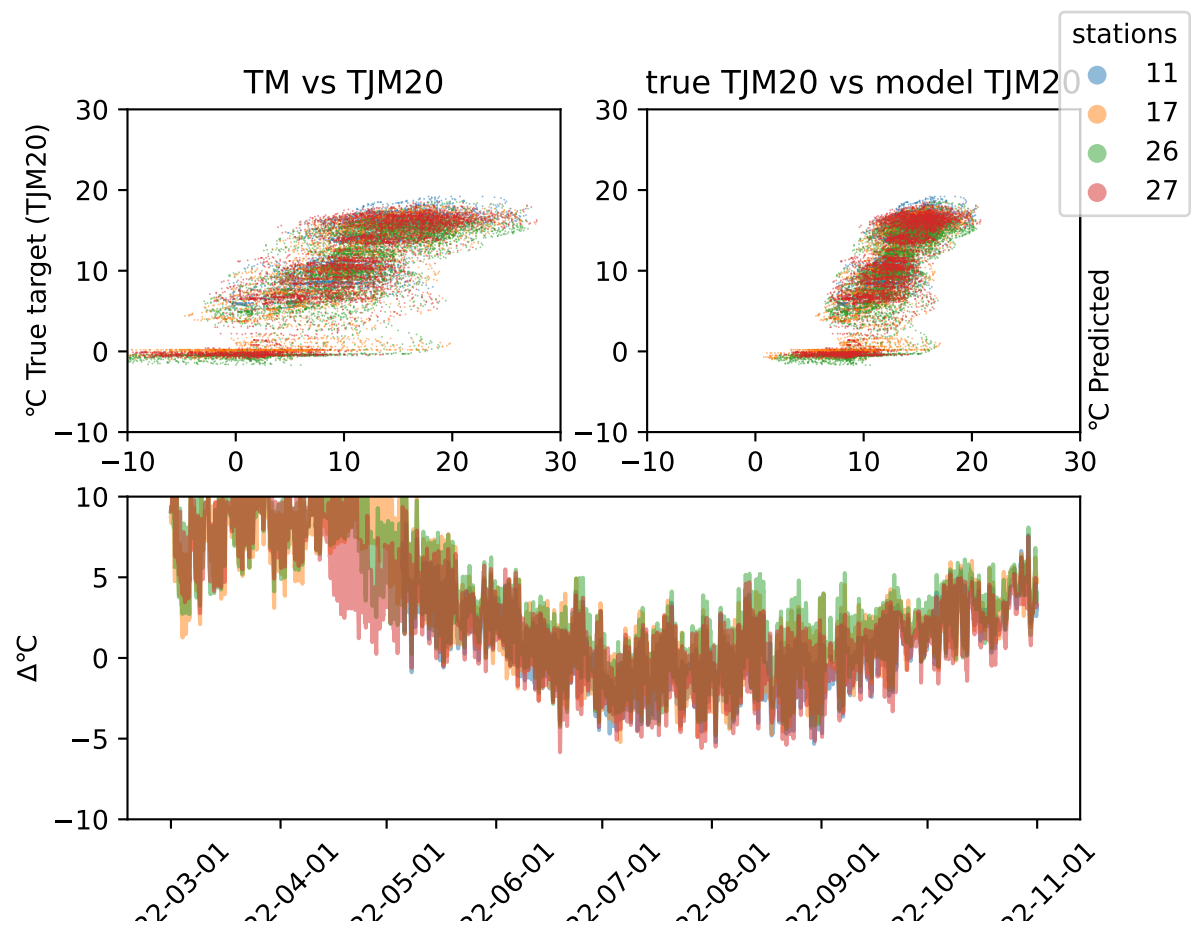


Figure 31: Difference plot for Linear Regression model in year 2022 and region Innlandet at depth 20. The station names can be found in table 1.

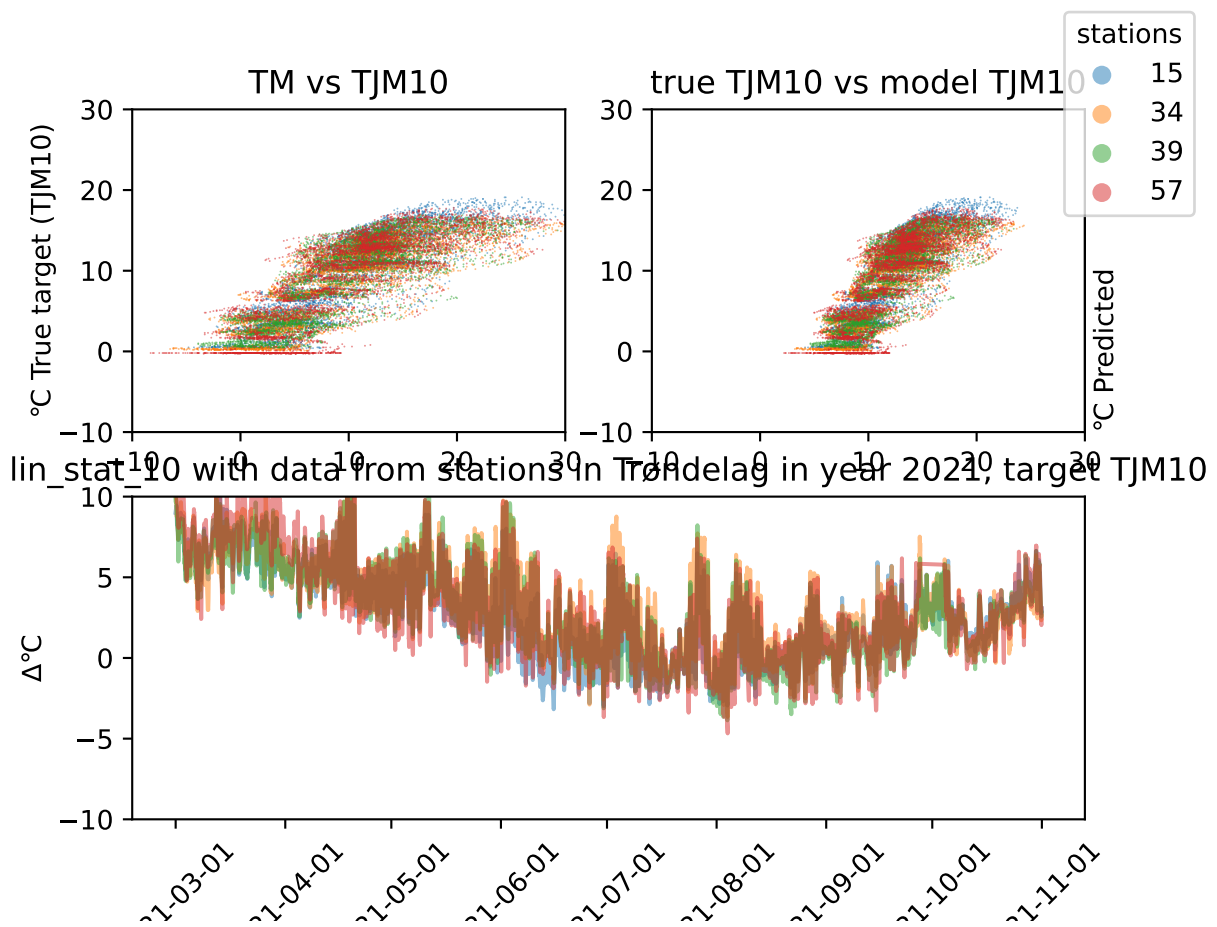


Figure 32: Difference plot for Linear Regression model in year 2021 and region Trøndelag at depth 10. The station names can be found in table 1.

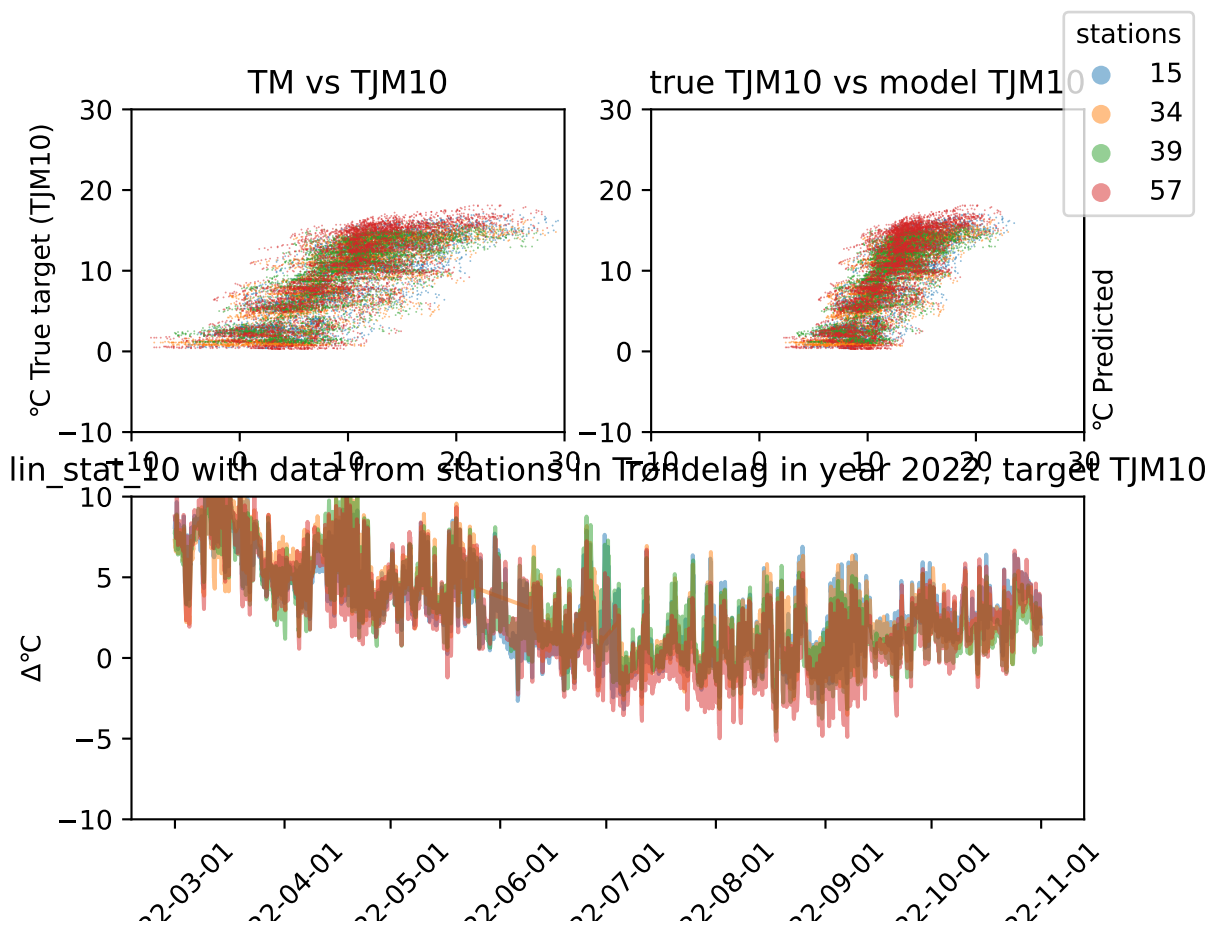


Figure 33: Difference plot for Linear Regression model in year 2022 and region Trøndelagat depth 10. The station names can be found in table 1.

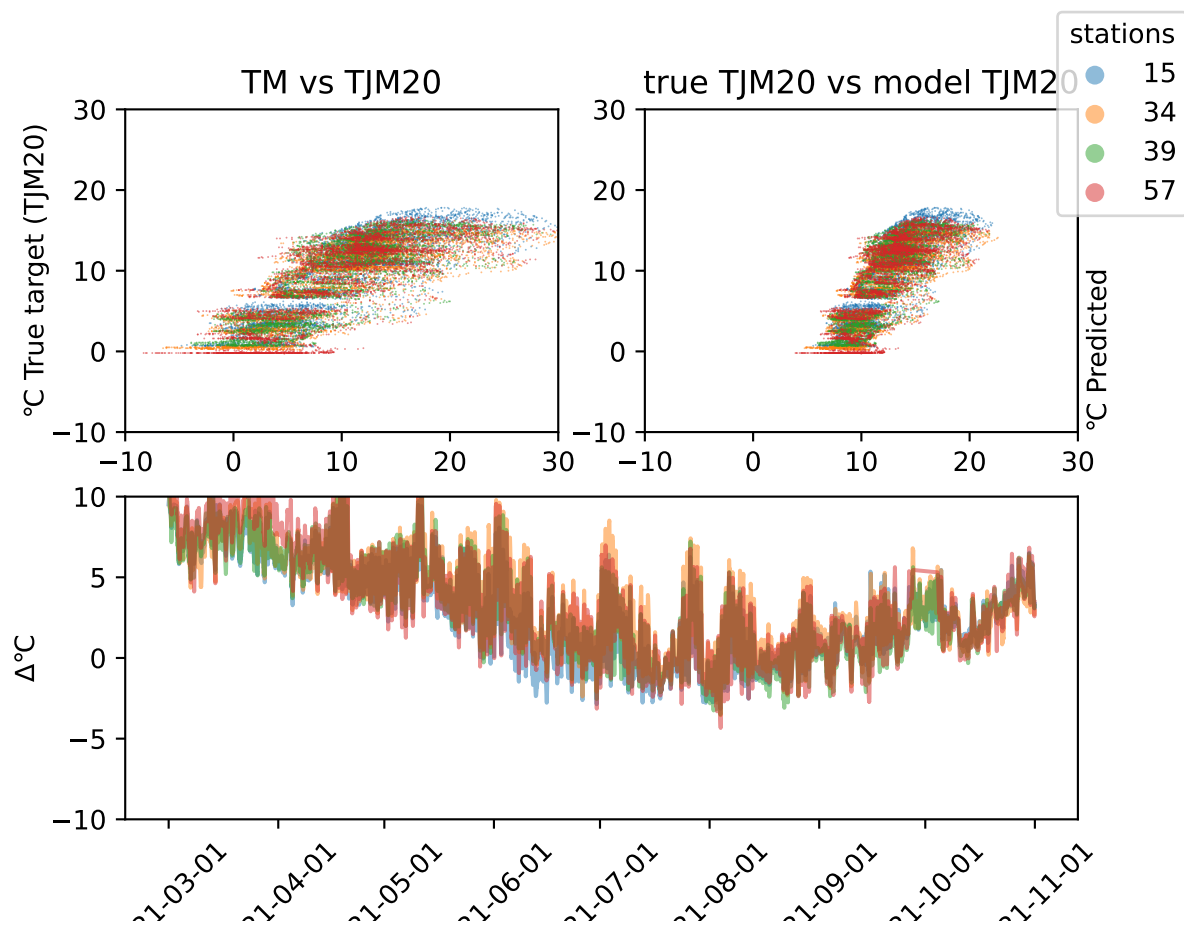


Figure 34: Difference plot for Linear Regression model in year 2021 and region Trøndelag at depth 20. The station names can be found in table 1.

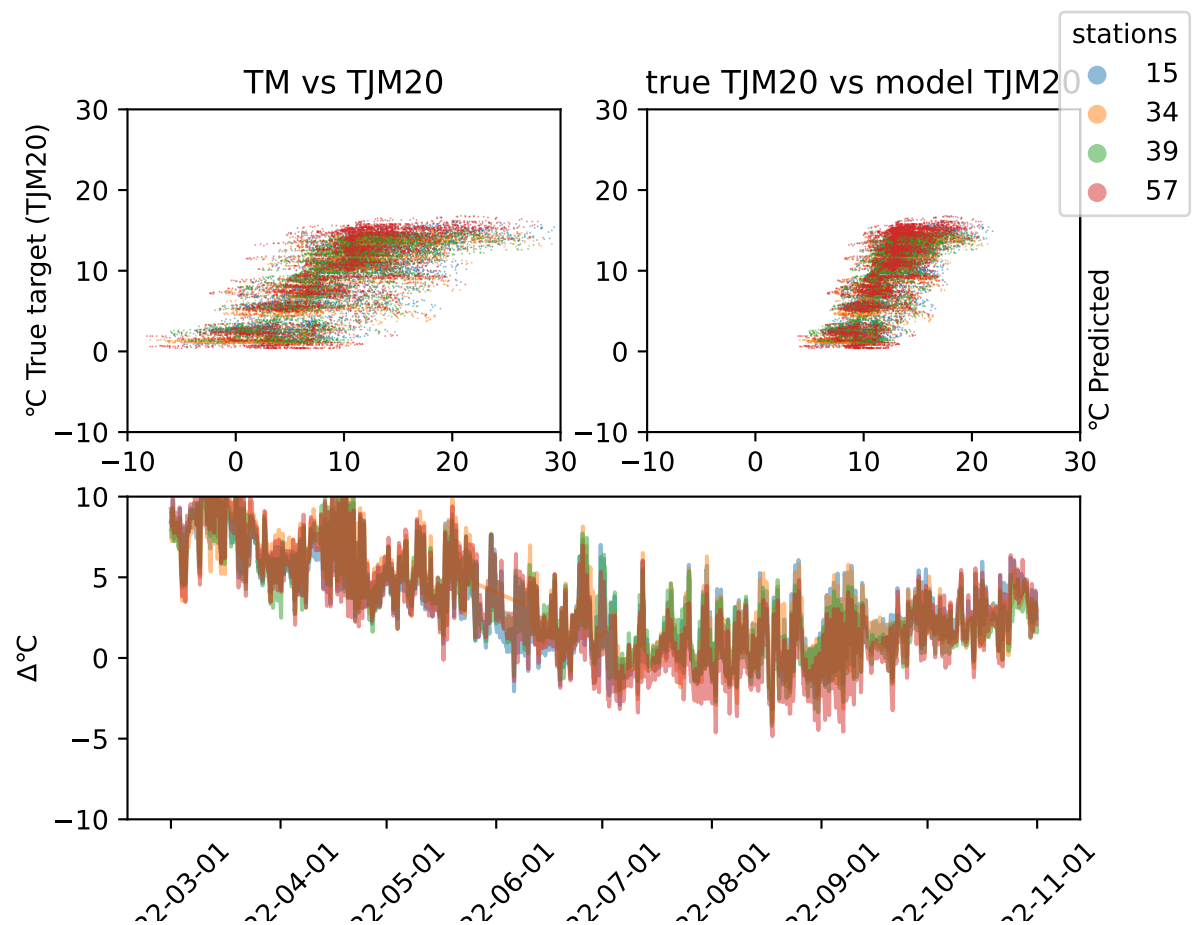


Figure 35: Difference plot for Linear Regression model in year 2022 and region Trøndelagat depth 20. The station names can be found in table 1.

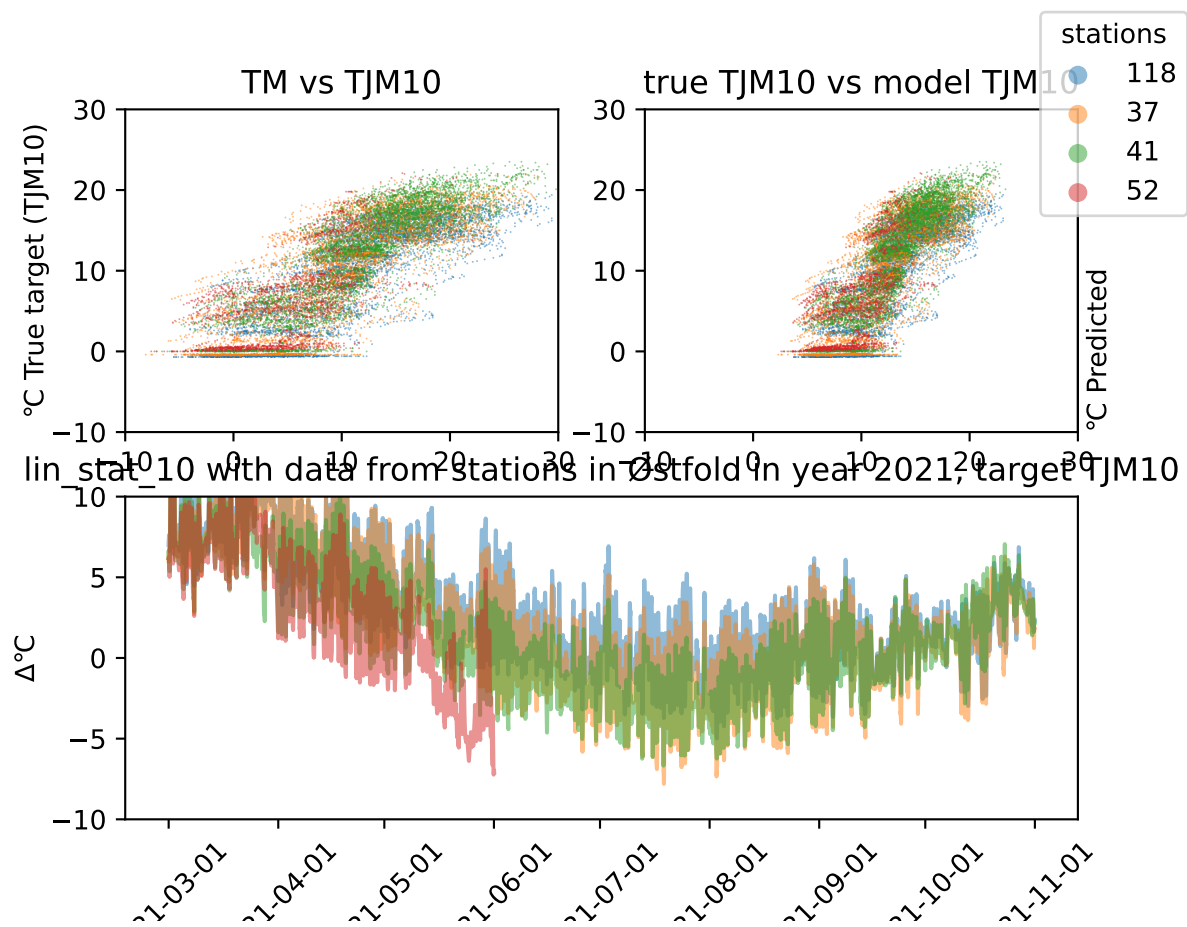


Figure 36: Difference plot for Linear Regression model in year 2021 and region Østfoldat depth 10. The station names can be found in table 1.

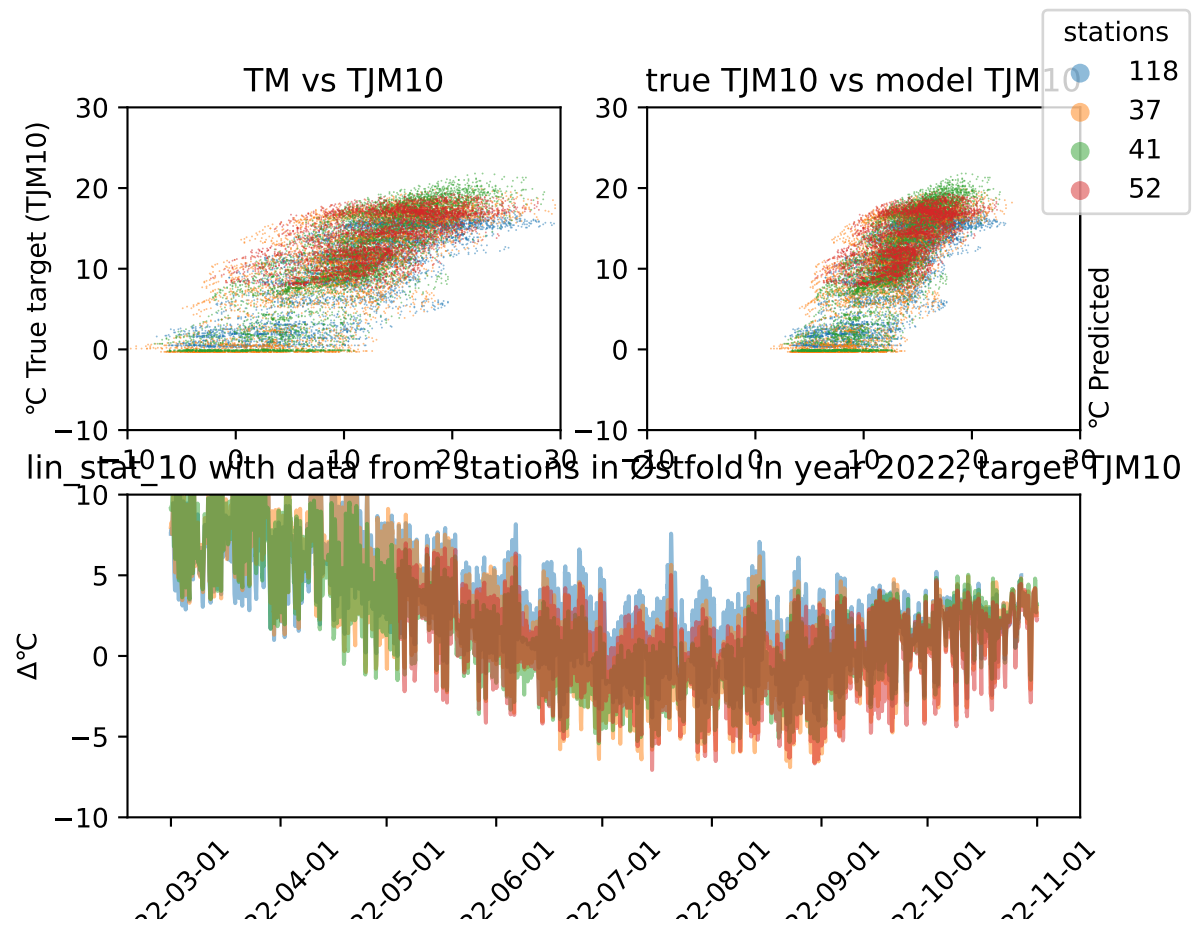


Figure 37: Difference plot for Linear Regression model in year 2022 and region Østfoldat depth 10. The station names can be found in table 1.

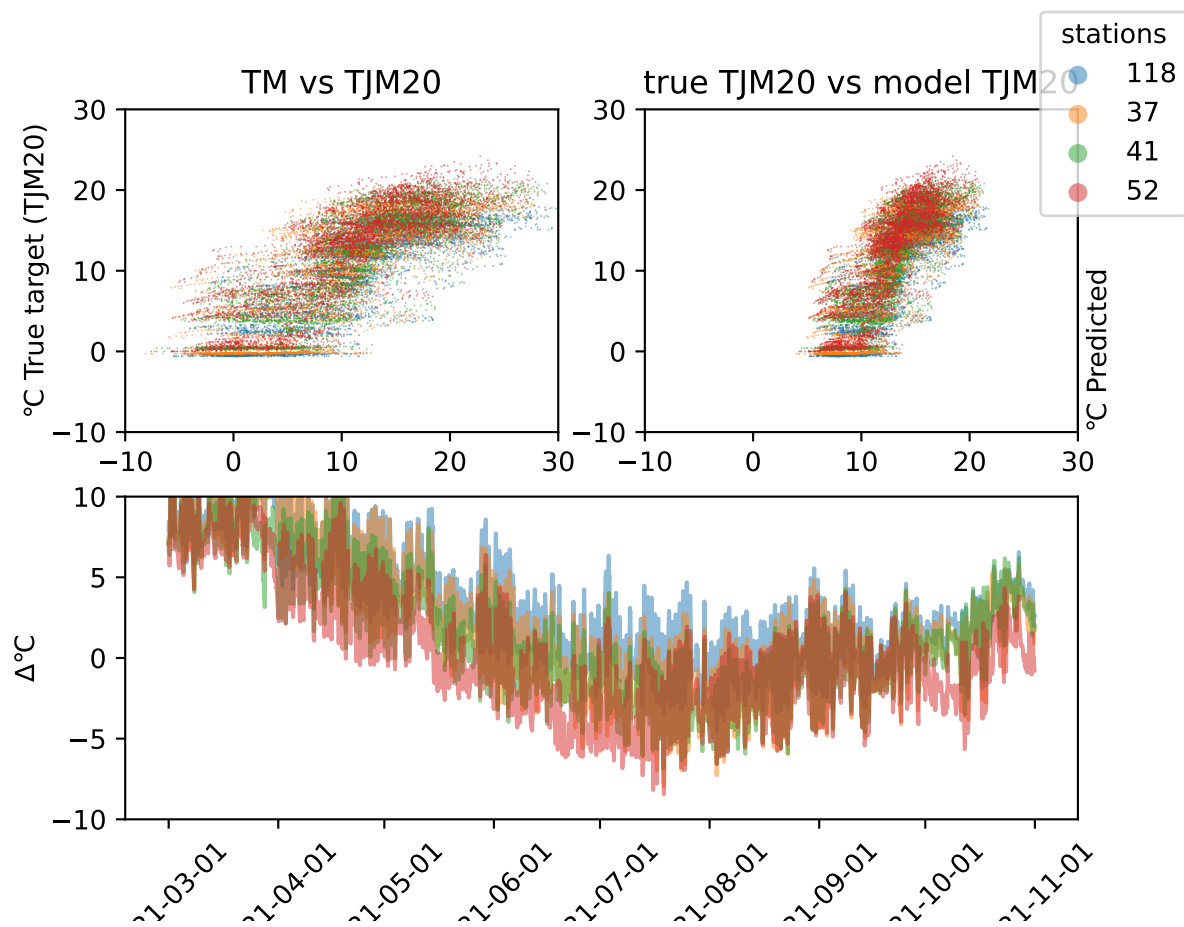


Figure 38: Difference plot for Linear Regression model in year 2021 and region Østfoldat depth 20. The station names can be found in table 1.

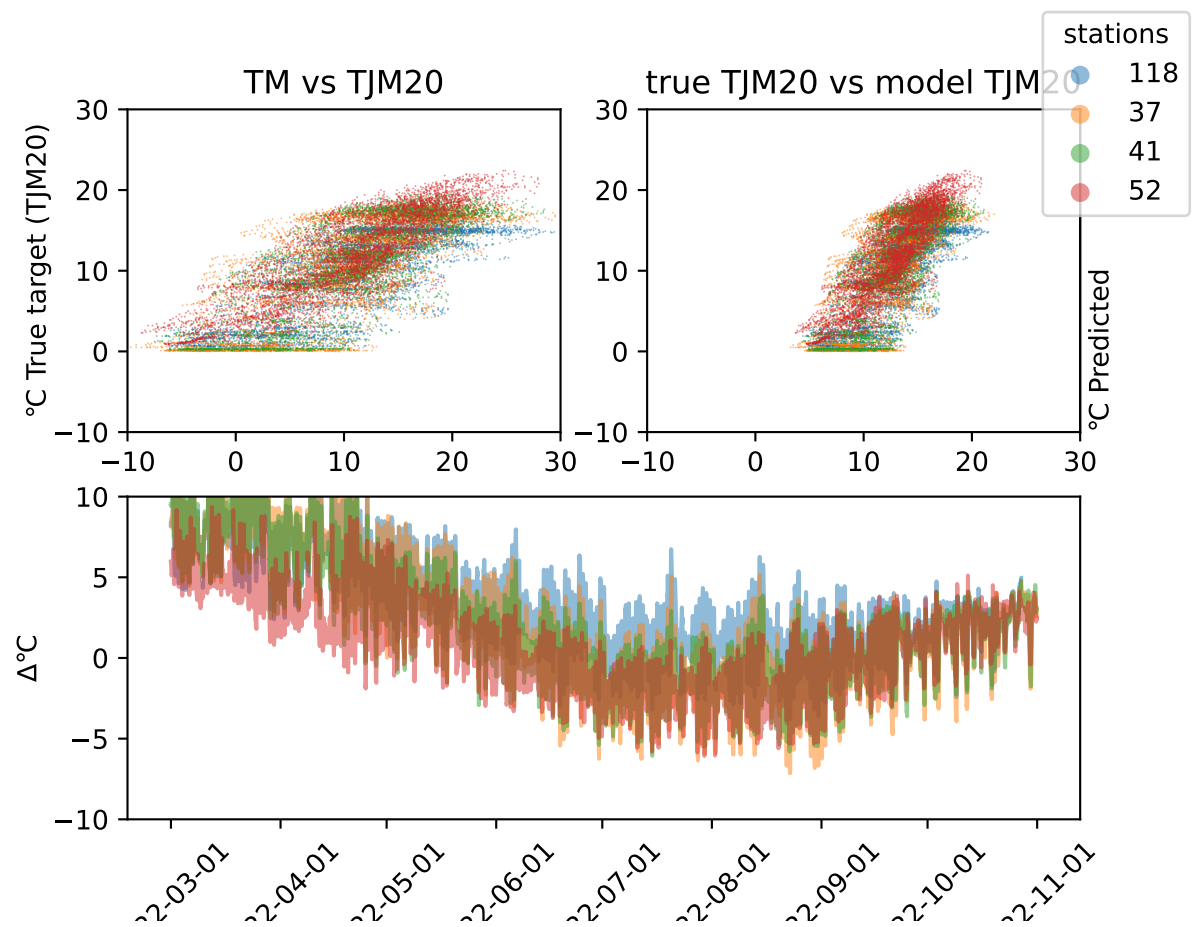


Figure 39: Difference plot for Linear Regression model in year 2022 and region Østfold at depth 20. The station names can be found in table 1.

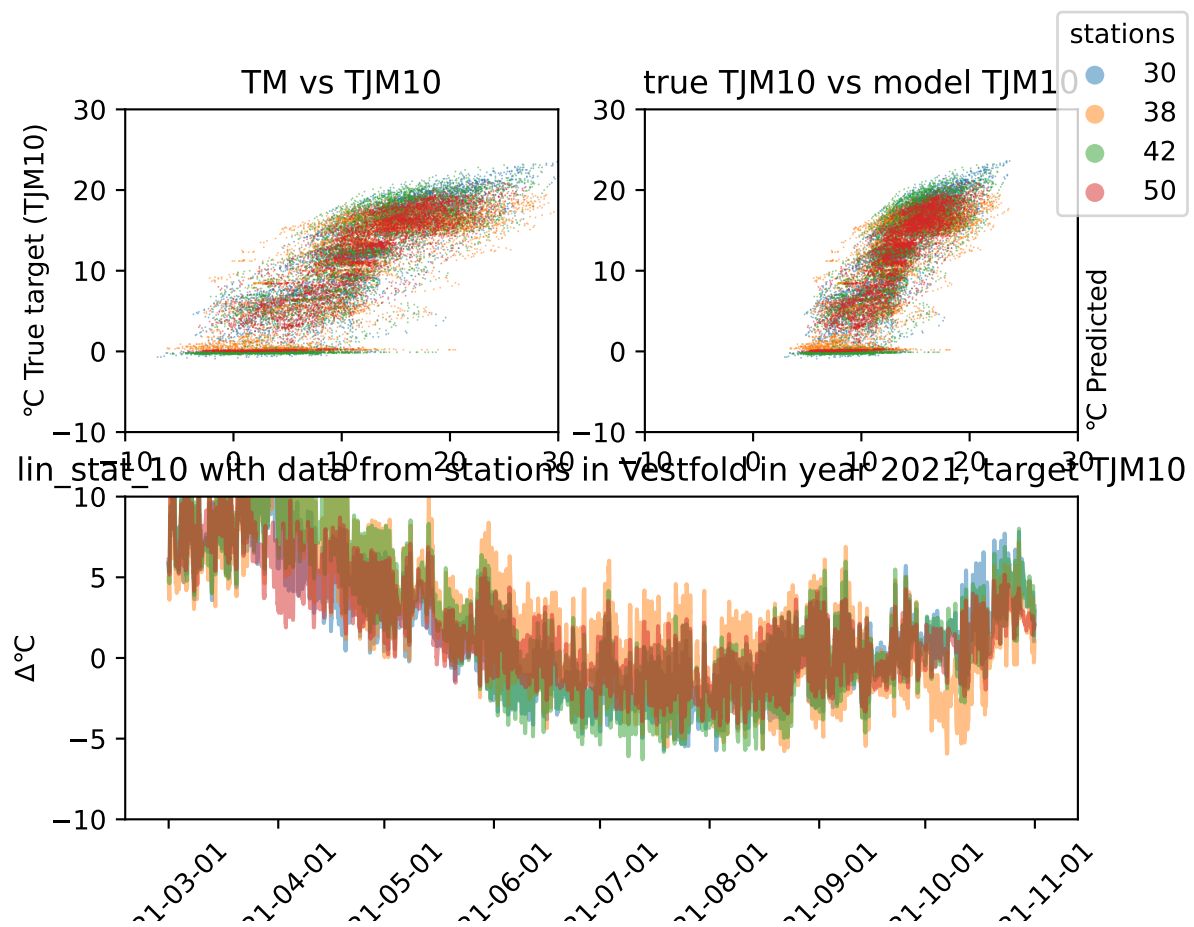


Figure 40: Difference plot for Linear Regression model in year 2021 and region Vestfoldat depth 10. The station names can be found in table 1.

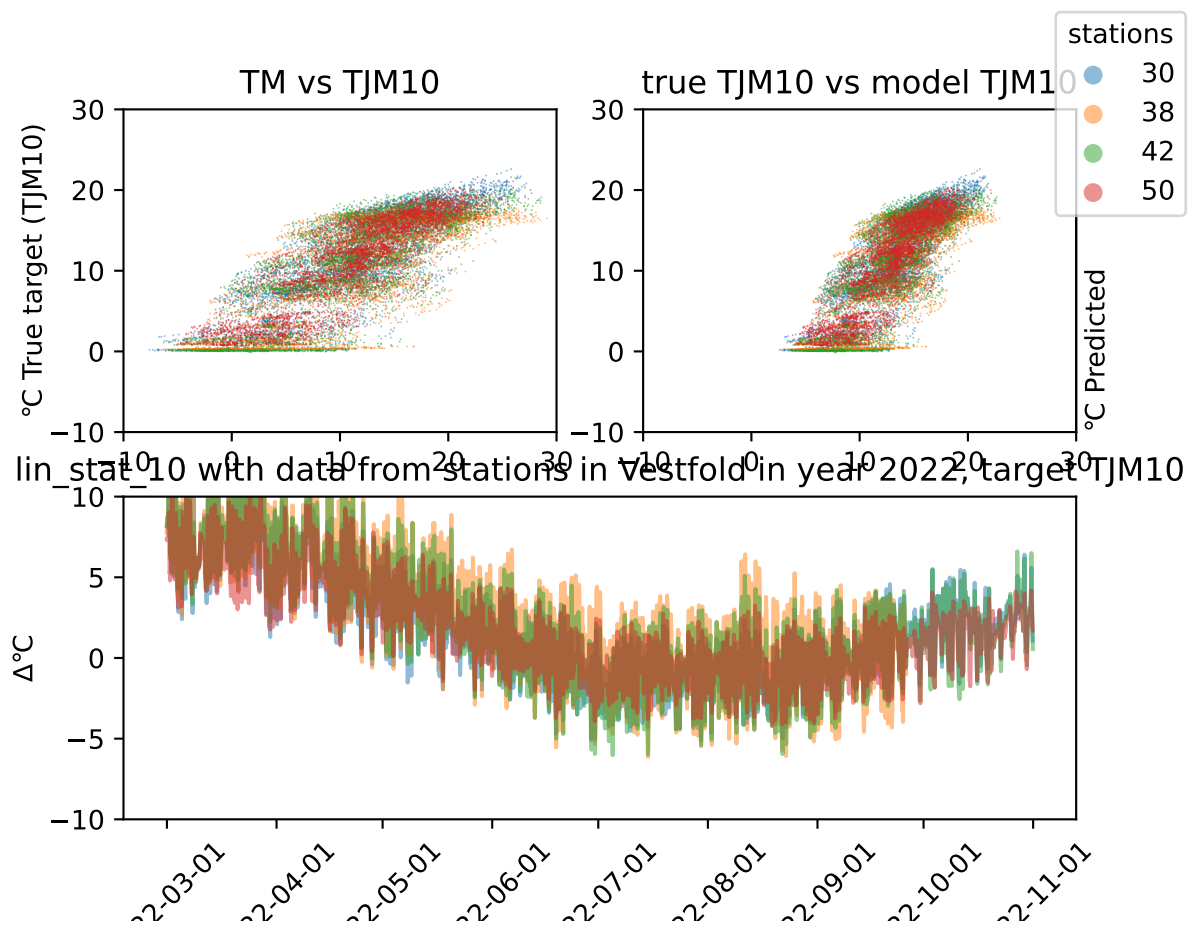


Figure 41: Difference plot for Linear Regression model in year 2022 and region Vestfoldat depth 10. The station names can be found in table 1.

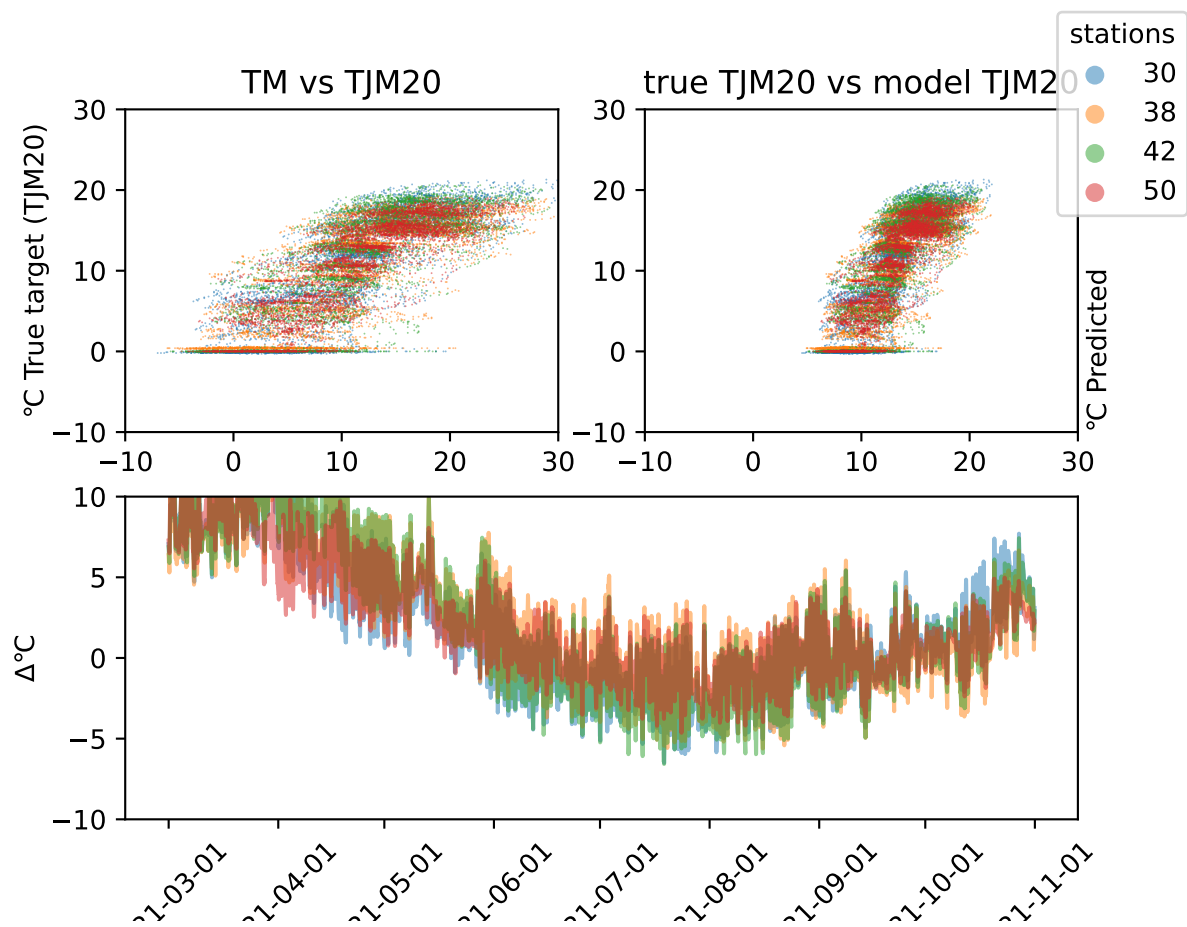


Figure 42: Difference plot for Linear Regression model in year 2021 and region Vestfoldat depth 20. The station names can be found in table 1.

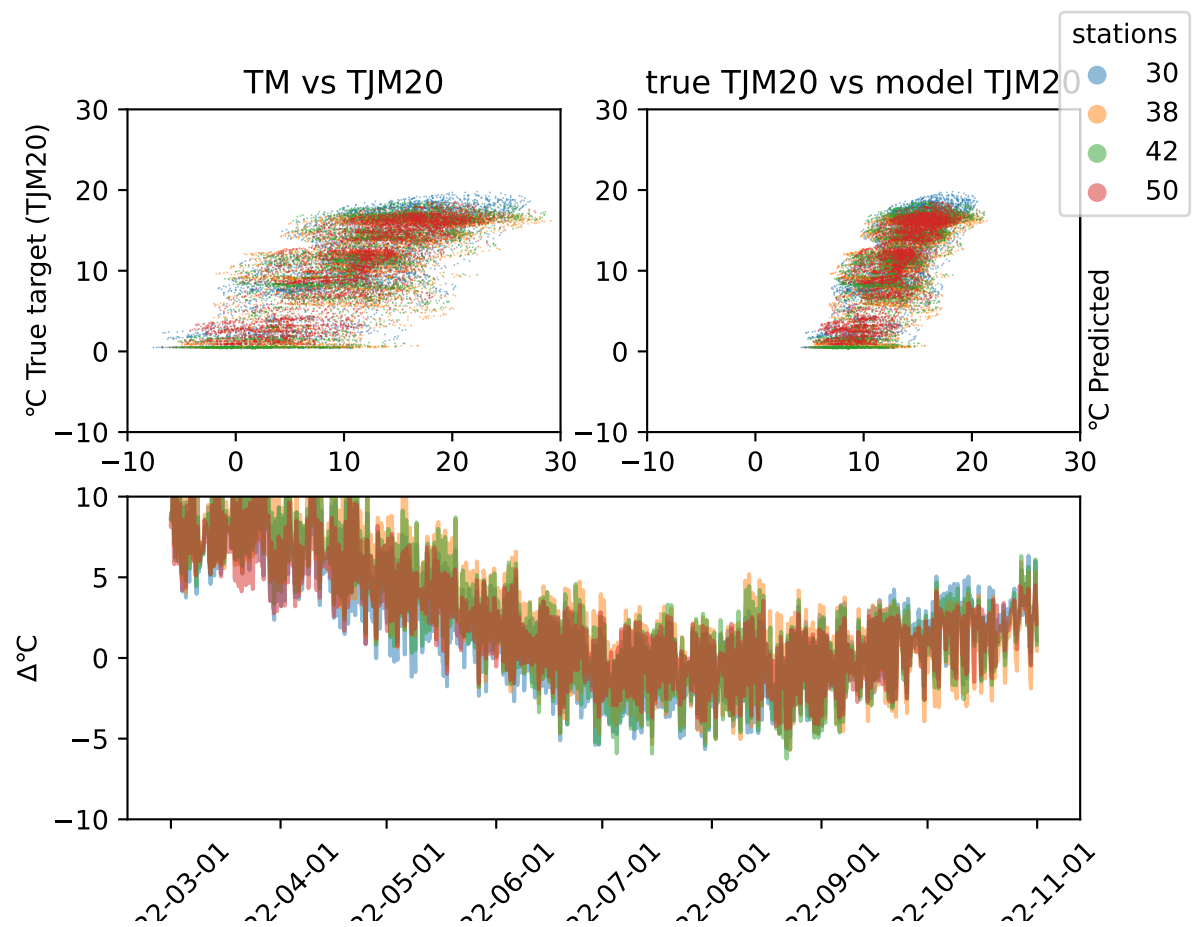


Figure 43: Difference plot for Linear Regression model in year 2022 and region Vestfoldat depth 20. The station names can be found in table 1.

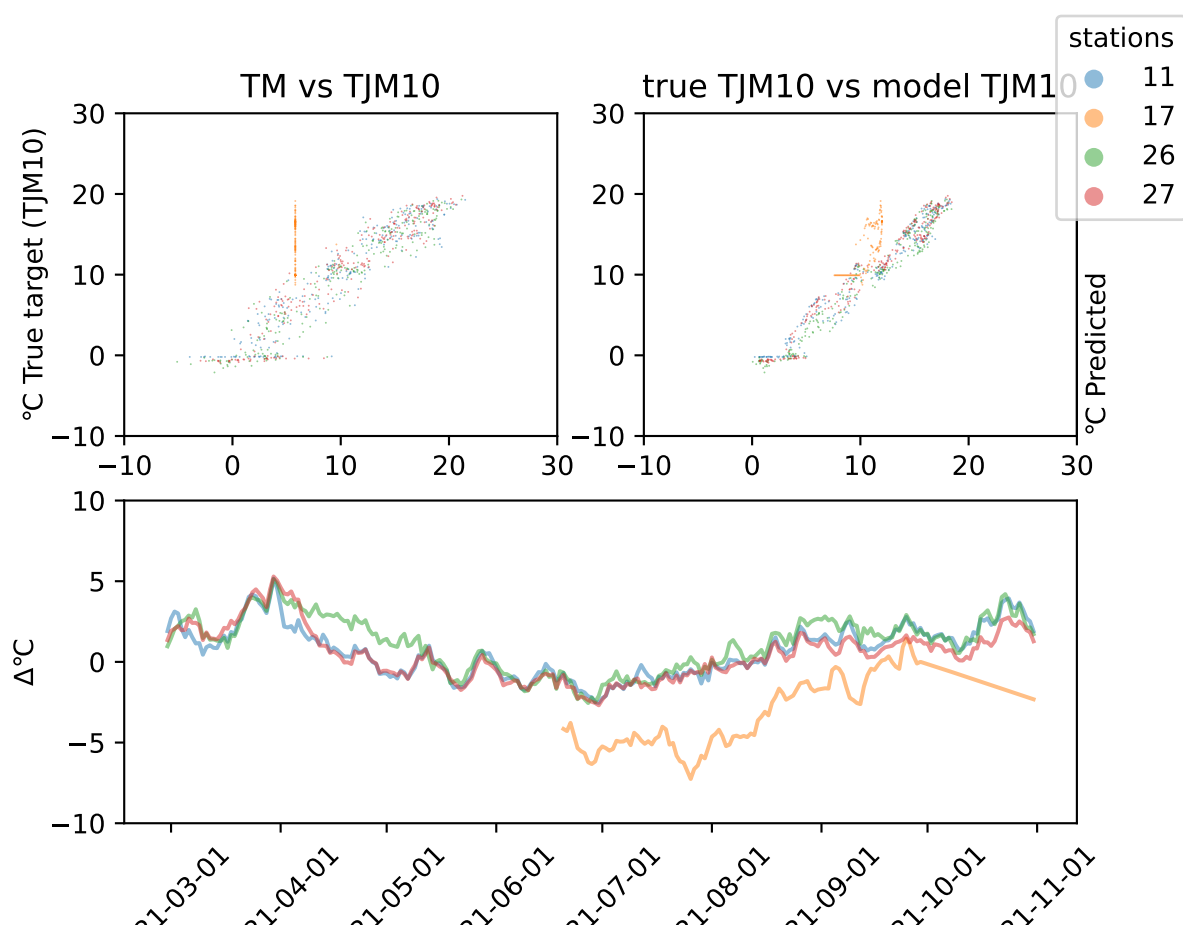


Figure 44: Difference plot for daily Plauborg model in year 2021 and region Innlandetat depth 10. The station names can be found in table 1.

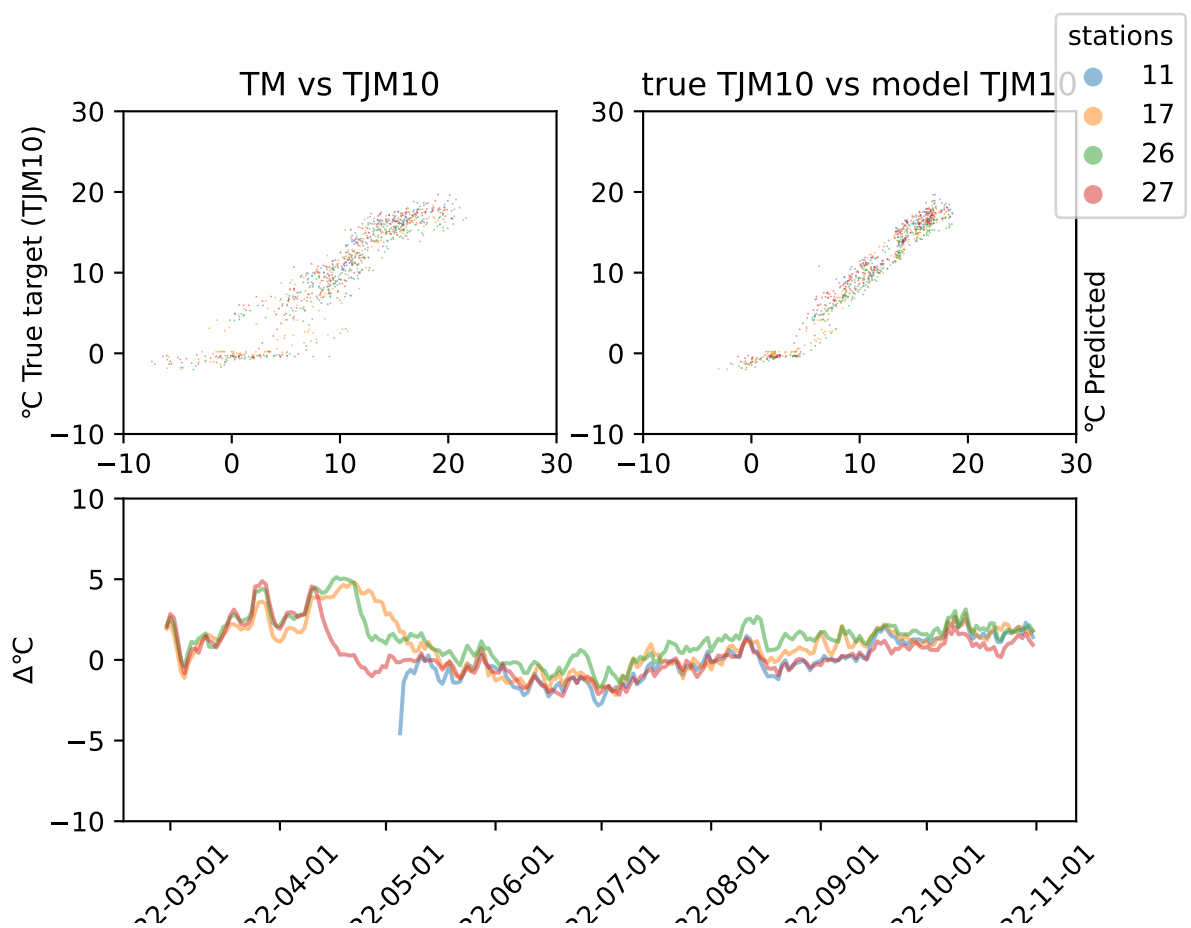


Figure 45: Difference plot for daily Plauborg model in year 2022 and region Innlandetat depth 10. The station names can be found in table 1.

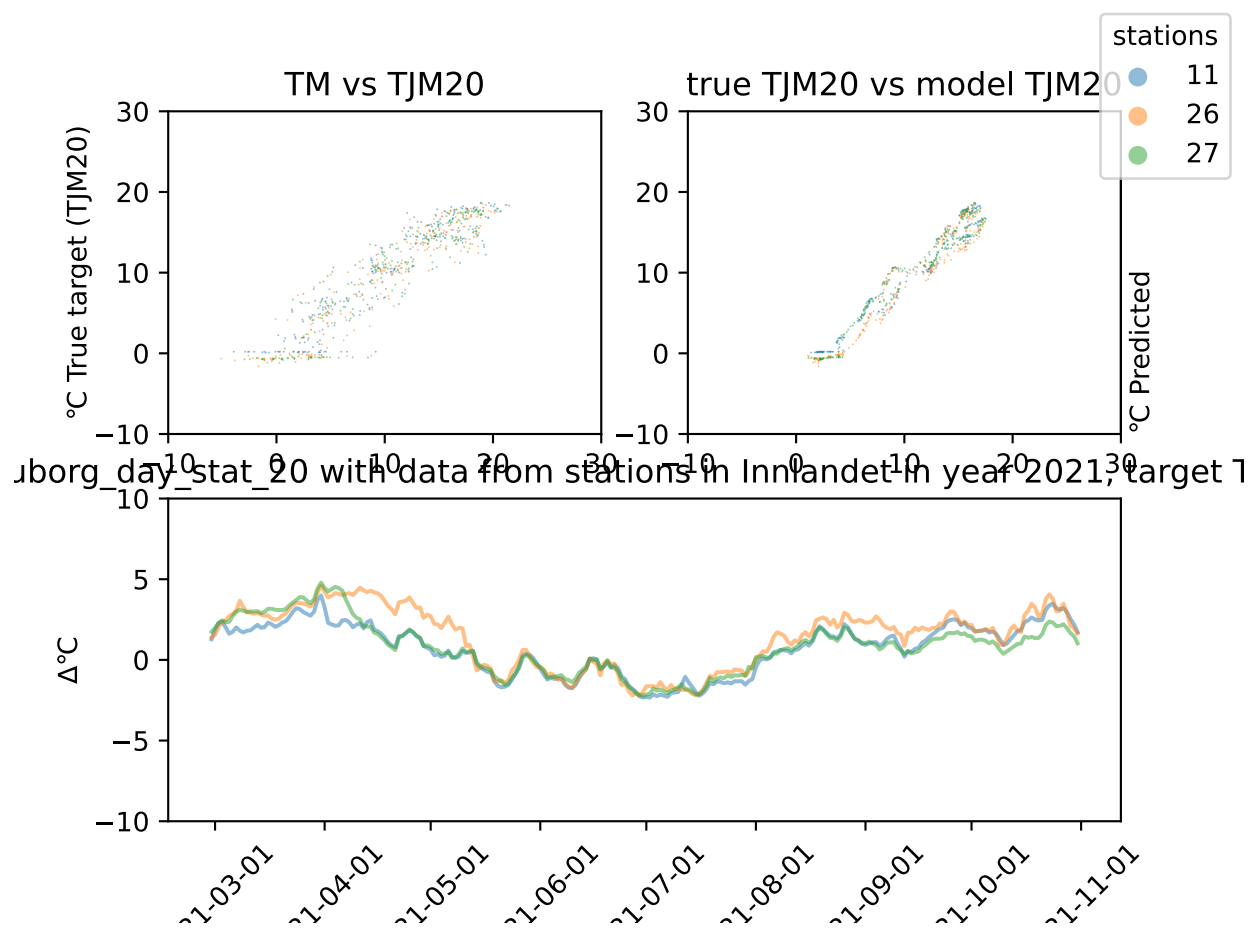


Figure 46: Difference plot for daily Plauborg model in year 2021 and region Innlandet depth 20. The station names can be found in table 1.

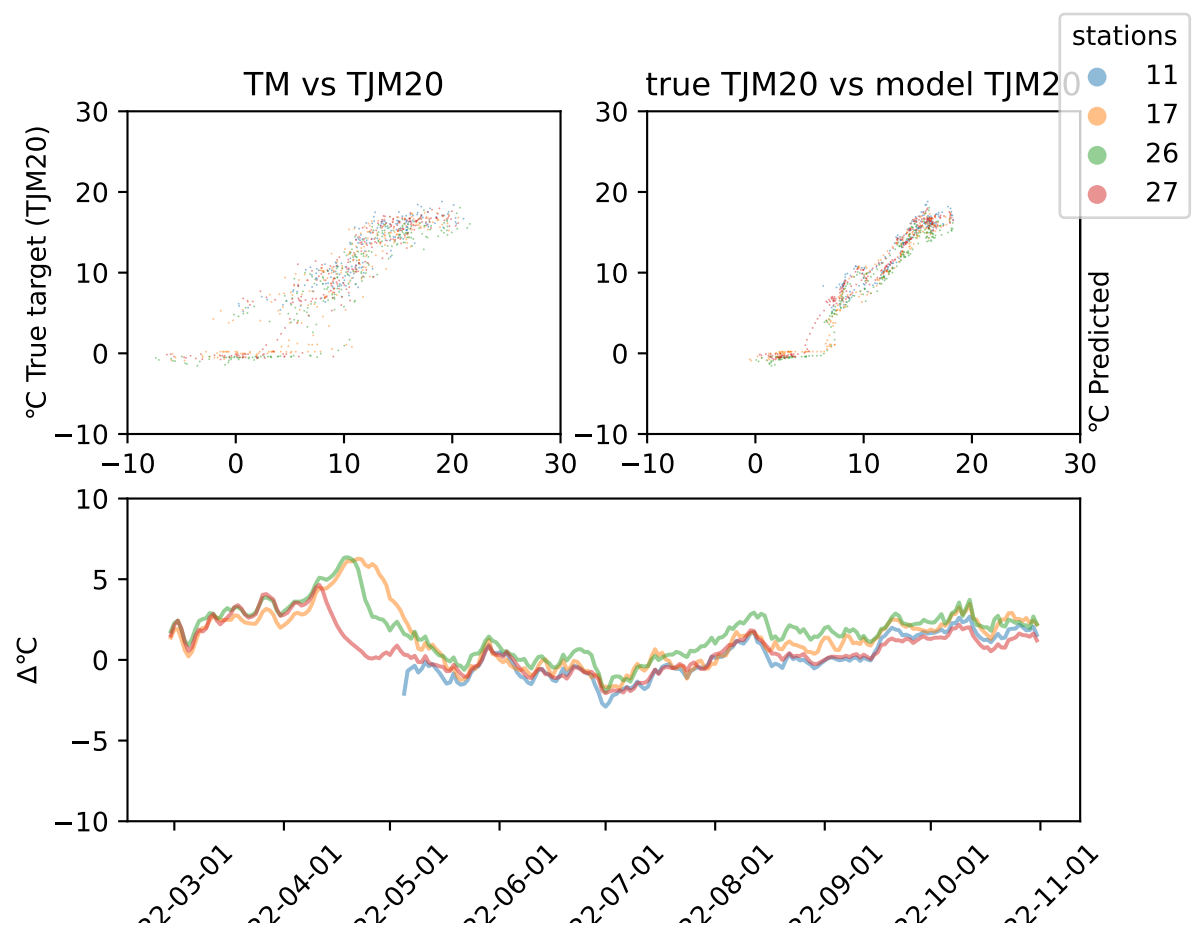


Figure 47: Difference plot for daily Plauborg model in year 2022 and region Innlandetat depth 20. The station names can be found in table 1.

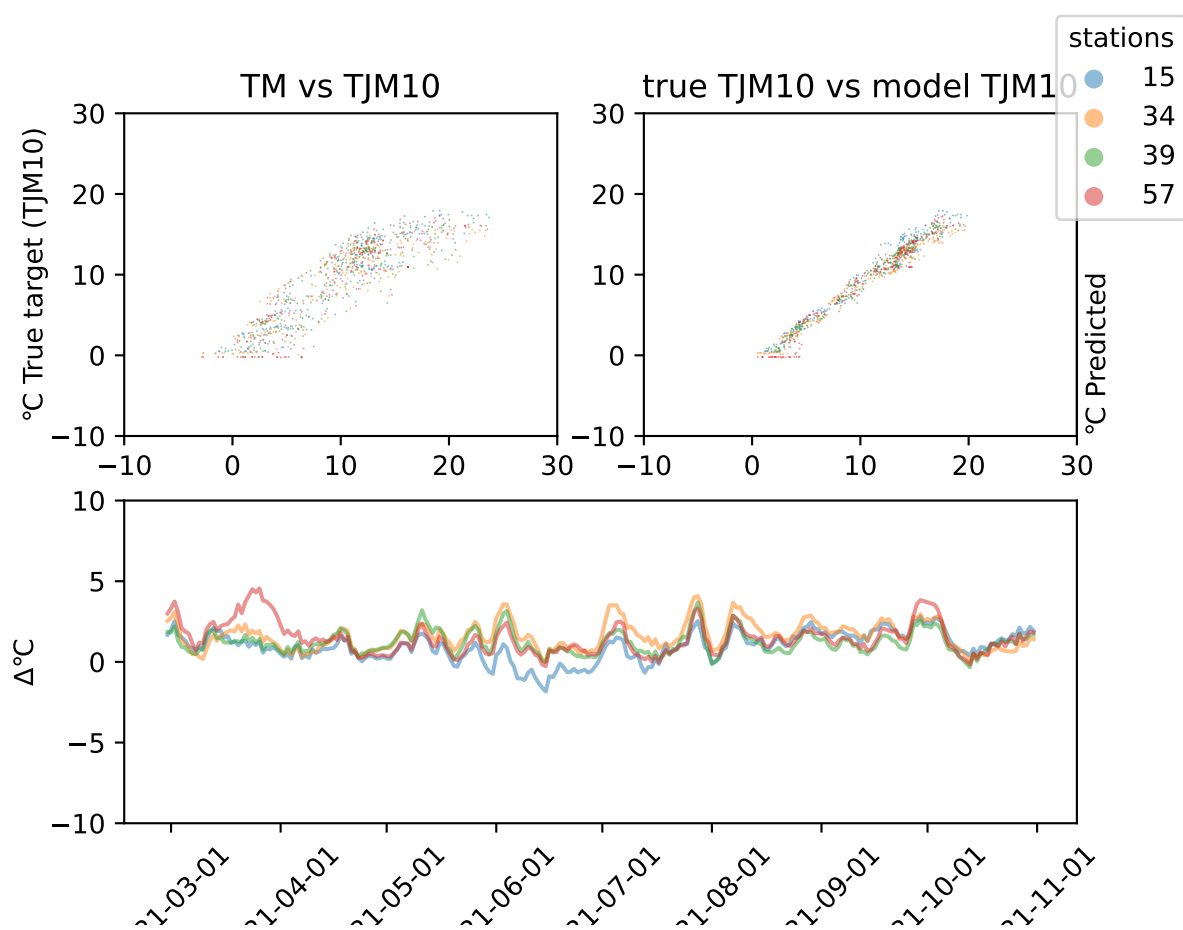


Figure 48: Difference plot for daily Plauborg model in year 2021 and region Trøndelagat depth 10. The station names can be found in table 1.

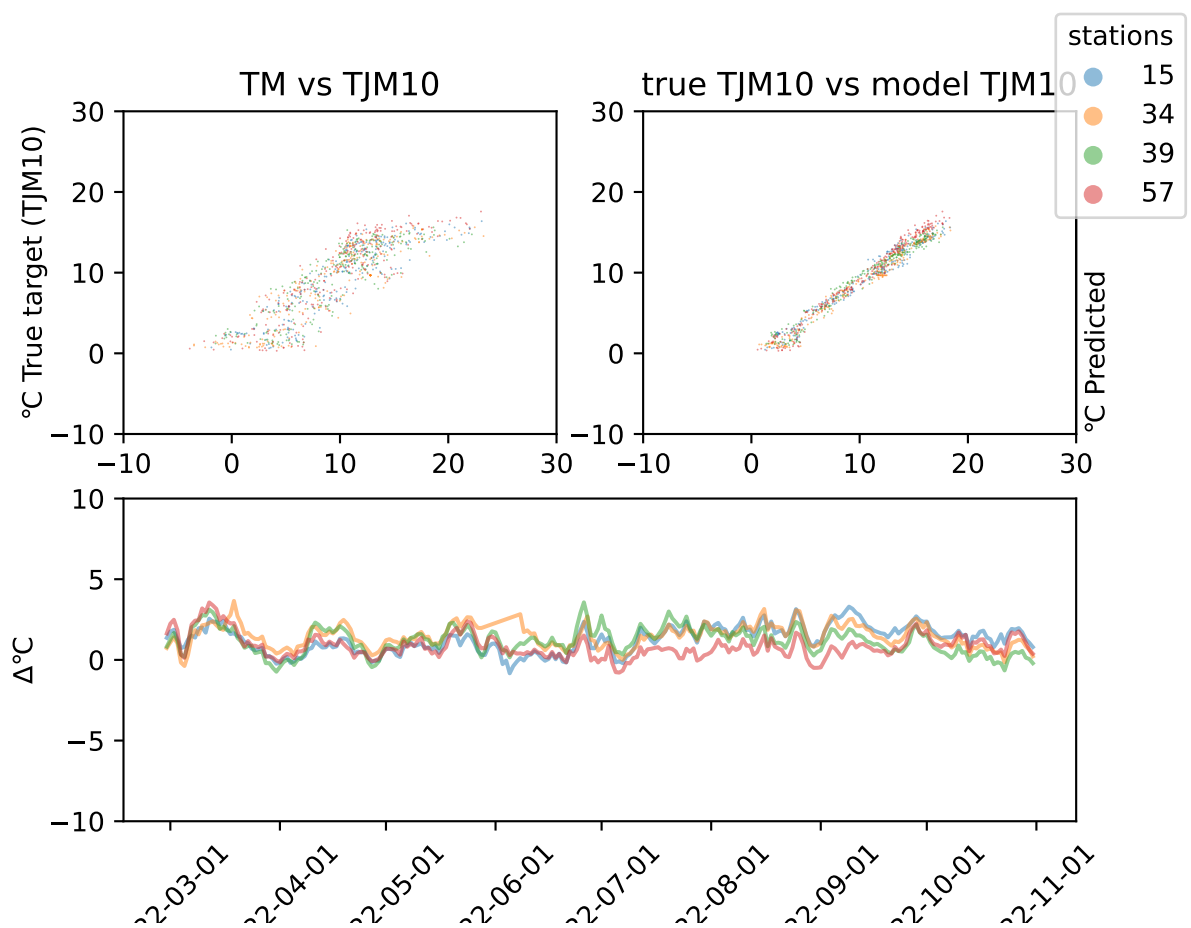


Figure 49: Difference plot for daily Plauborg model in year 2022 and region Trøndelagat depth 10. The station names can be found in table 1.

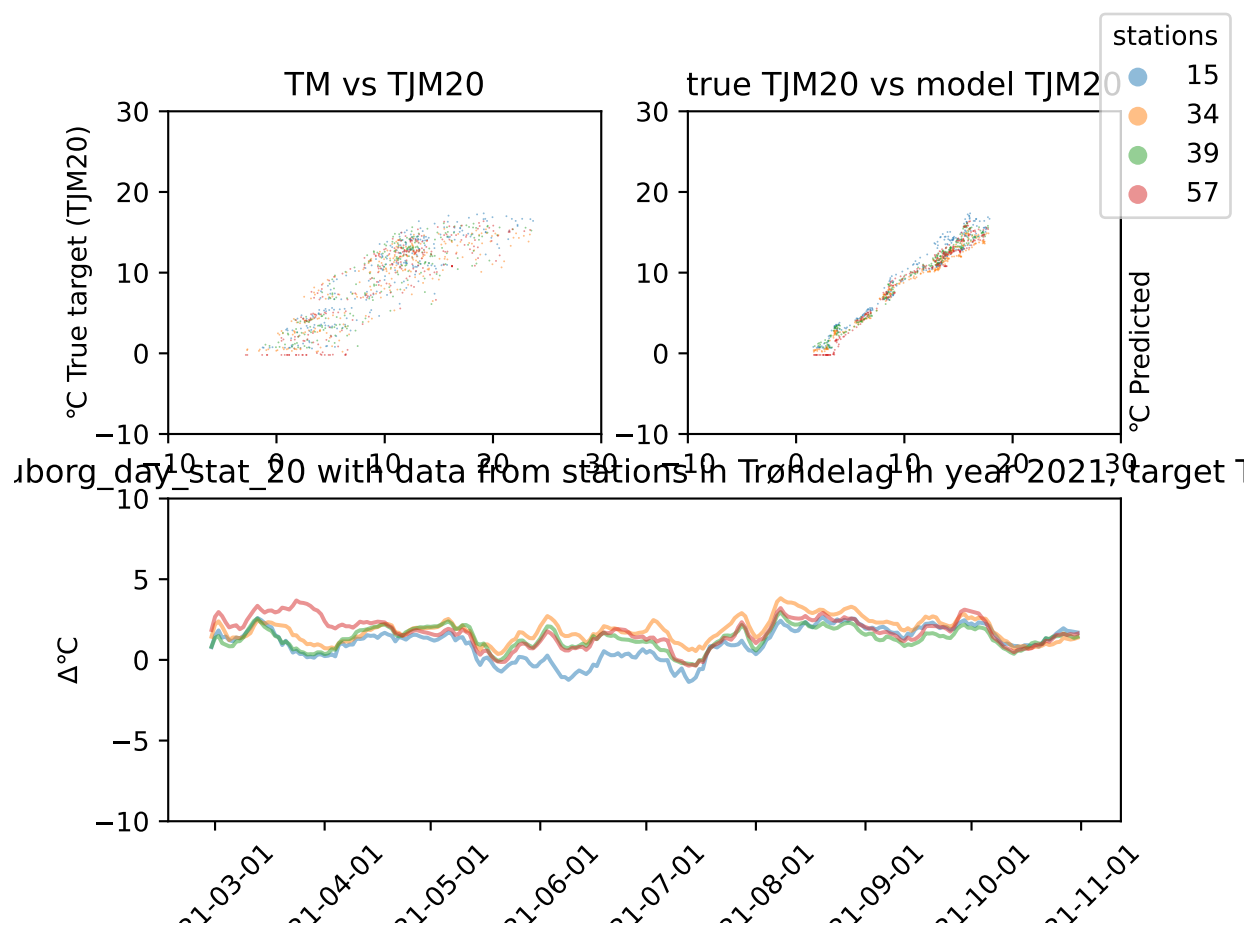


Figure 50: Difference plot for daily Plauborg model in year 2021 and region Trøndelagat depth 20. The station names can be found in table 1.

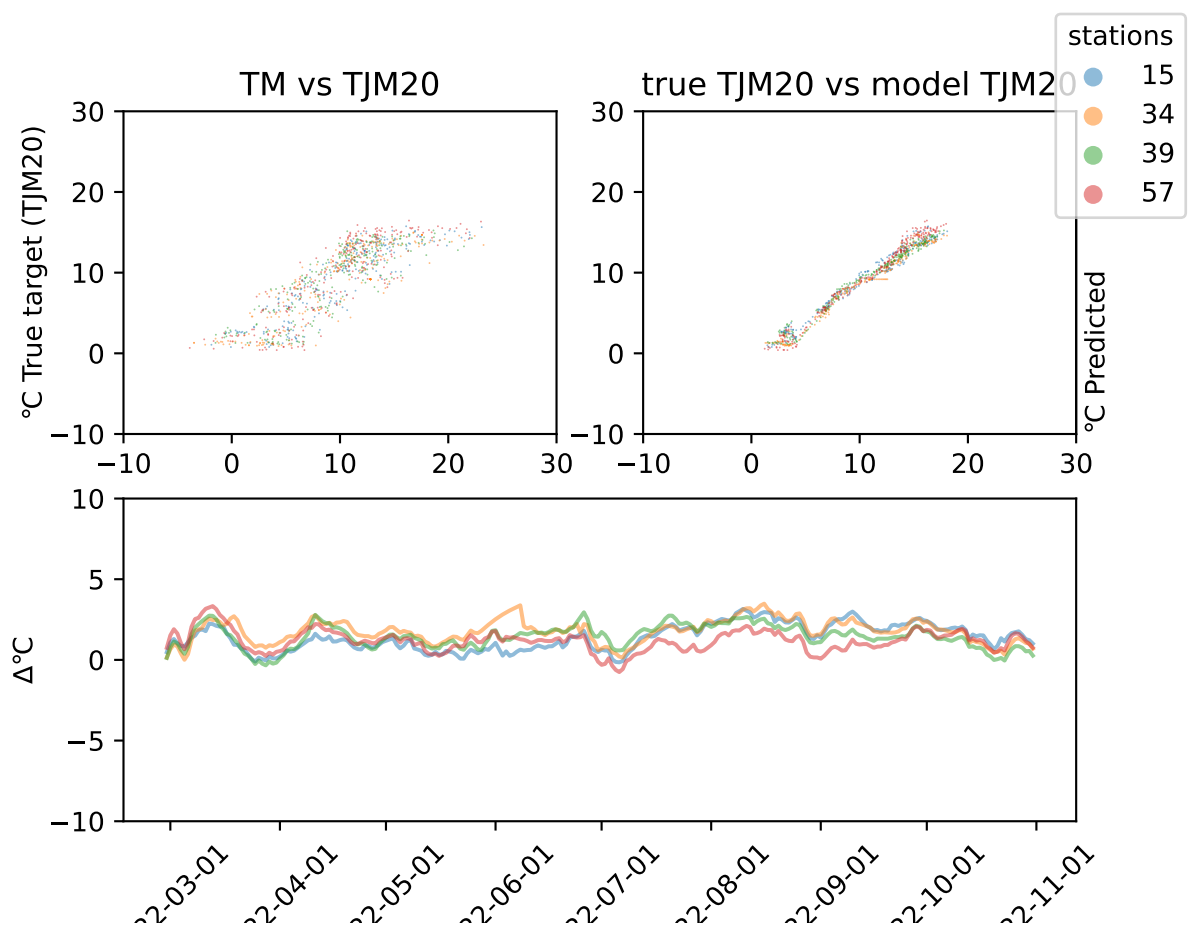


Figure 51: Difference plot for daily Plauborg model in year 2022 and region Trøndelagat depth 20. The station names can be found in table 1.

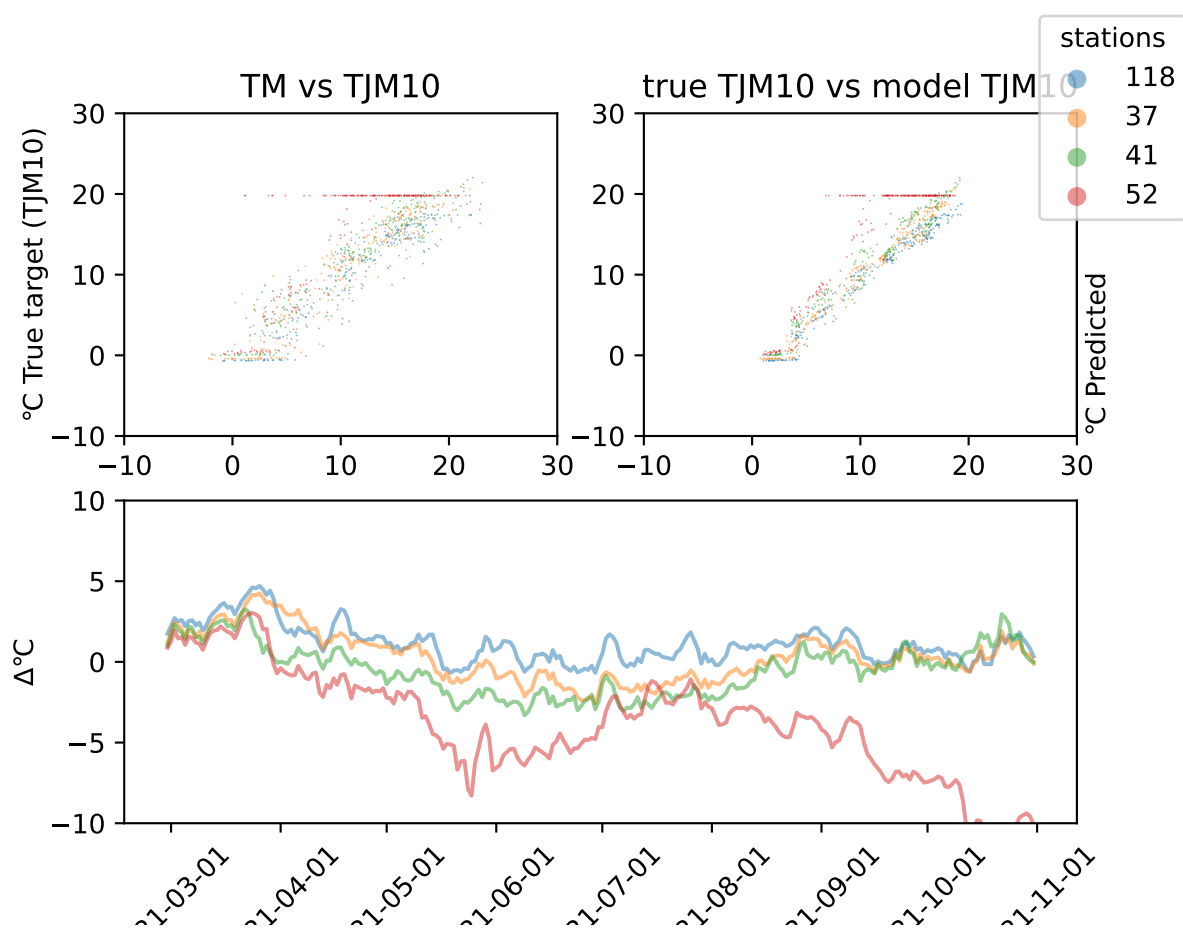


Figure 52: Difference plot for daily Plauborg model in year 2021 and region Østfoldat depth 10. The station names can be found in table 1.

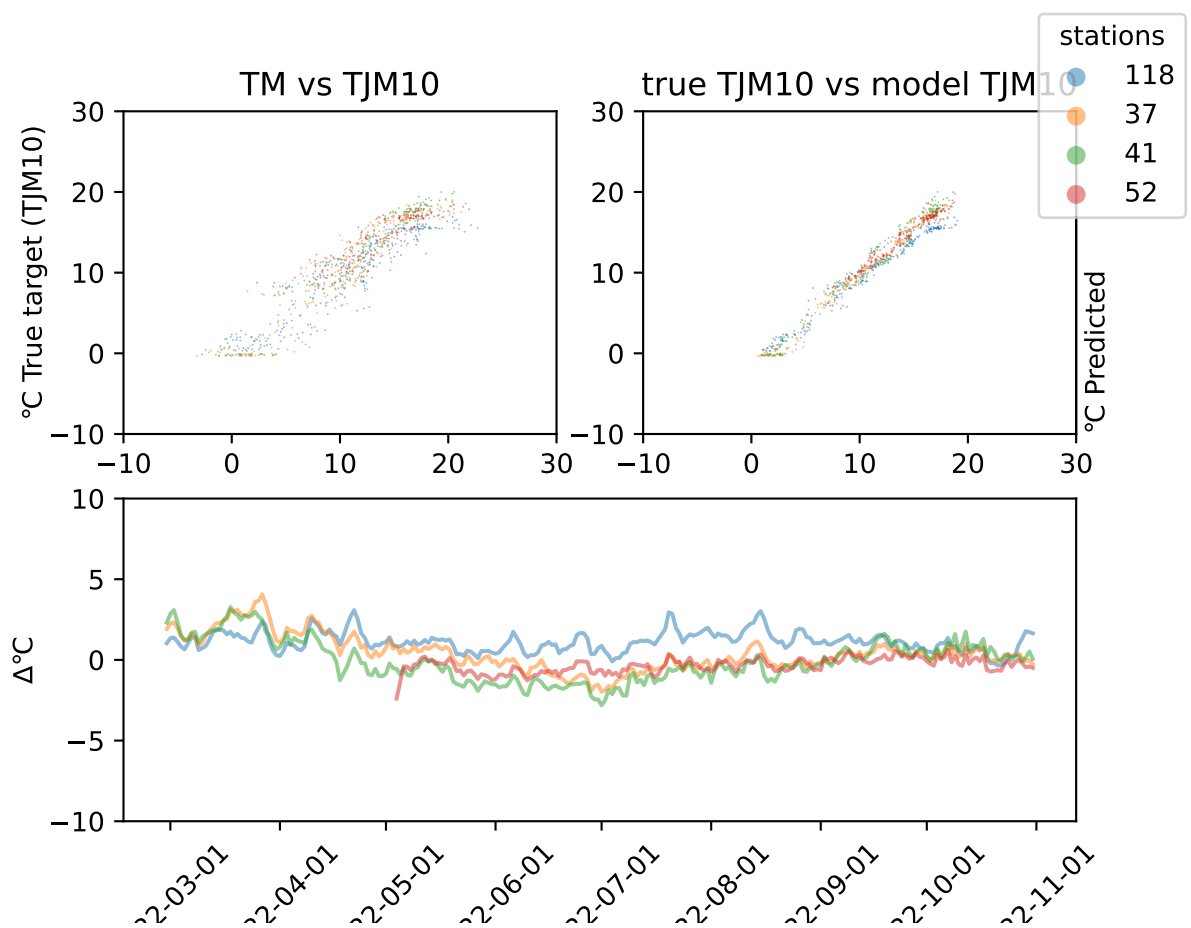


Figure 53: Difference plot for daily Plauborg model in year 2022 and region Østfoldat depth 10. The station names can be found in table 1.

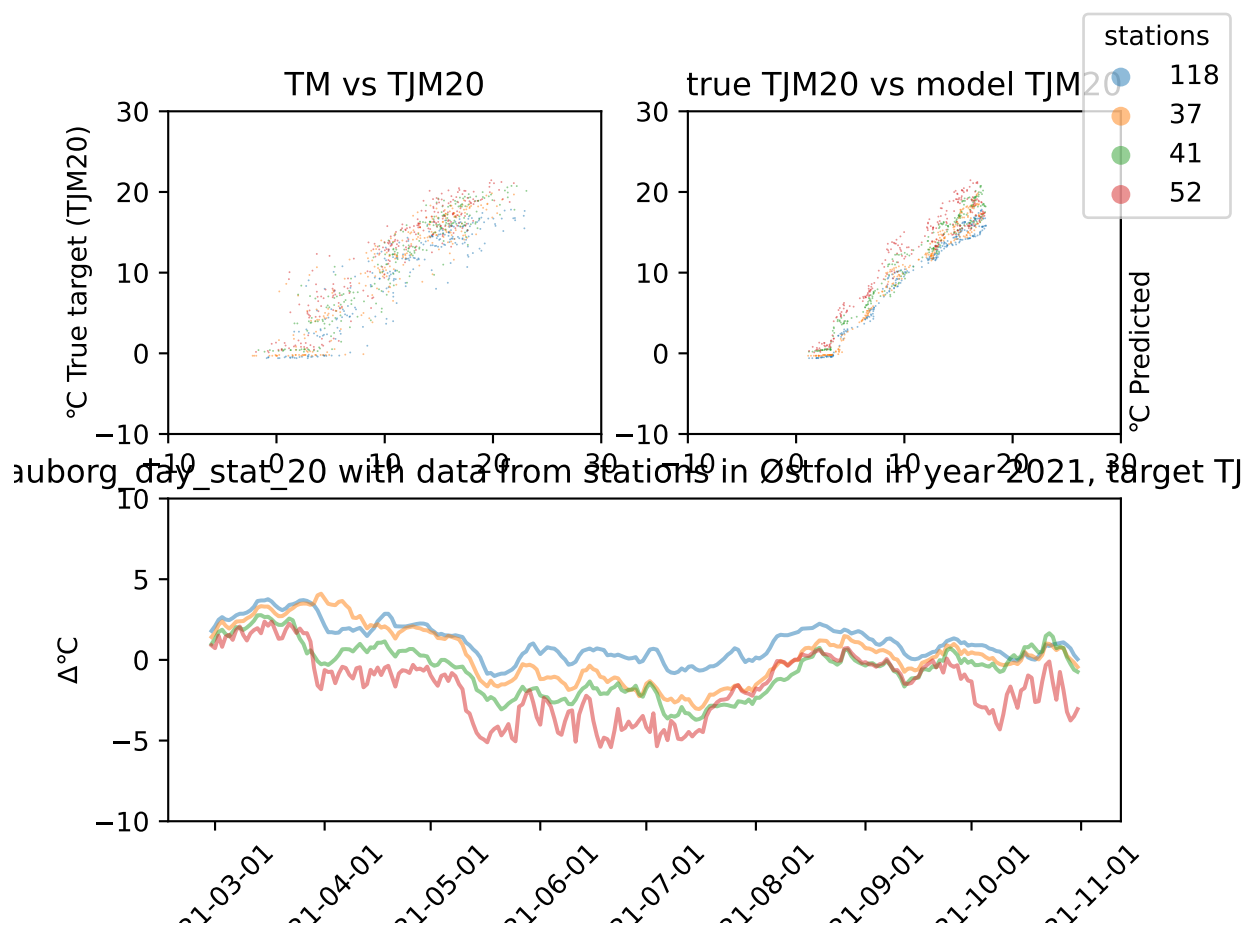


Figure 54: Difference plot for daily Plauborg model in year 2021 and region Østfoldat depth 20. The station names can be found in table 1.

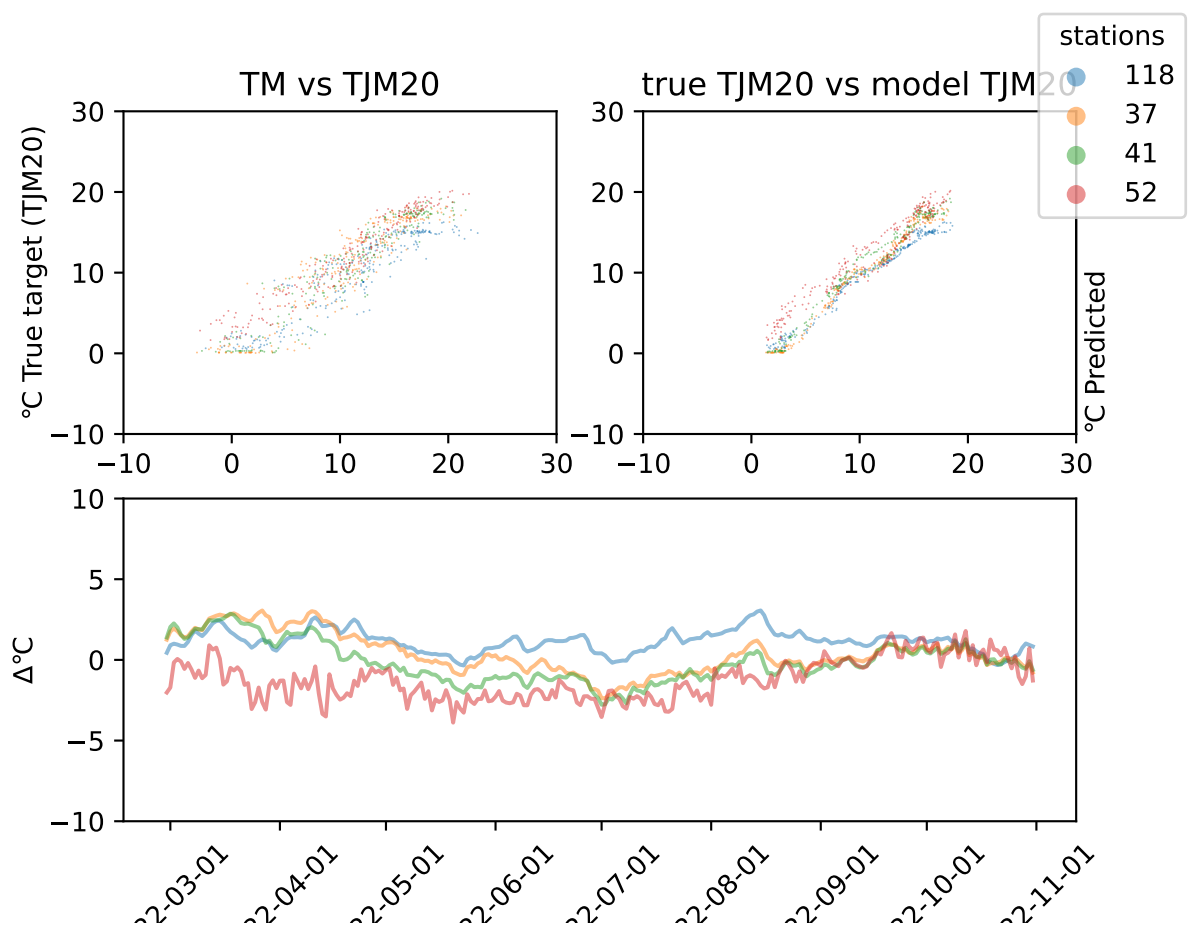


Figure 55: Difference plot for daily Plauborg model in year 2022 and region Østfoldat depth 20. The station names can be found in table 1.

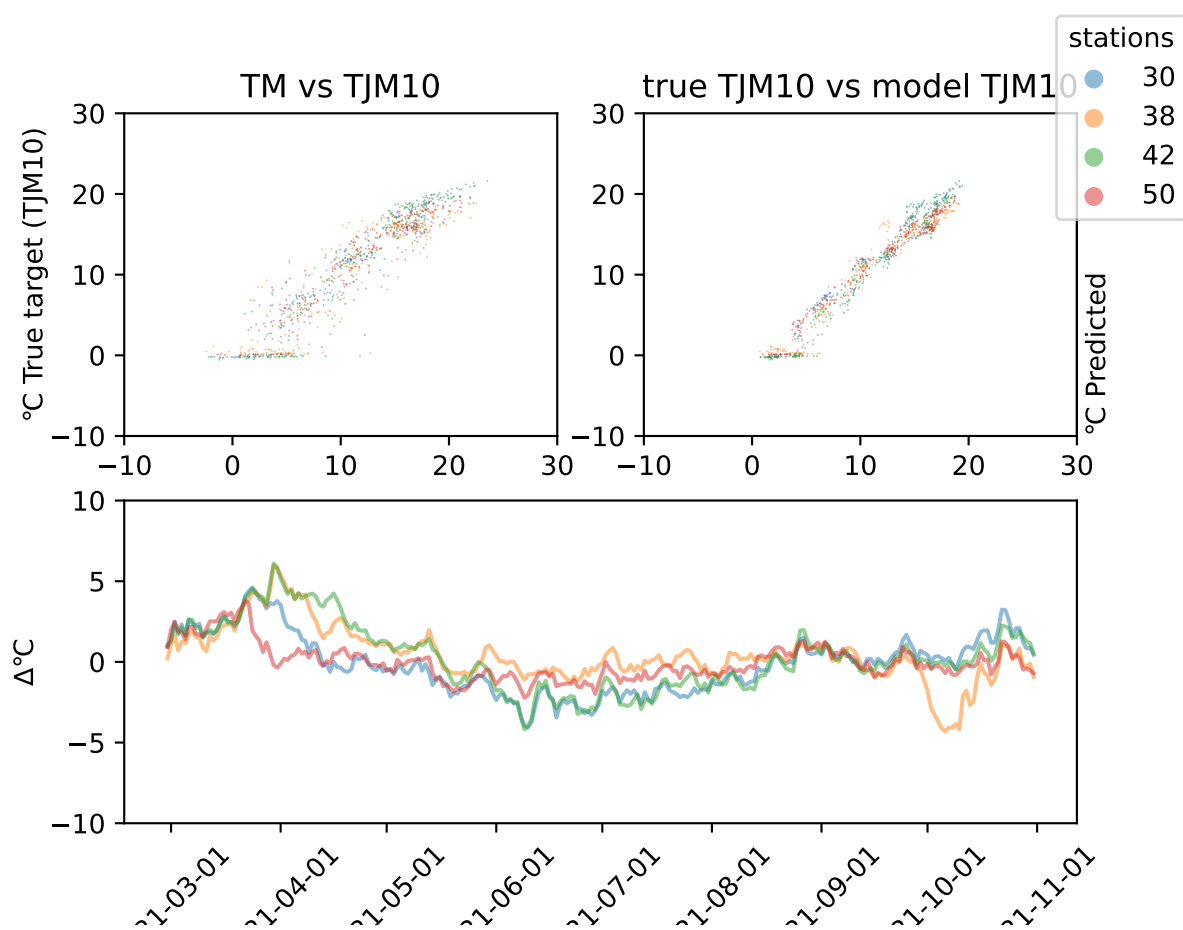


Figure 56: Difference plot for daily Plauborg model in year 2021 and region Vestfoldat depth 10. The station names can be found in table 1.

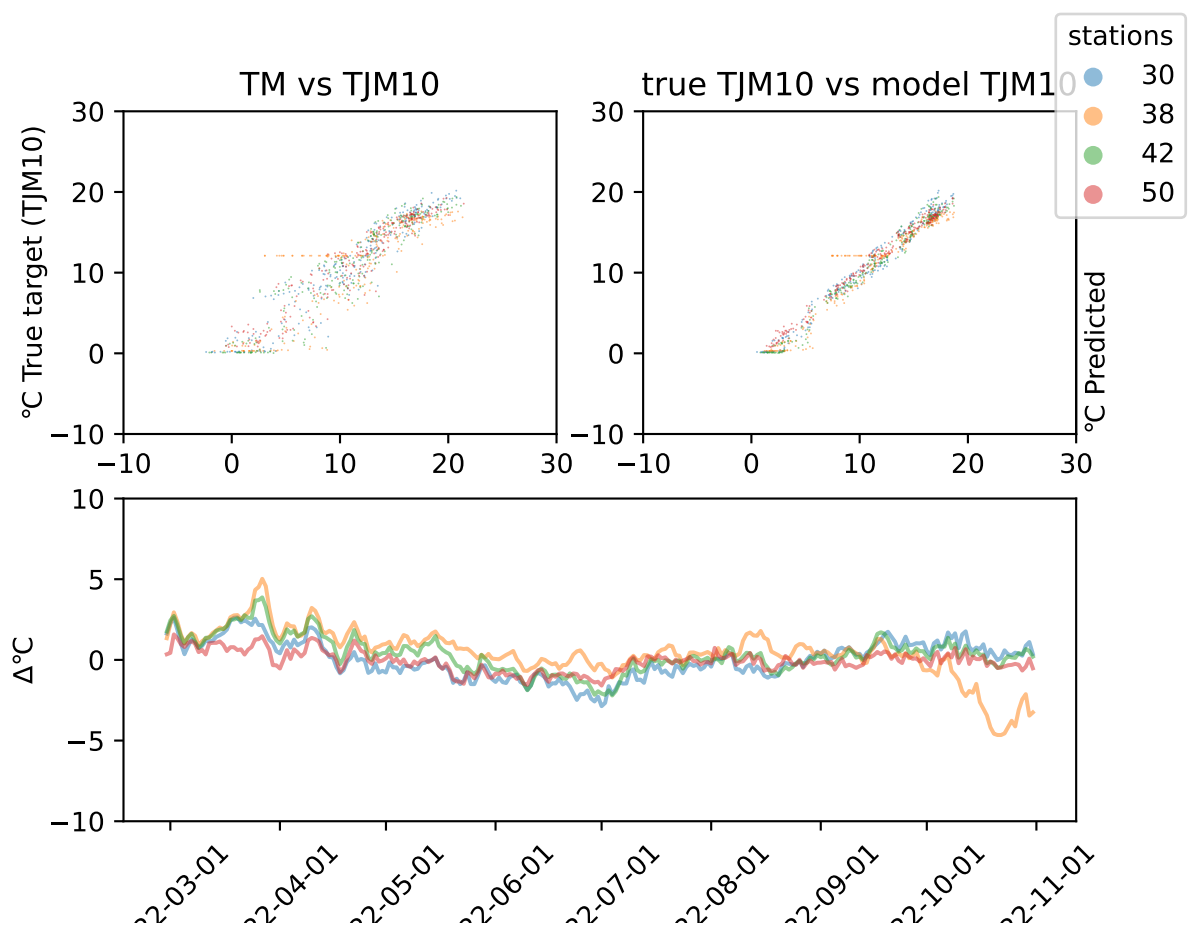


Figure 57: Difference plot for daily Plauborg model in year 2022 and region Vestfoldat depth 10. The station names can be found in table 1.

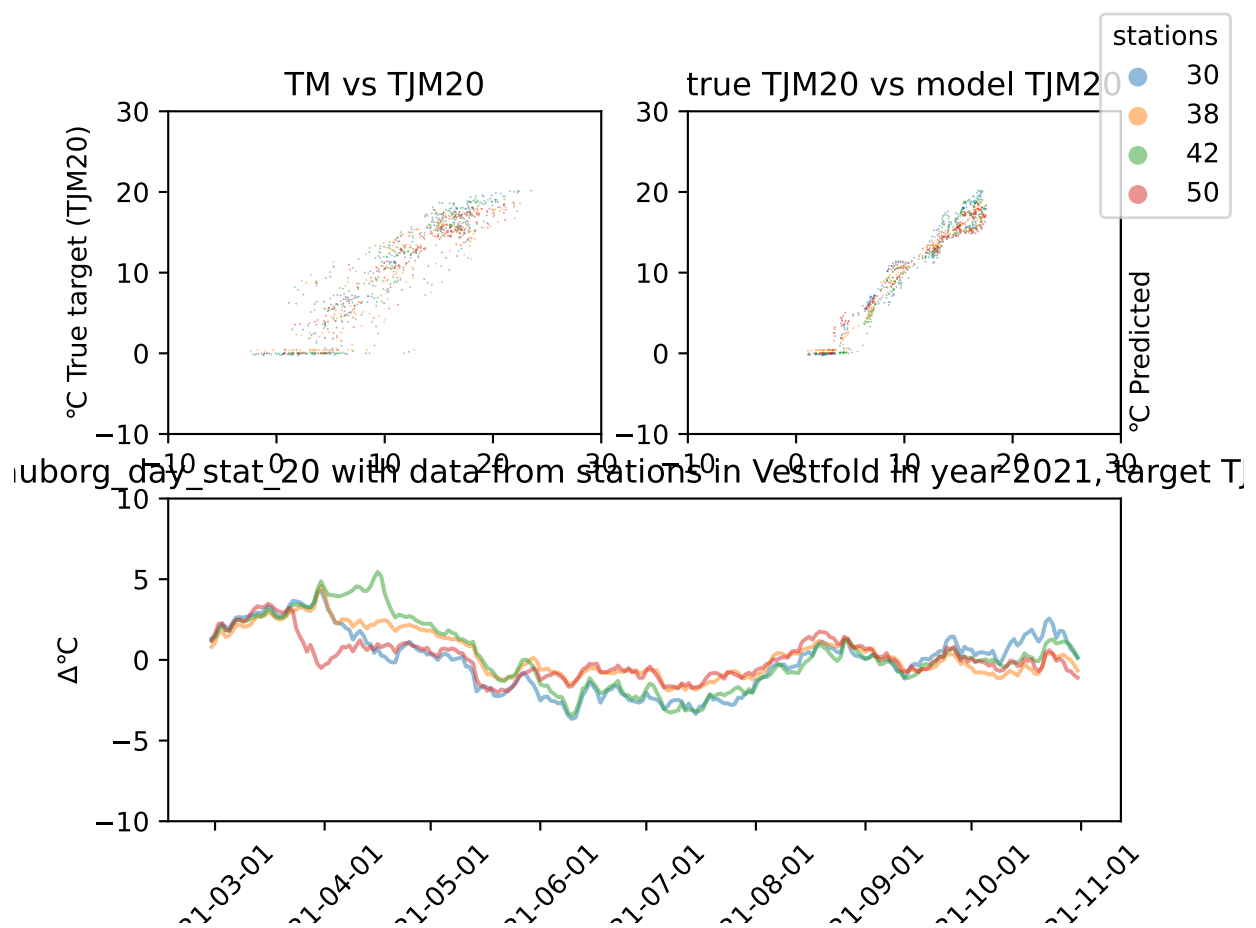


Figure 58: Difference plot for daily Plauborg model in year 2021 and region Vestfoldat depth 20. The station names can be found in table 1.

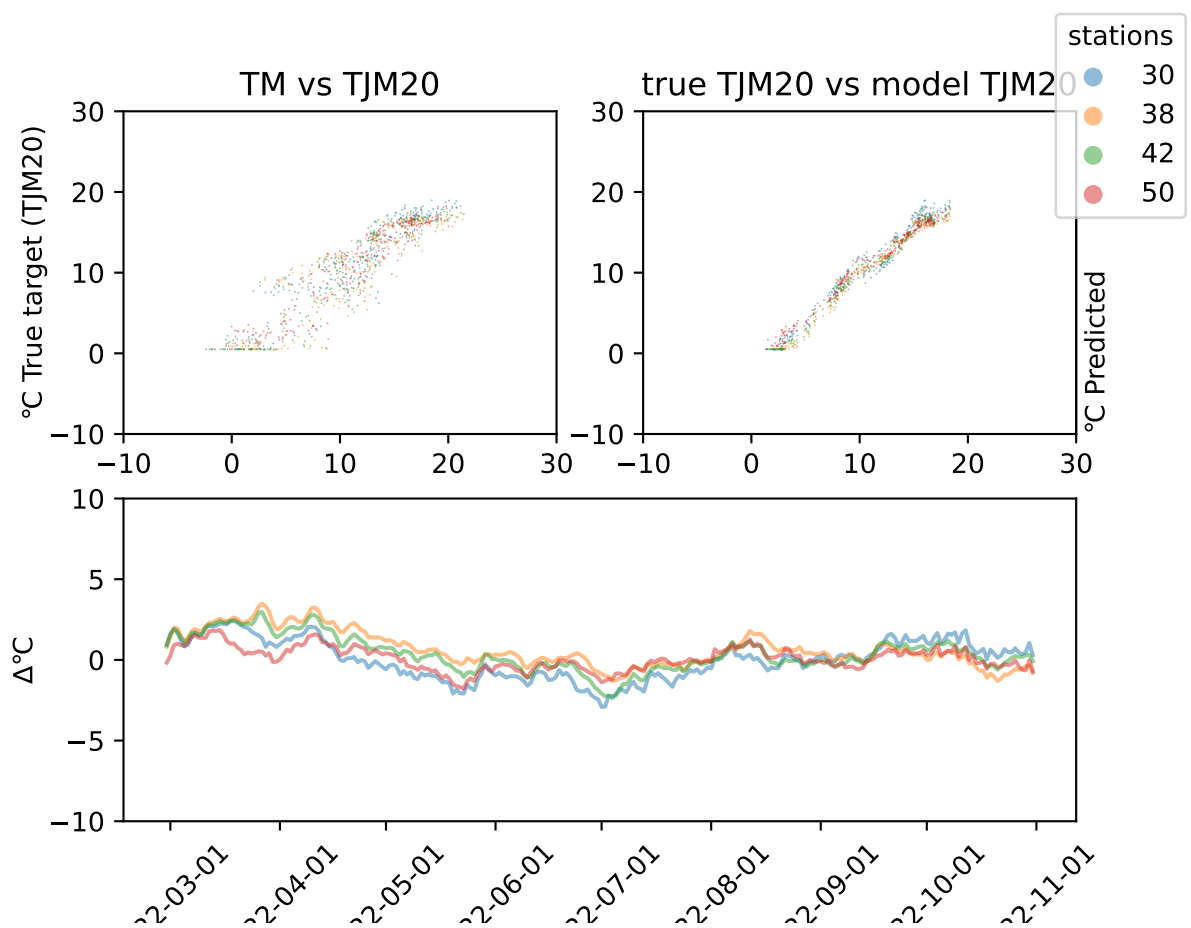


Figure 59: Difference plot for daily Plauborg model in year 2022 and region Vestfoldat depth 20. The station names can be found in table 1.

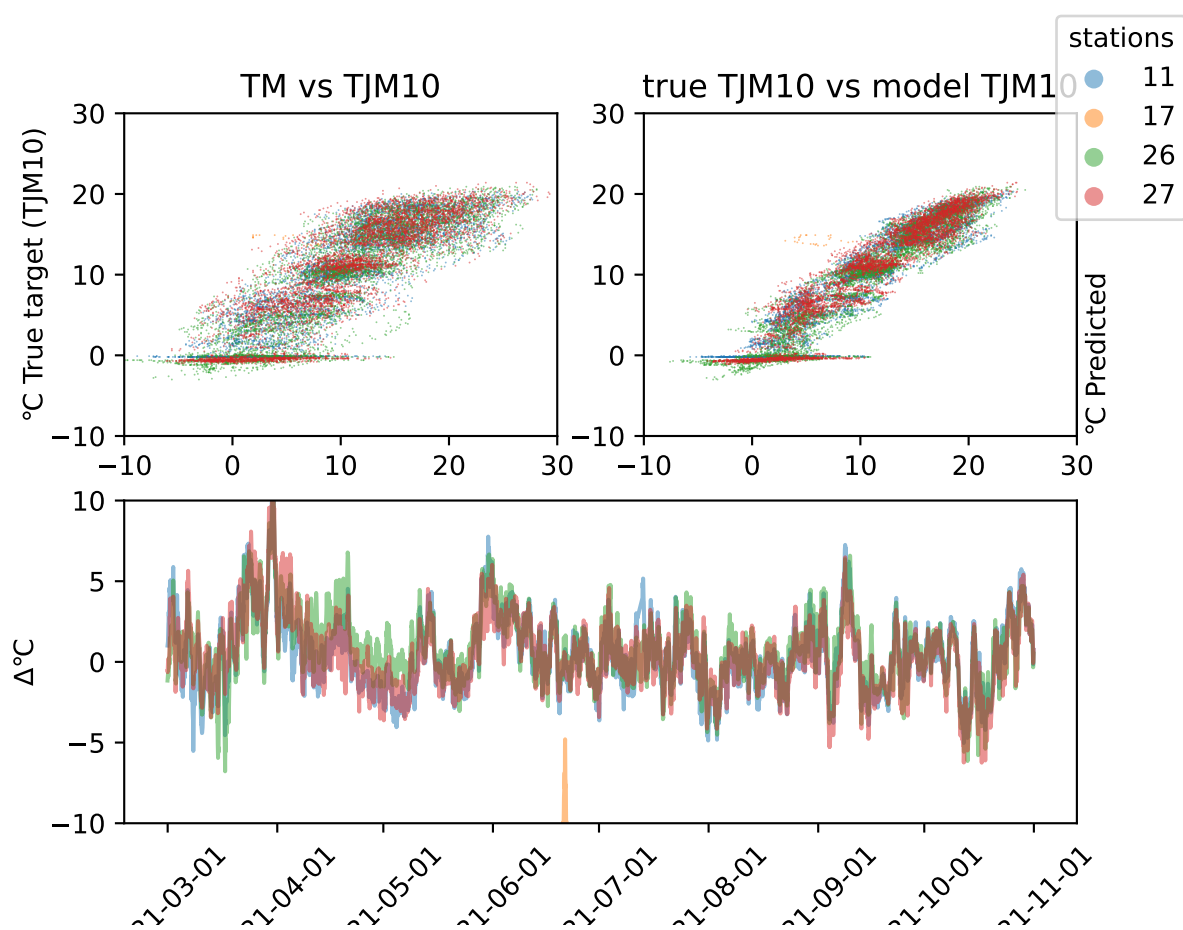


Figure 60: Difference plot for hourly Plauborg model in year 2021 and region Innlandetat depth 10. The station names can be found in table 1.

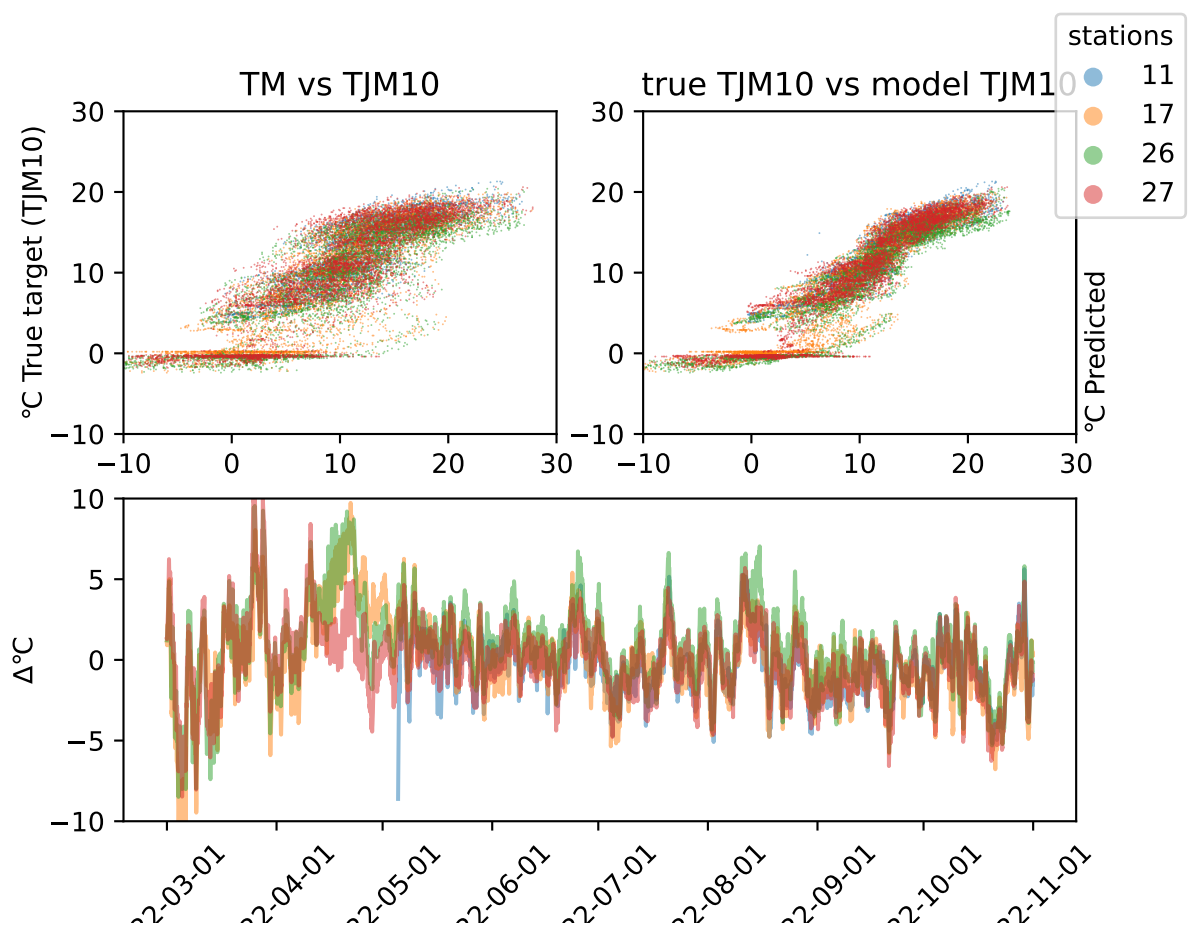


Figure 61: Difference plot for hourly Plauborg model in year 2022 and region Innlandetat depth 10. The station names can be found in table 1.

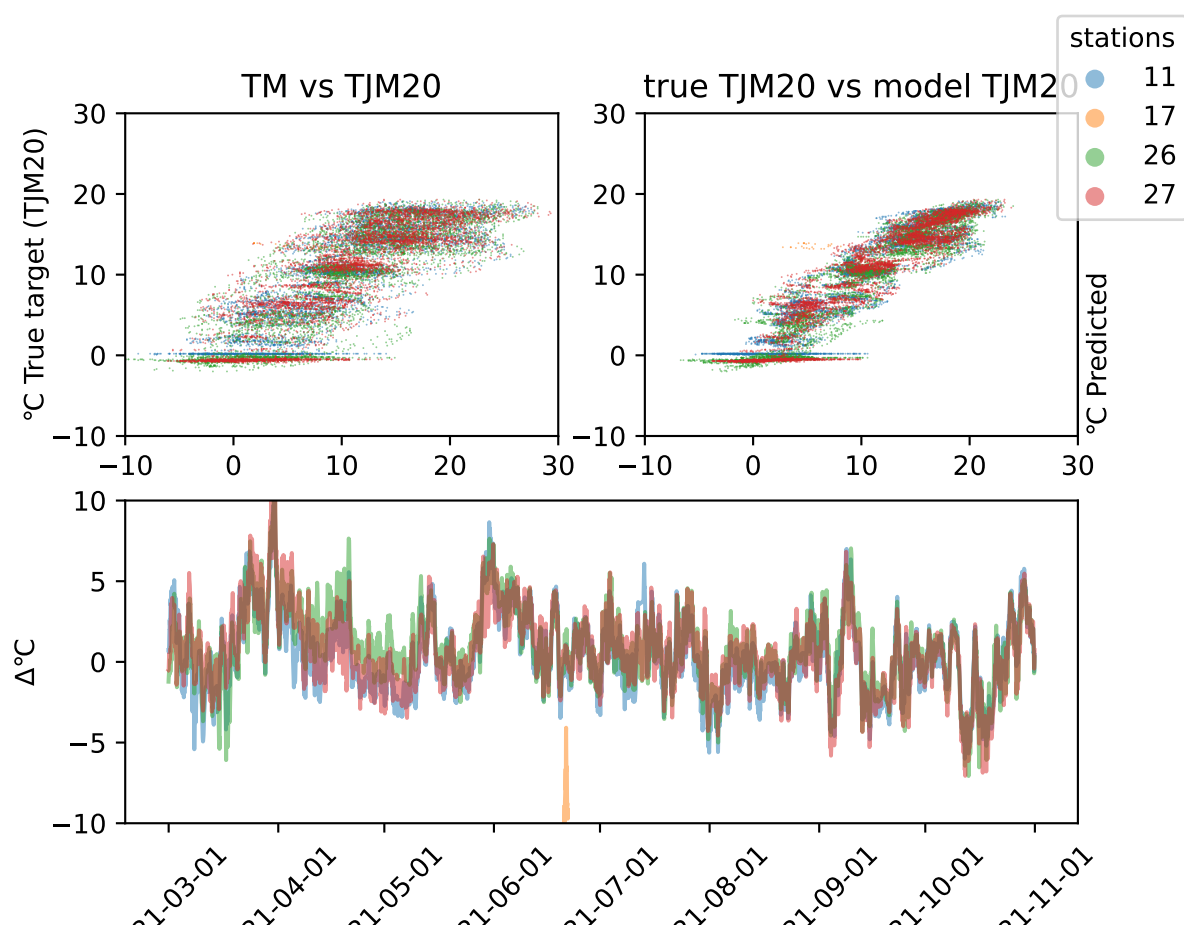


Figure 62: Difference plot for hourly Plauborg model in year 2021 and region Innlandetat depth 20. The station names can be found in table 1.

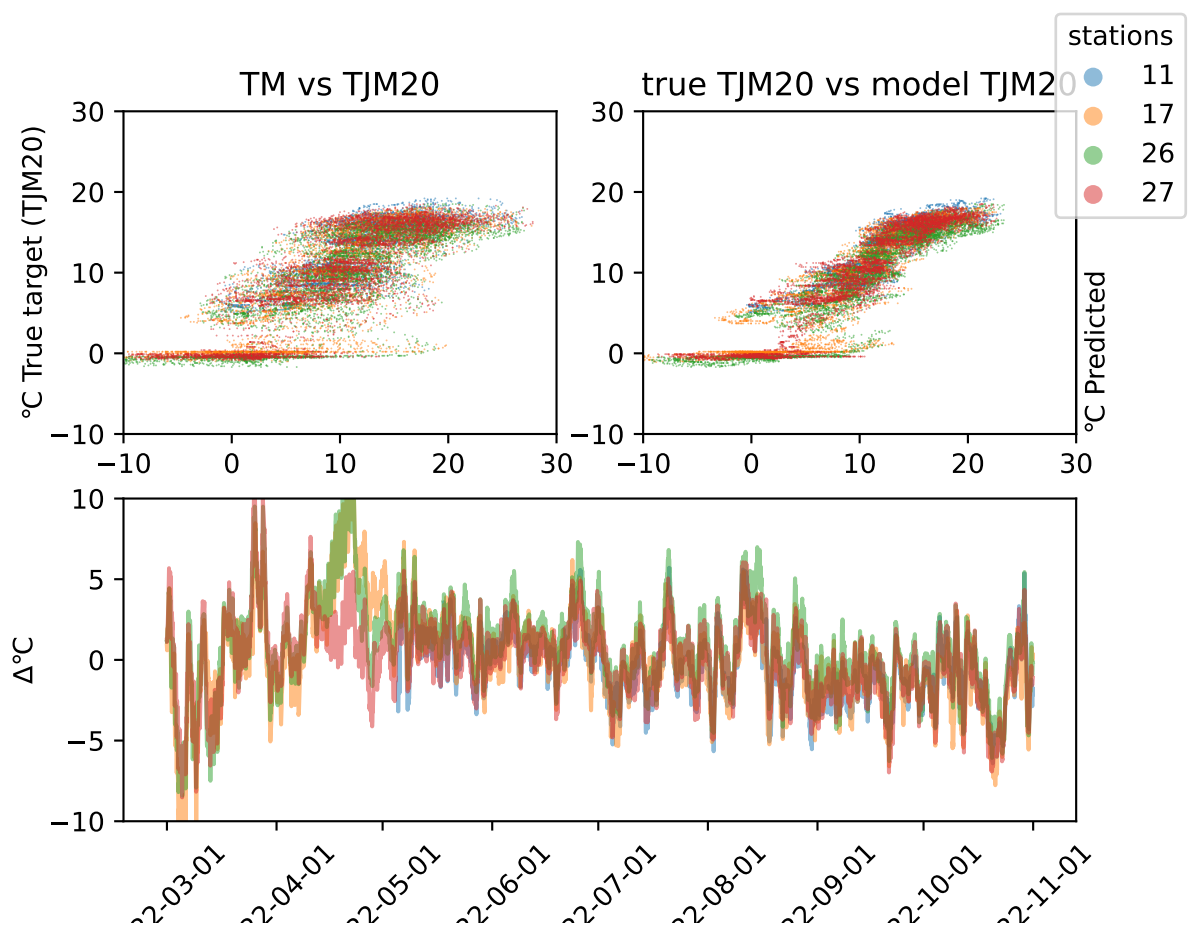


Figure 63: Difference plot for hourly Plauborg model in year 2022 and region Innlandetat depth 20. The station names can be found in table 1.

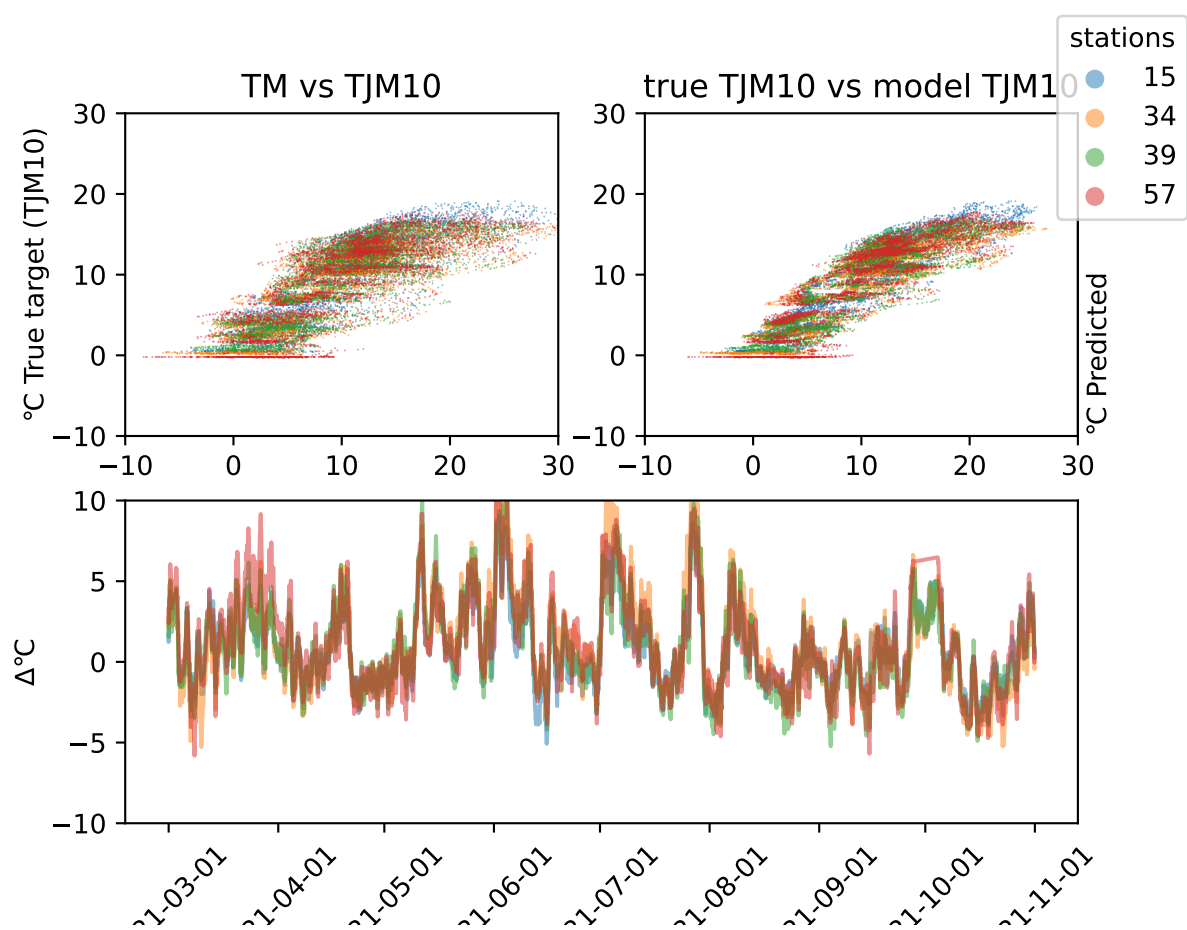


Figure 64: Difference plot for hourly Plauborg model in year 2021 and region Trøndelagat depth 10. The station names can be found in table 1.

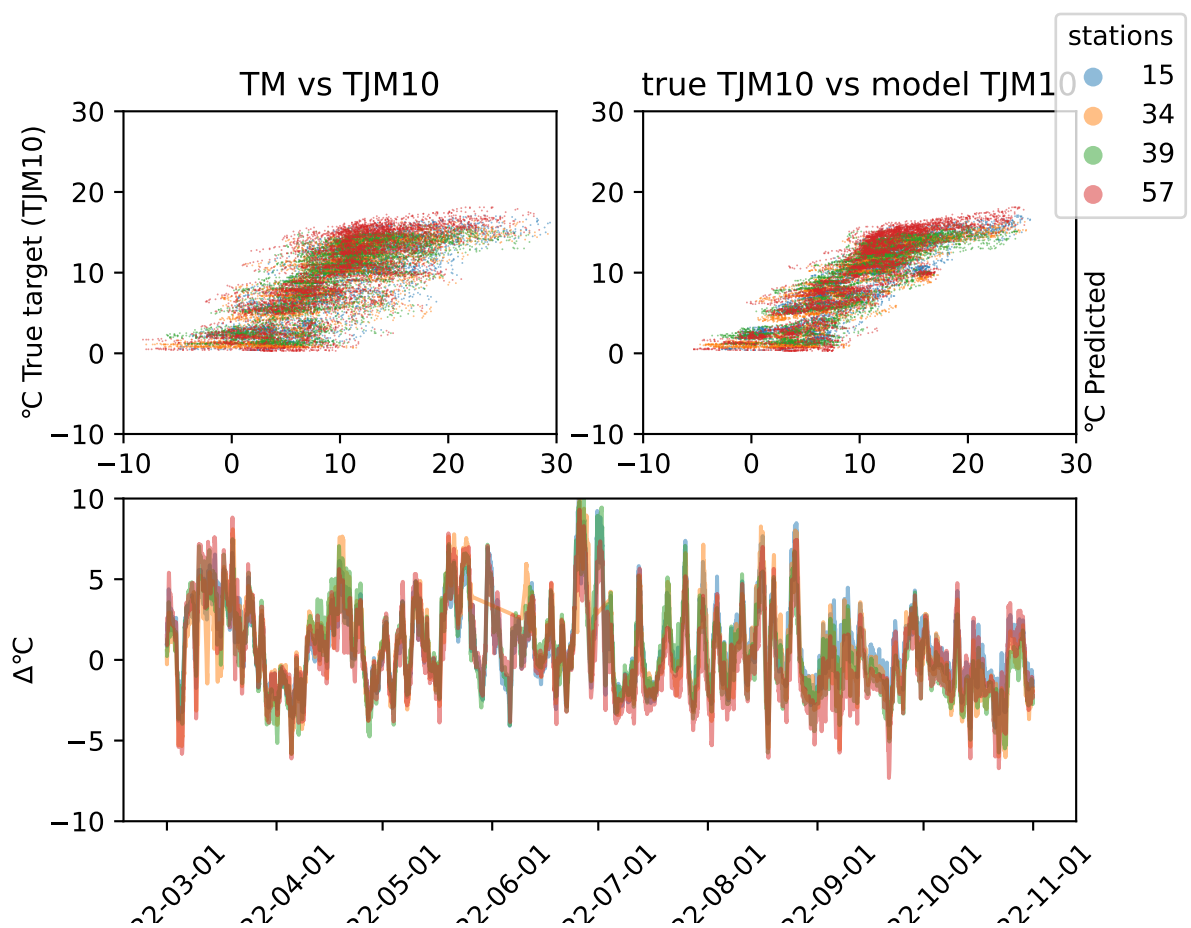


Figure 65: Difference plot for hourly Plauborg model in year 2022 and region Trøndelagat depth 10. The station names can be found in table 1.

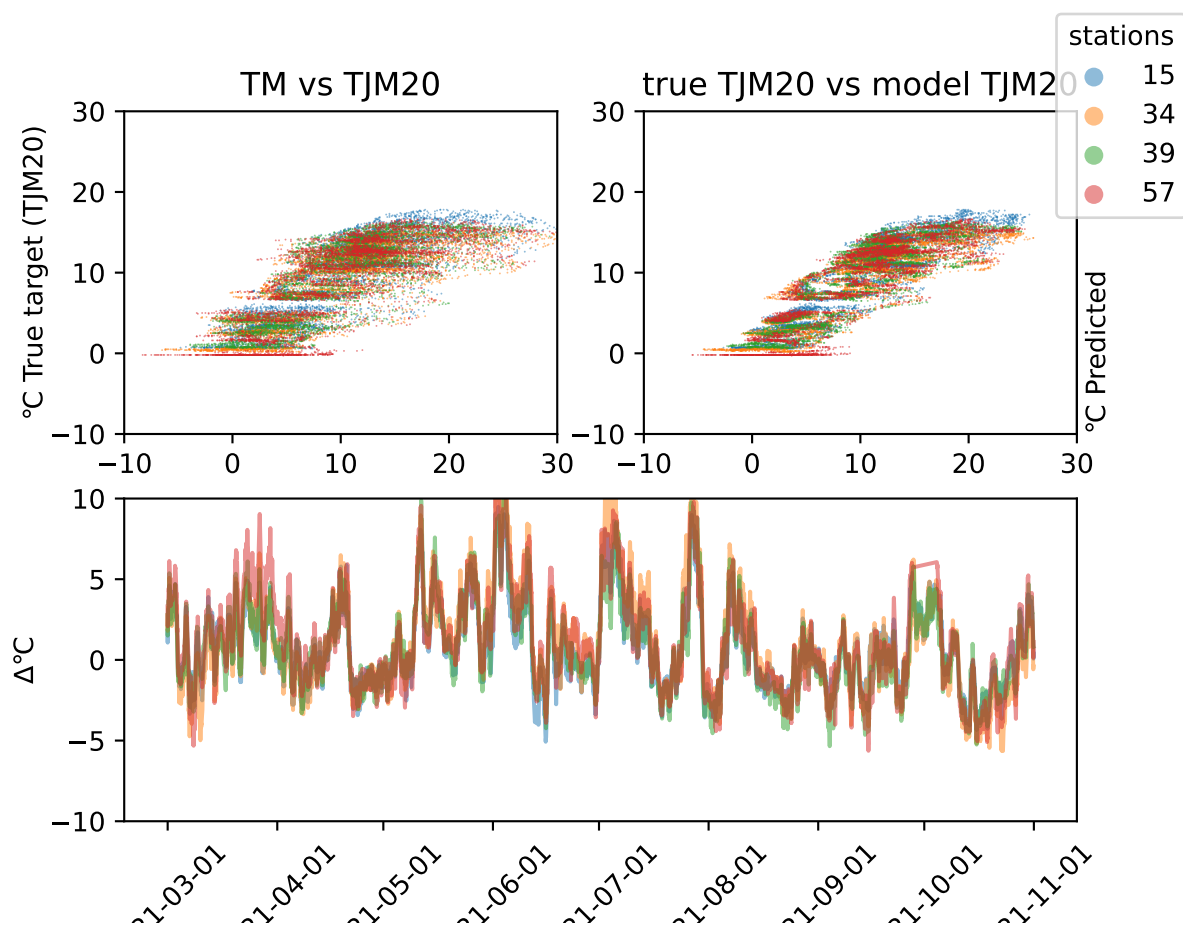


Figure 66: Difference plot for hourly Plauborg model in year 2021 and region Trøndelagat depth 20. The station names can be found in table 1.

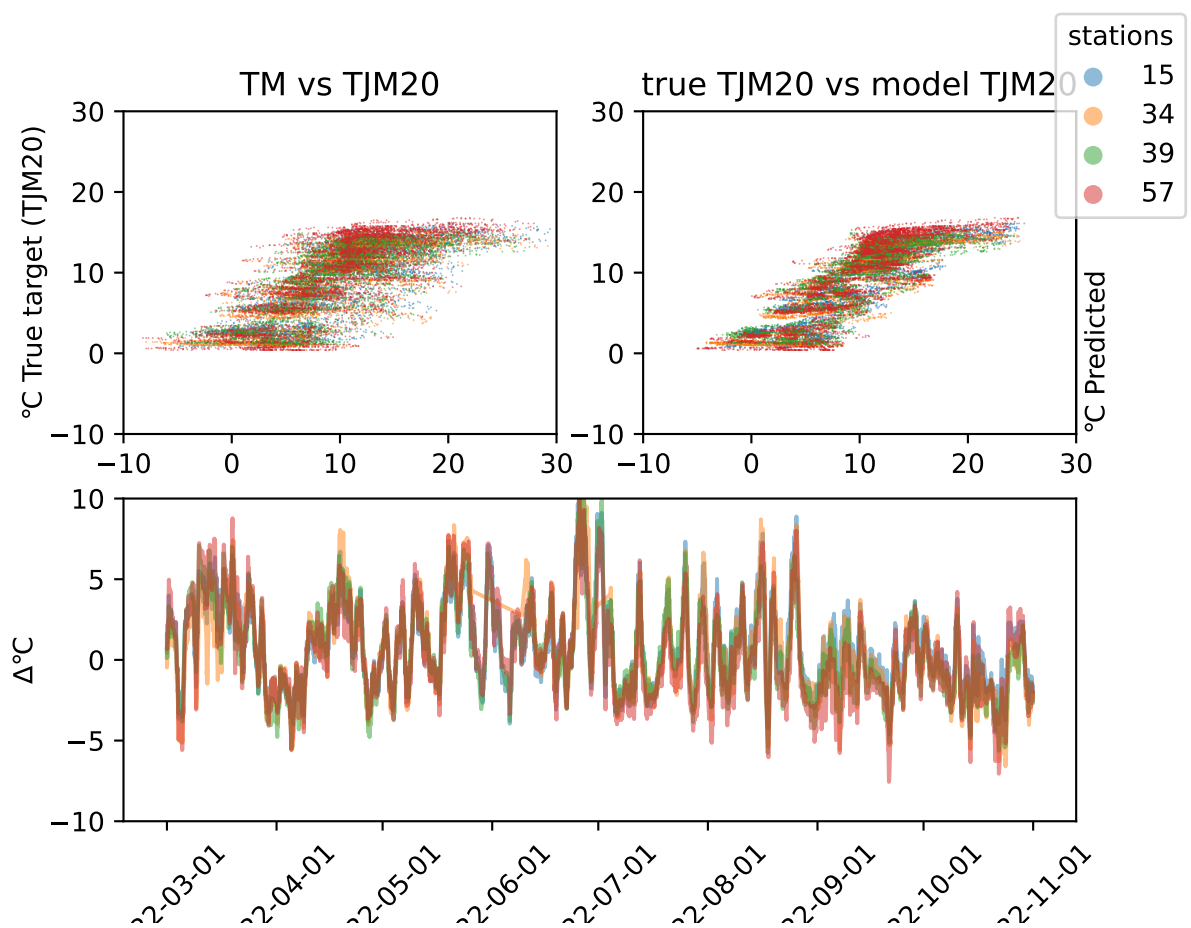


Figure 67: Difference plot for hourly Plauborg model in year 2022 and region Trøndelagat depth 20. The station names can be found in table 1.

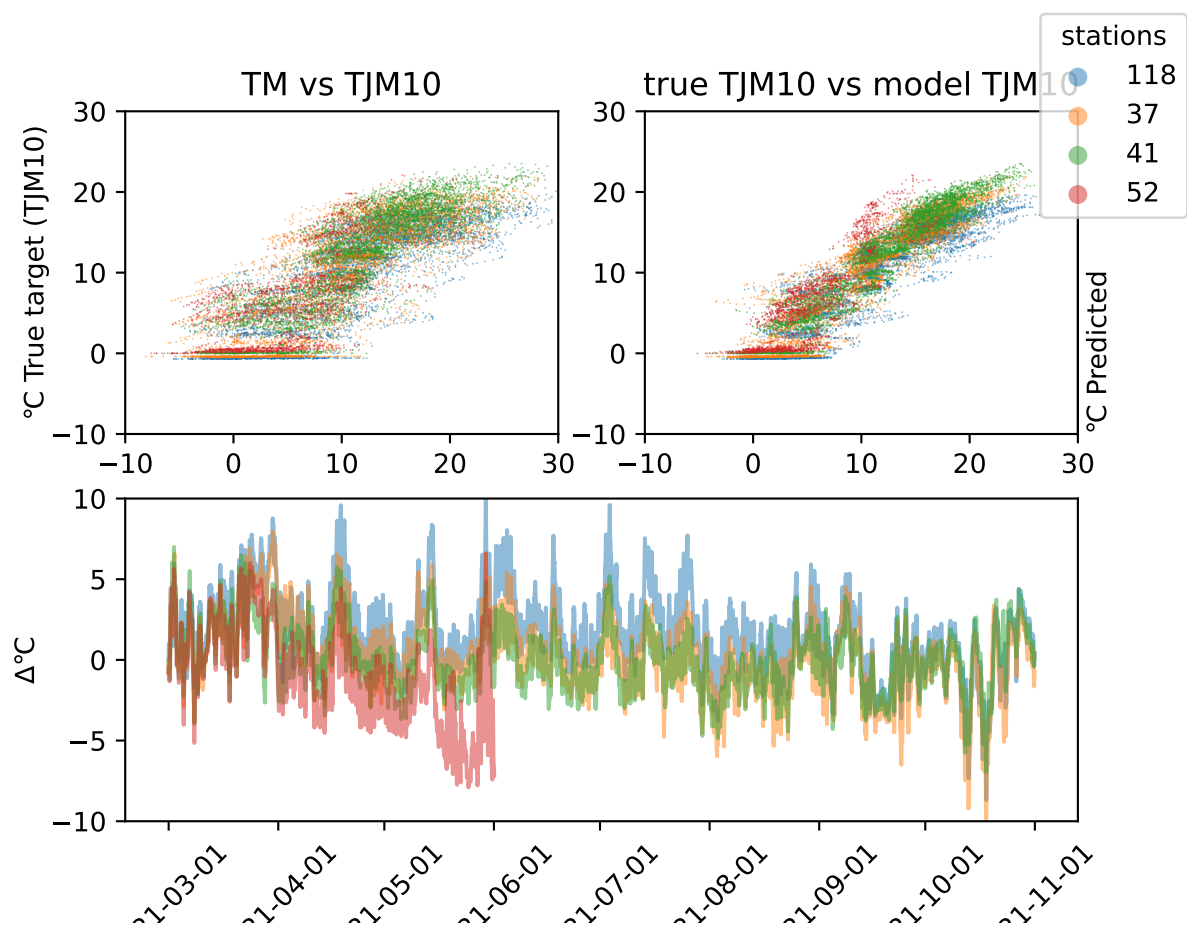


Figure 68: Difference plot for hourly Plauborg model in year 2021 and region Østfoldat depth 10. The station names can be found in table 1.

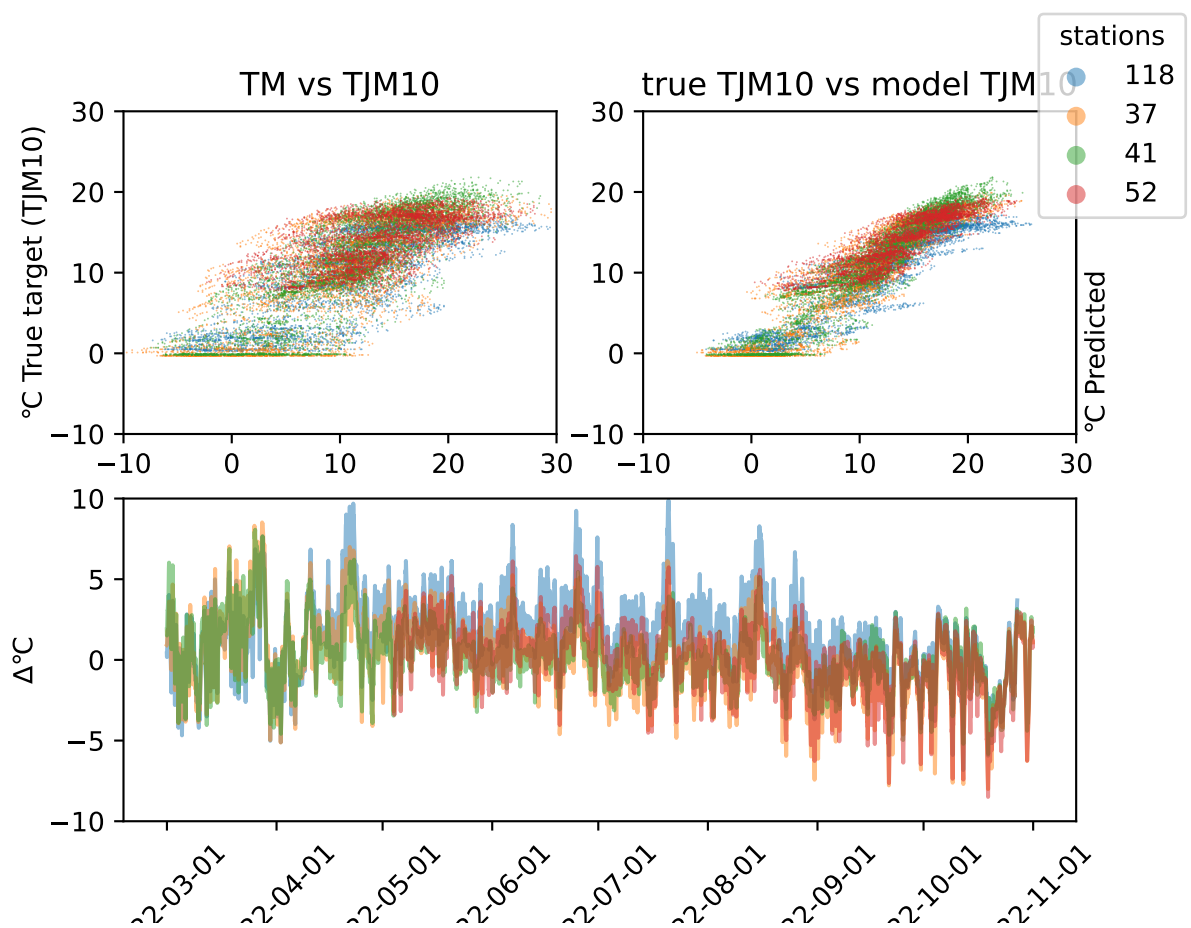


Figure 69: Difference plot for hourly Plauborg model in year 2022 and region Østfoldat depth 10. The station names can be found in table 1.

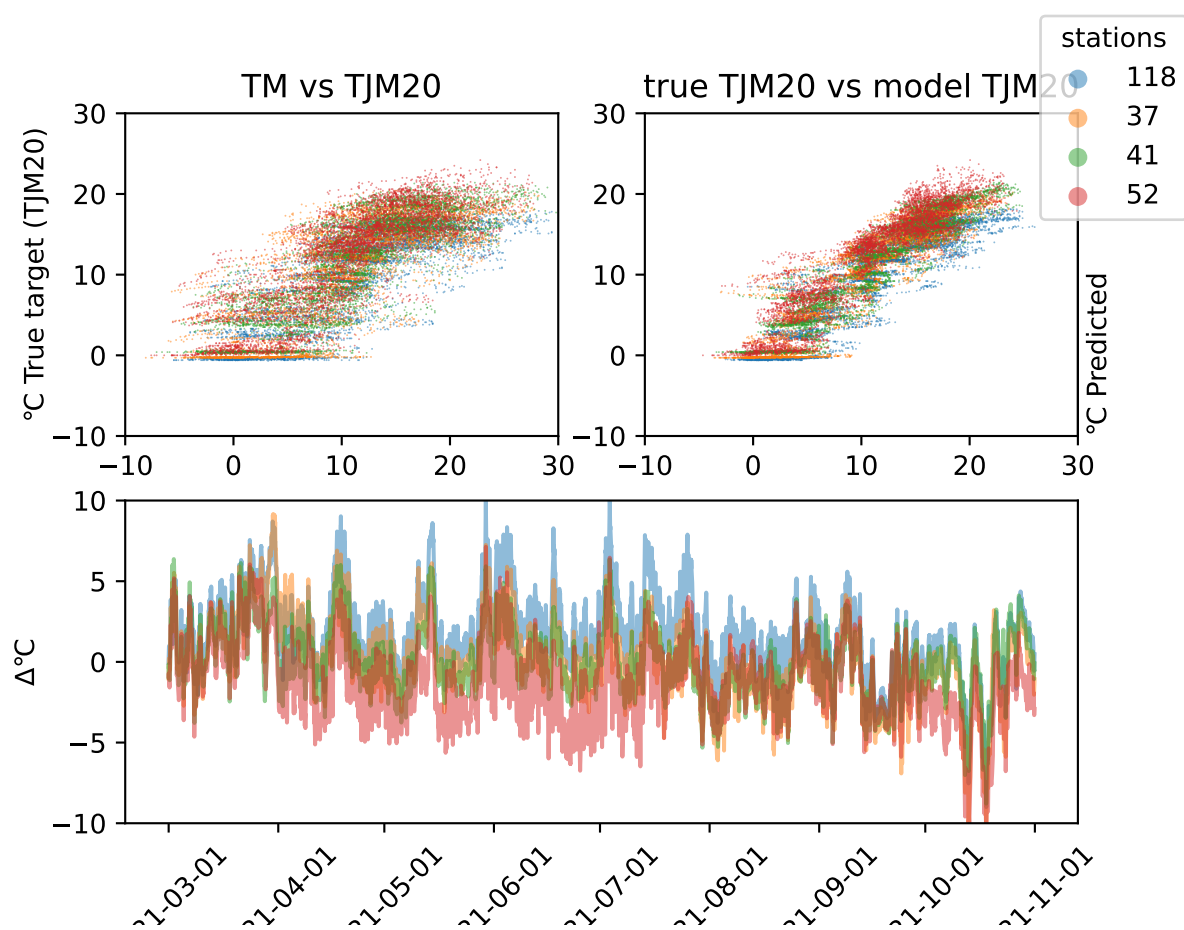


Figure 70: Difference plot for hourly Plauborg model in year 2021 and region Østfoldat depth 20. The station names can be found in table 1.

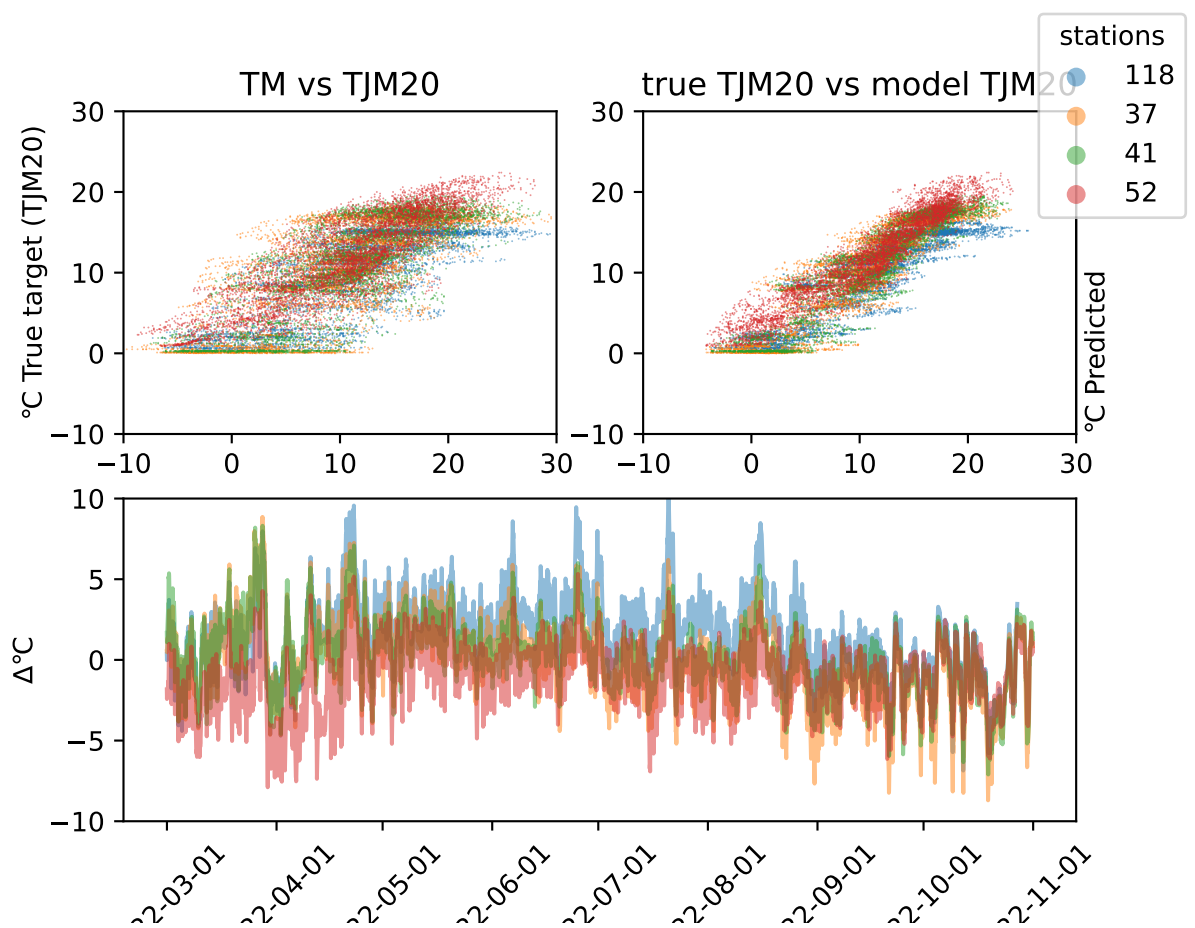


Figure 71: Difference plot for hourly Plauborg model in year 2022 and region Østfoldat depth 20. The station names can be found in table 1.

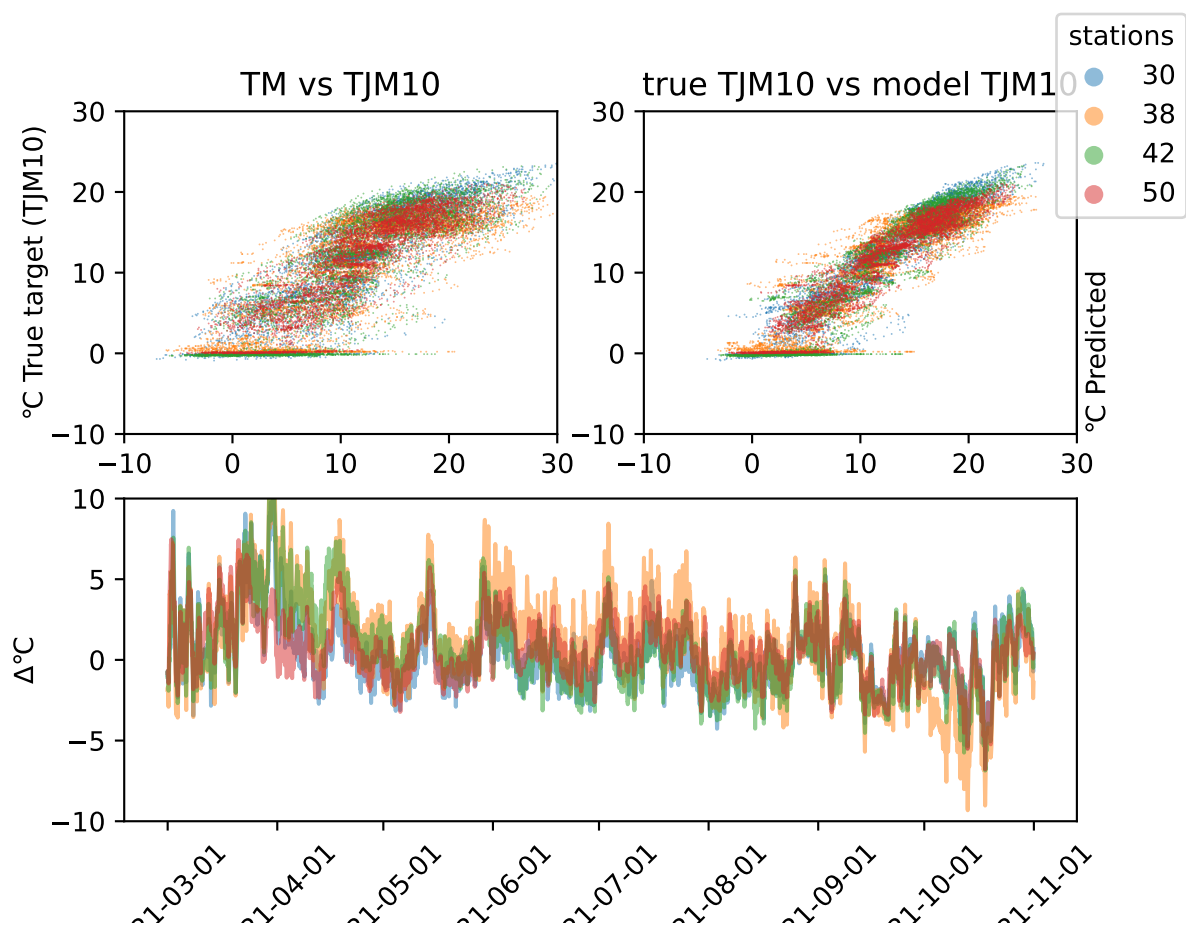


Figure 72: Difference plot for hourly Plauborg model in year 2021 and region Vestfoldat depth 10. The station names can be found in table 1.

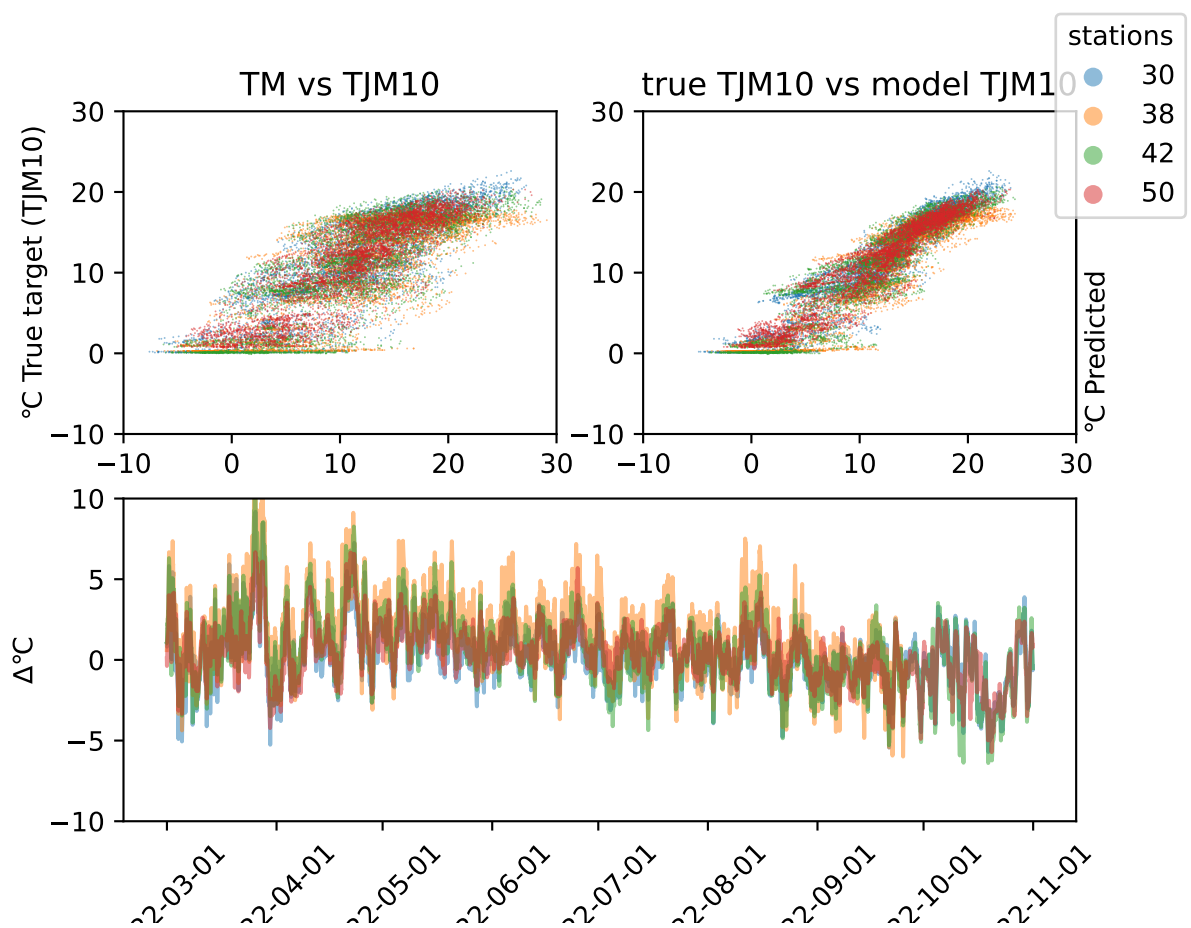


Figure 73: Difference plot for hourly Plauborg model in year 2022 and region Vestfoldat depth 10. The station names can be found in table 1.

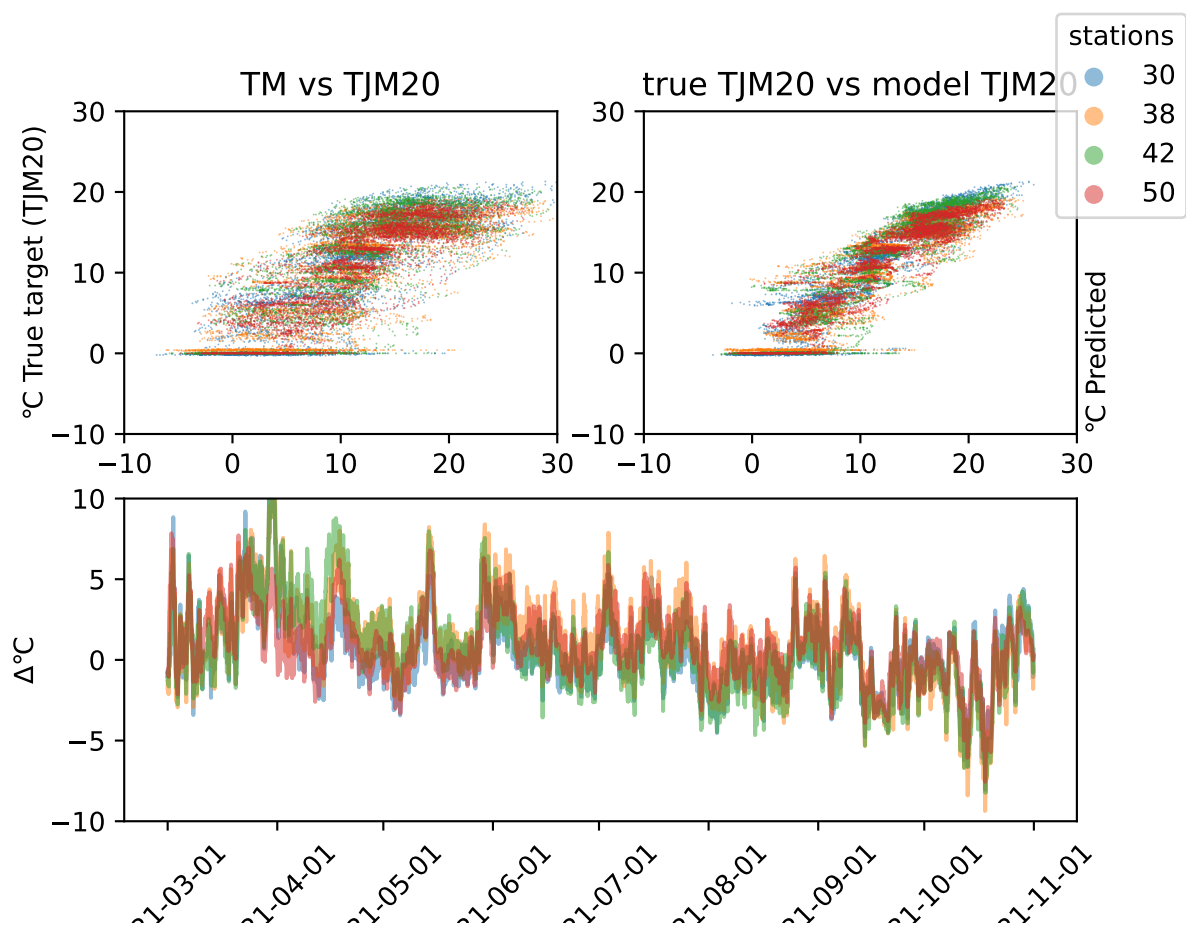


Figure 74: Difference plot for hourly Plauborg model in year 2021 and region Vestfoldat depth 20. The station names can be found in table 1.

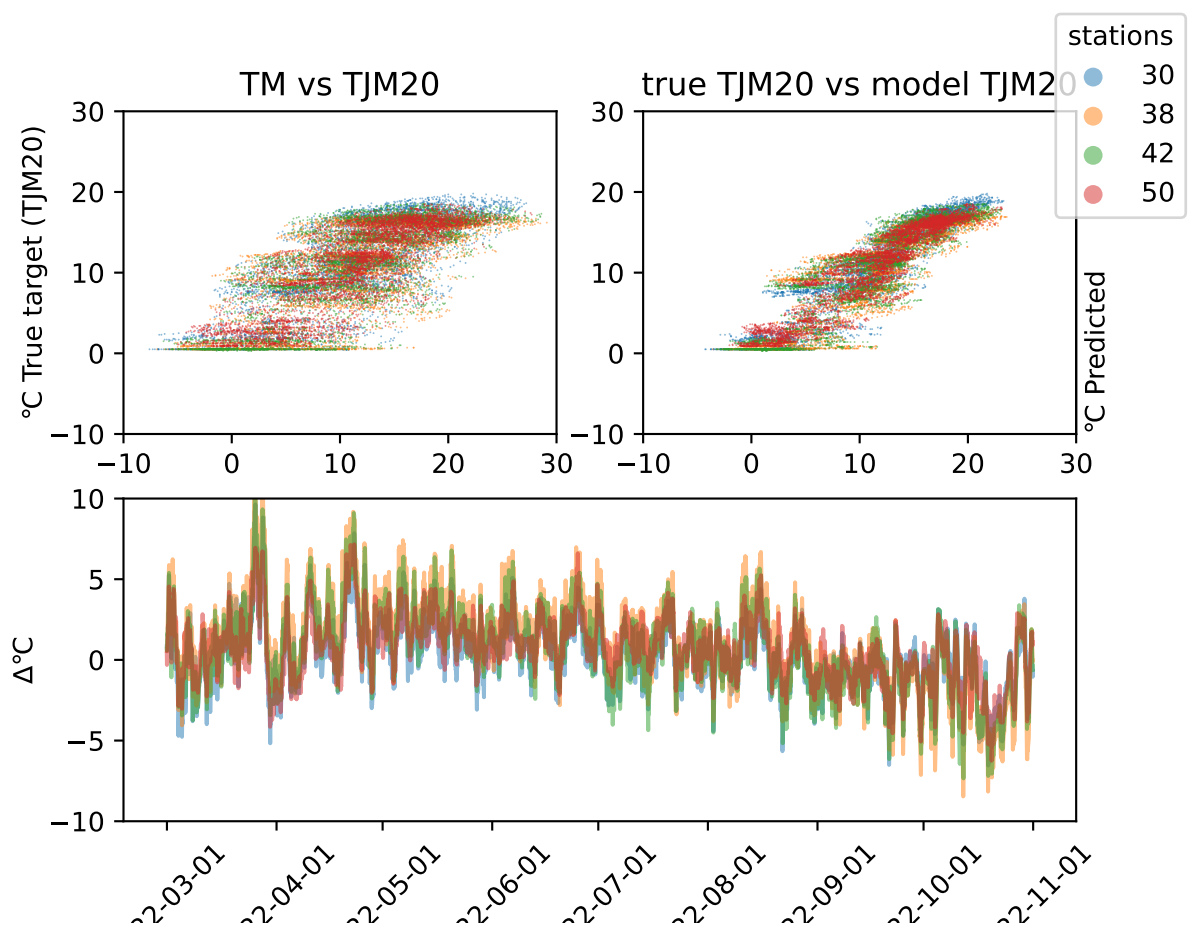


Figure 75: Difference plot for hourly Plauborg model in year 2022 and region Vestfoldat depth 20. The station names can be found in table 1.

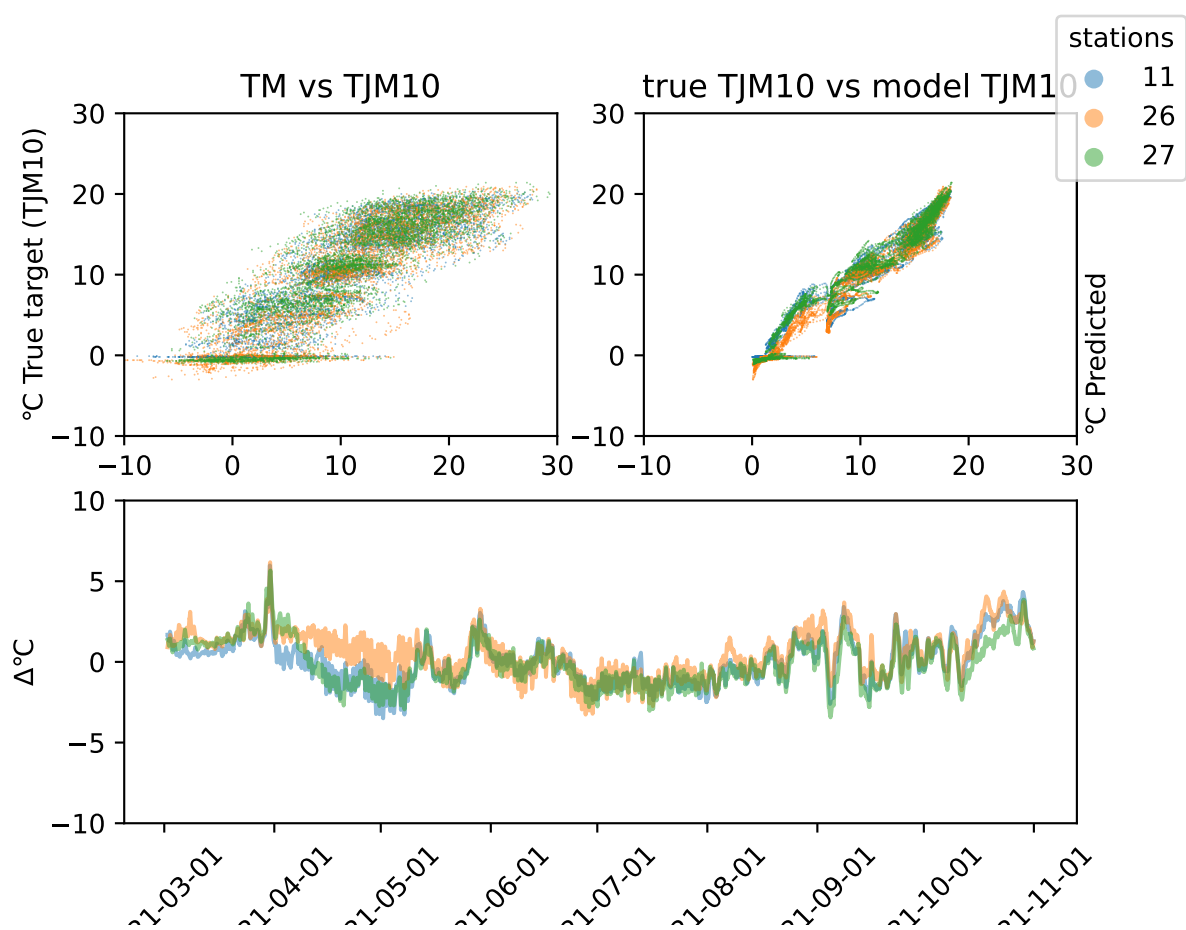


Figure 76: Difference plot for BiLSTM model in year 2021 and region Innlandet at depth 10. The station names can be found in table 1.

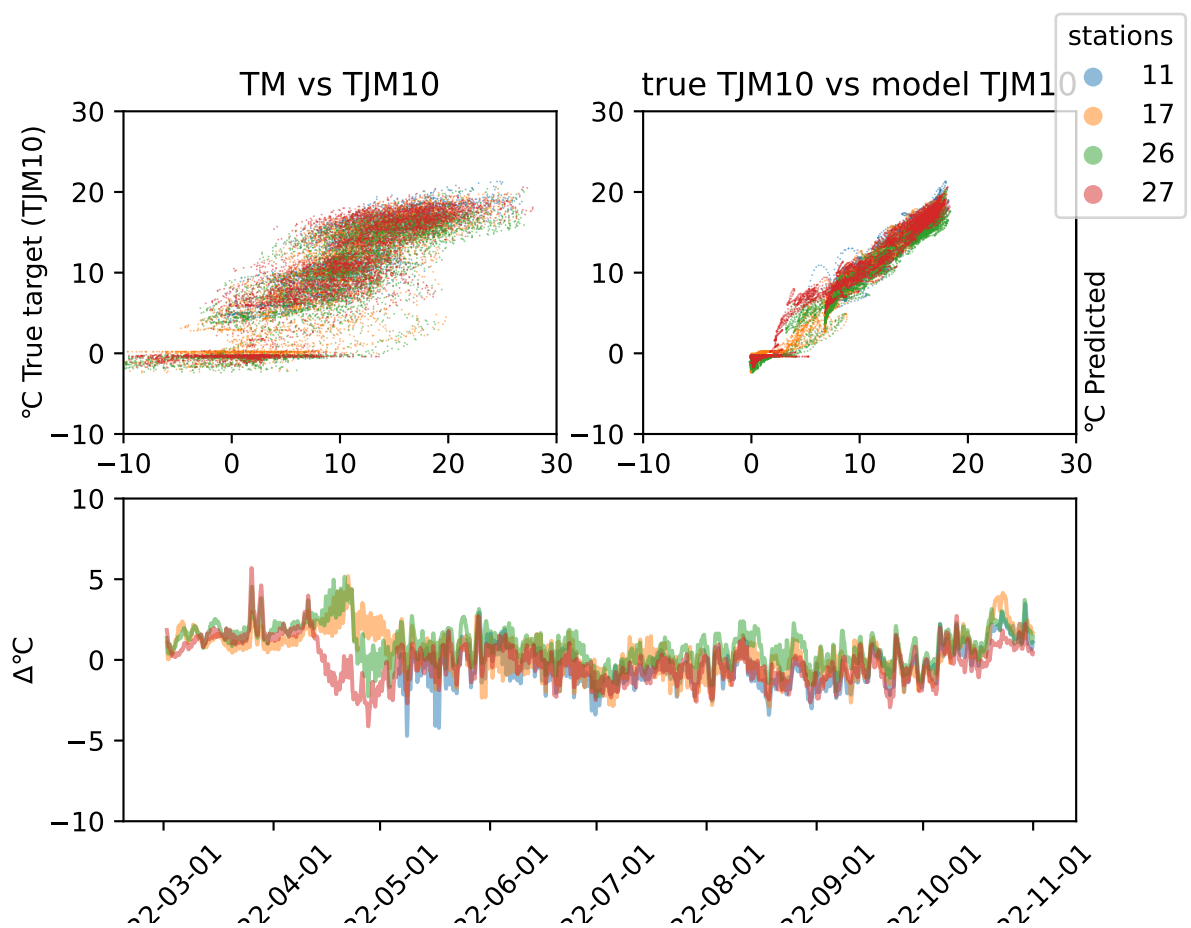


Figure 77: Difference plot for BiLSTM model in year 2022 and region Innlandet at depth 10. The station names can be found in table 1.

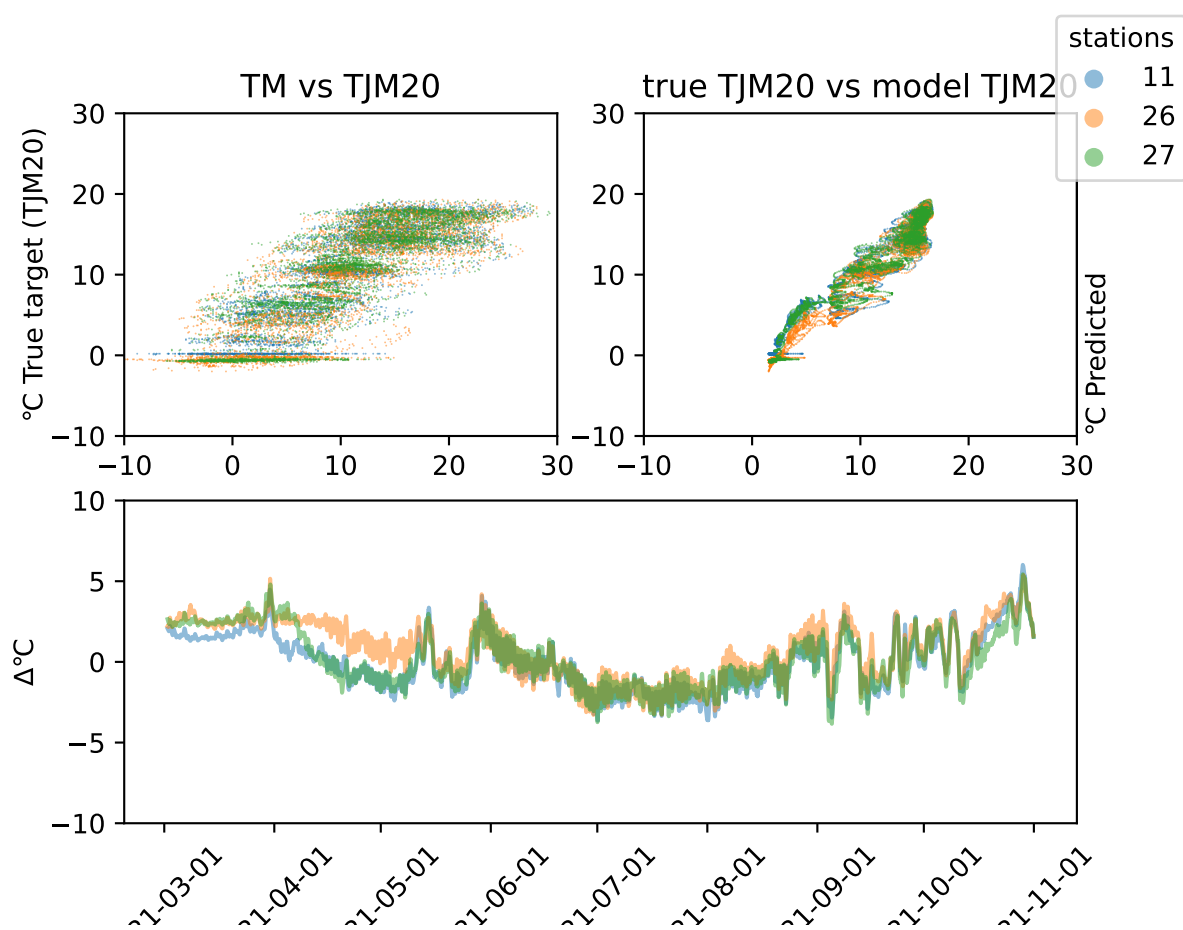


Figure 78: Difference plot for BiLSTM model in year 2021 and region Innlandetat depth 20. The station names can be found in table 1.

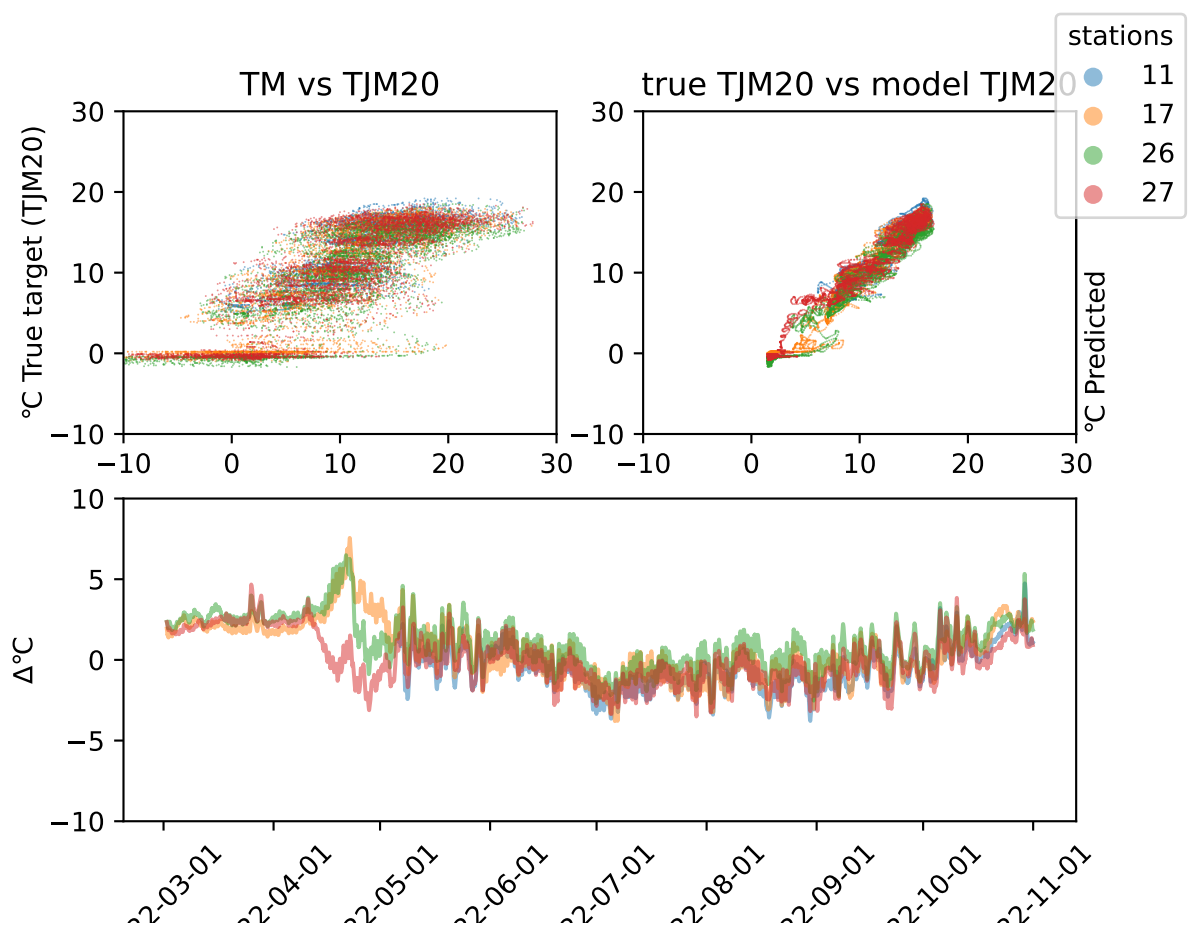


Figure 79: Difference plot for BiLSTM model in year 2022 and region Innlandetat depth 20. The station names can be found in table 1.

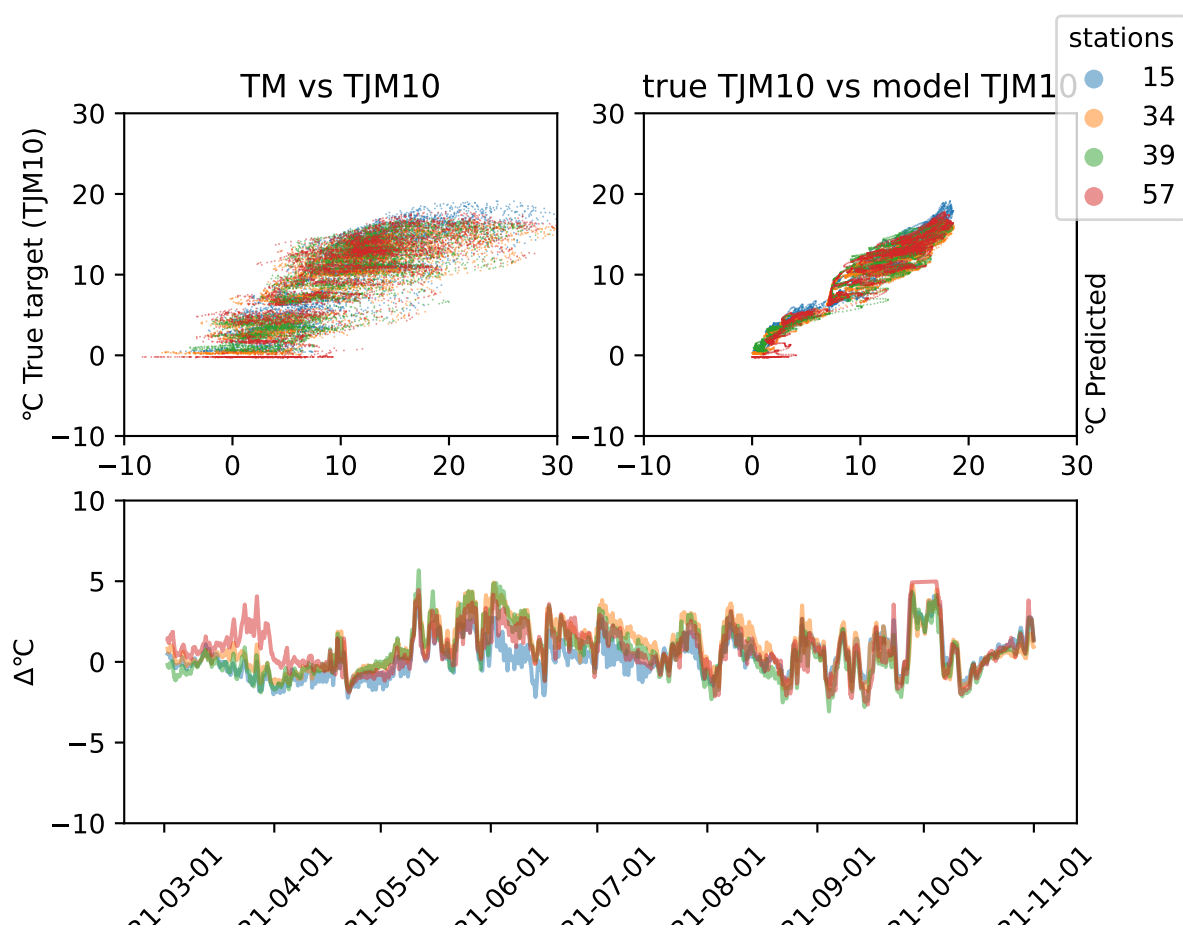


Figure 80: Difference plot for BiLSTM model in year 2021 and region Trøndelagat depth 10. The station names can be found in table 1.

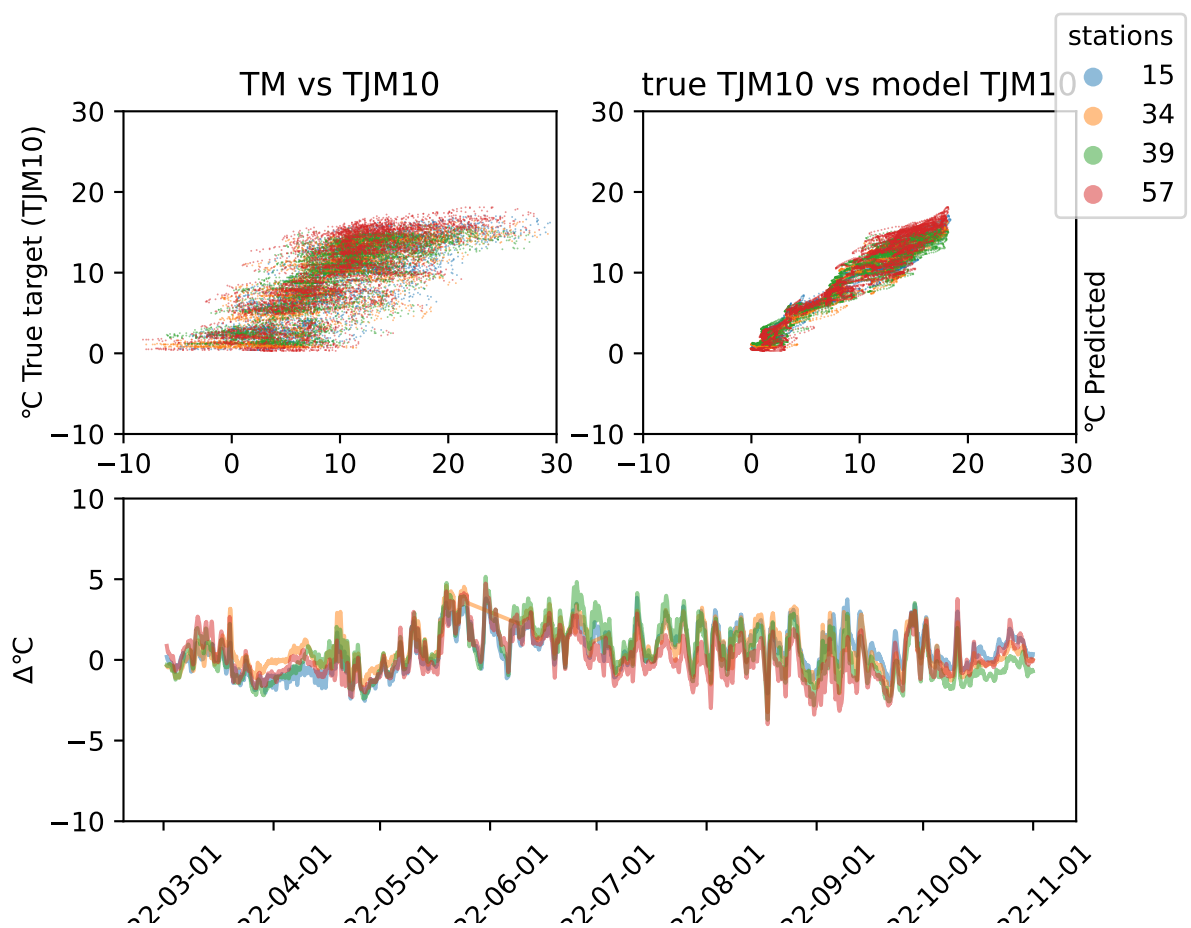


Figure 81: Difference plot for BiLSTM model in year 2022 and region Trøndelag at depth 10. The station names can be found in table 1.

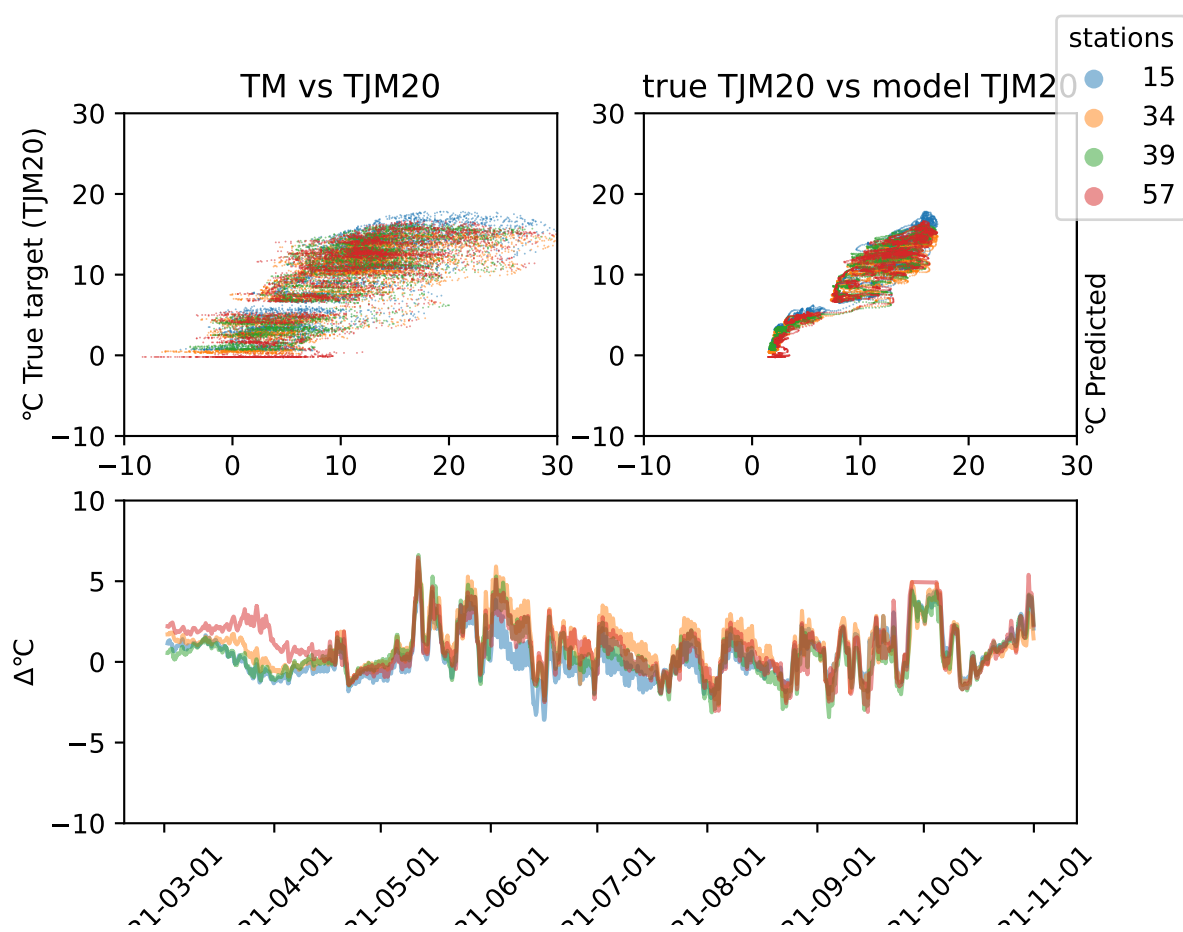


Figure 82: Difference plot for BiLSTM model in year 2021 and region Trøndelagat depth 20. The station names can be found in table 1.

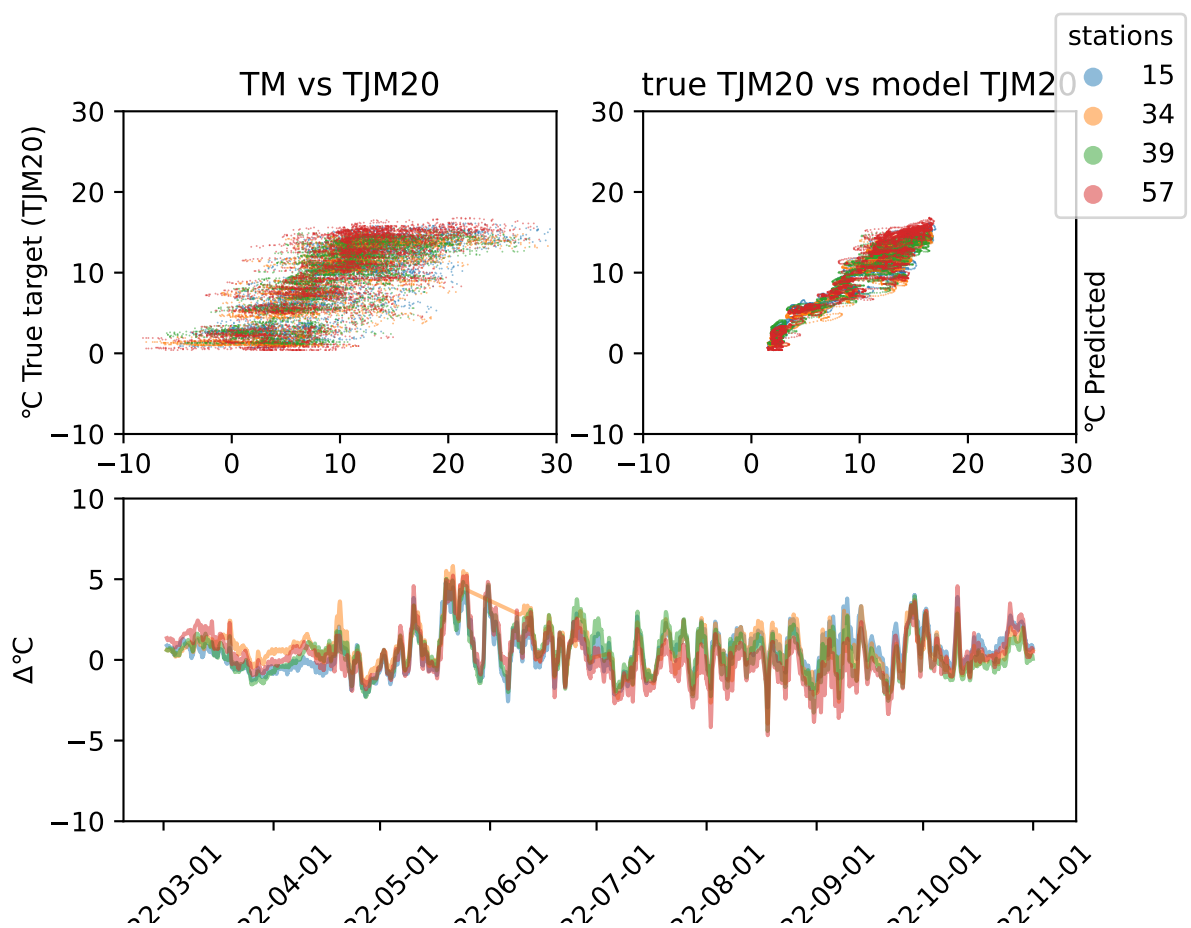


Figure 83: Difference plot for BiLSTM model in year 2022 and region Trøndelag at depth 20. The station names can be found in table 1.

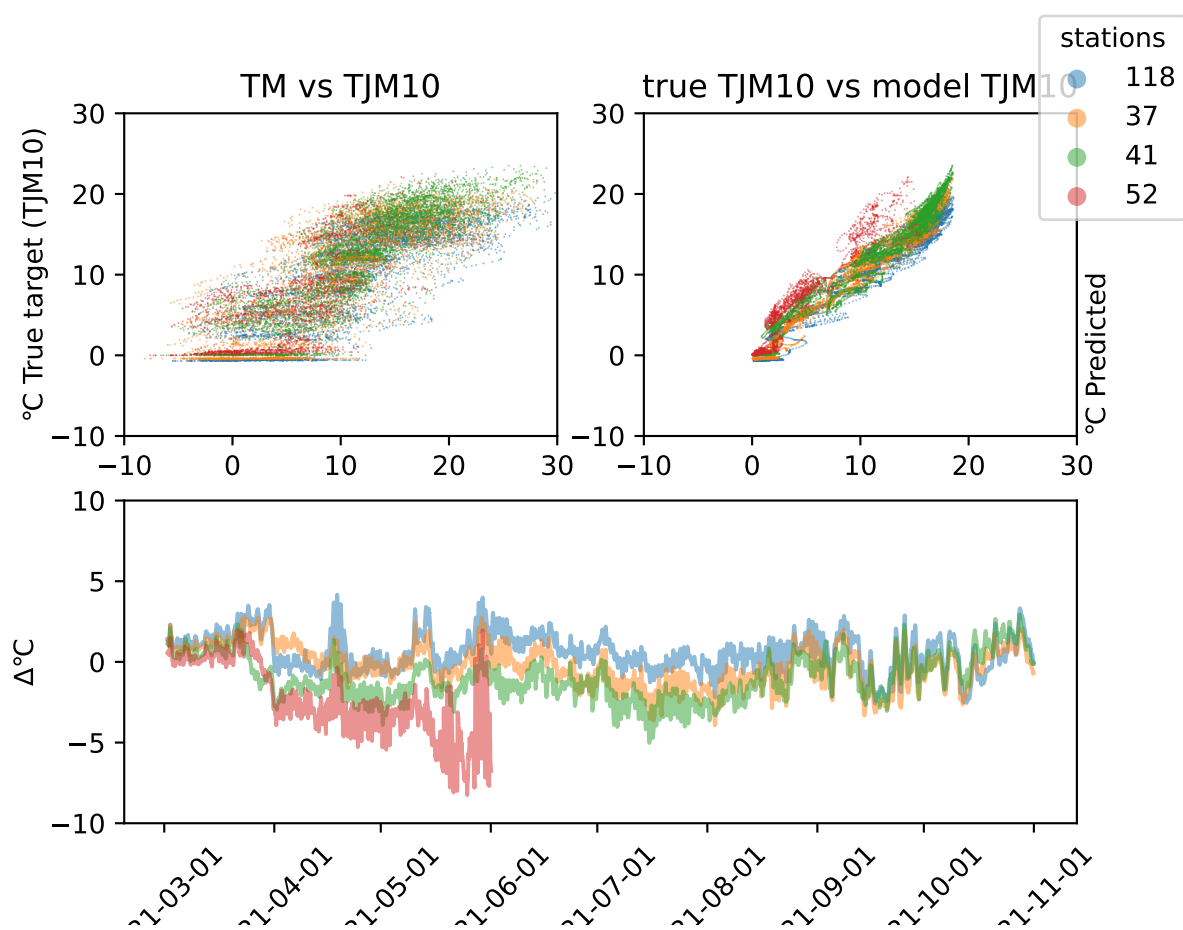


Figure 84: Difference plot for BiLSTM model in year 2021 and region Østfoldat depth 10. The station names can be found in table 1.

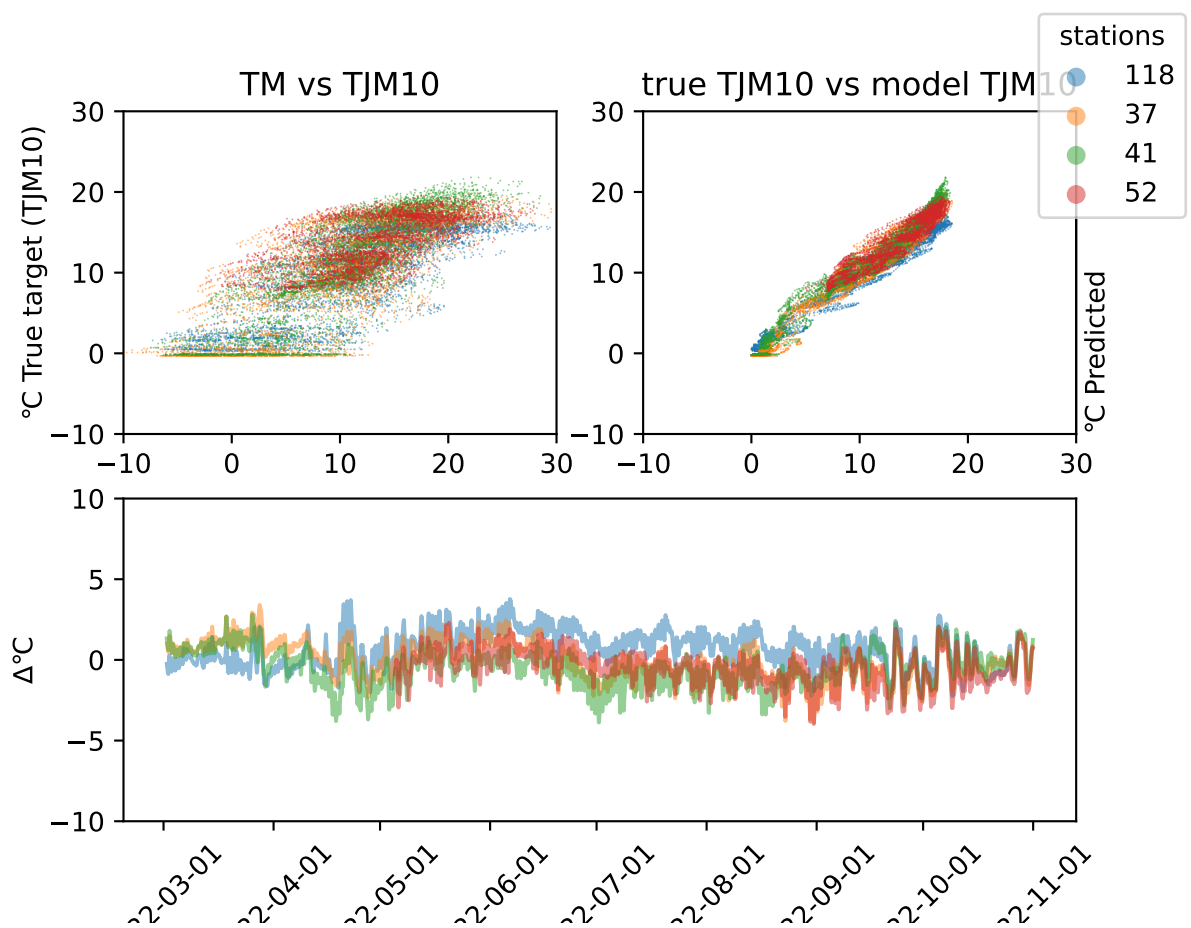


Figure 85: Difference plot for BiLSTM model in year 2022 and region Østfoldat depth 10. The station names can be found in table 1.

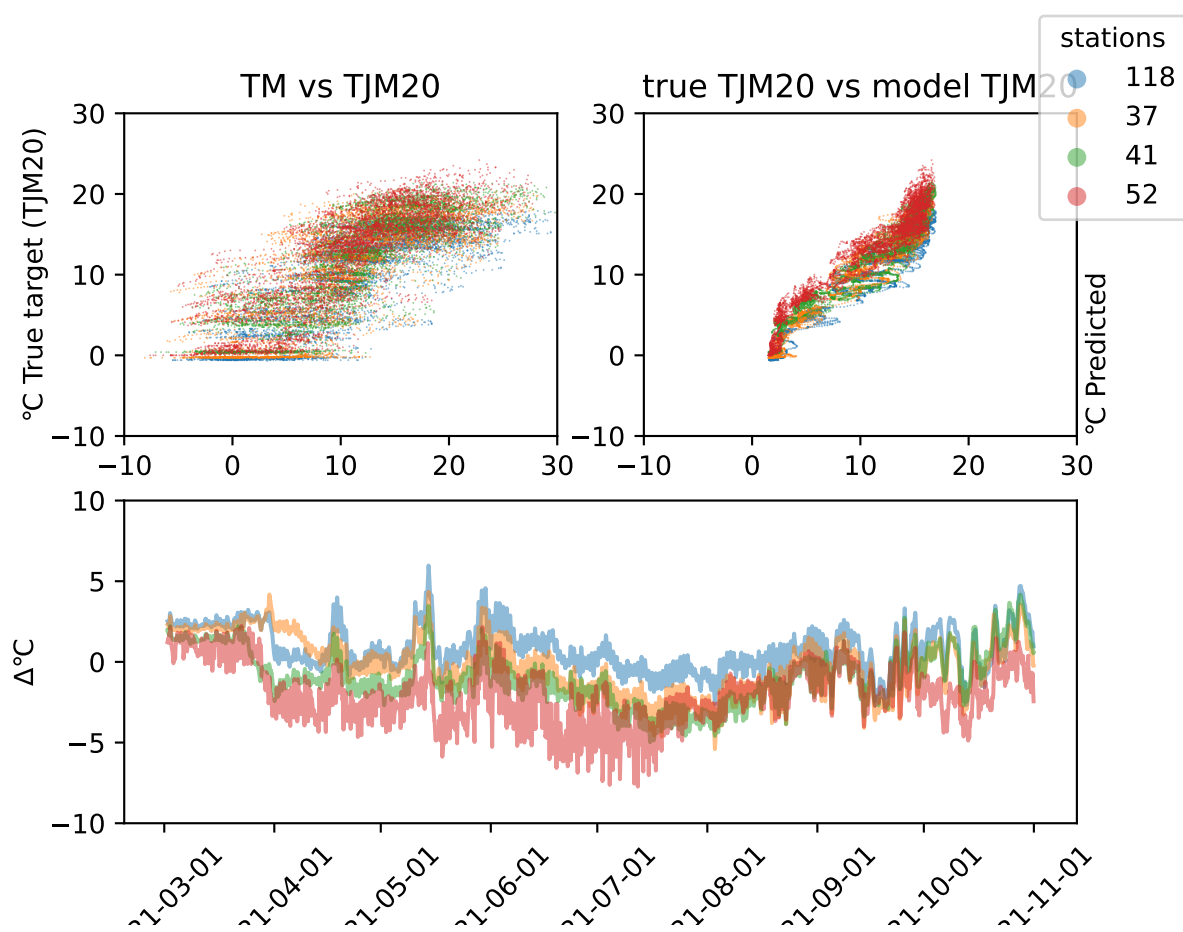


Figure 86: Difference plot for BiLSTM model in year 2021 and region Østfoldat depth 20. The station names can be found in table 1.

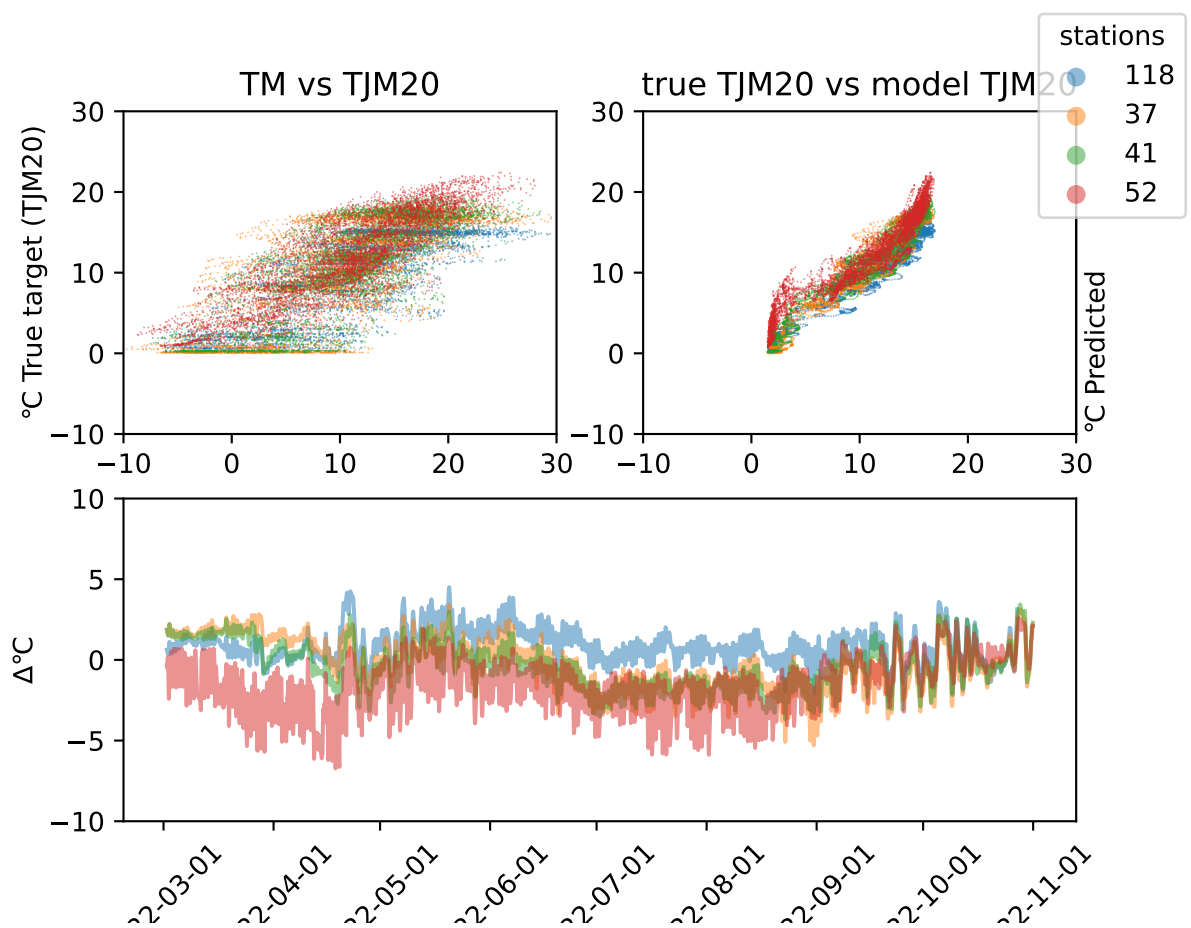


Figure 87: Difference plot for BiLSTM model in year 2022 and region Østfoldat depth 20. The station names can be found in table 1.

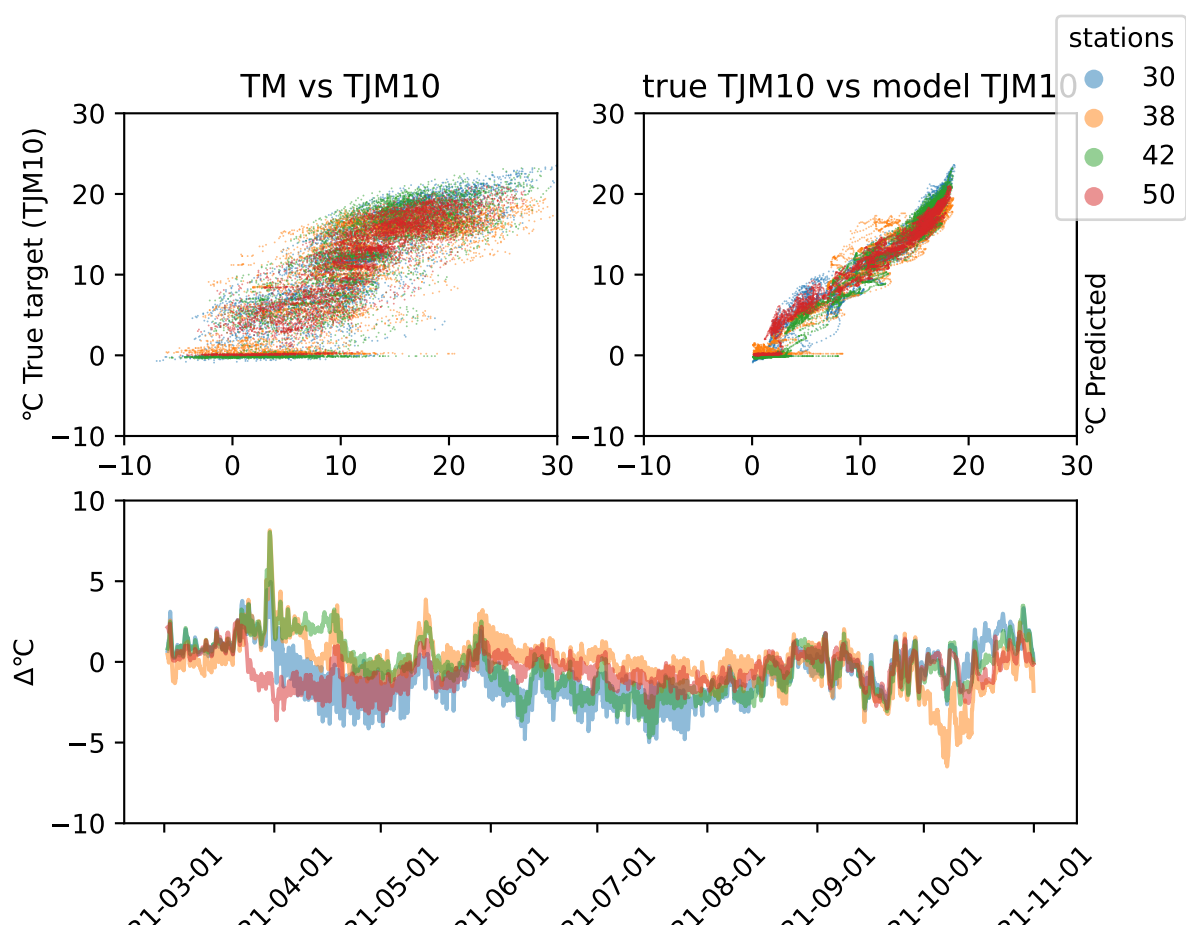


Figure 88: Difference plot for BiLSTM model in year 2021 and region Vestfoldat depth 10. The station names can be found in table 1.

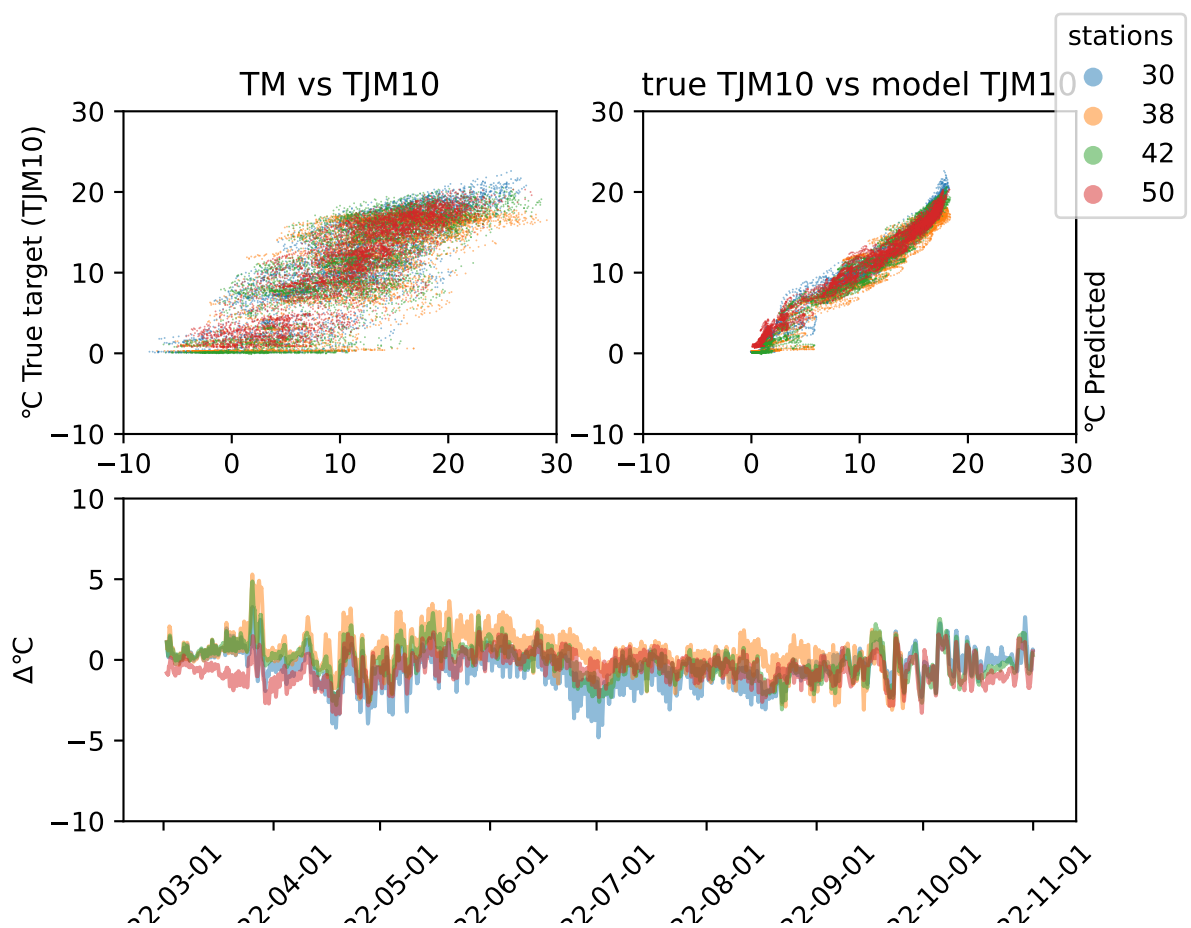


Figure 89: Difference plot for BiLSTM model in year 2022 and region Vestfoldat depth 10. The station names can be found in table 1.

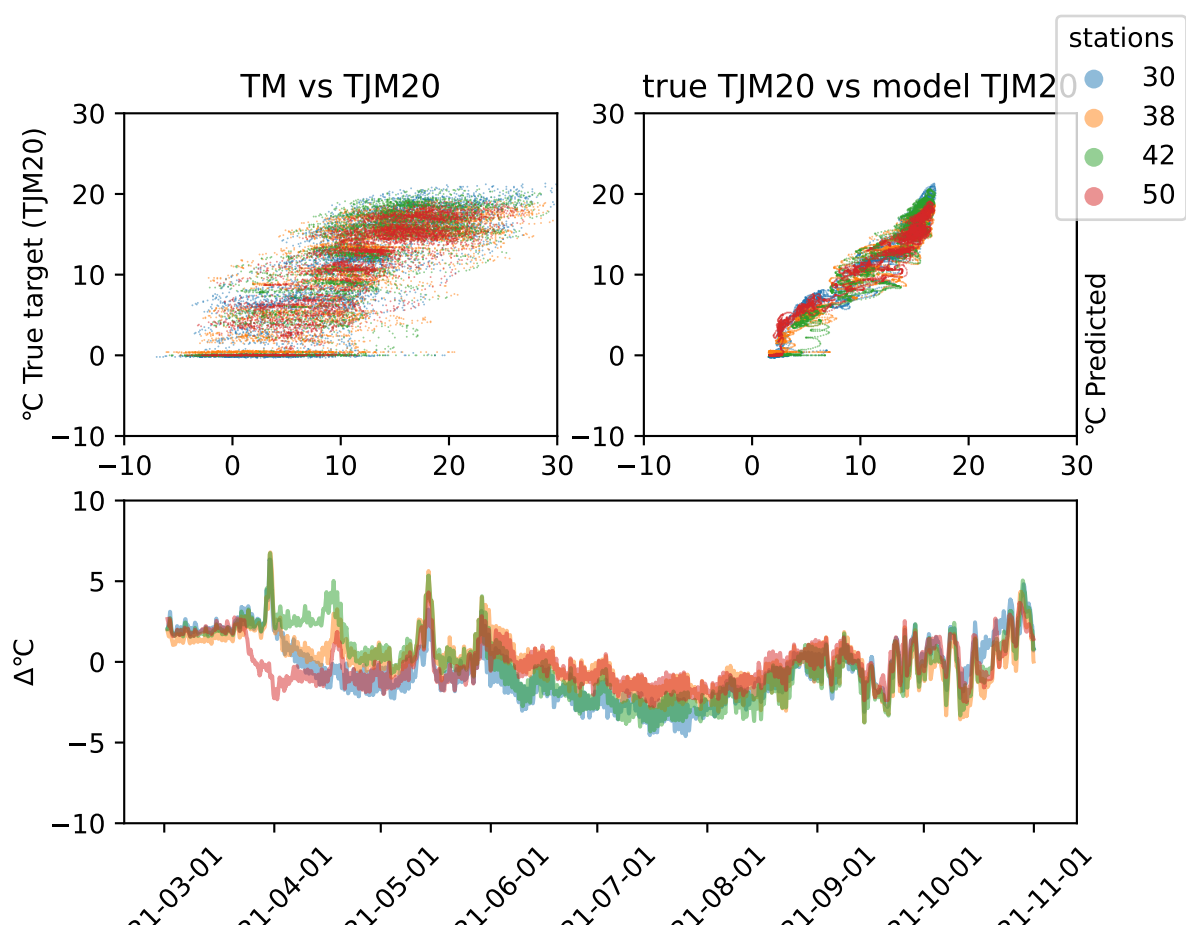


Figure 90: Difference plot for BiLSTM model in year 2021 and region Vestfoldat depth 20. The station names can be found in table 1.

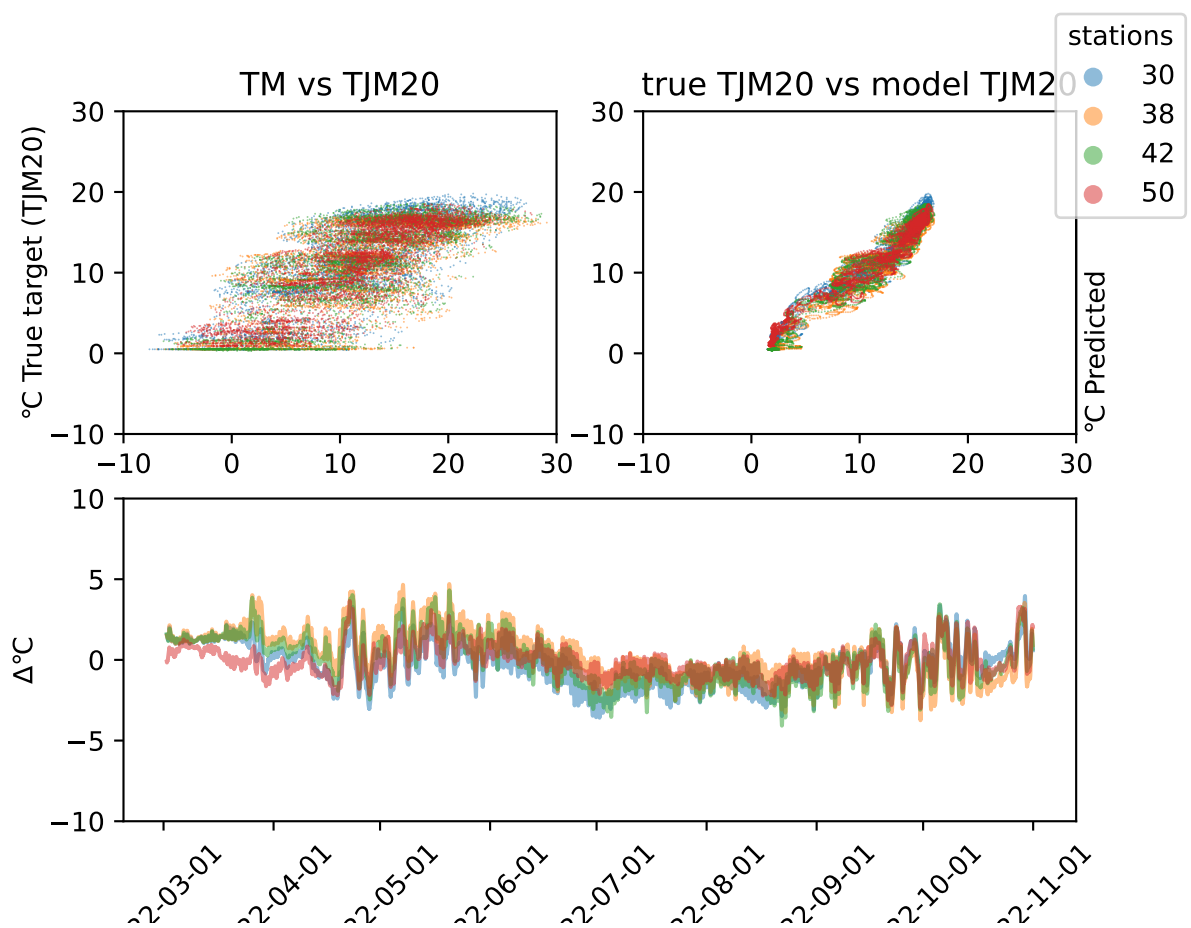


Figure 91: Difference plot for BiLSTM model in year 2022 and region Vestfoldat depth 20. The station names can be found in table 1.

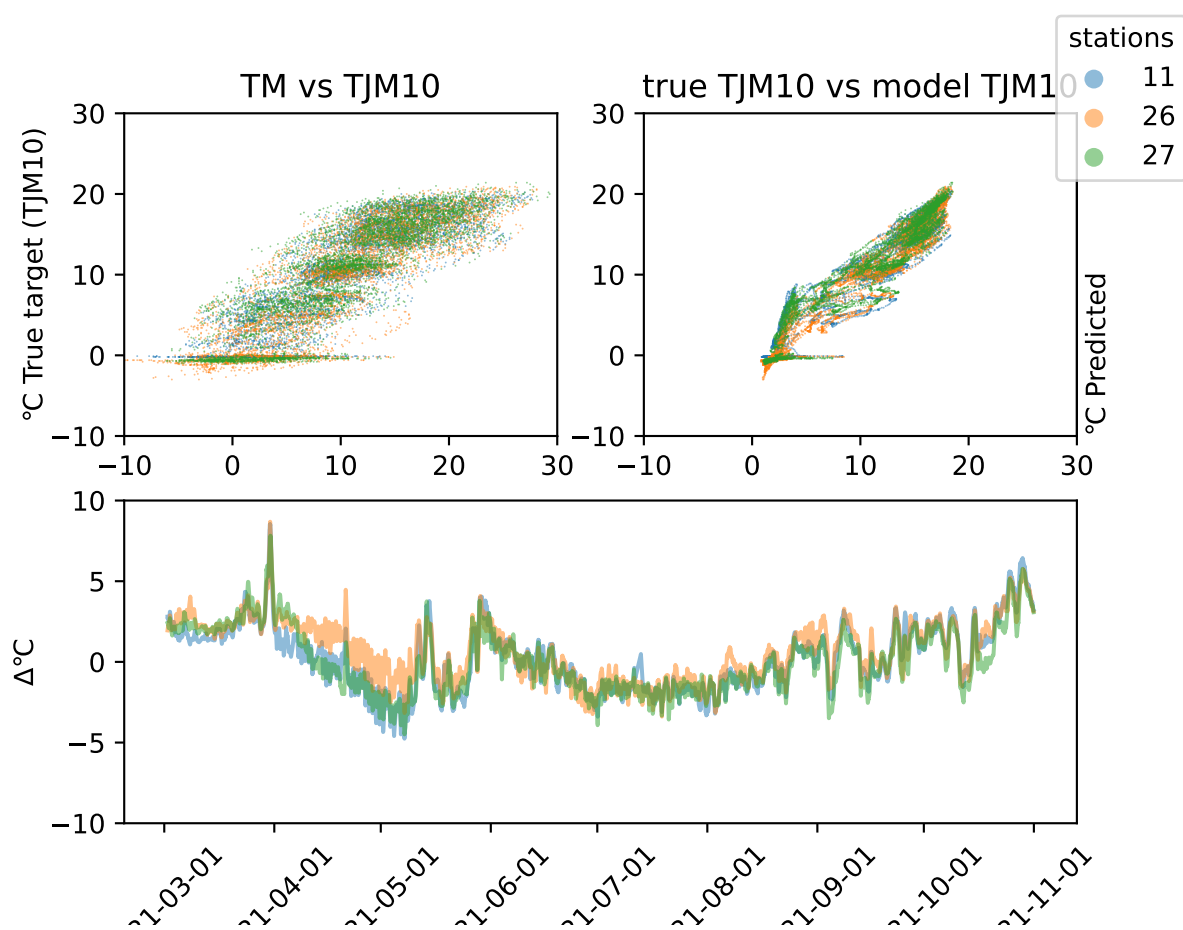


Figure 92: Difference plot for LSTM model in year 2021 and region Innlandet at depth 10. The station names can be found in table 1.

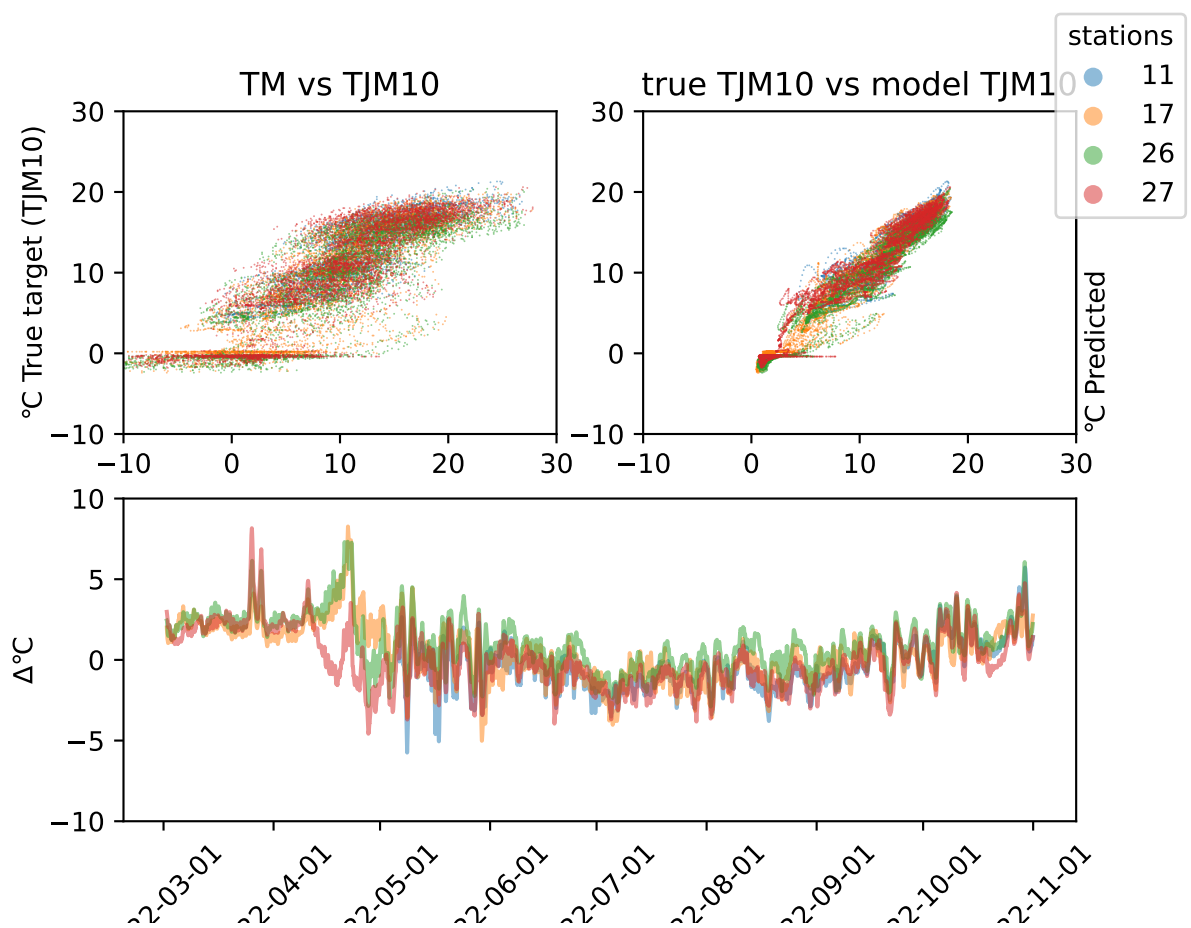


Figure 93: Difference plot for LSTM model in year 2022 and region Innlandet at depth 10. The station names can be found in table 1.

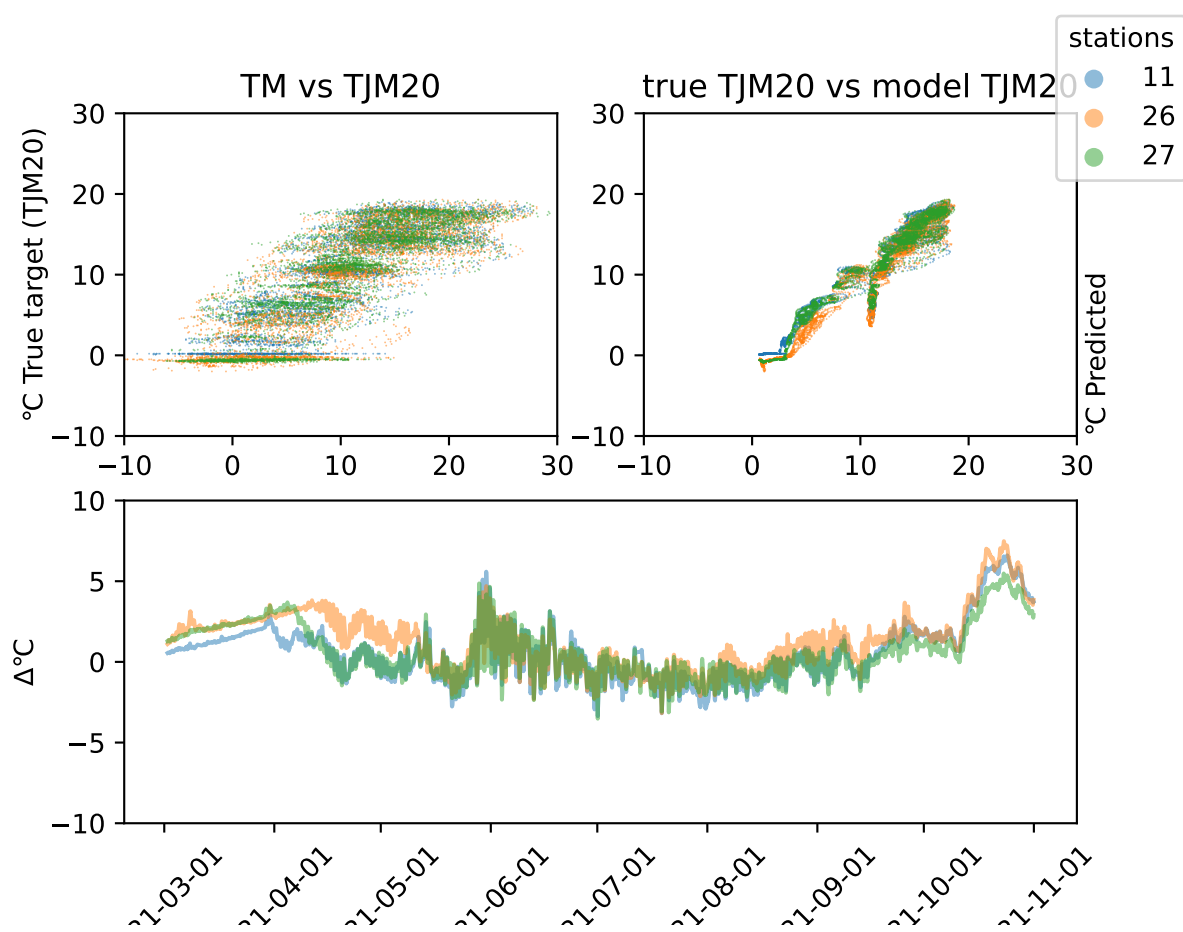


Figure 94: Difference plot for LSTM model in year 2021 and region Innlandet at depth 20. The station names can be found in table 1.

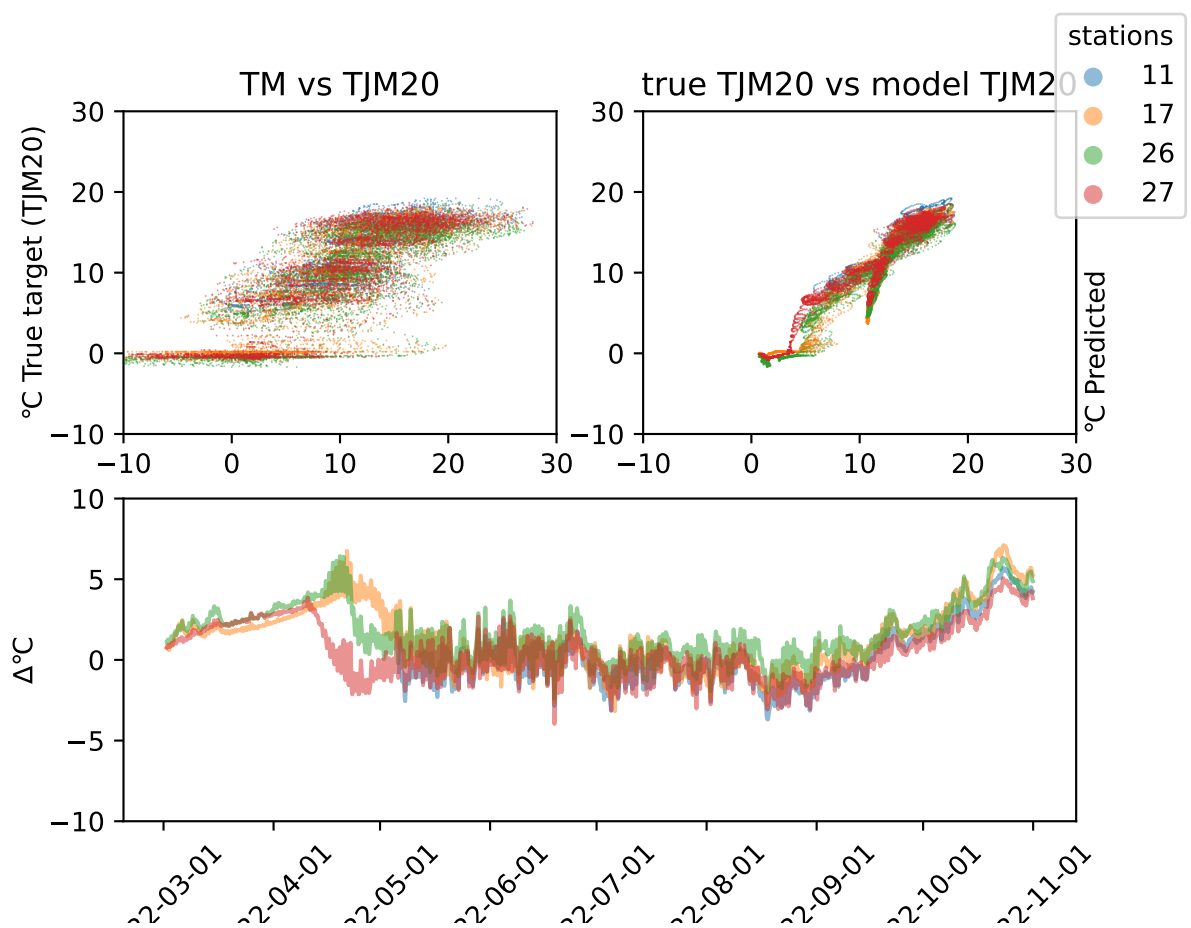


Figure 95: Difference plot for LSTM model in year 2022 and region Innlandetat depth 20. The station names can be found in table 1.

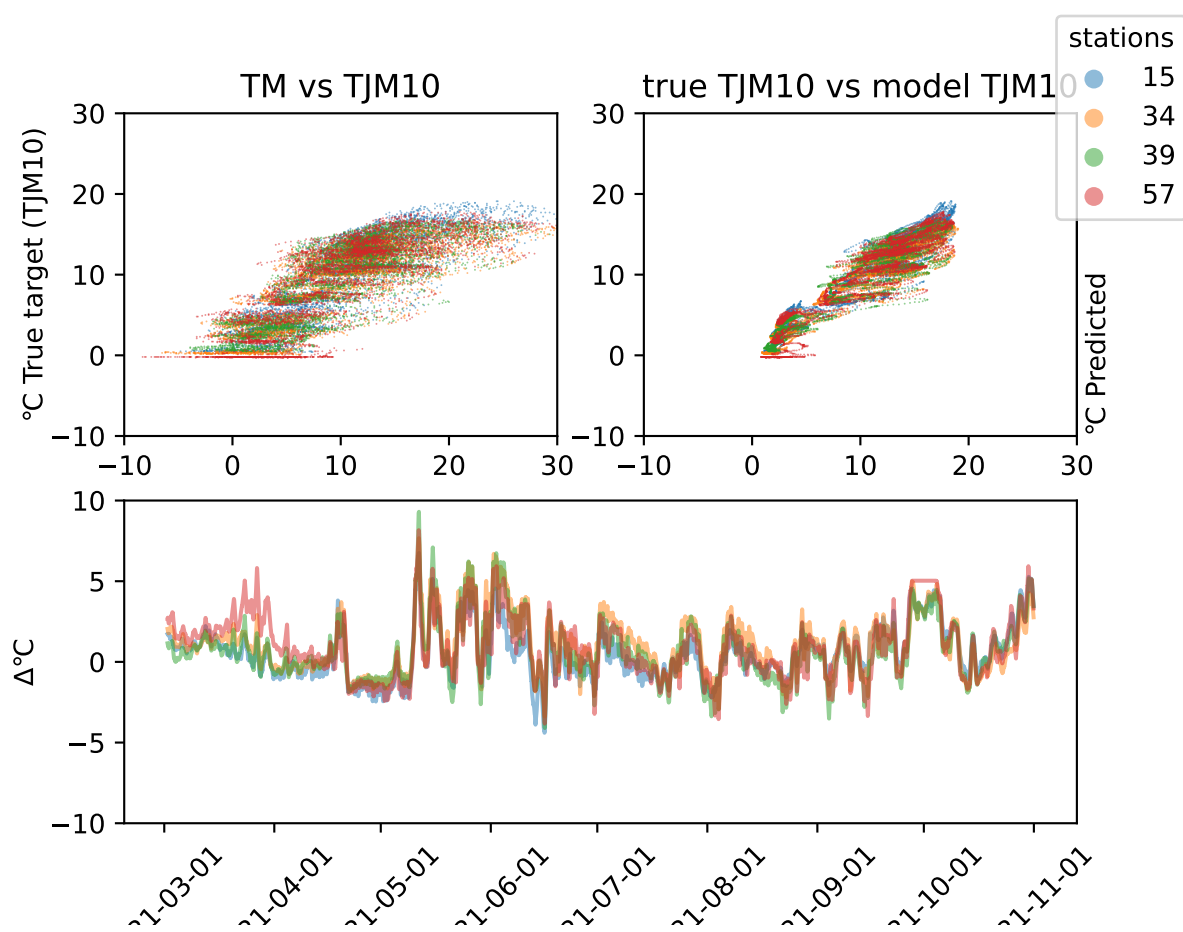


Figure 96: Difference plot for LSTM model in year 2021 and region Trøndelagat depth 10. The station names can be found in table 1.

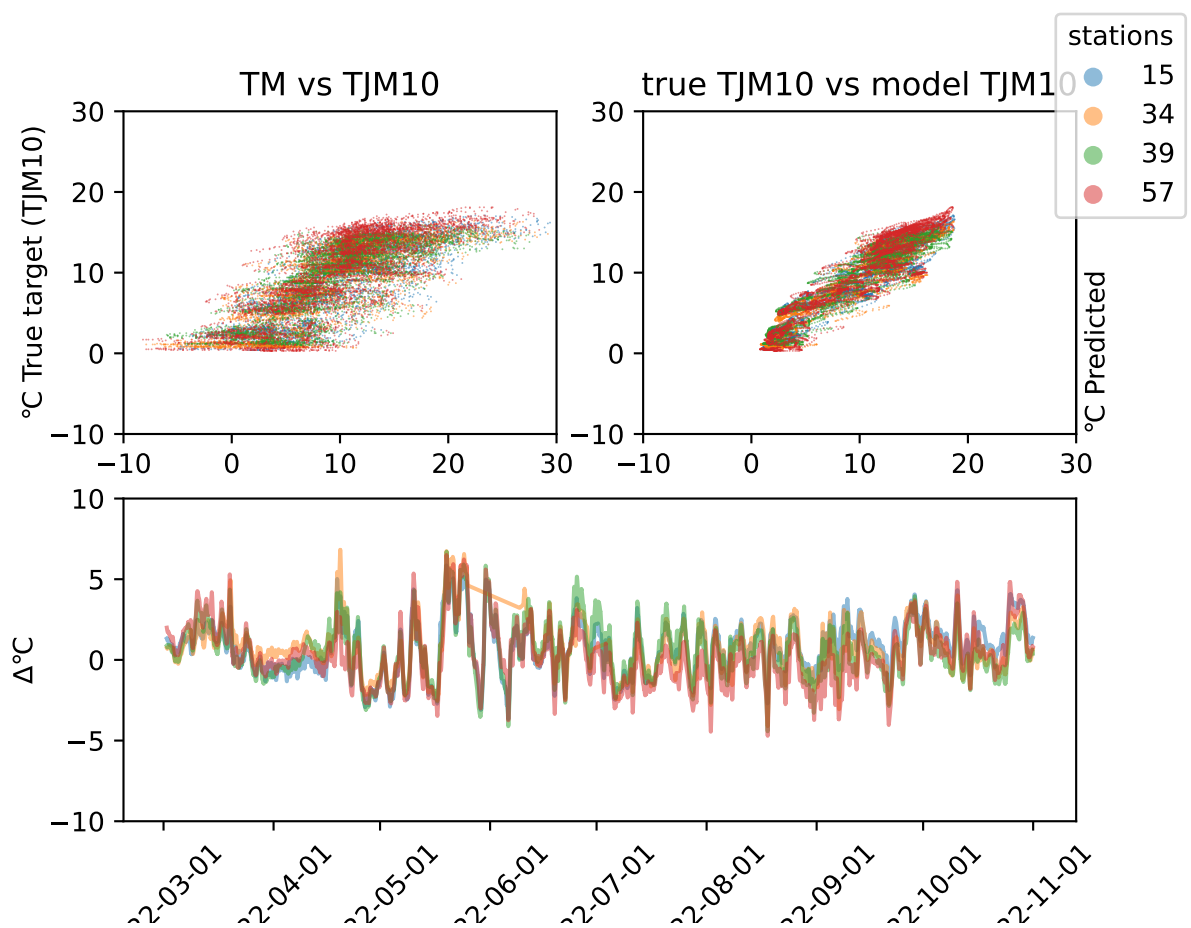


Figure 97: Difference plot for LSTM model in year 2022 and region Trøndelag at depth 10. The station names can be found in table 1.

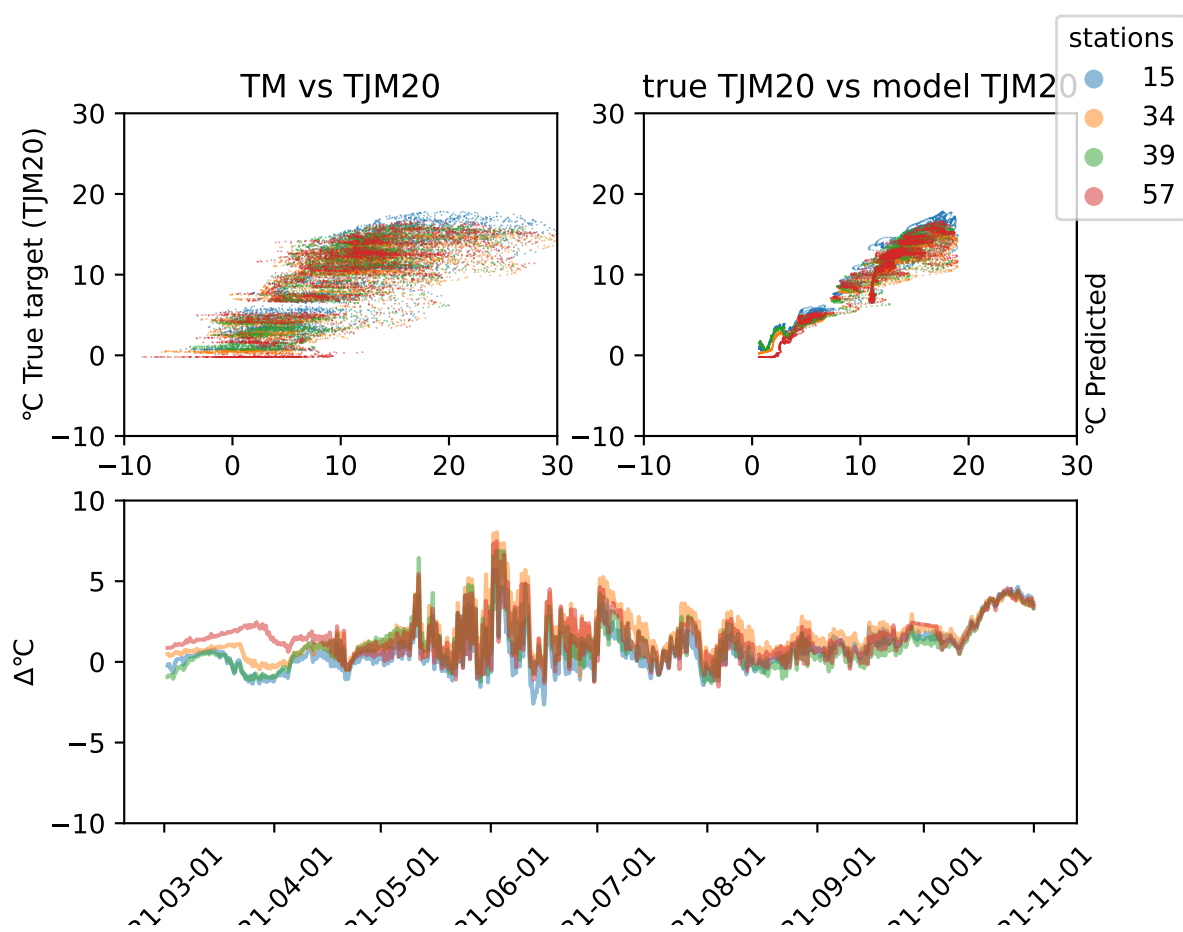


Figure 98: Difference plot for LSTM model in year 2021 and region Trøndelagat depth 20. The station names can be found in table 1.

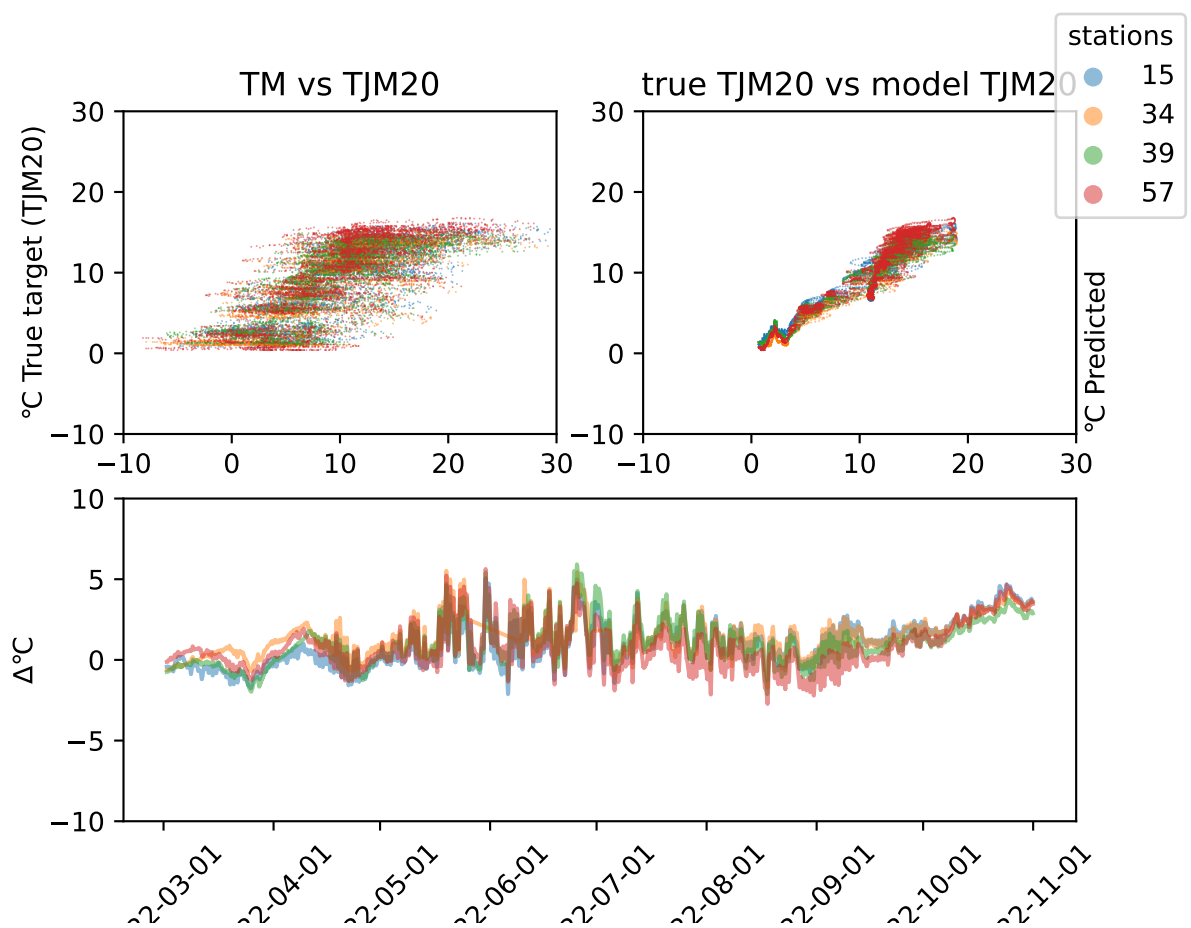


Figure 99: Difference plot for LSTM model in year 2022 and region Trøndelag at depth 20. The station names can be found in table 1.

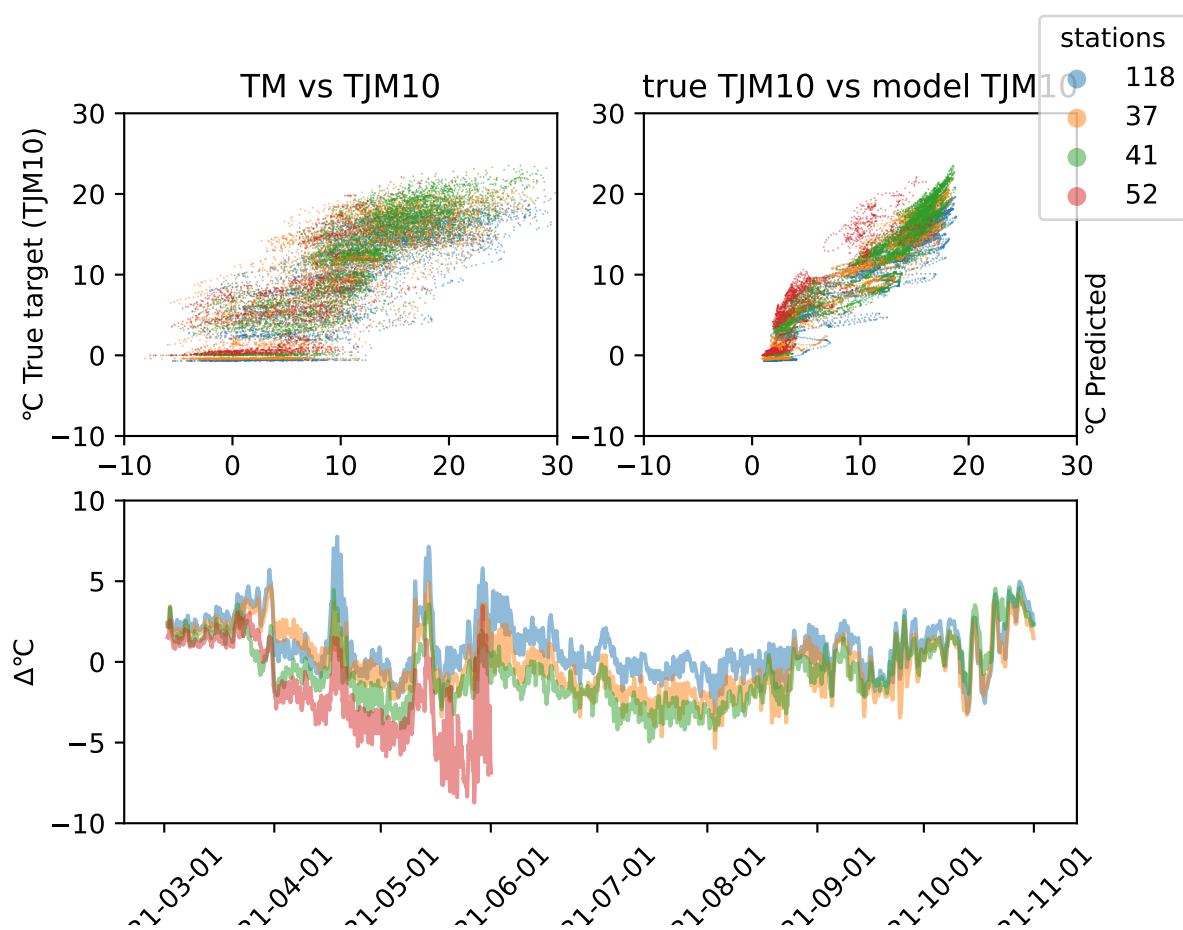


Figure 100: Difference plot for LSTM model in year 2021 and region Østfoldat depth 10. The station names can be found in table 1.

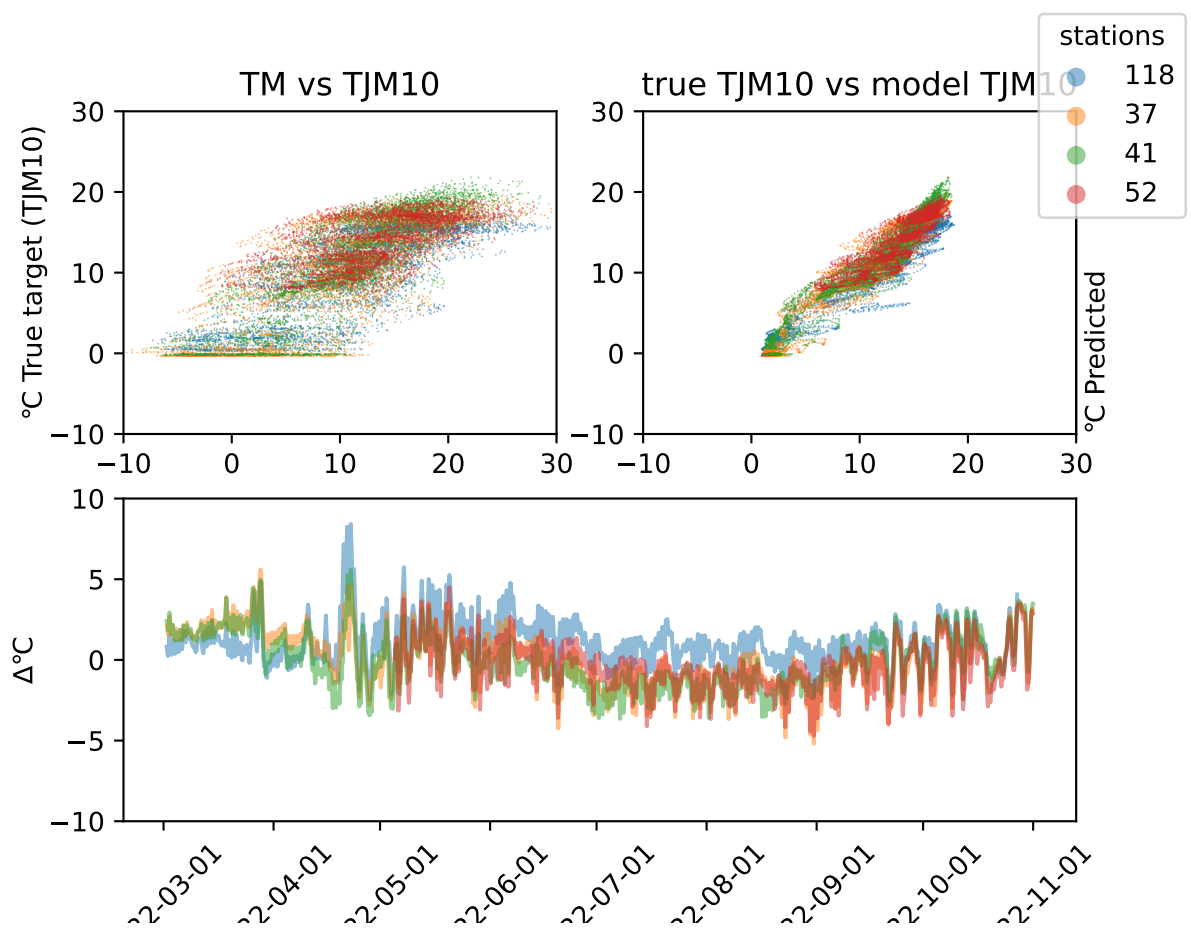


Figure 101: Difference plot for LSTM model in year 2022 and region Østfoldat depth 10. The station names can be found in table 1.

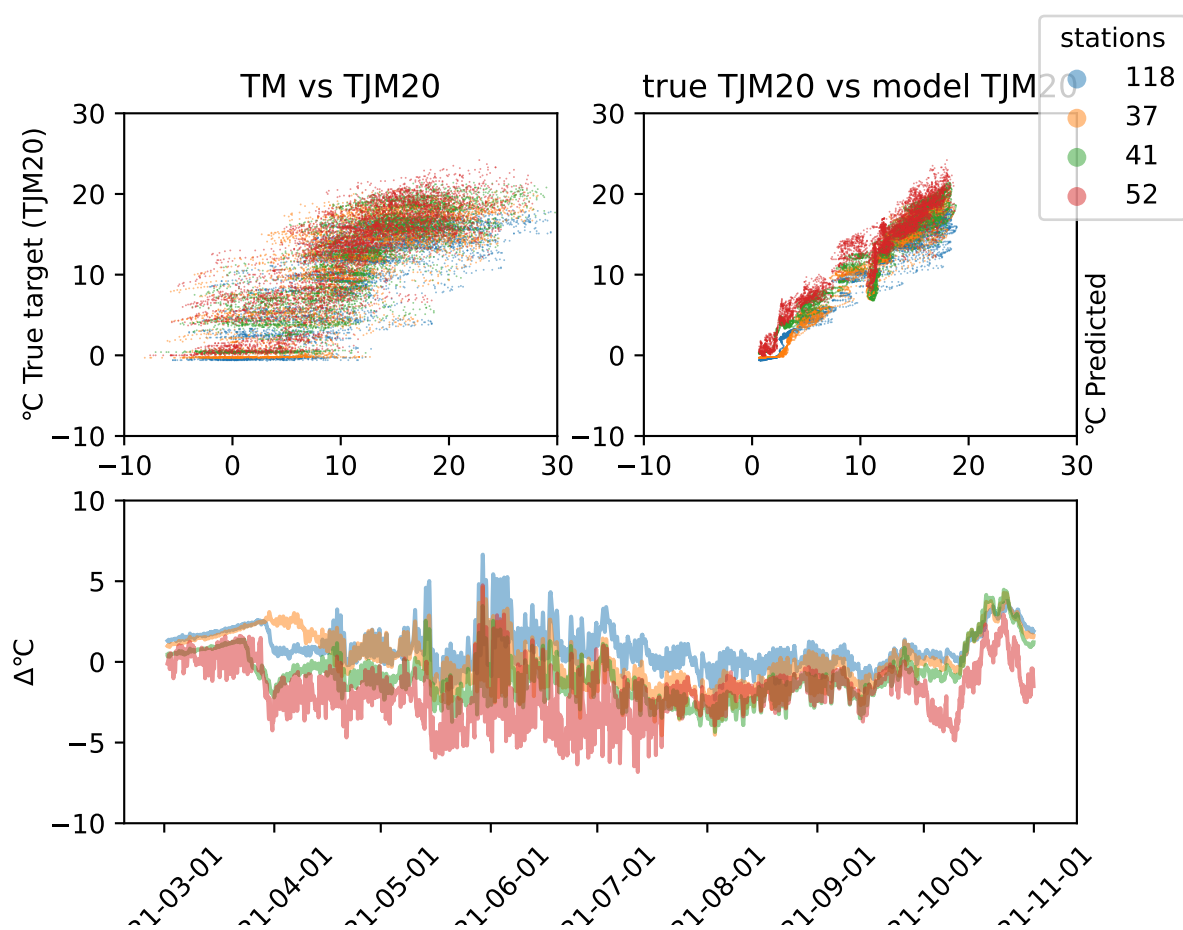


Figure 102: Difference plot for LSTM model in year 2021 and region Østfoldat depth 20. The station names can be found in table 1.

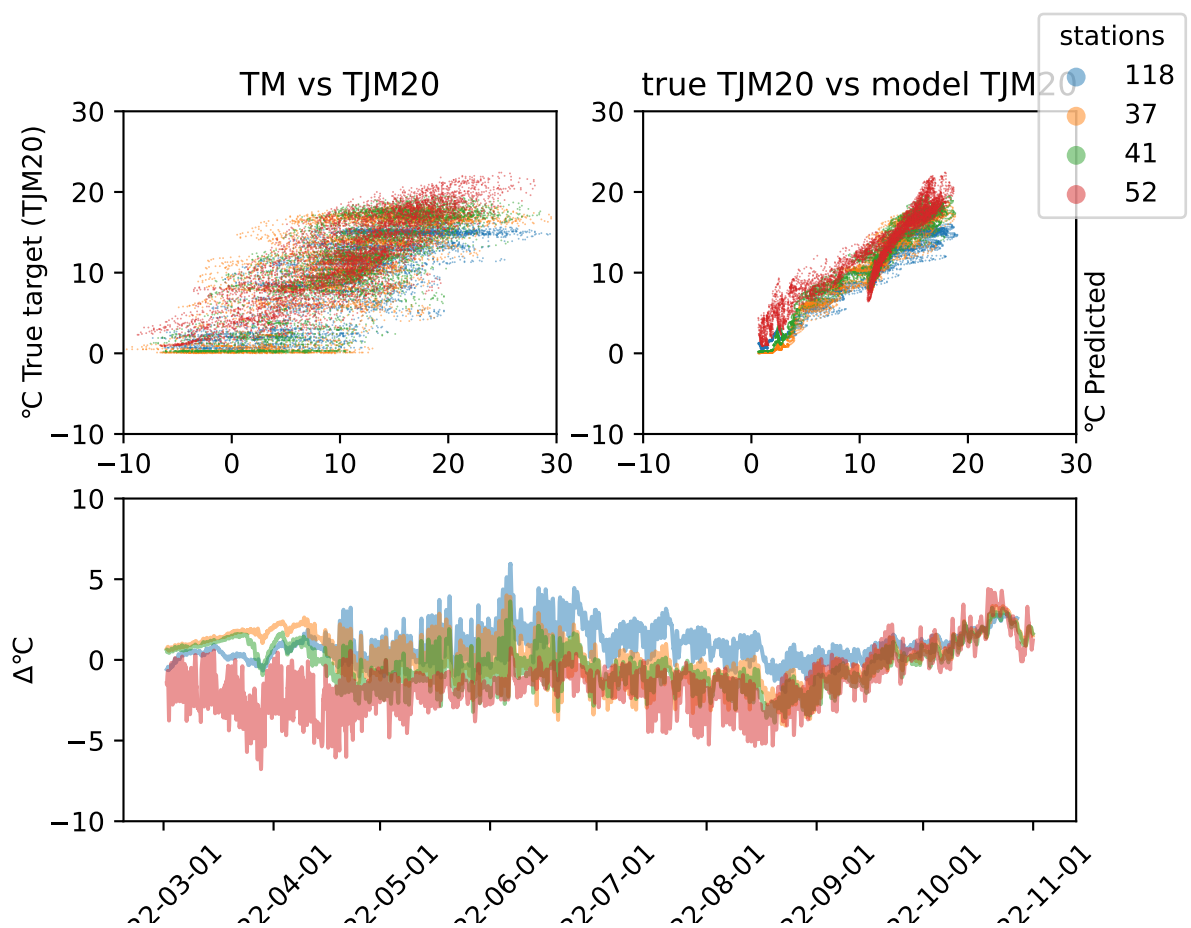


Figure 103: Difference plot for LSTM model in year 2022 and region Østfoldat depth 20. The station names can be found in table 1.

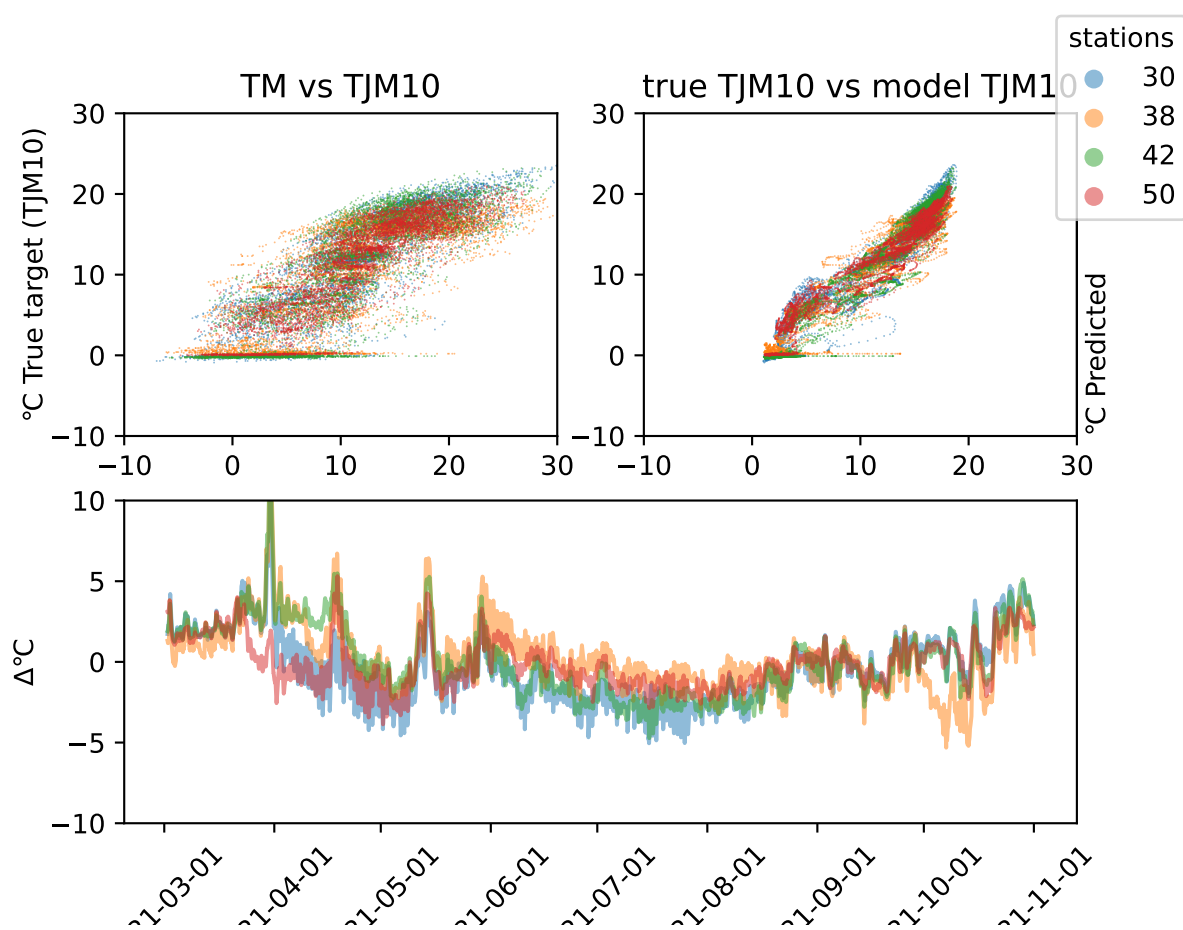


Figure 104: Difference plot for LSTM model in year 2021 and region Vestfoldat depth 10. The station names can be found in table 1.

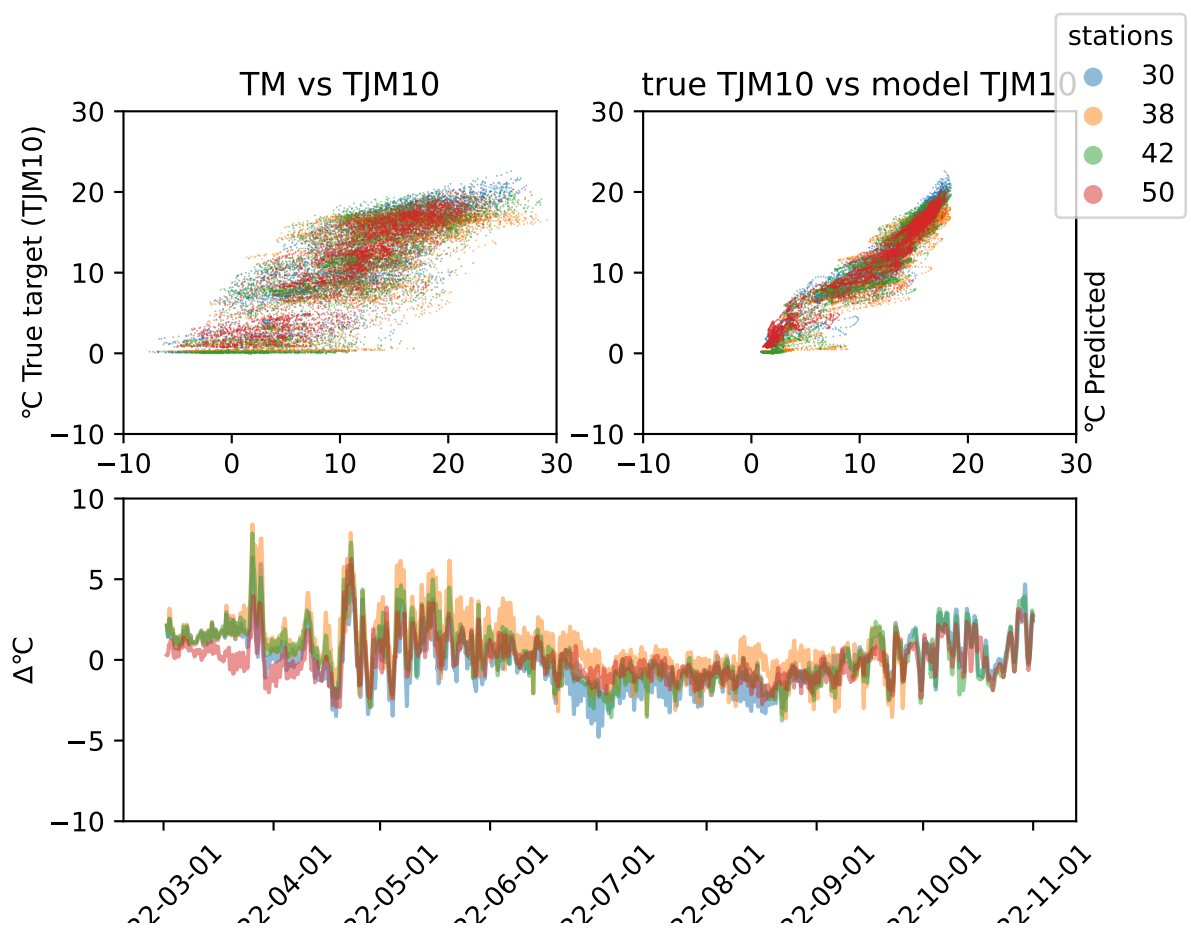


Figure 105: Difference plot for LSTM model in year 2022 and region Vestfoldat depth 10. The station names can be found in table 1.

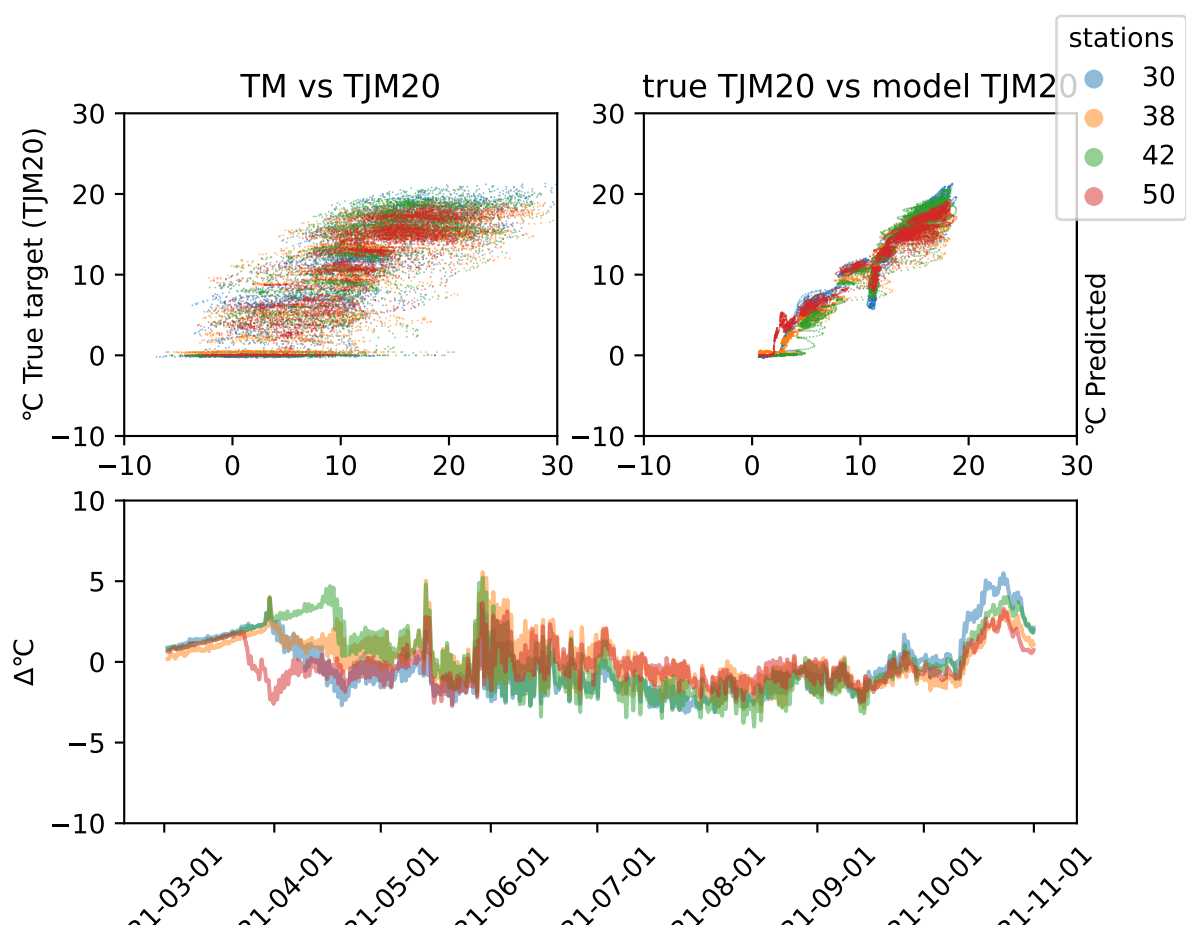


Figure 106: Difference plot for LSTM model in year 2021 and region Vestfoldat depth 20. The station names can be found in table 1.

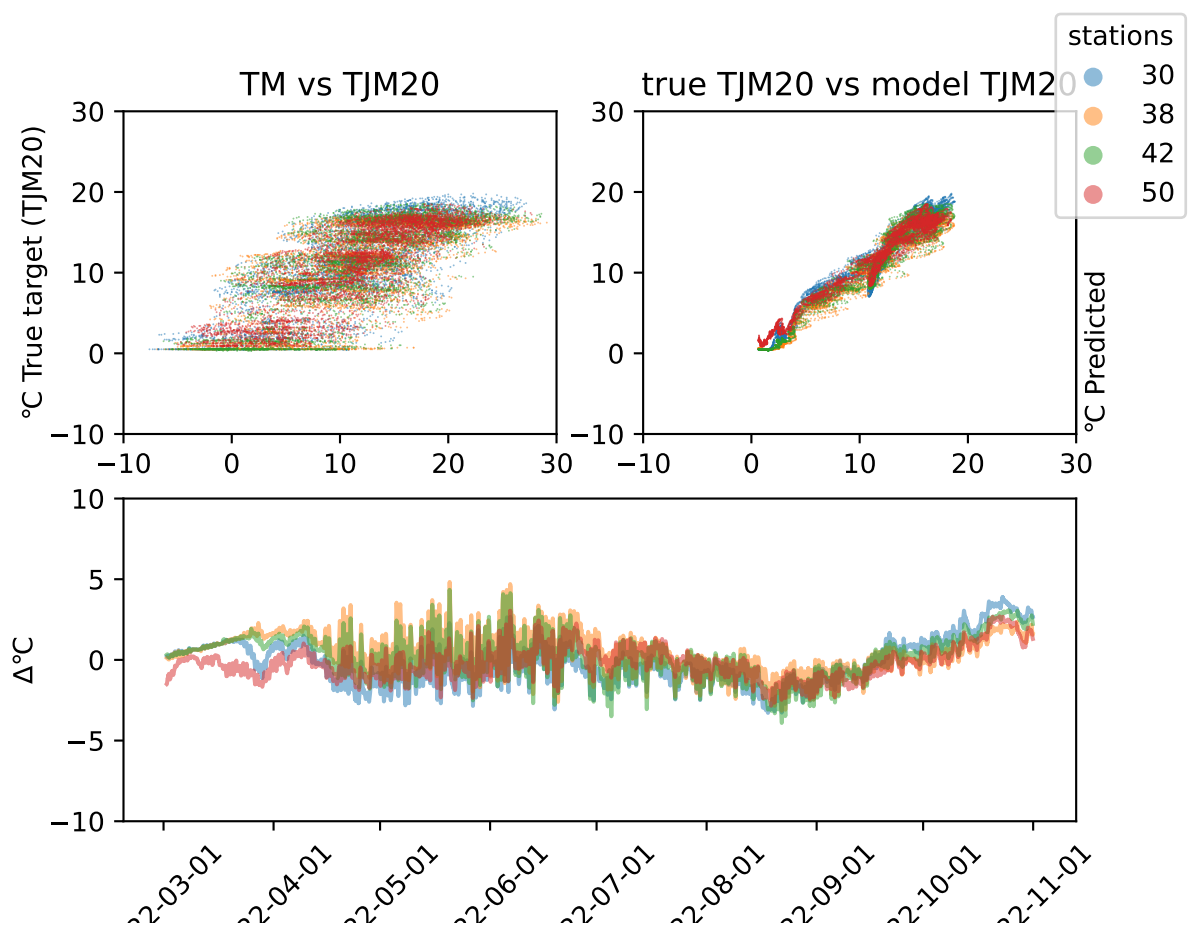


Figure 107: Difference plot for LSTM model in year 2022 and region Vestfoldat depth 20. The station names can be found in table 1.

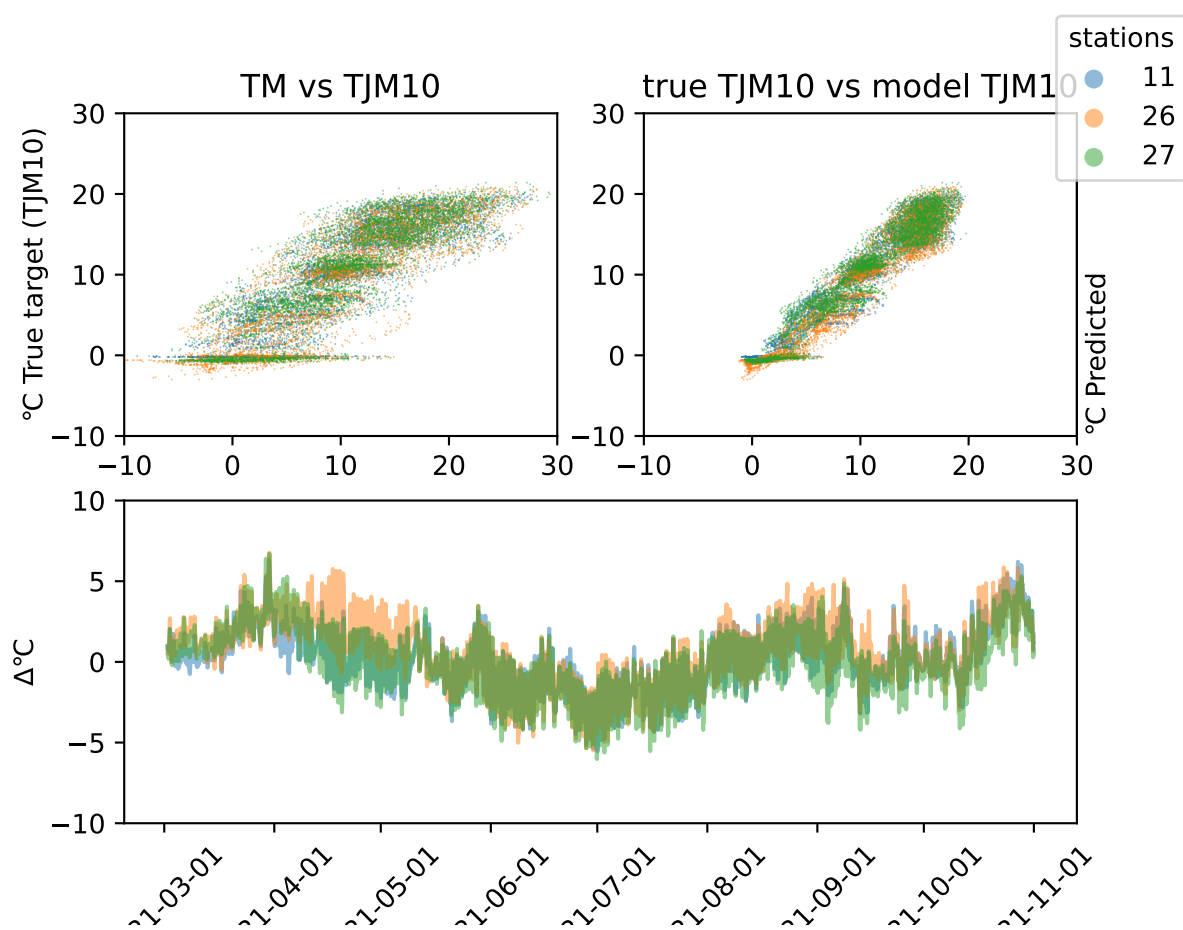


Figure 108: Difference plot for GRU model in year 2021 and region Innlandet at depth 10. The station names can be found in table 1.

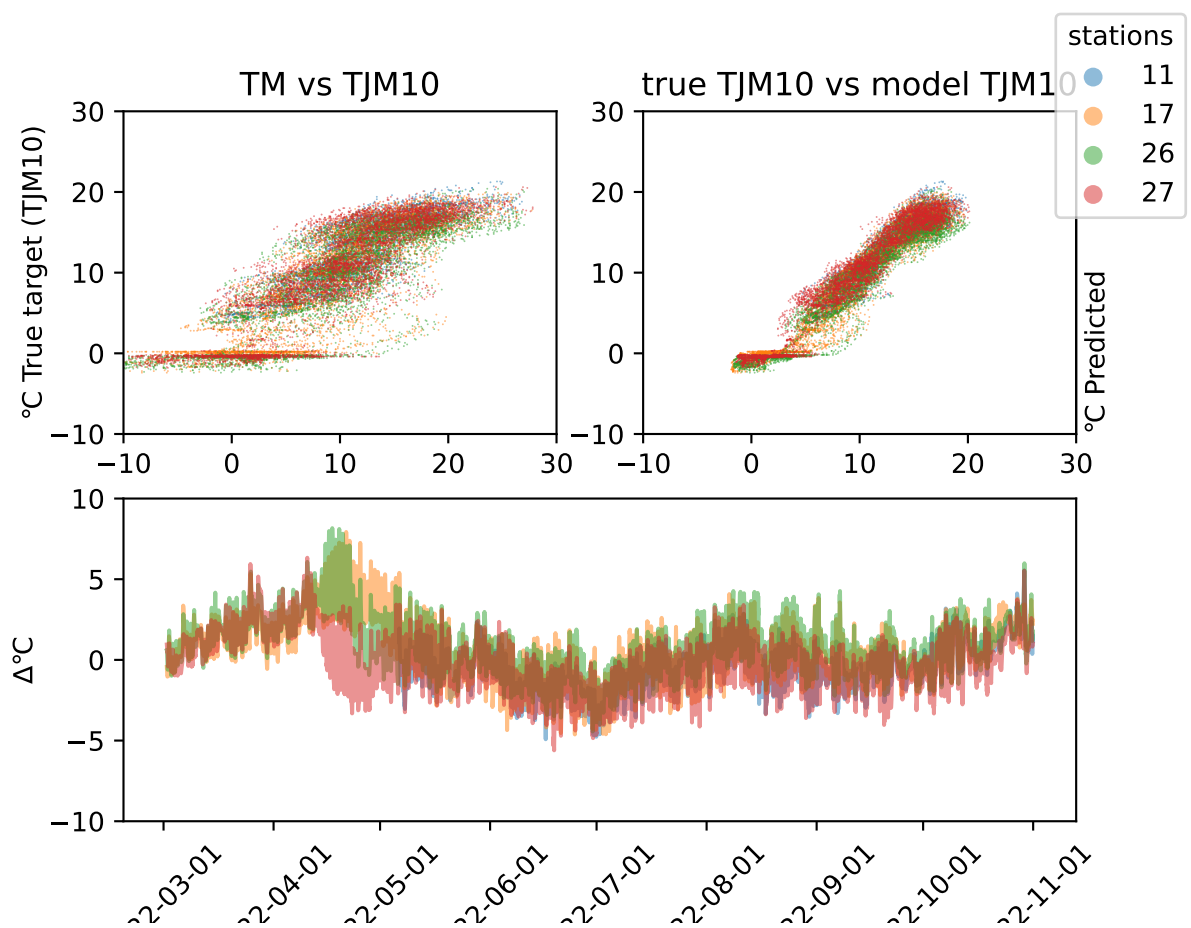


Figure 109: Difference plot for GRU model in year 2022 and region Innlandet at depth 10. The station names can be found in table 1.

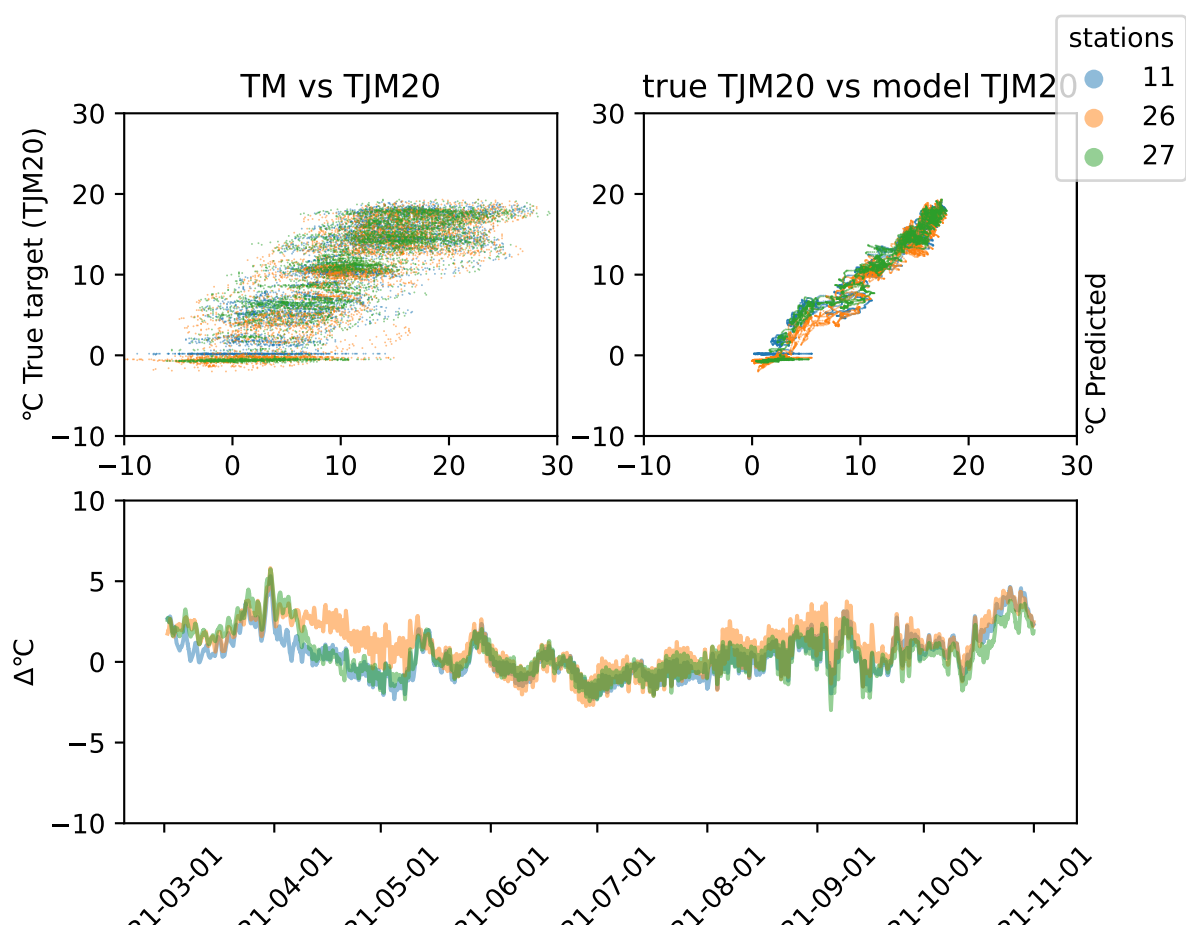


Figure 110: Difference plot for GRU model in year 2021 and region Innlandet at depth 20. The station names can be found in table 1.

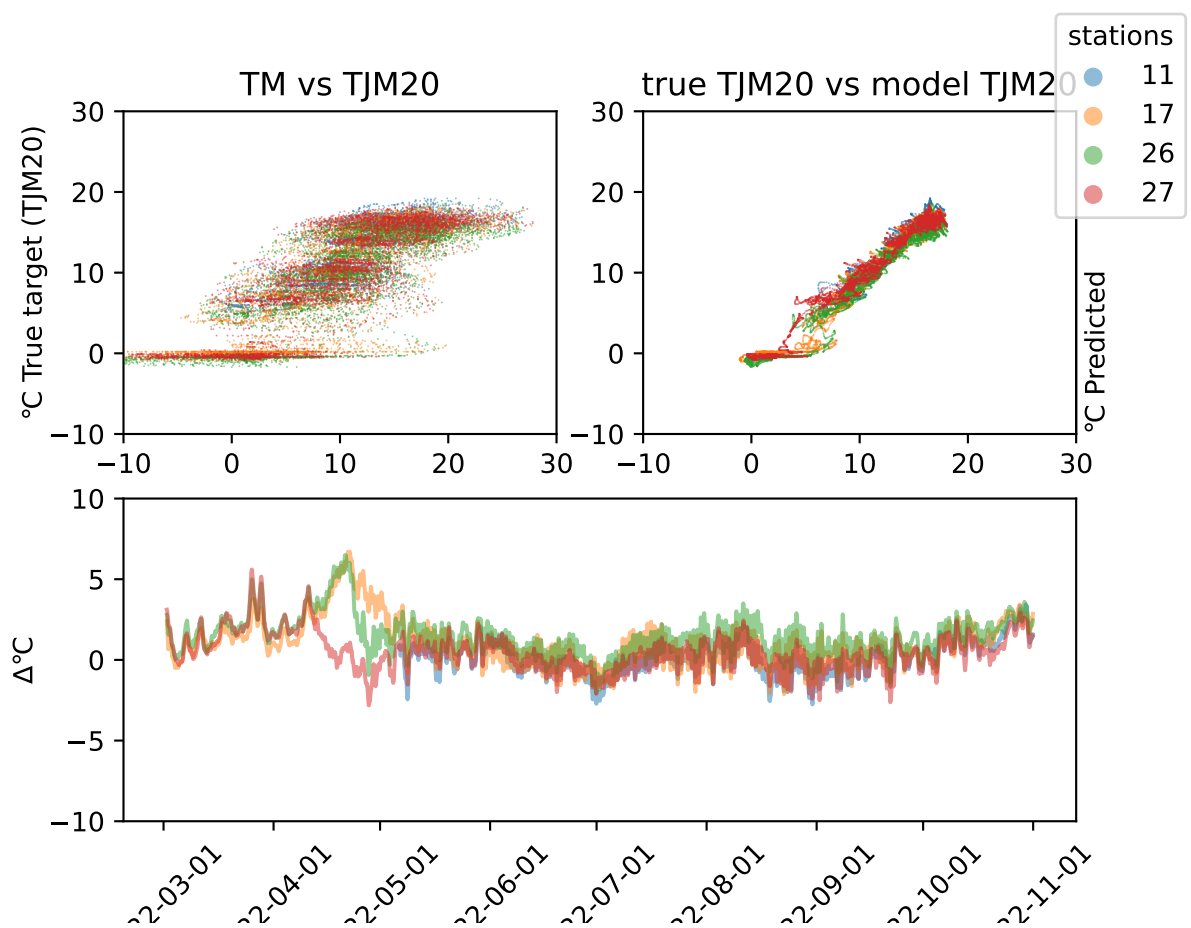


Figure 111: Difference plot for GRU model in year 2022 and region Innlandet at depth 20. The station names can be found in table 1.

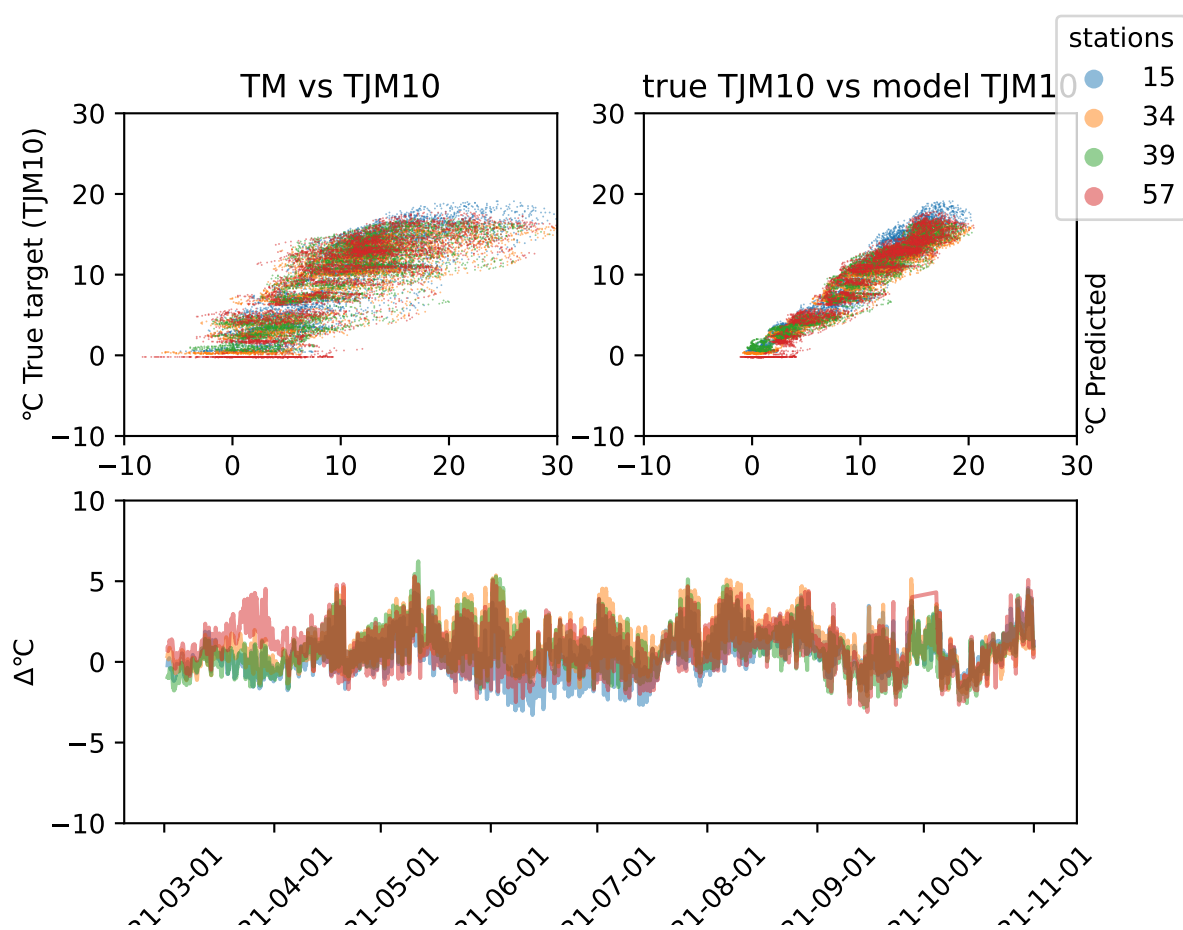


Figure 112: Difference plot for GRU model in year 2021 and region Trøndelagat depth 10. The station names can be found in table 1.

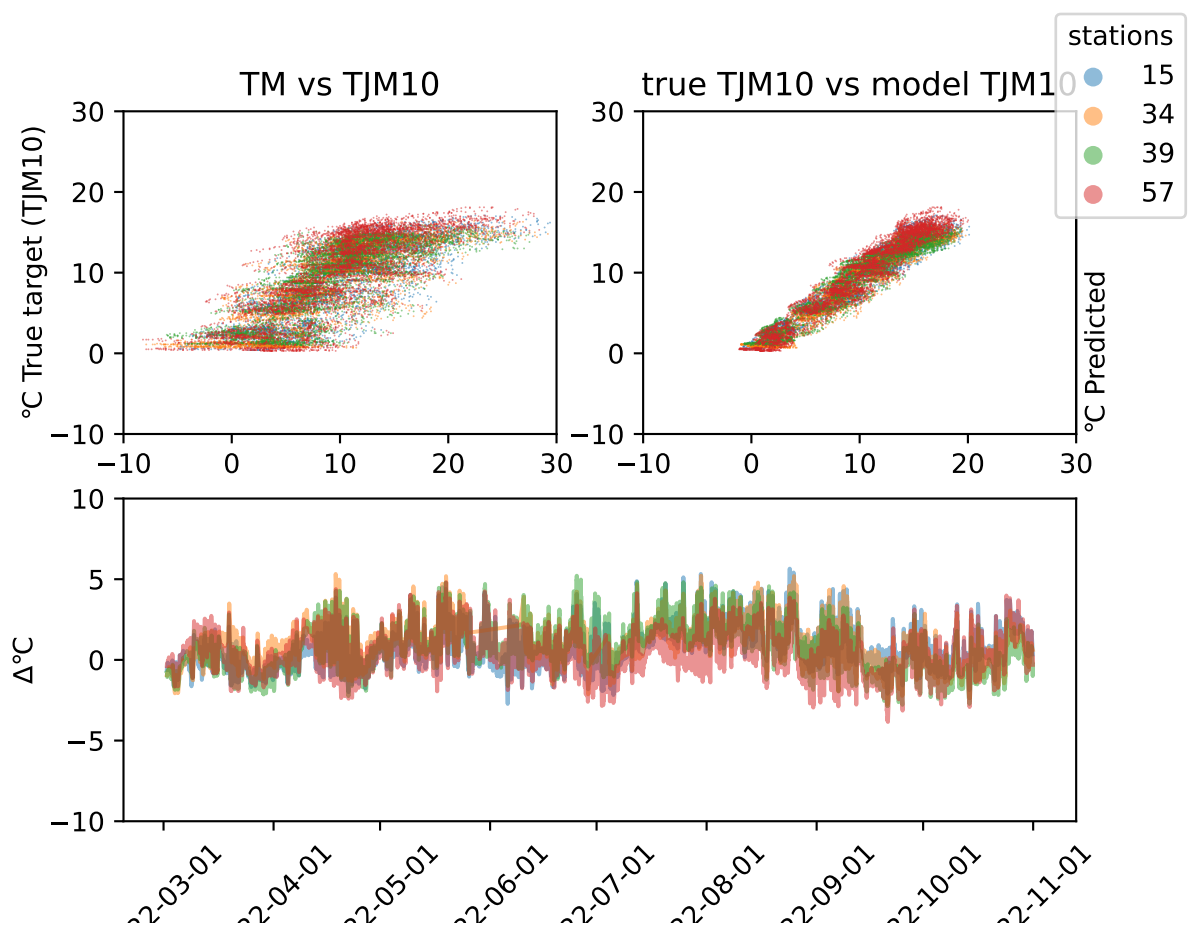


Figure 113: Difference plot for GRU model in year 2022 and region Trøndelag at depth 10. The station names can be found in table 1.

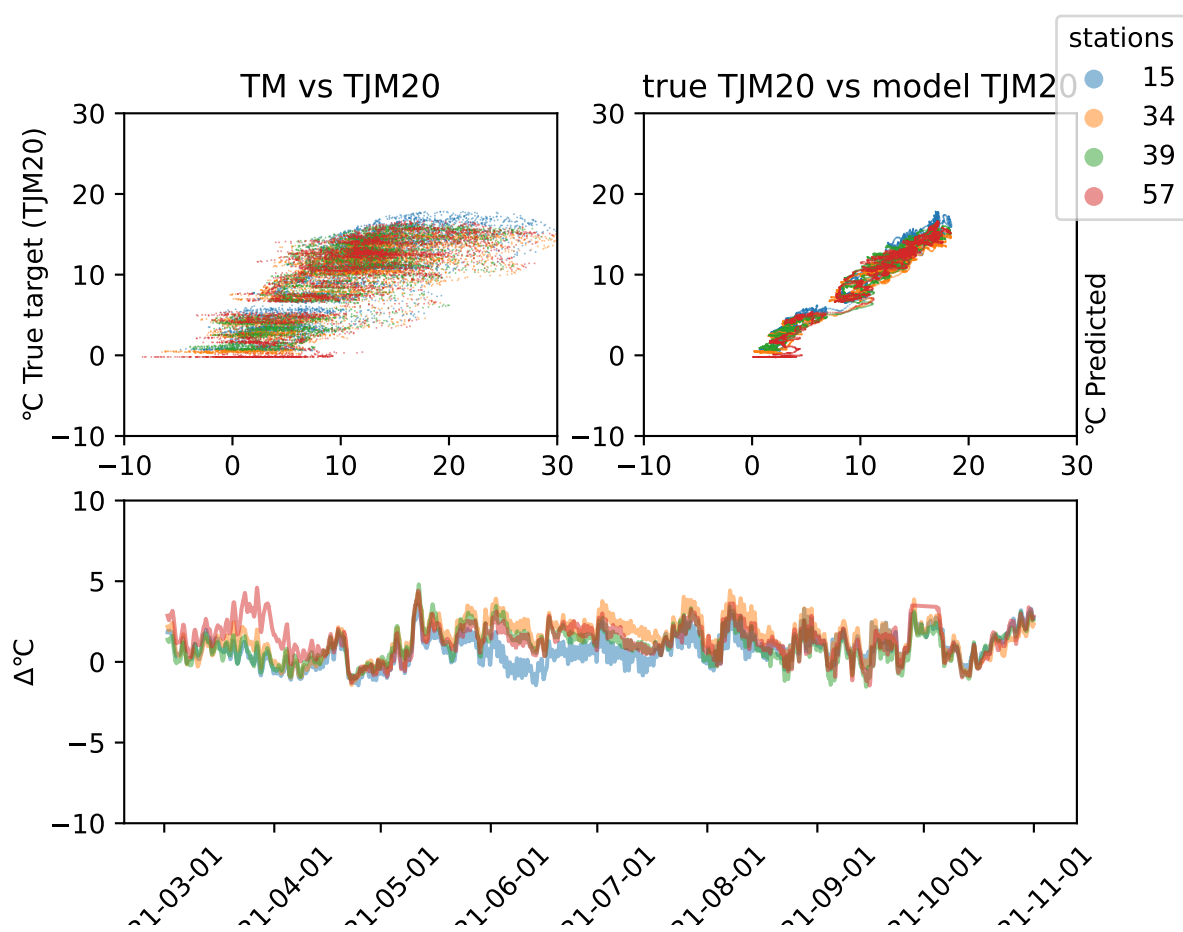


Figure 114: Difference plot for GRU model in year 2021 and region Trøndelagat depth 20. The station names can be found in table 1.

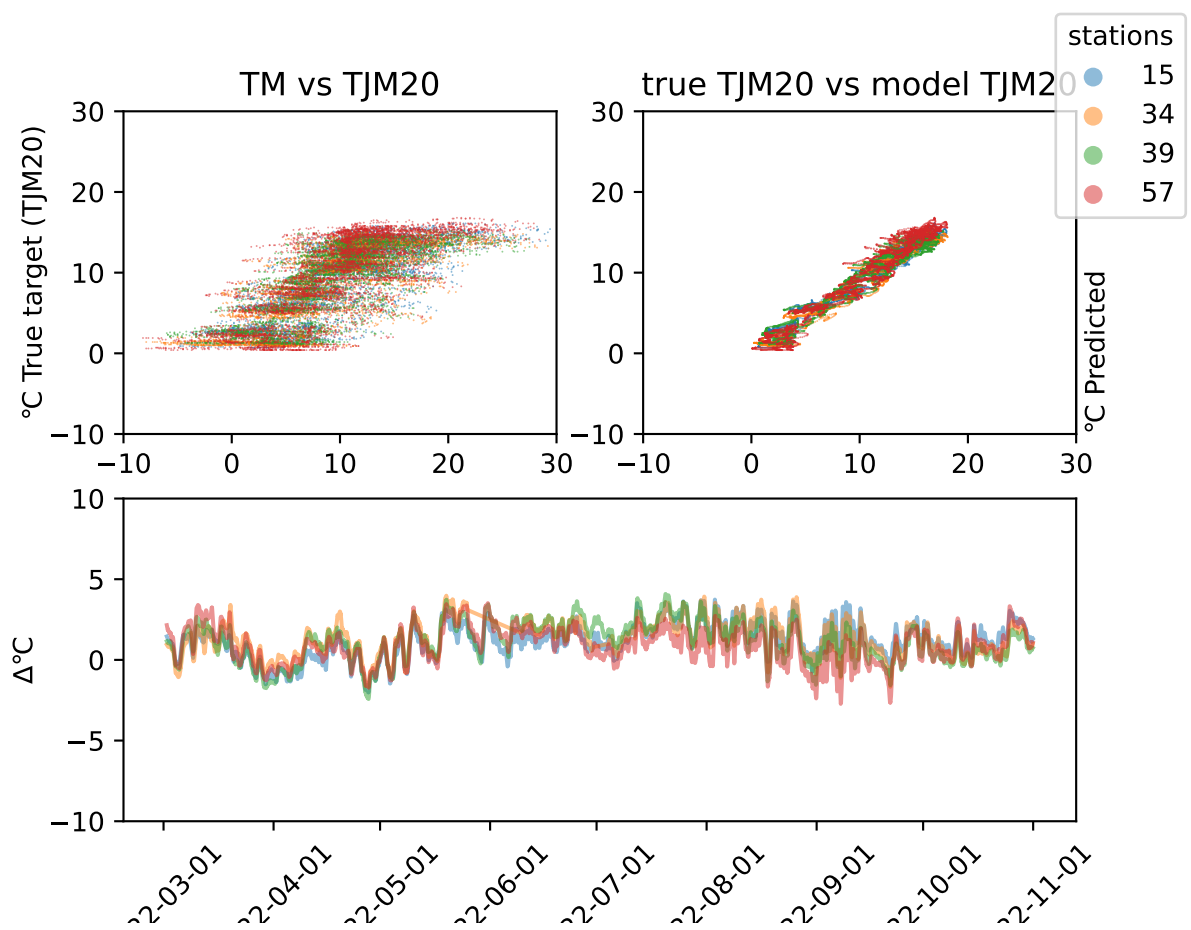


Figure 115: Difference plot for GRU model in year 2022 and region Trøndelag at depth 20. The station names can be found in table 1.

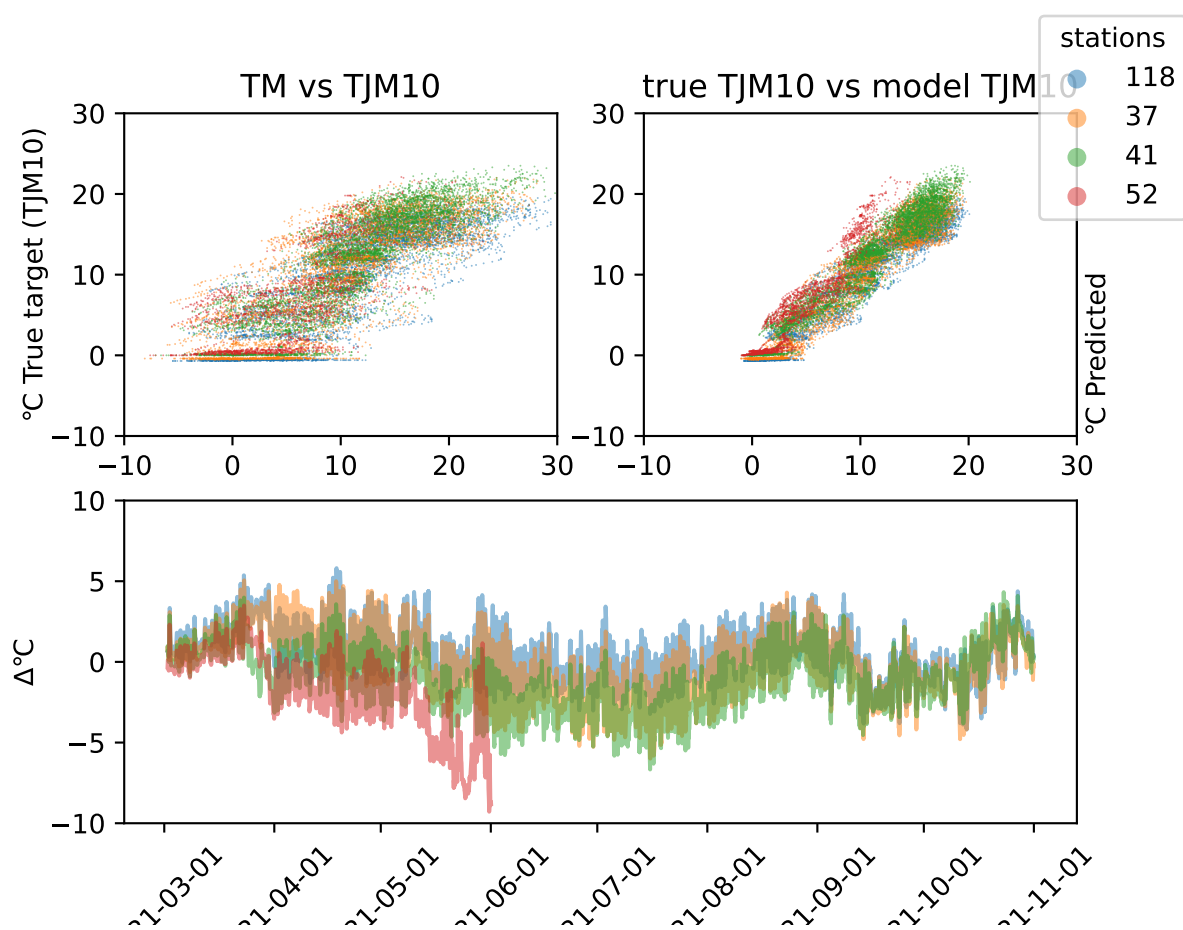


Figure 116: Difference plot for GRU model in year 2021 and region Østfoldat depth 10. The station names can be found in table 1.

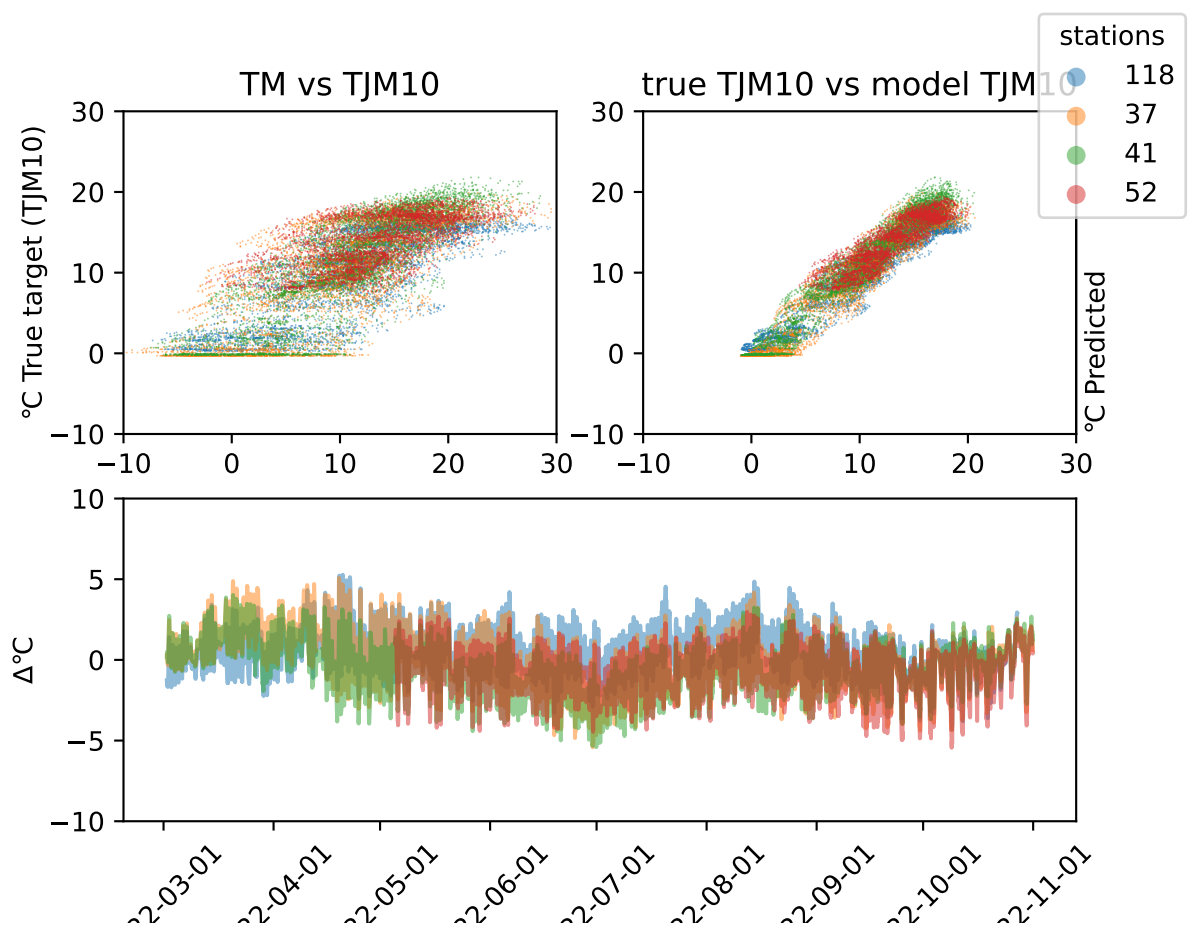


Figure 117: Difference plot for GRU model in year 2022 and region Østfoldat depth 10. The station names can be found in table 1.

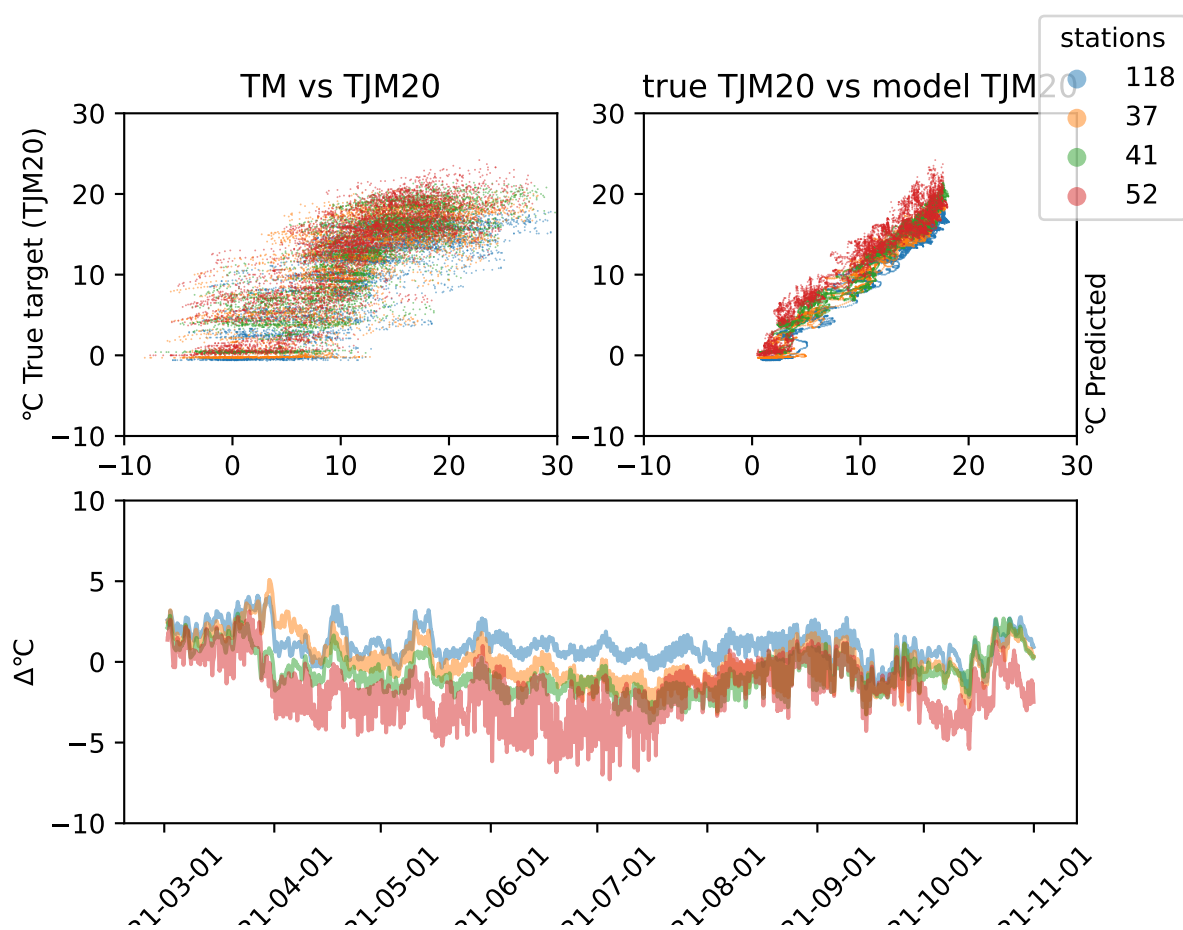


Figure 118: Difference plot for GRU model in year 2021 and region Østfoldat depth 20. The station names can be found in table 1.

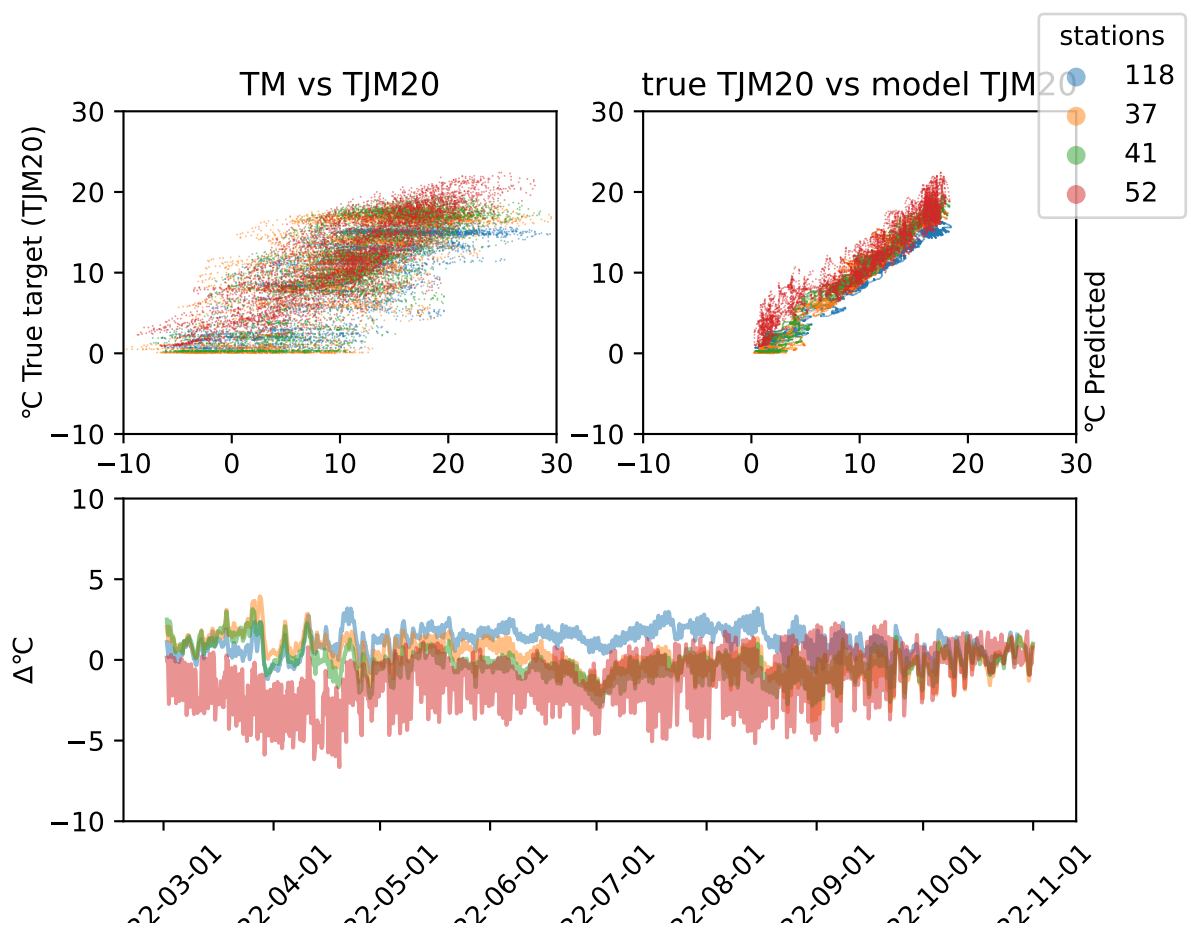


Figure 119: Difference plot for GRU model in year 2022 and region Østfoldat depth 20. The station names can be found in table 1.

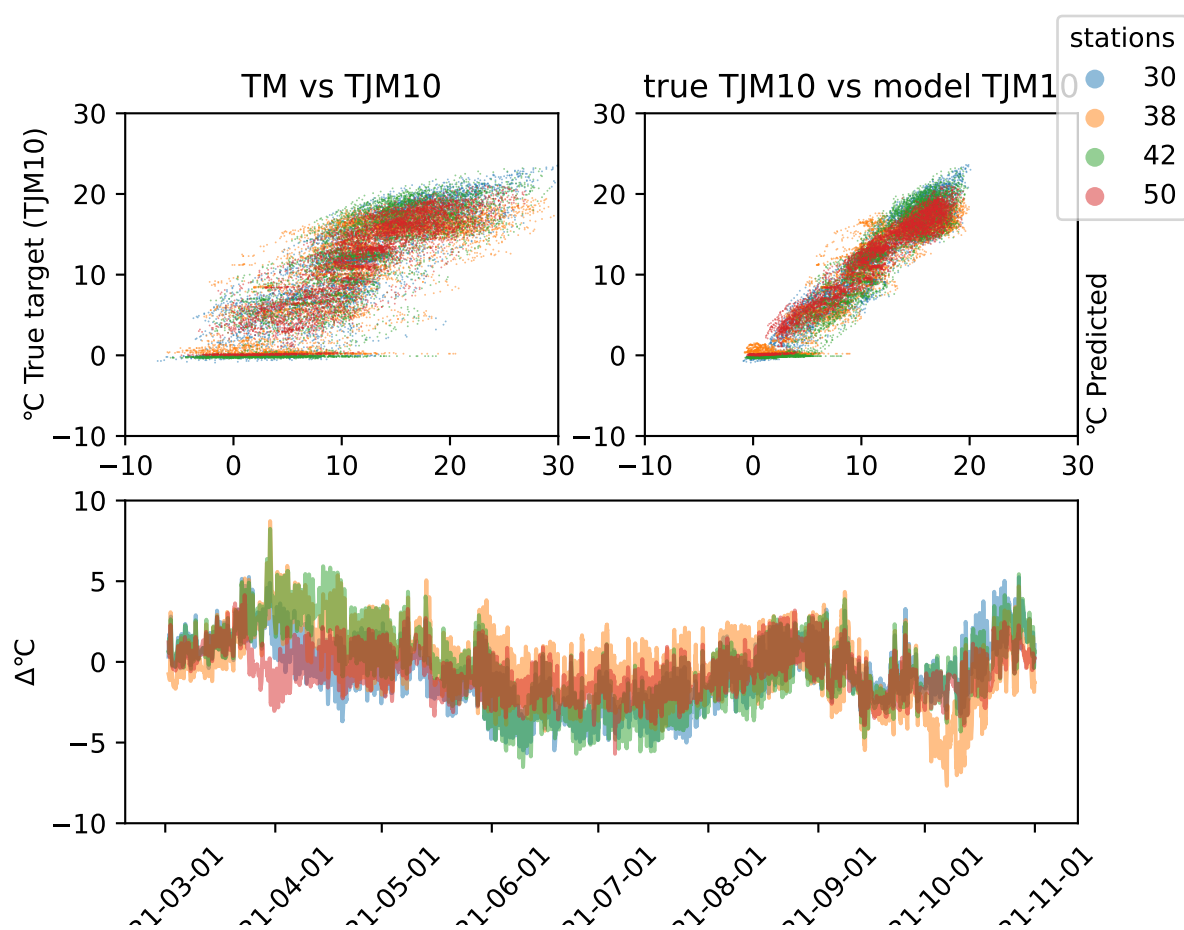


Figure 120: Difference plot for GRU model in year 2021 and region Vestfoldat depth 10. The station names can be found in table 1.

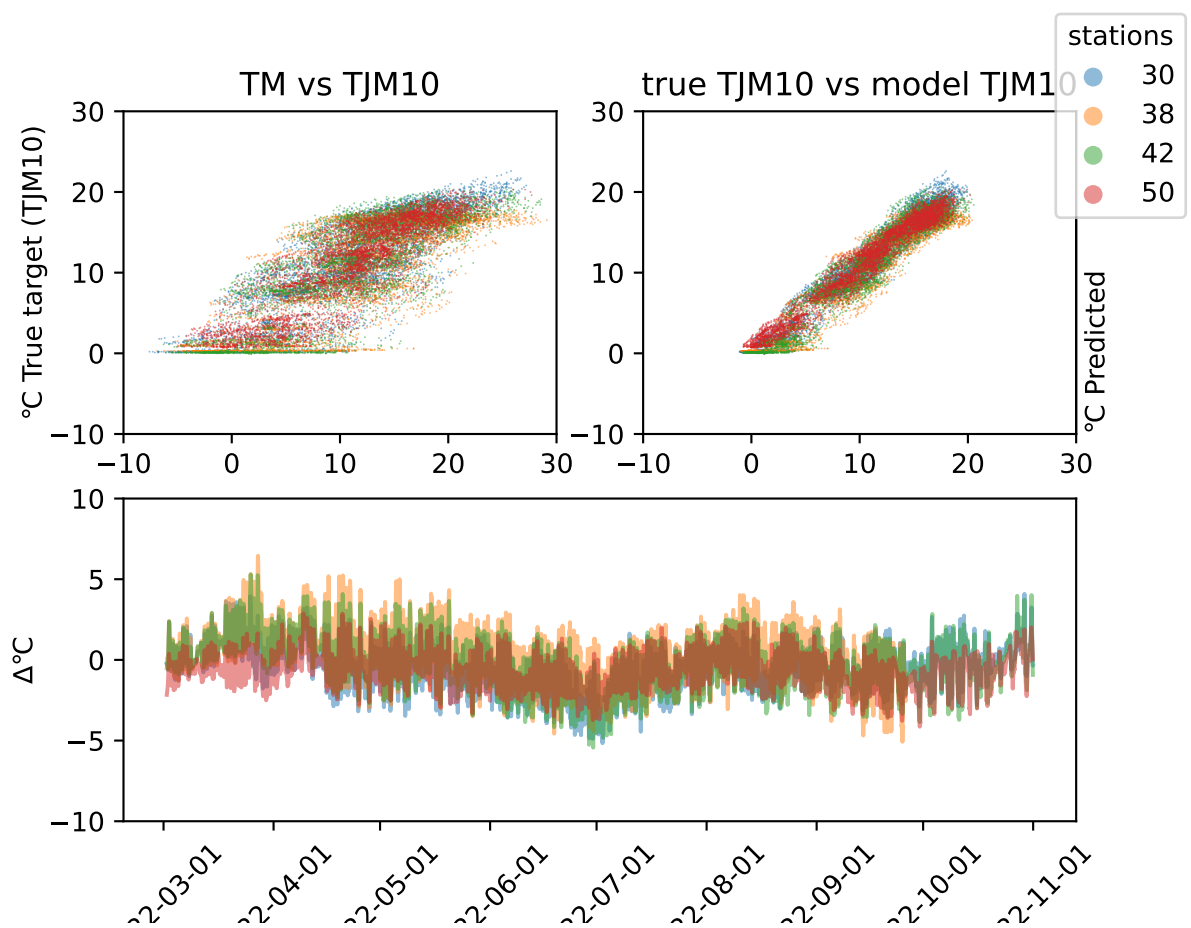


Figure 121: Difference plot for GRU model in year 2022 and region Vestfoldat depth 10. The station names can be found in table 1.

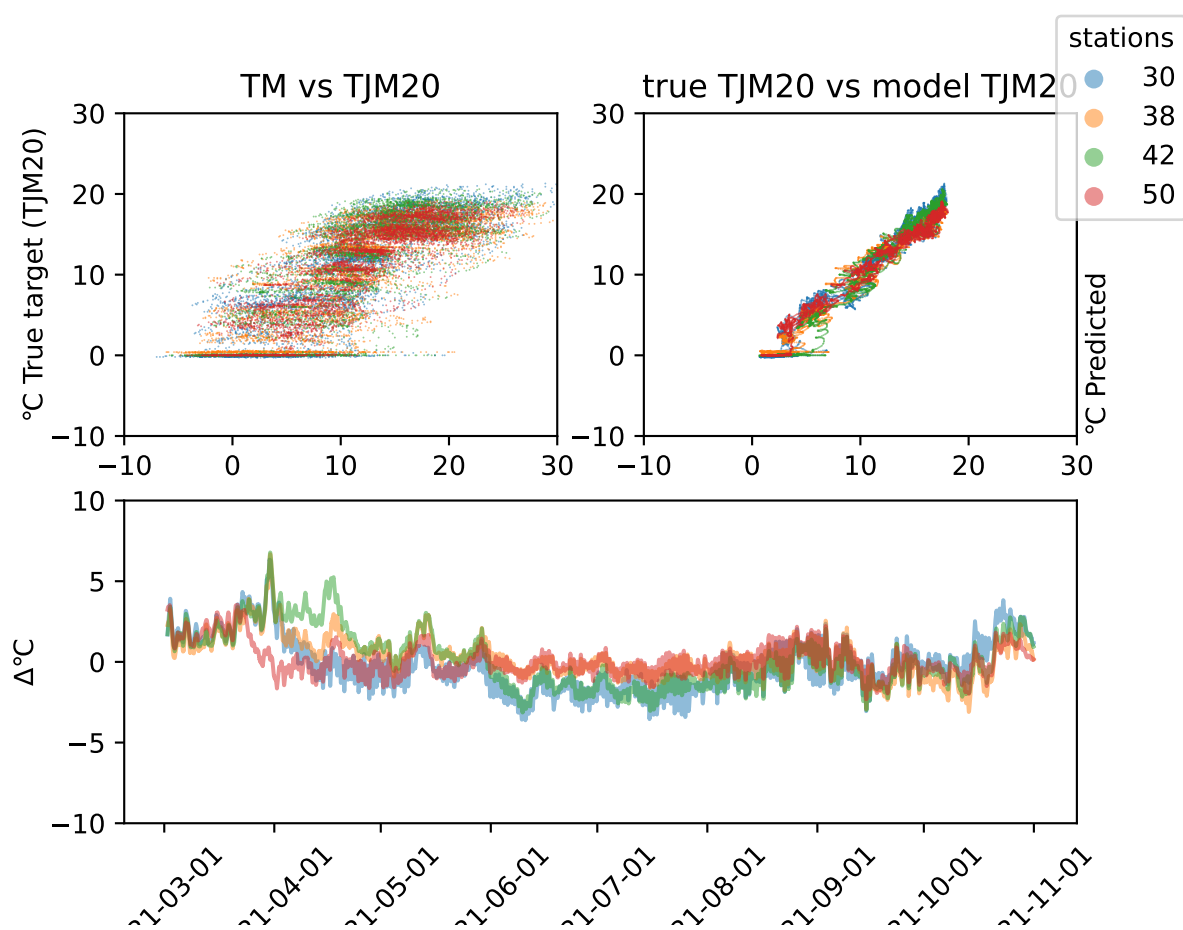


Figure 122: Difference plot for GRU model in year 2021 and region Vestfoldat depth 20. The station names can be found in table 1.

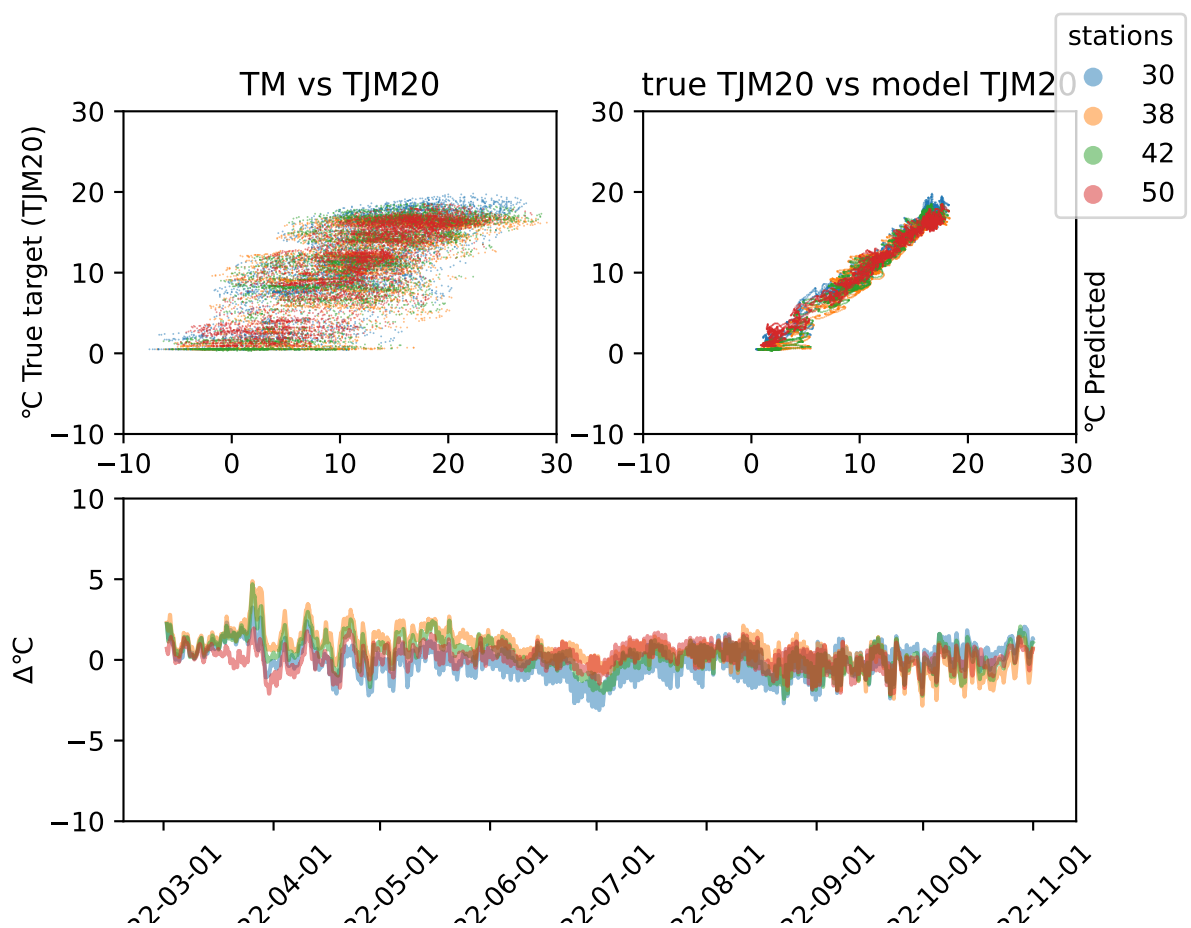


Figure 123: Difference plot for GRU model in year 2022 and region Vestfoldat depth 20. The station names can be found in table 1.



## A.2 Data visiulation of data before treatment

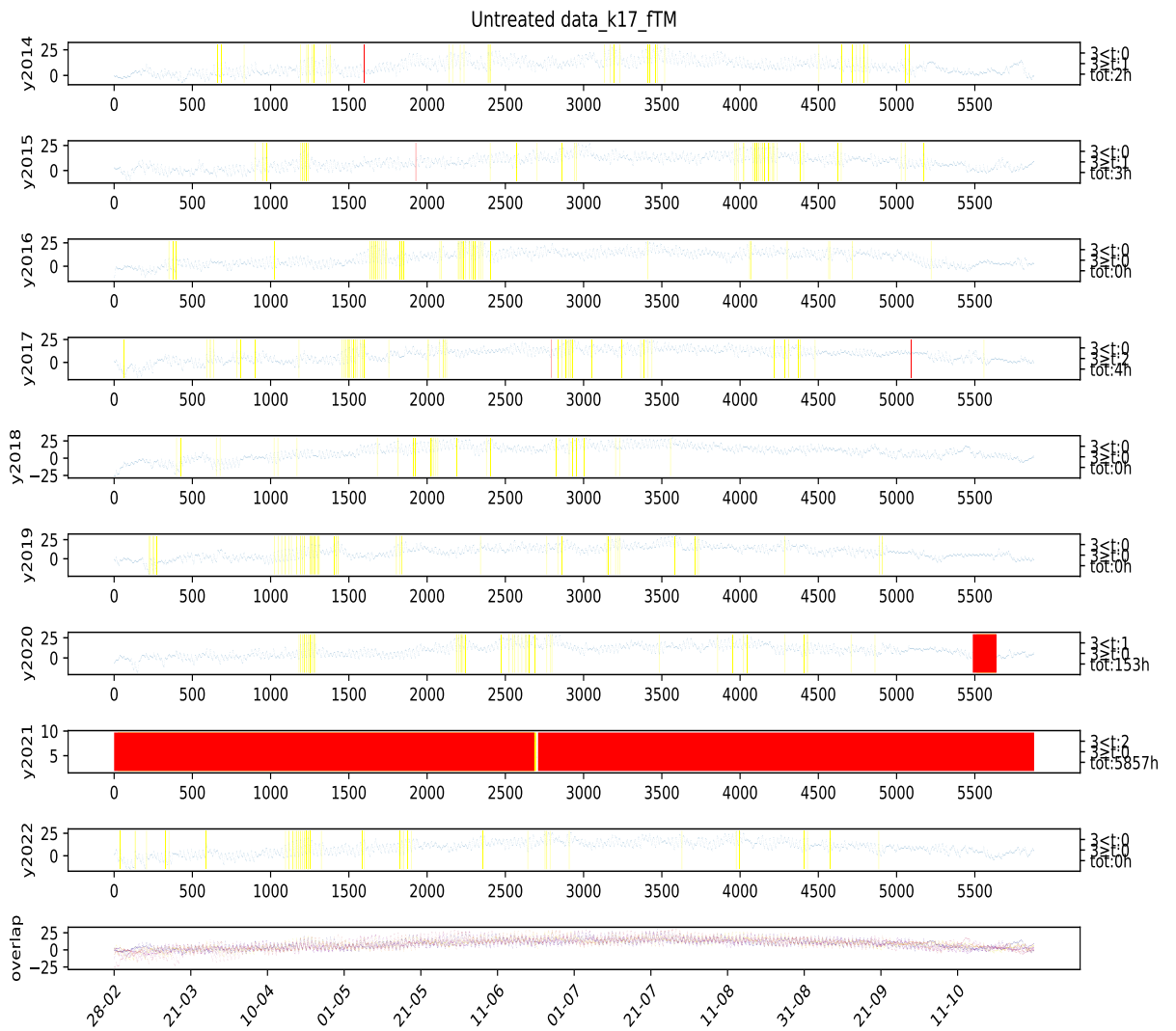


Figure 124: Visual representation of missing values at station 17 from 2014 to 2022 at the parameter "TM" after treating for outliers. The left numbers indicated how many hours that are missing and how many of them are shorter than or longer than 5 hours, however for this visualization they indicate the untreated version of the data. The yellow markings indicate possible outliers based on the given year, all markings was checked if they were actual outliers. The red colouring indicate missing values in the data (represented in the data with code "NULL"). The station names can be found in table 1.

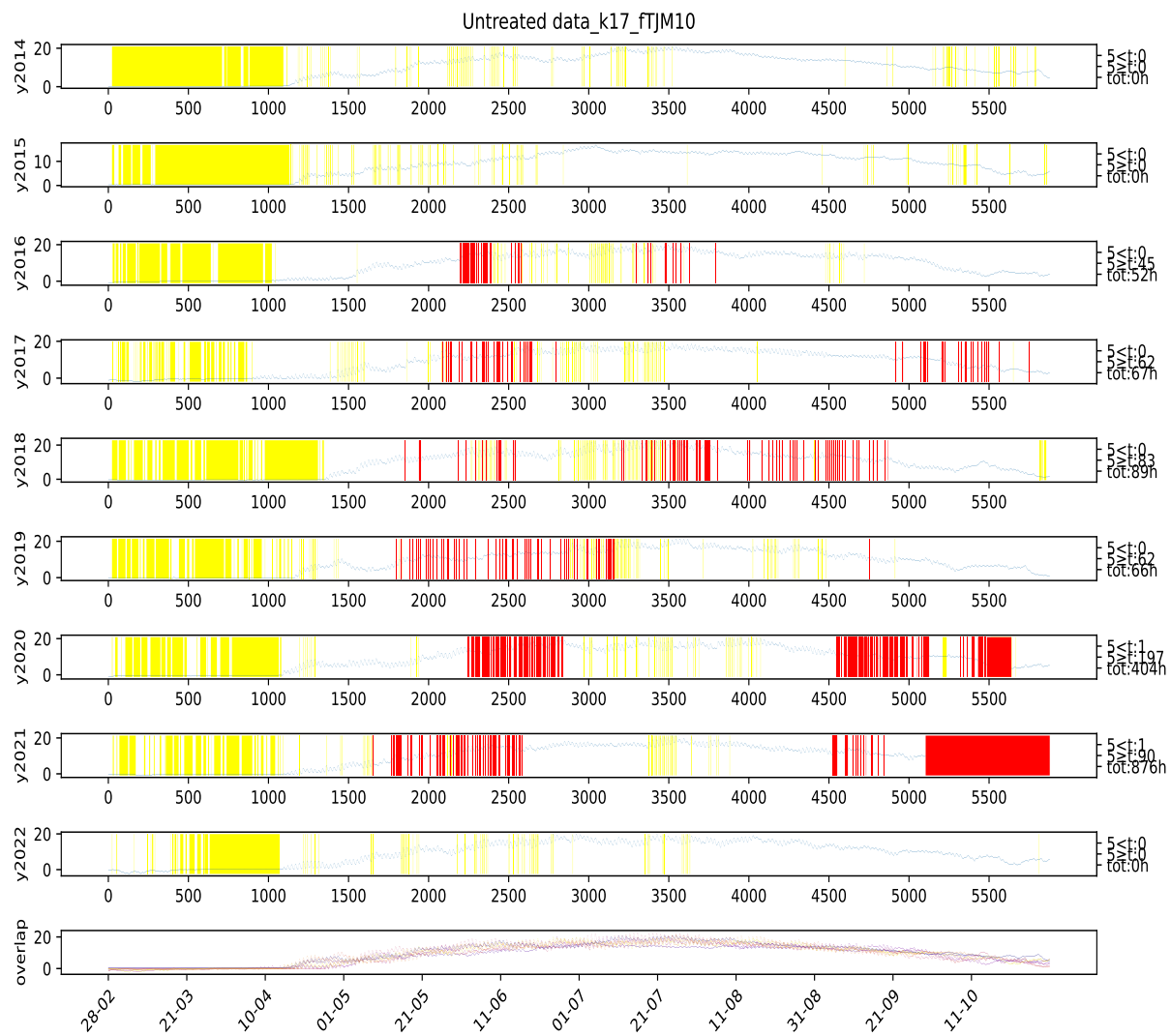


Figure 125: Visual representation of missing values at station 17 from 2014 to 2022 at the parameter "TJM10" after treating for outliers. The left numbers indicated how many hours that are missing and how many of them are shorter than or longer than 5 hours, however for this visualization they indicate the untreated version of the data. The yellow markings indicate possible outliers based on the given year, all markings was checked if they were actual outliers. The red colouring indicate missing values in the data (represented in the data with code "NULL").The station names can be found in table 1.

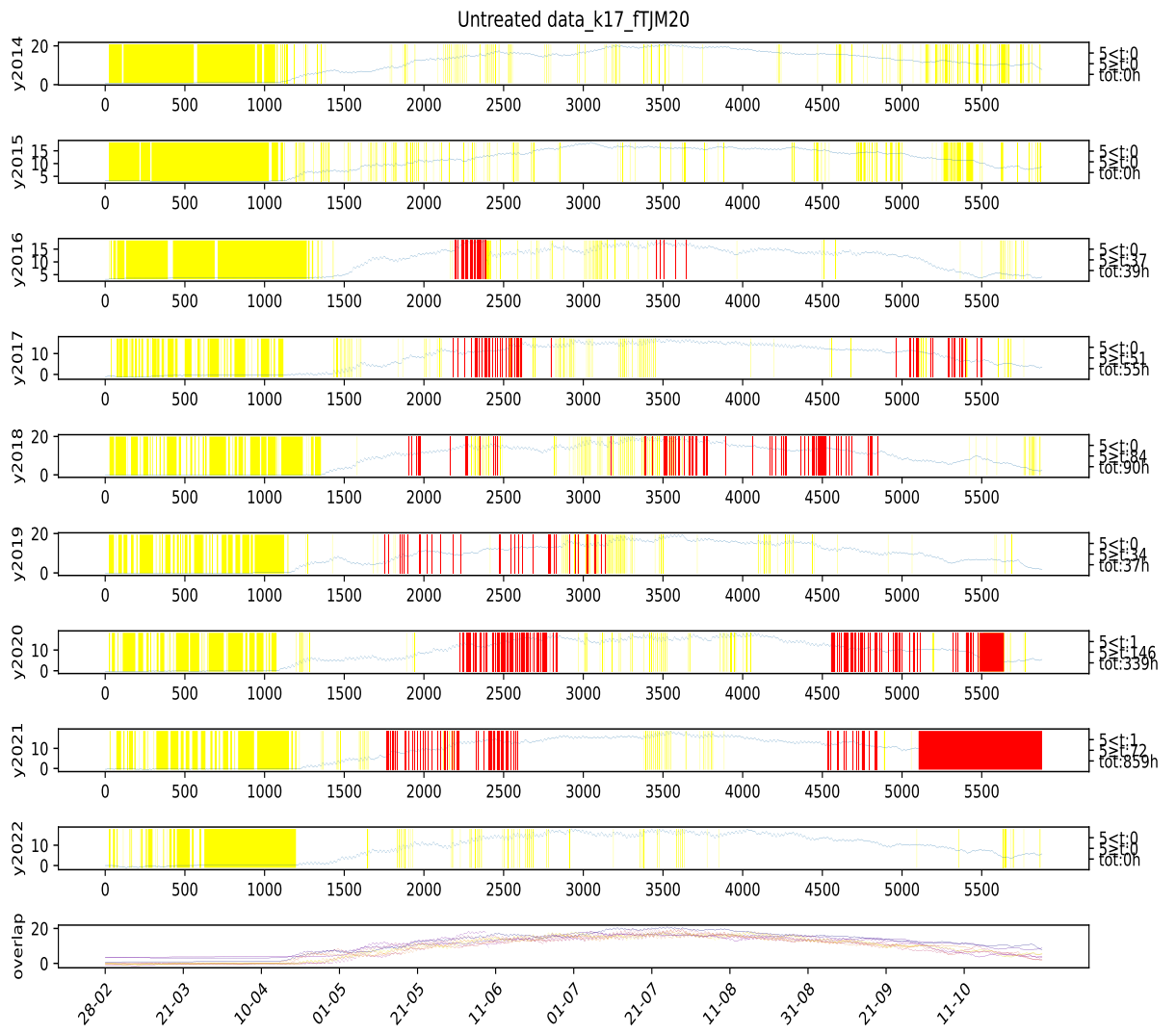


Figure 126: Visual representation of missing values at station 17 from 2014 to 2022 at the parameter "TJM20" after treating for outliers. The left numbers indicated how many hours that are missing and how many of them are shorter than or longer than 5 hours, however for this visualization they indicate the untreated version of the data. The yellow markings indicate possible outliers based on the given year, all markings was checked if they were actual outliers. The red colouring indicate missing values in the data (represented in the data with code "NULL"). The station names can be found in table 1.

## A PLOTS



Figure 127: Visual representation of missing values at station 11 from 2014 to 2022 at the parameter "TM" after treating for outliers. The left numbers indicated how many hours that are missing and how many of them are shorter than or longer than 5 hours, however for this visualization they indicate the untreated version of the data. The yellow markings indicate possible outliers based on the given year, all markings was checked if they were actual outliers. The red colouring indicate missing values in the data (represented in the data with code "NULL"). The station names can be found in table 1.

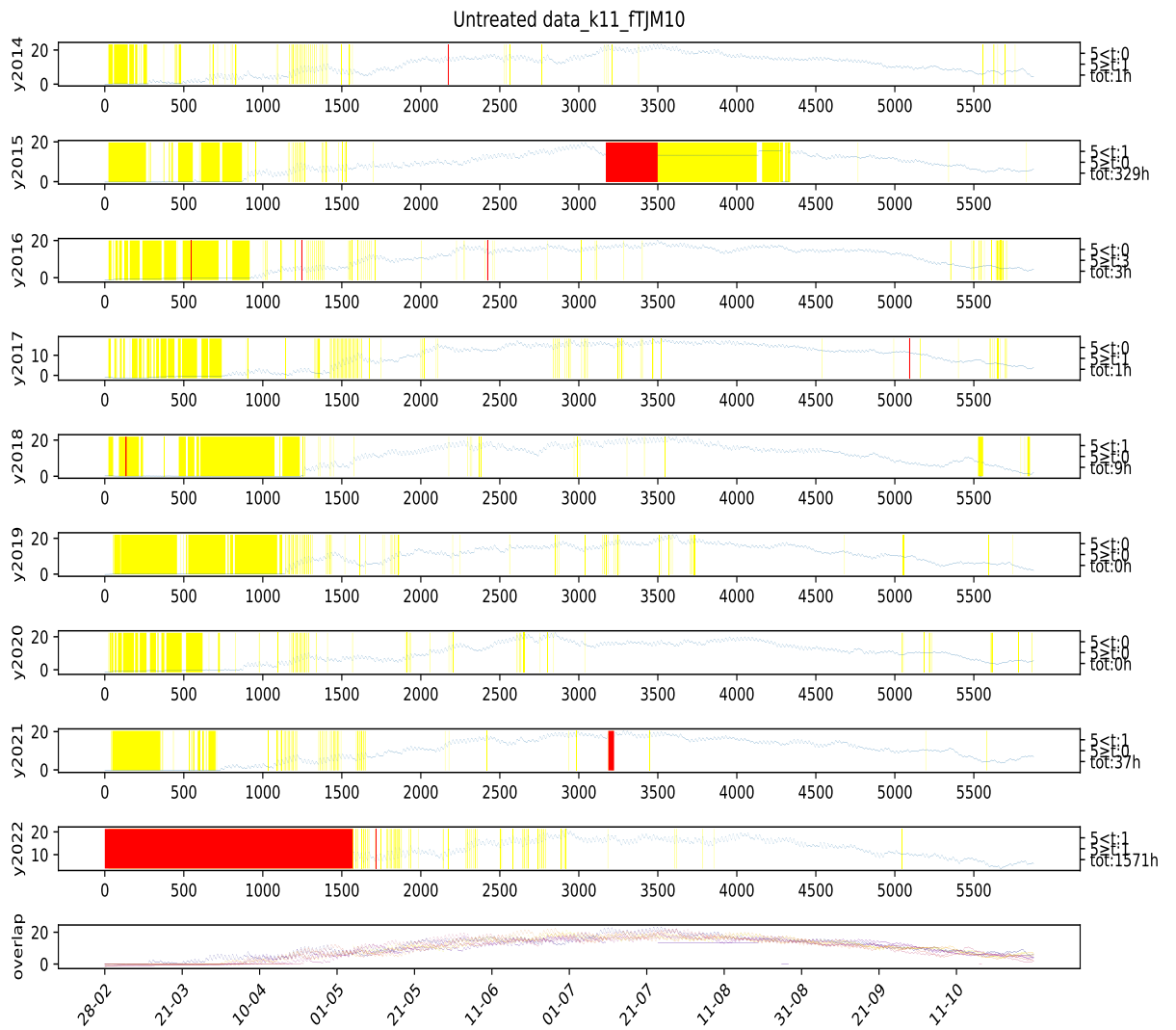


Figure 128: Visual representation of missing values at station 11 from 2014 to 2022 at the parameter "TJM10" after treating for outliers. The left numbers indicated how many hours that are missing and how many of them are shorter than or longer than 5 hours, however for this visualization they indicate the untreated version of the data. The yellow markings indicate possible outliers based on the given year, all markings was checked if they were actual outliers. The red colouring indicate missing values in the data (represented in the data with code "NULL"). The station names can be found in table 1.

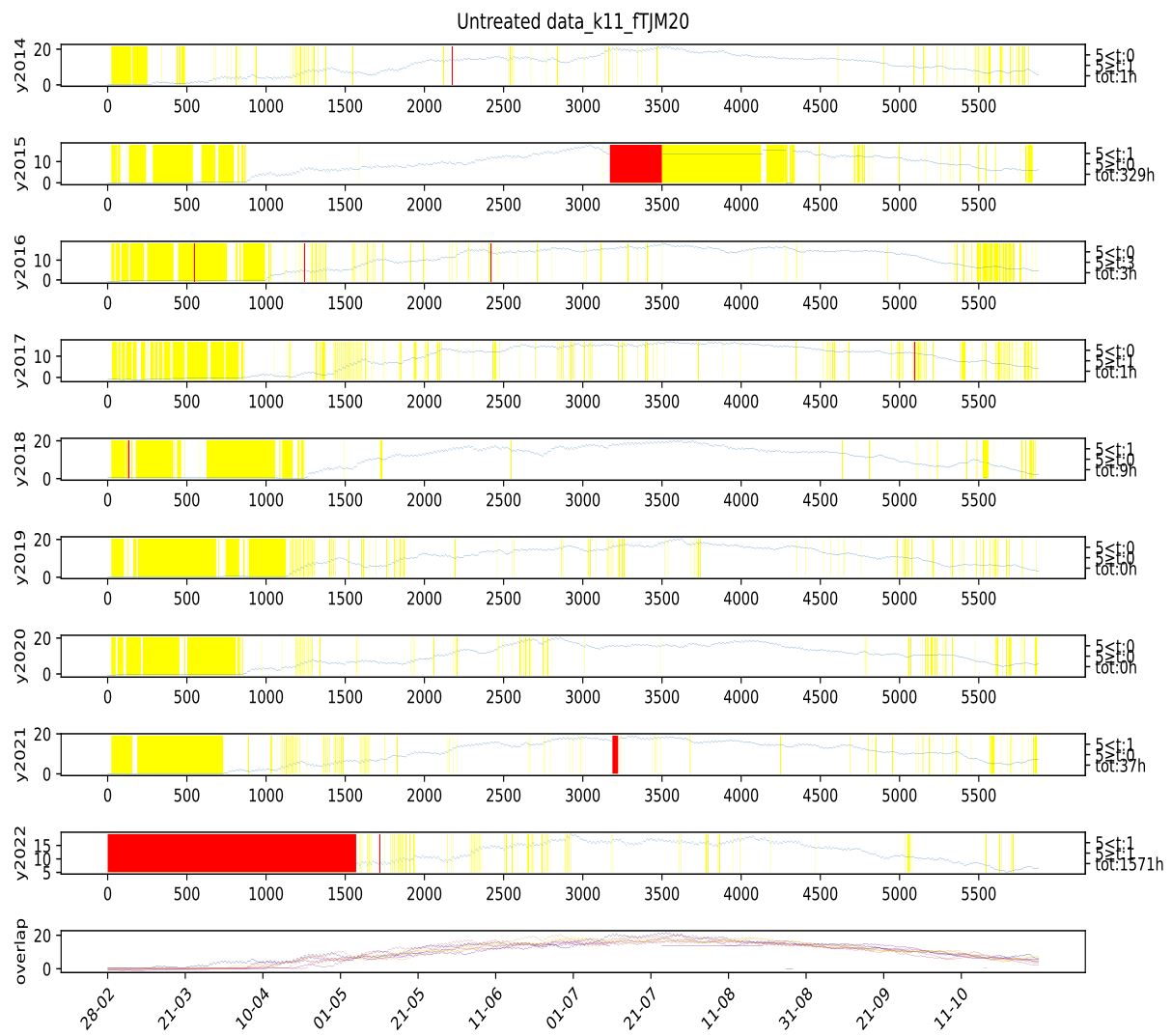


Figure 129: Visual representation of missing values at station 11 from 2014 to 2022 at the parameter "TJM20" after treating for outliers. The left numbers indicated how many hours that are missing and how many of them are shorter than or longer than 5 hours, however for this visualization they indicate the untreated version of the data. The yellow markings indicate possible outliers based on the given year, all markings was checked if they were actual outliers. The red colouring indicate missing values in the data (represented in the data with code "NULL"). The station names can be found in table 1.

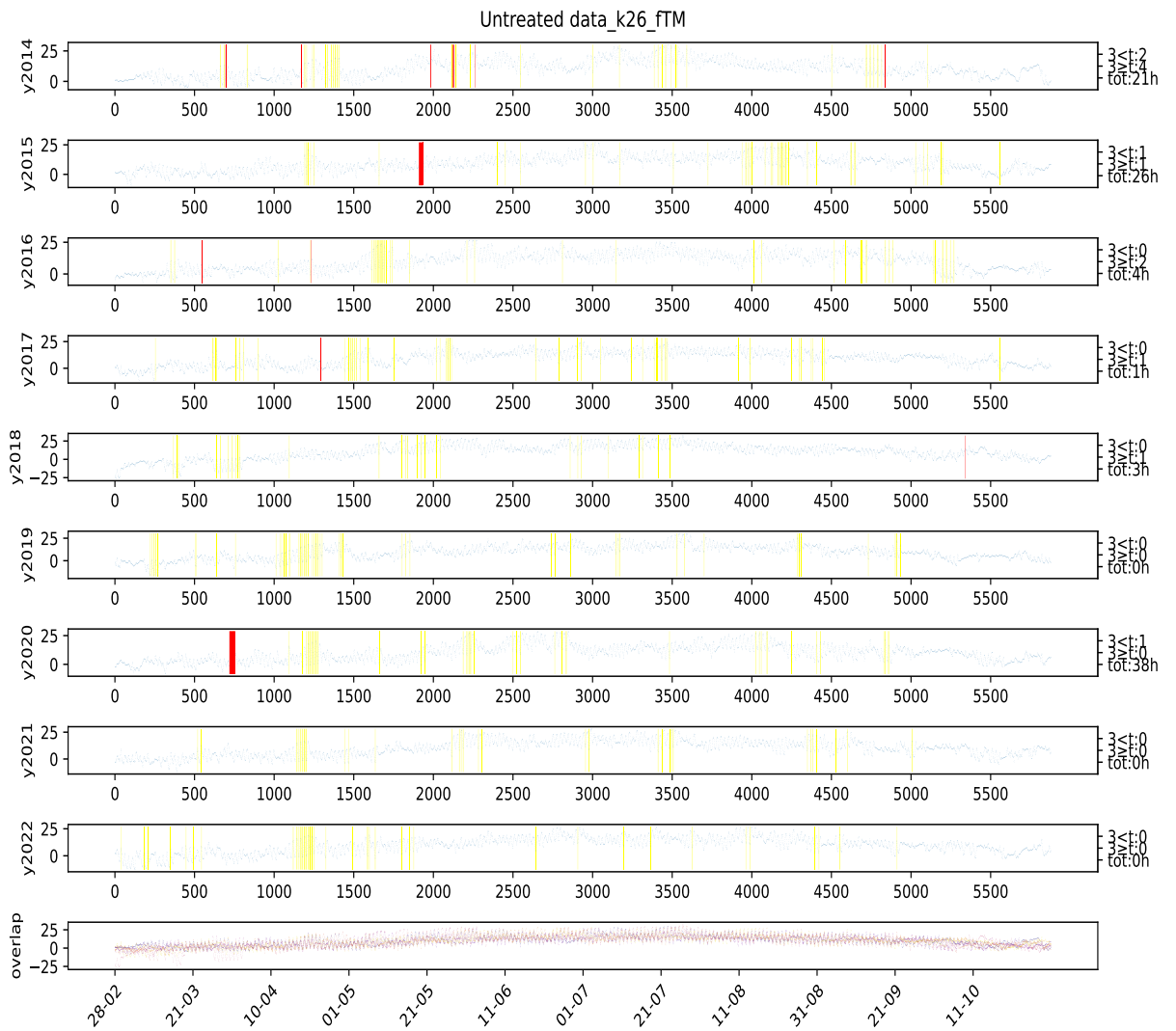


Figure 130: Visual representation of missing values at station 26 from 2014 to 2022 at the parameter "TM" after treating for outliers. The left numbers indicated how many hours that are missing and how many of them are shorter than or longer than 5 hours, however for this visualization they indicate the untreated version of the data. The yellow markings indicate possible outliers based on the given year, all markings was checked if they were actual outliers. The red colouring indicate missing values in the data (represented in the data with code "NULL"). The station names can be found in table 1.

## A PLOTS

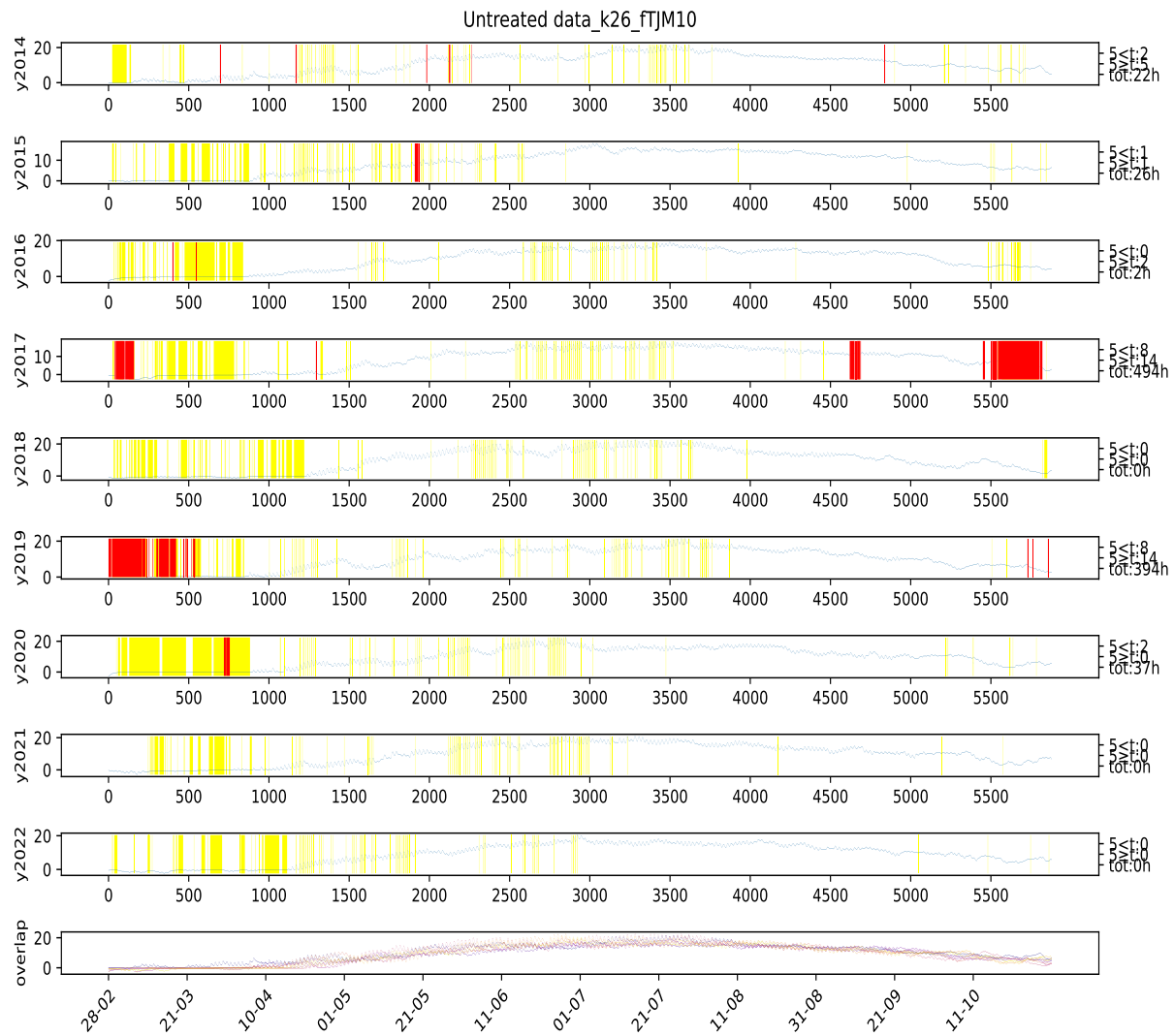


Figure 131: Visual representation of missing values at station 26 from 2014 to 2022 at the parameter "TJM10" after treating for outliers. The left numbers indicated how many hours that are missing and how many of them are shorter than or longer than 5 hours, however for this visualization they indicate the untreated version of the data. The yellow markings indicate possible outliers based on the given year, all markings was checked if they were actual outliers. The red colouring indicate missing values in the data (represented in the data with code "NULL"). The station names can be found in table 1.

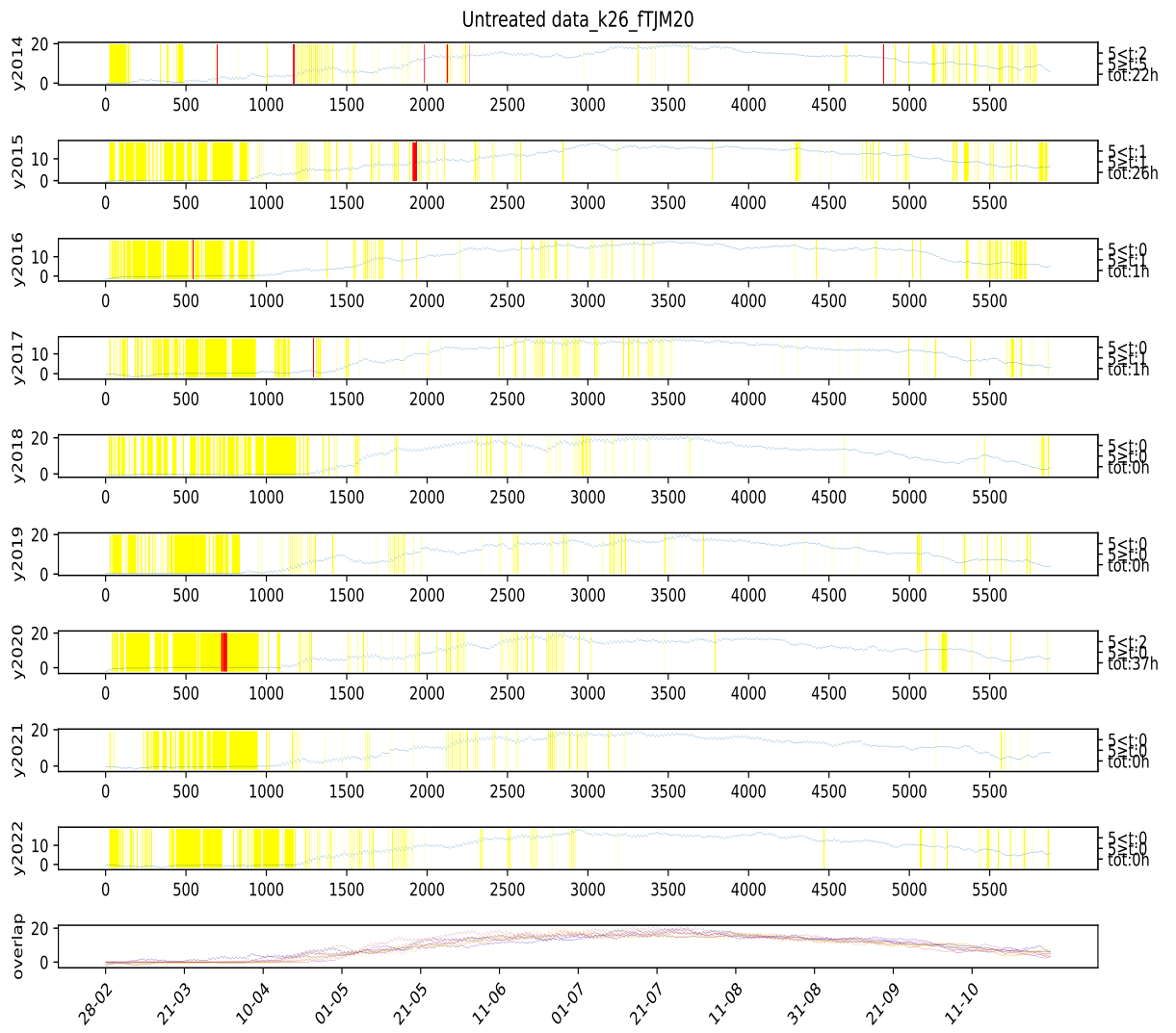


Figure 132: Visual representation of missing values at station 26 from 2014 to 2022 at the parameter "TJM20" after treating for outliers. The left numbers indicated how many hours that are missing and how many of them are shorter than or longer than 5 hours, however for this visualization they indicate the untreated version of the data. The yellow markings indicate possible outliers based on the given year, all markings was checked if they were actual outliers. The red colouring indicate missing values in the data (represented in the data with code "NULL"). The station names can be found in table 1.

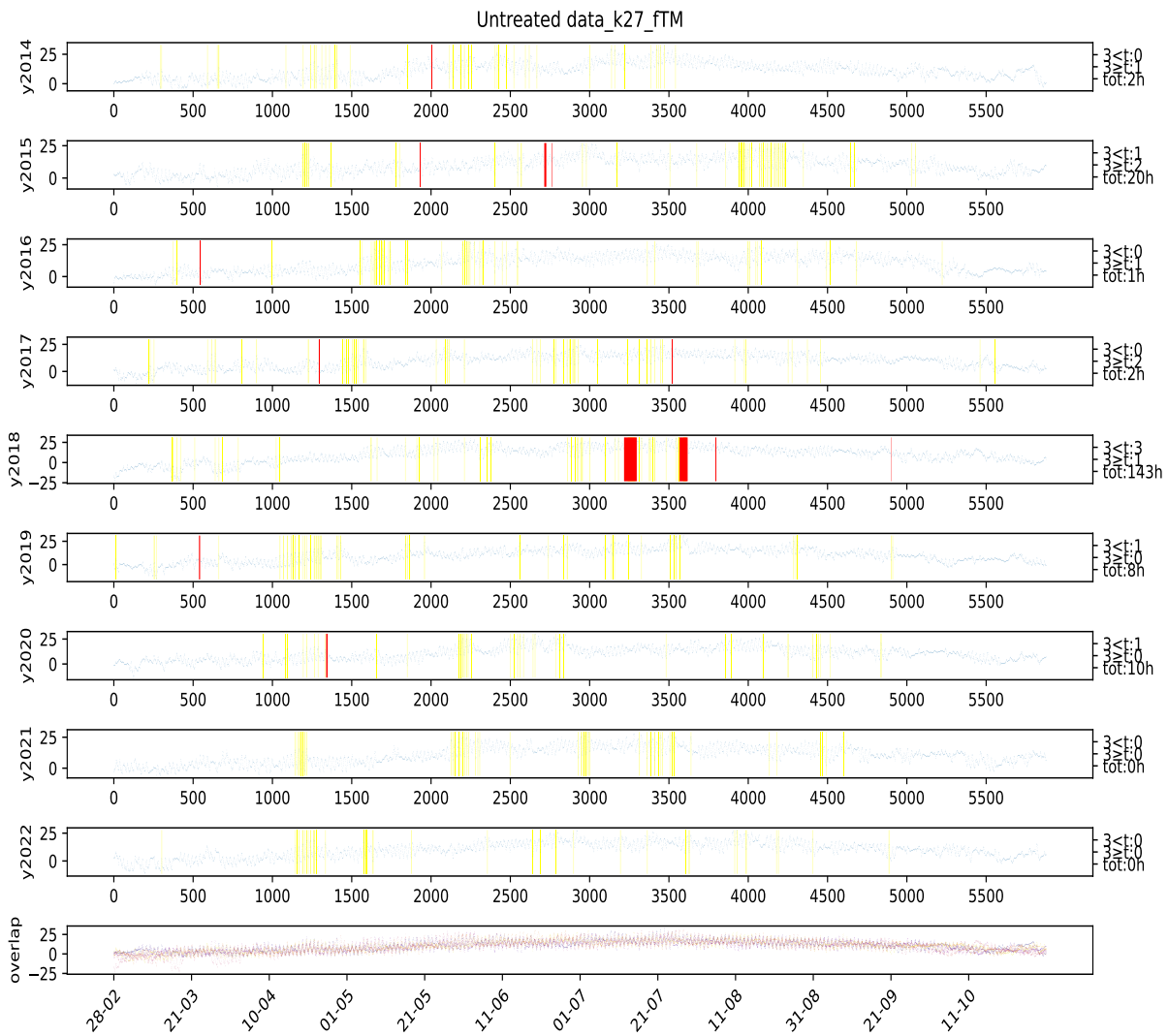


Figure 133: Visual representation of missing values at station 27 from 2014 to 2022 at the parameter "TM" after treating for outliers. The left numbers indicated how many hours that are missing and how many of them are shorter than or longer than 5 hours, however for this visualization they indicate the untreated version of the data. The yellow markings indicate possible outliers based on the given year, all markings was checked if they were actual outliers. The red colouring indicate missing values in the data (represented in the data with code "NULL"). The station names can be found in table 1.

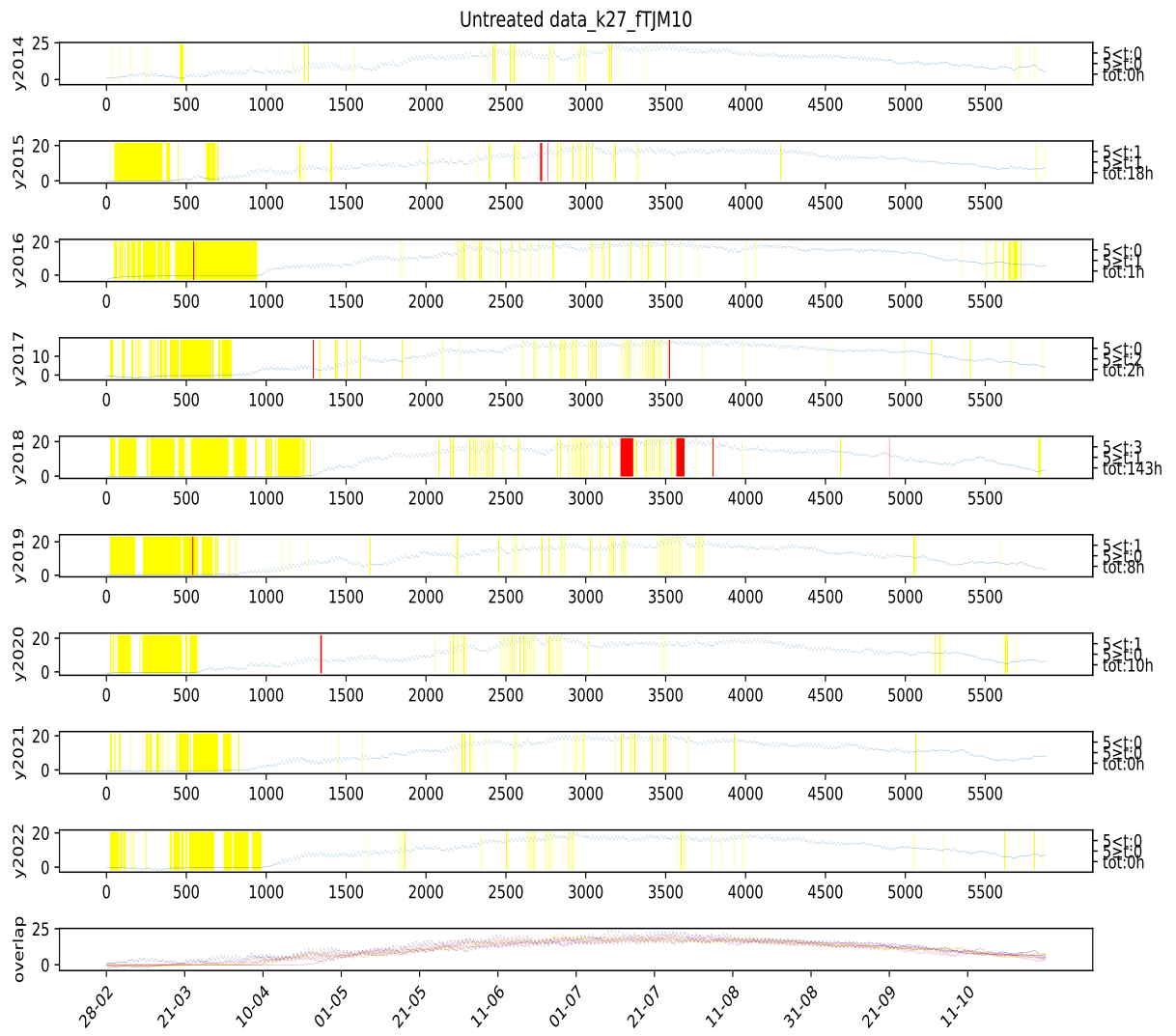


Figure 134: Visual representation of missing values at station 27 from 2014 to 2022 at the parameter "TJM10" after treating for outliers. The left numbers indicated how many hours that are missing and how many of them are shorter than or longer than 5 hours, however for this visualization they indicate the untreated version of the data. The yellow markings indicate possible outliers based on the given year, all markings was checked if they were actual outliers. The red colouring indicate missing values in the data (represented in the data with code "NULL"). The station names can be found in table 1.

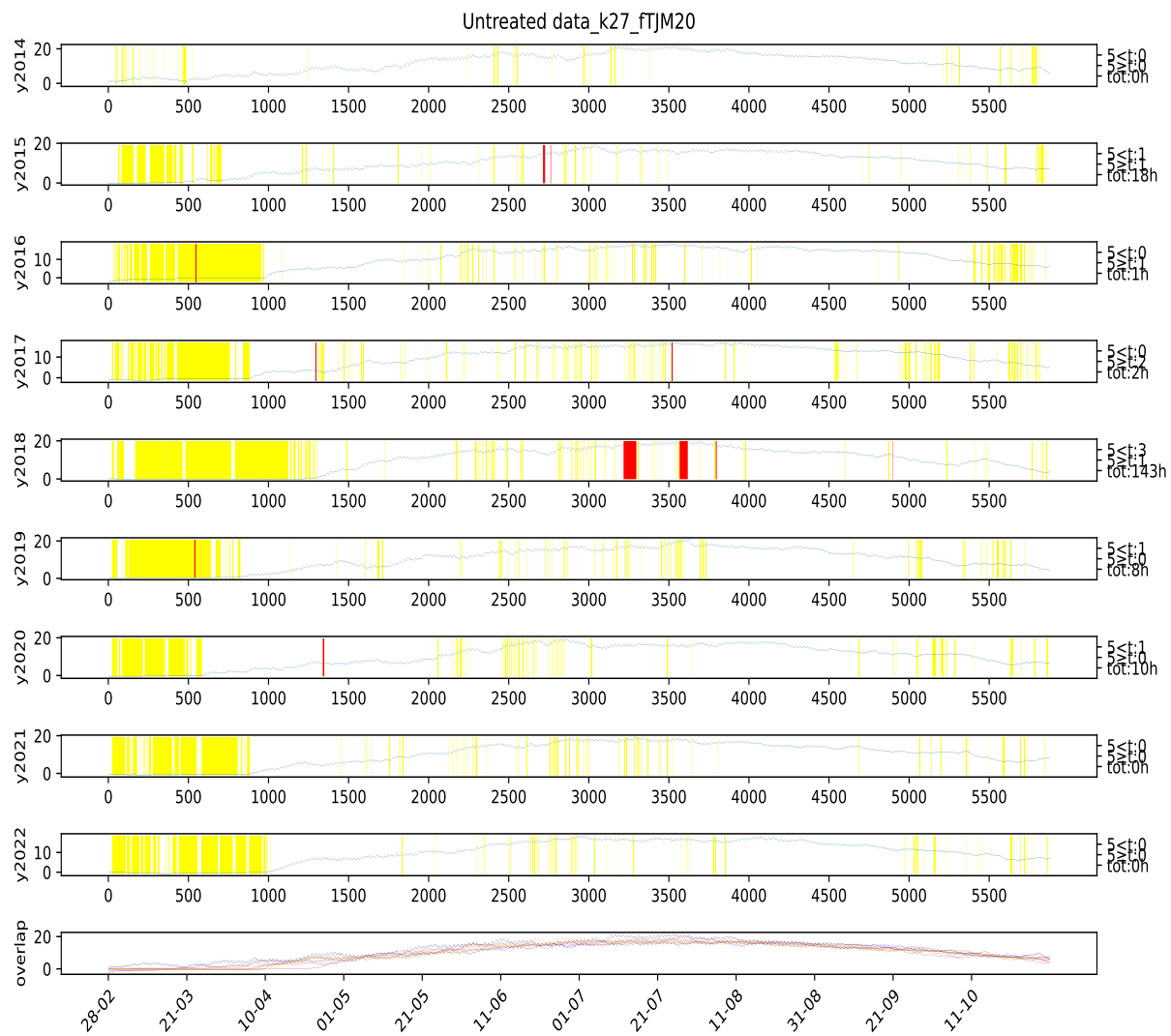


Figure 135: Visual representation of missing values at station 27 from 2014 to 2022 at the parameter "TJM20" after treating for outliers. The left numbers indicated how many hours that are missing and how many of them are shorter than or longer than 5 hours, however for this visualization they indicate the untreated version of the data. The yellow markings indicate possible outliers based on the given year, all markings was checked if they were actual outliers. The red colouring indicate missing values in the data (represented in the data with code "NULL"). The station names can be found in table 1.

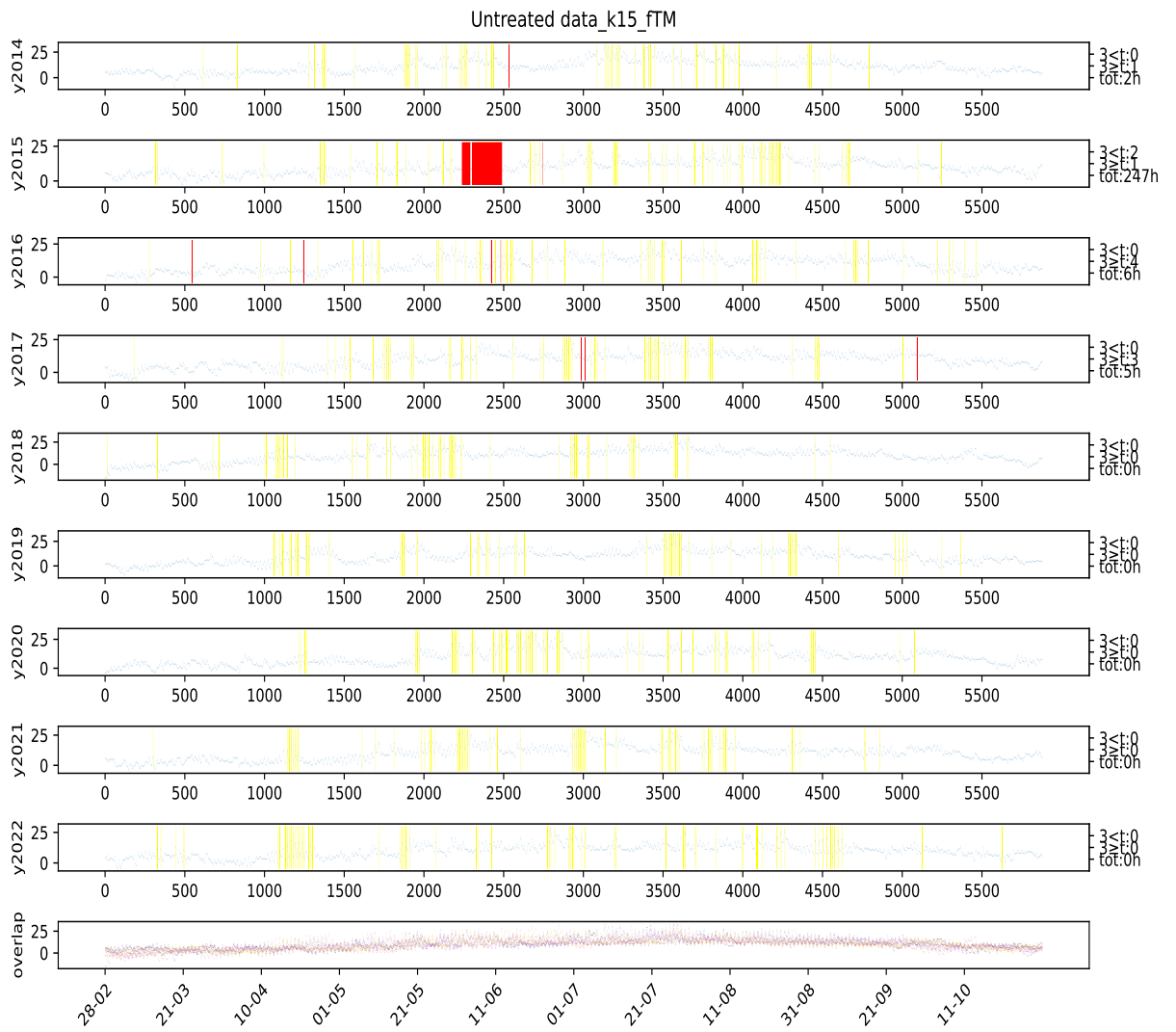


Figure 136: Visual representation of missing values at station 15 from 2014 to 2022 at the parameter "TM" after treating for outliers. The left numbers indicated how many hours that are missing and how many of them are shorter than or longer than 5 hours, however for this visualization they indicate the untreated version of the data. The yellow markings indicate possible outliers based on the given year, all markings was checked if they were actual outliers. The red colouring indicate missing values in the data (represented in the data with code "NULL"). The station names can be found in table 1.

## A PLOTS

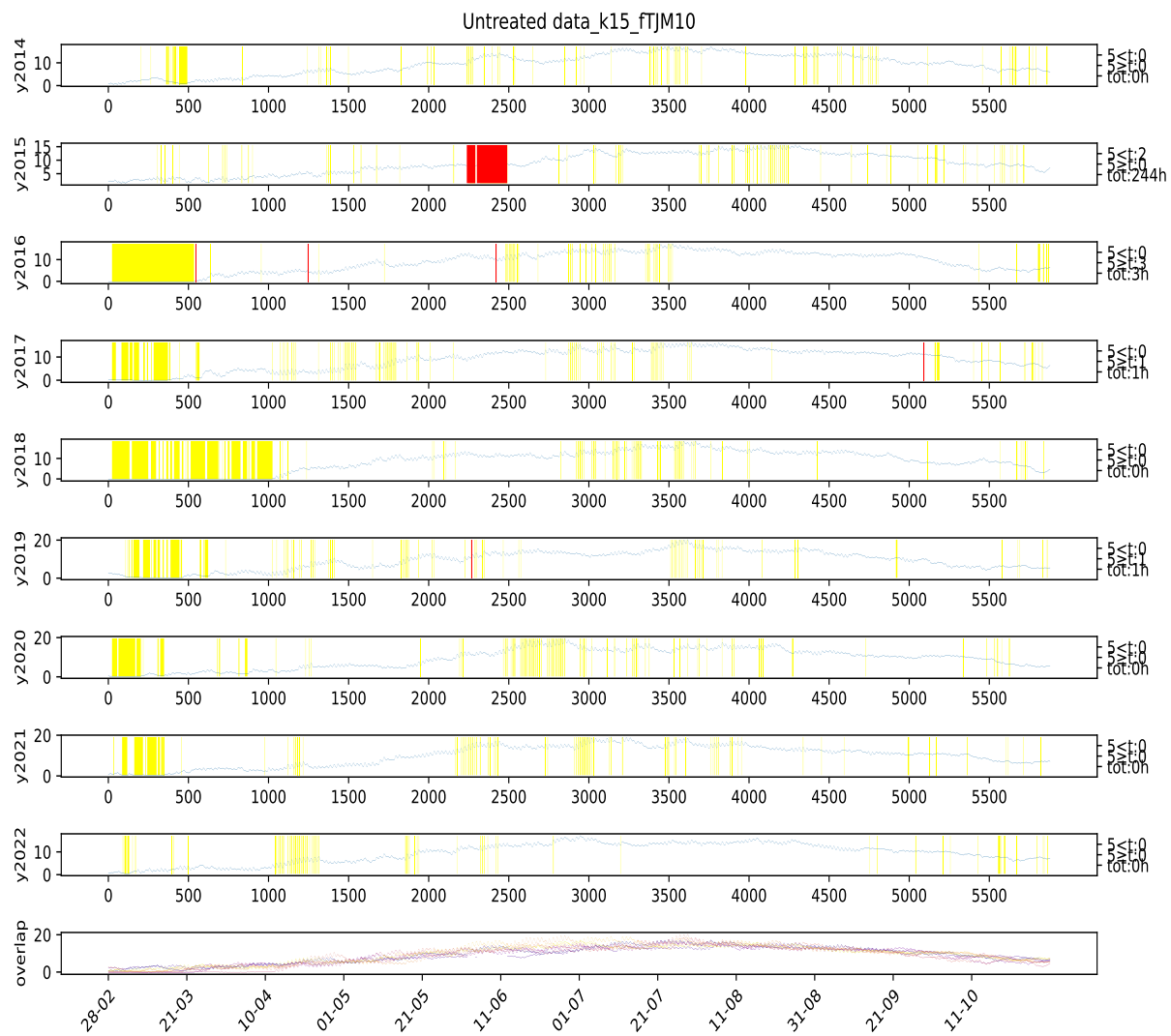


Figure 137: Visual representation of missing values at station 15 from 2014 to 2022 at the parameter "TJM10" after treating for outliers. The left numbers indicated how many hours that are missing and how many of them are shorter than or longer than 5 hours, however for this visualization they indicate the untreated version of the data. The yellow markings indicate possible outliers based on the given year, all markings was checked if they were actual outliers. The red colouring indicate missing values in the data (represented in the data with code "NULL"). The station names can be found in table 1.

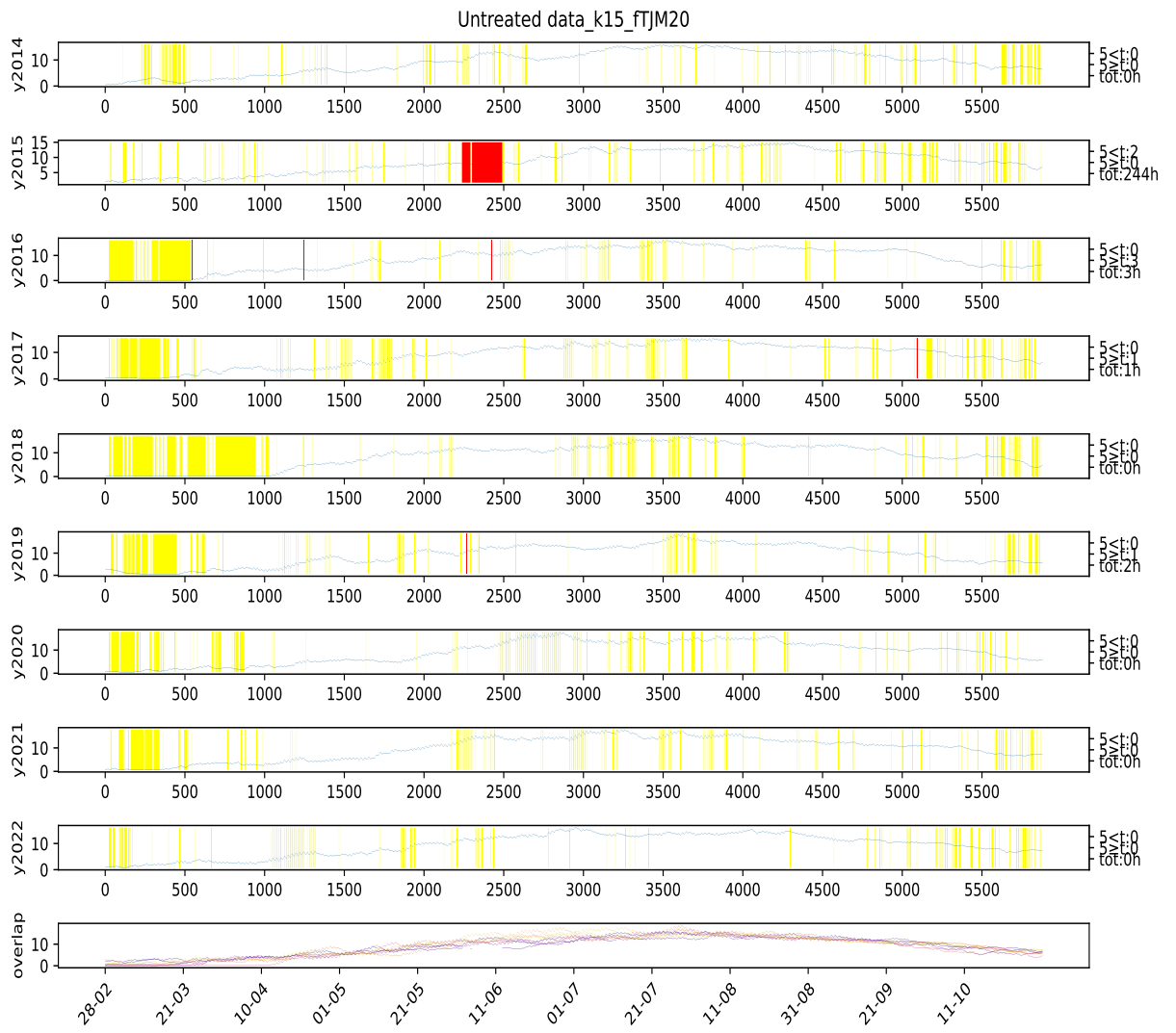


Figure 138: Visual representation of missing values at station 15 from 2014 to 2022 at the parameter "TJM20" after treating for outliers. The left numbers indicated how many hours that are missing and how many of them are shorter than or longer than 5 hours, however for this visualization they indicate the untreated version of the data. The yellow markings indicate possible outliers based on the given year, all markings was checked if they were actual outliers. The red colouring indicate missing values in the data (represented in the data with code "NULL"). The station names can be found in table 1.

## A PLOTS

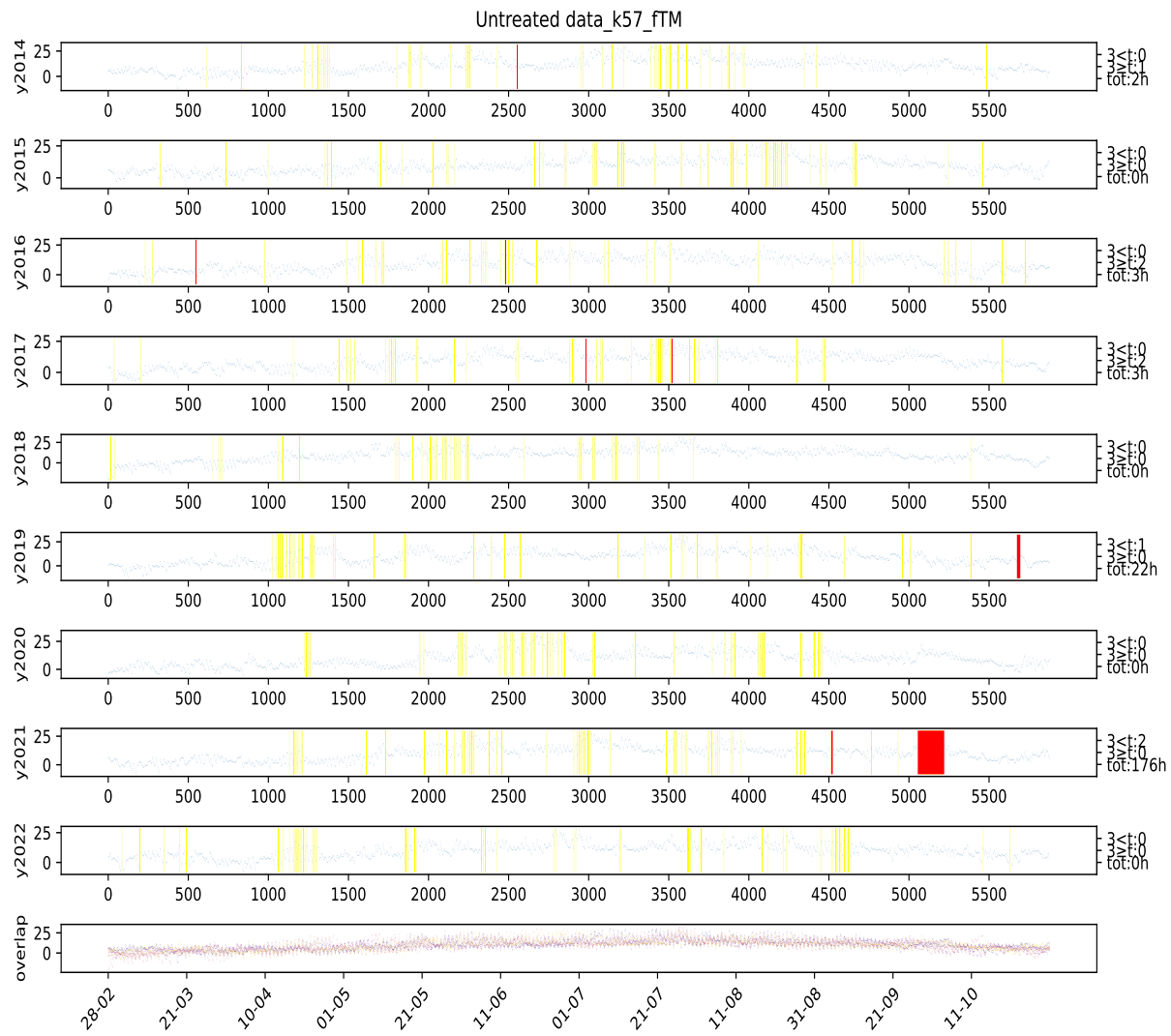


Figure 139: Visual representation of missing values at station 57 from 2014 to 2022 at the parameter "TM" after treating for outliers. The left numbers indicated how many hours that are missing and how many of them are shorter than or longer than 5 hours, however for this visualization they indicate the untreated version of the data. The yellow markings indicate possible outliers based on the given year, all markings was checked if they were actual outliers. The red colouring indicate missing values in the data (represented in the data with code "NULL"). The station names can be found in table 1.

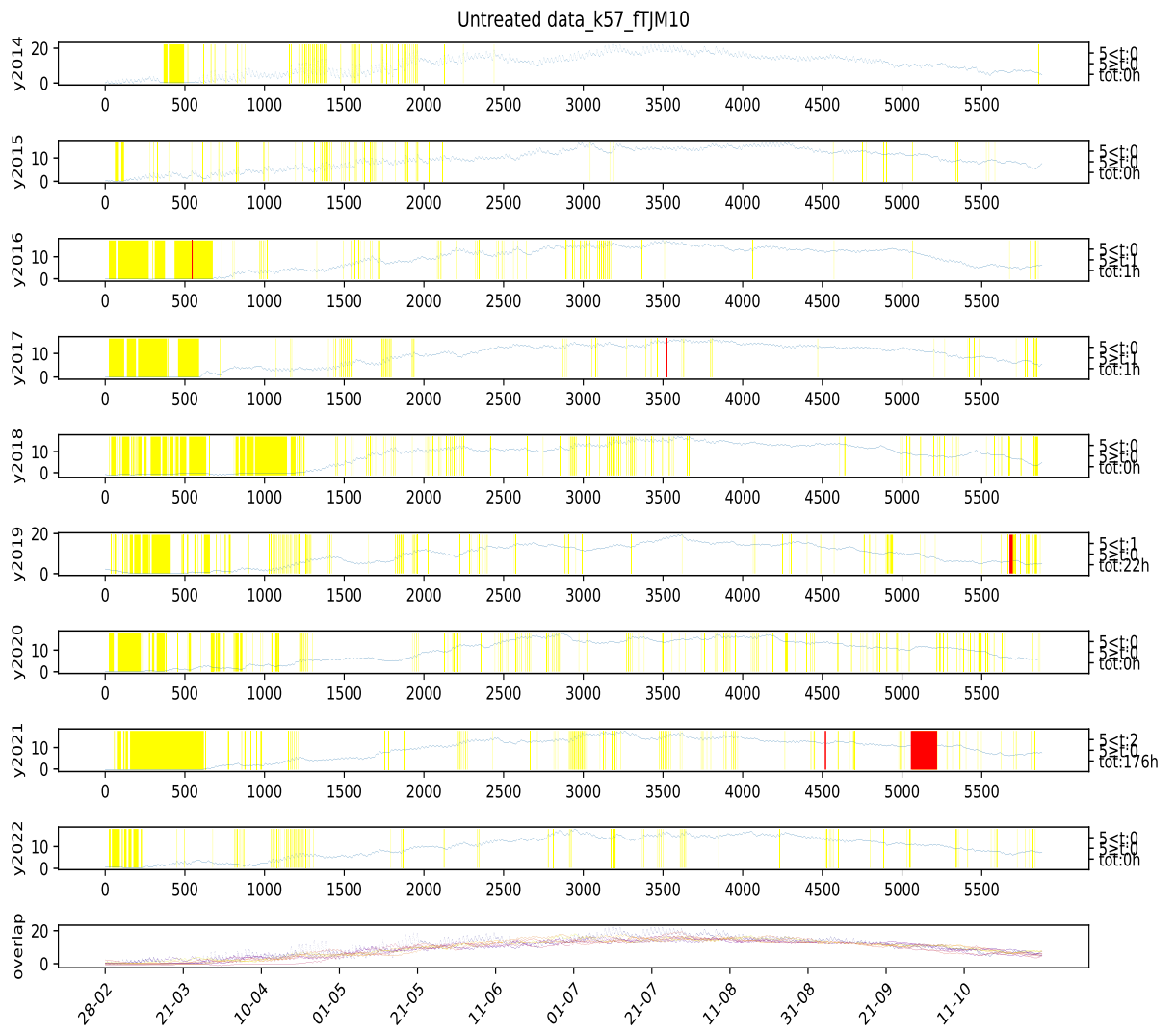


Figure 140: Visual representation of missing values at station 57 from 2014 to 2022 at the parameter "TJM10" after treating for outliers. The left numbers indicated how many hours that are missing and how many of them are shorter than or longer than 5 hours, however for this visualization they indicate the untreated version of the data. The yellow markings indicate possible outliers based on the given year, all markings was checked if they were actual outliers. The red colouring indicate missing values in the data (represented in the data with code "NULL"). The station names can be found in table 1.

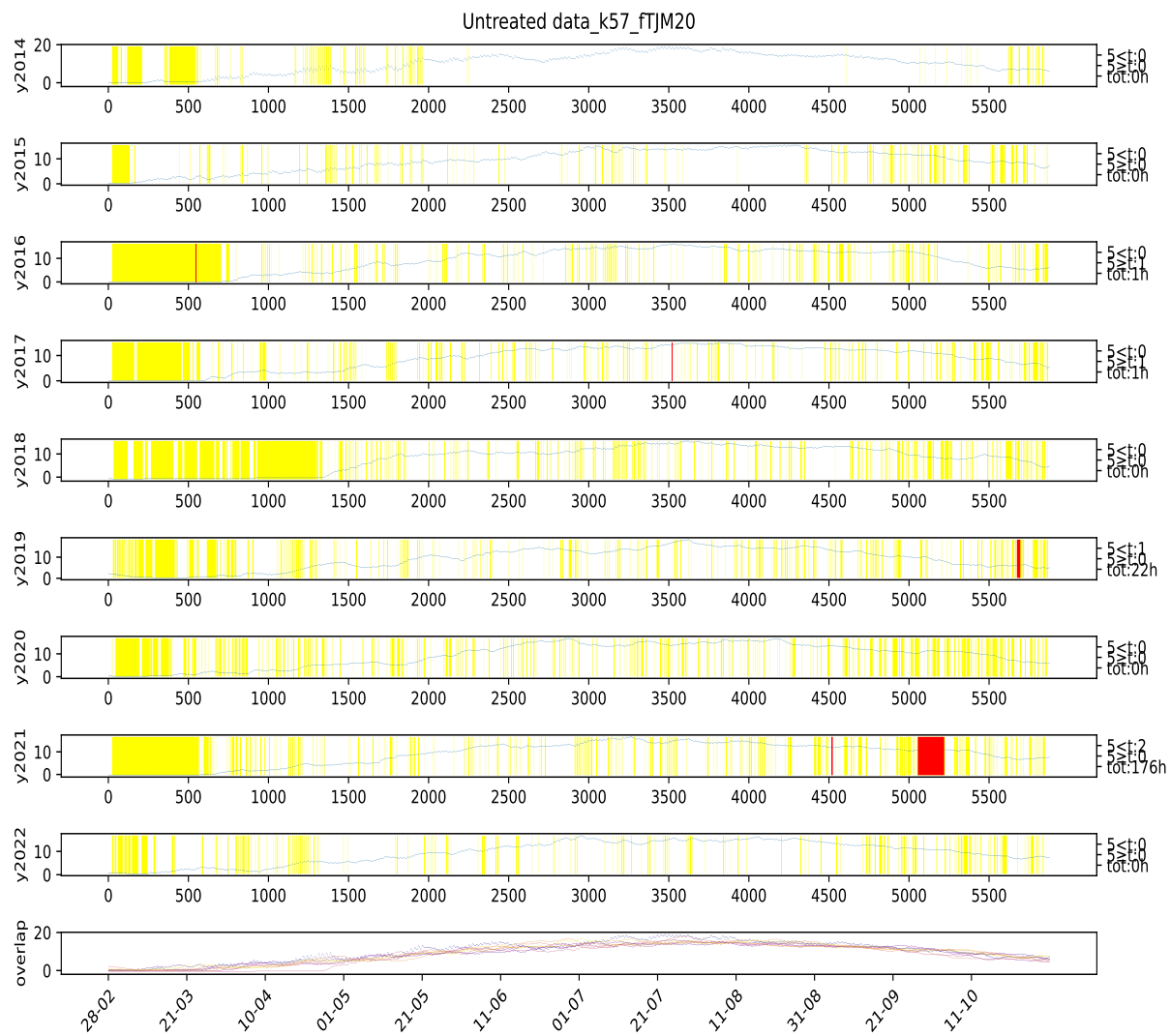


Figure 141: Visual representation of missing values at station 57 from 2014 to 2022 at the parameter "TJM20" after treating for outliers. The left numbers indicated how many hours that are missing and how many of them are shorter than or longer than 5 hours, however for this visualization they indicate the untreated version of the data. The yellow markings indicate possible outliers based on the given year, all markings was checked if they were actual outliers. The red colouring indicate missing values in the data (represented in the data with code "NULL"). The station names can be found in table 1.

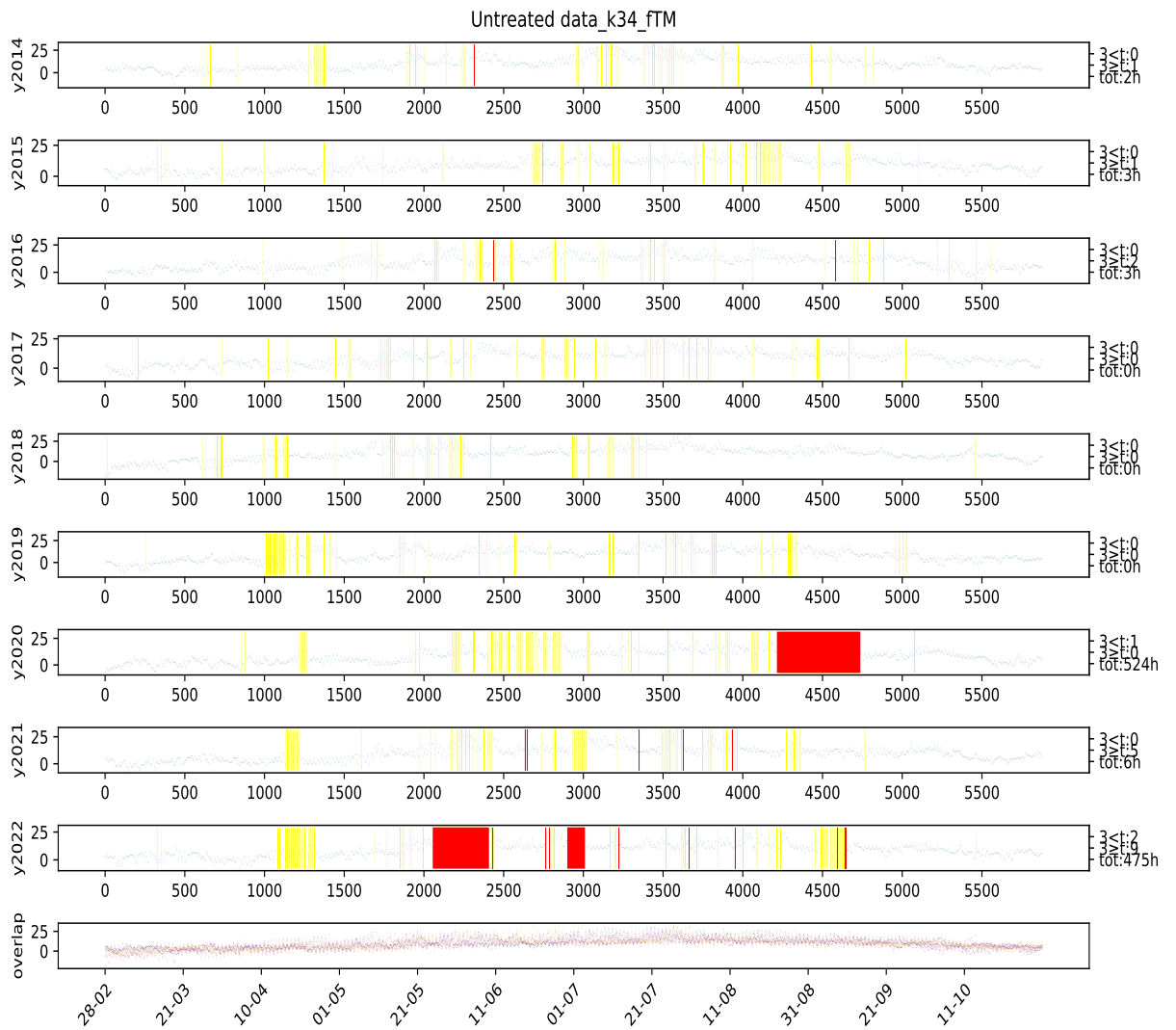


Figure 142: Visual representation of missing values at station 34 from 2014 to 2022 at the parameter "TM" after treating for outliers. The left numbers indicated how many hours that are missing and how many of them are shorter than or longer than 5 hours, however for this visualization they indicate the untreated version of the data. The yellow markings indicate possible outliers based on the given year, all markings was checked if they were actual outliers. The red colouring indicate missing values in the data (represented in the data with code "NULL"). The station names can be found in table 1.

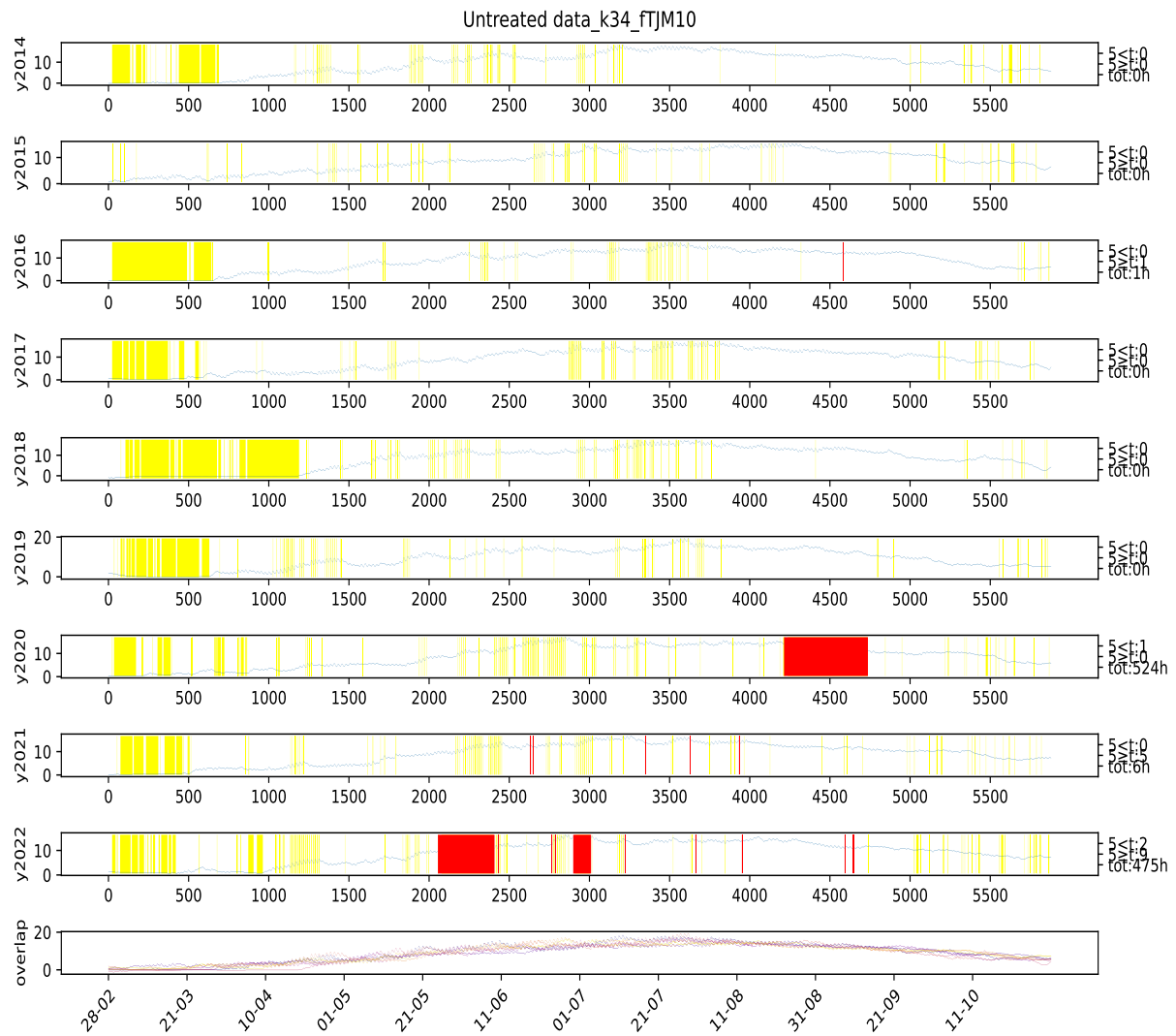


Figure 143: Visual representation of missing values at station 34 from 2014 to 2022 at the parameter "TJM10" after treating for outliers. The left numbers indicated how many hours that are missing and how many of them are shorter than or longer than 5 hours, however for this visualization they indicate the untreated version of the data. The yellow markings indicate possible outliers based on the given year, all markings was checked if they were actual outliers. The red colouring indicate missing values in the data (represented in the data with code "NULL").The station names can be found in table 1.

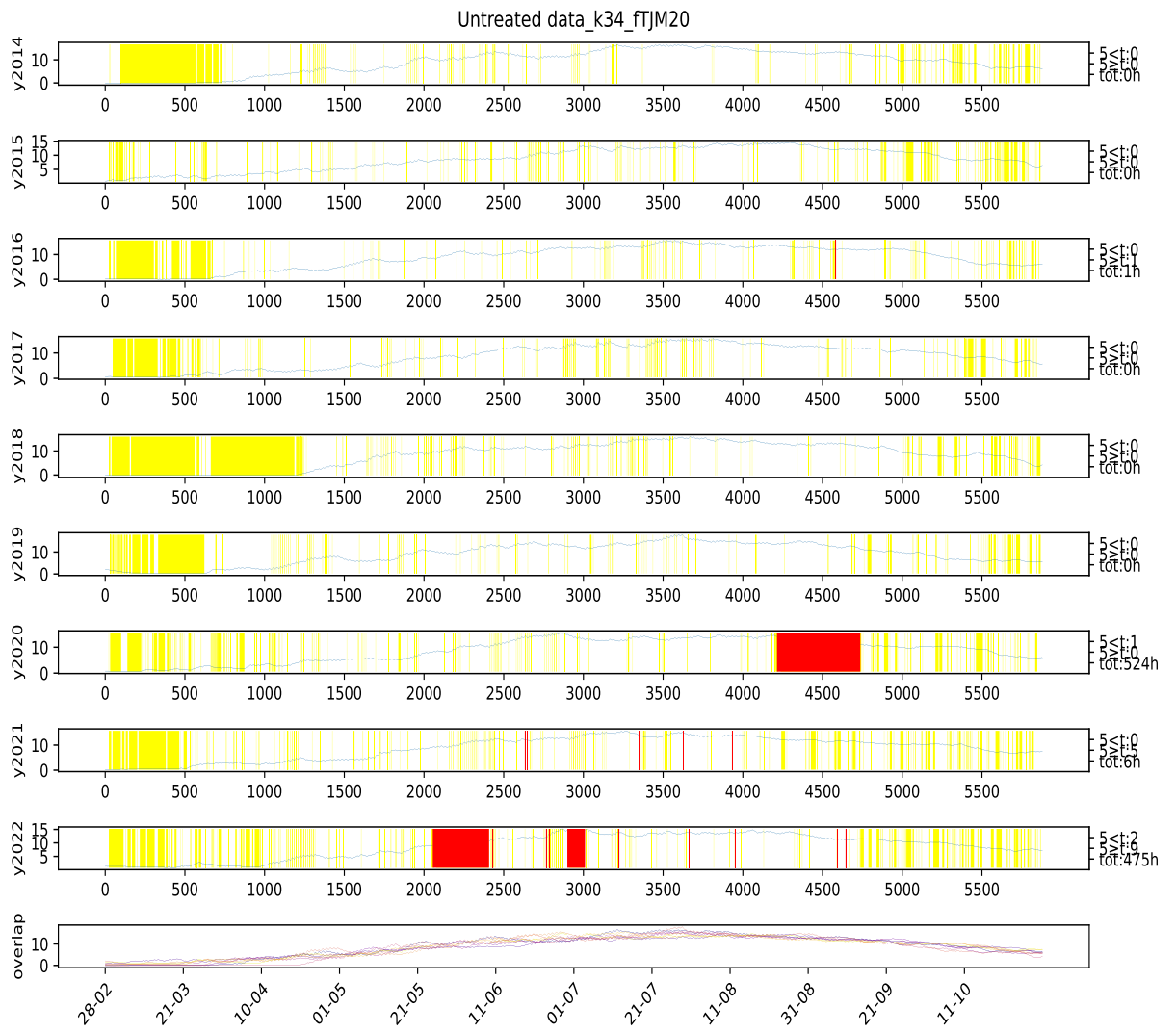


Figure 144: Visual representation of missing values at station 34 from 2014 to 2022 at the parameter "TJM20" after treating for outliers. The left numbers indicated how many hours that are missing and how many of them are shorter than or longer than 5 hours, however for this visualization they indicate the untreated version of the data. The yellow markings indicate possible outliers based on the given year, all markings was checked if they were actual outliers. The red colouring indicate missing values in the data (represented in the data with code "NULL"). The station names can be found in table 1.

## A PLOTS

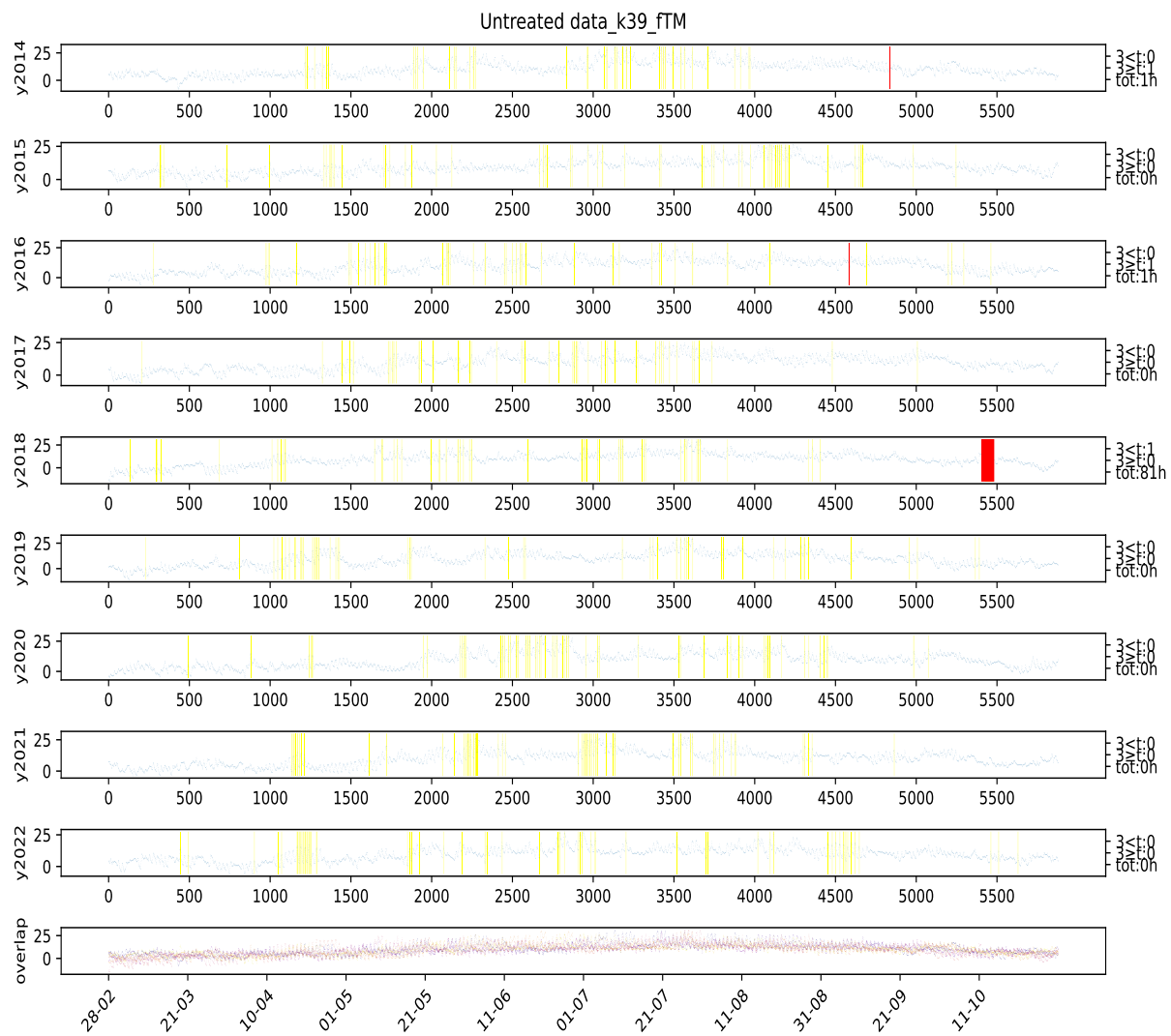


Figure 145: Visual representation of missing values at station 39 from 2014 to 2022 at the parameter "TM" after treating for outliers. The left numbers indicated how many hours that are missing and how many of them are shorter than or longer than 5 hours, however for this visualization they indicate the untreated version of the data. The yellow markings indicate possible outliers based on the given year, all markings was checked if they were actual outliers. The red colouring indicate missing values in the data (represented in the data with code "NULL"). The station names can be found in table 1.

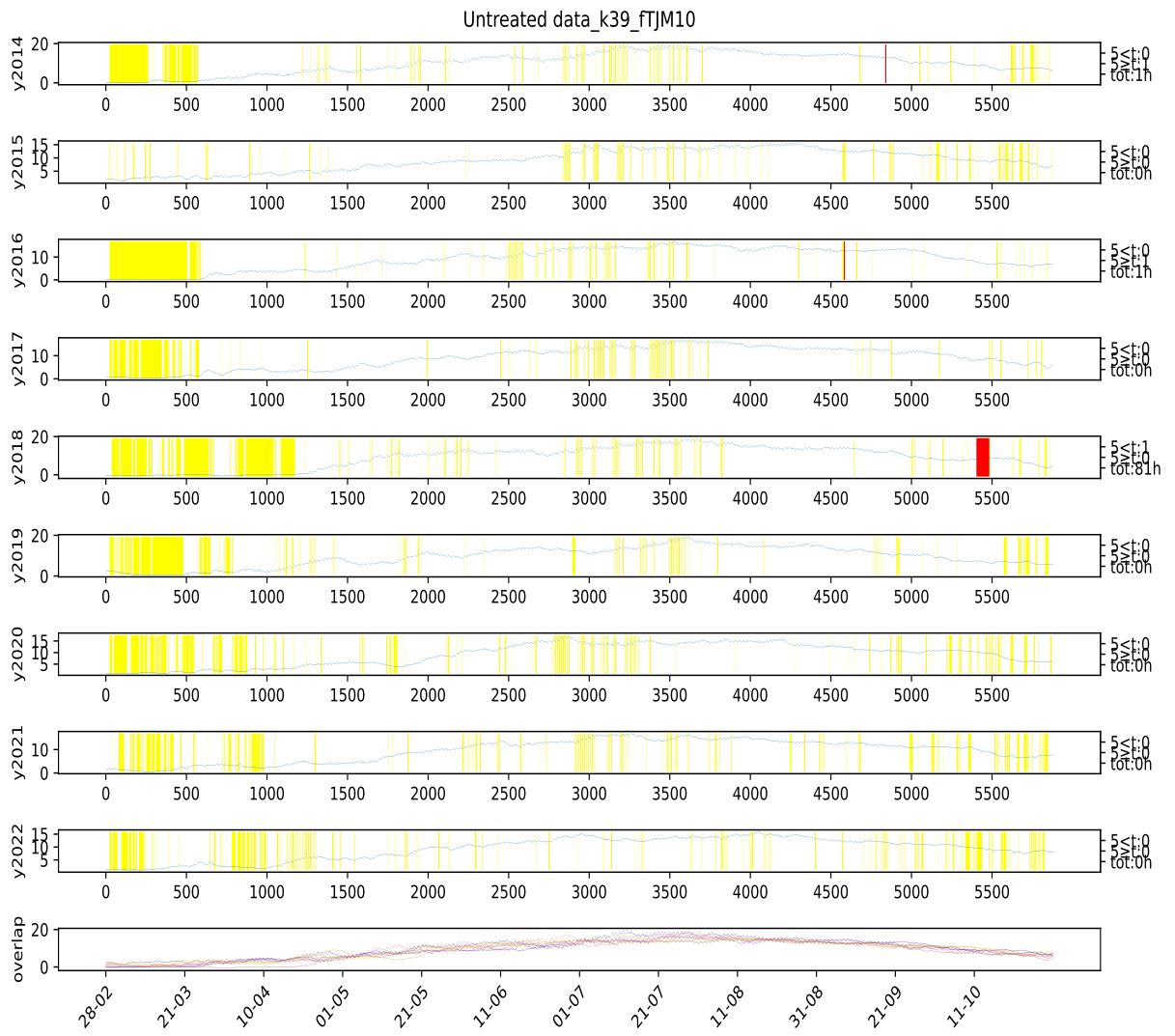


Figure 146: Visual representation of missing values at station 39 from 2014 to 2022 at the parameter "TJM10" after treating for outliers. The left numbers indicated how many hours that are missing and how many of them are shorter than or longer than 5 hours, however for this visualization they indicate the untreated version of the data. The yellow markings indicate possible outliers based on the given year, all markings was checked if they were actual outliers. The red colouring indicate missing values in the data (represented in the data with code "NULL"). The station names can be found in table 1.

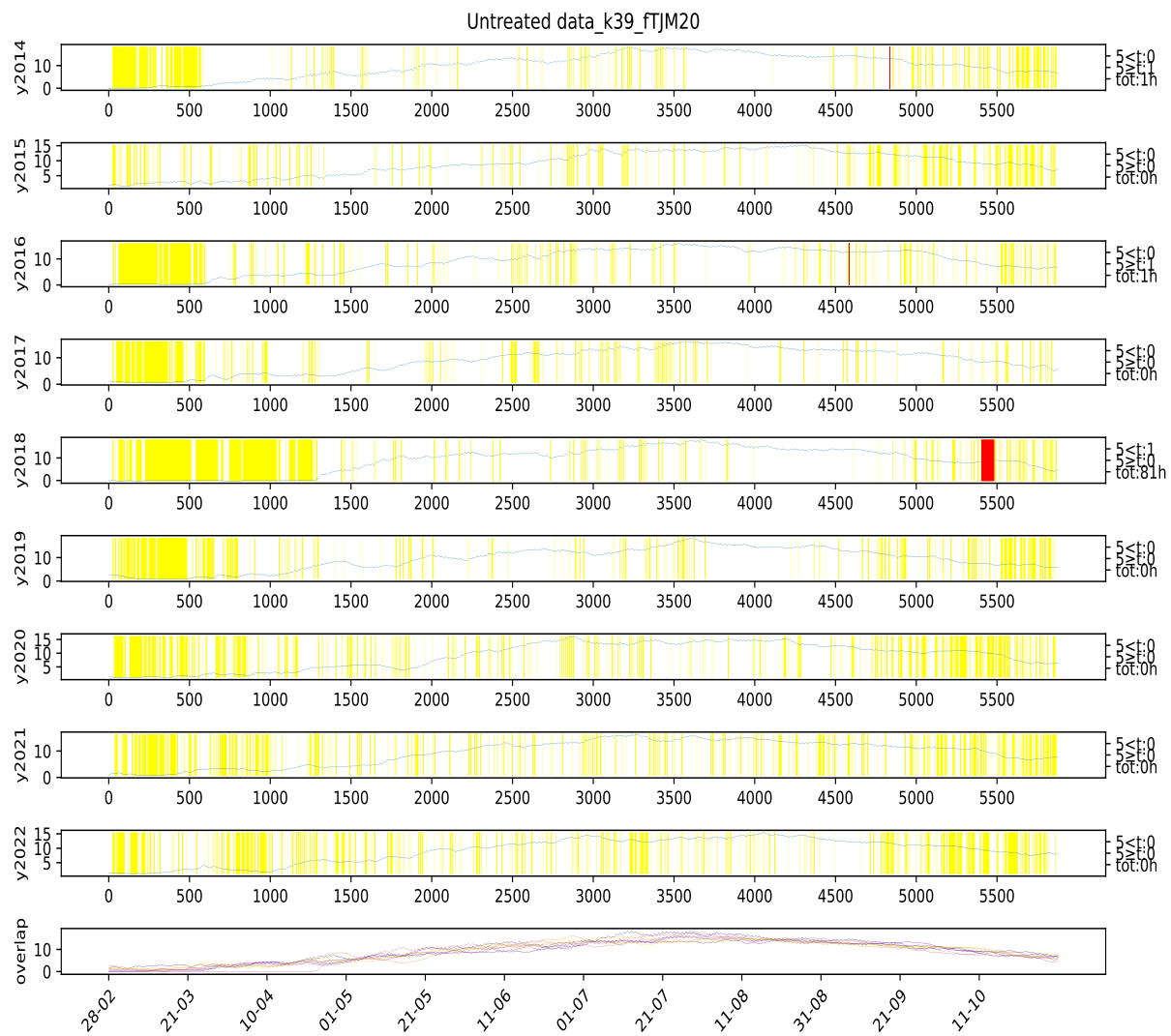


Figure 147: Visual representation of missing values at station 39 from 2014 to 2022 at the parameter "TJM20" after treating for outliers. The left numbers indicated how many hours that are missing and how many of them are shorter than or longer than 5 hours, however for this visualization they indicate the untreated version of the data. The yellow markings indicate possible outliers based on the given year, all markings was checked if they were actual outliers. The red colouring indicate missing values in the data (represented in the data with code "NULL").The station names can be found in table 1.

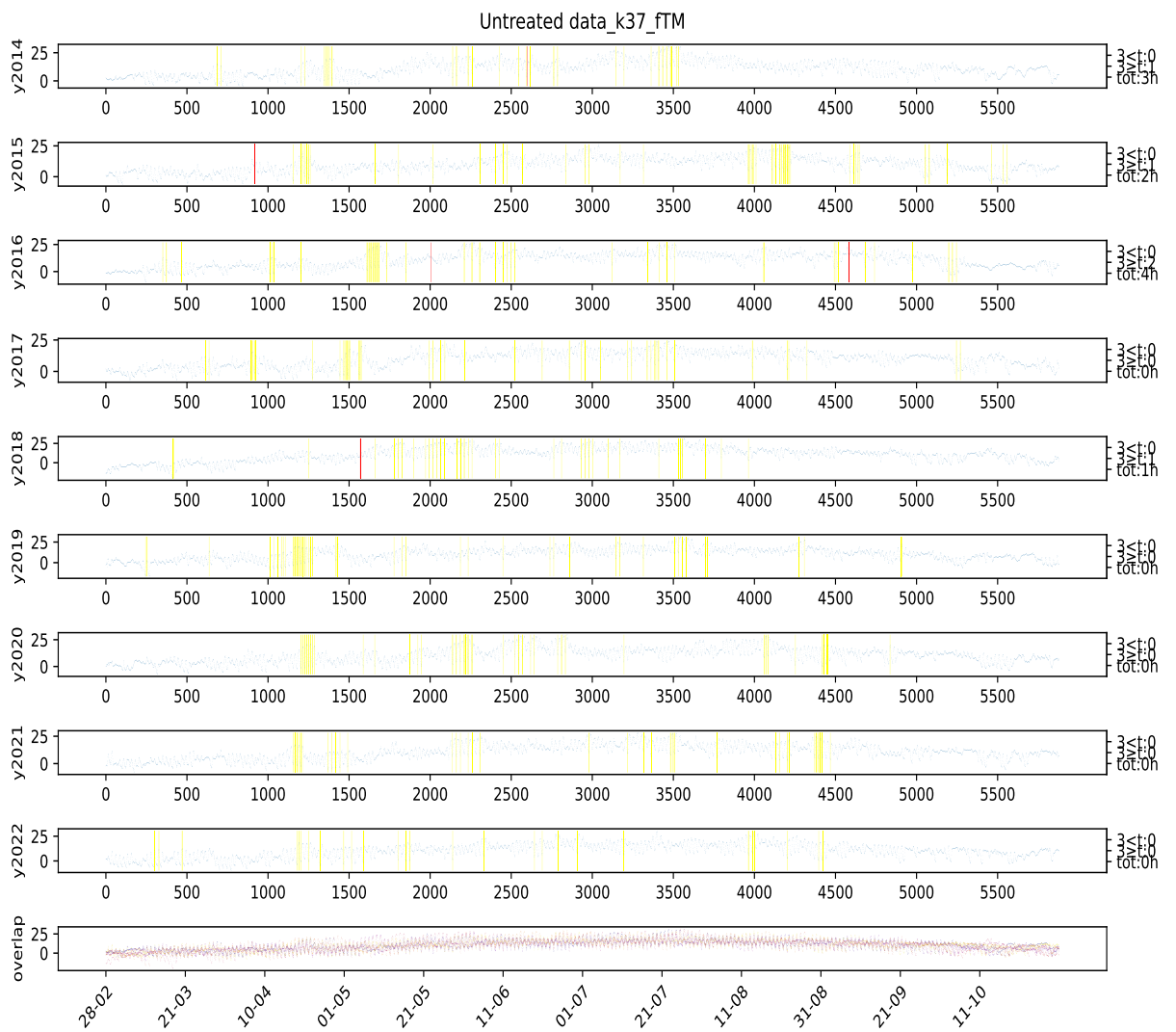


Figure 148: Visual representation of missing values at station 37 from 2014 to 2022 at the parameter "TM" after treating for outliers. The left numbers indicated how many hours that are missing and how many of them are shorter than or longer than 5 hours, however for this visualization they indicate the untreated version of the data. The yellow markings indicate possible outliers based on the given year, all markings was checked if they were actual outliers. The red colouring indicate missing values in the data (represented in the data with code "NULL"). The station names can be found in table 1.

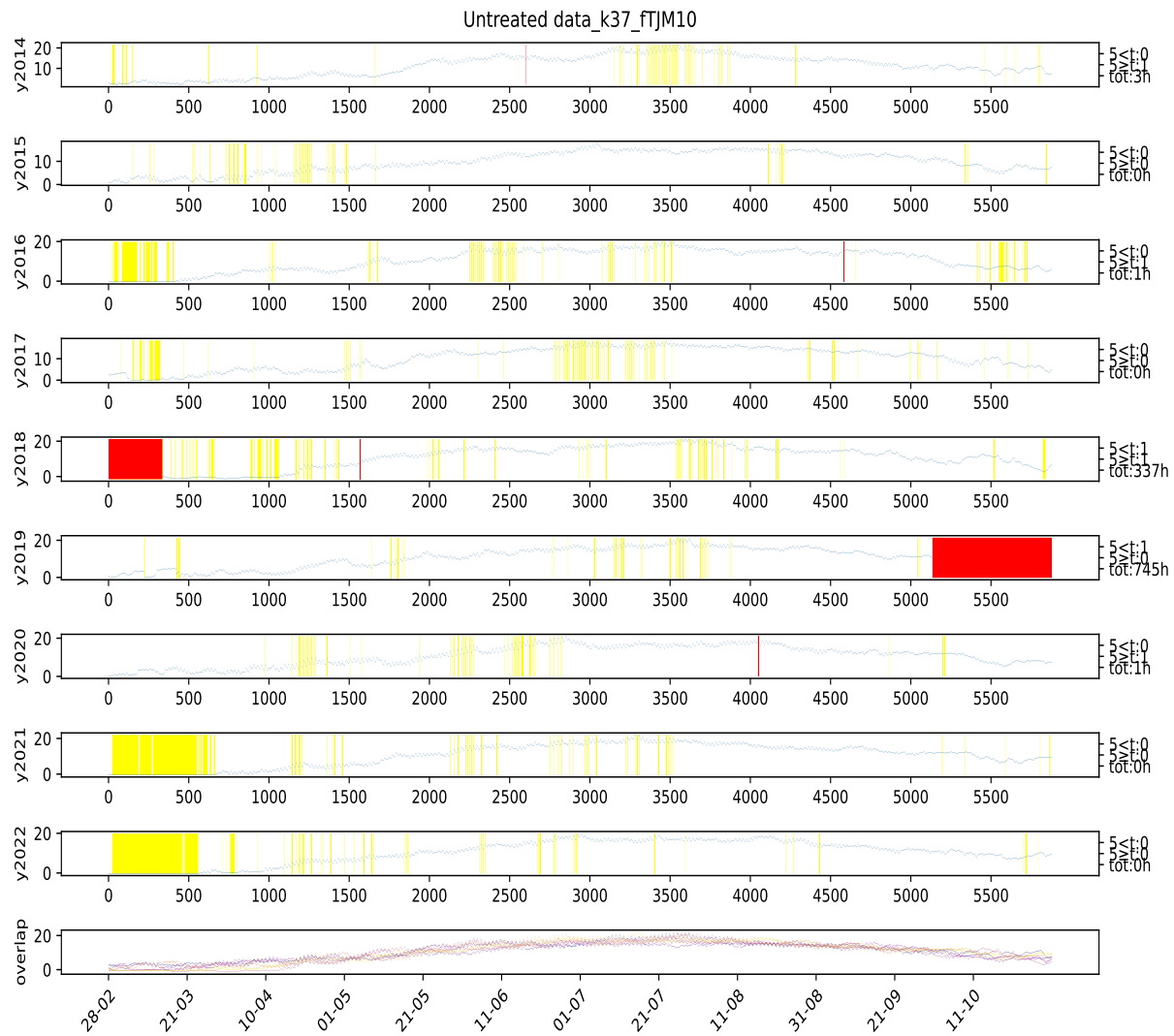


Figure 149: Visual representation of missing values at station 37 from 2014 to 2022 at the parameter "TJM10" after treating for outliers. The left numbers indicated how many hours that are missing and how many of them are shorter than or longer than 5 hours, however for this visualization they indicate the untreated version of the data. The yellow markings indicate possible outliers based on the given year, all markings was checked if they were actual outliers. The red colouring indicate missing values in the data (represented in the data with code "NULL").The station names can be found in table 1.

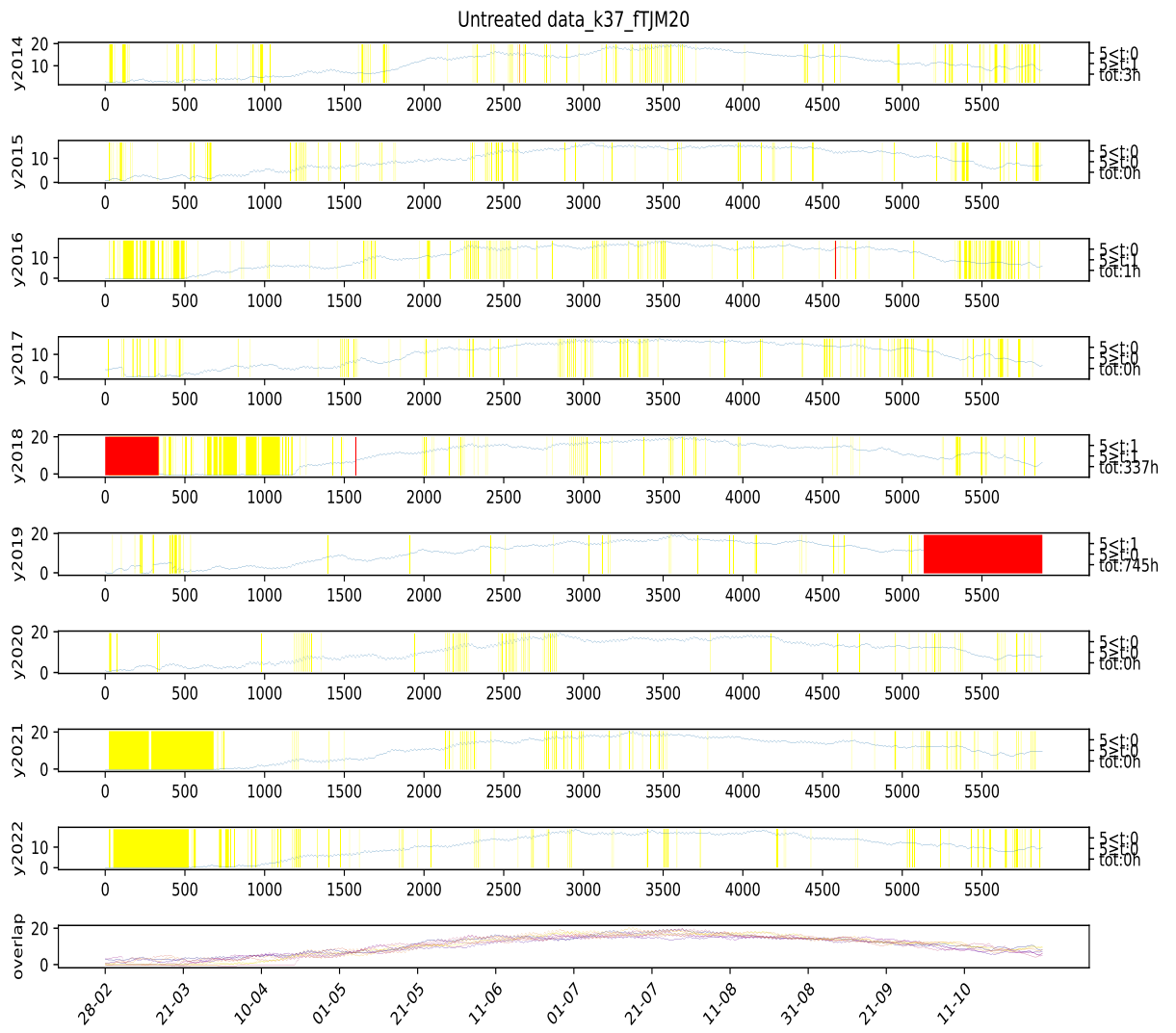


Figure 150: Visual representation of missing values at station 37 from 2014 to 2022 at the parameter "TJM20" after treating for outliers. The left numbers indicated how many hours that are missing and how many of them are shorter than or longer than 5 hours, however for this visualization they indicate the untreated version of the data. The yellow markings indicate possible outliers based on the given year, all markings was checked if they were actual outliers. The red colouring indicate missing values in the data (represented in the data with code "NULL"). The station names can be found in table 1.

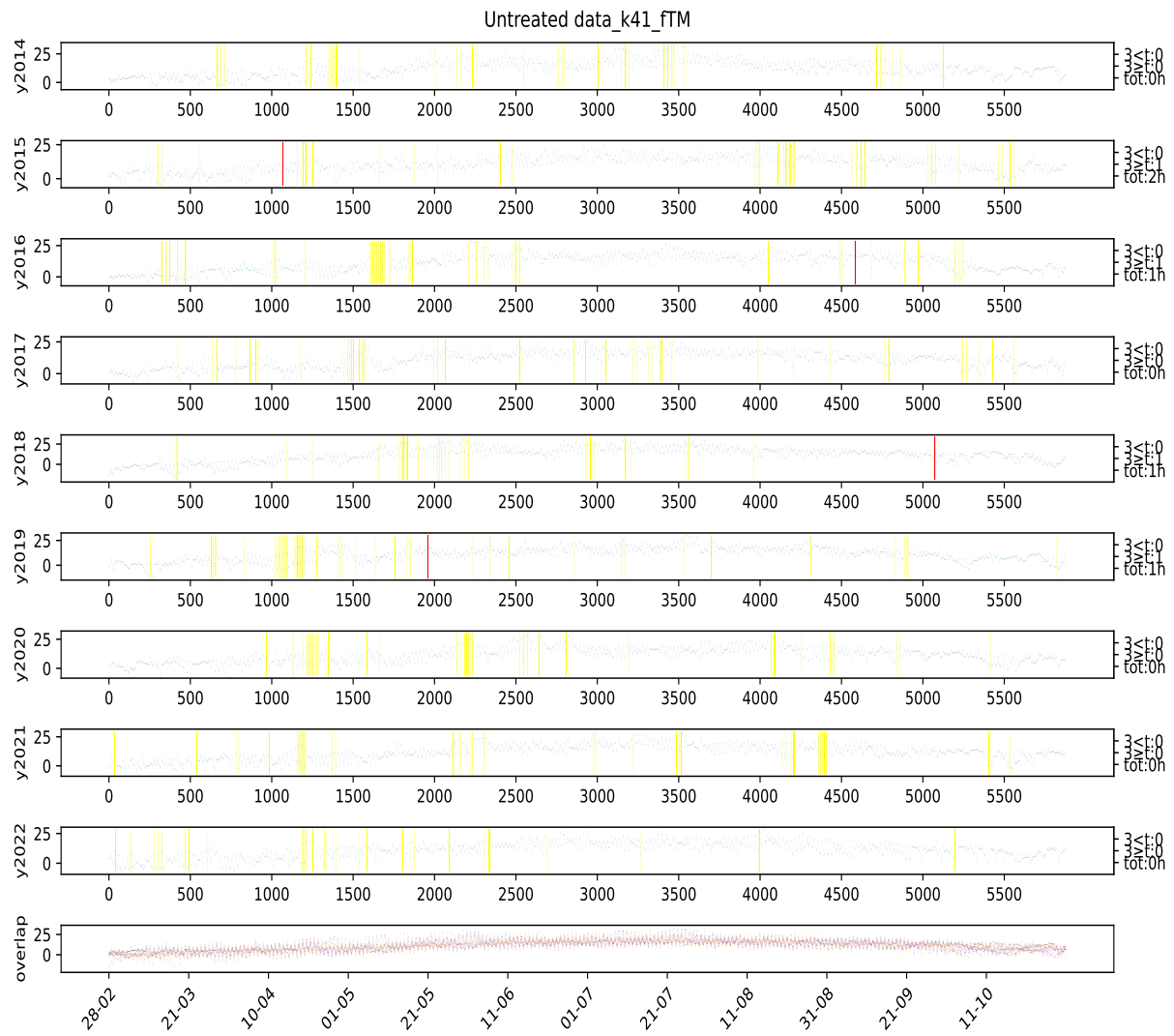


Figure 151: Visual representation of missing values at station 41 from 2014 to 2022 at the parameter "TM" after treating for outliers. The left numbers indicated how many hours that are missing and how many of them are shorter than or longer than 5 hours, however for this visualization they indicate the untreated version of the data. The yellow markings indicate possible outliers based on the given year, all markings was checked if they were actual outliers. The red colouring indicate missing values in the data (represented in the data with code "NULL"). The station names can be found in table 1.

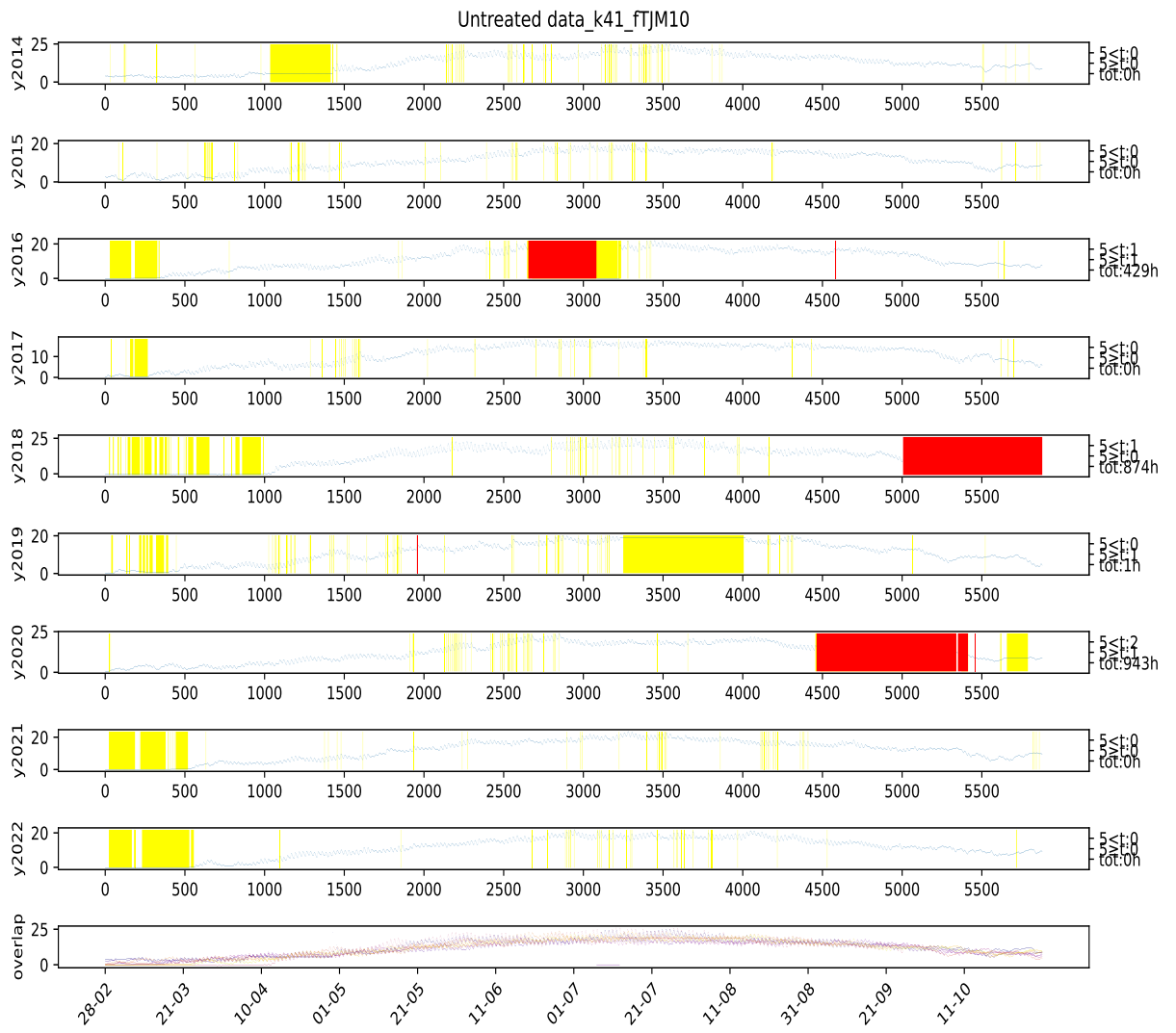


Figure 152: Visual representation of missing values at station 41 from 2014 to 2022 at the parameter "TJM10" after treating for outliers. The left numbers indicated how many hours that are missing and how many of them are shorter than or longer than 5 hours, however for this visualization they indicate the untreated version of the data. The yellow markings indicate possible outliers based on the given year, all markings was checked if they were actual outliers. The red colouring indicate missing values in the data (represented in the data with code "NULL"). The station names can be found in table 1.

## A PLOTS

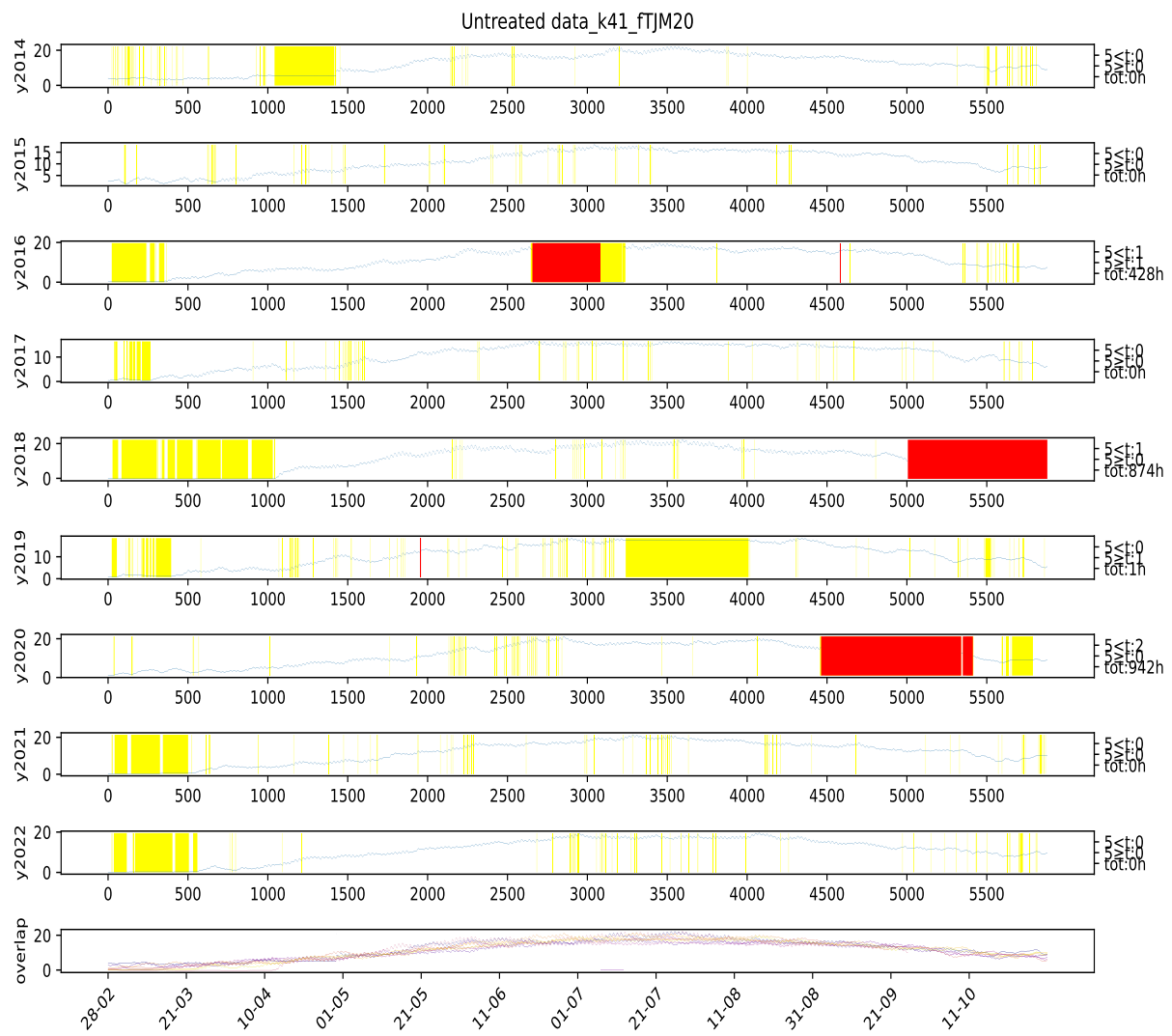


Figure 153: Visual representation of missing values at station 41 from 2014 to 2022 at the parameter "TJM20" after treating for outliers. The left numbers indicated how many hours that are missing and how many of them are shorter than or longer than 5 hours, however for this visualization they indicate the untreated version of the data. The yellow markings indicate possible outliers based on the given year, all markings was checked if they were actual outliers. The red colouring indicate missing values in the data (represented in the data with code "NULL"). The station names can be found in table 1.

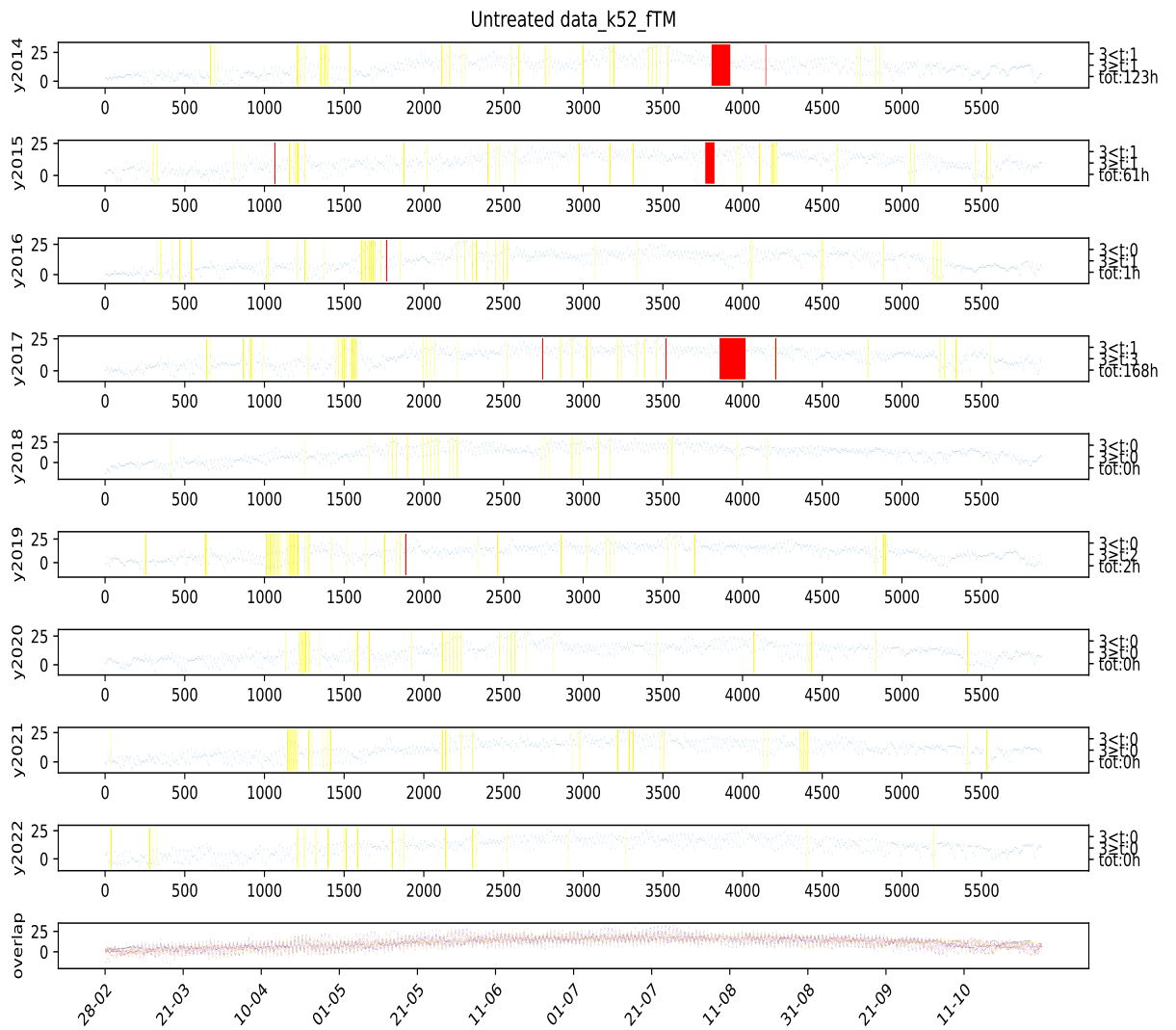


Figure 154: Visual representation of missing values at station 52 from 2014 to 2022 at the parameter "TM" after treating for outliers. The left numbers indicated how many hours that are missing and how many of them are shorter than or longer than 5 hours, however for this visualization they indicate the untreated version of the data. The yellow markings indicate possible outliers based on the given year, all markings was checked if they were actual outliers. The red colouring indicate missing values in the data (represented in the data with code "NULL"). The station names can be found in table 1.

## A PLOTS

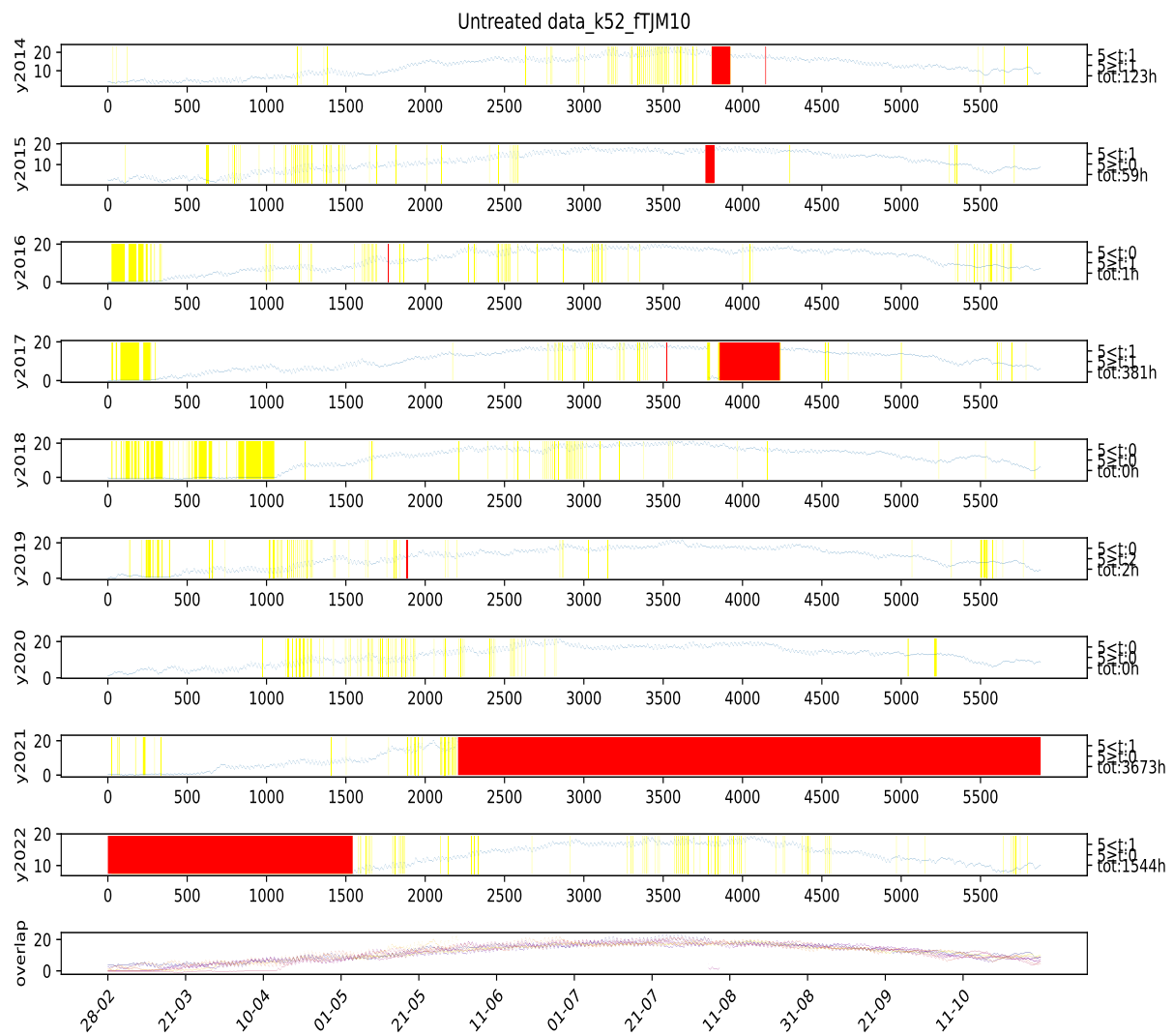


Figure 155: Visual representation of missing values at station 52 from 2014 to 2022 at the parameter "TJM10" after treating for outliers. The left numbers indicated how many hours that are missing and how many of them are shorter than or longer than 5 hours, however for this visualization they indicate the untreated version of the data. The yellow markings indicate possible outliers based on the given year, all markings was checked if they were actual outliers. The red colouring indicate missing values in the data (represented in the data with code "NULL"). The station names can be found in table 1.

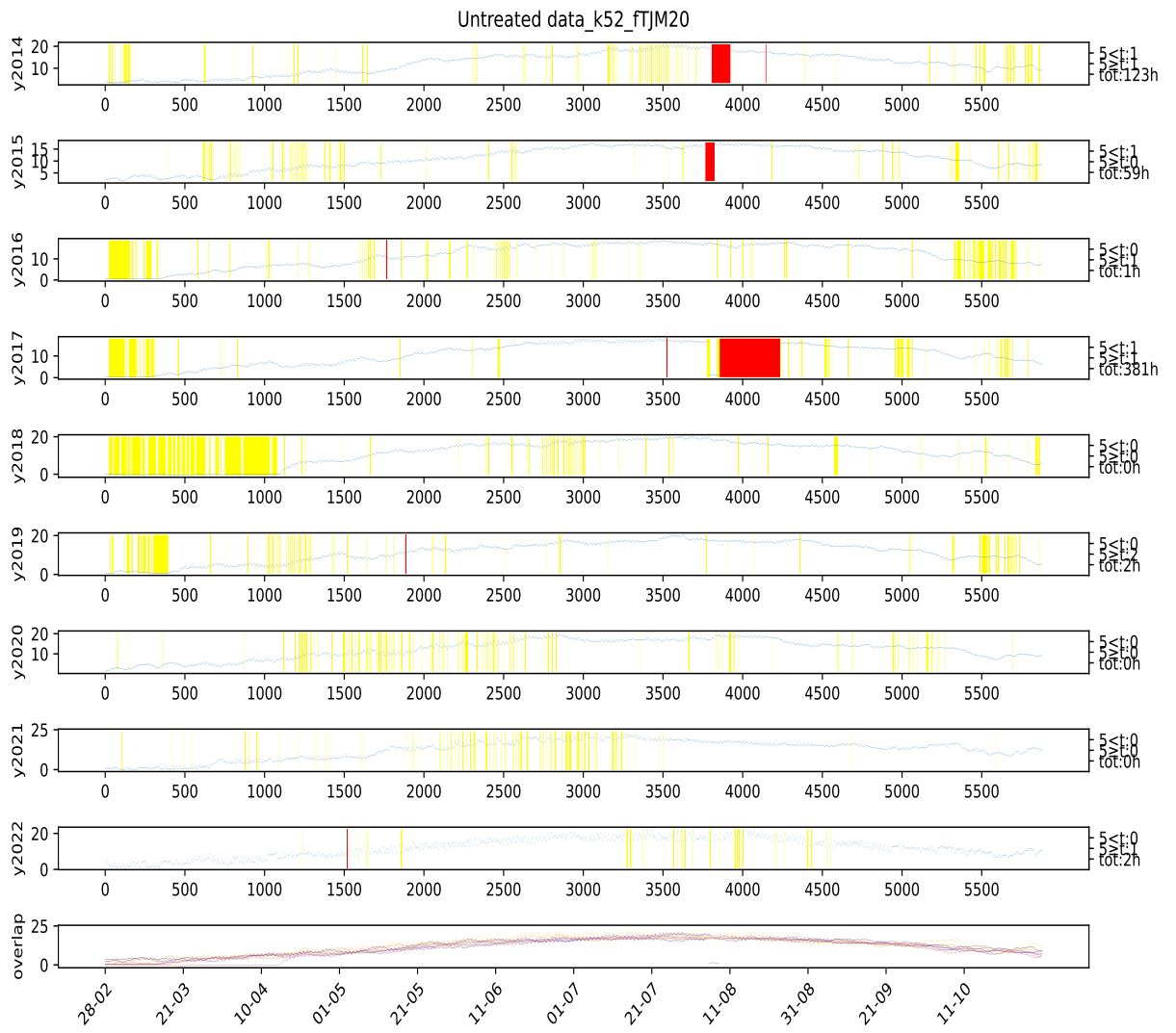


Figure 156: Visual representation of missing values at station 52 from 2014 to 2022 at the parameter "TJM20" after treating for outliers. The left numbers indicated how many hours that are missing and how many of them are shorter than or longer than 5 hours, however for this visualization they indicate the untreated version of the data. The yellow markings indicate possible outliers based on the given year, all markings was checked if they were actual outliers. The red colouring indicate missing values in the data (represented in the data with code "NULL"). The station names can be found in table 1.

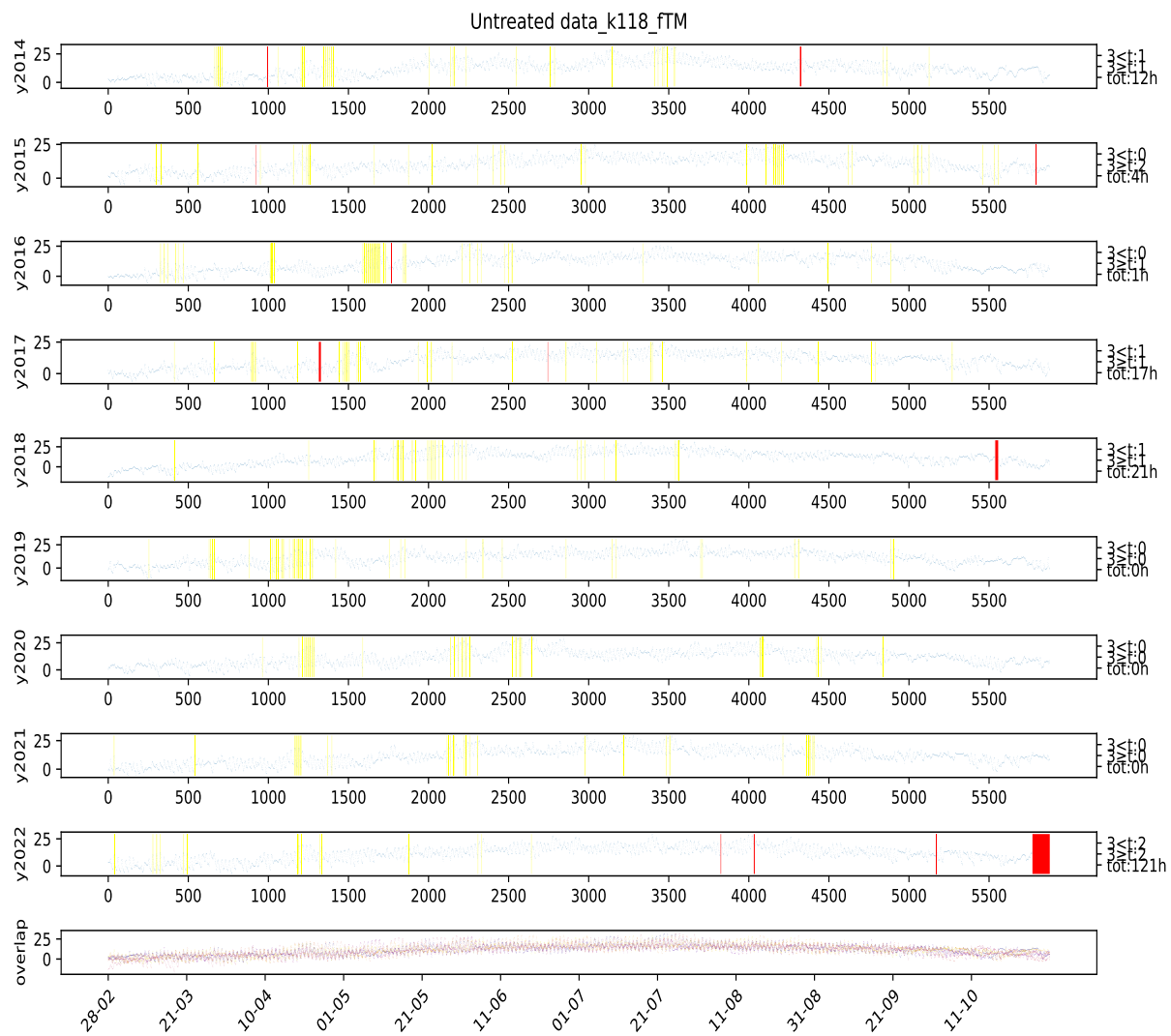


Figure 157: Visual representation of missing values at station 118 from 2014 to 2022 at the parameter "TM" after treating for outliers. The left numbers indicated how many hours that are missing and how many of them are shorter than or longer than 5 hours, however for this visualization they indicate the untreated version of the data. The yellow markings indicate possible outliers based on the given year, all markings was checked if they were actual outliers. The red colouring indicate missing values in the data (represented in the data with code "NULL"). The station names can be found in table 1.

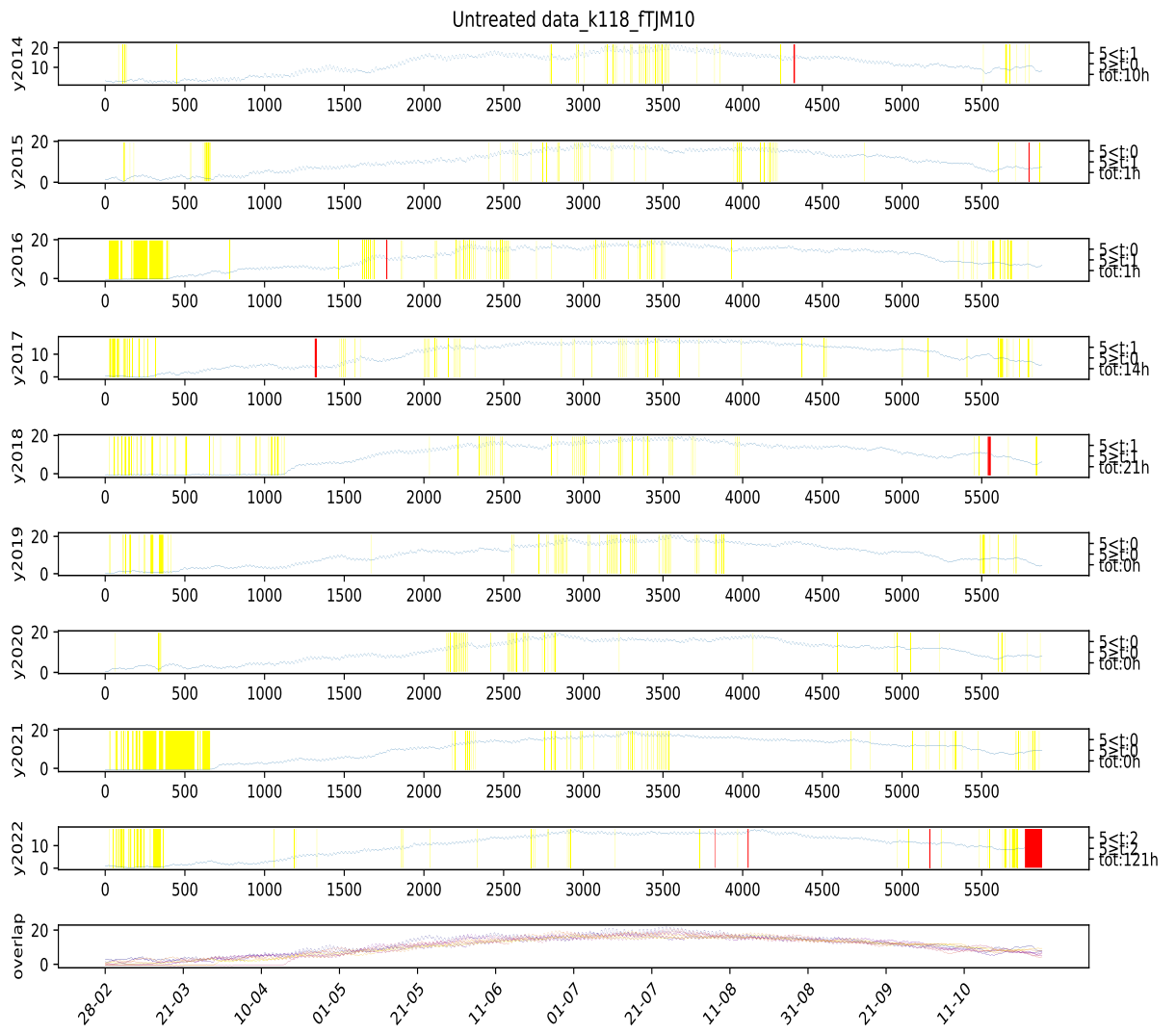


Figure 158: Visual representation of missing values at station 118 from 2014 to 2022 at the parameter "TJM10" after treating for outliers. The left numbers indicated how many hours that are missing and how many of them are shorter than or longer than 5 hours, however for this visualization they indicate the untreated version of the data. The yellow markings indicate possible outliers based on the given year, all markings was checked if they were actual outliers. The red colouring indicate missing values in the data (represented in the data with code "NULL"). The station names can be found in table 1.

## A PLOTS

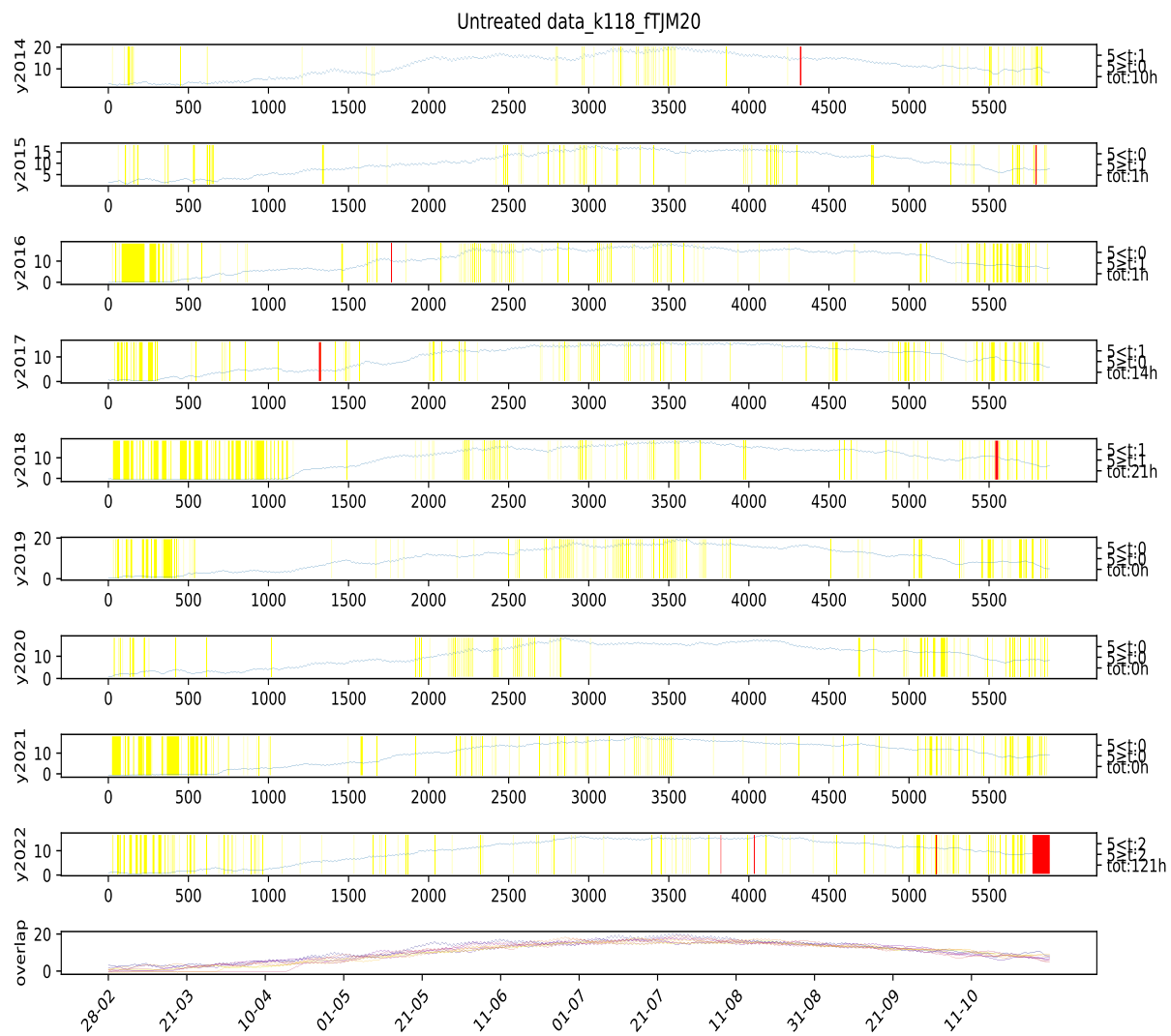


Figure 159: Visual representation of missing values at station 118 from 2014 to 2022 at the parameter "TJM20" after treating for outliers. The left numbers indicated how many hours that are missing and how many of them are shorter than or longer than 5 hours, however for this visualization they indicate the untreated version of the data. The yellow markings indicate possible outliers based on the given year, all markings was checked if they were actual outliers. The red colouring indicate missing values in the data (represented in the data with code "NULL"). The station names can be found in table 1.

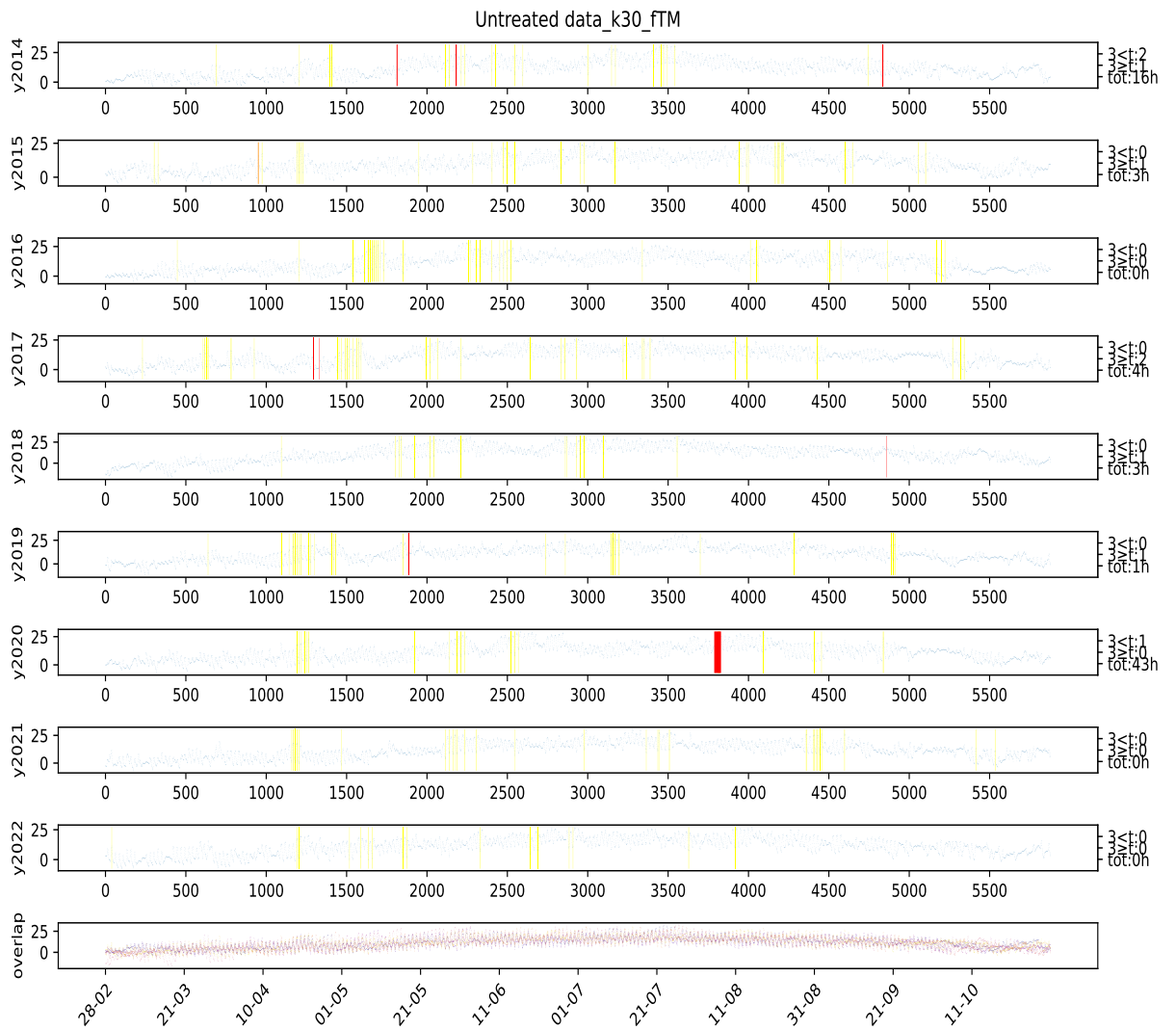


Figure 160: Visual representation of missing values at station 30 from 2014 to 2022 at the parameter "TM" after treating for outliers. The left numbers indicated how many hours that are missing and how many of them are shorter than or longer than 5 hours, however for this visualization they indicate the untreated version of the data. The yellow markings indicate possible outliers based on the given year, all markings was checked if they were actual outliers. The red colouring indicate missing values in the data (represented in the data with code "NULL"). The station names can be found in table 1.

## A PLOTS

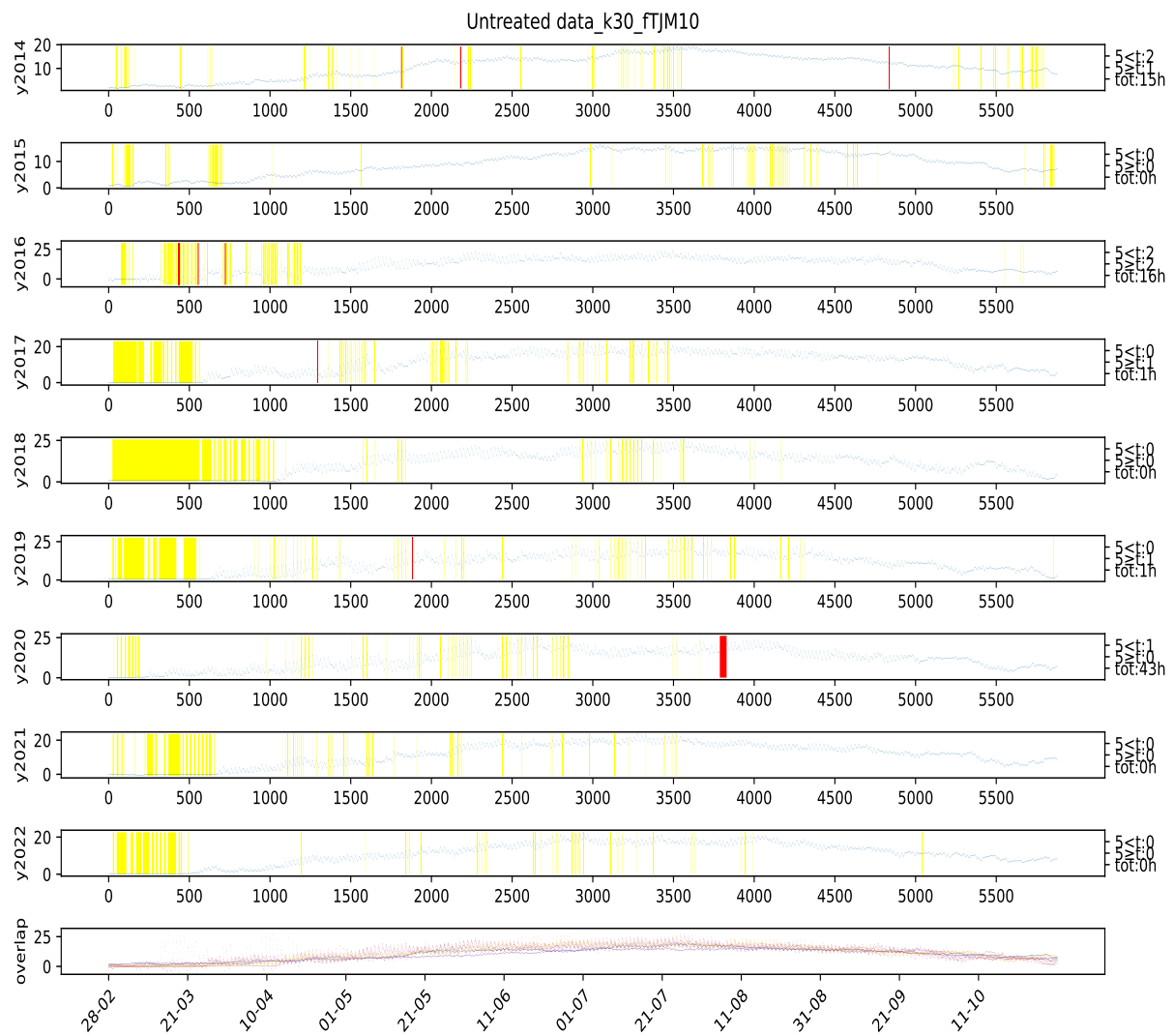


Figure 161: Visual representation of missing values at station 30 from 2014 to 2022 at the parameter "TJM10" after treating for outliers. The left numbers indicated how many hours that are missing and how many of them are shorter than or longer than 5 hours, however for this visualization they indicate the untreated version of the data. The yellow markings indicate possible outliers based on the given year, all markings was checked if they were actual outliers. The red colouring indicate missing values in the data (represented in the data with code "NULL"). The station names can be found in table 1.

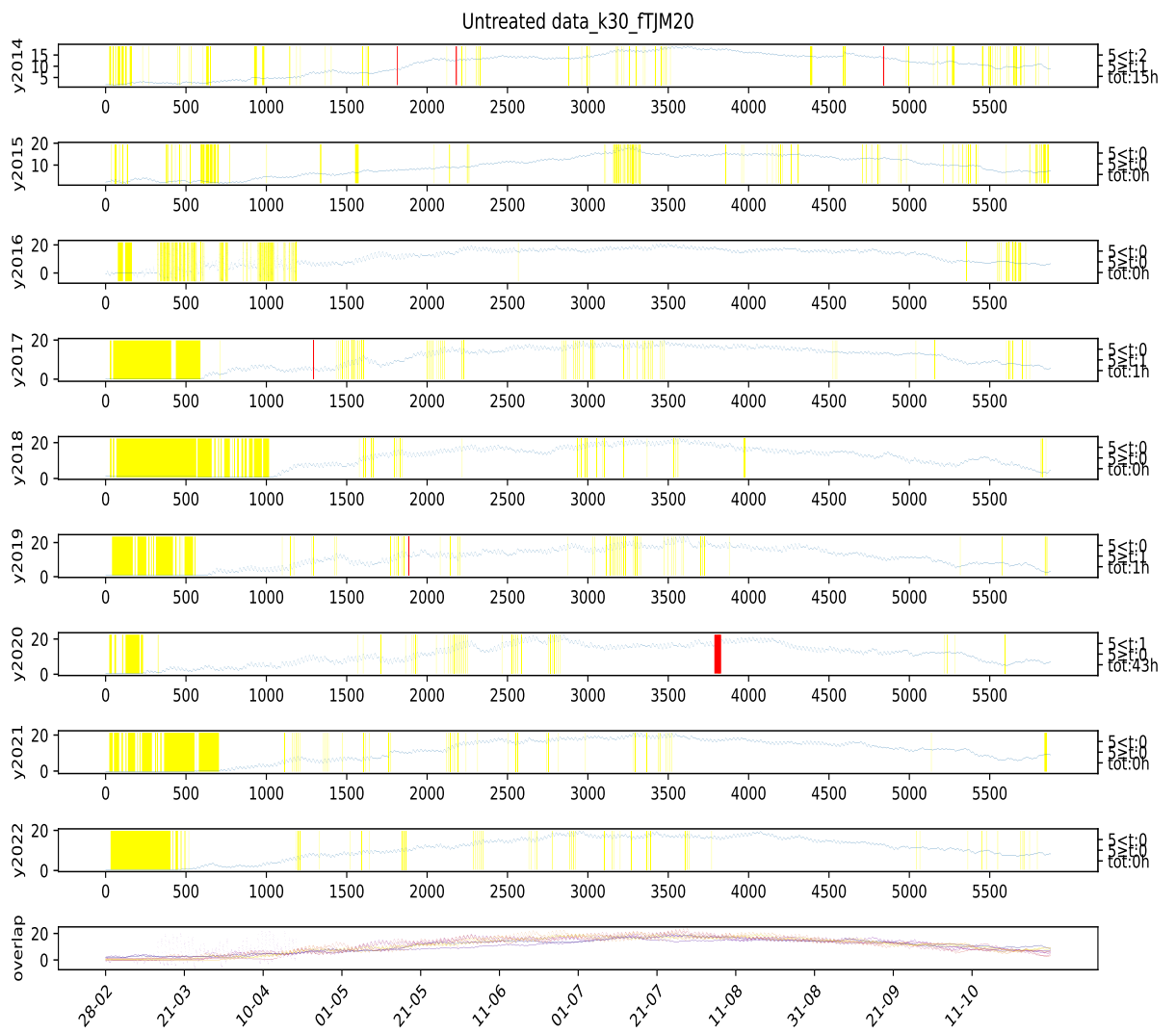


Figure 162: Visual representation of missing values at station 30 from 2014 to 2022 at the parameter "TJM20" after treating for outliers. The left numbers indicated how many hours that are missing and how many of them are shorter than or longer than 5 hours, however for this visualization they indicate the untreated version of the data. The yellow markings indicate possible outliers based on the given year, all markings was checked if they were actual outliers. The red colouring indicate missing values in the data (represented in the data with code "NULL"). The station names can be found in table 1.

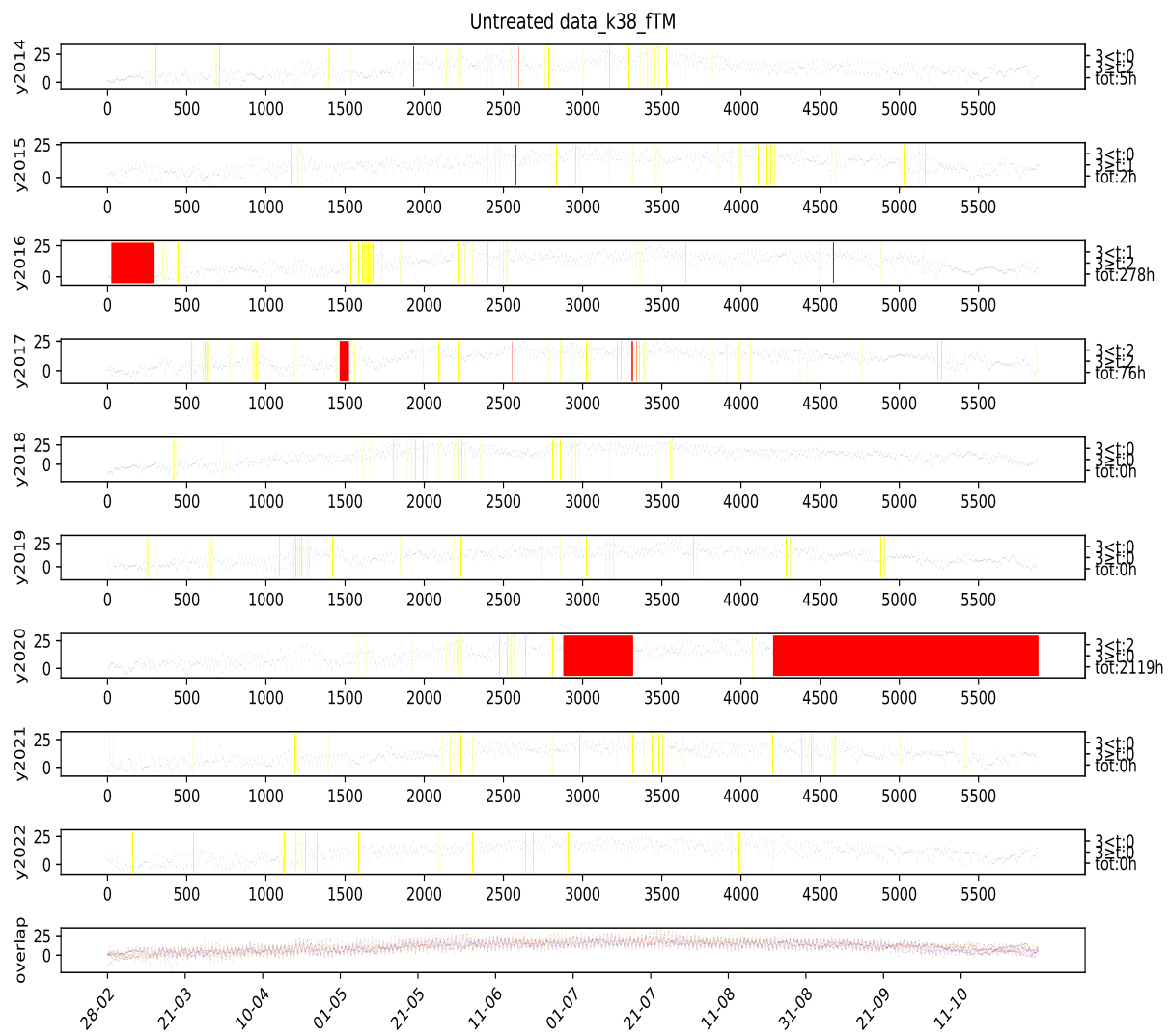


Figure 163: Visual representation of missing values at station 38 from 2014 to 2022 at the parameter "TM" after treating for outliers. The left numbers indicated how many hours that are missing and how many of them are shorter than or longer than 5 hours, however for this visualization they indicate the untreated version of the data. The yellow markings indicate possible outliers based on the given year, all markings was checked if they were actual outliers. The red colouring indicate missing values in the data (represented in the data with code "NULL"). The station names can be found in table 1.

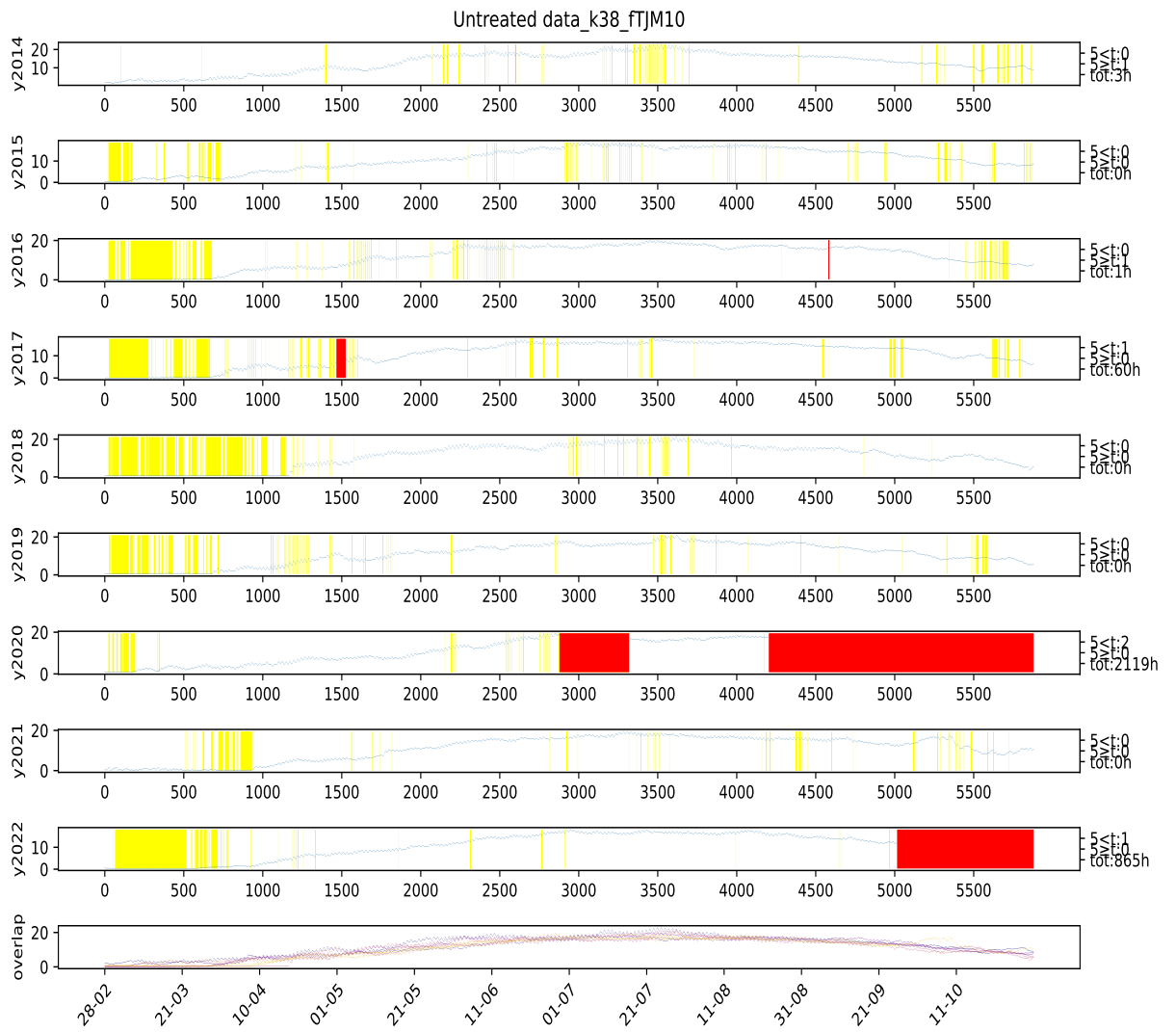


Figure 164: Visual representation of missing values at station 38 from 2014 to 2022 at the parameter "TJM10" after treating for outliers. The left numbers indicated how many hours that are missing and how many of them are shorter than or longer than 5 hours, however for this visualization they indicate the untreated version of the data. The yellow markings indicate possible outliers based on the given year, all markings was checked if they were actual outliers. The red colouring indicate missing values in the data (represented in the data with code "NULL"). The station names can be found in table 1.

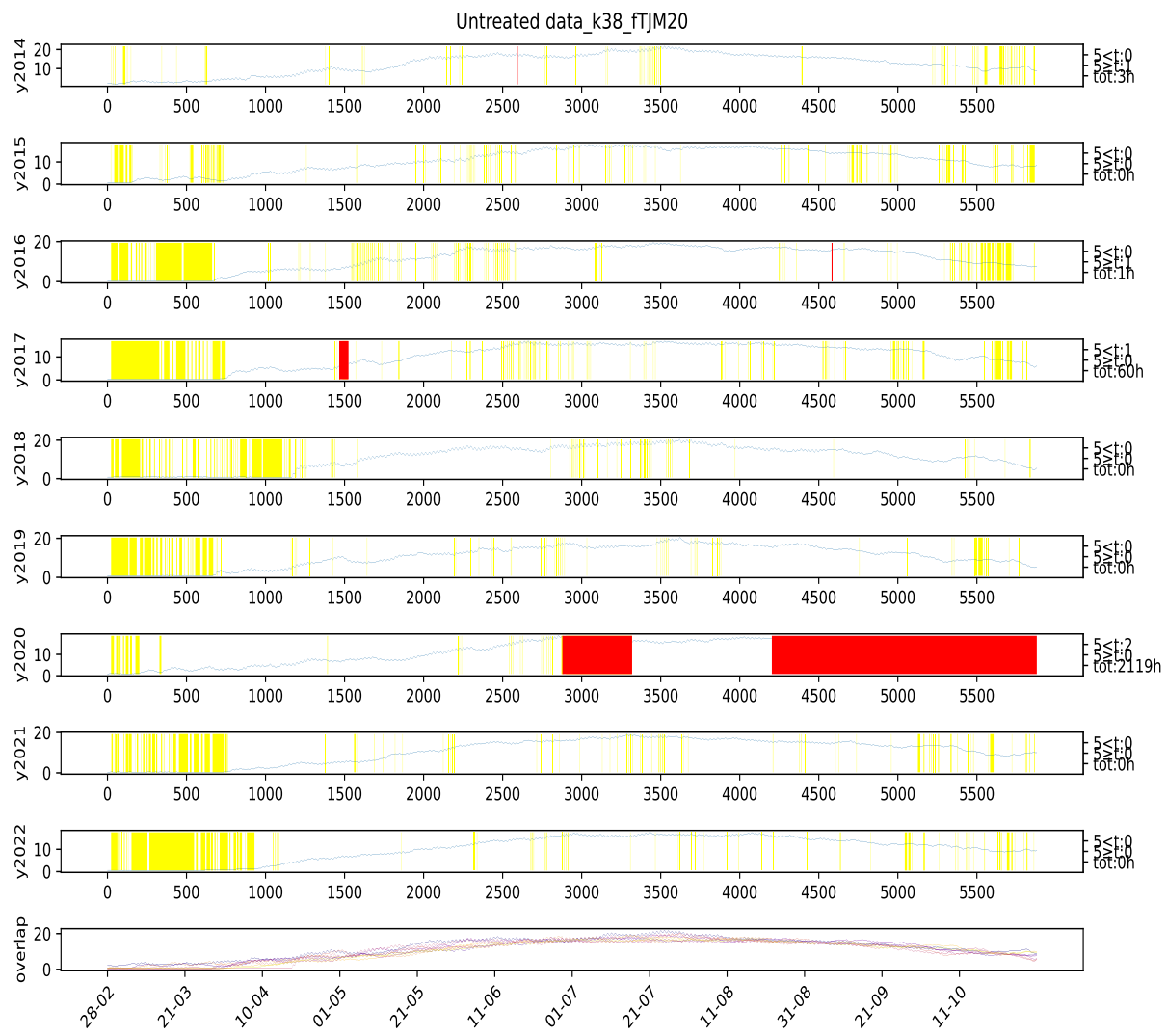


Figure 165: Visual representation of missing values at station 38 from 2014 to 2022 at the parameter "TJM20" after treating for outliers. The left numbers indicated how many hours that are missing and how many of them are shorter than or longer than 5 hours, however for this visualization they indicate the untreated version of the data. The yellow markings indicate possible outliers based on the given year, all markings was checked if they were actual outliers. The red colouring indicate missing values in the data (represented in the data with code "NULL"). The station names can be found in table 1.

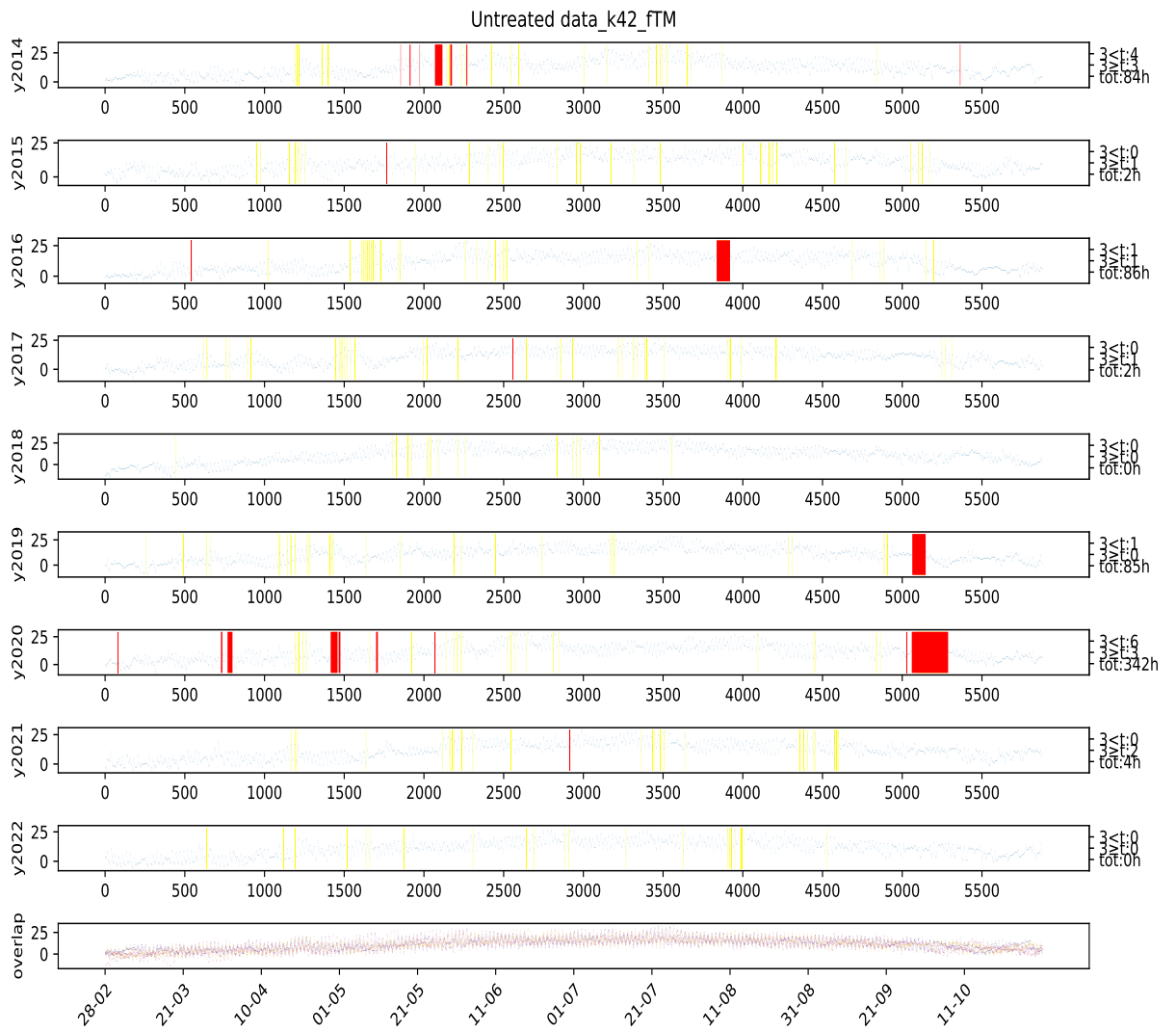


Figure 166: Visual representation of missing values at station 42 from 2014 to 2022 at the parameter "TM" after treating for outliers. The left numbers indicated how many hours that are missing and how many of them are shorter than or longer than 5 hours, however for this visualization they indicate the untreated version of the data. The yellow markings indicate possible outliers based on the given year, all markings was checked if they were actual outliers. The red colouring indicate missing values in the data (represented in the data with code "NULL"). The station names can be found in table 1.

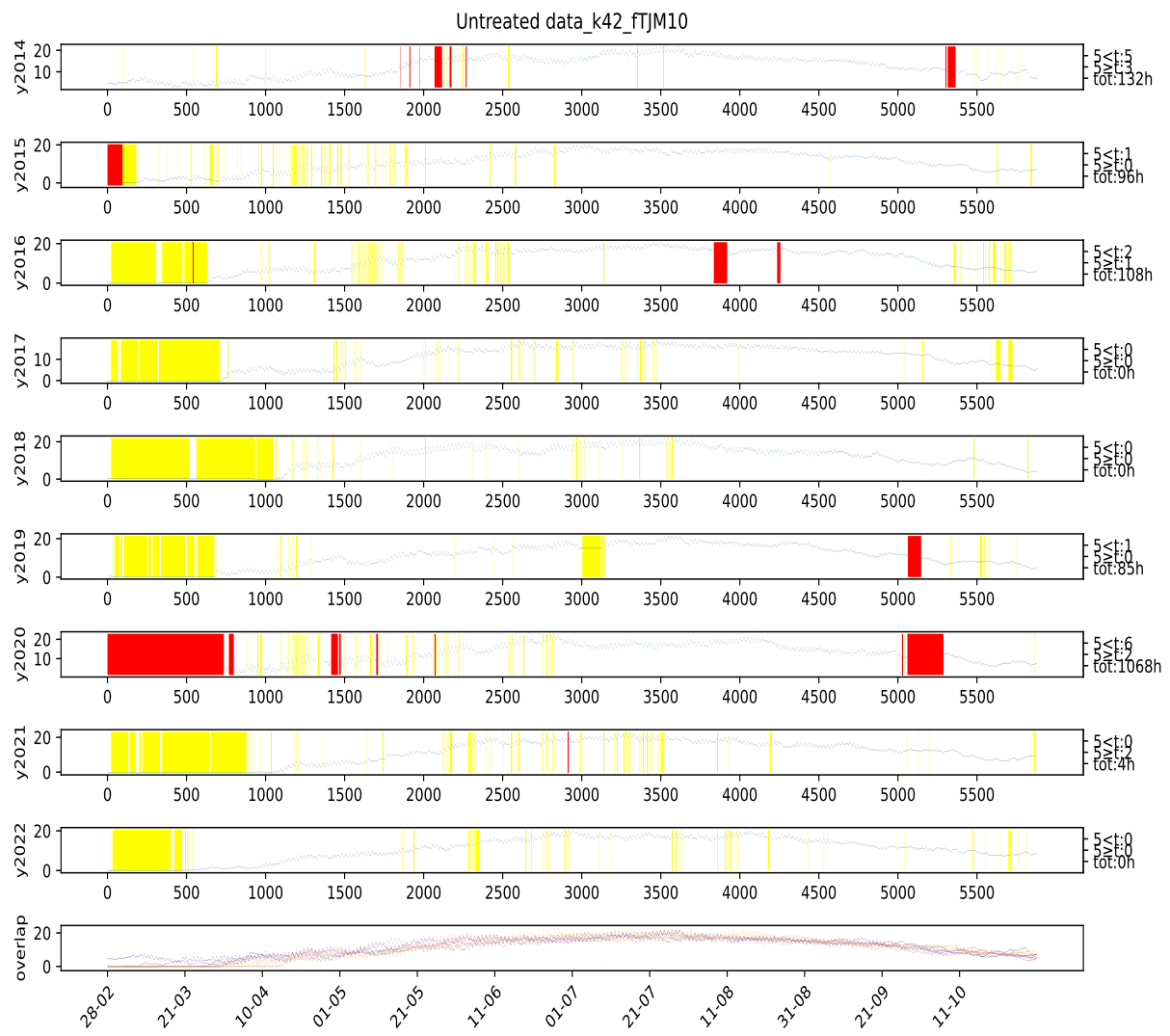


Figure 167: Visual representation of missing values at station 42 from 2014 to 2022 at the parameter "TJM10" after treating for outliers. The left numbers indicated how many hours that are missing and how many of them are shorter than or longer than 5 hours, however for this visualization they indicate the untreated version of the data. The yellow markings indicate possible outliers based on the given year, all markings was checked if they were actual outliers. The red colouring indicate missing values in the data (represented in the data with code "NULL"). The station names can be found in table 1.

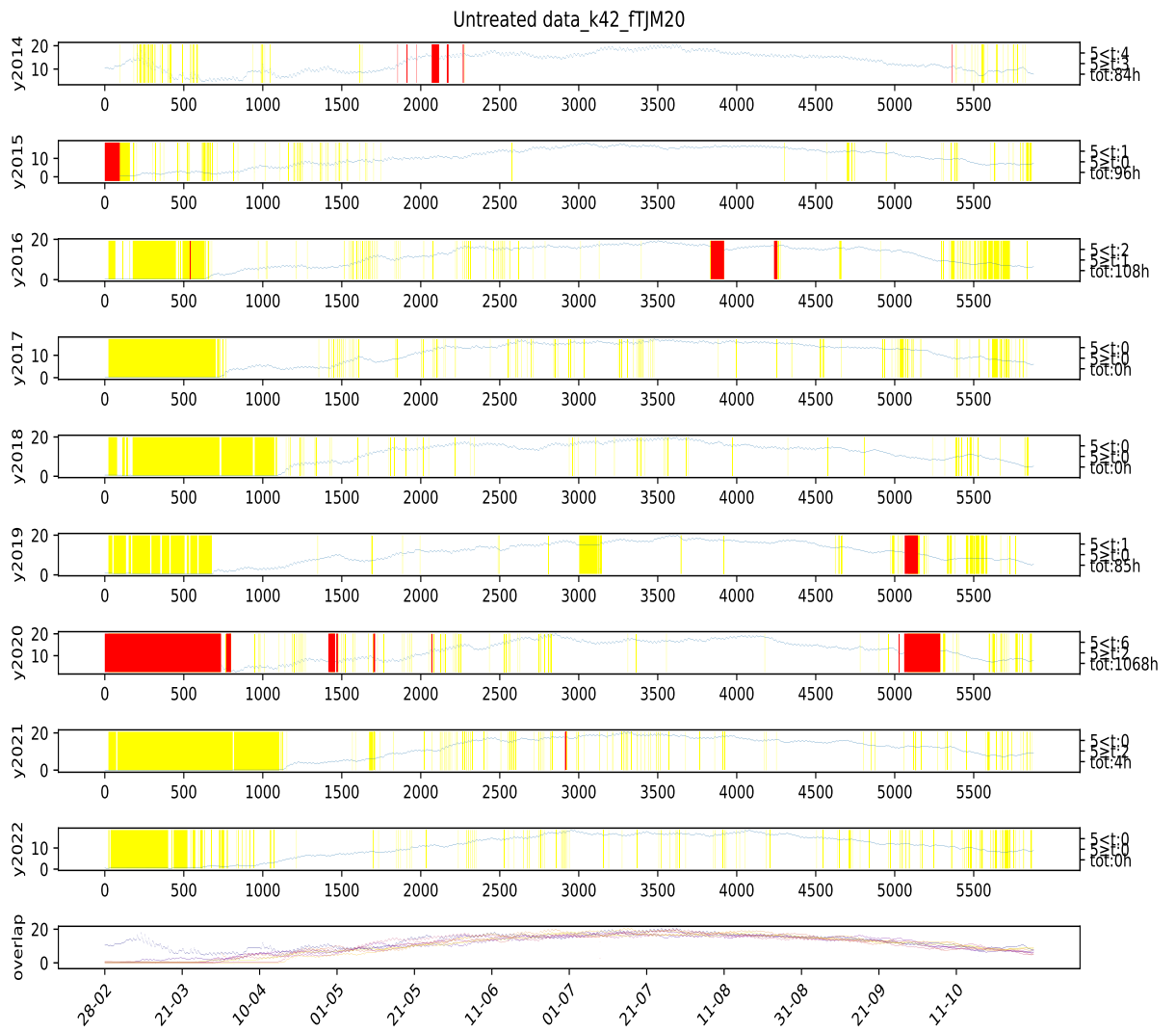


Figure 168: Visual representation of missing values at station 42 from 2014 to 2022 at the parameter "TJM20" after treating for outliers. The left numbers indicated how many hours that are missing and how many of them are shorter than or longer than 5 hours, however for this visualization they indicate the untreated version of the data. The yellow markings indicate possible outliers based on the given year, all markings was checked if they were actual outliers. The red colouring indicate missing values in the data (represented in the data with code "NULL"). The station names can be found in table 1.

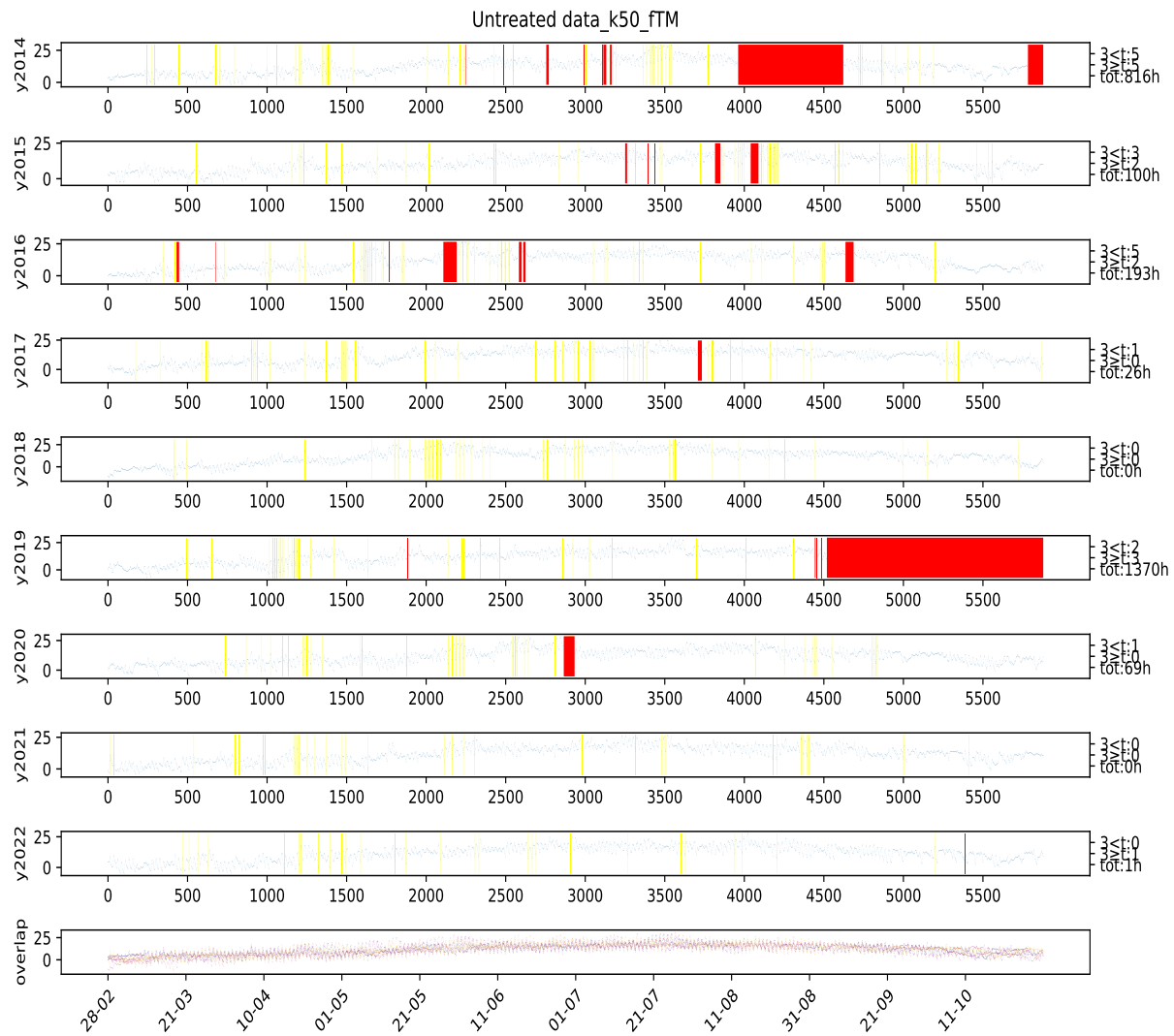


Figure 169: Visual representation of missing values at station 50 from 2014 to 2022 at the parameter "TM" after treating for outliers. The left numbers indicated how many hours that are missing and how many of them are shorter than or longer than 5 hours, however for this visualization they indicate the untreated version of the data. The yellow markings indicate possible outliers based on the given year, all markings was checked if they were actual outliers. The red colouring indicate missing values in the data (represented in the data with code "NULL"). The station names can be found in table 1.

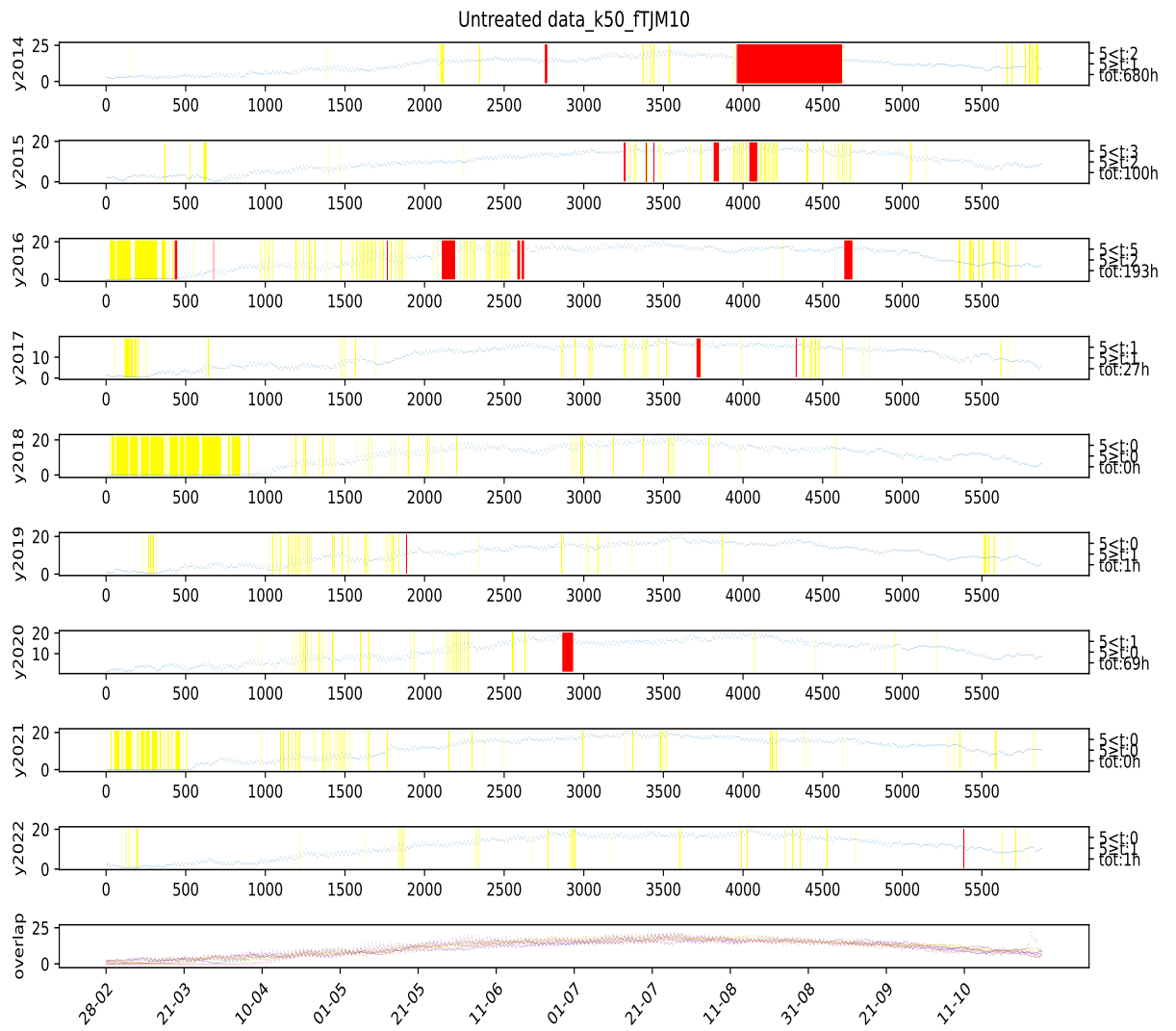


Figure 170: Visual representation of missing values at station 50 from 2014 to 2022 at the parameter "TJM10" after treating for outliers. The left numbers indicated how many hours that are missing and how many of them are shorter than or longer than 5 hours, however for this visualization they indicate the untreated version of the data. The yellow markings indicate possible outliers based on the given year, all markings was checked if they were actual outliers. The red colouring indicate missing values in the data (represented in the data with code "NULL"). The station names can be found in table 1.

## A PLOTS

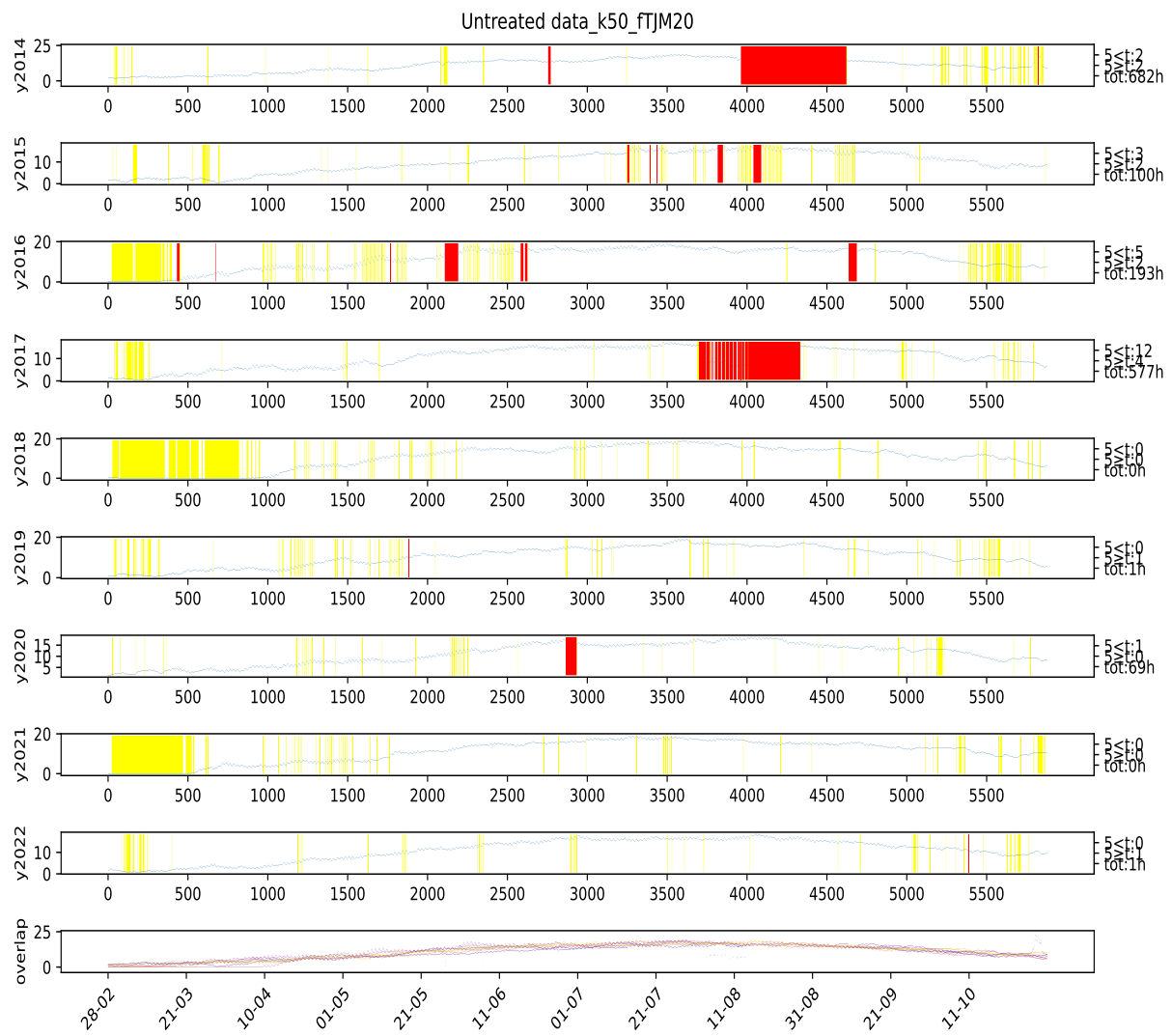


Figure 171: Visual representation of missing values at station 50 from 2014 to 2022 at the parameter "TJM20" after treating for outliers. The left numbers indicated how many hours that are missing and how many of them are shorter than or longer than 5 hours, however for this visualization they indicate the untreated version of the data. The yellow markings indicate possible outliers based on the given year, all markings was checked if they were actual outliers. The red colouring indicate missing values in the data (represented in the data with code "NULL"). The station names can be found in table 1.

### A.3 Data visiulation of data after treatment

## A PLOTS

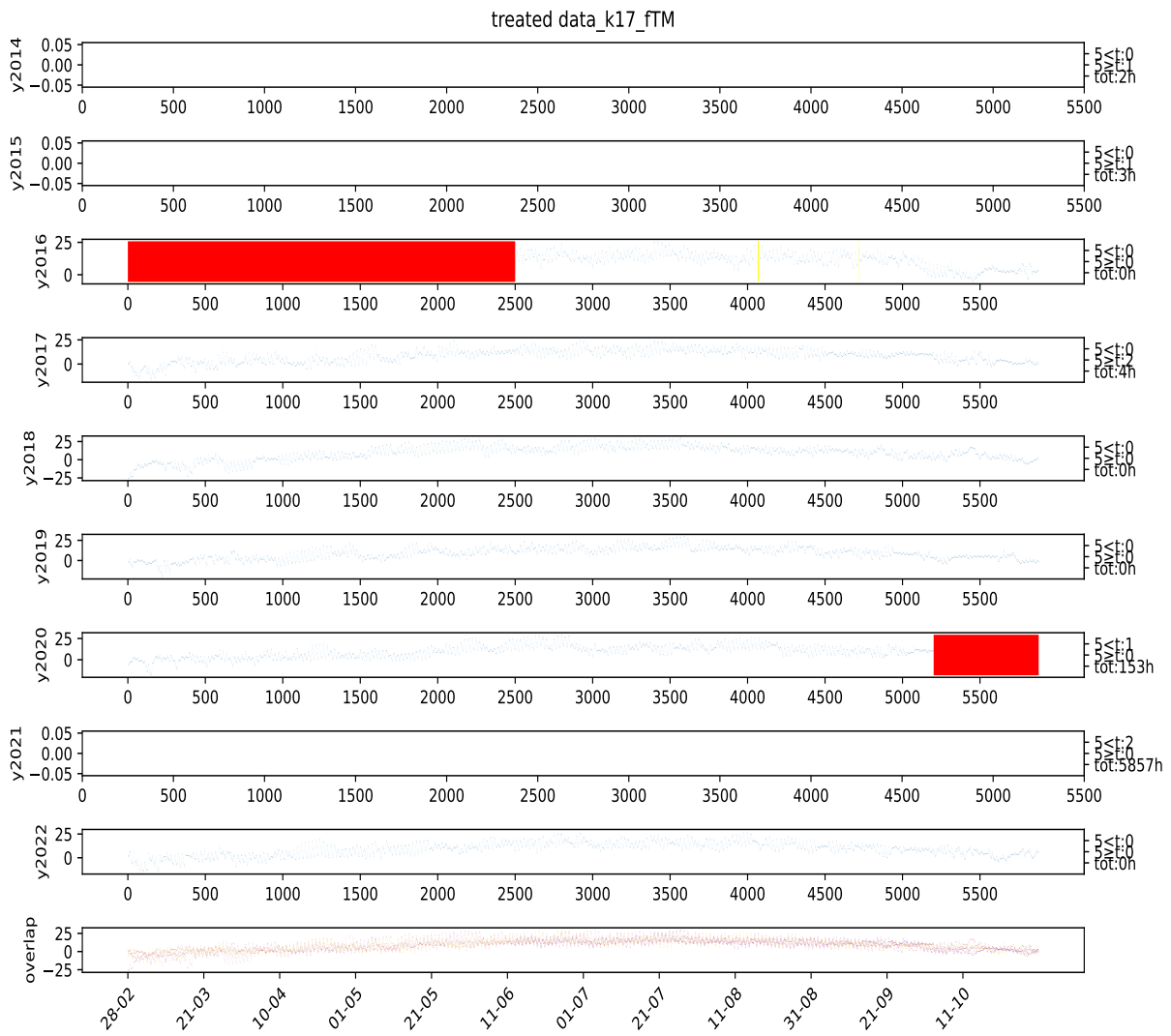


Figure 172: Visual representation of missing values at station 17 from 2014 to 2022 at the parameter "TM" after treating for outliers. The left numbers indicated how many hours that are missing and how many of them are shorter than or longer than 5 hours, however for this visualization they indicate the untreated version of the data. The yellow markings indicate possible outliers based on the given year, all markings was checked if they were actual outliers. The red colouring indicate missing values in the data (represented in the data with code "NULL"). The station names can be found in table 1.

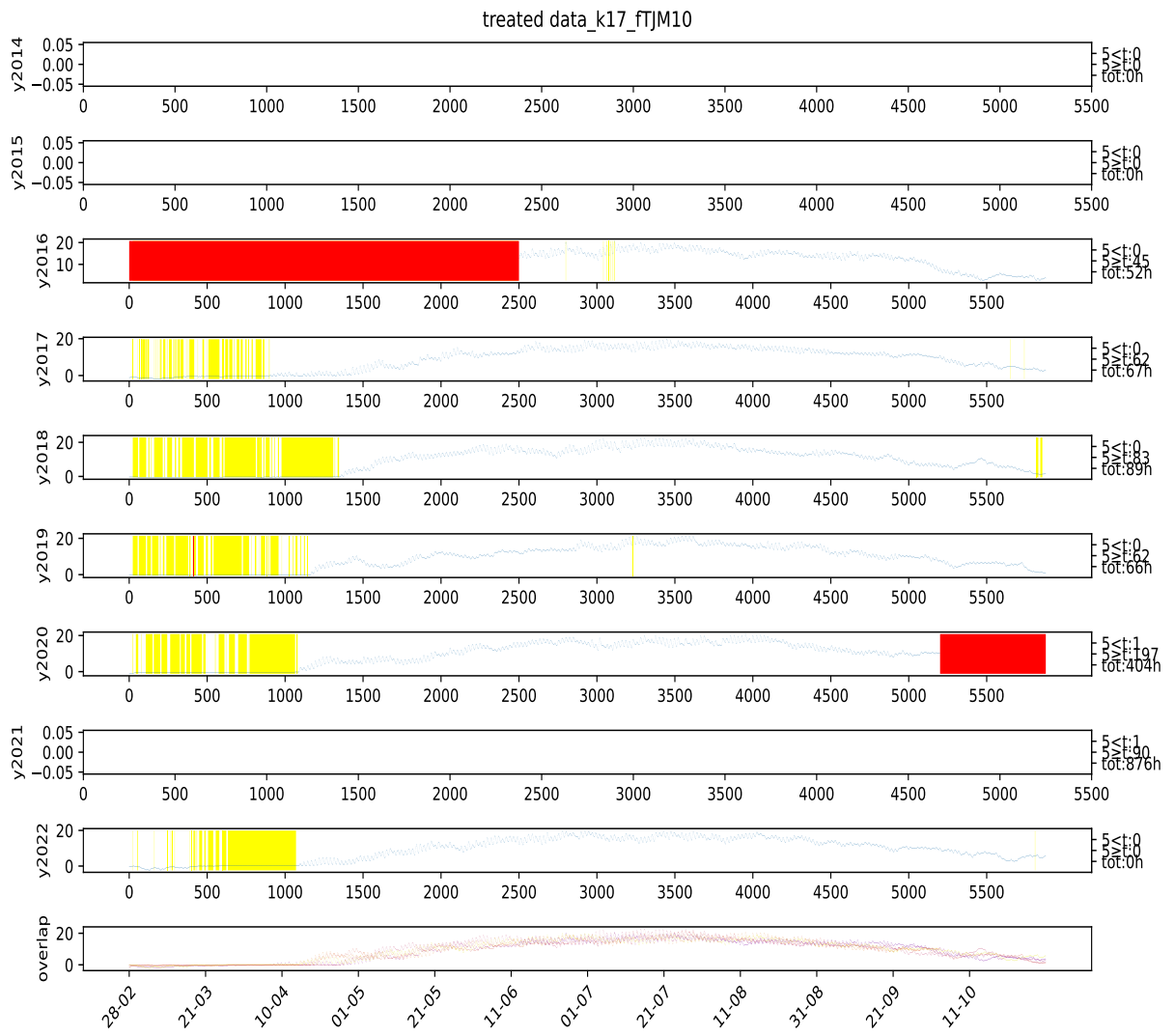


Figure 173: Visual representation of missing values at station 17 from 2014 to 2022 at the parameter "TJM10" after treating for outliers. The left numbers indicated how many hours that are missing and how many of them are shorter than or longer than 5 hours, however for this visualization they indicate the untreated version of the data. The yellow markings indicate possible outliers based on the given year, all markings was checked if they were actual outliers. The red colouring indicate missing values in the data (represented in the data with code "NULL"). The station names can be found in table 1.

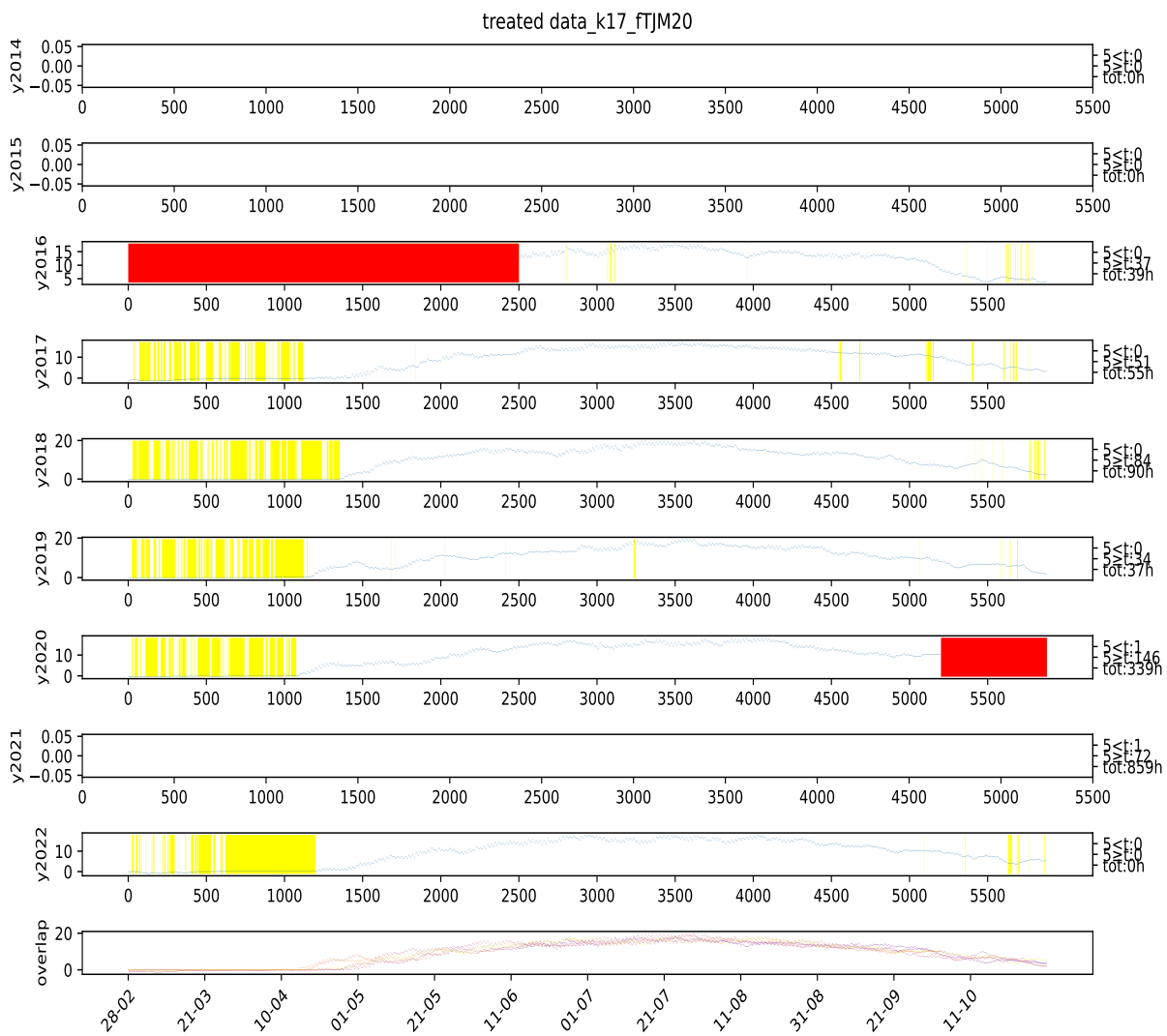


Figure 174: Visual representation of missing values at station 17 from 2014 to 2022 at the parameter "TJM20" after treating for outliers. The left numbers indicated how many hours that are missing and how many of them are shorter than or longer than 5 hours, however for this visualization they indicate the untreated version of the data. The yellow markings indicate possible outliers based on the given year, all markings was checked if they were actual outliers. The red colouring indicate missing values in the data (represented in the data with code "NULL"). The station names can be found in table 1.

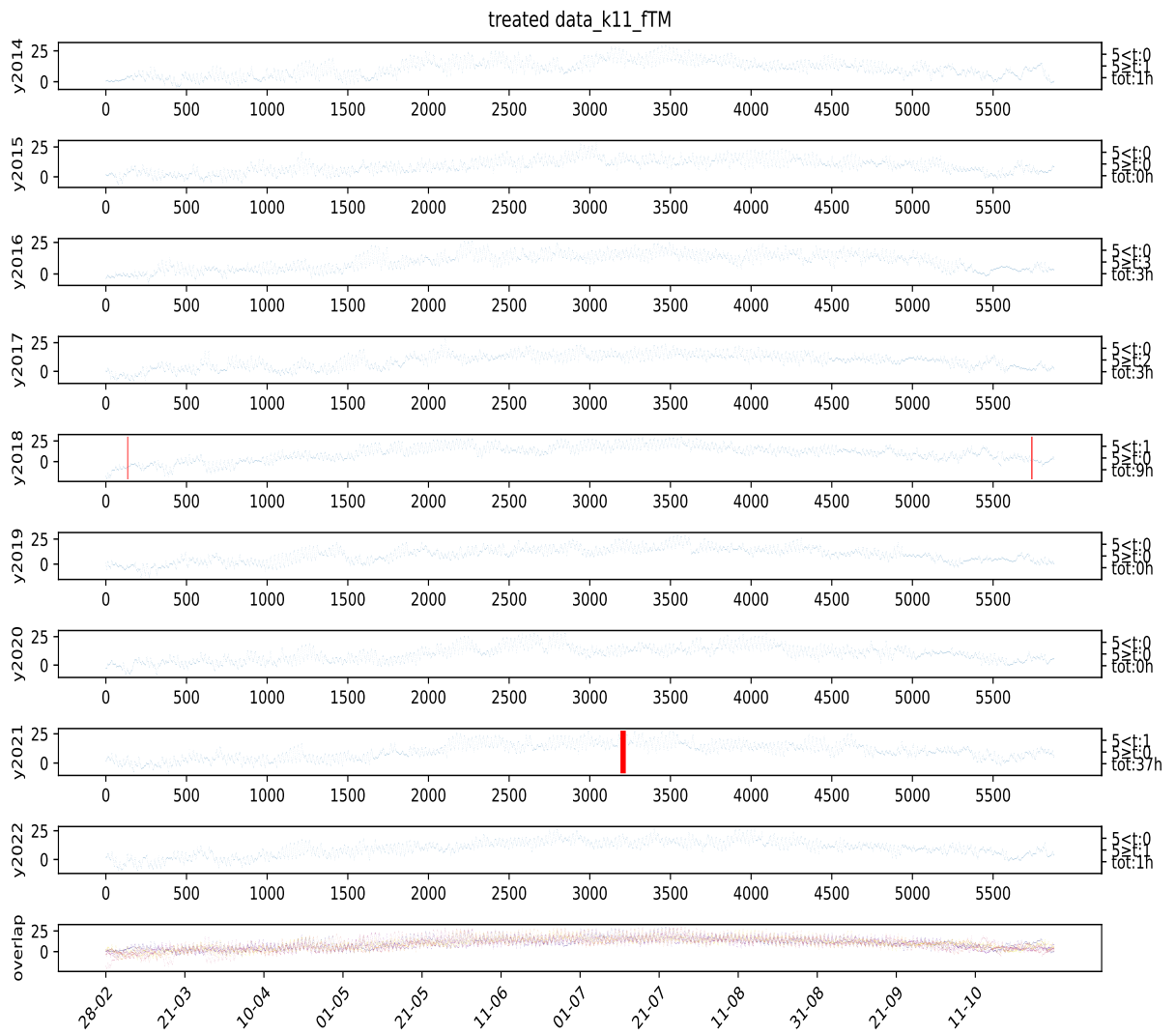


Figure 175: Visual representation of missing values at station 11 from 2014 to 2022 at the parameter "TM" after treating for outliers. The left numbers indicated how many hours that are missing and how many of them are shorter than or longer than 5 hours, however for this visualization they indicate the untreated version of the data. The yellow markings indicate possible outliers based on the given year, all markings was checked if they were actual outliers. The red colouring indicate missing values in the data (represented in the data with code "NULL"). The station names can be found in table 1.

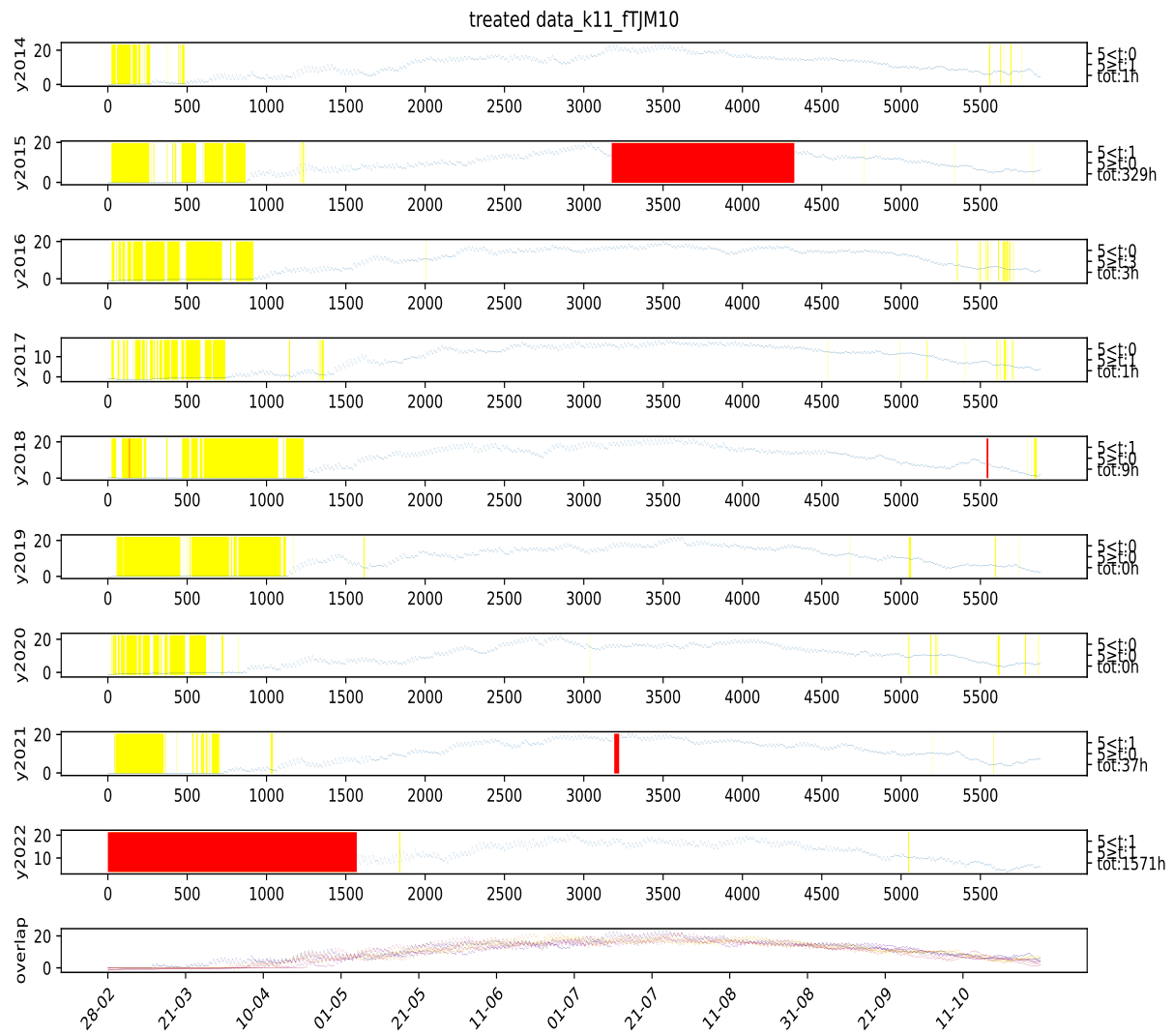


Figure 176: Visual representation of missing values at station 11 from 2014 to 2022 at the parameter "TJM10" after treating for outliers. The left numbers indicated how many hours that are missing and how many of them are shorter than or longer than 5 hours, however for this visualization they indicate the untreated version of the data. The yellow markings indicate possible outliers based on the given year, all markings was checked if they were actual outliers. The red colouring indicate missing values in the data (represented in the data with code "NULL"). The station names can be found in table 1.

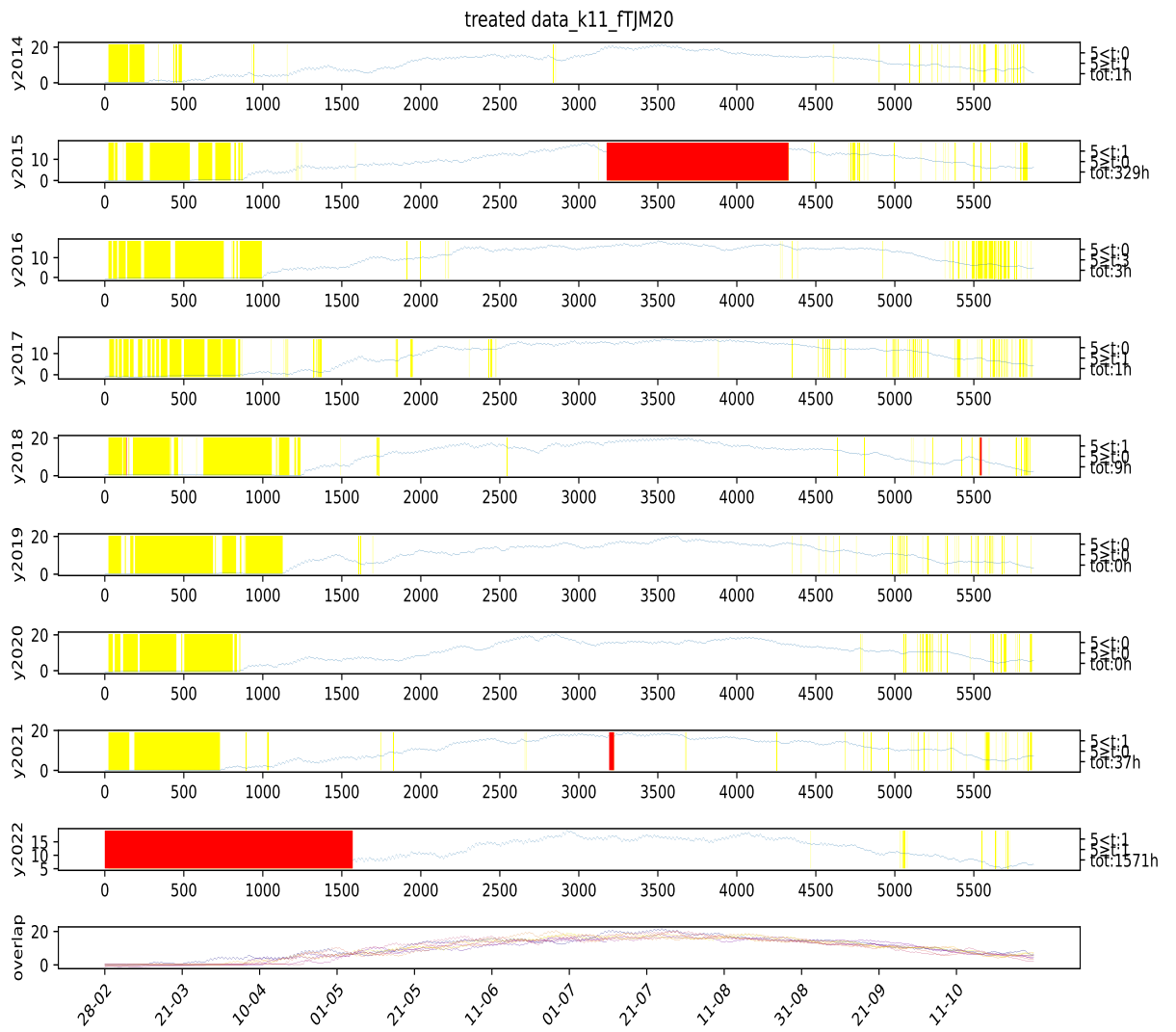


Figure 177: Visual representation of missing values at station 11 from 2014 to 2022 at the parameter "TJM20" after treating for outliers. The left numbers indicated how many hours that are missing and how many of them are shorter than or longer than 5 hours, however for this visualization they indicate the untreated version of the data. The yellow markings indicate possible outliers based on the given year, all markings was checked if they were actual outliers. The red colouring indicate missing values in the data (represented in the data with code "NULL"). The station names can be found in table 1.

## A PLOTS

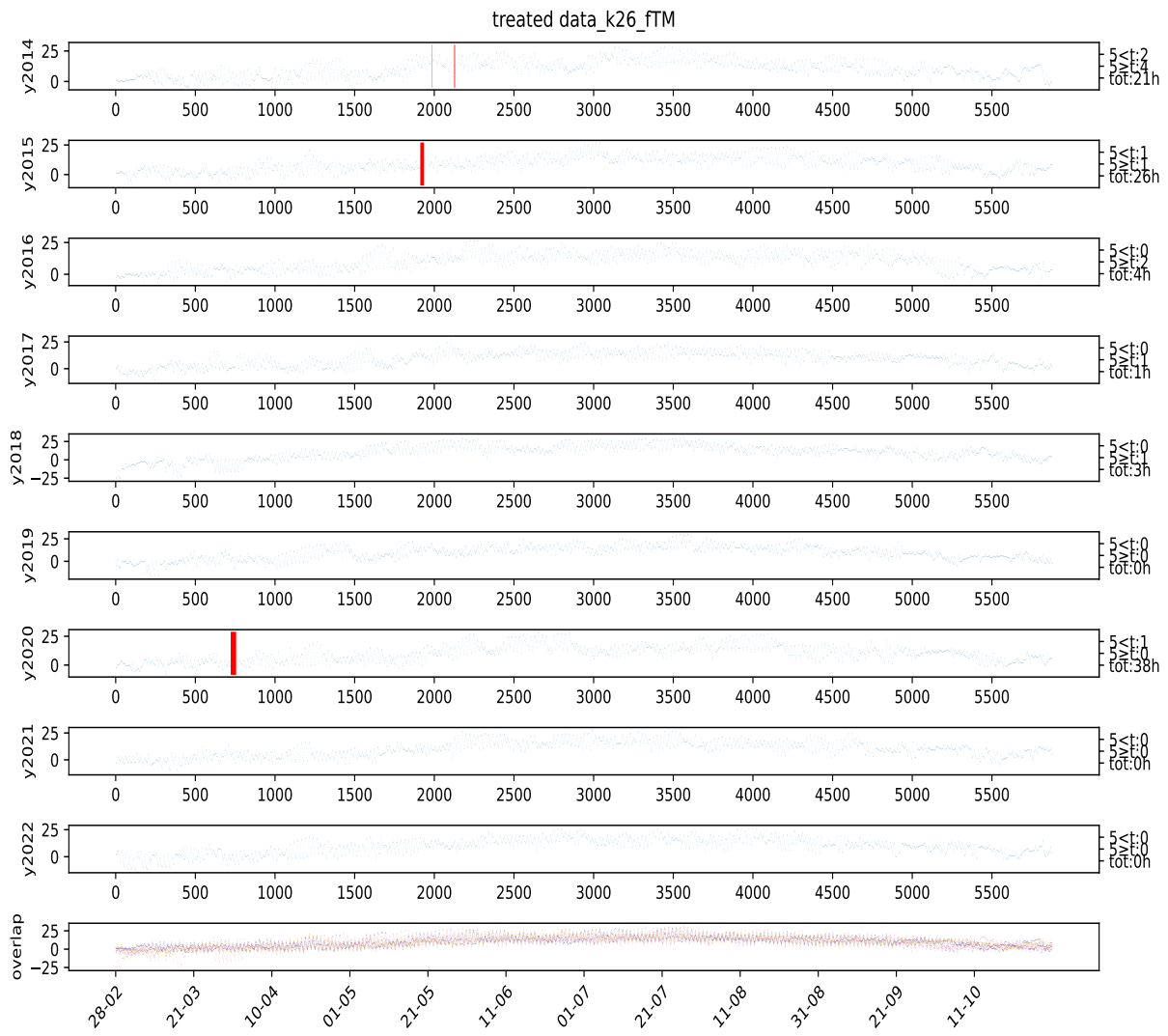


Figure 178: Visual representation of missing values at station 26 from 2014 to 2022 at the parameter "TM" after treating for outliers. The left numbers indicated how many hours that are missing and how many of them are shorter than or longer than 5 hours, however for this visualization they indicate the untreated version of the data. The yellow markings indicate possible outliers based on the given year, all markings was checked if they were actual outliers. The red colouring indicate missing values in the data (represented in the data with code "NULL"). The station names can be found in table 1.

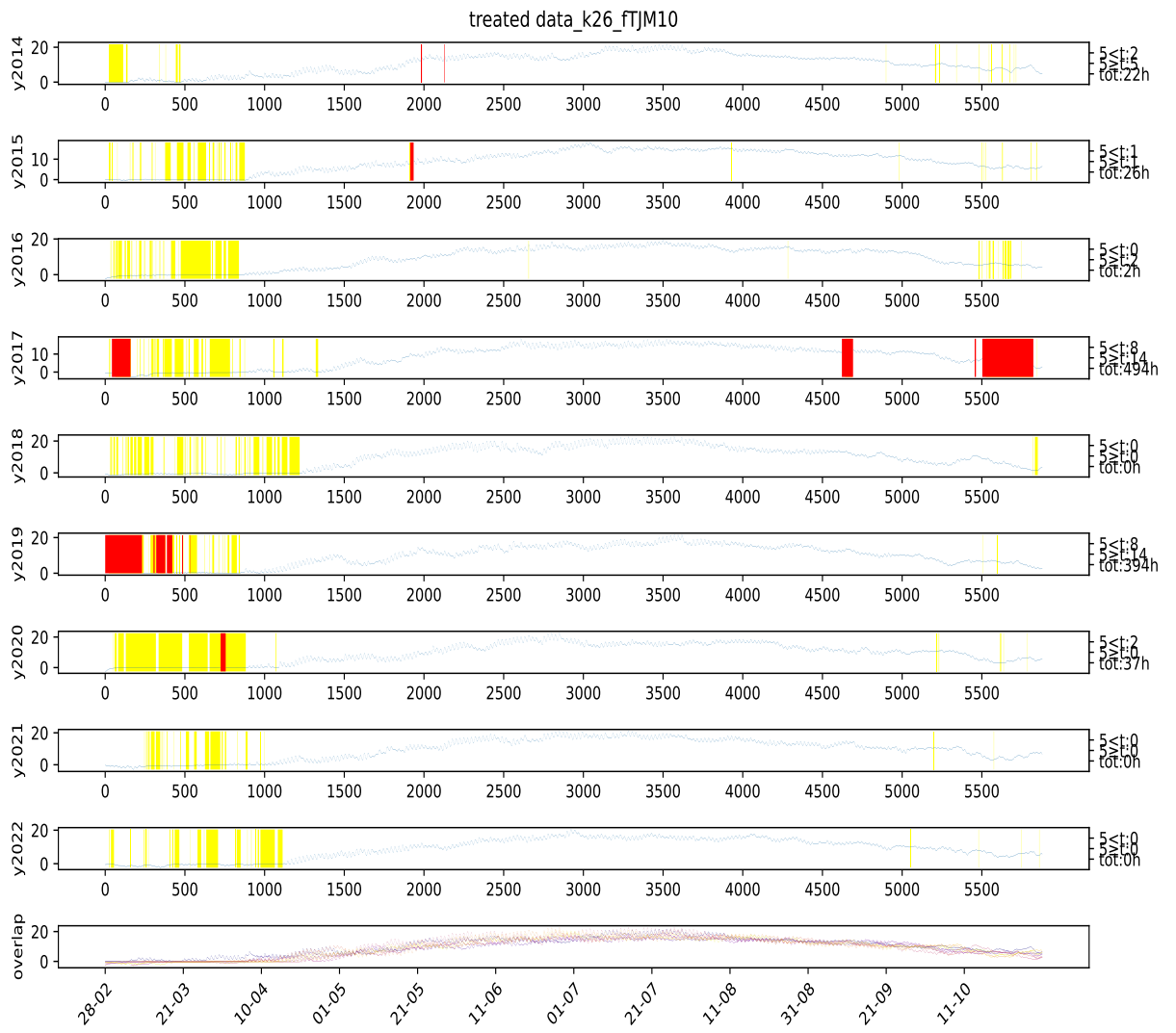


Figure 179: Visual representation of missing values at station 26 from 2014 to 2022 at the parameter "TJM10" after treating for outliers. The left numbers indicated how many hours that are missing and how many of them are shorter than or longer than 5 hours, however for this visualization they indicate the untreated version of the data. The yellow markings indicate possible outliers based on the given year, all markings was checked if they were actual outliers. The red colouring indicate missing values in the data (represented in the data with code "NULL"). The station names can be found in table 1.

## A PLOTS

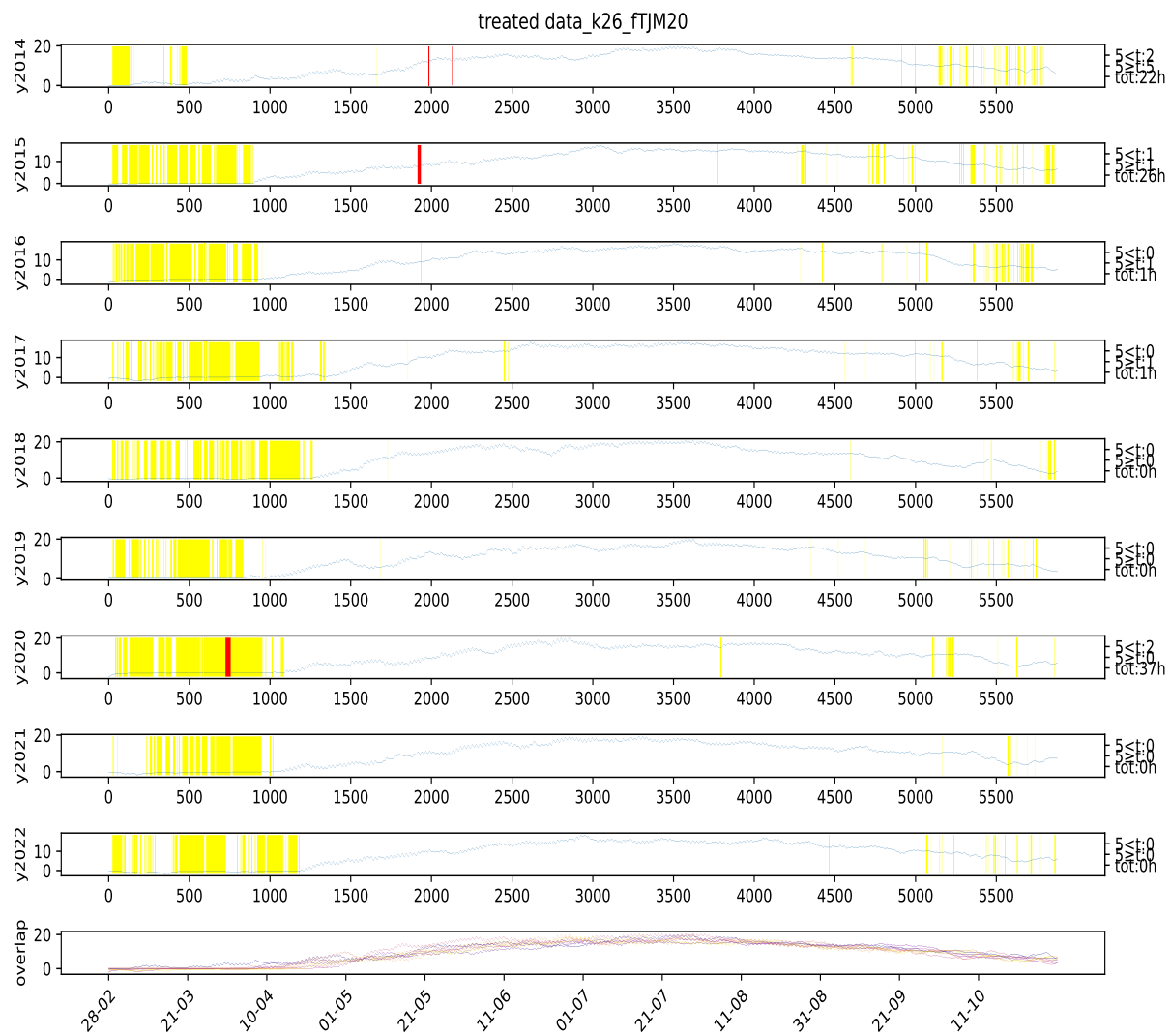


Figure 180: Visual representation of missing values at station 26 from 2014 to 2022 at the parameter "TJM20" after treating for outliers. The left numbers indicated how many hours that are missing and how many of them are shorter than or longer than 5 hours, however for this visualization they indicate the untreated version of the data. The yellow markings indicate possible outliers based on the given year, all markings was checked if they were actual outliers. The red colouring indicate missing values in the data (represented in the data with code "NULL").The station names can be found in table 1.

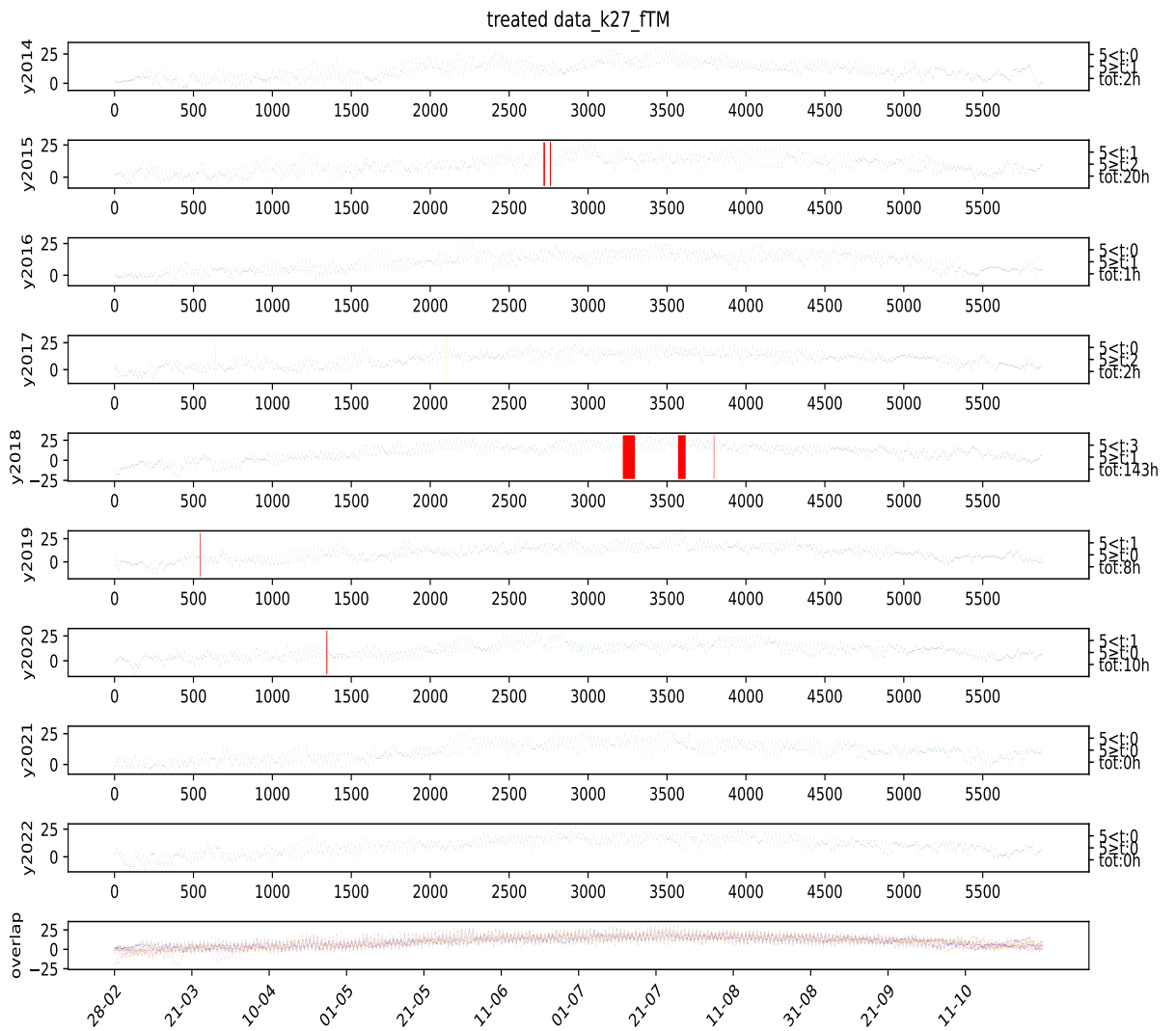


Figure 181: Visual representation of missing values at station 27 from 2014 to 2022 at the parameter "TM" after treating for outliers. The left numbers indicated how many hours that are missing and how many of them are shorter than or longer than 5 hours, however for this visualization they indicate the untreated version of the data. The yellow markings indicate possible outliers based on the given year, all markings was checked if they were actual outliers. The red colouring indicate missing values in the data (represented in the data with code "NULL"). The station names can be found in table 1.

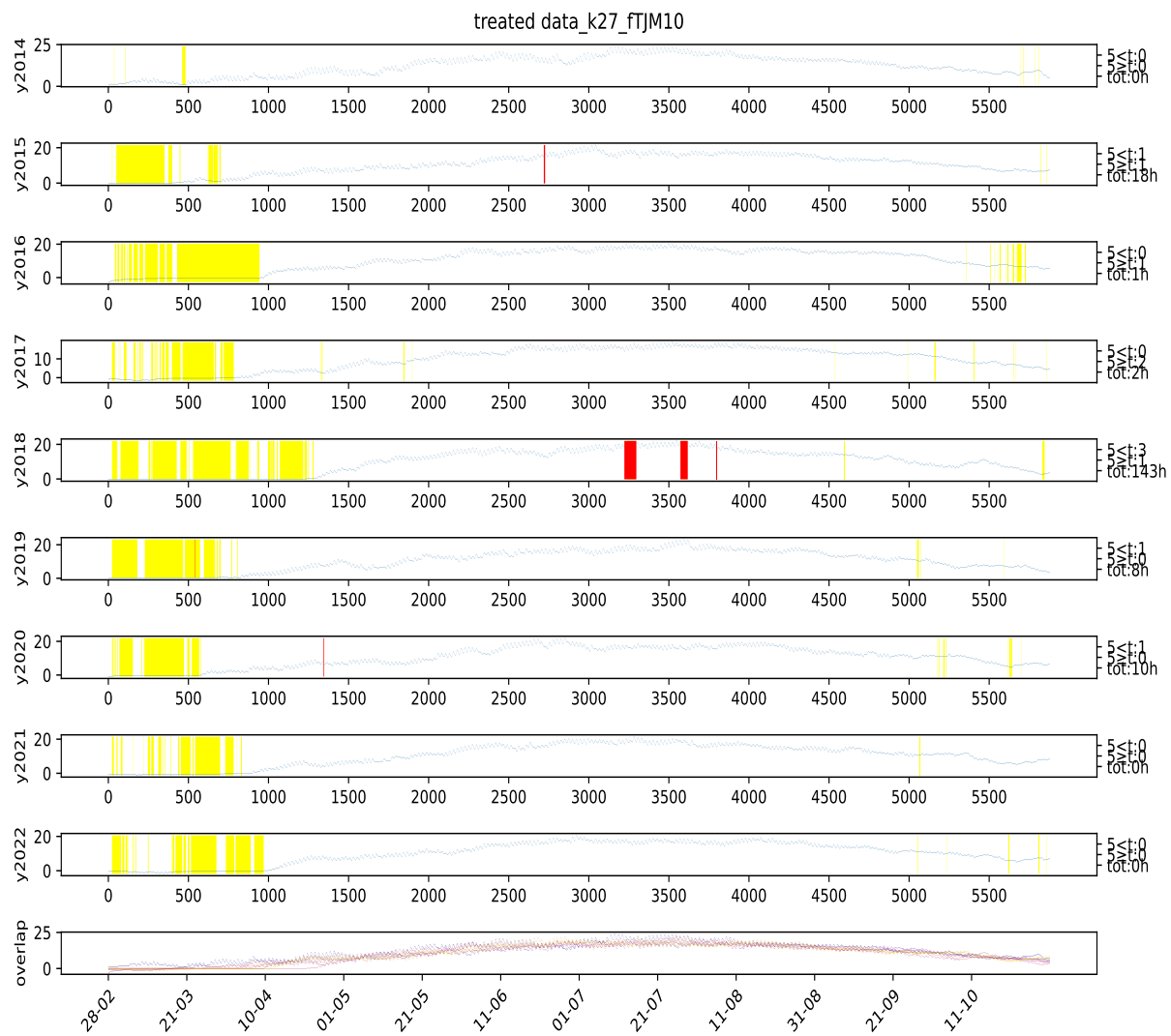


Figure 182: Visual representation of missing values at station 27 from 2014 to 2022 at the parameter "TJM10" after treating for outliers. The left numbers indicated how many hours that are missing and how many of them are shorter than or longer than 5 hours, however for this visualization they indicate the untreated version of the data. The yellow markings indicate possible outliers based on the given year, all markings was checked if they were actual outliers. The red colouring indicate missing values in the data (represented in the data with code "NULL"). The station names can be found in table 1.

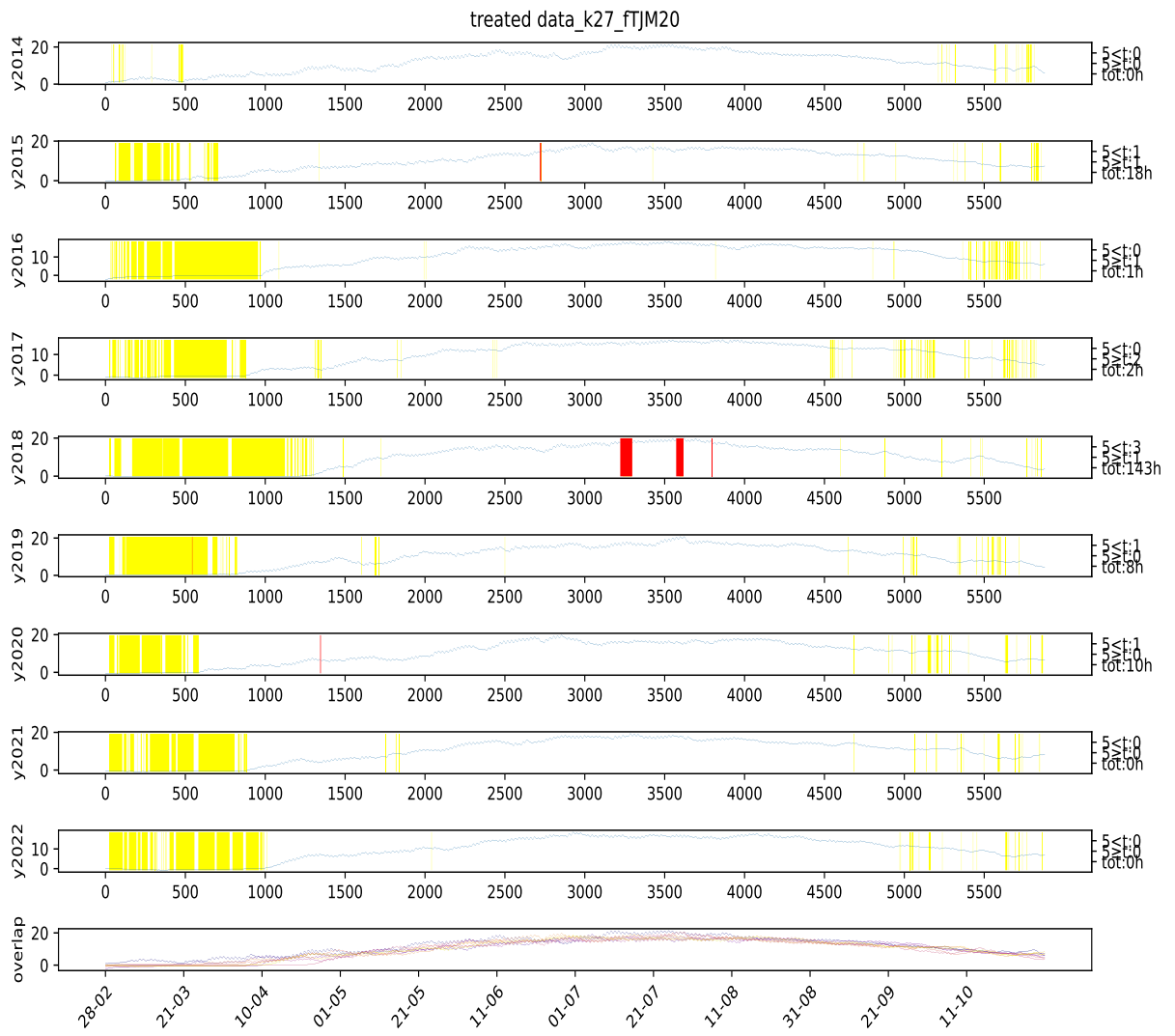


Figure 183: Visual representation of missing values at station 27 from 2014 to 2022 at the parameter "TJM20" after treating for outliers. The left numbers indicated how many hours that are missing and how many of them are shorter than or longer than 5 hours, however for this visualization they indicate the untreated version of the data. The yellow markings indicate possible outliers based on the given year, all markings was checked if they were actual outliers. The red colouring indicate missing values in the data (represented in the data with code "NULL"). The station names can be found in table 1.

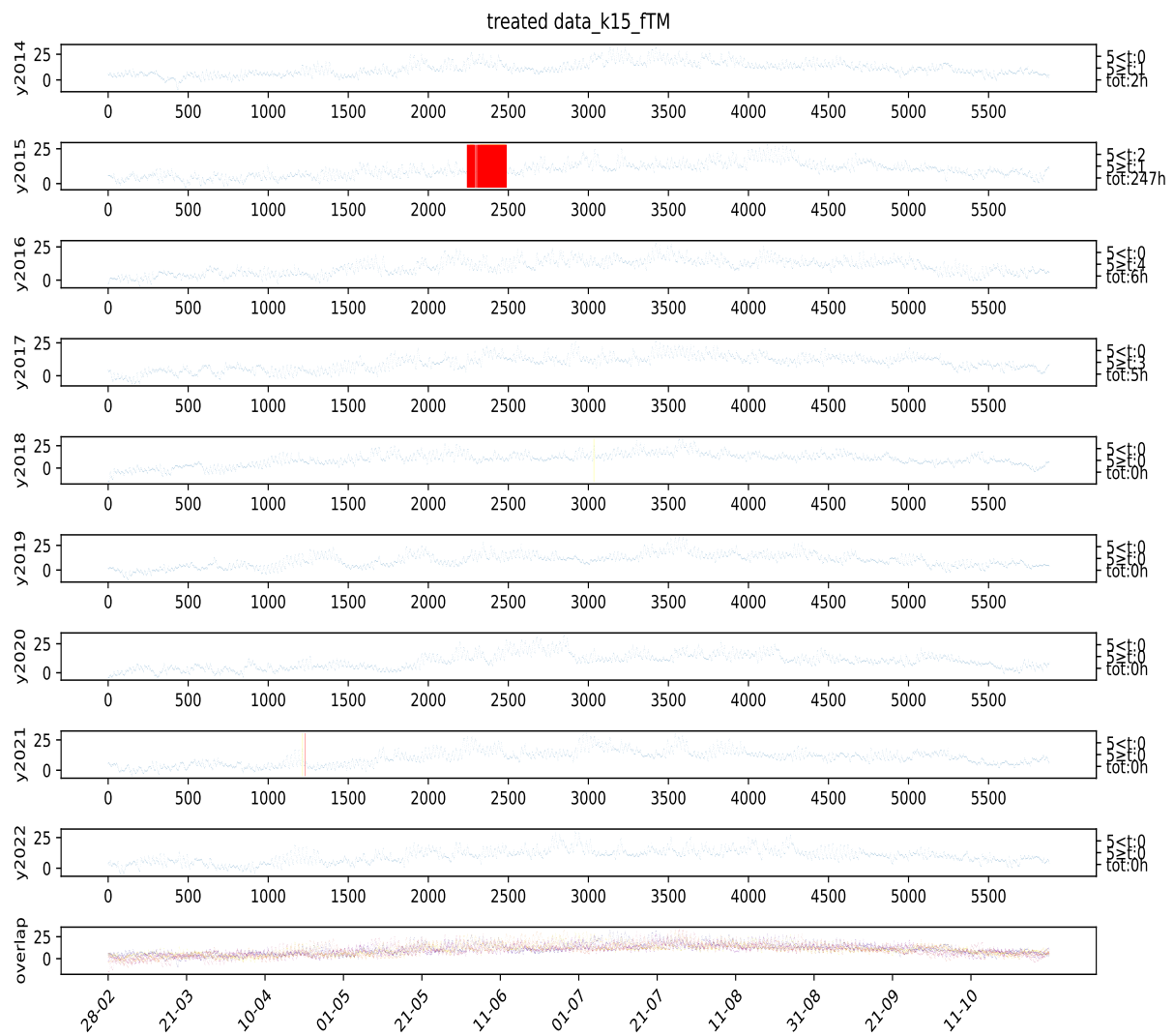


Figure 184: Visual representation of missing values at station 15 from 2014 to 2022 at the parameter "TM" after treating for outliers. The left numbers indicated how many hours that are missing and how many of them are shorter than or longer than 5 hours, however for this visualization they indicate the untreated version of the data. The yellow markings indicate possible outliers based on the given year, all markings was checked if they were actual outliers. The red colouring indicate missing values in the data (represented in the data with code "NULL"). The station names can be found in table 1.

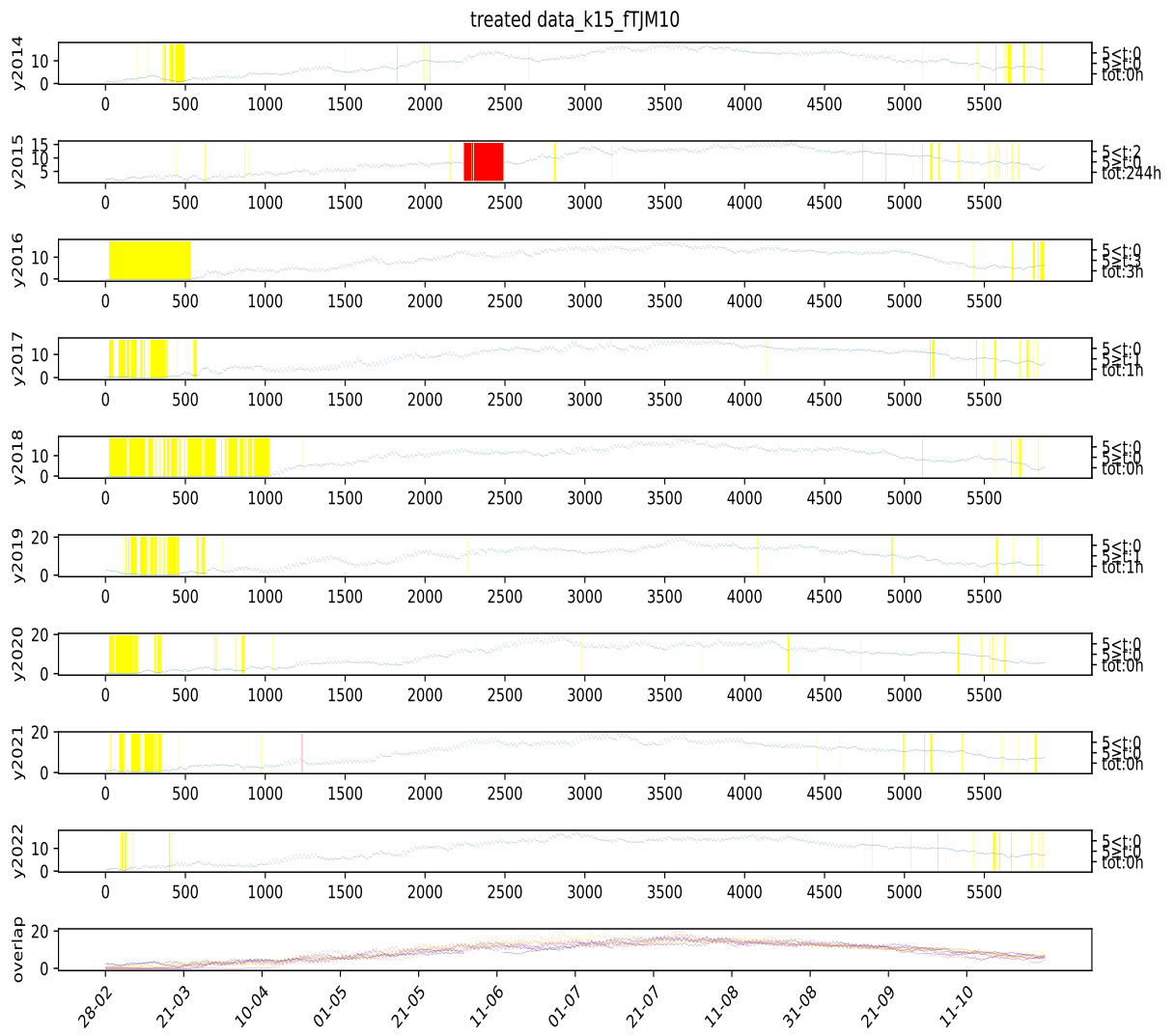


Figure 185: Visual representation of missing values at station 15 from 2014 to 2022 at the parameter "TJM10" after treating for outliers. The left numbers indicated how many hours that are missing and how many of them are shorter than or longer than 5 hours, however for this visualization they indicate the untreated version of the data. The yellow markings indicate possible outliers based on the given year, all markings was checked if they were actual outliers. The red colouring indicate missing values in the data (represented in the data with code "NULL"). The station names can be found in table 1.

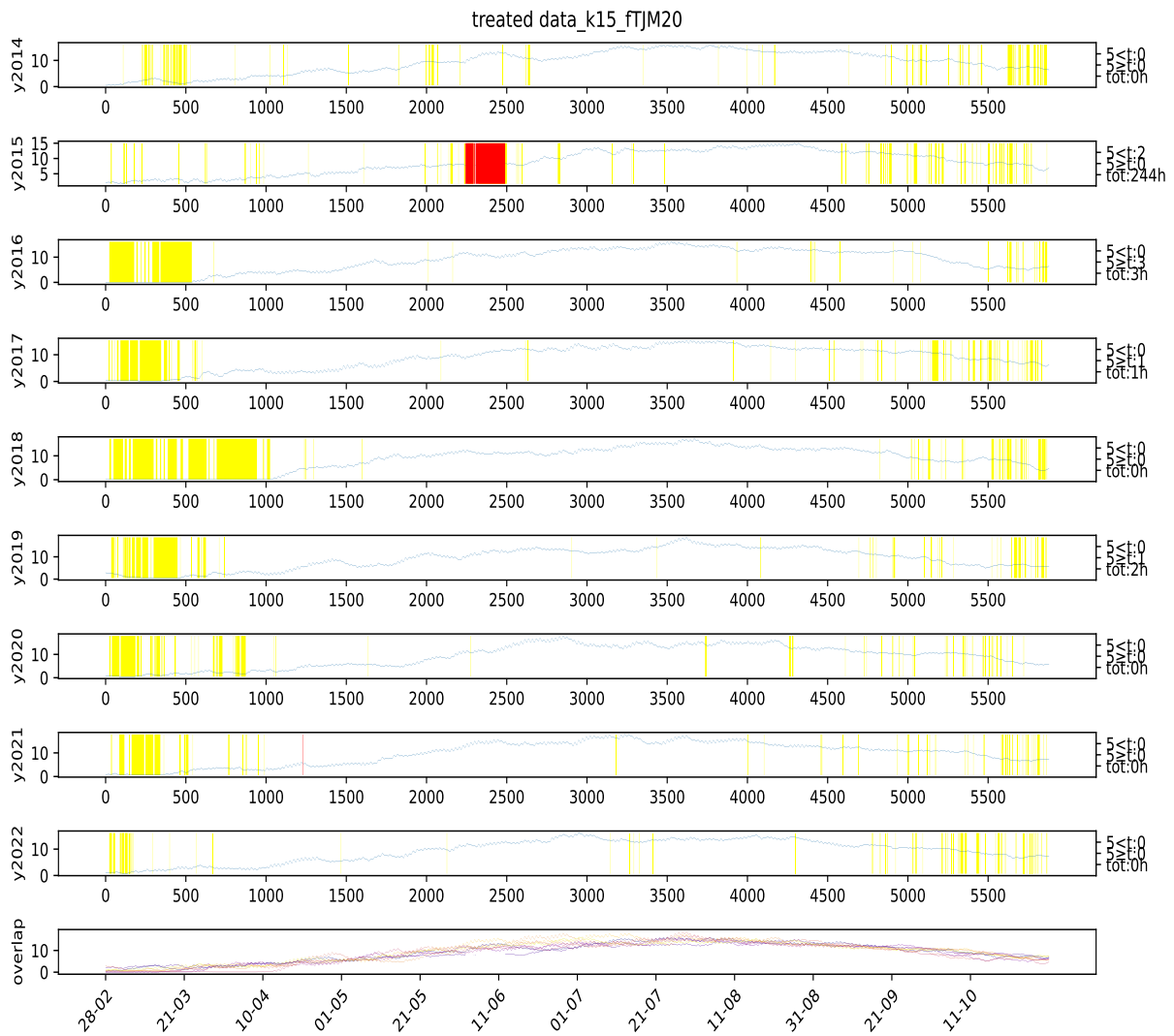


Figure 186: Visual representation of missing values at station 15 from 2014 to 2022 at the parameter "TJM20" after treating for outliers. The left numbers indicated how many hours that are missing and how many of them are shorter than or longer than 5 hours, however for this visualization they indicate the untreated version of the data. The yellow markings indicate possible outliers based on the given year, all markings was checked if they were actual outliers. The red colouring indicate missing values in the data (represented in the data with code "NULL"). The station names can be found in table 1.

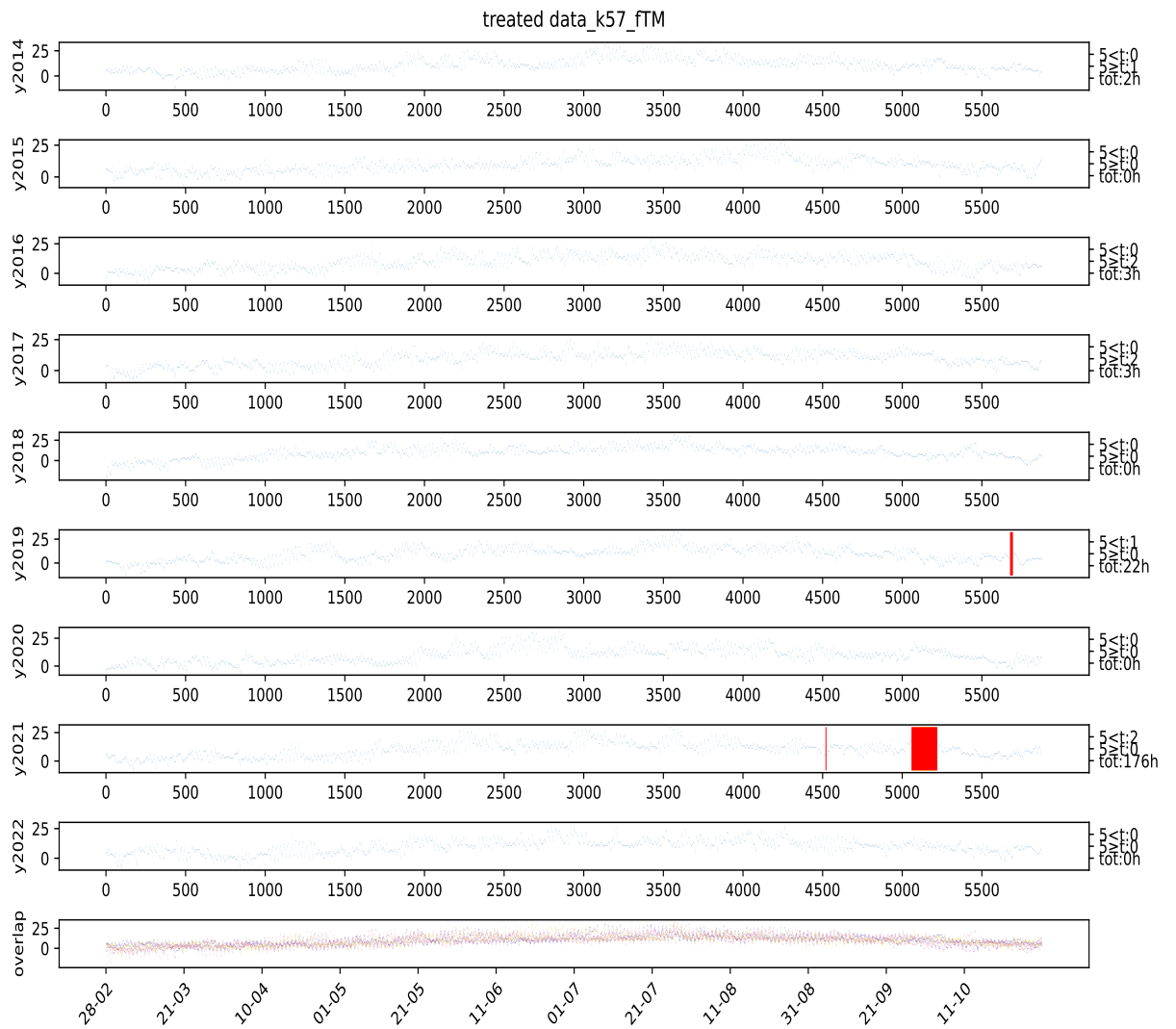


Figure 187: Visual representation of missing values at station 57 from 2014 to 2022 at the parameter "TM" after treating for outliers. The left numbers indicated how many hours that are missing and how many of them are shorter than or longer than 5 hours, however for this visualization they indicate the untreated version of the data. The yellow markings indicate possible outliers based on the given year, all markings was checked if they were actual outliers. The red colouring indicate missing values in the data (represented in the data with code "NULL"). The station names can be found in table 1.

## A PLOTS

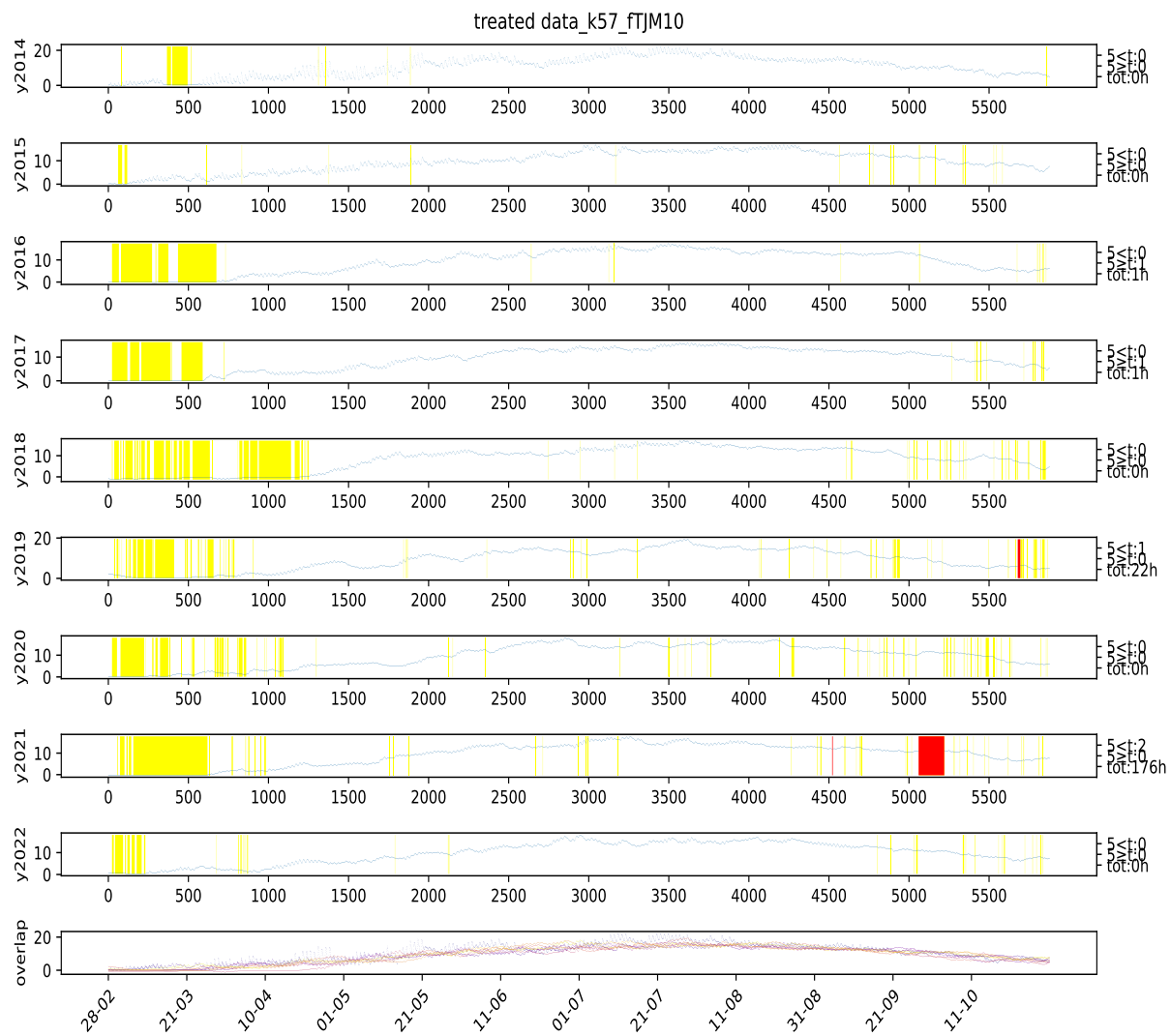


Figure 188: Visual representation of missing values at station 57 from 2014 to 2022 at the parameter "TJM10" after treating for outliers. The left numbers indicated how many hours that are missing and how many of them are shorter than or longer than 5 hours, however for this visualization they indicate the untreated version of the data. The yellow markings indicate possible outliers based on the given year, all markings was checked if they were actual outliers. The red colouring indicate missing values in the data (represented in the data with code "NULL"). The station names can be found in table 1.

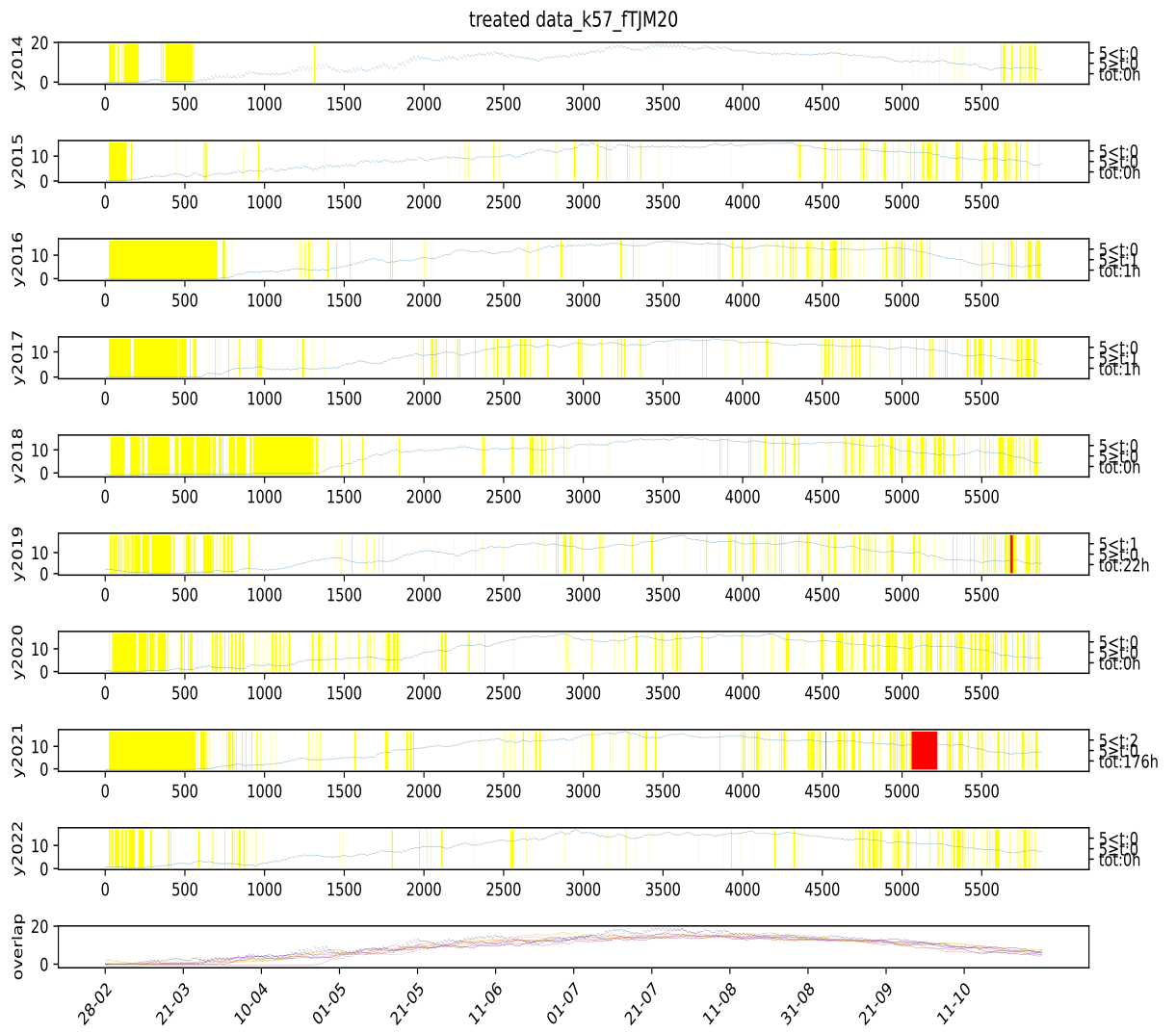


Figure 189: Visual representation of missing values at station 57 from 2014 to 2022 at the parameter "TJM20" after treating for outliers. The left numbers indicated how many hours that are missing and how many of them are shorter than or longer than 5 hours, however for this visualization they indicate the untreated version of the data. The yellow markings indicate possible outliers based on the given year, all markings was checked if they were actual outliers. The red colouring indicate missing values in the data (represented in the data with code "NULL"). The station names can be found in table 1.

## A PLOTS

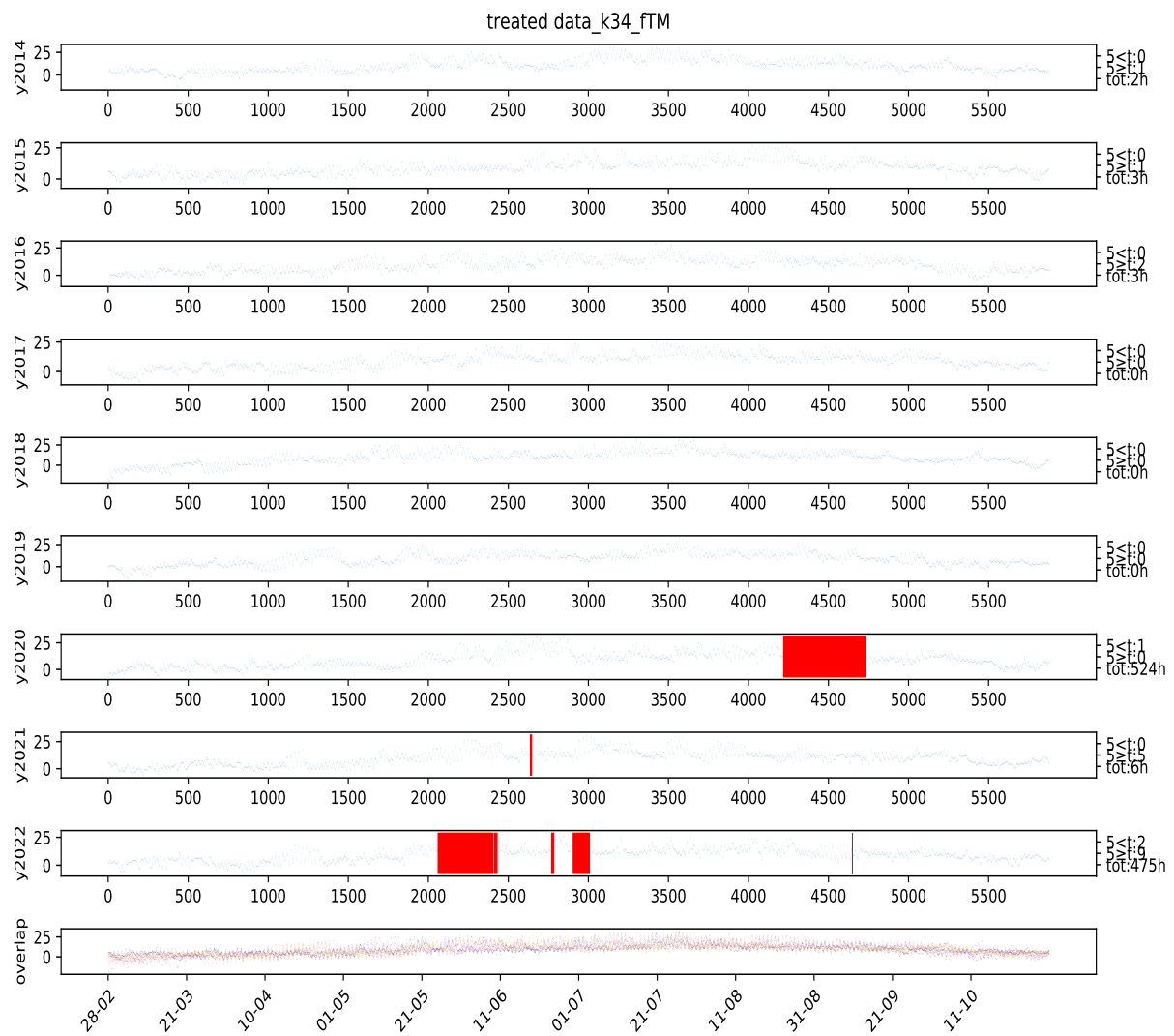


Figure 190: Visual representation of missing values at station 34 from 2014 to 2022 at the parameter "TM" after treating for outliers. The left numbers indicated how many hours that are missing and how many of them are shorter than or longer than 5 hours, however for this visualization they indicate the untreated version of the data. The yellow markings indicate possible outliers based on the given year, all markings was checked if they were actual outliers. The red colouring indicate missing values in the data (represented in the data with code "NULL"). The station names can be found in table 1.

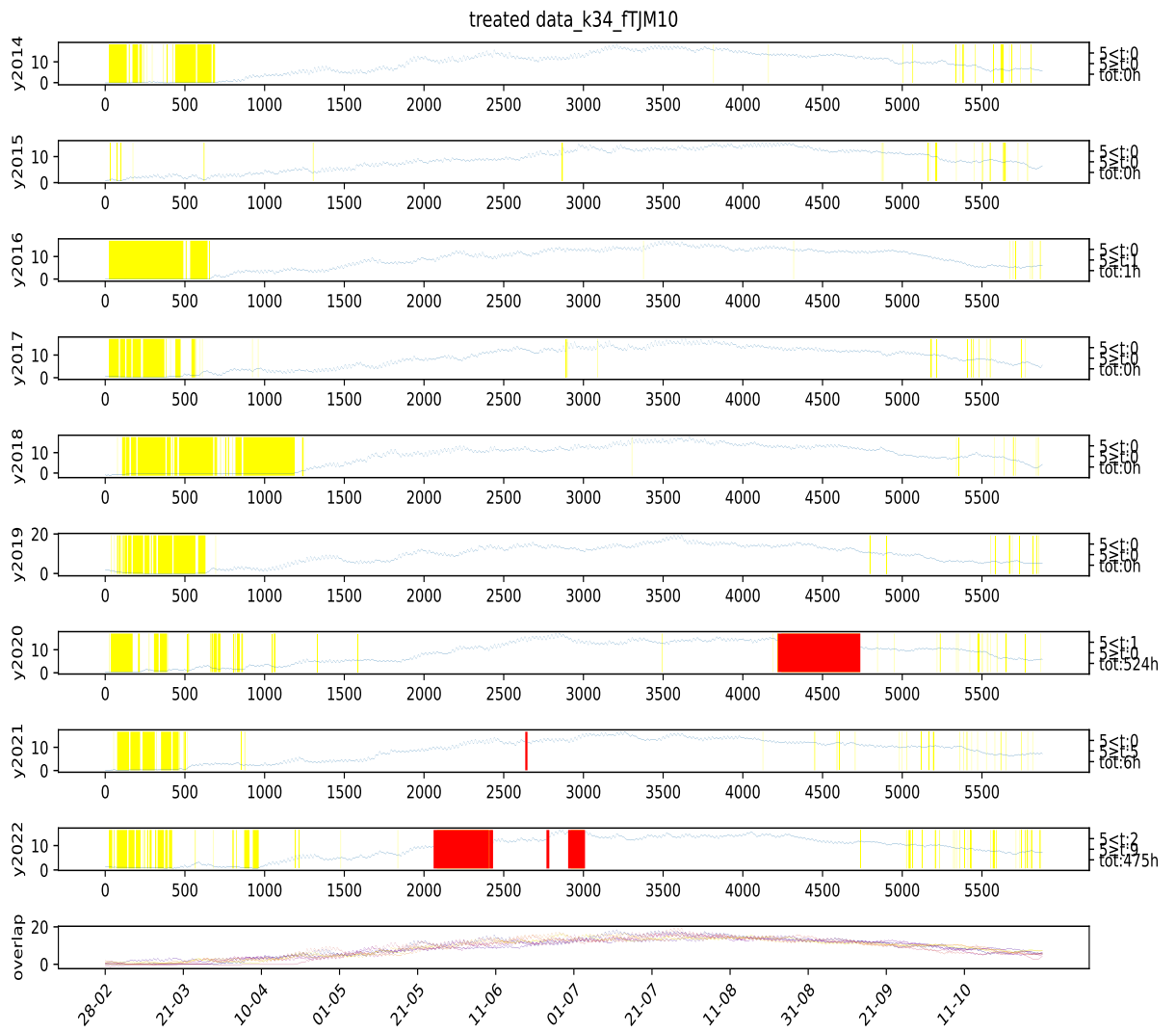


Figure 191: Visual representation of missing values at station 34 from 2014 to 2022 at the parameter "TJM10" after treating for outliers. The left numbers indicated how many hours that are missing and how many of them are shorter than or longer than 5 hours, however for this visualization they indicate the untreated version of the data. The yellow markings indicate possible outliers based on the given year, all markings was checked if they were actual outliers. The red colouring indicate missing values in the data (represented in the data with code "NULL"). The station names can be found in table 1.

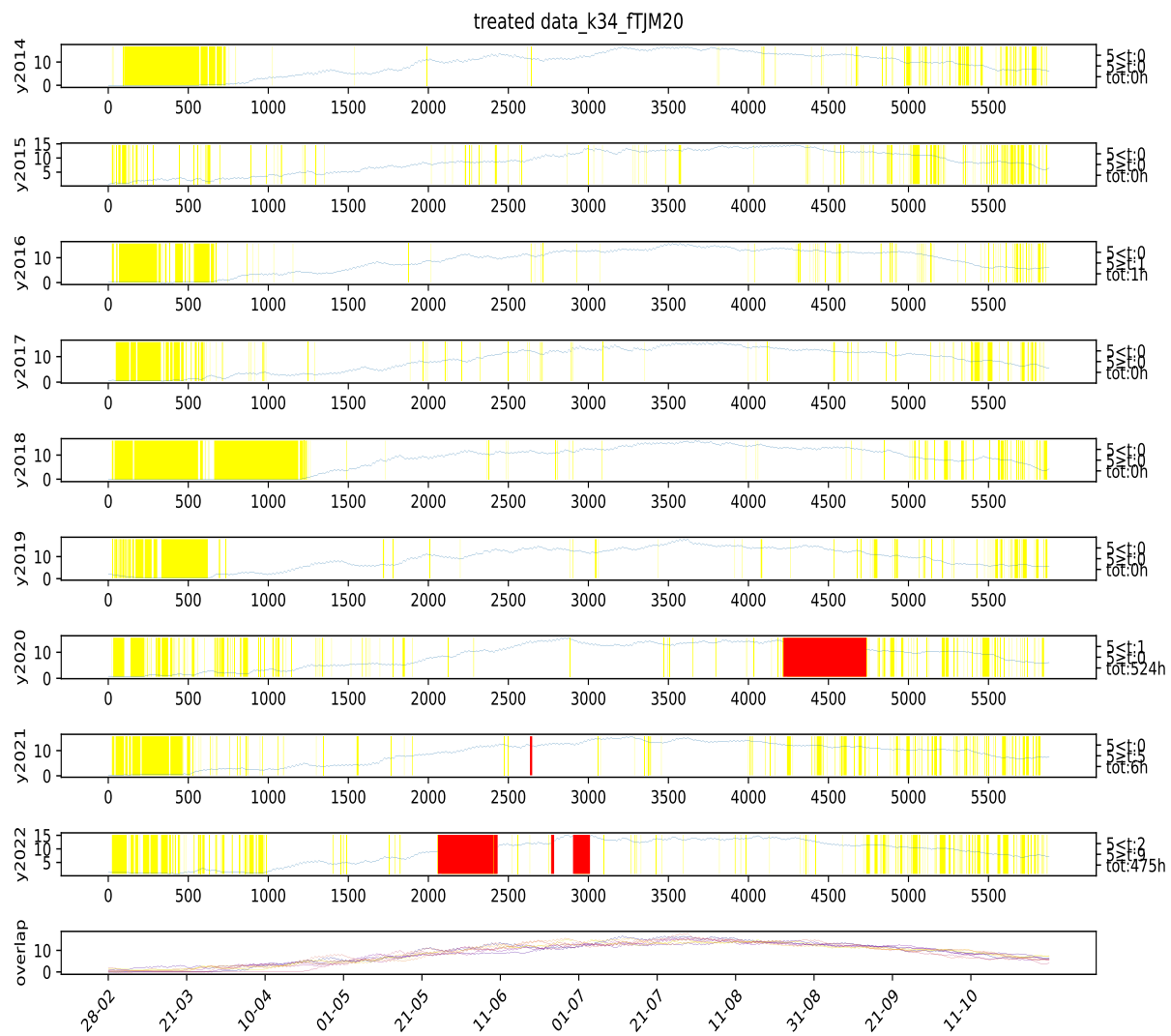


Figure 192: Visual representation of missing values at station 34 from 2014 to 2022 at the parameter "TJM20" after treating for outliers. The left numbers indicated how many hours that are missing and how many of them are shorter than or longer than 5 hours, however for this visualization they indicate the untreated version of the data. The yellow markings indicate possible outliers based on the given year, all markings was checked if they were actual outliers. The red colouring indicate missing values in the data (represented in the data with code "NULL"). The station names can be found in table 1.

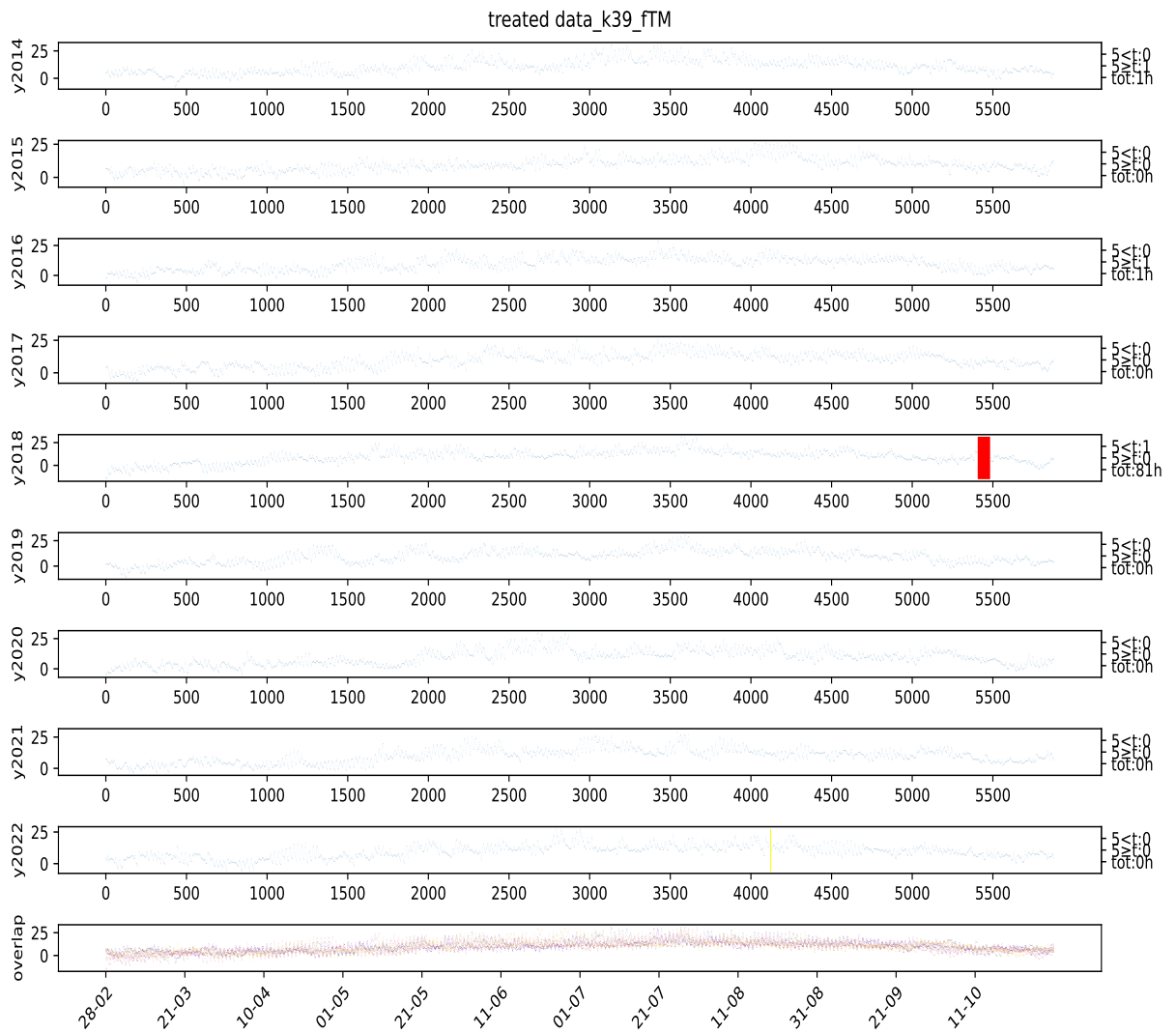


Figure 193: Visual representation of missing values at station 39 from 2014 to 2022 at the parameter "TM" after treating for outliers. The left numbers indicated how many hours that are missing and how many of them are shorter than or longer than 5 hours, however for this visualization they indicate the untreated version of the data. The yellow markings indicate possible outliers based on the given year, all markings was checked if they were actual outliers. The red colouring indicate missing values in the data (represented in the data with code "NULL"). The station names can be found in table 1.

## A PLOTS

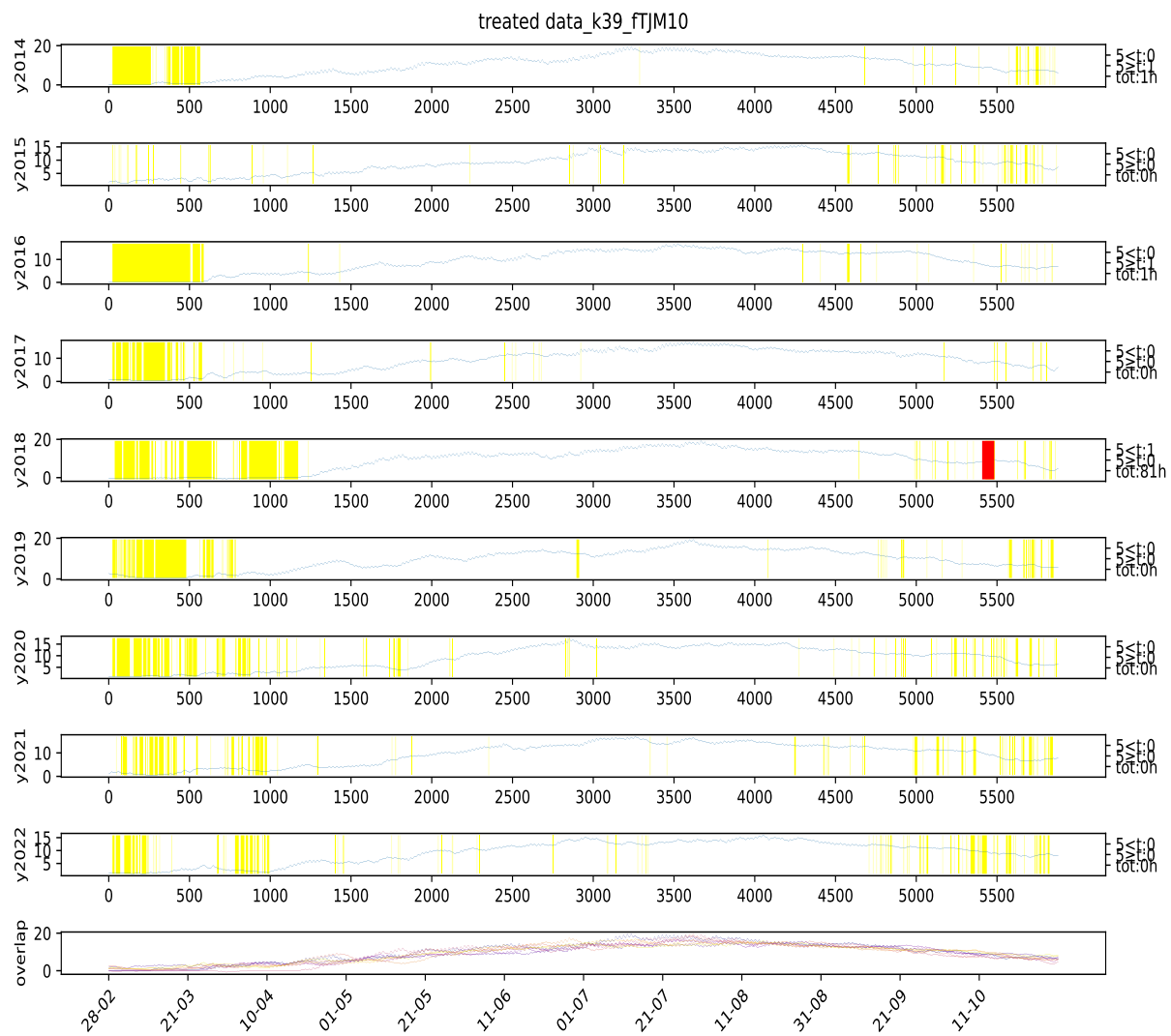


Figure 194: Visual representation of missing values at station 39 from 2014 to 2022 at the parameter "TJM10" after treating for outliers. The left numbers indicated how many hours that are missing and how many of them are shorter than or longer than 5 hours, however for this visualization they indicate the untreated version of the data. The yellow markings indicate possible outliers based on the given year, all markings was checked if they were actual outliers. The red colouring indicate missing values in the data (represented in the data with code "NULL"). The station names can be found in table 1.

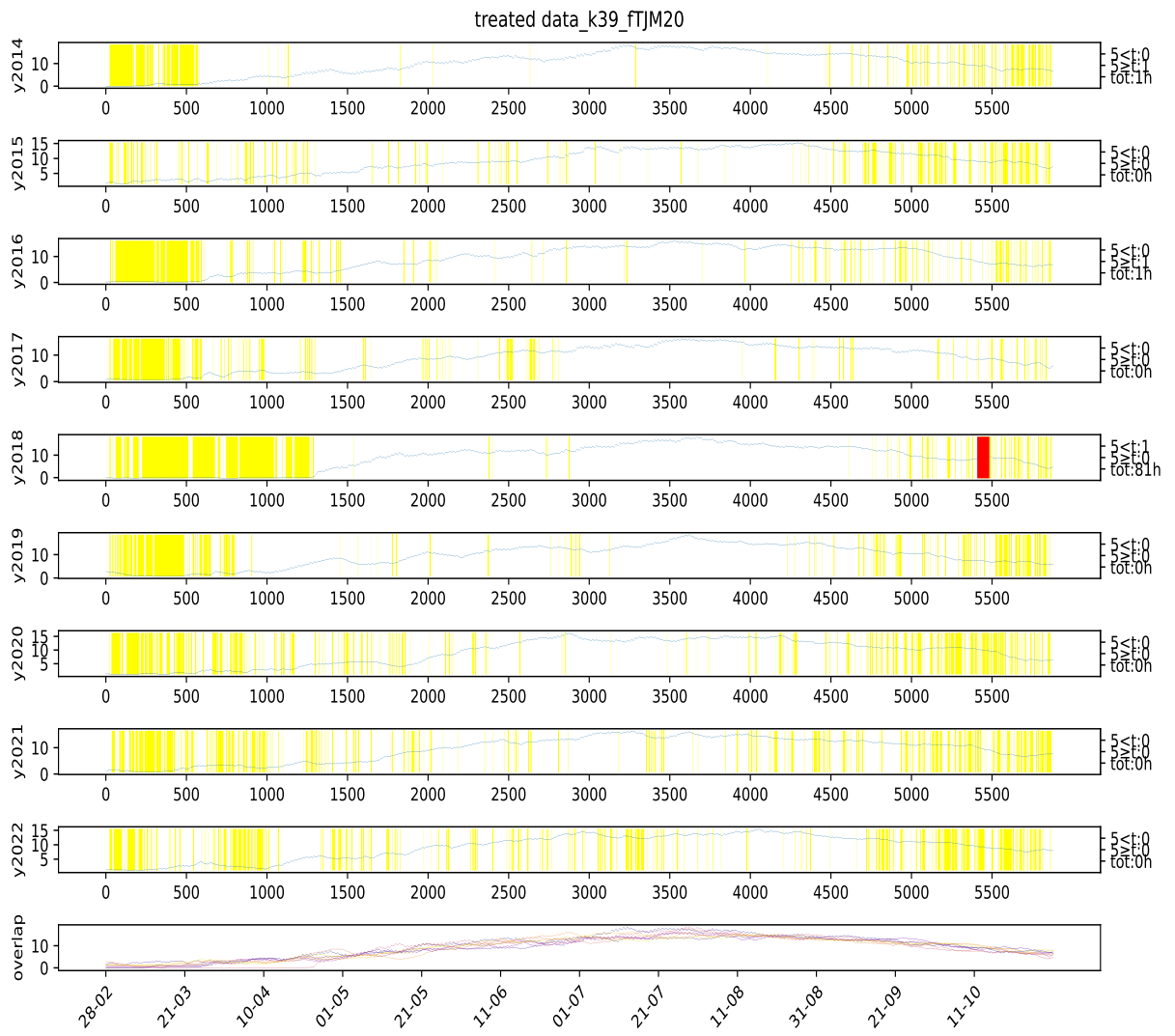


Figure 195: Visual representation of missing values at station 39 from 2014 to 2022 at the parameter "TJM20" after treating for outliers. The left numbers indicated how many hours that are missing and how many of them are shorter than or longer than 5 hours, however for this visualization they indicate the untreated version of the data. The yellow markings indicate possible outliers based on the given year, all markings was checked if they were actual outliers. The red colouring indicate missing values in the data (represented in the data with code "NULL"). The station names can be found in table 1.

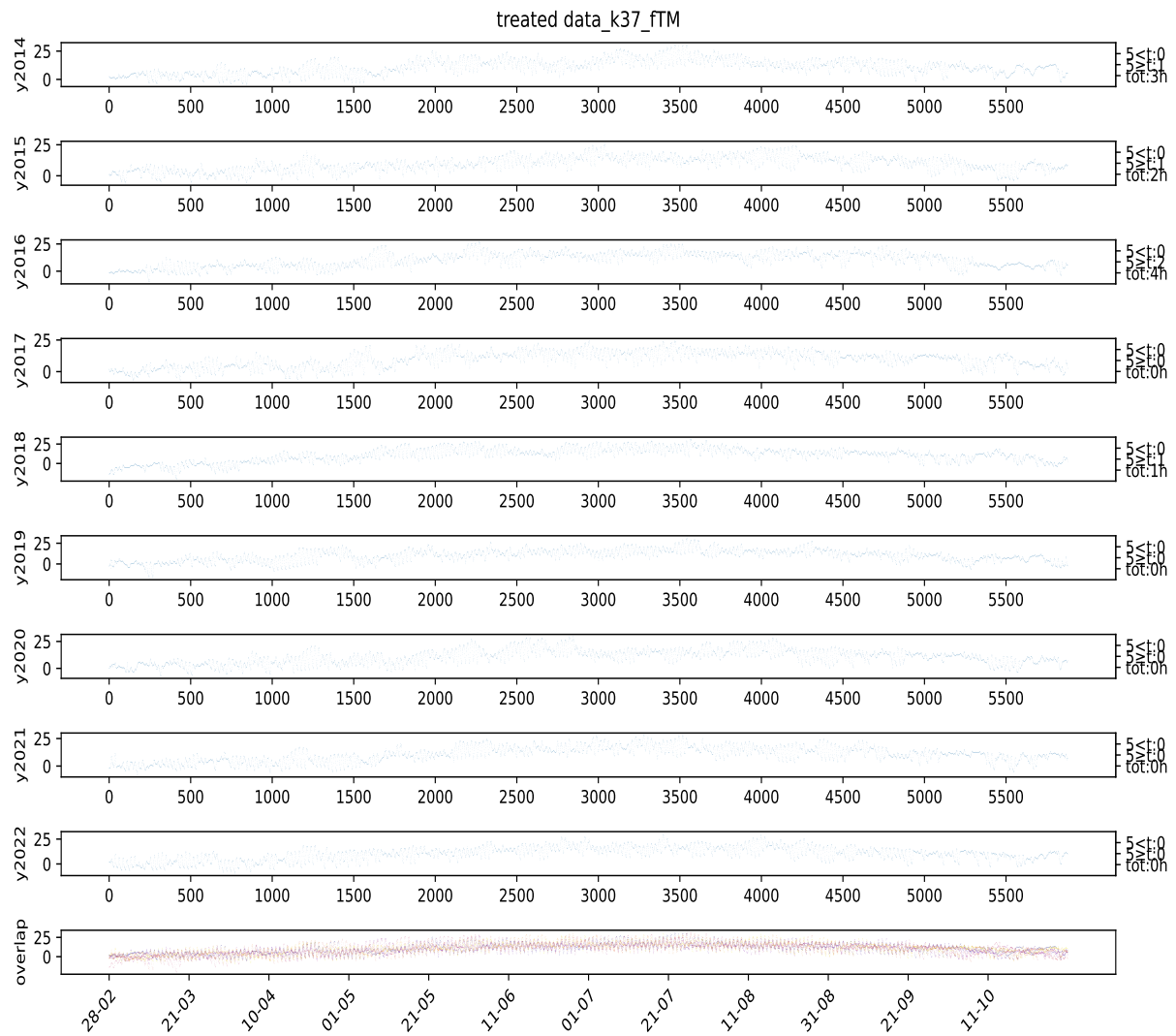


Figure 196: Visual representation of missing values at station 37 from 2014 to 2022 at the parameter "TM" after treating for outliers. The left numbers indicated how many hours that are missing and how many of them are shorter than or longer than 5 hours, however for this visualization they indicate the untreated version of the data. The yellow markings indicate possible outliers based on the given year, all markings was checked if they were actual outliers. The red colouring indicate missing values in the data (represented in the data with code "NULL"). The station names can be found in table 1.

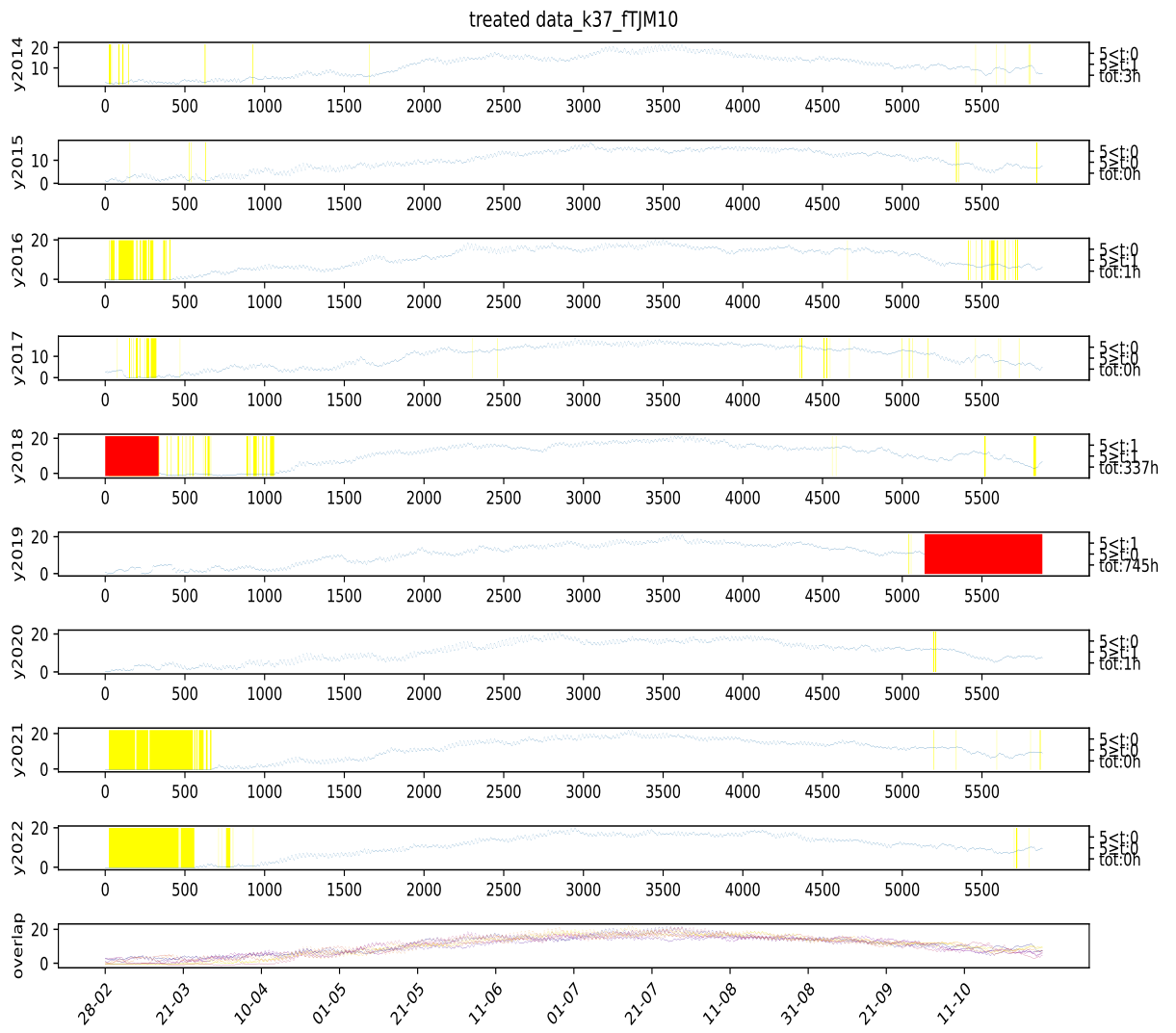


Figure 197: Visual representation of missing values at station 37 from 2014 to 2022 at the parameter "TJM10" after treating for outliers. The left numbers indicated how many hours that are missing and how many of them are shorter than or longer than 5 hours, however for this visualization they indicate the untreated version of the data. The yellow markings indicate possible outliers based on the given year, all markings was checked if they were actual outliers. The red colouring indicate missing values in the data (represented in the data with code "NULL"). The station names can be found in table 1.

## A PLOTS

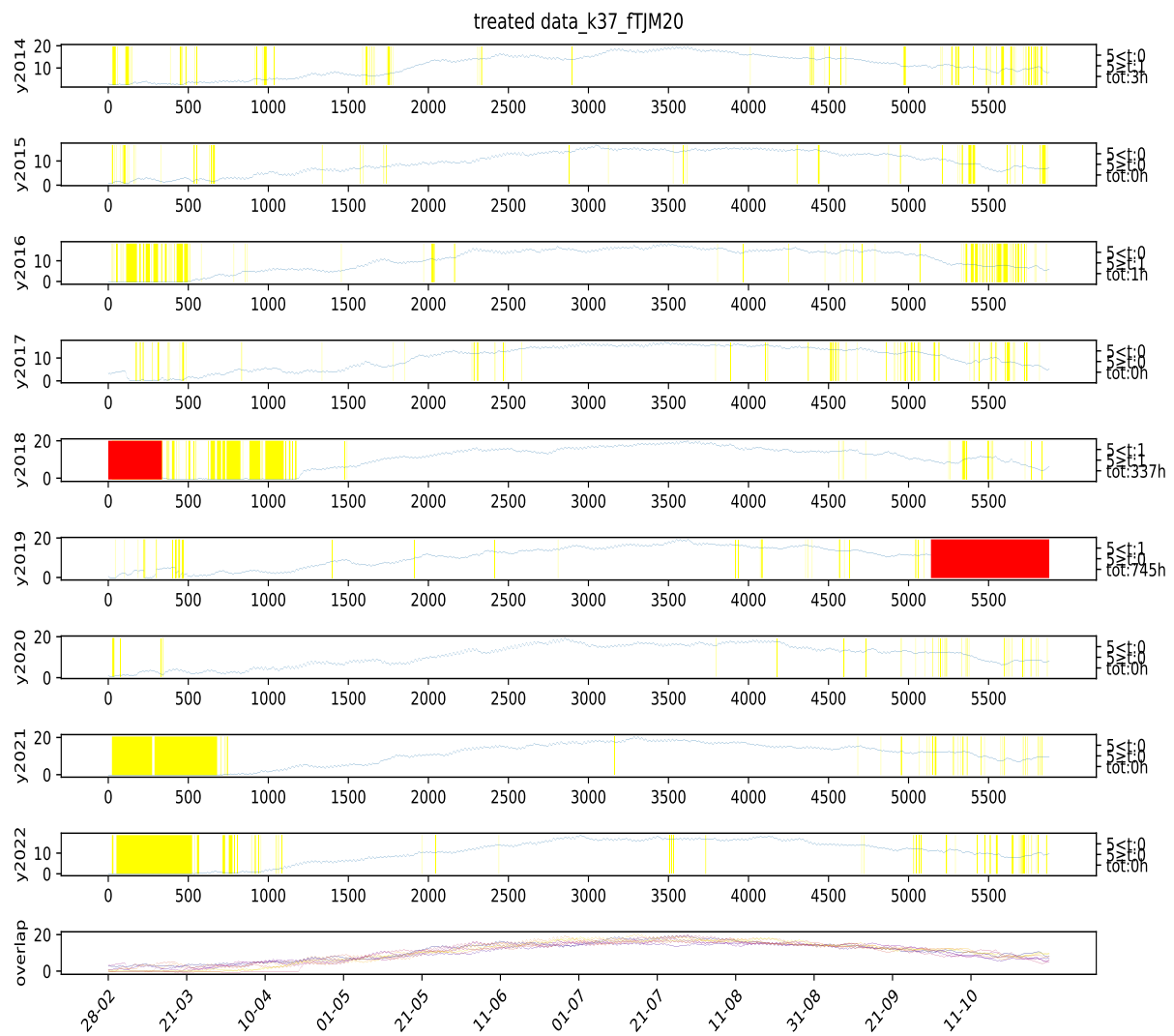


Figure 198: Visual representation of missing values at station 37 from 2014 to 2022 at the parameter "TJM20" after treating for outliers. The left numbers indicated how many hours that are missing and how many of them are shorter than or longer than 5 hours, however for this visualization they indicate the untreated version of the data. The yellow markings indicate possible outliers based on the given year, all markings was checked if they were actual outliers. The red colouring indicate missing values in the data (represented in the data with code "NULL"). The station names can be found in table 1.

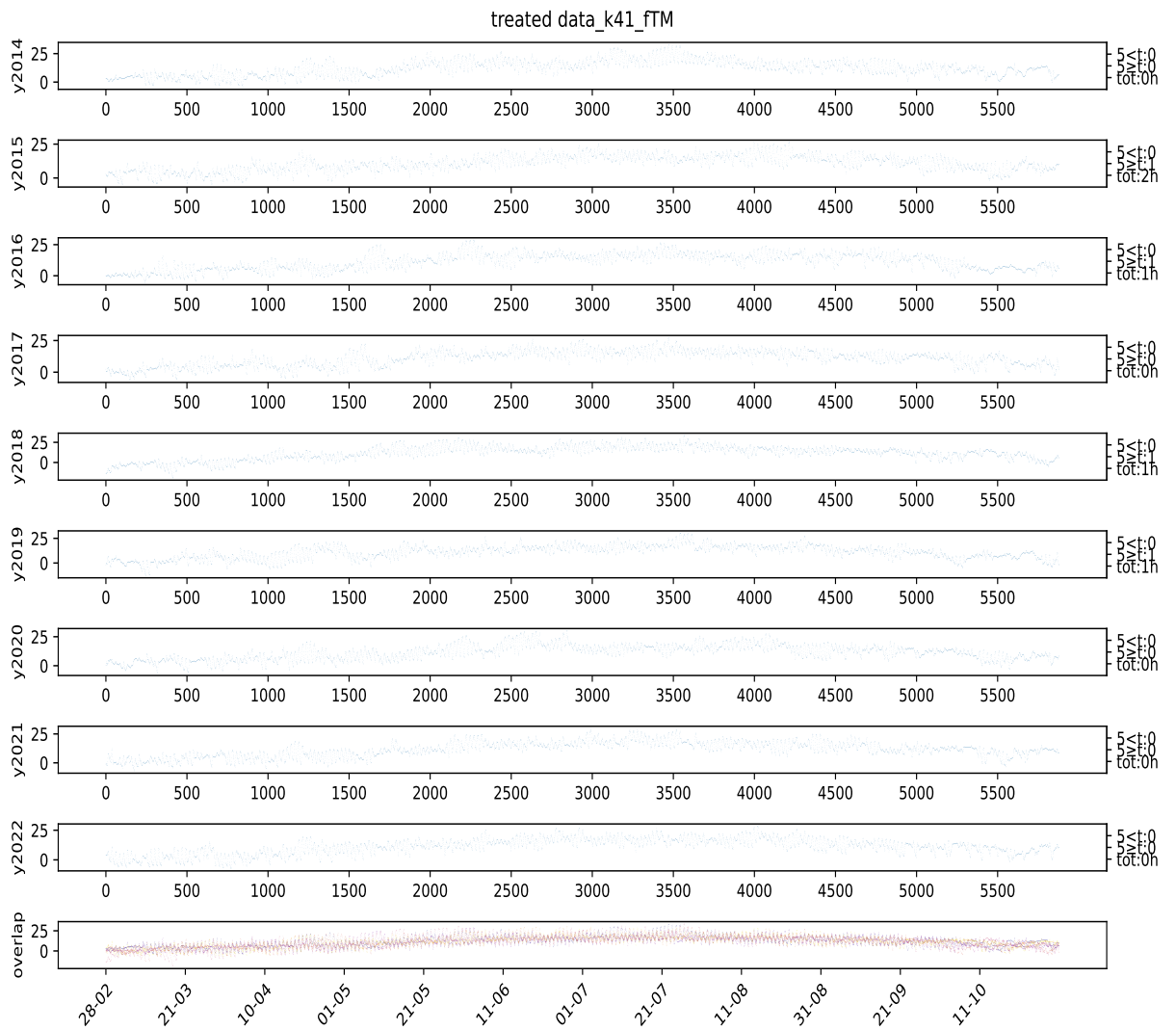


Figure 199: Visual representation of missing values at station 41 from 2014 to 2022 at the parameter "TM" after treating for outliers. The left numbers indicated how many hours that are missing and how many of them are shorter than or longer than 5 hours, however for this visualization they indicate the untreated version of the data. The yellow markings indicate possible outliers based on the given year, all markings was checked if they were actual outliers. The red colouring indicate missing values in the data (represented in the data with code "NULL"). The station names can be found in table 1.

## A PLOTS

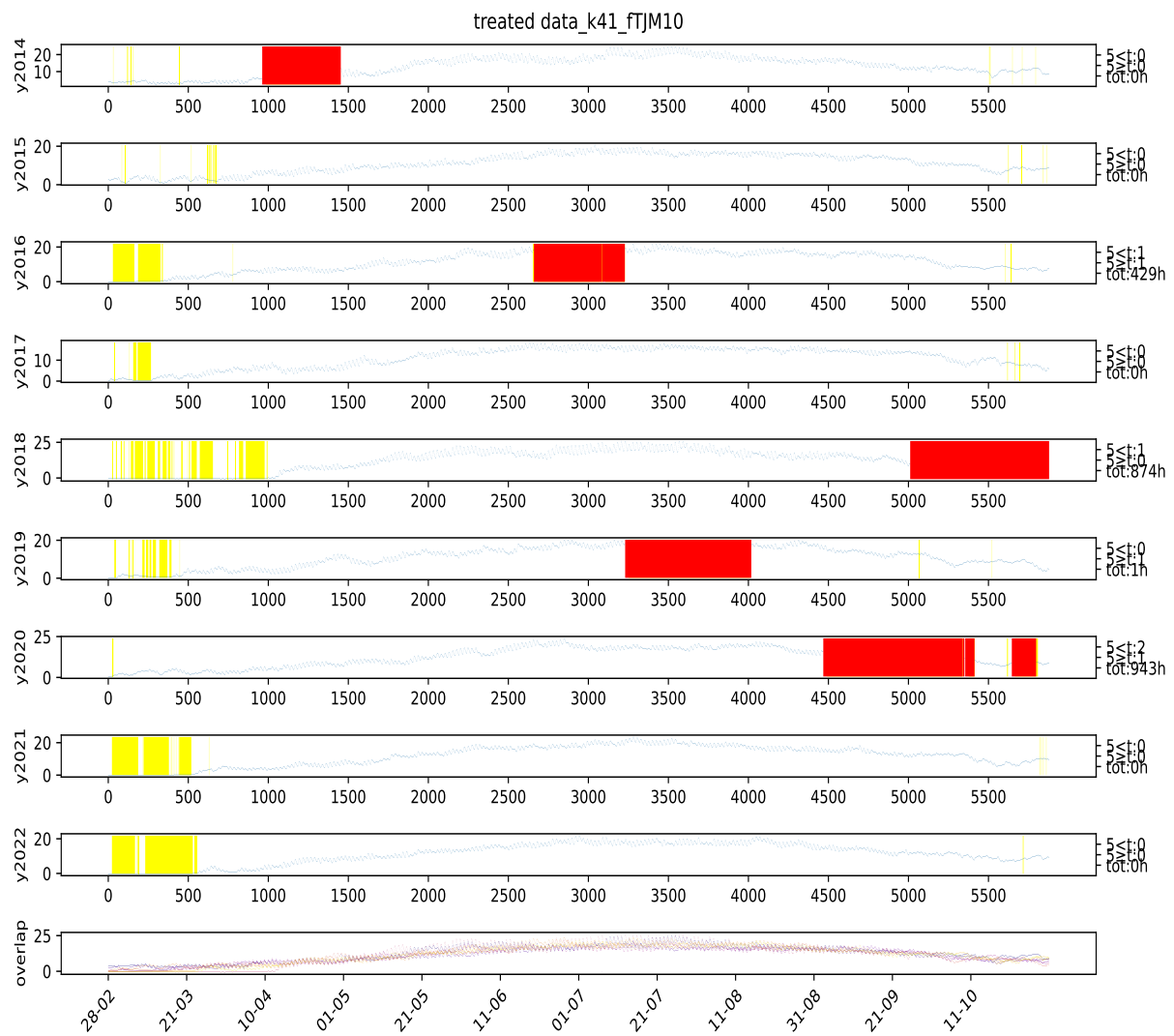


Figure 200: Visual representation of missing values at station 41 from 2014 to 2022 at the parameter "TJM10" after treating for outliers. The left numbers indicated how many hours that are missing and how many of them are shorter than or longer than 5 hours, however for this visualization they indicate the untreated version of the data. The yellow markings indicate possible outliers based on the given year, all markings was checked if they were actual outliers. The red colouring indicate missing values in the data (represented in the data with code "NULL"). The station names can be found in table 1.

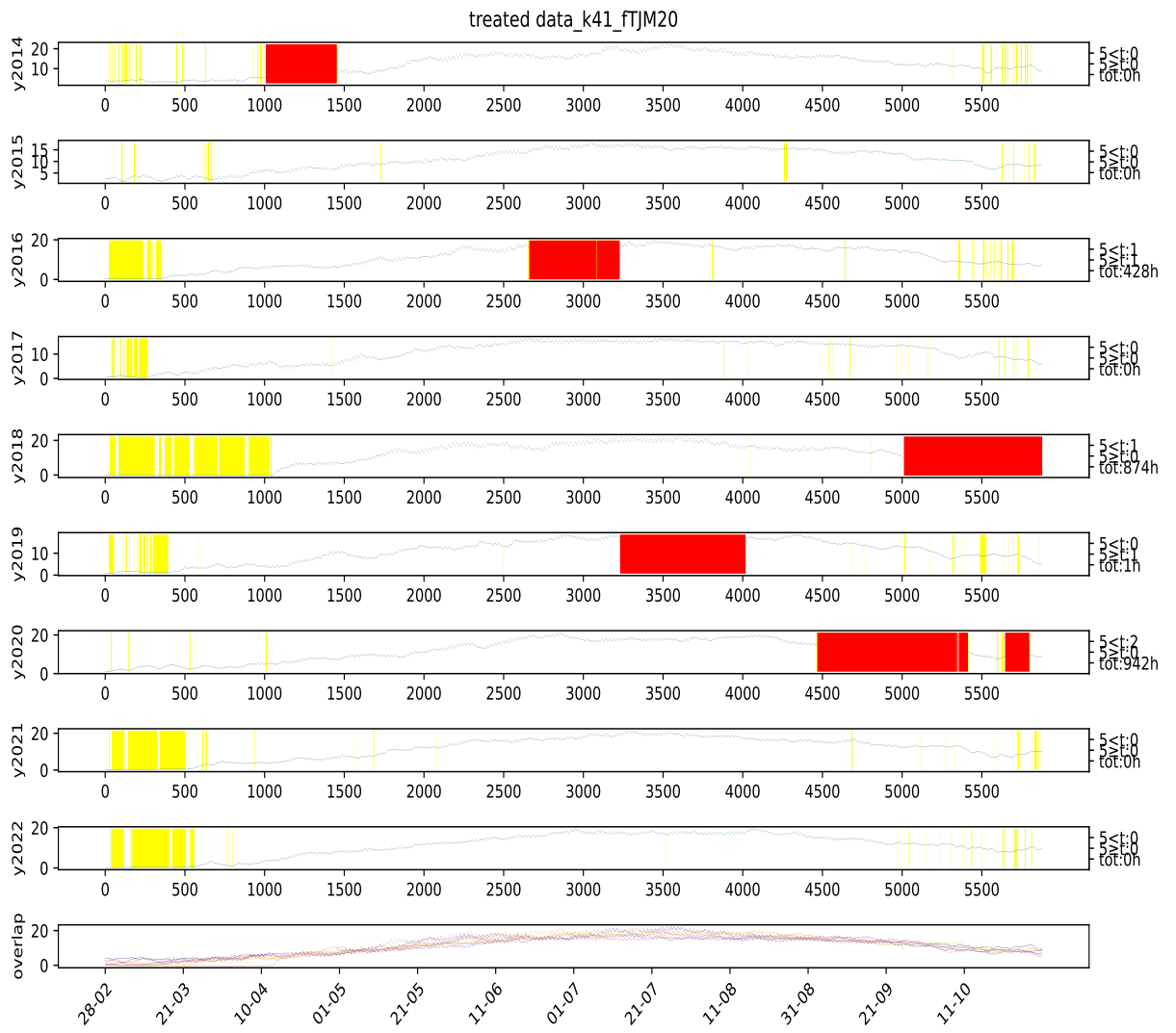


Figure 201: Visual representation of missing values at station 41 from 2014 to 2022 at the parameter "TJM20" after treating for outliers. The left numbers indicated how many hours that are missing and how many of them are shorter than or longer than 5 hours, however for this visualization they indicate the untreated version of the data. The yellow markings indicate possible outliers based on the given year, all markings was checked if they were actual outliers. The red colouring indicate missing values in the data (represented in the data with code "NULL"). The station names can be found in table 1.

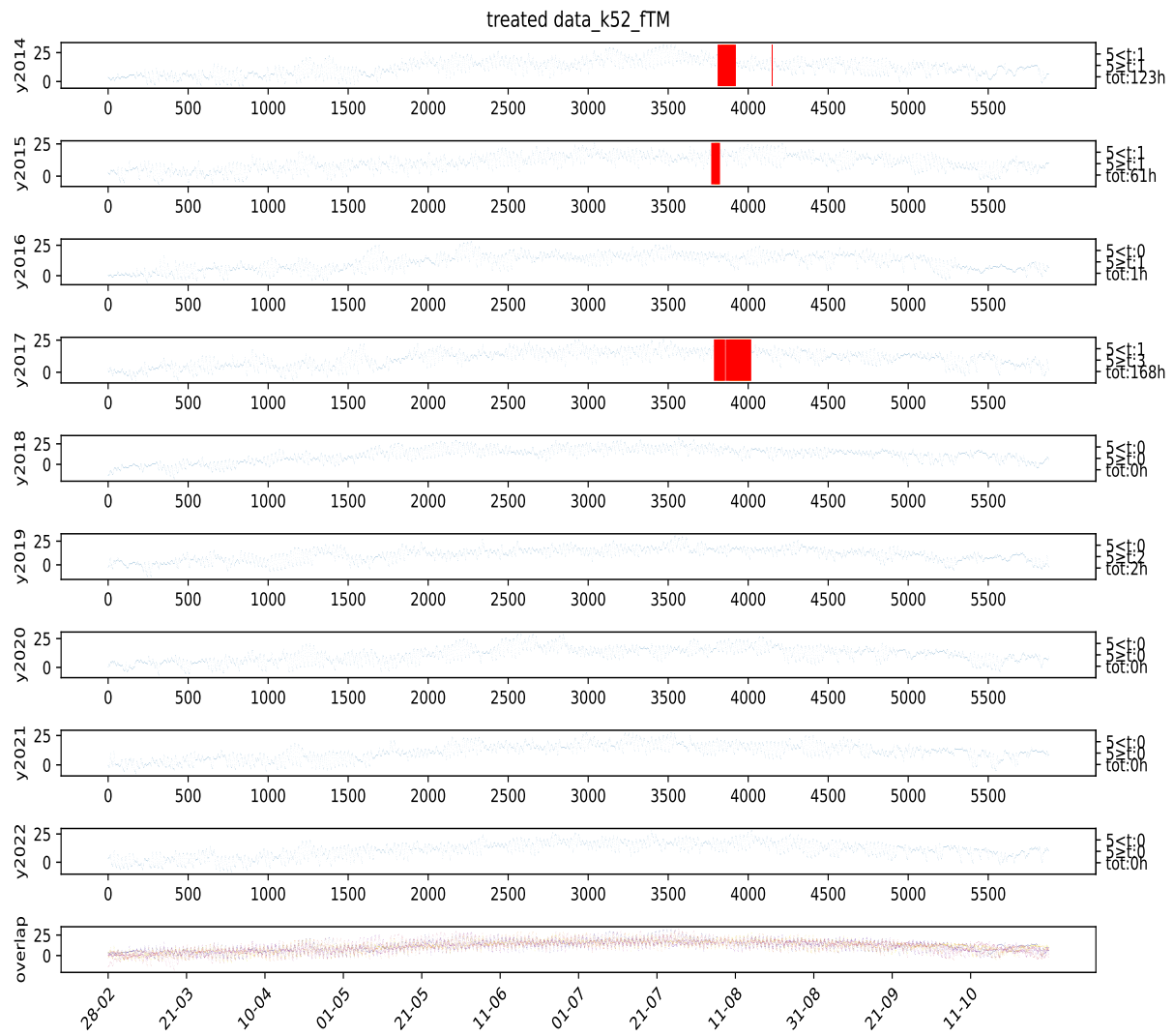


Figure 202: Visual representation of missing values at station 52 from 2014 to 2022 at the parameter "TM" after treating for outliers. The left numbers indicated how many hours that are missing and how many of them are shorter than or longer than 5 hours, however for this visualization they indicate the untreated version of the data. The yellow markings indicate possible outliers based on the given year, all markings was checked if they were actual outliers. The red colouring indicate missing values in the data (represented in the data with code "NULL"). The station names can be found in table 1.

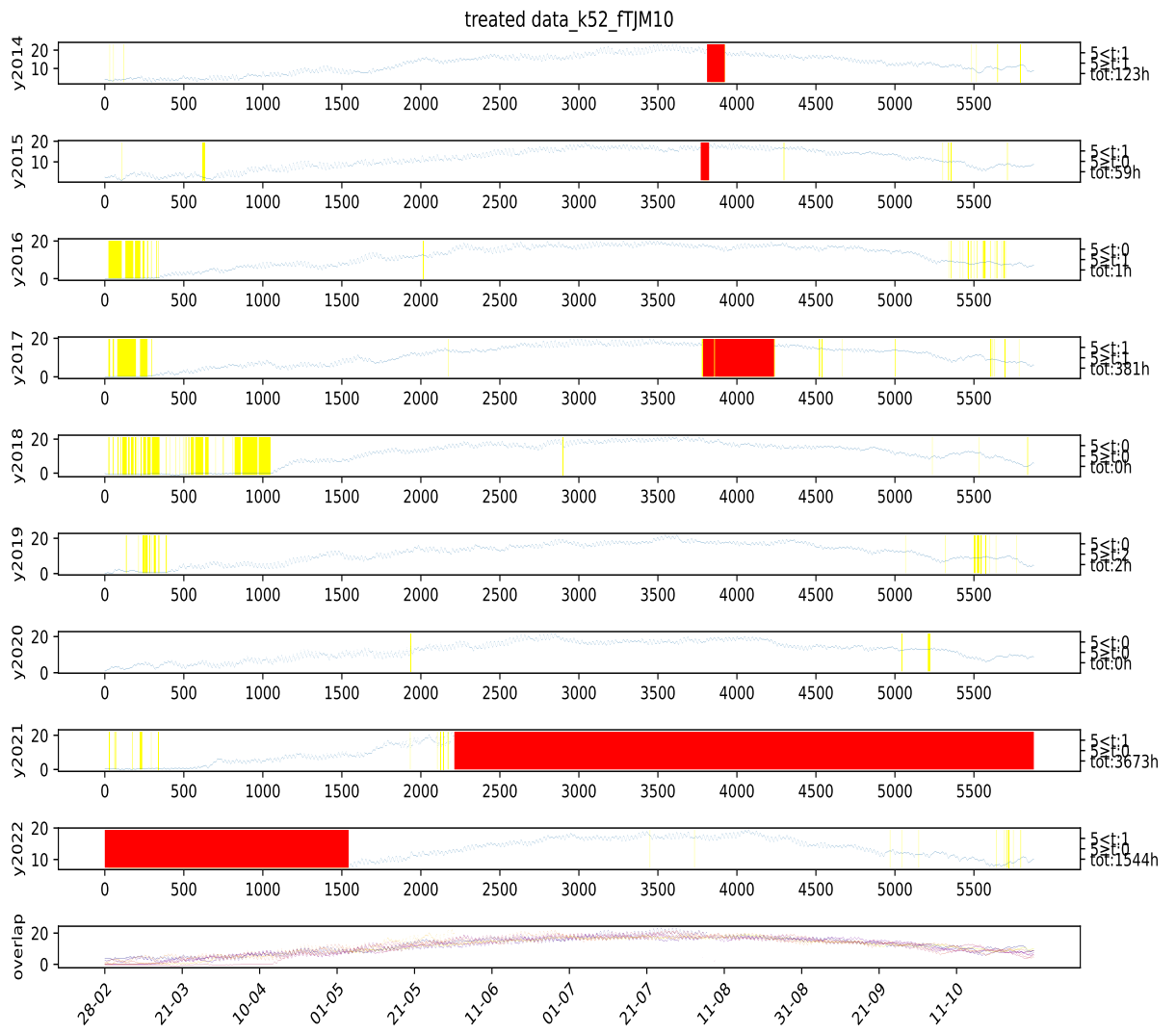


Figure 203: Visual representation of missing values at station 52 from 2014 to 2022 at the parameter "TJM10" after treating for outliers. The left numbers indicated how many hours that are missing and how many of them are shorter than or longer than 5 hours, however for this visualization they indicate the untreated version of the data. The yellow markings indicate possible outliers based on the given year, all markings was checked if they were actual outliers. The red colouring indicate missing values in the data (represented in the data with code "NULL"). The station names can be found in table 1.

## A PLOTS

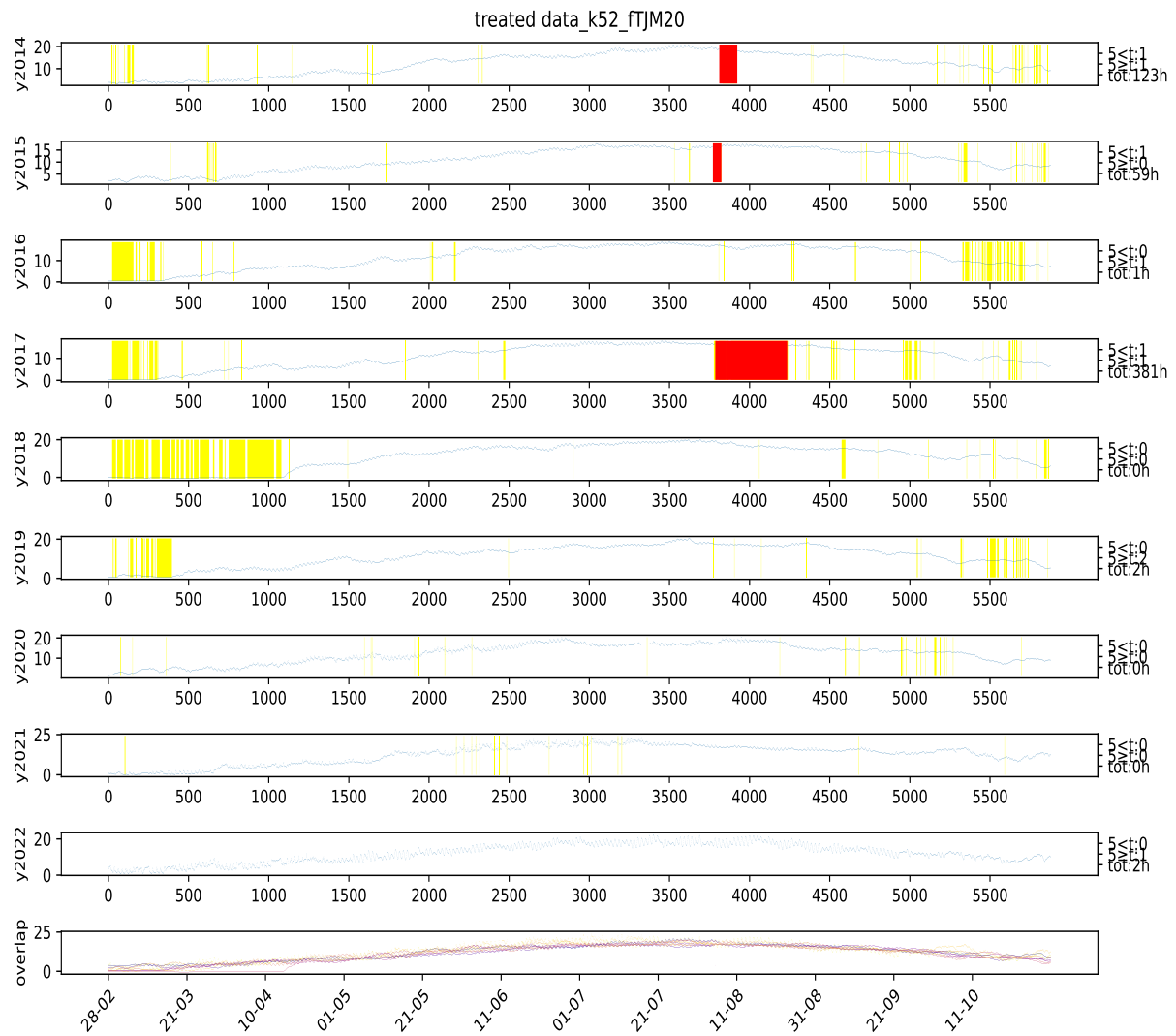


Figure 204: Visual representation of missing values at station 52 from 2014 to 2022 at the parameter "TJM20" after treating for outliers. The left numbers indicated how many hours that are missing and how many of them are shorter than or longer than 5 hours, however for this visualization they indicate the untreated version of the data. The yellow markings indicate possible outliers based on the given year, all markings was checked if they were actual outliers. The red colouring indicate missing values in the data (represented in the data with code "NULL"). The station names can be found in table 1.

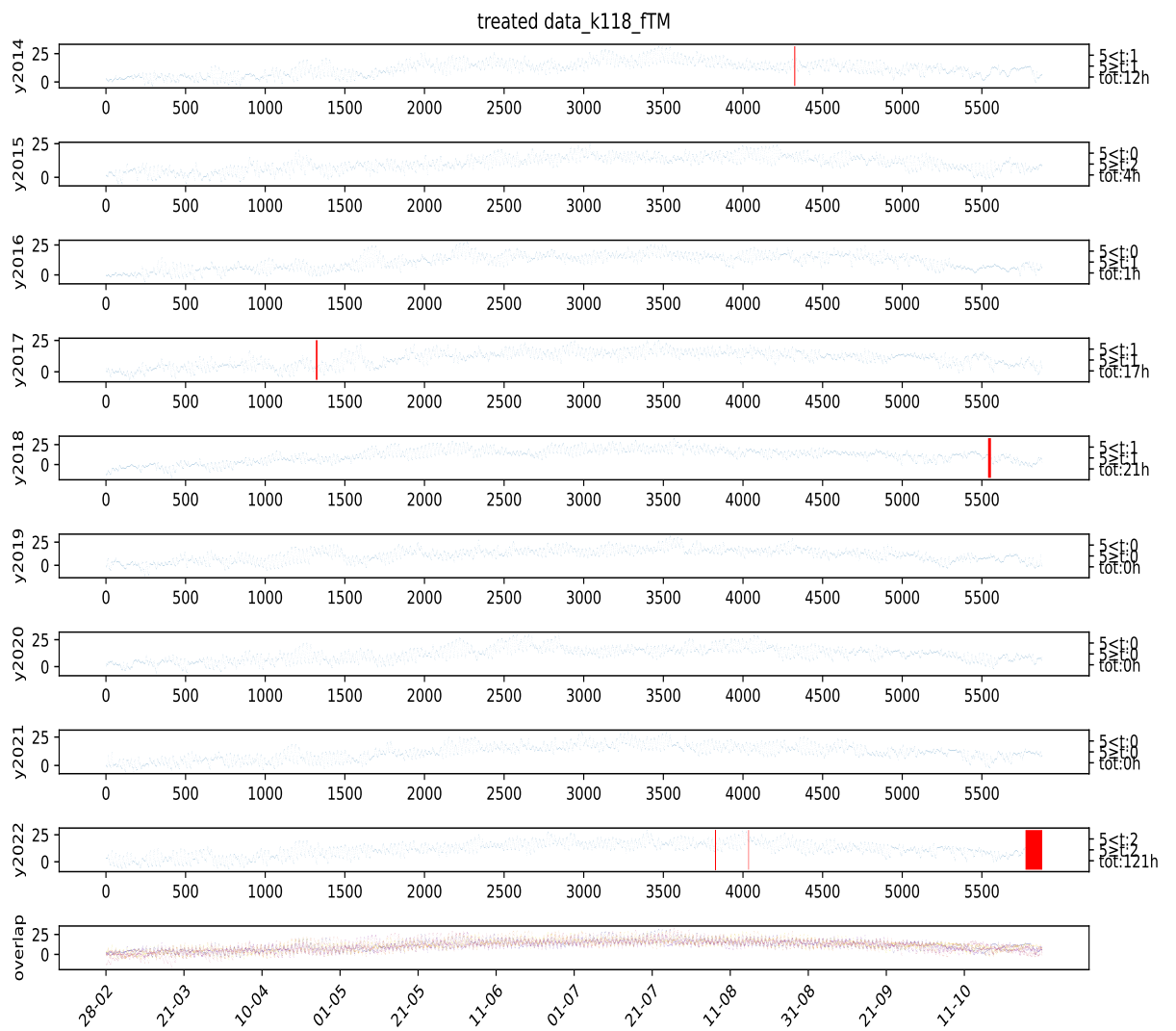


Figure 205: Visual representation of missing values at station 118 from 2014 to 2022 at the parameter "TM" after treating for outliers. The left numbers indicated how many hours that are missing and how many of them are shorter than or longer than 5 hours, however for this visualization they indicate the untreated version of the data. The yellow markings indicate possible outliers based on the given year, all markings was checked if they were actual outliers. The red colouring indicate missing values in the data (represented in the data with code "NULL"). The station names can be found in table 1.

## A PLOTS

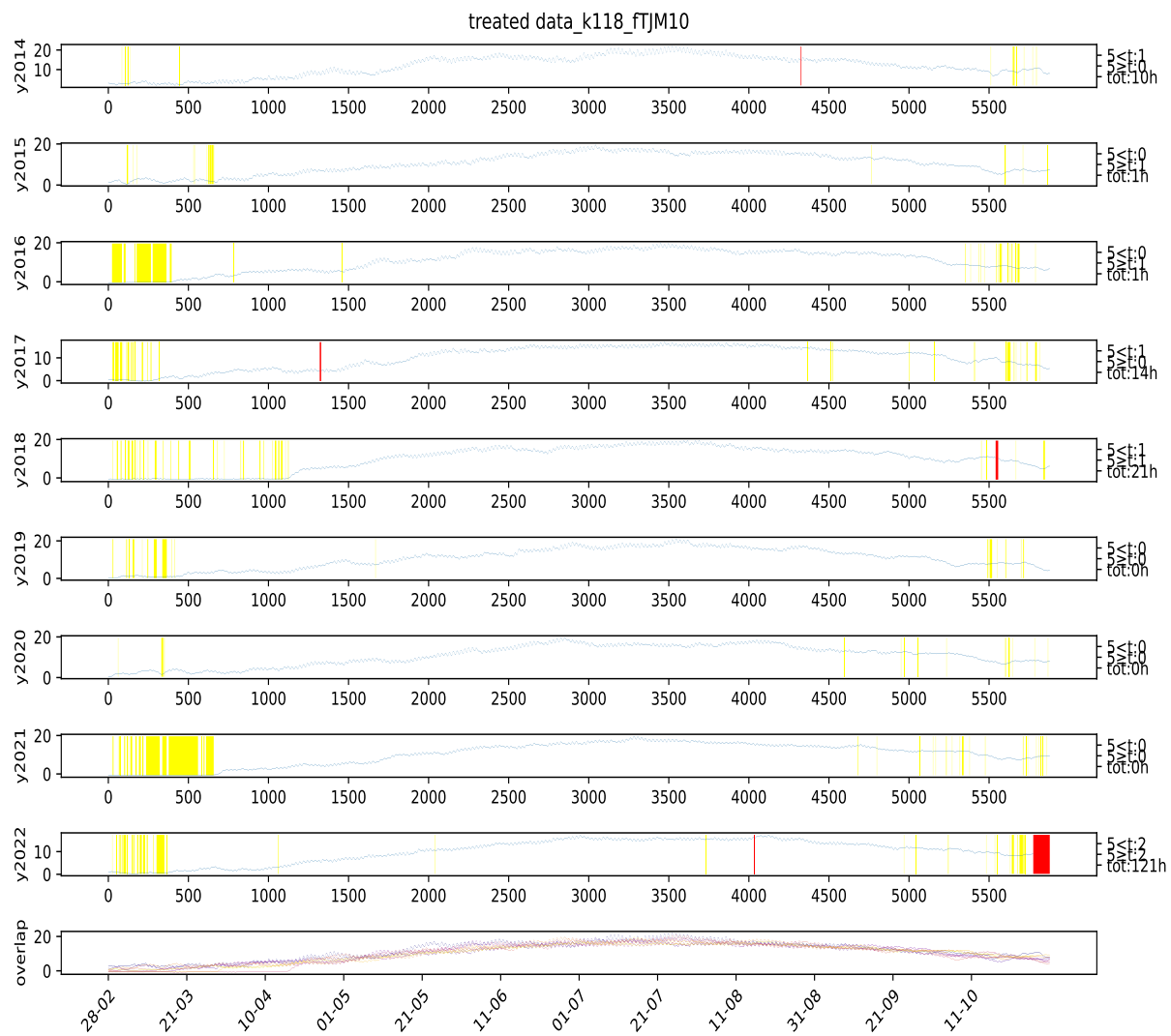


Figure 206: Visual representation of missing values at station 118 from 2014 to 2022 at the parameter "TJM10" after treating for outliers. The left numbers indicated how many hours that are missing and how many of them are shorter than or longer than 5 hours, however for this visualization they indicate the untreated version of the data. The yellow markings indicate possible outliers based on the given year, all markings was checked if they were actual outliers. The red colouring indicate missing values in the data (represented in the data with code "NULL"). The station names can be found in table 1.

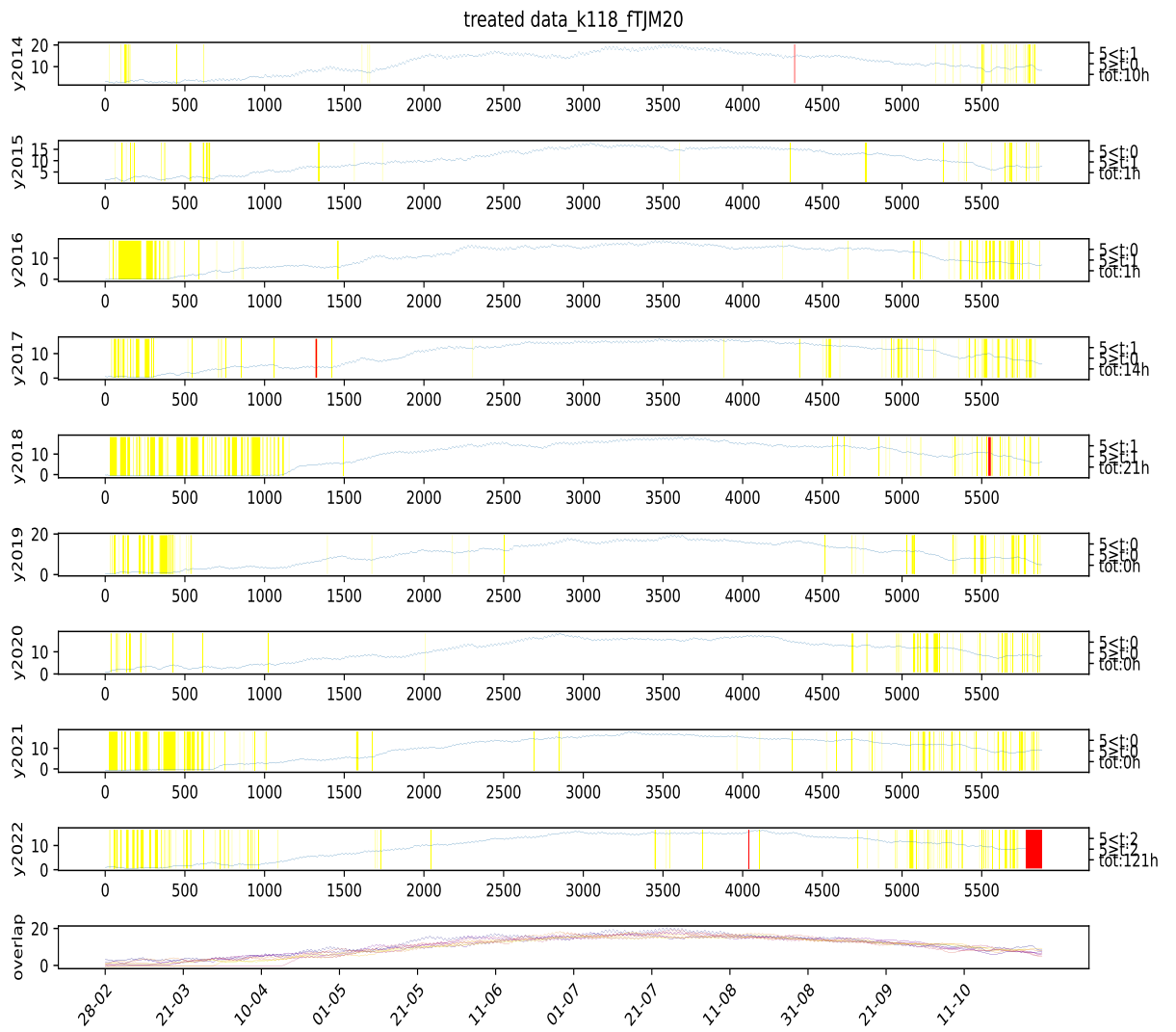


Figure 207: Visual representation of missing values at station 118 from 2014 to 2022 at the parameter "TJM20" after treating for outliers. The left numbers indicated how many hours that are missing and how many of them are shorter than or longer than 5 hours, however for this visualization they indicate the untreated version of the data. The yellow markings indicate possible outliers based on the given year, all markings was checked if they were actual outliers. The red colouring indicate missing values in the data (represented in the data with code "NULL"). The station names can be found in table 1.

## A PLOTS

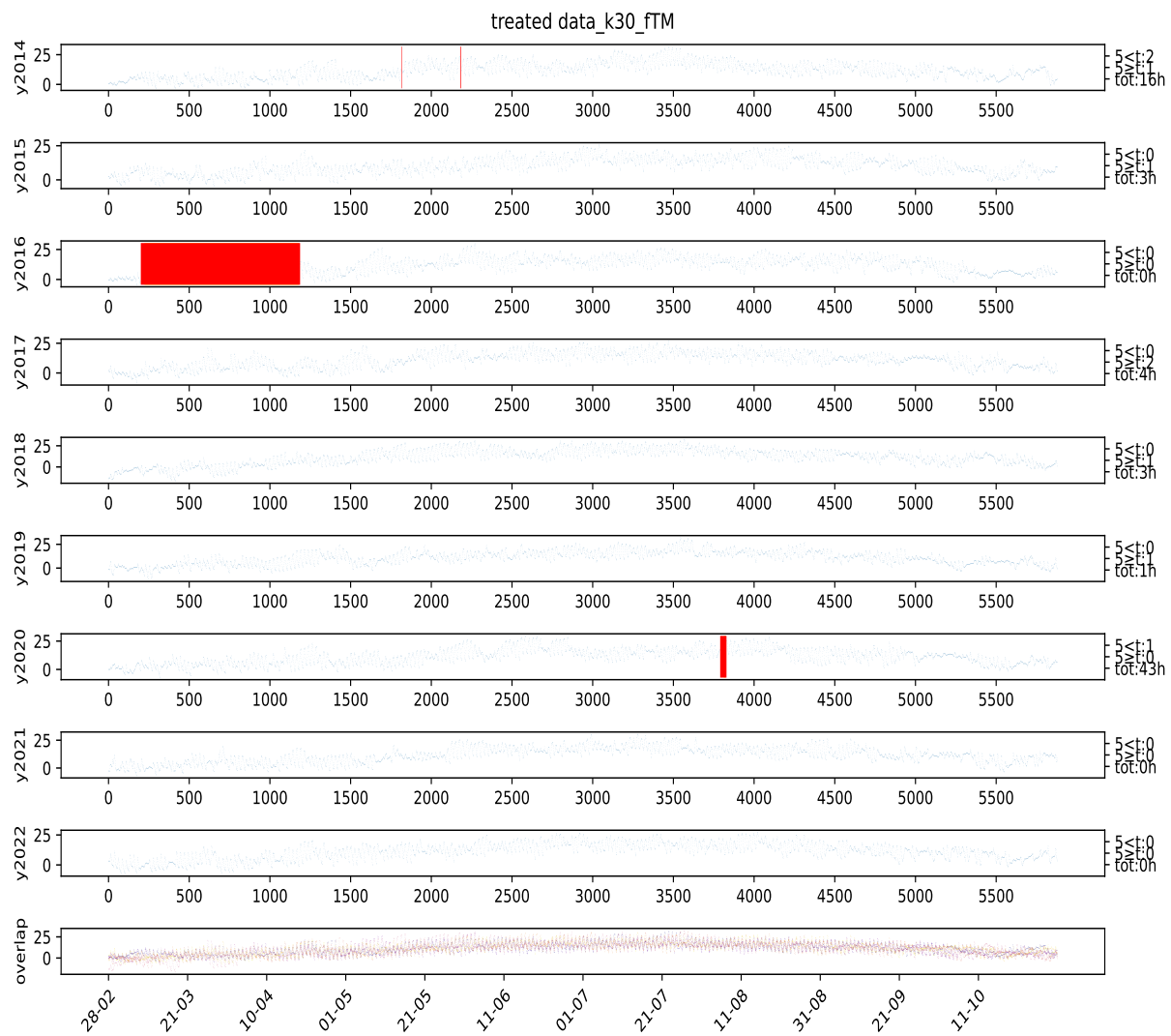


Figure 208: Visual representation of missing values at station 30 from 2014 to 2022 at the parameter "TM" after treating for outliers. The left numbers indicated how many hours that are missing and how many of them are shorter than or longer than 5 hours, however for this visualization they indicate the untreated version of the data. The yellow markings indicate possible outliers based on the given year, all markings was checked if they were actual outliers. The red colouring indicate missing values in the data (represented in the data with code "NULL"). The station names can be found in table 1.

## A PLOTS

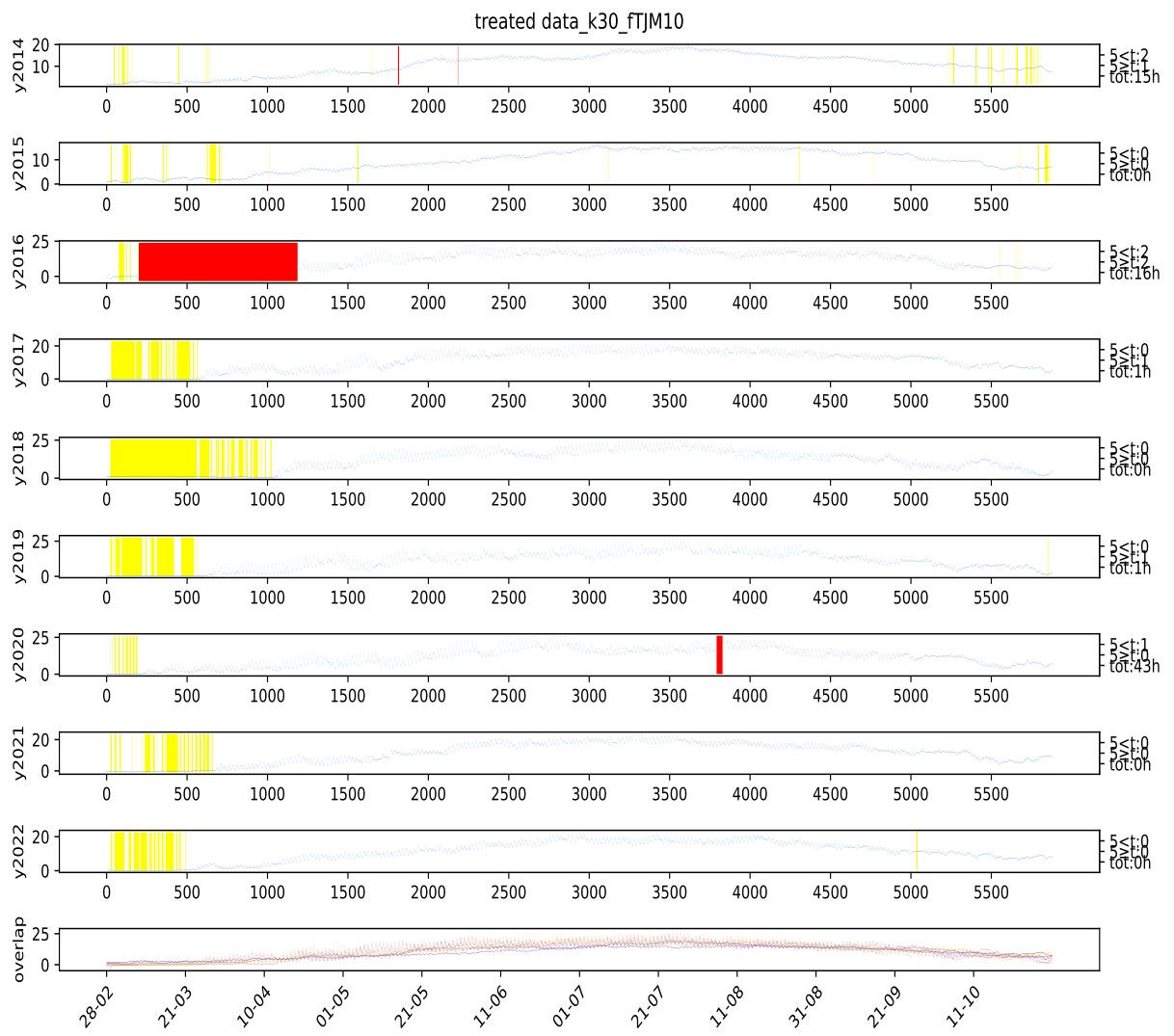


Figure 209: Visual representation of missing values at station 30 from 2014 to 2022 at the parameter "TJM10" after treating for outliers. The left numbers indicated how many hours that are missing and how many of them are shorter than or longer than 5 hours, however for this visualization they indicate the untreated version of the data. The yellow markings indicate possible outliers based on the given year, all markings was checked if they were actual outliers. The red colouring indicate missing values in the data (represented in the data with code "NULL").The station names can be found in table 1.

## A PLOTS

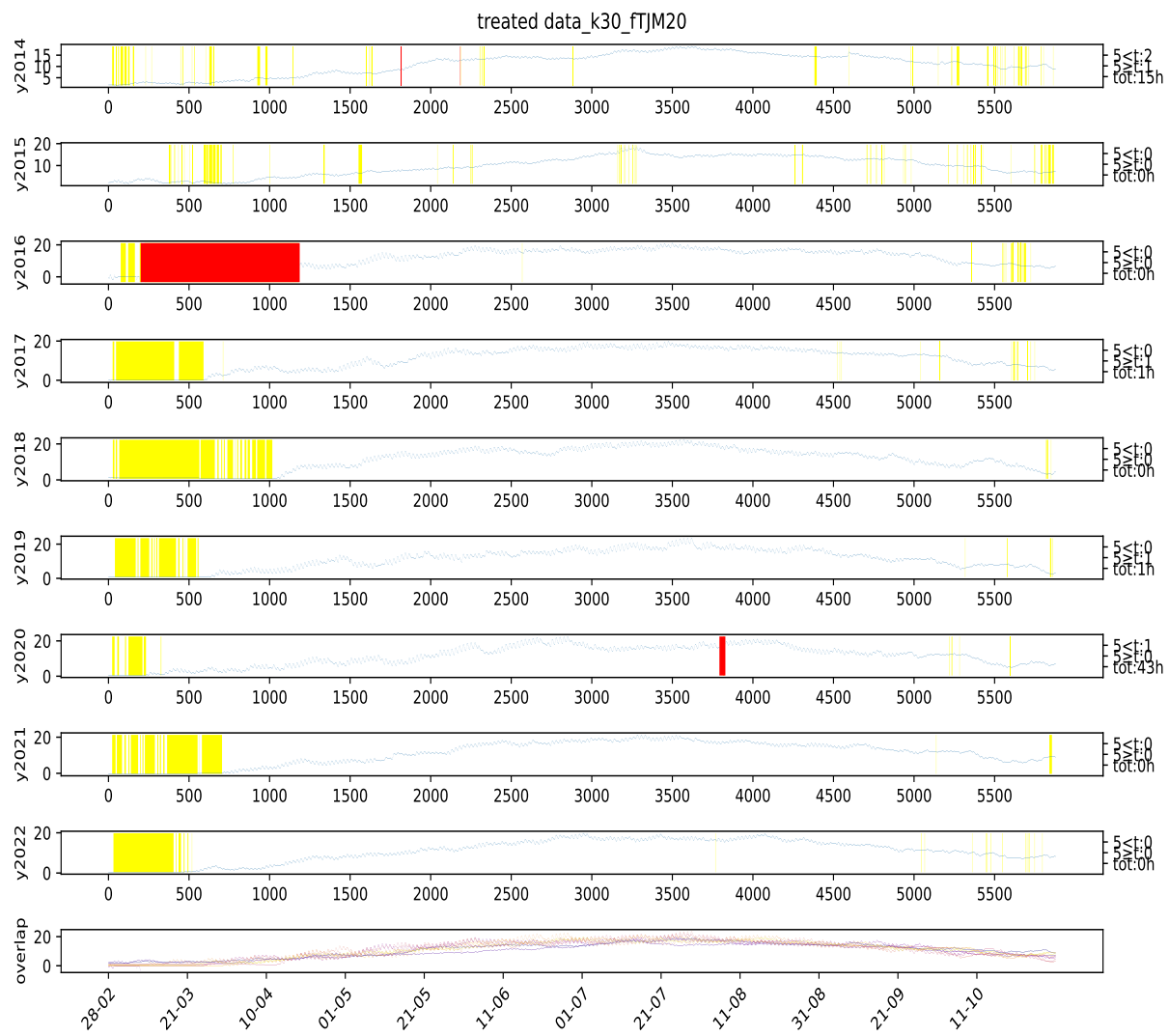


Figure 210: Visual representation of missing values at station 30 from 2014 to 2022 at the parameter "TJM20" after treating for outliers. The left numbers indicated how many hours that are missing and how many of them are shorter than or longer than 5 hours, however for this visualization they indicate the untreated version of the data. The yellow markings indicate possible outliers based on the given year, all markings was checked if they were actual outliers. The red colouring indicate missing values in the data (represented in the data with code "NULL"). The station names can be found in table 1.

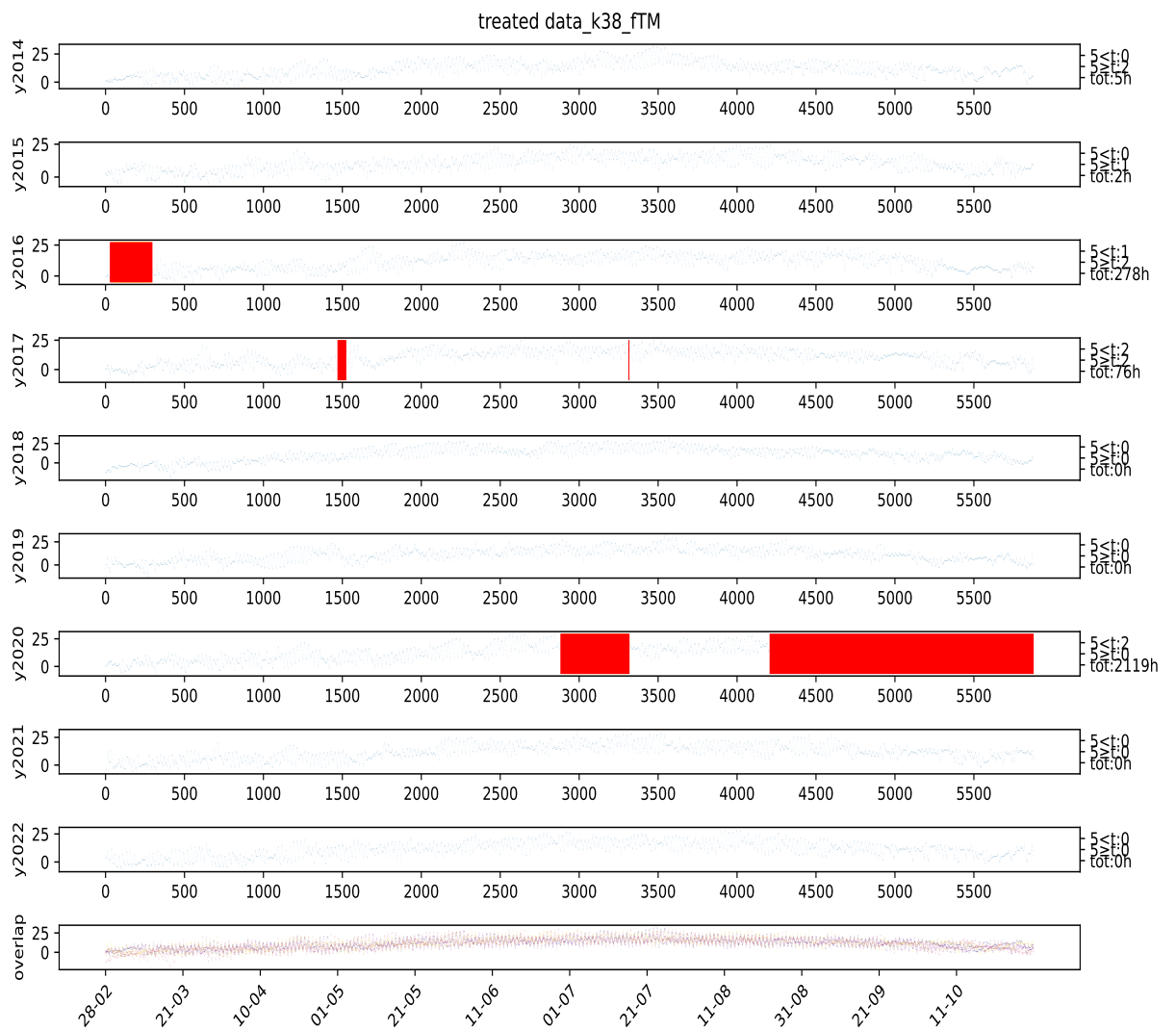


Figure 211: Visual representation of missing values at station 38 from 2014 to 2022 at the parameter "TM" after treating for outliers. The left numbers indicated how many hours that are missing and how many of them are shorter than or longer than 5 hours, however for this visualization they indicate the untreated version of the data. The yellow markings indicate possible outliers based on the given year, all markings was checked if they were actual outliers. The red colouring indicate missing values in the data (represented in the data with code "NULL"). The station names can be found in table 1.

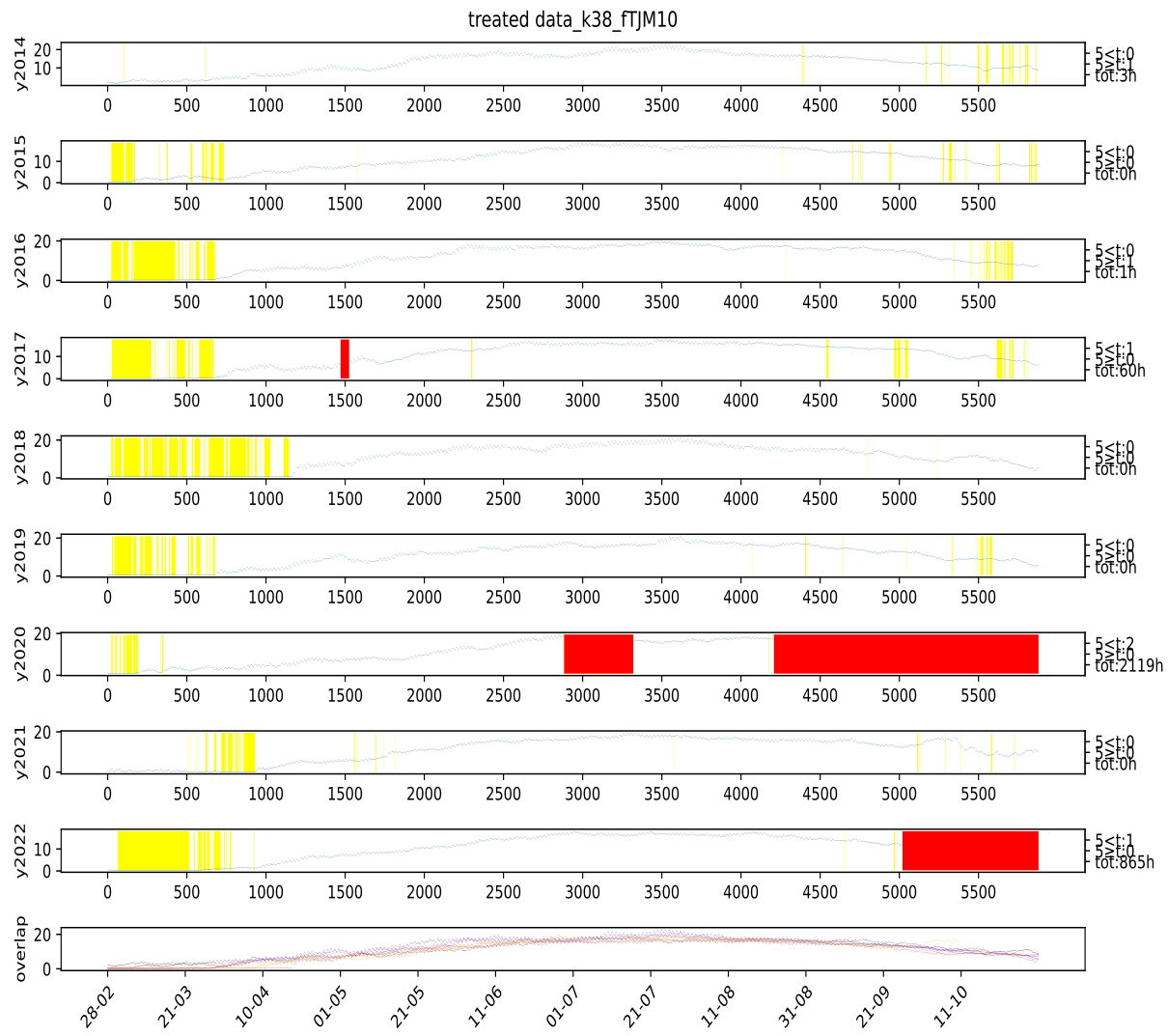


Figure 212: Visual representation of missing values at station 38 from 2014 to 2022 at the parameter "TJM10" after treating for outliers. The left numbers indicated how many hours that are missing and how many of them are shorter than or longer than 5 hours, however for this visualization they indicate the untreated version of the data. The yellow markings indicate possible outliers based on the given year, all markings was checked if they were actual outliers. The red colouring indicate missing values in the data (represented in the data with code "NULL"). The station names can be found in table 1.

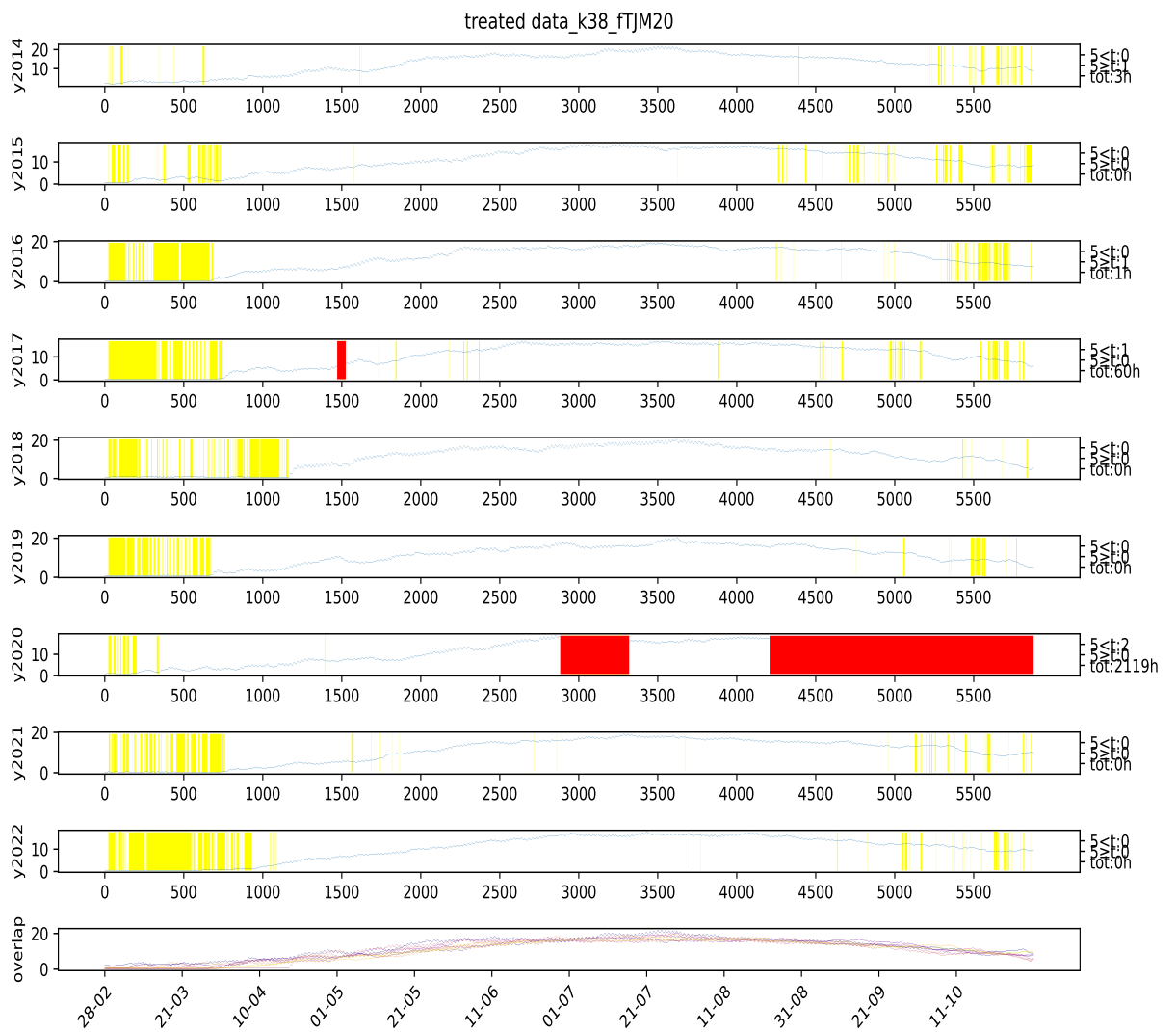


Figure 213: Visual representation of missing values at station 38 from 2014 to 2022 at the parameter "TJM20" after treating for outliers. The left numbers indicated how many hours that are missing and how many of them are shorter than or longer than 5 hours, however for this visualization they indicate the untreated version of the data. The yellow markings indicate possible outliers based on the given year, all markings was checked if they were actual outliers. The red colouring indicate missing values in the data (represented in the data with code "NULL"). The station names can be found in table 1.

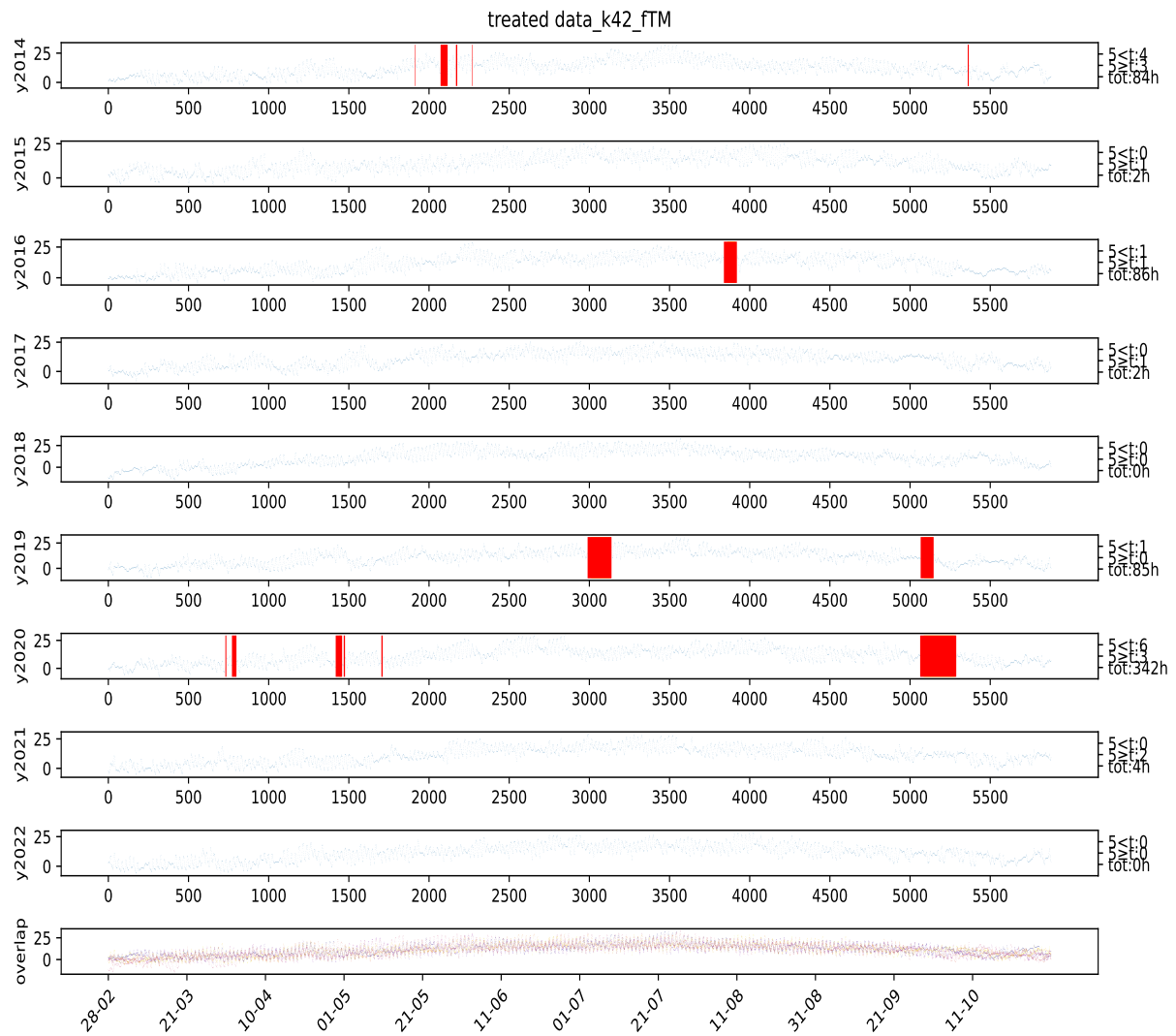


Figure 214: Visual representation of missing values at station 42 from 2014 to 2022 at the parameter "TM" after treating for outliers. The left numbers indicated how many hours that are missing and how many of them are shorter than or longer than 5 hours, however for this visualization they indicate the untreated version of the data. The yellow markings indicate possible outliers based on the given year, all markings was checked if they were actual outliers. The red colouring indicate missing values in the data (represented in the data with code "NULL"). The station names can be found in table 1.

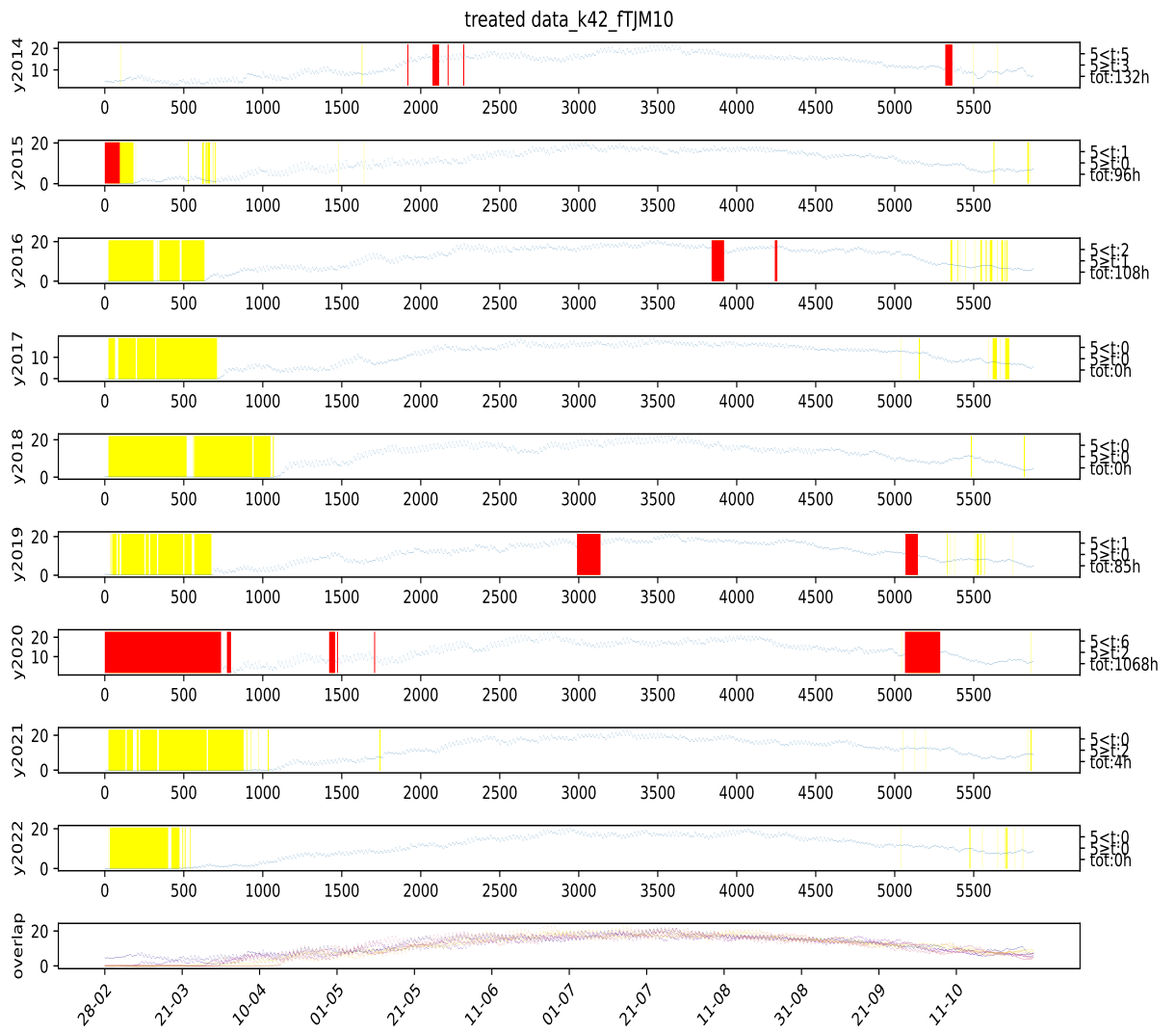


Figure 215: Visual representation of missing values at station 42 from 2014 to 2022 at the parameter "TJM10" after treating for outliers. The left numbers indicated how many hours that are missing and how many of them are shorter than or longer than 5 hours, however for this visualization they indicate the untreated version of the data. The yellow markings indicate possible outliers based on the given year, all markings was checked if they were actual outliers. The red colouring indicate missing values in the data (represented in the data with code "NULL"). The station names can be found in table 1.

## A PLOTS

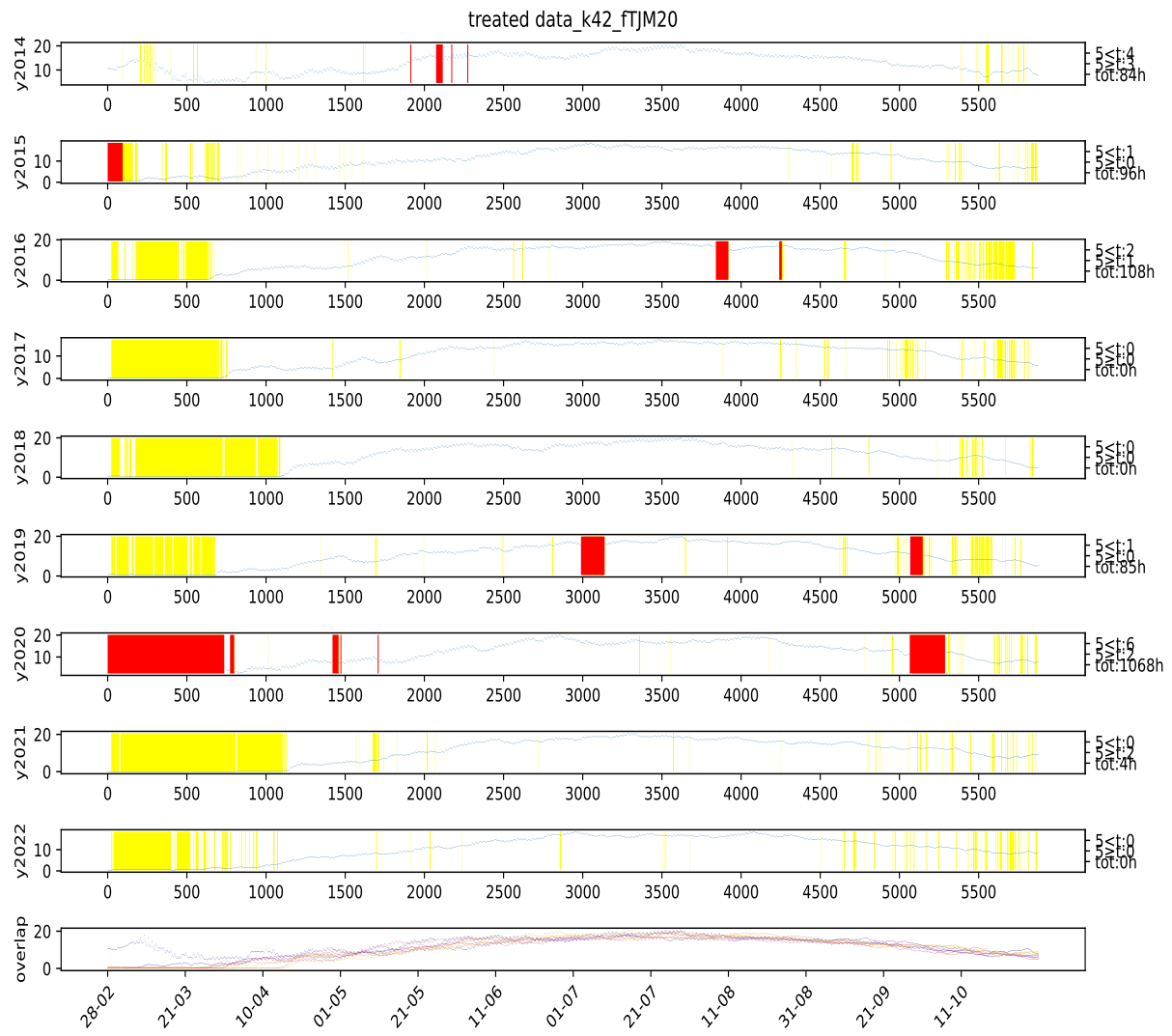


Figure 216: Visual representation of missing values at station 42 from 2014 to 2022 at the parameter "TJM20" after treating for outliers. The left numbers indicated how many hours that are missing and how many of them are shorter than or longer than 5 hours, however for this visualization they indicate the untreated version of the data. The yellow markings indicate possible outliers based on the given year, all markings was checked if they were actual outliers. The red colouring indicate missing values in the data (represented in the data with code "NULL"). The station names can be found in table 1.

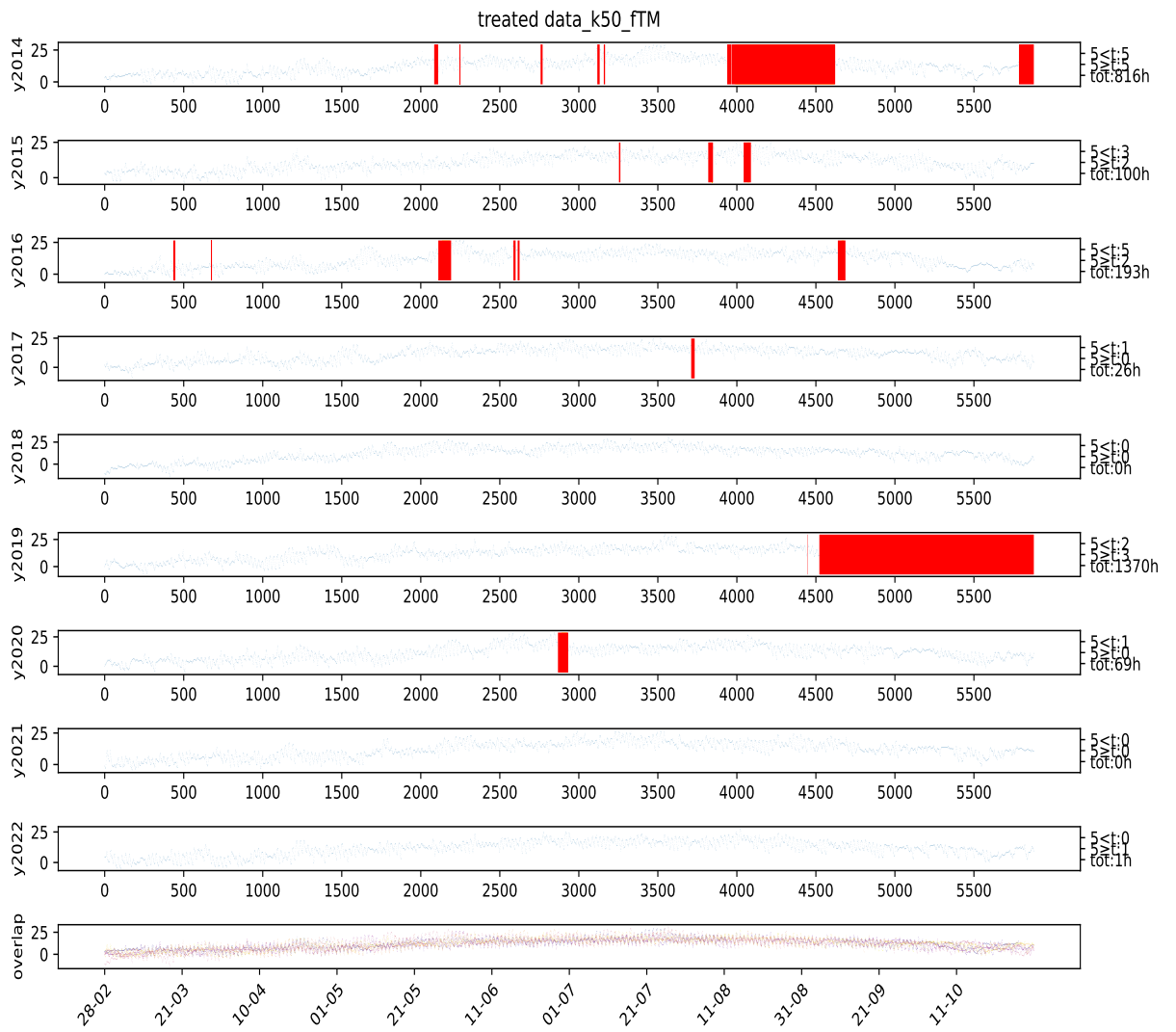


Figure 217: Visual representation of missing values at station 50 from 2014 to 2022 at the parameter "TM" after treating for outliers. The left numbers indicated how many hours that are missing and how many of them are shorter than or longer than 5 hours, however for this visualization they indicate the untreated version of the data. The yellow markings indicate possible outliers based on the given year, all markings was checked if they were actual outliers. The red colouring indicate missing values in the data (represented in the data with code "NULL"). The station names can be found in table 1.

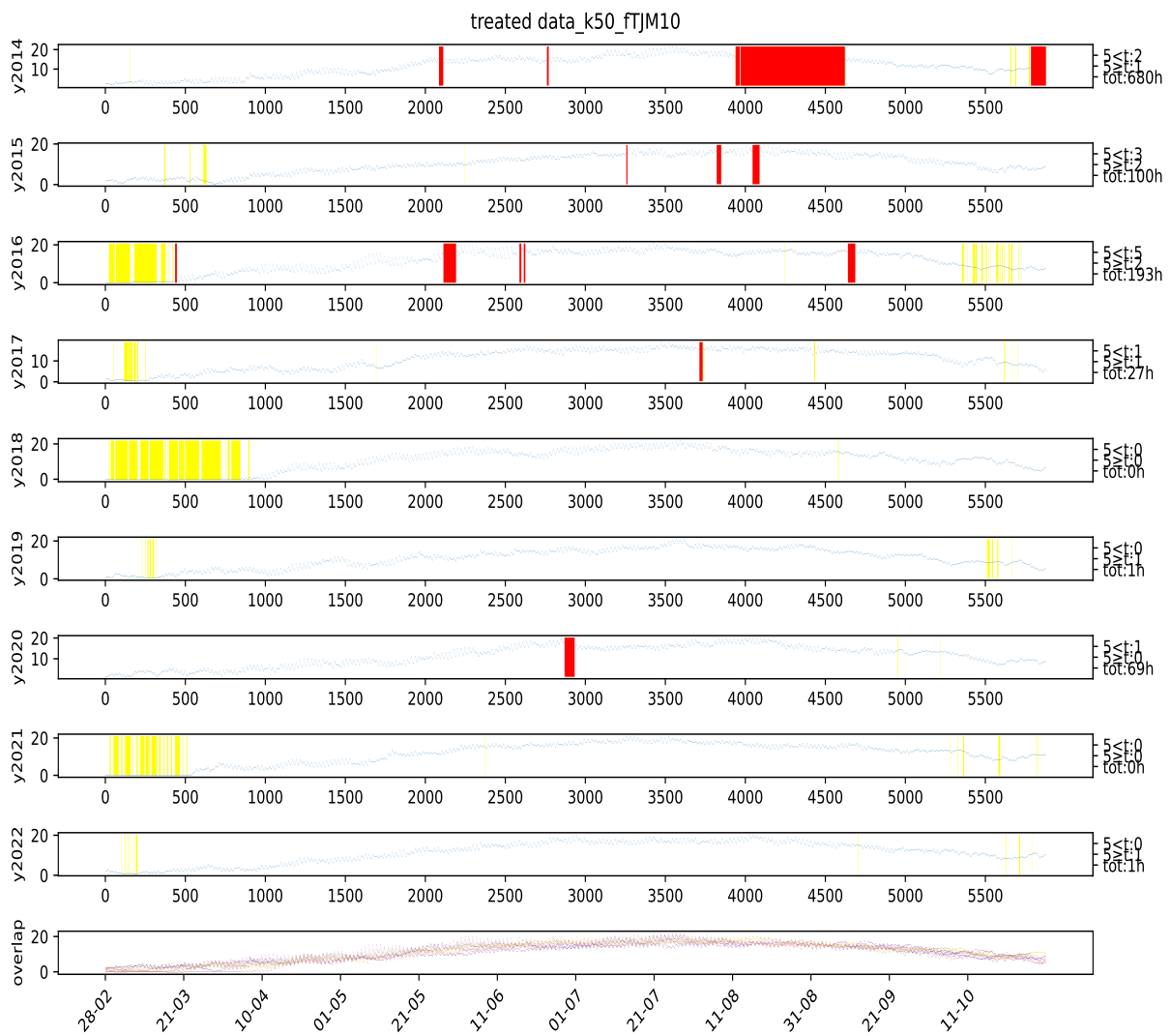


Figure 218: Visual representation of missing values at station 50 from 2014 to 2022 at the parameter "TJM10" after treating for outliers. The left numbers indicated how many hours that are missing and how many of them are shorter than or longer than 5 hours, however for this visualization they indicate the untreated version of the data. The yellow markings indicate possible outliers based on the given year, all markings was checked if they were actual outliers. The red colouring indicate missing values in the data (represented in the data with code "NULL").The station names can be found in table 1.

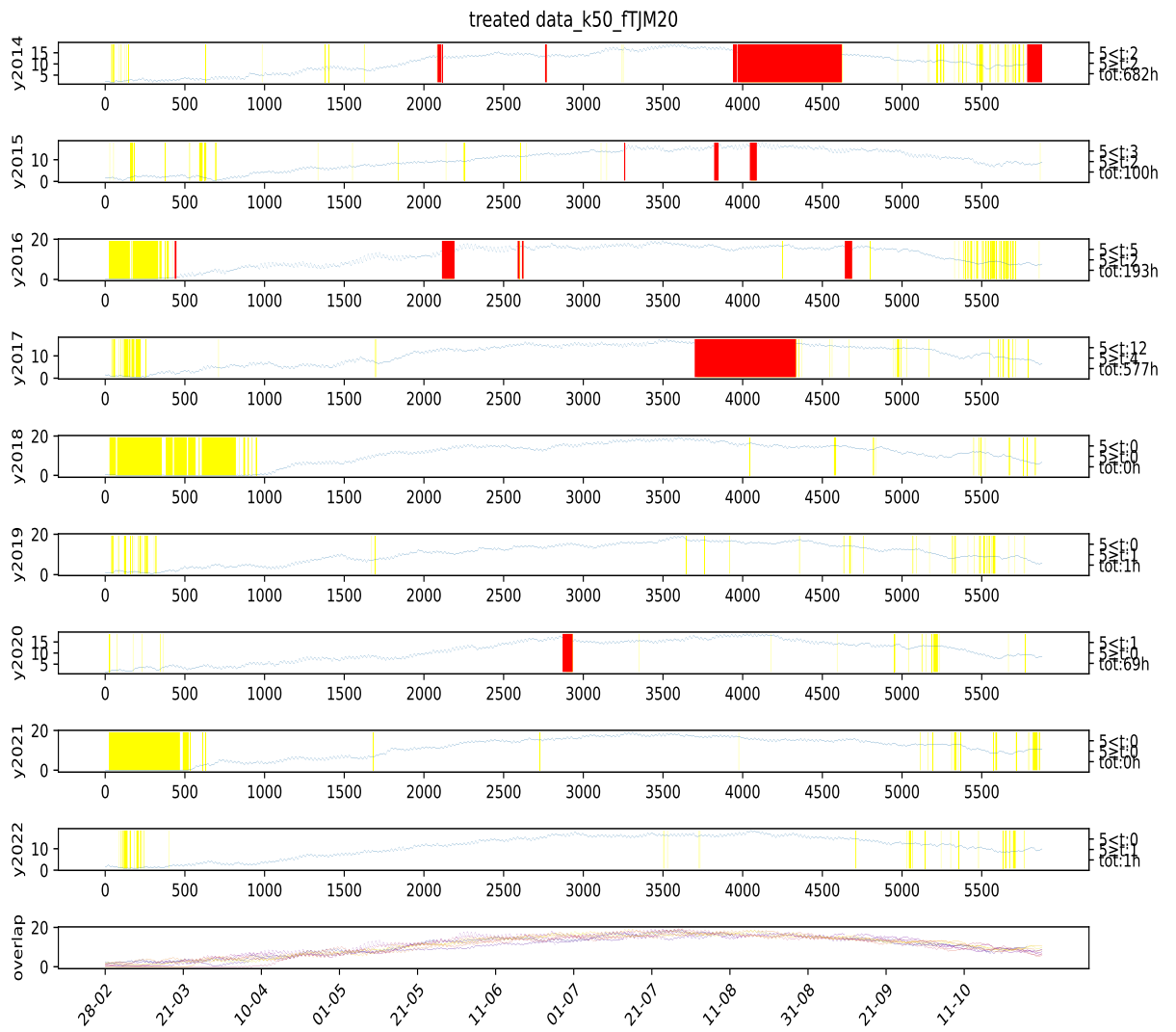


Figure 219: Visual representation of missing values at station 50 from 2014 to 2022 at the parameter "TJM20" after treating for outliers. The left numbers indicated how many hours that are missing and how many of them are shorter than or longer than 5 hours, however for this visualization they indicate the untreated version of the data. The yellow markings indicate possible outliers based on the given year, all markings was checked if they were actual outliers. The red colouring indicate missing values in the data (represented in the data with code "NULL"). The station names can be found in table 1.

## B Tables

### B.1 Model performance

scope	spesific scope	RMSE °C	MAE°C	bias °C	log( $\kappa$ (model))	digit sensitivity	R <sup>2</sup>
global	—	2.676	2.06	0.528	-0.328	-1	0.756
region	Østfold	2.564	2	0.176	-0.324	-1	0.8
region	Vestfold	2.565	1.958	0.785	-0.317	-1	0.81
region	Trøndelag	2.938	2.279	0.75	-0.321	-1	0.477
region	Innlandet	2.612	1.997	0.379	-0.32	-1	0.799
local	52	2.504	1.976	-1.2	-0.327	-1	0.803
local	41	2.135	1.665	0.13	-0.322	-1	0.872
local	37	2.513	1.938	0.067	-0.322	-1	0.83
local	118	3.029	2.422	1.722	-0.323	-1	0.656
local	50	2.176	1.7	0.815	-0.327	-1	0.836
local	42	2.739	2.099	0.746	-0.323	-1	0.807
local	38	2.983	2.323	1.149	-0.333	-1	0.736
local	30	2.276	1.708	0.428	-0.328	-1	0.859
local	57	3.079	2.419	0.744	-0.33	-1	0.617
local	39	2.79	2.186	0.633	-0.322	-1	0.615
local	34	3.163	2.427	0.797	-0.329	-1	-0.547
local	15	2.706	2.094	0.827	-0.329	-1	0.484
local	27	2.455	1.885	0.335	-0.328	-1	0.839
local	26	2.757	2.105	0.892	-0.324	-1	0.801
local	17	3.023	2.265	0.137	-0.33	-1	0.762
local	11	2.346	1.847	-0.023	-0.33	-1	0.755

Table 22: Results from hourly version of the Plauborg model for 20cm depth. The station names can be found in table 1.

scope	spesific scope	RMSE °C	MAE°C	bias °C	log( $\kappa$ (model))	digit sensitivity	R <sup>2</sup>
global	—	2.529	1.926	0.597	-0.449	-1	0.794
region	Østfold	2.448	1.894	0.512	-0.45	-1	0.816
region	Vestfold	2.412	1.81	0.733	-0.43	-1	0.846
region	Trøndelag	2.822	2.176	0.781	-0.439	-1	0.547
region	Innlandet	2.382	1.805	0.312	-0.448	-1	0.847
local	52	2.514	1.964	-0.349	-0.446	-1	0.636
local	41	1.938	1.519	0.151	-0.445	-1	0.903
local	37	2.344	1.804	0.237	-0.446	-1	0.857
local	118	2.928	2.322	1.639	-0.442	-1	0.706
local	50	1.908	1.472	0.558	-0.442	-1	0.884
local	42	2.501	1.885	0.703	-0.447	-1	0.852
local	38	3.055	2.368	1.363	-0.447	-1	0.754
local	30	2.072	1.555	0.354	-0.441	-1	0.892
local	57	2.906	2.263	0.677	-0.443	-1	0.677
local	39	2.77	2.151	0.701	-0.44	-1	0.633
local	34	3.013	2.306	0.845	-0.446	-1	-0.193
local	15	2.589	1.991	0.903	-0.444	-1	0.562
local	27	2.277	1.724	0.163	-0.444	-1	0.872
local	26	2.532	1.918	0.821	-0.442	-1	0.843
local	17	2.649	1.979	0.065	-0.44	-1	0.828
local	11	2.146	1.666	0.038	-0.443	-1	0.823

Table 23: Results from hourly version of the Plauborg model for 10cm depth. The station names can be found in table 1.

## B TABLES

scope	spesific scope	RMSE °C	MAE°C	bias °C	log( $\kappa$ (model))	digit sensitivity	R <sup>2</sup>
global	—	1.91	1.536	0.644	-1.918	-2	0.876
region	Østfold	1.94	1.541	-0.073	-1.917	-2	0.885
region	Vestfold	1.71	1.341	0.236	-1.899	-2	0.915
region	Trøndelag	1.843	1.56	1.461	-1.913	-2	0.794
region	Innlandet	2.16	1.735	1.02	-1.909	-2	0.863
local	52	2.33	1.873	-1.402	-1.908	-2	0.83
local	41	1.748	1.409	-0.371	-1.902	-2	0.914
local	37	1.877	1.496	0.353	-1.913	-2	0.905
local	118	1.742	1.384	1.139	-1.917	-2	0.886
local	50	1.251	0.985	0.096	-1.912	-2	0.946
local	42	1.966	1.54	0.346	-1.917	-2	0.901
local	38	1.721	1.367	0.515	-1.906	-2	0.912
local	30	1.817	1.471	-0.014	-1.918	-2	0.91
local	57	1.841	1.538	1.427	-1.919	-2	0.863
local	39	1.729	1.468	1.402	-1.912	-2	0.852
local	34	2.104	1.836	1.816	-1.91	-2	0.316
local	15	1.681	1.411	1.215	-1.903	-2	0.801
local	27	1.924	1.534	0.753	-1.905	-2	0.901
local	26	2.528	2.101	1.578	-1.912	-2	0.833
local	17	2.448	1.911	1.401	-1.912	-2	0.844
local	11	1.735	1.443	0.463	-1.91	-2	0.866

Table 24: Results from daily version of the Plauborg model for 20cm depth. The station names can be found in table 1.

scope	spesific scope	RMSE °C	MAE°C	bias °C	log( $\kappa$ (model))	digit sensitivity	R <sup>2</sup>
global	—	2.074	1.621	0.608	-1.261	-2	0.861
region	Østfold	2.168	1.704	0.24	-1.27	-2	0.856
region	Vestfold	2.022	1.564	0.219	-1.263	-2	0.892
region	Trøndelag	1.957	1.528	1.235	-1.257	-2	0.782
region	Innlandet	2.165	1.71	0.714	-1.269	-2	0.873
local	52	2.418	1.837	-0.636	-1.265	-2	0.664
local	41	1.975	1.587	-0.293	-1.266	-2	0.9
local	37	2.206	1.755	0.373	-1.26	-2	0.873
local	118	2.165	1.697	1.137	-1.263	-2	0.839
local	50	1.395	1.105	-0.046	-1.265	-2	0.938
local	42	2.239	1.75	0.333	-1.266	-2	0.881
local	38	2.42	1.908	0.667	-1.261	-2	0.845
local	30	1.914	1.519	-0.046	-1.271	-2	0.908
local	57	1.978	1.547	1.108	-1.266	-2	0.85
local	39	1.896	1.455	1.193	-1.266	-2	0.828
local	34	2.143	1.687	1.535	-1.261	-2	0.397
local	15	1.806	1.428	1.114	-1.262	-2	0.787
local	27	2.063	1.627	0.396	-1.266	-2	0.895
local	26	2.43	1.937	1.251	-1.267	-2	0.855
local	17	2.26	1.78	0.921	-1.263	-2	0.875
local	11	1.879	1.504	0.339	-1.262	-2	0.864

Table 25: Results from daily version of the Plauborg model for 10cm depth. The station names can be found in table 1.

## B TABLES

scope	spesific scope	RMSE °C	MAE°C	bias °C	log( $\kappa$ (model))	digit sensitivity	R <sup>2</sup>
global	—	4.504	3.474	2.487	-0.796	-1	0.308
region	Østfold	4.348	3.363	1.901	-0.796	-1	0.424
region	Vestfold	4.564	3.47	2.297	-0.796	-1	0.397
region	Trøndelag	4.438	3.508	3.175	-0.796	-1	-0.194
region	Innlandet	4.688	3.568	2.601	-0.796	-1	0.353
local	52	3.556	2.841	0.559	-0.796	-1	0.604
local	41	4.248	3.286	1.677	-0.796	-1	0.491
local	37	4.754	3.675	2.174	-0.796	-1	0.391
local	118	4.726	3.654	3.208	-0.796	-1	0.162
local	50	4.048	3.025	2.207	-0.796	-1	0.434
local	42	4.863	3.741	2.364	-0.796	-1	0.393
local	38	4.832	3.682	2.601	-0.796	-1	0.308
local	30	4.465	3.433	2.015	-0.796	-1	0.456
local	57	4.655	3.636	3.153	-0.796	-1	0.125
local	39	4.31	3.39	3.083	-0.796	-1	0.081
local	34	4.583	3.675	3.471	-0.796	-1	-2.248
local	15	4.198	3.342	3.006	-0.796	-1	-0.241
local	27	4.672	3.547	2.535	-0.796	-1	0.415
local	26	5.17	4.009	3.282	-0.796	-1	0.302
local	17	5.049	3.84	2.939	-0.796	-1	0.336
local	11	3.821	2.924	1.692	-0.796	-1	0.35

Table 26: Results from the Linear Regression model for 20cm depth. The station names can be found in table 1.

scope	spesific scope	RMSE °C	MAE°C	bias °C	log( $\kappa$ (model))	digit sensitivity	R <sup>2</sup>
global	—	4.231	3.267	2.303	-0.638	-1	0.423
region	Østfold	4.236	3.28	2.015	-0.638	-1	0.45
region	Vestfold	4.277	3.26	2.019	-0.638	-1	0.517
region	Trøndelag	4.133	3.274	2.893	-0.638	-1	0.028
region	Innlandet	4.282	3.254	2.246	-0.638	-1	0.504
local	52	3.679	2.889	1.226	-0.638	-1	0.221
local	41	3.976	3.07	1.494	-0.638	-1	0.593
local	37	4.501	3.503	2.07	-0.638	-1	0.473
local	118	4.5	3.486	2.93	-0.638	-1	0.306
local	50	3.611	2.702	1.766	-0.638	-1	0.584
local	42	4.571	3.525	2.109	-0.638	-1	0.506
local	38	4.815	3.741	2.502	-0.638	-1	0.388
local	30	4.053	3.106	1.733	-0.638	-1	0.588
local	57	4.293	3.356	2.775	-0.638	-1	0.295
local	39	4.057	3.193	2.835	-0.638	-1	0.213
local	34	4.262	3.415	3.176	-0.638	-1	-1.386
local	15	3.918	3.141	2.799	-0.638	-1	-0.003
local	27	4.272	3.236	2.078	-0.638	-1	0.551
local	26	4.714	3.651	2.902	-0.638	-1	0.456
local	17	4.518	3.432	2.506	-0.638	-1	0.501
local	11	3.567	2.713	1.529	-0.638	-1	0.51

Table 27: Results from the Linear Regression model for 10cm depth. The station names can be found in table 1.

## B TABLES

scope	spesific scope	RMSE [°C]	MAE [°C]	bias [°C]	log( $\kappa$ (model))	digit sensitivity	R <sup>2</sup>
global	—	1.7	1.294	0.244	-2.662	-3	0.901
region	Østfold	1.778	1.405	-0.482	-2.682	-3	0.903
region	Vestfold	1.417	1.118	-0.152	-2.646	-3	0.941
region	Trøndelag	1.622	1.255	0.993	-2.65	-3	0.841
region	Innlandet	1.979	1.419	0.706	-2.654	-3	0.884
local	52	2.517	2.148	-1.806	-2.633	-3	0.8
local	41	1.638	1.358	-0.779	-2.665	-3	0.924
local	37	1.414	1.146	-0.036	-2.639	-3	0.946
local	118	1.258	0.955	0.727	-2.629	-3	0.941
local	50	1.06	0.854	-0.355	-2.641	-3	0.961
local	42	1.628	1.307	-0.032	-2.655	-3	0.931
local	38	1.224	0.985	0.145	-2.664	-3	0.955
local	30	1.66	1.325	-0.368	-2.657	-3	0.924
local	57	1.575	1.194	0.982	-2.642	-3	0.899
local	39	1.563	1.217	0.917	-2.66	-3	0.878
local	34	1.831	1.489	1.339	-2.684	-3	0.502
local	15	1.518	1.138	0.763	-2.63	-3	0.836
local	27	1.626	1.2	0.362	-2.652	-3	0.929
local	26	2.187	1.595	1.246	-2.667	-3	0.874
local	17	2.335	1.634	1.106	-2.663	-3	0.857
local	11	1.869	1.344	0.244	-2.627	-3	0.844

Table 28: Results from the GRU model for 20cm depth for each region, and station. The "Global" category covers data from all monitoring stations, "Regional" uses stations within a specific area, and "Local" details the results from individual stations. The station names can be found in table 1.

scope	spesific scope	RMSE [°C]	MAE [°C]	bias [°C]	$\log(\kappa(\text{model}))$	digit sensitivity	R <sup>2</sup>
global	—	1.807	1.418	0.027	-0.013	-1	0.894
region	Østfold	1.917	1.507	-0.377	-0.042	-1	0.887
region	Vestfold	1.861	1.474	-0.435	-0.044	-1	0.908
region	Trøndelag	1.537	1.199	0.699	0.014	-1	0.866
region	Innlandet	1.911	1.513	0.212	-0.03	-1	0.901
local	52	2.289	1.686	-1.195	-0.034	-1	0.696
local	41	1.983	1.6	-0.937	0.008	-1	0.898
local	37	1.89	1.528	-0.155	-0.027	-1	0.906
local	118	1.619	1.288	0.439	-0.002	-1	0.911
local	50	1.442	1.183	-0.719	-0.036	-1	0.933
local	42	2.062	1.645	-0.309	-0.032	-1	0.899
local	38	2.005	1.569	0.018	-0.013	-1	0.893
local	30	1.881	1.507	-0.695	-0.029	-1	0.91
local	57	1.5	1.19	0.589	-0.045	-1	0.914
local	39	1.553	1.214	0.671	-0.014	-1	0.884
local	34	1.69	1.315	1.031	-0.033	-1	0.639
local	15	1.404	1.086	0.533	-0.028	-1	0.87
local	27	1.853	1.486	-0.139	-0.021	-1	0.915
local	26	2.081	1.654	0.765	-0.011	-1	0.893
local	17	1.976	1.54	0.499	-0.002	-1	0.904
local	11	1.722	1.367	-0.189	-0.027	-1	0.885

Table 29: Results from the GRU model for 10cm depth for each region, and station. The "Global" category covers data from all monitoring stations, "Regional" uses stations within a specific area, and "Local" details the results from individual stations. The station names can be found in table 1.

## B TABLES

scope	spesific scope	RMSE [°C]	MAE [°C]	bias [°C]	log( $\kappa$ (model))	digit sensitivity	R <sup>2</sup>
global	—	1.575	1.236	0.012	-2.01	-3	0.915
region	Østfold	1.828	1.452	-0.583	-1.981	-2	0.898
region	Vestfold	1.409	1.112	-0.149	-1.981	-2	0.942
region	Trøndelag	1.456	1.141	0.584	-1.953	-2	0.872
region	Innlandet	1.572	1.236	0.247	-1.997	-2	0.927
local	52	2.565	2.131	-1.905	-2.004	-3	0.792
local	41	1.574	1.319	-0.749	-1.96	-2	0.93
local	37	1.562	1.283	-0.397	-1.996	-2	0.934
local	118	1.351	1.063	0.756	-1.943	-2	0.932
local	50	1.051	0.825	-0.151	-1.97	-2	0.961
local	42	1.585	1.259	-0.096	-2	-2	0.935
local	38	1.381	1.088	0.113	-1.996	-2	0.943
local	30	1.553	1.275	-0.464	-1.981	-2	0.934
local	57	1.527	1.198	0.549	-1.965	-2	0.905
local	39	1.404	1.095	0.514	-1.952	-2	0.902
local	34	1.578	1.228	0.807	-1.969	-2	0.63
local	15	1.311	1.052	0.486	-2.003	-3	0.878
local	27	1.52	1.205	0.037	-1.971	-2	0.938
local	26	1.677	1.314	0.763	-1.99	-2	0.926
local	17	1.629	1.208	0.434	-1.962	-2	0.931
local	11	1.467	1.199	-0.219	-1.975	-2	0.904

Table 30: Results from the BiGRU model for 20cm depth for each region, and station. The "Global" category covers data from all monitoring stations, "Regional" uses stations within a specific area, and "Local" details the results from individual stations. The station names can be found in table 1.

## B TABLES

scope	spesific scope	RMSE [°C]	MAE [°C]	bias [°C]	$\log(\kappa(\text{model}))$	digit sensitivity	R <sup>2</sup>
global	—	1.722	1.36	-0.037	-1.734	-2	0.904
region	Østfold	1.793	1.408	-0.277	-1.717	-2	0.901
region	Vestfold	1.673	1.32	-0.211	-1.685	-2	0.925
region	Trøndelag	1.672	1.313	0.345	-1.7	-2	0.842
region	Innlandet	1.758	1.411	-0.023	-1.68	-2	0.916
local	52	2.31	1.687	-1.149	-1.7	-2	0.69
local	41	1.81	1.498	-0.716	-1.719	-2	0.915
local	37	1.659	1.369	-0.313	-1.705	-2	0.928
local	118	1.552	1.196	0.709	-1.681	-2	0.918
local	50	1.288	1.049	-0.397	-1.696	-2	0.947
local	42	1.818	1.455	-0.139	-1.709	-2	0.921
local	38	1.777	1.34	0.229	-1.731	-2	0.916
local	30	1.76	1.436	-0.507	-1.702	-2	0.922
local	57	1.736	1.377	0.226	-1.719	-2	0.884
local	39	1.659	1.286	0.283	-1.735	-2	0.867
local	34	1.732	1.336	0.554	-1.709	-2	0.621
local	15	1.562	1.256	0.334	-1.74	-2	0.839
local	27	1.774	1.438	-0.304	-1.716	-2	0.922
local	26	1.739	1.386	0.51	-1.658	-2	0.925
local	17	1.693	1.311	0.077	-1.705	-2	0.93
local	11	1.796	1.467	-0.375	-1.704	-2	0.875

Table 31: Results from the BiGRU model for 10cm depth for each region, and station. The "Global" category covers data from all monitoring stations, "Regional" uses stations within a specific area, and "Local" details the results from individual stations. The station names can be found in table 1.

## B TABLES

scope	spesific scope	RMSE [°C]	MAE [°C]	bias [°C]	log( $\kappa$ (model))	digit sensitivity	R <sup>2</sup>
global	—	1.695	1.349	0.068	-1.797	-2	0.901
region	Østfold	1.902	1.532	-0.479	-1.831	-2	0.889
region	Vestfold	1.563	1.268	-0.093	-1.796	-2	0.929
region	Trøndelag	1.538	1.166	0.557	-1.787	-2	0.856
region	Innlandet	1.76	1.444	0.339	-1.786	-2	0.908
local	52	2.495	2.067	-1.788	-1.819	-2	0.803
local	41	1.745	1.455	-0.675	-1.755	-2	0.913
local	37	1.716	1.439	-0.255	-1.813	-2	0.92
local	118	1.497	1.162	0.82	-1.814	-2	0.915
local	50	1.201	0.986	-0.131	-1.832	-2	0.95
local	42	1.781	1.463	-0.034	-1.814	-2	0.918
local	38	1.54	1.244	0.189	-1.808	-2	0.929
local	30	1.67	1.379	-0.396	-1.818	-2	0.923
local	57	1.6	1.233	0.534	-1.823	-2	0.896
local	39	1.504	1.123	0.464	-1.83	-2	0.887
local	34	1.64	1.233	0.808	-1.819	-2	0.589
local	15	1.405	1.08	0.435	-1.807	-2	0.86
local	27	1.664	1.385	0.13	-1.822	-2	0.925
local	26	1.91	1.567	0.894	-1.801	-2	0.904
local	17	1.884	1.508	0.589	-1.835	-2	0.907
local	11	1.607	1.333	-0.207	-1.805	-2	0.885

Table 32: Results from the BiLSTM model for 20cm depth for each region, and station. The "Global" category covers data from all monitoring stations, "Regional" uses stations within a specific area, and "Local" details the results from individual stations. The station names can be found in table 1.

## B TABLES

scope	spesific scope	RMSE [°C]	MAE [°C]	bias [°C]	$\log(\kappa(\text{model}))$	digit sensitivity	R <sup>2</sup>
global	—	1.423	1.111	0.06	-1.858	-2	0.934
region	Østfold	1.483	1.154	-0.252	-1.869	-2	0.932
region	Vestfold	1.341	1.03	-0.264	-1.832	-2	0.952
region	Trøndelag	1.467	1.133	0.524	-1.864	-2	0.877
region	Innlandet	1.4	1.135	0.225	-1.896	-2	0.947
local	52	2.08	1.479	-1.078	-1.838	-2	0.749
local	41	1.473	1.203	-0.757	-1.891	-2	0.944
local	37	1.221	1.006	-0.167	-1.88	-2	0.961
local	118	1.324	1.071	0.64	-1.893	-2	0.94
local	50	1.061	0.858	-0.475	-1.859	-2	0.964
local	42	1.403	1.103	-0.169	-1.861	-2	0.953
local	38	1.429	1.026	0.178	-1.878	-2	0.946
local	30	1.443	1.132	-0.559	-1.87	-2	0.947
local	57	1.405	1.106	0.419	-1.813	-2	0.924
local	39	1.592	1.239	0.496	-1.84	-2	0.878
local	34	1.557	1.171	0.749	-1.829	-2	0.685
local	15	1.3	1.018	0.445	-1.836	-2	0.888
local	27	1.356	1.126	-0.115	-1.836	-2	0.954
local	26	1.487	1.2	0.744	-1.848	-2	0.946
local	17	1.401	1.112	0.459	-1.875	-2	0.952
local	11	1.344	1.084	-0.118	-1.869	-2	0.93

Table 33: Results from the BiLSTM model for 10cm depth for each region, and station. The "Global" category covers data from all monitoring stations, "Regional" uses stations within a specific area, and "Local" details the results from individual stations. The station names can be found in table 1.

## B TABLES

scope	spesific scope	RMSE [°C]	MAE [°C]	bias [°C]	log( $\kappa$ (model))	digit sensitivity	R <sup>2</sup>
global	—	1.762	1.363	0.423	-2.168	-3	0.893
region	Østfold	1.781	1.432	-0.288	-2.108	-3	0.902
region	Vestfold	1.433	1.153	0.033	-2.169	-3	0.94
region	Trøndelag	1.758	1.329	1.116	-2.177	-3	0.812
region	Innlandet	2.073	1.572	0.925	-2.165	-3	0.873
local	52	2.346	1.985	-1.611	-2.156	-3	0.826
local	41	1.609	1.339	-0.577	-2.15	-3	0.926
local	37	1.547	1.281	0.131	-2.132	-3	0.935
local	118	1.48	1.119	0.921	-2.149	-3	0.917
local	50	1.092	0.88	-0.165	-2.167	-3	0.958
local	42	1.637	1.343	0.163	-2.173	-3	0.931
local	38	1.326	1.082	0.31	-2.173	-3	0.947
local	30	1.606	1.308	-0.176	-2.147	-3	0.929
local	57	1.766	1.334	1.113	-2.133	-3	0.873
local	39	1.678	1.253	1.006	-2.158	-3	0.859
local	34	1.959	1.538	1.48	-2.165	-3	0.413
local	15	1.624	1.203	0.887	-2.173	-3	0.812
local	27	1.772	1.363	0.597	-2.137	-3	0.915
local	26	2.318	1.798	1.491	-2.153	-3	0.859
local	17	2.374	1.797	1.304	-2.103	-3	0.853
local	11	1.903	1.419	0.428	-2.164	-3	0.838

Table 34: Results from the LSTM model for 20cm depth for each region, and station. The "Global" category covers data from all monitoring stations, "Regional" uses stations within a specific area, and "Local" details the results from individual stations. The station names can be found in table 1.

scope	spesific scope	RMSE [°C]	MAE [°C]	bias [°C]	$\log(\kappa(\text{model}))$	digit sensitivity	R <sup>2</sup>
global	—	1.871	1.472	0.302	-1.544	-2	0.886
region	Østfold	1.904	1.522	0.067	-1.571	-2	0.888
region	Vestfold	1.834	1.422	0.119	-1.565	-2	0.91
region	Trøndelag	1.859	1.423	0.675	-1.57	-2	0.803
region	Innlandet	1.893	1.534	0.328	-1.552	-2	0.903
local	52	2.254	1.725	-0.807	-1.544	-2	0.705
local	41	1.85	1.544	-0.372	-1.581	-2	0.911
local	37	1.773	1.495	0.023	-1.565	-2	0.917
local	118	1.872	1.412	1.047	-1.6	-2	0.879
local	50	1.388	1.106	-0.047	-1.593	-2	0.938
local	42	2.002	1.591	0.199	-1.517	-2	0.905
local	38	2.014	1.477	0.537	-1.559	-2	0.892
local	30	1.876	1.518	-0.182	-1.581	-2	0.911
local	57	1.906	1.463	0.549	-1.592	-2	0.86
local	39	1.855	1.397	0.616	-1.596	-2	0.834
local	34	1.923	1.466	0.877	-1.609	-2	0.52
local	15	1.754	1.371	0.669	-1.581	-2	0.797
local	27	1.894	1.561	0.043	-1.568	-2	0.911
local	26	1.964	1.585	0.869	-1.568	-2	0.905
local	17	1.809	1.433	0.464	-1.535	-2	0.92
local	11	1.854	1.503	-0.048	-1.553	-2	0.867

Table 35: Results from the LSTM model for 10cm depth for each region, and station. The "Global" category covers data from all monitoring stations, "Regional" uses stations within a specific area, and "Local" details the results from individual stations. The station id can be found in table 1

## B.2 Data summary

	38	34	27	42				
2014	$\mu:11.71$ $\sigma:6.4$	max:31.8 min:-4.0	$\mu:10.54$ $\sigma:6.89$	max:31.4 min:-14.5	$\mu:10.99$ $\sigma:6.56$	max:33.0 min:-4.2	$\mu:12.0$ $\sigma:6.46$	max:32.2 min:-3.1
2015	$\mu:10.38$ $\sigma:5.69$	max:25.0 min:-5.7	$\mu:9.21$ $\sigma:5.42$	max:27.4 min:-5.9	$\mu:9.42$ $\sigma:5.91$	max:27.1 min:-6.8	$\mu:10.42$ $\sigma:5.87$	max:25.4 min:-4.8
2016	$\mu:11.34$ $\sigma:5.92$	max:27.4 min:-5.2	$\mu:9.34$ $\sigma:6.1$	max:29.4 min:-8.4	$\mu:10.1$ $\sigma:6.51$	max:27.8 min:-6.6	$\mu:11.04$ $\sigma:6.48$	max:29.4 min:-4.2
2017	$\mu:10.35$ $\sigma:6.1$	max:25.2 min:-9.2	$\mu:8.88$ $\sigma:5.99$	max:25.6 min:-9.5	$\mu:9.32$ $\sigma:6.34$	max:29.7 min:-10.8	$\mu:10.56$ $\sigma:6.21$	max:26.8 min:-8.5
2018	$\mu:11.03$ $\sigma:8.81$	max:32.3 min:-19.7	$\mu:9.29$ $\sigma:7.73$	max:31.6 min:-19.5	$\mu:9.69$ $\sigma:9.47$	max:31.1 min:-23.2	$\mu:11.4$ $\sigma:8.93$	max:33.0 min:-14.5
2019	$\mu:10.94$ $\sigma:6.83$	max:31.6 min:-12.0	$\mu:8.94$ $\sigma:7.02$	max:32.7 min:-14.3	$\mu:9.56$ $\sigma:7.08$	max:31.1 min:-15.9	$\mu:10.47$ $\sigma:6.82$	max:30.9 min:-9.8
2020	$\mu:11.28$ $\sigma:7.45$	max:29.7 min:-6.8	$\mu:9.05$ $\sigma:7.0$	max:31.3 min:-7.5	$\mu:10.33$ $\sigma:6.64$	max:30.3 min:-13.6	$\mu:11.03$ $\sigma:6.67$	max:29.4 min:-7.5
2021	$\mu:11.72$ $\sigma:6.79$	max:30.3 min:-6.1	$\mu:9.72$ $\sigma:6.48$	max:31.7 min:-6.5	$\mu:10.46$ $\sigma:6.83$	max:29.3 min:-6.1	$\mu:11.35$ $\sigma:6.75$	max:29.2 min:-5.8
2022	$\mu:11.33$ $\sigma:6.79$	max:29.1 min:-6.9	$\mu:8.99$ $\sigma:5.87$	max:29.2 min:-7.9	$\mu:9.87$ $\sigma:6.89$	max:27.8 min:-11.6	$\mu:11.09$ $\sigma:6.68$	max:28.6 min:-6.3

Table 36: The table shows the statistics of each station for each feature, except for Time as it is a strictly monotonic increasing sequence, for each year. The station names can be found in table 1.  $\mu$  Denotes the mean temperature,  $\sigma$  denotes the standard deviation, "min" is the minimum temperature, and "max" is the maximum temperature. All values in the table have the unit degree Celsius.

	38	34	27	42				
2014	$\mu:12.79$ $\sigma:5.56$	$\max:22.8$ $\min:1.5$	$\mu:9.23$ $\sigma:5.27$	$\max:18.4$ $\min:-0.1$	$\mu:12.24$ $\sigma:5.92$	$\max:23.9$ $\min:0.9$	$\mu:12.3$ $\sigma:4.89$	$\max:21.8$ $\min:2.7$
2015	$\mu:10.99$ $\sigma:5.32$	$\max:18.7$ $\min:0.4$	$\mu:8.78$ $\sigma:4.09$	$\max:15.4$ $\min:0.6$	$\mu:10.5$ $\sigma:5.58$	$\max:21.5$ $\min:-0.2$	$\mu:10.96$ $\sigma:5.29$	$\max:20.3$ $\min:0.1$
2016	$\mu:11.67$ $\sigma:6.07$	$\max:19.9$ $\min:0.1$	$\mu:8.69$ $\sigma:4.85$	$\max:17.0$ $\min:-0.1$	$\mu:10.58$ $\sigma:6.46$	$\max:20.3$ $\min:-2.7$	$\mu:11.29$ $\sigma:6.04$	$\max:20.7$ $\min:-0.1$
2017	$\mu:10.55$ $\sigma:5.47$	$\max:17.6$ $\min:0.1$	$\mu:8.71$ $\sigma:4.78$	$\max:17.1$ $\min:0.1$	$\mu:9.84$ $\sigma:6.07$	$\max:18.8$ $\min:-1.6$	$\mu:10.46$ $\sigma:5.74$	$\max:19.0$ $\min:-0.3$
2018	$\mu:11.12$ $\sigma:6.32$	$\max:21.2$ $\min:0.5$	$\mu:8.44$ $\sigma:5.49$	$\max:17.6$ $\min:-1.3$	$\mu:10.03$ $\sigma:6.86$	$\max:22.0$ $\min:-0.2$	$\mu:11.05$ $\sigma:6.59$	$\max:22.0$ $\min:0.0$
2019	$\mu:10.96$ $\sigma:5.67$	$\max:21.0$ $\min:0.4$	$\mu:9.08$ $\sigma:5.11$	$\max:19.3$ $\min:-0.2$	$\mu:10.5$ $\sigma:6.15$	$\max:23.1$ $\min:0.2$	$\mu:10.67$ $\sigma:6.06$	$\max:21.4$ $\min:0.1$
2020	$\mu:9.97$ $\sigma:5.87$	$\max:19.5$ $\min:0.8$	$\mu:8.53$ $\sigma:4.84$	$\max:17.0$ $\min:0.3$	$\mu:10.57$ $\sigma:6.1$	$\max:21.9$ $\min:-0.9$	$\mu:13.18$ $\sigma:4.76$	$\max:22.8$ $\min:1.6$
2021	$\mu:11.01$ $\sigma:6.18$	$\max:19.5$ $\min:0.1$	$\mu:8.94$ $\sigma:4.72$	$\max:16.7$ $\min:0.1$	$\mu:10.42$ $\sigma:6.44$	$\max:21.4$ $\min:-1.1$	$\mu:11.0$ $\sigma:7.0$	$\max:23.2$ $\min:-0.4$
2022	$\mu:10.62$ $\sigma:6.13$	$\max:18.1$ $\min:0.3$	$\mu:8.69$ $\sigma:4.76$	$\max:16.4$ $\min:0.6$	$\mu:10.31$ $\sigma:6.31$	$\max:20.6$ $\min:-1.8$	$\mu:10.84$ $\sigma:5.97$	$\max:20.6$ $\min:-0.1$

Table 37: The table shows the statistics of each station for each feature, except for Time as it is a strictly monotonic increasing sequence, for each year. The station names can be found in table 1.  $\mu$  Denotes the mean temperature,  $\sigma$  denotes the standard deviation, "min" is the minimum temperature, and "max" is the maximum temperature. All values in the table have the unit degree Celsius.

	38	34	27	42				
2014	$\mu:12.52$ $\sigma:5.42$	max:21.7 min:1.7	$\mu:9.04$ $\sigma:5.11$	max:16.7 min:-0.1	$\mu:11.86$ $\sigma:5.59$	max:21.4 min:0.9	$\mu:12.97$ $\sigma:4.05$	max:20.6 min:4.6
2015	$\mu:10.85$ $\sigma:5.14$	max:17.9 min:0.6	$\mu:8.69$ $\sigma:3.98$	max:14.6 min:0.8	$\mu:10.2$ $\sigma:5.33$	max:19.1 min:-0.1	$\mu:10.77$ $\sigma:5.04$	max:18.6 min:0.4
2016	$\mu:11.56$ $\sigma:5.92$	max:19.4 min:0.3	$\mu:8.62$ $\sigma:4.69$	max:15.7 min:0.0	$\mu:10.21$ $\sigma:6.22$	max:18.5 min:-2.2	$\mu:11.11$ $\sigma:5.78$	max:19.3 min:0.2
2017	$\mu:10.37$ $\sigma:5.43$	max:16.9 min:0.3	$\mu:8.63$ $\sigma:4.61$	max:15.7 min:0.4	$\mu:9.49$ $\sigma:5.87$	max:17.1 min:-1.3	$\mu:10.32$ $\sigma:5.5$	max:17.3 min:0.1
2018	$\mu:11.09$ $\sigma:6.15$	max:20.5 min:0.6	$\mu:8.31$ $\sigma:5.27$	max:16.0 min:-0.2	$\mu:9.66$ $\sigma:6.44$	max:19.9 min:-0.1	$\mu:10.86$ $\sigma:6.19$	max:19.9 min:0.3
2019	$\mu:10.87$ $\sigma:5.55$	max:20.4 min:0.8	$\mu:9.03$ $\sigma:4.91$	max:17.9 min:0.2	$\mu:10.19$ $\sigma:5.84$	max:20.7 min:0.3	$\mu:10.52$ $\sigma:5.77$	max:19.9 min:0.5
2020	$\mu:9.76$ $\sigma:5.75$	max:18.7 min:0.8	$\mu:8.45$ $\sigma:4.62$	max:15.6 min:0.6	$\mu:10.21$ $\sigma:5.83$	max:19.7 min:-0.5	$\mu:12.79$ $\sigma:4.49$	max:20.1 min:2.5
2021	$\mu:10.77$ $\sigma:6.01$	max:19.2 min:0.3	$\mu:8.79$ $\sigma:4.56$	max:15.7 min:0.2	$\mu:10.03$ $\sigma:6.19$	max:19.3 min:-0.9	$\mu:10.75$ $\sigma:6.74$	max:20.6 min:-0.1
2022	$\mu:10.39$ $\sigma:5.6$	max:17.6 min:0.5	$\mu:8.61$ $\sigma:4.62$	max:15.2 min:0.8	$\mu:9.99$ $\sigma:6.02$	max:18.5 min:-0.8	$\mu:10.6$ $\sigma:5.69$	max:18.5 min:0.3

Table 38: The table shows the statistics of each station for each feature, except for Time as it is a strictly monotonic increasing sequence, for each year. The station names can be found in table 1.  $\mu$  Denotes the mean temperature,  $\sigma$  denotes the standard deviation, "min" is the minimum temperature, and "max" is the maximum temperature. All values in the table have the unit degree Celsius.

	30	41	39	50				
2014	$\mu:11.49$ $\sigma:6.47$	$\max:31.8$ $\min:-3.3$	$\mu:12.2$ $\sigma:6.63$	$\max:33.0$ $\min:-4.5$	$\mu:10.76$ $\sigma:6.24$	$\max:30.7$ $\min:-8.0$	$\mu:11.87$ $\sigma:5.69$	$\max:29.4$ $\min:-1.9$
2015	$\mu:10.15$ $\sigma:5.81$	$\max:25.7$ $\min:-4.9$	$\mu:10.61$ $\sigma:5.68$	$\max:26.4$ $\min:-5.1$	$\mu:9.52$ $\sigma:5.07$	$\max:26.2$ $\min:-5.8$	$\mu:10.58$ $\sigma:5.24$	$\max:24.9$ $\min:-3.3$
2016	$\mu:12.43$ $\sigma:6.28$	$\max:30.4$ $\min:-4.4$	$\mu:11.22$ $\sigma:6.41$	$\max:28.8$ $\min:-5.5$	$\mu:9.51$ $\sigma:5.45$	$\max:29.0$ $\min:-6.4$	$\mu:11.35$ $\sigma:6.02$	$\max:26.5$ $\min:-4.9$
2017	$\mu:10.69$ $\sigma:6.37$	$\max:26.7$ $\min:-8.4$	$\mu:10.71$ $\sigma:6.08$	$\max:27.3$ $\min:-6.4$	$\mu:9.48$ $\sigma:5.69$	$\max:26.2$ $\min:-6.4$	$\mu:11.01$ $\sigma:5.67$	$\max:24.7$ $\min:-9.5$
2018	$\mu:11.32$ $\sigma:9.11$	$\max:32.5$ $\min:-16.8$	$\mu:11.55$ $\sigma:8.63$	$\max:33.7$ $\min:-19.2$	$\mu:9.25$ $\sigma:6.88$	$\max:31.4$ $\min:-15.1$	$\mu:11.73$ $\sigma:7.94$	$\max:31.3$ $\min:-14.0$
2019	$\mu:10.6$ $\sigma:6.99$	$\max:32.0$ $\min:-11.9$	$\mu:10.84$ $\sigma:6.68$	$\max:30.4$ $\min:-12.8$	$\mu:9.19$ $\sigma:6.45$	$\max:30.8$ $\min:-10.9$	$\mu:11.73$ $\sigma:6.32$	$\max:29.5$ $\min:-7.3$
2020	$\mu:11.02$ $\sigma:6.7$	$\max:29.6$ $\min:-7.2$	$\mu:11.32$ $\sigma:6.32$	$\max:30.2$ $\min:-6.6$	$\mu:9.44$ $\sigma:6.22$	$\max:29.8$ $\min:-5.3$	$\mu:11.44$ $\sigma:5.97$	$\max:28.6$ $\min:-5.3$
2021	$\mu:11.42$ $\sigma:6.89$	$\max:30.5$ $\min:-7.0$	$\mu:11.52$ $\sigma:6.55$	$\max:29.8$ $\min:-7.1$	$\mu:9.91$ $\sigma:5.8$	$\max:30.0$ $\min:-3.9$	$\mu:11.77$ $\sigma:6.1$	$\max:26.9$ $\min:-4.8$
2022	$\mu:11.13$ $\sigma:6.84$	$\max:27.2$ $\min:-7.6$	$\mu:11.19$ $\sigma:6.63$	$\max:28.5$ $\min:-7.5$	$\mu:9.5$ $\sigma:5.25$	$\max:27.5$ $\min:-6.0$	$\mu:11.5$ $\sigma:6.0$	$\max:27.7$ $\min:-5.0$

Table 39: The table shows the statistics of each station for each feature, except for Time as it is a strictly monotonic increasing sequence, for each year. The station names can be found in table 1.  $\mu$  Denotes the mean temperature,  $\sigma$  denotes the standard deviation, "min" is the minimum temperature, and "max" is the maximum temperature. All values in the table have the unit degree Celsius.

	30	41	39	50				
2014	$\mu:10.76$ $\sigma:4.84$	max:19.2 min:1.6	$\mu:13.38$ $\sigma:5.72$	max:24.8 min:2.4	$\mu:10.05$ $\sigma:5.34$	max:19.6 min:0.0	$\mu:11.19$ $\sigma:5.04$	max:21.6 min:1.5
	$\mu:9.37$ $\sigma:4.52$	max:16.3 min:0.5	$\mu:11.1$ $\sigma:4.95$	max:20.6 min:0.8	$\mu:9.12$ $\sigma:4.11$	max:15.7 min:1.2	$\mu:10.27$ $\sigma:4.81$	max:19.5 min:0.2
2015	$\mu:13.31$ $\sigma:5.3$	max:23.9 min:-3.3	$\mu:11.17$ $\sigma:5.78$	max:21.9 min:-0.1	$\mu:9.11$ $\sigma:4.87$	max:16.9 min:0.1	$\mu:11.61$ $\sigma:5.56$	max:20.7 min:0.0
	$\mu:11.17$ $\sigma:5.97$	max:23.0 min:-0.2	$\mu:11.0$ $\sigma:4.96$	max:18.5 min:0.3	$\mu:9.0$ $\sigma:4.75$	max:16.9 min:0.3	$\mu:10.9$ $\sigma:4.83$	max:19.0 min:0.3
2018	$\mu:11.53$ $\sigma:6.86$	max:25.6 min:0.4	$\mu:12.44$ $\sigma:7.82$	max:25.9 min:-0.8	$\mu:9.08$ $\sigma:5.86$	max:19.2 min:-0.9	$\mu:10.92$ $\sigma:6.26$	max:21.9 min:-0.3
	$\mu:11.16$ $\sigma:6.38$	max:27.6 min:0.4	$\mu:10.49$ $\sigma:5.4$	max:20.3 min:0.2	$\mu:9.39$ $\sigma:4.91$	max:19.4 min:0.5	$\mu:10.78$ $\sigma:5.08$	max:21.0 min:0.3
2020	$\mu:11.59$ $\sigma:6.17$	max:26.1 min:0.1	$\mu:12.21$ $\sigma:6.33$	max:23.9 min:0.6	$\mu:9.11$ $\sigma:4.85$	max:17.6 min:1.0	$\mu:11.33$ $\sigma:4.97$	max:20.2 min:1.3
	$\mu:11.46$ $\sigma:6.65$	max:23.6 min:-0.9	$\mu:11.89$ $\sigma:6.34$	max:23.5 min:0.0	$\mu:9.44$ $\sigma:4.79$	max:16.9 min:0.5	$\mu:11.51$ $\sigma:5.81$	max:21.0 min:0.0
2022	$\mu:11.19$ $\sigma:5.96$	max:22.6 min:0.1	$\mu:11.32$ $\sigma:6.12$	max:21.8 min:-0.2	$\mu:9.27$ $\sigma:4.35$	max:15.9 min:1.0	$\mu:11.47$ $\sigma:5.39$	max:20.3 min:0.7

Table 40: The table shows the statistics of each station for each feature, except for Time as it is a strictly monotonic increasing sequence, for each year. The station names can be found in table 1.  $\mu$  Denotes the mean temperature,  $\sigma$  denotes the standard deviation, "min" is the minimum temperature, and "max" is the maximum temperature. All values in the table have the unit degree Celsius.

	30	41	39	50
2014	$\mu:11.02$ $\sigma:4.89$	$\mu:12.91$ $\sigma:5.34$	$\mu:9.9$ $\sigma:5.22$	$\mu:10.51$ $\sigma:4.77$
	max:18.9 min:1.6	max:22.2 min:2.6	max:18.4 min:0.0	max:18.8 min:1.8
2015	$\mu:9.66$ $\sigma:4.49$	$\mu:10.83$ $\sigma:4.71$	$\mu:9.02$ $\sigma:4.02$	$\mu:9.87$ $\sigma:4.79$
	max:19.5 min:1.7	max:18.2 min:1.4	max:15.3 min:1.4	max:17.9 min:0.4
2016	$\mu:13.17$ $\sigma:4.83$	$\mu:10.83$ $\sigma:5.51$	$\mu:9.01$ $\sigma:4.76$	$\mu:11.44$ $\sigma:5.37$
	max:21.1 min:-3.3	max:19.7 min:0.0	max:16.1 min:0.1	max:19.2 min:0.3
2017	$\mu:10.92$ $\sigma:5.69$	$\mu:10.63$ $\sigma:4.75$	$\mu:8.92$ $\sigma:4.64$	$\mu:10.24$ $\sigma:4.67$
	max:19.8 min:-0.1	max:16.4 min:0.4	max:16.2 min:0.5	max:17.5 min:0.5
2018	$\mu:11.36$ $\sigma:6.4$	$\mu:11.76$ $\sigma:7.33$	$\mu:8.93$ $\sigma:5.75$	$\mu:10.59$ $\sigma:5.96$
	max:22.3 min:0.6	max:22.2 min:-0.3	max:18.2 min:-0.3	max:19.3 min:0.0
2019	$\mu:11.03$ $\sigma:5.87$	$\mu:10.37$ $\sigma:5.12$	$\mu:9.31$ $\sigma:4.77$	$\mu:10.57$ $\sigma:4.9$
	max:23.5 min:0.7	max:18.5 min:0.7	max:18.5 min:0.7	max:19.3 min:0.5
2020	$\mu:11.37$ $\sigma:5.73$	$\mu:11.8$ $\sigma:6.0$	$\mu:9.02$ $\sigma:4.73$	$\mu:11.05$ $\sigma:4.78$
	max:22.5 min:0.4	max:21.2 min:1.0	max:16.3 min:1.1	max:18.6 min:1.5
2021	$\mu:11.12$ $\sigma:6.41$	$\mu:11.7$ $\sigma:6.08$	$\mu:9.35$ $\sigma:4.71$	$\mu:11.05$ $\sigma:5.6$
	max:21.3 min:-0.3	max:21.4 min:0.2	max:16.4 min:0.6	max:19.1 min:0.0
2022	$\mu:10.98$ $\sigma:5.68$	$\mu:11.15$ $\sigma:5.83$	$\mu:9.15$ $\sigma:4.27$	$\mu:11.0$ $\sigma:5.14$
	max:19.8 min:0.4	max:19.5 min:0.1	max:15.5 min:1.1	max:18.5 min:0.8

Table 41: The table shows the statistics of each station for each feature, except for Time as it is a strictly monotonic increasing sequence, for each year. The station names can be found in table 1.  $\mu$  Denotes the mean temperature,  $\sigma$  denotes the standard deviation, "min" is the minimum temperature, and "max" is the maximum temperature. All values in the table have the unit degree Celsius.

	26	57	118	37				
2014	$\mu:10.33$ $\sigma:6.83$	max:30.2 min:-5.1	$\mu:10.92$ $\sigma:6.59$	max:31.2 min:-11.9	$\mu:11.79$ $\sigma:6.38$	max:31.5 min:-3.5	$\mu:10.8$ $\sigma:6.44$	max:30.7 min:-4.6
2015	$\mu:8.99$ $\sigma:6.13$	max:27.1 min:-9.3	$\mu:9.57$ $\sigma:5.37$	max:27.5 min:-6.7	$\mu:10.28$ $\sigma:5.48$	max:24.6 min:-4.9	$\mu:9.36$ $\sigma:5.74$	max:26.2 min:-6.0
2016	$\mu:9.74$ $\sigma:6.73$	max:26.7 min:-7.2	$\mu:9.54$ $\sigma:6.02$	max:28.6 min:-8.1	$\mu:10.99$ $\sigma:6.22$	max:27.3 min:-5.8	$\mu:10.16$ $\sigma:6.44$	max:26.9 min:-9.8
2017	$\mu:8.93$ $\sigma:6.48$	max:28.5 min:-11.8	$\mu:9.41$ $\sigma:5.9$	max:27.1 min:-8.0	$\mu:10.43$ $\sigma:5.9$	max:25.2 min:-6.4	$\mu:9.48$ $\sigma:6.11$	max:24.6 min:-7.0
2018	$\mu:9.95$ $\sigma:10.0$	max:32.4 min:-26.3	$\mu:9.59$ $\sigma:7.61$	max:32.0 min:-21.4	$\mu:11.34$ $\sigma:8.46$	max:33.1 min:-16.6	$\mu:10.51$ $\sigma:8.76$	max:31.3 min:-20.1
2019	$\mu:9.24$ $\sigma:7.48$	max:30.4 min:-17.4	$\mu:9.31$ $\sigma:6.98$	max:32.4 min:-13.0	$\mu:11.06$ $\sigma:6.72$	max:31.5 min:-11.3	$\mu:9.97$ $\sigma:7.08$	max:31.6 min:-16.6
2020	$\mu:9.95$ $\sigma:6.9$	max:28.9 min:-8.5	$\mu:9.62$ $\sigma:6.62$	max:32.8 min:-6.2	$\mu:11.44$ $\sigma:6.45$	max:30.2 min:-6.6	$\mu:10.4$ $\sigma:6.7$	max:29.7 min:-7.4
2021	$\mu:10.08$ $\sigma:7.17$	max:28.1 min:-12.0	$\mu:9.89$ $\sigma:6.38$	max:29.9 min:-8.3	$\mu:11.59$ $\sigma:6.59$	max:29.4 min:-5.5	$\mu:10.51$ $\sigma:6.81$	max:28.2 min:-8.1
2022	$\mu:9.56$ $\sigma:7.24$	max:27.0 min:-12.8	$\mu:9.72$ $\sigma:5.79$	max:28.4 min:-8.2	$\mu:11.4$ $\sigma:6.71$	max:29.4 min:-7.3	$\mu:10.16$ $\sigma:6.92$	max:30.5 min:-9.7

Table 42: The table shows the statistics of each station for each feature, except for Time as it is a strictly monotonic increasing sequence, for each year. The station names can be found in table 1.  $\mu$  Denotes the mean temperature,  $\sigma$  denotes the standard deviation, "min" is the minimum temperature, and "max" is the maximum temperature. All values in the table have the unit degree Celsius.

	26	57	118	37
2014	$\mu:10.52$ $\sigma:5.78$	$\mu:10.6$ $\sigma:5.7$	$\mu:11.9$ $\sigma:5.26$	$\mu:11.24$ $\sigma:5.15$
	max:21.7 min:-0.2	max:22.2 min:0.0	max:21.8 min:1.9	max:21.6 min:2.0
2015	$\mu:8.86$ $\sigma:5.28$	$\mu:9.55$ $\sigma:4.38$	$\mu:10.51$ $\sigma:5.02$	$\mu:9.76$ $\sigma:4.51$
	max:18.2 min:-0.5	max:16.7 min:0.1	max:19.5 min:0.5	max:17.8 min:0.5
2016	$\mu:9.26$ $\sigma:6.05$	$\mu:9.15$ $\sigma:5.25$	$\mu:10.87$ $\sigma:5.6$	$\mu:10.59$ $\sigma:5.56$
	max:19.1 min:-2.3	max:17.4 min:-0.2	max:19.6 min:-0.4	max:19.8 min:-0.4
2017	$\mu:8.9$ $\sigma:6.11$	$\mu:9.04$ $\sigma:4.87$	$\mu:10.1$ $\sigma:4.97$	$\mu:10.15$ $\sigma:5.15$
	max:18.5 min:-2.7	max:16.3 min:-0.1	max:16.9 min:-0.2	max:18.5 min:-0.2
2018	$\mu:9.85$ $\sigma:7.19$	$\mu:8.46$ $\sigma:5.6$	$\mu:10.15$ $\sigma:6.35$	$\mu:11.1$ $\sigma:6.22$
	max:22.6 min:-1.4	max:17.1 min:-1.3	max:19.4 min:-0.9	max:21.2 min:-1.5
2019	$\mu:10.17$ $\sigma:5.66$	$\mu:9.2$ $\sigma:5.27$	$\mu:10.67$ $\sigma:5.49$	$\mu:10.77$ $\sigma:5.61$
	max:21.4 min:0.0	max:19.4 min:0.1	max:20.9 min:0.1	max:21.4 min:-0.2
2020	$\mu:9.52$ $\sigma:6.26$	$\mu:9.55$ $\sigma:5.29$	$\mu:10.82$ $\sigma:5.07$	$\mu:10.81$ $\sigma:5.29$
	max:22.5 min:-2.5	max:18.0 min:0.1	max:19.6 min:0.4	max:21.0 min:0.0
2021	$\mu:9.59$ $\sigma:6.59$	$\mu:9.21$ $\sigma:5.32$	$\mu:10.28$ $\sigma:5.91$	$\mu:10.59$ $\sigma:6.4$
	max:20.9 min:-3.0	max:17.8 min:-0.3	max:19.6 min:-0.7	max:22.0 min:-0.5
2022	$\mu:9.1$ $\sigma:6.18$	$\mu:9.71$ $\sigma:4.97$	$\mu:10.22$ $\sigma:5.15$	$\mu:10.34$ $\sigma:5.99$
	max:20.4 min:-2.4	max:18.1 min:0.3	max:17.4 min:0.2	max:19.9 min:-0.3

Table 43: The table shows the statistics of each station for each feature, except for Time as it is a strictly monotonic increasing sequence, for each year. The station names can be found in table 1.  $\mu$  Denotes the mean temperature,  $\sigma$  denotes the standard deviation, "min" is the minimum temperature, and "max" is the maximum temperature. All values in the table have the unit degree Celsius.

	26	57	118	37				
2014	$\mu:10.49$ $\sigma:5.59$	max:19.7 min:0.1	$\mu:10.15$ $\sigma:5.36$	max:19.1 min:-0.1	$\mu:11.67$ $\sigma:5.0$	max:20.3 min:2.4	$\mu:11.15$ $\sigma:4.94$	max:19.7 min:2.3
2015	$\mu:9.01$ $\sigma:5.33$	max:17.5 min:-0.2	$\mu:9.34$ $\sigma:4.32$	max:15.5 min:0.2	$\mu:10.4$ $\sigma:4.73$	max:18.0 min:0.9	$\mu:9.72$ $\sigma:4.53$	max:16.6 min:0.6
2016	$\mu:9.59$ $\sigma:6.09$	max:18.4 min:-1.6	$\mu:8.95$ $\sigma:5.12$	max:16.2 min:0.0	$\mu:10.77$ $\sigma:5.26$	max:18.3 min:-0.1	$\mu:10.39$ $\sigma:5.42$	max:18.3 min:-0.4
2017	$\mu:9.1$ $\sigma:6.18$	max:17.7 min:-1.8	$\mu:8.8$ $\sigma:4.74$	max:15.2 min:0.1	$\mu:9.99$ $\sigma:4.77$	max:16.0 min:0.2	$\mu:10.12$ $\sigma:5.04$	max:16.9 min:0.0
2018	$\mu:10.14$ $\sigma:7.06$	max:20.6 min:-0.8	$\mu:8.11$ $\sigma:5.41$	max:15.6 min:-0.9	$\mu:9.93$ $\sigma:6.07$	max:18.3 min:-0.6	$\mu:10.89$ $\sigma:6.13$	max:20.0 min:-0.7
2019	$\mu:9.87$ $\sigma:5.89$	max:19.9 min:0.3	$\mu:9.02$ $\sigma:5.12$	max:18.3 min:0.2	$\mu:10.45$ $\sigma:5.27$	max:19.4 min:0.3	$\mu:10.46$ $\sigma:5.43$	max:19.3 min:-0.3
2020	$\mu:9.24$ $\sigma:6.06$	max:20.1 min:-2.2	$\mu:9.37$ $\sigma:5.17$	max:16.8 min:0.1	$\mu:10.61$ $\sigma:4.84$	max:18.3 min:0.8	$\mu:10.83$ $\sigma:5.16$	max:19.4 min:0.5
2021	$\mu:9.35$ $\sigma:6.37$	max:19.3 min:-2.0	$\mu:8.96$ $\sigma:5.18$	max:16.6 min:-0.3	$\mu:10.0$ $\sigma:5.67$	max:18.1 min:-0.7	$\mu:10.52$ $\sigma:6.31$	max:20.5 min:-0.3
2022	$\mu:8.85$ $\sigma:6.0$	max:18.5 min:-1.7	$\mu:9.48$ $\sigma:4.84$	max:16.8 min:0.4	$\mu:9.93$ $\sigma:4.95$	max:16.5 min:0.5	$\mu:10.38$ $\sigma:5.87$	max:18.7 min:0.0

Table 44: The table shows the statistics of each station for each feature, except for Time as it is a strictly monotonic increasing sequence, for each year. The station names can be found in table 1.  $\mu$  Denotes the mean temperature,  $\sigma$  denotes the standard deviation, "min" is the minimum temperature, and "max" is the maximum temperature. All values in the table have the unit degree Celsius.

	52	11	15	17				
2014	$\mu:11.96$ $\sigma:6.68$	$\max:31.9$ $\min:-4.0$	$\mu:10.66$ $\sigma:6.47$	$\max:30.0$ $\min:-4.5$	$\mu:11.17$ $\sigma:6.3$	$\max:32.4$ $\min:-9.4$	$\mu:\text{nan}$ $\sigma:\text{nan}$	$\max:\text{nan}$ $\min:\text{nan}$
2015	$\mu:10.45$ $\sigma:5.93$	$\max:25.8$ $\min:-6.4$	$\mu:9.12$ $\sigma:5.76$	$\max:28.6$ $\min:-7.1$	$\mu:9.86$ $\sigma:5.17$	$\max:27.9$ $\min:-2.9$	$\mu:\text{nan}$ $\sigma:\text{nan}$	$\max:\text{nan}$ $\min:\text{nan}$
2016	$\mu:11.1$ $\sigma:6.46$	$\max:28.4$ $\min:-5.7$	$\mu:9.84$ $\sigma:6.49$	$\max:26.4$ $\min:-7.4$	$\mu:9.98$ $\sigma:5.58$	$\max:28.1$ $\min:-4.2$	$\mu:11.34$ $\sigma:6.03$	$\max:25.8$ $\min:-5.5$
2017	$\mu:10.37$ $\sigma:6.16$	$\max:25.6$ $\min:-6.7$	$\mu:9.05$ $\sigma:6.17$	$\max:28.5$ $\min:-8.7$	$\mu:9.67$ $\sigma:5.6$	$\max:26.5$ $\min:-6.1$	$\mu:8.24$ $\sigma:6.65$	$\max:25.2$ $\min:-16.7$
2018	$\mu:11.45$ $\sigma:8.54$	$\max:32.6$ $\min:-18.0$	$\mu:10.17$ $\sigma:9.32$	$\max:30.2$ $\min:-21.4$	$\mu:9.88$ $\sigma:7.04$	$\max:32.6$ $\min:-15.4$	$\mu:9.07$ $\sigma:9.79$	$\max:29.8$ $\min:-25.9$
2019	$\mu:10.7$ $\sigma:6.75$	$\max:30.6$ $\min:-13.2$	$\mu:9.28$ $\sigma:7.08$	$\max:29.4$ $\min:-13.2$	$\mu:9.7$ $\sigma:6.67$	$\max:33.5$ $\min:-10.0$	$\mu:8.75$ $\sigma:7.46$	$\max:29.9$ $\min:-20.4$
2020	$\mu:11.07$ $\sigma:6.5$	$\max:28.9$ $\min:-7.1$	$\mu:9.92$ $\sigma:6.66$	$\max:28.5$ $\min:-9.0$	$\mu:9.94$ $\sigma:6.46$	$\max:32.5$ $\min:-4.5$	$\mu:9.64$ $\sigma:7.22$	$\max:29.4$ $\min:-18.3$
2021	$\mu:11.06$ $\sigma:6.62$	$\max:27.7$ $\min:-7.6$	$\mu:10.18$ $\sigma:6.76$	$\max:27.7$ $\min:-8.8$	$\mu:10.38$ $\sigma:6.12$	$\max:30.6$ $\min:-4.8$	$\mu:\text{nan}$ $\sigma:\text{nan}$	$\max:\text{nan}$ $\min:\text{nan}$
2022	$\mu:10.88$ $\sigma:6.85$	$\max:28.0$ $\min:-8.7$	$\mu:9.64$ $\sigma:6.65$	$\max:26.8$ $\min:-10.3$	$\mu:10.03$ $\sigma:5.5$	$\max:30.2$ $\min:-4.8$	$\mu:9.07$ $\sigma:7.16$	$\max:27.7$ $\min:-15.0$

Table 45: The table shows the statistics of each station for each feature, except for Time as it is a strictly monotonic increasing sequence, for each year. The station names can be found in table 1.  $\mu$  Denotes the mean temperature,  $\sigma$  denotes the standard deviation, "min" is the minimum temperature, and "max" is the maximum temperature. All values in the table have the unit degree Celsius.

	52	11	15	17				
2014	$\mu:12.46$ $\sigma:5.16$	max:23.2 min:2.6	$\mu:11.15$ $\sigma:5.98$	max:23.3 min:0.1	$\mu:9.38$ $\sigma:4.48$	max:17.2 min:0.5	$\mu:\text{nan}$ $\sigma:\text{nan}$	max:nan min:nan
2015	$\mu:11.31$ $\sigma:4.86$	max:19.4 min:1.1	$\mu:8.04$ $\sigma:5.15$	max:19.7 min:-0.2	$\mu:8.81$ $\sigma:3.98$	max:15.6 min:1.5	$\mu:\text{nan}$ $\sigma:\text{nan}$	max:nan min:nan
2016	$\mu:11.95$ $\sigma:5.67$	max:20.2 min:0.1	$\mu:10.03$ $\sigma:6.29$	max:20.0 min:-1.3	$\mu:8.88$ $\sigma:4.8$	max:17.3 min:-0.2	$\mu:12.88$ $\sigma:4.55$	max:20.7 min:2.5
2017	$\mu:10.89$ $\sigma:5.34$	max:19.7 min:0.1	$\mu:9.31$ $\sigma:6.13$	max:18.3 min:-1.4	$\mu:8.93$ $\sigma:4.52$	max:16.3 min:-0.1	$\mu:8.66$ $\sigma:6.31$	max:19.7 min:-1.9
2018	$\mu:11.39$ $\sigma:6.8$	max:21.2 min:-1.0	$\mu:10.31$ $\sigma:6.95$	max:21.9 min:0.0	$\mu:8.82$ $\sigma:5.22$	max:18.5 min:-0.1	$\mu:9.55$ $\sigma:6.99$	max:22.8 min:-0.5
2019	$\mu:11.66$ $\sigma:5.5$	max:21.7 min:0.3	$\mu:9.73$ $\sigma:6.26$	max:22.0 min:-0.1	$\mu:9.24$ $\sigma:4.97$	max:20.2 min:0.2	$\mu:9.09$ $\sigma:6.32$	max:21.4 min:-0.5
2020	$\mu:12.33$ $\sigma:4.97$	max:21.7 min:0.8	$\mu:9.93$ $\sigma:6.39$	max:22.4 min:-1.6	$\mu:9.29$ $\sigma:5.11$	max:19.6 min:0.2	$\mu:9.71$ $\sigma:6.53$	max:20.8 min:-1.2
2021	$\mu:6.95$ $\sigma:5.75$	max:22.1 min:0.0	$\mu:10.11$ $\sigma:6.25$	max:20.4 min:-0.3	$\mu:9.9$ $\sigma:5.1$	max:19.1 min:0.4	$\mu:\text{nan}$ $\sigma:\text{nan}$	max:nan min:nan
2022	$\mu:14.0$ $\sigma:3.07$	max:19.4 min:7.4	$\mu:13.18$ $\sigma:3.95$	max:21.3 min:3.9	$\mu:9.42$ $\sigma:4.41$	max:17.1 min:0.4	$\mu:9.33$ $\sigma:6.4$	max:19.9 min:-2.4

Table 46: The table shows the statistics of each station for each feature, except for Time as it is a strictly monotonic increasing sequence, for each year. The station names can be found in table 1.  $\mu$  Denotes the mean temperature,  $\sigma$  denotes the standard deviation, "min" is the minimum temperature, and "max" is the maximum temperature. All values in the table have the unit degree Celsius.

	52	11	15	17
2014	$\mu:12.15$ $\sigma:4.93$	$\mu:10.92$ $\sigma:5.76$	$\mu:9.21$ $\sigma:4.35$	$\mu:\text{nan}$ $\sigma:\text{nan}$
	max:20.9 min:3.3	max:21.6 min:0.3	max:16.0 min:0.5	max:nan min:nan
2015	$\mu:11.08$ $\sigma:4.7$	$\mu:7.92$ $\sigma:4.91$	$\mu:8.71$ $\sigma:3.88$	$\mu:\text{nan}$ $\sigma:\text{nan}$
	max:17.8 min:1.6	max:17.9 min:0.0	max:15.0 min:1.7	max:nan min:nan
2016	$\mu:11.67$ $\sigma:5.44$	$\mu:9.84$ $\sigma:6.06$	$\mu:8.75$ $\sigma:4.63$	$\mu:12.63$ $\sigma:4.0$
	max:18.7 min:0.4	max:18.5 min:-0.7	max:16.1 min:0.0	max:18.0 min:3.6
2017	$\mu:10.64$ $\sigma:5.15$	$\mu:9.1$ $\sigma:5.99$	$\mu:8.8$ $\sigma:4.38$	$\mu:8.31$ $\sigma:6.08$
	max:18.0 min:0.2	max:16.8 min:-1.1	max:15.4 min:0.2	max:17.2 min:-1.4
2018	$\mu:11.08$ $\sigma:6.52$	$\mu:10.15$ $\sigma:6.54$	$\mu:8.7$ $\sigma:5.03$	$\mu:9.22$ $\sigma:6.46$
	max:20.0 min:-0.6	max:20.3 min:0.2	max:17.1 min:0.1	max:19.9 min:-0.3
2019	$\mu:11.38$ $\sigma:5.3$	$\mu:9.67$ $\sigma:5.96$	$\mu:9.12$ $\sigma:4.75$	$\mu:8.89$ $\sigma:5.97$
	max:20.4 min:0.5	max:20.4 min:0.3	max:18.7 min:0.5	max:19.4 min:-0.3
2020	$\mu:12.26$ $\sigma:4.77$	$\mu:9.82$ $\sigma:6.13$	$\mu:9.17$ $\sigma:4.9$	$\mu:9.35$ $\sigma:6.15$
	max:20.4 min:1.2	max:20.5 min:-0.7	max:17.9 min:0.5	max:18.3 min:-0.4
2021	$\mu:12.57$ $\sigma:6.03$	$\mu:10.01$ $\sigma:5.99$	$\mu:9.78$ $\sigma:4.93$	$\mu:\text{nan}$ $\sigma:\text{nan}$
	max:24.2 min:0.0	max:19.1 min:0.1	max:17.8 min:0.6	max:nan min:nan
2022	$\mu:12.15$ $\sigma:5.25$	$\mu:12.99$ $\sigma:3.61$	$\mu:9.34$ $\sigma:4.29$	$\mu:9.09$ $\sigma:6.2$
	max:22.4 min:0.9	max:19.2 min:5.1	max:16.1 min:0.7	max:18.0 min:-1.1

Table 47: The table shows the statistics of each station for each feature, except for Time as it is a strictly monotonic increasing sequence, for each year. The station names can be found in table 1.  $\mu$  Denotes the mean temperature,  $\sigma$  denotes the standard deviation, "min" is the minimum temperature, and "max" is the maximum temperature. All values in the table have the unit degree Celsius.





Norges miljø- og biovitenskapelige universitet  
Noregs miljø- og biovitenskapslelege universitet  
Norwegian University of Life Sciences

Postboks 5003  
NO-1432 Ås  
Norway